

THE UNIVERSITY OF CHICAGO

RAPIDLY INTRODUCING MOLECULAR COMPLEXITY:
REACTION DEVELOPMENT AND APPLICATION TO HYDROCARBON AND
HETEROCYCLIC FRAMEWORKS

A DISSERTATION SUBMITTED TO
THE FACULTY OF THE DIVISION OF THE PHYSICAL SCIENCES
IN CANDIDACY FOR THE DEGREE OF
DOCTOR OF PHILOSOPHY

DEPARTMENT OF CHEMISTRY

BY

CHARLES JAMES FREDERICK COLE

CHICAGO, ILLINOIS

JUNE 2021

“The unique challenge which chemical synthesis provides for the creative imagination and the skilled hand ensures that it will endure as long as men write books, paint pictures, and fashion things which are beautiful, or practical, or both.”

– R. B. Woodward

TABLE OF CONTENTS

List of Schemes	vi
List of Figures	xi
List of Tables	xiii
List of Abbreviations	xiv
Acknowledgements	xvii
Abstract	xxi
Chapter 1. Preparation and Application of Novel Disulfanium Salts to Polyene Cyclizations	1
1.1. Introduction	2
1.2. Modular Preparation of Novel Alkyl and Aryl Disulfanium Salts	8
1.3. Applications to Polyene Cyclizations and Initial Asymmetric Studies	9
1.4. Conclusion	13
1.5. References	14
1.6. Experimental Section	16
1.7. ¹ H and ¹³ C NMR Data	26
1.8. HPLC Traces	48
Chapter 2. Total Syntheses of Spiroviolene and Spirograterpene A	49
2.1. Introduction	50
2.2. Pursuing New Targets	53
2.3. Proposed Biosynthesis of Spiroviolene and Spirograterpene A	55
2.4. Total Synthesis of Spiroviolene	58
2.5. Total Synthesis of Spirograterpene A	60

2.6. Evidence for the Structural Reassignment of 21	63
2.7. Revised Biosynthesis of Spiroviolene	65
2.8. Conclusion	67
2.9. References	68
2.10. Experimental Section	71
2.11. ¹ H and ¹³ C NMR Data	93
Chapter 3. Development of an Asymmetric Pyrone Diels–Alder Reaction Mediated by Dienamine Catalysis	124
3.1. Introduction	125
3.2. The Pyrone Diels–Alder Reaction in Total Synthesis	126
3.3. Asymmetric Pyrone Diels–Alder Reactions	131
3.4. Dienamine Catalysis and the Diels–Alder Reaction	134
3.5. Initial Discovery and Reaction Optimization	136
3.6. Exploring and Understanding the Reaction Scope	140
3.7. Derivatization of Bicyclic Lactone Products	145
3.8. Initial Studies Towards the Gardmutine Alkaloids	147
3.9. Application to the Pyridone Diels–Alder Reaction	152
3.10. Conclusion	155
3.11. References	156
3.12. Experimental Section	160
3.13. ¹ H and ¹³ C NMR Data	194
3.14. HPLC Traces	291
3.15. X-Ray Crystallographic Data	334

Chapter 4. Study Towards the Total Synthesis of Nareline	343
4.1. Introduction	344
4.2. Biosynthesis of the Akuammiline Alkaloids	345
4.3. Selected Total Syntheses of the Akuammiline Family of Natural Products	346
4.4. A Modular Approach to Indole Alkaloid Natural Products	352
4.5. Isolation and Structural Determination of Nareline	357
4.6. Retrosynthesis of Nareline	358
4.7. Initial Approach: β -Carboline Propargylation	359
4.8. Pictet–Spengler Approach to the [Au]-Cyclization Precursor	362
4.9. Imposing Structural Rigidity	364
4.10. Attempts to Close the E-Ring with Furoindole 131	369
4.11. Studies on Conjugate Additions to 145	371
4.12. Current Progress and Future Outlook	373
4.13. Conclusion	376
4.14. References	378
4.15. Experimental Section	382
4.16. ^1H NMR Data	398

LIST OF SCHEMES

Scheme 1.1. (a) Block and Rittenberg study on link between cholesterol (2) and acetic acid; (b) Stork and (c) Eschenmoser studies on the mechanism of polyene cyclizations	2
Scheme 1.2. (a) Enzyme-mediated polyene cyclization of squalene (10); (b) Early example of polyene cyclizations in total synthesis	4
Scheme 1.3. Potent electrophilic halonium sources 18-20 and application of 18 to the total synthesis of peyssonol A (23).....	5
Scheme 1.4. Pioneering examples of thiiranium-promoted in both racemic and asymmetric fashions.....	6
Scheme 1.5. (a) Alkyl disulfanium salts synthesized previously and the proposed mechanism for their formation; (b) Chiral disulfanium salts which served as key inspiration for developed method.....	7
Scheme 1.6. Modular preparation of disulfanium salts 47-53 from commercially available materials	9
Scheme 1.7. Initial exploration of chiral disulfanium salts 75-77	12
Scheme 2.1. Utilizing quaternary carbons to guide and expedite the total synthesis of non-functionalized terpenes as in 17-20	53
Scheme 2.2. (a) Structural similarities between non-functionalized terpenes 21, 22 and 23 ; (b) Retrosynthetic analysis of 21 and 22	54
Scheme 2.3. (a) Literature-precedent for the 1,3-trans-stereochemistry as set by the Heck cyclization; (b) Stereodetermining step of the Heck cyclization to afford 24	55
Scheme 2.4. Proposed biosynthesis of 21 from GGPP (28).....	56
Scheme 2.5. Proposed biosynthesis of 22 and 38 from GGPP.....	57
Scheme 2.6. Asymmetric preparation of sidechain 27	58
Scheme 2.7. Total synthesis of spiroviolene (21) starting from known intermediate 48	59

Scheme 2.8. Total synthesis of spirograterpene A (22) starting from known intermediate 53	61
Scheme 2.9. Synthetic and NMR support for the structural reassignment of spiroviolene (21).....	63
Scheme 2.10. Revised biosynthesis for the formation of 21 that also provides reasonable access to 22 and 23	66
Scheme 3.1. Pyrone Diels–Alder reaction.....	125
Scheme 3.2. Pyrone Diels–Alder reactions as a means to access arene and bridged frameworks	126
Scheme 3.3. Pyrone Diels–Alder reactions used in total synthesis to (a) install a bicyclic lactone, (b) form a diene for further functionalization and (c) set key relative stereochemistry.....	128
Scheme 3.4. Previous work from the Snyder group in pyrone Diels–Alder chemistry	130
Scheme 3.5. Initial approaches to controlling absolute stereochemistry in the pyrone Diels–Alder reaction	131
Scheme 3.6. Literature precedented normal electron-demand asymmetric pyrone Diels–Alder reaction	132
Scheme 3.7. Literature precedented inverse electron-demand pyrone Diels–Alder reaction and the application to the synthesis of (+)-MK7607	133
Scheme 3.8. Reactivity patterns common to dienamine catalysis.....	134
Scheme 3.9. Literature precedent for dienamine- and trienamine-catalyzed Diels–Alder reactions.....	135
Scheme 3.10. Generic proposal for dienamine-catalyzed pyrone Diels–Alder reaction.....	136
Scheme 3.11. Accounting for observed substrate trends initial screening	138

Scheme 3.12. Studying the regioisomeric outcome from the reaction of 35 with citral (116)	142
Scheme 3.13. Selected derivatization of Diels–Alder products	146
Scheme 3.14. Conversion of cyanopyrone 146 to protected diol 149.....	149
Scheme 3.15. Early attempts at forming the gem-dihalocyclopropane.....	150
Scheme 3.16. Installation of gem-dibromocyclopropane and attempts at Ag-promoted ring opening.....	151
Scheme 3.17. Pyridone Diels–Alder reaction.....	152
Scheme 3.18. Examples of normal and inverse electron-demand pyridone Diels–Alder reactions.....	153
Scheme 3.19. First example of a catalytic asymmetric pyridone Diels–Alder reaction.....	153
Scheme 4.1. Proposed biosynthesis of the akuammiline alkaloids through key intermediate geissoschizine (17)	346
Scheme 4.2. MacMillan synthesis of vincorine (8).....	347
Scheme 4.3. Ma synthesis of aspidophylline A (2).....	348
Scheme 4.4. Zhu synthesis of strictamine (3).....	350
Scheme 4.5. Garg synthesis of picrinine (4) and formal synthesis of strictamine (3).....	351
Scheme 4.6. Common approach to indole alkaloid natural products with selected examples	352
Scheme 4.7. Modular approach to indole alkaloid natural products	354
Scheme 4.8. Concise formal synthesis of strictamine (3) by Snyder	355
Scheme 4.9. Snyder synthesis of arboridinine (60).....	355
Scheme 4.10. Snyder synthesis of arborisidine (61)	356
Scheme 4.11. Proposed biosynthesis of nareline (5) from akuammiline (1).....	358
Scheme 4.12. Proposed route to nareline (5).....	359

Scheme 4.13. Initial explorations into propargylation of β -carboline 94	360
Scheme 4.14. Aminoalcohol approach to Au-cyclization product 103	361
Scheme 4.15. Pictet–Spengler approach to 6- <i>endo</i> -dig cyclization product 111	362
Scheme 4.16. 6- <i>endo</i> -dig cyclization of <i>cis</i> - and <i>trans</i> - 112	363
Scheme 4.17. Attempt at Ni-mediated 6- <i>exo</i> -dig cyclization with 116	364
Scheme 4.18. Proposed bicyclic lactone intermediate and observed undesired rearrangement product (124)	366
Scheme 4.19. Chemoselective ester hydrolysis and failed attempt at intramolecular lactonization	366
Scheme 4.20. Common 5-membered ring motif found in many akuammiline alkaloids and proposed installation of furoindole ring in 129	367
Scheme 4.21. Proposed connection between picrinine (4) and nareline (5).....	368
Scheme 4.22. Preparation of α -aminonitrile and failed attempt at retro-Strecker reaction to form furoindole 140	368
Scheme 4.23. One-pot Barton decarboxylation/oxidation sequence to afford furoindole 131	369
Scheme 4.24. Studies on the 6- <i>exo</i> -dig cyclization of furoindole 138	370
Scheme 4.25. Attempts at intramolecular Michael addition	371
Scheme 4.26. Unsuccessful conjugate additions to 145 and an example from our group	371
Scheme 4.27. Conjugate addition of cyanide to 145 and rationale for observed stereoselectivity	373
Scheme 4.28. Observed epimerization of nitrile 149 and α -functionalization to introduce desired sidechain	375
Scheme 4.29. Alkylation of secondary amine 156 with various alkyl halides.....	375
Scheme 4.30. Proposed end-game strategy to access picrinine (4).....	376

Scheme 4.31. **111** as a proposed intermediate to access a wide variety of akuammiline
alkaloids..... 377

LIST OF FIGURES

Figure 2.1. Quaternary centers in (a) biologically relevant natural products, (b) ligands relevant to stereoselective transformations, and (c) medicinal chemistry.....	50
Figure 2.2. Potential Energy Surface for both α - and β -face hydroboration of simplified substrate 69 indicating a kinetic preference via TS1. Calculated at the B3LYP/aug-cc-pvDZ level of theory in the gas phase, values are zero-point energy corrected total energies [$\Delta H_{\text{rel}}(0\text{K})(\text{kcal/mol})$].....	64
Figure 2.3. ^1H NMR comparison of the Barton product (top) to synthetic 21 (bottom).....	90
Figure 2.4. ^{13}C NMR comparison of the Barton product (top) to synthetic 21 (bottom).....	90
Figure 2.5. ^1H NMR comparison of the Double Barton product (top) to synthetic 21	92
Figure 2.6. ^{13}C NMR comparison of the Double Barton product (top) to synthetic 21	92
Figure 3.1. Natural products accessed via key pyrone Diels–Alder reactions	127
Figure 3.2. Transition state analysis to account for <i>dr</i> outcomes	145
Figure 3.3. (a) Gardmutine alkaloids and shared structural framework with pyrone Diels–Alder product. (b) Proposed key ring expansion to form core azabicyclic 145	148
Figure 3.4. ORTEP representation of <i>Endo</i> - 88	334
Figure 3.5. ORTEP representation of <i>Endo</i> - 106	335
Figure 3.6. ORTEP representation of <i>Endo</i> - 110	336
Figure 3.7. ORTEP representation of <i>Endo</i> - 114	337
Figure 3.8. ORTEP representation of <i>Endo</i> - 115	338
Figure 3.9. ORTEP representation of <i>Exo</i> - 115	340
Figure 3.10. ORTEP representation of 128	341
Figure 3.11. ORTEP representation of 138	342
Figure 4.1. The diverse members of the akuammiline alkaloid family of natural products..	344
Figure 4.2. Structural features common to many indole alkaloid natural product	353

Figure 4.3. Conformation about the bridged piperidine ring and the implication on the potential for cyclization.....	365
--	-----

LIST OF TABLES

Table 1.1. Thiiranium-promoted polyene cyclization of homogeranyl benzene (28) with disulfanium salts 47-43	10
Table 1.2. Scope of monoalkene and polyene cyclizations as effected by ethyl disulfanium salt 48	11
Table 2.1. Conditions screened to effect olefin isomerization to 60	62
Table 2.2. Comparison of ¹ H NMR data of spiroviolene (21) between our synthetic sample and the natural isolate.....	76
Table 2.3. Comparison of ¹³ C NMR data of spiroviolene (21) between our synthetic sample and the natural isolate.....	78
Table 2.4. Comparison of ¹ H NMR data of spirograterpene A (22) between our synthetic sample and the natural isolate.....	86
Table 2.5. Comparison of ¹³ C NMR data of spirograterpene (22) between our synthetic sample and the natural isolate.....	87
Table 3.1. Initial reaction discovery and substrate screening.....	137
Table 3.2. Exploration of various catalyst scaffolds to promote the pyrone Diels–Alder reaction.....	139
Table 3.3. Exploration of diarylprolinol scaffolds to promote the Diels–Alder reaction.....	140
Table 3.4. Exploring the scope of compatible enal partners.....	141
Table 3.5. Exploring the effect of ester positioning on the reactivity of the pyrone partner.....	143
Table 3.6. Exploring the scope of 2-pyrones as dienes.....	144
Table 3.7. Initial substrate screen for the dienamine catalyzed pyridone Diels–Alder reaction.....	155
Table 4.1. Screening conditions for selective nitrile reduction.....	374

LIST OF ABBREVIATIONS

Ac	acetyl
ACHN	1,1'-azobis(cyclohexanecarbonitrile)
AIBN	1,1'-azobisisobutyronitrile
Alloc	allyloxycarbonyl
Ar	aryl
BDSB	bromodiethylsulfonium bromopentachloroantimonate(V)
BHT	2,6-di- <i>tert</i> -butyl-4-methylphenol
Boc	<i>tert</i> -butoxycarbonyl
Bn	benzyl
brsm	based on recovered starting material
Bz	benzoyl
CDI	1,1'-carbonyldiimidazole
COD	1,4-cyclooctadiene
COSY	correlated spectroscopy
DBU	1,8-Diazabicyclo[5.4.0]undec-7-ene
DCE	dichloroethane
DEA	<i>N,N</i> -diethylacetamide
DIBAL-H	diisobutylaluminium hydride
DIPEA	diisopropylethylamine
DMA	<i>N,N</i> -dimethylacetamide
DMAP	4-(<i>N,N</i> -dimethylamino)pyridine
DMF	<i>N,N</i> -dimethylformamide
DMP	Dess–Martin periodinane

DMSO	dimethylsulfoxide
DNs	2,4-dinitrophenylsulfonyl
<i>dr</i>	diastereomeric ratio
EDC	1-ethyl-3-(3-dimethylaminopropyl)carbodiimide
<i>ee</i>	enantiomeric excess
Et	ethyl
HAT	hydrogen-atom transfer
HFIP	1,1,1,3,3,3-hexafluoroisopropanol
HMDS	hexamethyldisilazide
HMPA	hexamethylphosphoramide
HRMS	high-resolution mass spectrometry
<i>i</i> -Bu	<i>iso</i> -butyl
IBX	2-iodoxybenzoic acid
<i>i</i> -Pr	<i>iso</i> -propyl
IR	infrared
LDA	lithium diisopropylamide
<i>m</i> CPBA	<i>meta</i> -chloroperbenzoic acid
Me	methyl
Mes	mesityl
Mn(dpm) ₃	tris(2,2,6,6-tetramethyl-3,5-heptanedionato)manganese(III)
Ms	methanesulfonyl
MS	molecular sieves
MVK	methyl vinyl ketone
<i>n</i> -Bu	butyl
NHC	<i>N</i> -heterocyclic carbene

NMM	<i>N</i> -methylmorpholine
NMO	<i>N</i> -methylmorpholine <i>N</i> -oxide
NMR	nuclear magnetic resonance
NOESY	nuclear Overhauser effect spectroscopy
NR	no reaction
<i>o</i> -Ns	<i>ortho</i> -nitrophenylsulfonyl
<i>o</i> -DCB	<i>ortho</i> -dichlorobenzene
Ph	phenyl
pin	pinacolato
<i>p</i> -Ns	<i>para</i> -nitrophenylsulfonyl
PPTS	pyridinium <i>para</i> -toluenesulfonate
<i>p</i> -TsOH	<i>para</i> -toluenesulfonic acid
Ra-Ni	Raney Nickel
<i>t</i> -Bu	<i>tert</i> -butyl
TBS	<i>tert</i> -butyldimethylsilyl
TCDI	1,1'-thiocarbonyldiimidazole
TES	triethylsilyl
Tf	trifluoromethanesulfonyl
TFA	trifluoroacetic acid
TFAA	trifluoroacetic anhydride
THF	tetrahydrofuran
TIPS	triisopropylsilyl
TMS	trimethylsilyl
TPP	tetraphenylporphyrin
Ts	<i>para</i> -toluenesulfonyl

ACKNOWLEDGEMENTS

While preparing this dissertation, I have taken the time to reminisce about the last four and a half years. I have identified the research questions and experiments that deserved more of my time, and those on which too much of my time was spent. I have reflected on all that I have been able to achieve and recalled the all too ambitious, and somewhat unrealistic, goals that I made at the outset. A PhD is by no means an endeavor to be taken lightly, and the last few years have presented some of the most daunting challenges I have faced. But they have also given me some of the most exciting and memorable times of my life. Through it all, there are three key lessons that I have learned: 1) Every result is an important one, 2) There is no such thing as a key step, and 3) Never lose sight of your ultimate goal. Each of these, although quite obvious, are often difficult to keep in mind when you are in the trenches, and even more difficult when you feel like you are on the losing end of the battle. But when things seemed most challenging, they served as a reassuring mantra, inspiring me to fight another day.

Of course, the knowledge of these things alone is by no means all that is required. So many people have played an integral role in my journey to this point and to thank each and every one of them would likely require a document of equal length to the dissertation enclosed here. And so, to any of those not mentioned below, with the brevity that fails to encompass my true gratitude, thank you.

First and foremost, I would like to thank my advisor, Professor Scott Snyder. Your approach to mentorship has granted me the freedom to take academic risks and pursue the directions I thought most pertinent. I realize that every conversation had, every question asked, and every decision made was used to shape me into the independent researcher that I am today. Under your guidance, I have learned more than just organic chemistry. Your commitment, approach to problem solving and unwavering standards, have been just as integral in my development. Please know that every single opportunity that you have given me, has not gone

unappreciated. Being a part of the grant writing and review process, allowing me to mentor junior students and vesting me with certain levels of responsibility, have all lent themselves to my personal and professional growth. I will be forever grateful for the role that you have played in my time here.

In addition to one's mentor, the people that you work with every day make up a large part of your support system. Over the past four years in the Snyder Group, I have been lucky enough to be surrounded by a number of intelligent, talented and diligent chemists, all of whom have created an environment of creativity, kindness and encouragement to enable me to thrive, thank you all. I would, in particular, like to thank Phil Gemmel for being a major part of my support system during my time here. Thank you for always making me want to be better. I would not have reached this point without the care, reassurance and motivation that you give me every day. Throughout my time at the University of Chicago, I have also made a number of life-long friendships. I would like to thank Tessa Lynch-Colameta, Cooper Taylor, Russell Kielawa, Jon Keim, Dr. Lilia Fuentes, Dr. Vlad Lisnyak, Dr. Alison Gao, Dr. Pengfei Hu, Professor Hyung Min Chi, Dr. Zhiyao Zhou and Dr. Yu-An Zhang. You have all played important roles in my time here, from helpful discussions about the problems of the day to memorable nights in the campus pub. I have truly treasured my time with every one of you and can't wait until we meet again. I would also like to thank Phil, Lilia, Zhiyao, Pengfei, Hyung Min and Cooper for being great collaborators and playing vital roles in the projects we undertook together. Russell, Cooper, Tessa, Jon, Phil and my mother are thanked for reading various chapters of my thesis and providing important feedback and suggestions.

There have also been a number of undergraduates that I had the joy of mentoring. Ken DeBacker, Jenna Reisler, Lindsey Jay, Mark Chen and Julien Heberling, thank you all for your hard-work and I wish you all the best in the future.

I would also like to thank Professor Viresh Rawal and Professor Mark Levin for serving as my committee members and taking the time to go through this dissertation, in an effort to provide critical insight and propositions to further improve my work.

There are also a number of people that play significant roles behind the scenes to ensure that everything proceeds as smoothly as possible, and they, too, deserve recognition. I would like to thank Laura Luburich and Mike Reedy for keeping Searle running, night and day. I would like to thank Dr. Antoni Jurkiewicz, Dr. Josh Kurutz, Dr. Jin Qin, Dr. Alex Filatov, Dr. Andrew McNeece and Kate Jesse for maintaining all of the facilities crucial to a synthetic chemist and for all of your assistance with structure elucidation. I would like to thank Dr. Vera Dragisich and Melinda Moore for playing vital roles in my student life and handling all associated problems with a personalized level of care. I would like to thank Dr. Val Keller for being a great resource during my time as a Teaching Assistant and always being ready for a friendly chat, no matter how much time had passed since our last.

My decision to pursue a PhD was fostered as an undergraduate student in the Chemistry Department at McGill University and, as such, I must thank Professor Scott Bohle for providing me with my first research position and introducing me to synthetic chemistry. I must also thank Professor Youla Tsantrizos. Working in your group taught me a lot more than practical skills; I learned the importance of work ethic and a joy for organic chemistry that propelled me into a PhD program. Despite only being in your group a short time, you have been and will be an important mentor and role model for years to come.

Certainly, I would be remiss not to acknowledge those who made their impact on my journey much earlier in its course. My interest in science was first nurtured at The Lodge School in Barbados, where the collection of hard-working and dedicated teachers continuously challenged me and encouraged me to be better, while at the same time being sure to put me in my place, if necessary. In particular, I would like to thank Ms. Sandra Wiltshire and Ms.

Rebecca Chewitt, two women who took a sincere and committed interest in my education and worked to guarantee that I would always perform at my best.

And, of course, I would like to thank my family. Mum, Dad and Vic, you have always supported me in all of my endeavors, always trusting that you had instilled in me the values and principles I needed to succeed, always offering support in any way you could and from any distance. I will be forever grateful to have you in my life and I hope that I have made you proud.

ABSTRACT

Rapidly Introducing Molecular Complexity: Reaction Development and Application to Hydrocarbon and Heterocyclic Frameworks

Charles James Frederick Cole

Natural product total synthesis, as a field, has sought to provide access to complex and intriguing structures as a means to further chemical knowledge, support biological studies and inspire therapeutic design. However, such access is limited by the tools made available to synthetic chemists, and as such, a leading goal within the community is the development and application of novel reactions to expedite the synthesis of targets of interest. Over the years the chemical toolbox, as it is informally known, has been consistently expanded from more traditional functional group interconversions and strategies, to reactions which can rapidly introduce stereochemical complexity and those which promote activation of chemical bonds typically viewed as inert. The dissertation herein reports the study of reactions which take achiral materials or materials with minimal chiral elements and rapidly introduce molecular complexity in both hydrocarbon and heterocyclic frameworks.

Chapter 1 serves to introduce our group's work on unique electrophile transfer reagents, in particular the development of a series of electrophilic sulfur transfer reagents, which can be used to promote polyene cyclizations in several substrates with varying steric and electronic demands. Initial studies on chiral forms of these reagents are also briefly discussed.

Subsequently, Chapter 2 presents the synthesis of the terpenes spiroviolene and spirograterpene A. Such minimally functionalized structures have been a focus of our group from the perspective of using quaternary centers to guide and expedite synthetic planning. Starting from a previously established intermediate, we perform a series of transformations

which, in short order, build in key stereocenters and bond connections, granting access, in a modular fashion, to both targets. In addition, experimental, spectral and computational data is used to rationalize the proposed structural reassignment of a key stereocenter in spiroviolene to match more closely the structure of spirograterpene A.

Chapter 3 then turns attention to the development of a novel asymmetric pyrone Diels–Alder reaction. Despite the fact that this reaction has been widely studied, due to the broad utility of the bicyclic lactone products as well as their derivatives, enantioselective methods are quite limited. This chapter seeks to demonstrate our approach to the development of an inverse electron-demand pyrone Diels–Alder reaction, enabled by dienamine catalysis. The broad scope of this transformation is detailed, as well as relevant derivatizations of various reaction products. In addition, key transition state proposals are put forward to account for the enantio- and diastereoselectivity observed for this process. Following this, we present a brief study towards the gardmutine alkaloids, taking advantage of the relative stereochemistry imparted by the pyrone Diels–Alder reaction, as well as the advancement of this method to include 2-pyridones as competent diene partners.

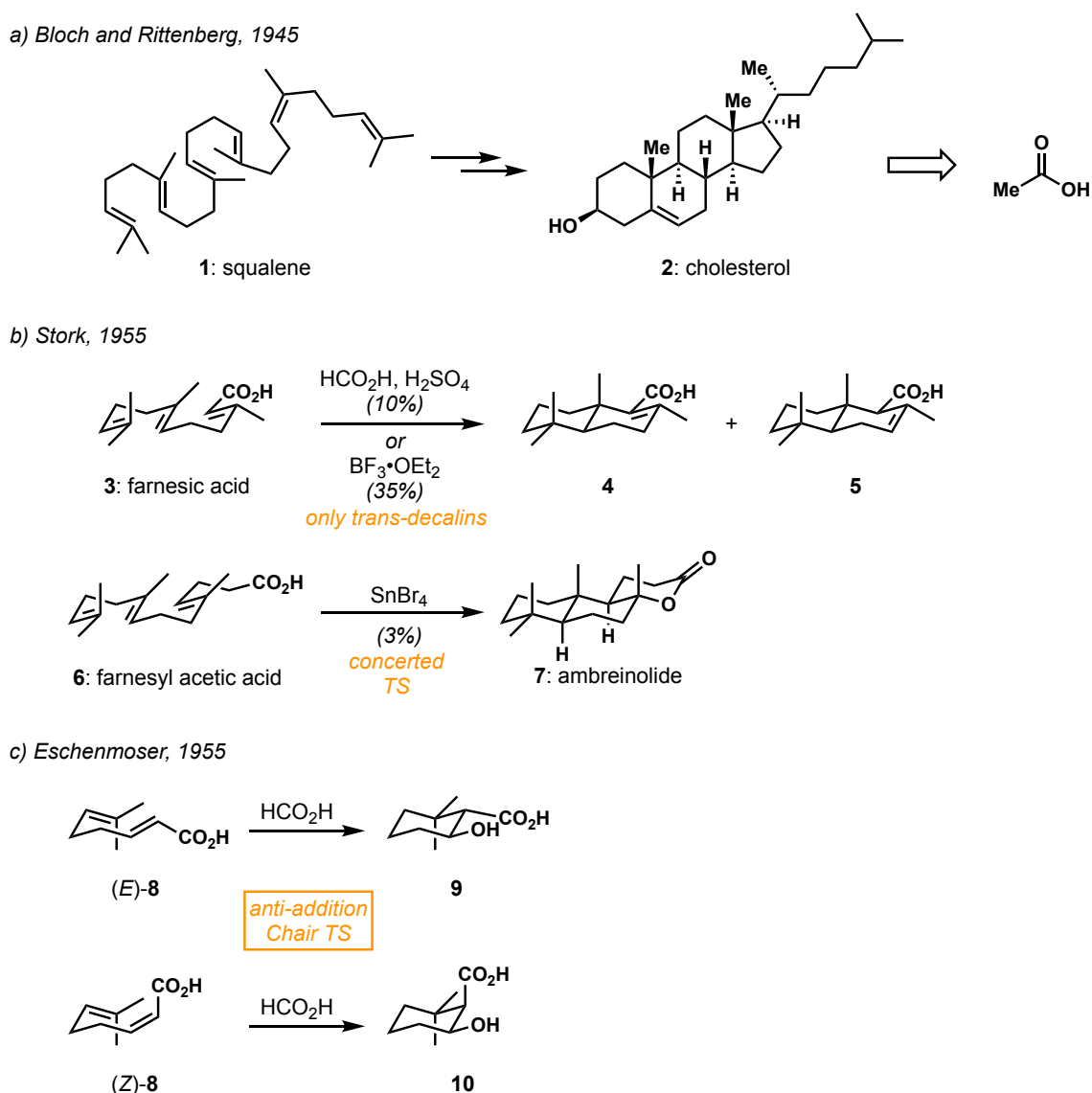
Finally, Chapter 4 details our synthetic approaches to the indole alkaloids nareline and picrinine. We discuss the modular strategy developed by our group, which has been used to successfully tackle a number of indole alkaloids. Application of this approach has rendered many highly functionalized late-stage intermediates to date, requiring a single ring forming event to access the desired target. Included in these studies are key transformations that serve to build significant structural complexity, such as a Au-catalyzed 6-*endo*-dig cyclization to construct the dihydrocarbazole backbone, as well as a one-pot Barton decarboxylation/oxidation sequence to form the requisite furoindole motif. Proposals for the completion of this target from the advanced intermediates disclosed here are also discussed.

CHAPTER 1

PREPARATION AND APPLICATION OF NOVEL DISULFANIUM SALTS TO POLYENE CYCLIZATIONS

1.1 Introduction

Currently, there are two major benchmarks for any new chemical method. The first is the ability to perform site selective transformations on unactivated bonds in complex substrates, while the other is the ability to construct molecular complexity from precursors with minimal, if any, stereochemical information. Furthermore, in the realm of total synthesis, the efficiency of individual transformations or even entire synthetic routes, is often compared to processes employed by nature herself. One area where both of these concepts intersect is polyene cyclizations: transformations in which a series of olefins within a long-chain hydrocarbon

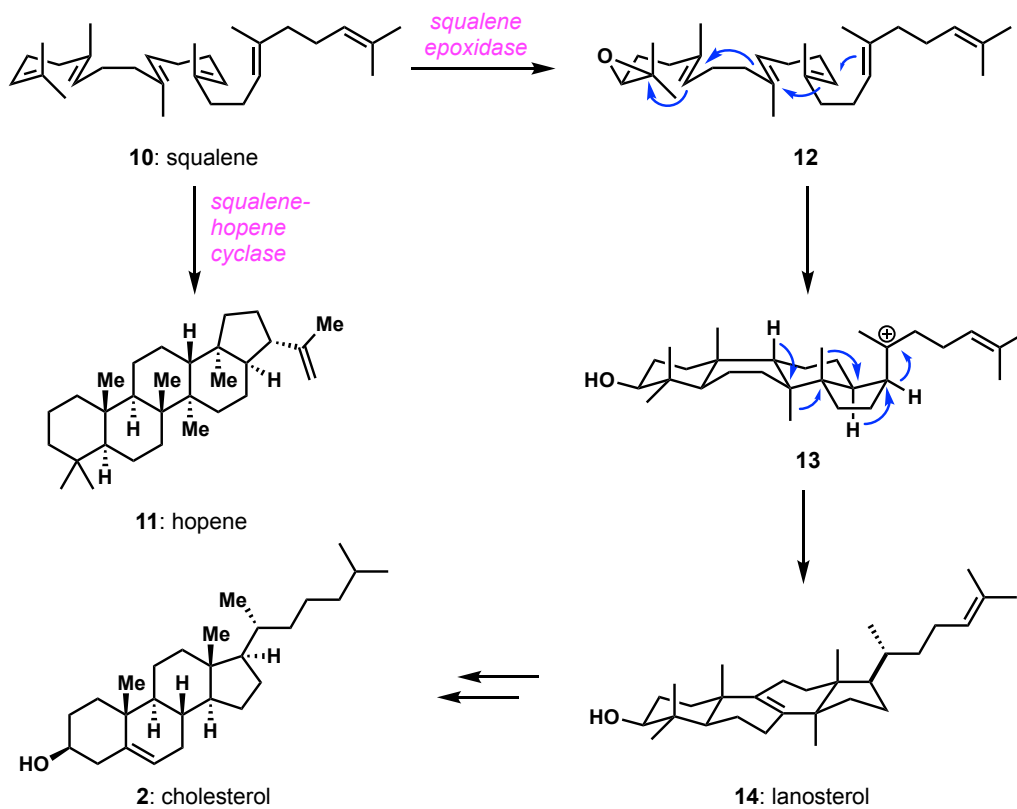


Scheme 1.1. (a) Bloch and Rittenberg study on link between cholesterol (2) and acetic acid; (b) Stork and (c) Eschenmoser studies on the mechanism of polyene cyclizations.

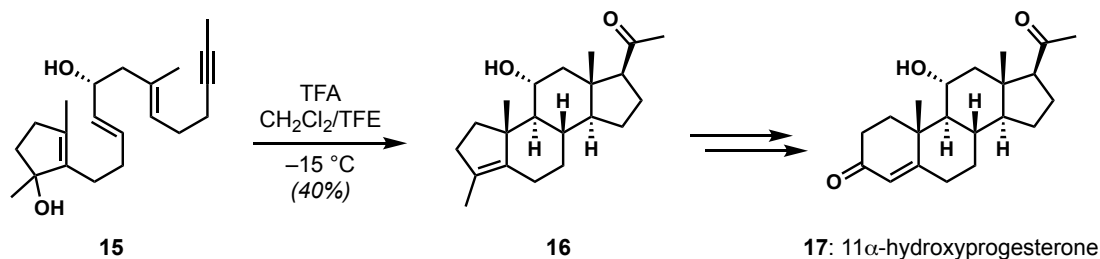
associate into chair transition states and undergo a concerted cyclization process to generate fused polycycles.^{1,2}

This concept was first discussed as a process through which squalene could be converted biosynthetically to a number of steroid architectures such as cholesterol (**2**). Early work from Bloch and Rittenberg, in which isotopic labelling confirmed acetic acid as a precursor to both squalene and cholesterol, disproved the original belief that fatty acids, such as arachidonic acid, served as the requisite starting material, and paved the way for the key experimental studies that would fully illuminate this biogenic process.³ Subsequent work by Stork on the cyclization of farnesic acid showed that only *trans*-decalins could be obtained under both Lewis and Brønsted acidic conditions, and additional studies on the polycyclization of farnesyl acetic acid indicated that not only does such a mechanism proceed in an *anti*-addition fashion but that the process is likely concerted, lacking any discrete carbocations.⁴ This conclusion was further supported in studies by Eschenmoser, where *E*- and *Z*-1,5-dienes (**8**) were subjected to HCO₂H under heating. In these cases, the transformations were stereospecific, with the conformation about the olefin proximal to the carboxylic acid moiety guiding the final stereo-outcome.⁵ These results supported the Stork proposition of a concerted *anti*-addition across the alkenes and further posited that such transformations must occur through a chair transition state. This led to what is commonly now known as the Stork-Eschenmoser Hypothesis and is the basis for all polyene cyclization strategies used to date, including in particular the enzyme catalyzed polycyclization of oxidosqualene (**12**) to lanosterol (**14**), a precursor to cholesterol. One of the first synthetic applications of this proposal was by Johnson in 1977, where an enantiopure polyene (**15**) was subjected to TFA at low temperature to promote the corresponding polyene cyclization to build the requisite 5/6/6/5 fused ring system and provide methyl ketone **16**, which could then be further advanced to 11- α -hydroxyprogesterone (**17**).⁶

a) Biosynthesis of hopene (11) and lanosterol (14)



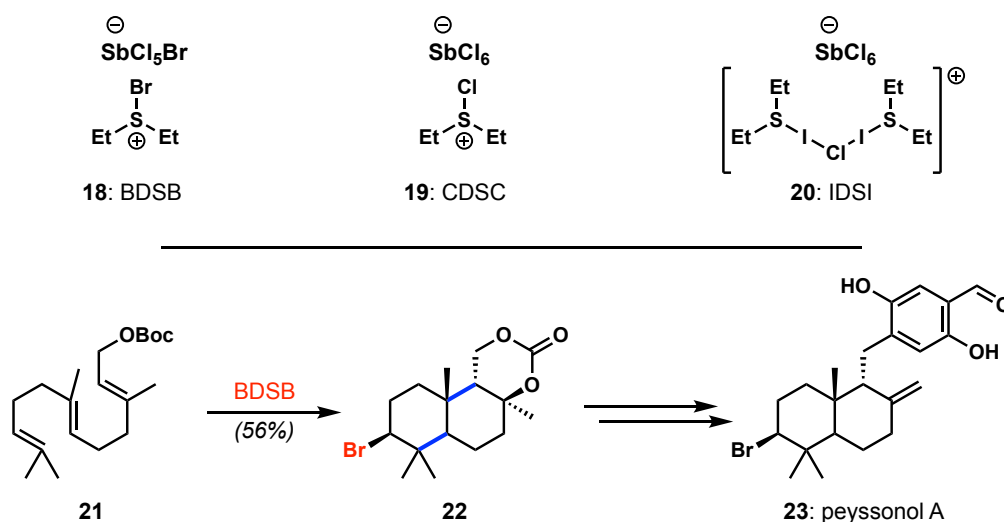
b) Johnson, 1977



Scheme 1.2. (a) Enzyme-mediated polyene cyclization of squalene (10); (b) Early example of polyene cyclizations in total synthesis.

Within the realm of polyene cyclizations, our group has taken particular interest in the species used to initiate such cascades. In a biosynthetic sense, these polycyclizations are initiated using simple protons, as in the case of the cyclization of squalene to hopene, or epoxides as in the conversion of squalene to lanosterol as discussed above (Scheme 1.2). However, synthetic chemists have broadened this arena to include other initiators. One of the more common alternatives is the use of halonium ion sources, an area in which our group has made significant headway with the development of reagents such as BDSB (18), CDSC (19)

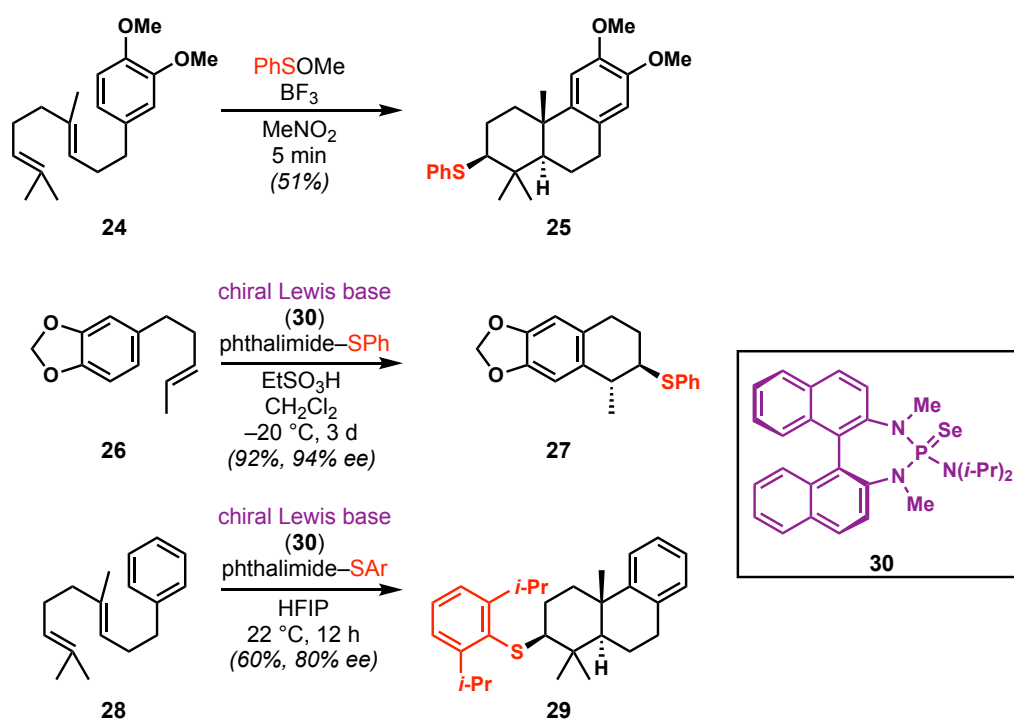
and IDSI (**20**): highly potent halonium ion sources capable of promoting a number of cation- π -cyclizations.⁷ Outside of the myriad of applications to analogous transformations mediated by electrophilic halonium reagents such as NBS or TBCO, a clear example of the utility of such species is the total synthesis of peyssonol A (**23**).^{7b} Here, Boc-protected farnesol **21** undergoes a polyene cyclization, promoted by BDSB and terminated by the Boc group to provide the *trans*-decalin **22**, containing a secondary bromide and cyclic carbonate. Not only does this transformation construct the necessary decalin frame from the completely linear precursor, but through careful choice of initiator and terminating group, the requisite functionalities are put in place to expedite the completion of this target following standard functional group interconversions. It is worth noting that the potential of these species is by no means limited to applications in polyene cyclizations and has been applied to more exotic systems, such as cyclization-ring expansion sequences to form 8-membered cyclic bromoethers, a gateway to a number of brominated marine natural products.⁸



Scheme 1.3. Potent electrophilic halonium sources **18-20** and application of **18** to the total synthesis of peyssonol A (**23**).

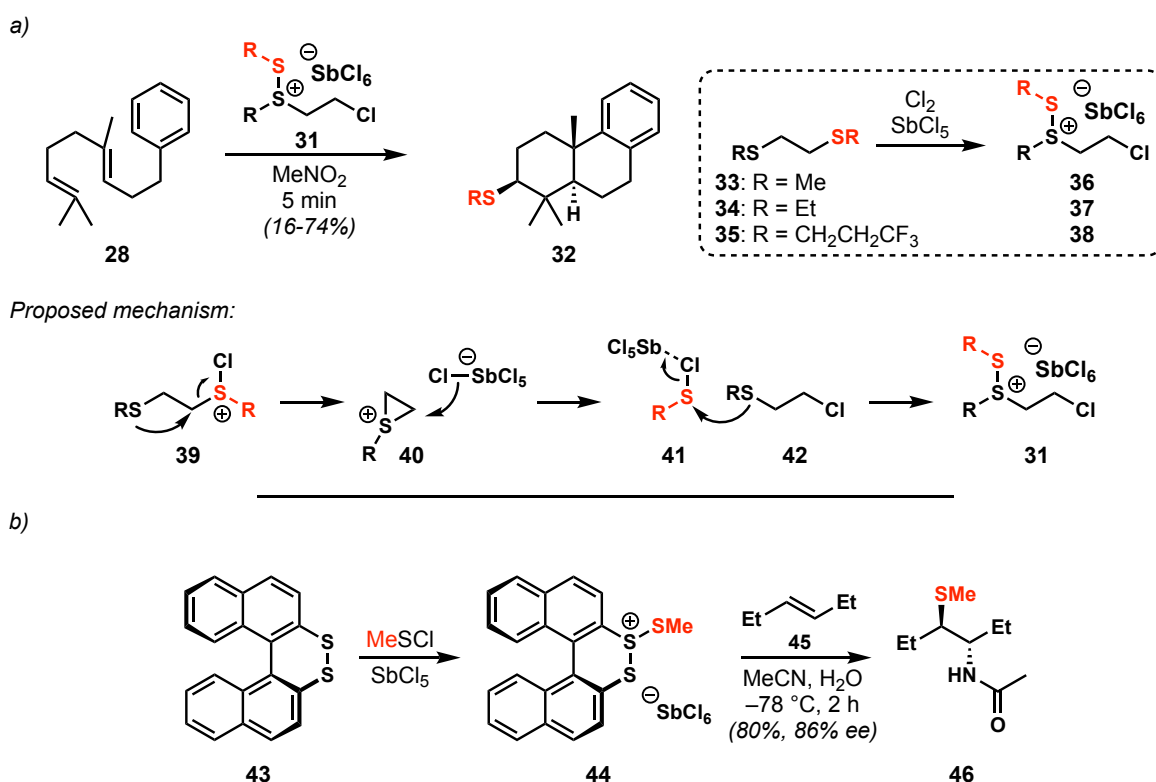
Along with the previously mentioned halonium sources, electrophilic sulfur reagents have also been used to promote such cascades, in this case via the formation of a thiiranium ion at the most distal olefin (Scheme 1.4). These sulfur-promoted polycyclizations are an area into which much effort has been placed, not only understanding the extent to which such

transformations are possible in the construction of complex thioethers, but also the ability to do so asymmetrically. Pioneering work within this field is attributed to B. M. Trost with the development of dimethyl(methylthio)sulfonium tetrafluoroborate (DMTSF), in which the initial potential of this reagent was viewed from the perspective of functionalizing individual olefins with a diverse array of nucleophiles, and which is currently used as a benchmark for novel electrophilic sulfur reagents.⁹ Shortly thereafter, Livinghouse demonstrated that aryl sulfenates such as PhSOMe, or the corresponding sulfenyl chloride, could in fact promote polyene cyclizations on a wide variety of substrates (e.g. **24**→**25**, Scheme 1.4).¹⁰ This work was later advanced by Denmark *et al.* in which a carefully designed Lewis base, in the form of a chiral selenophosphoramidate catalyst (**30**), permits the formation of a configurationally stable aryl thiiranium ion-catalyst complex.¹¹ The extensive chiral environment created around this electrophilic sulfur species then allows for a chiral transfer to the olefin of interest and provides the corresponding mono or polycyclization product in an asymmetric fashion. It is worth noting that this represents the first case of an asymmetric thiiranium-promoted polyene cyclization.



Scheme 1.4. Pioneering examples of thiiranium-promoted polyene cyclizations in both racemic and asymmetric fashions.

Despite the significant advances made in this field, in both racemic and asymmetric fashions, one shortfall is the limited availability of alkyl-sulfur based systems to perform such transformations. Our group made a significant contribution to this field while pursuing novel analogues of the electrophilic chlorine transfer reagent CDSC (**19**).¹² It was discovered that the combination of dithioethers with SbCl_5 in the presence of Cl_2 provided an isolable solid, whose structure was determined by X-ray crystallographic analysis. A proposed mechanism for the formation of **31** is provided in Scheme 1.5, wherein it is believed that one of the sulfur atoms associates with the electrophilic chlorine atom to form a positively charged chlorosulfonium intermediate. The second thioether moiety can then initiate a cyclization to form the strained thiiranium species **40**, which can be ring opened via the nucleophilic chloride to give chlorothioether **42**. Finally, the resulting thioether can attack the electrophilic sulfenyl chloride to form the disulfanium salt **31**.¹³ It was shown that these species were capable of performing polyene cyclizations with a number of electron rich and electron neutral systems in moderate to good yield. However, there were two major limitations to these reagents. First, they did not



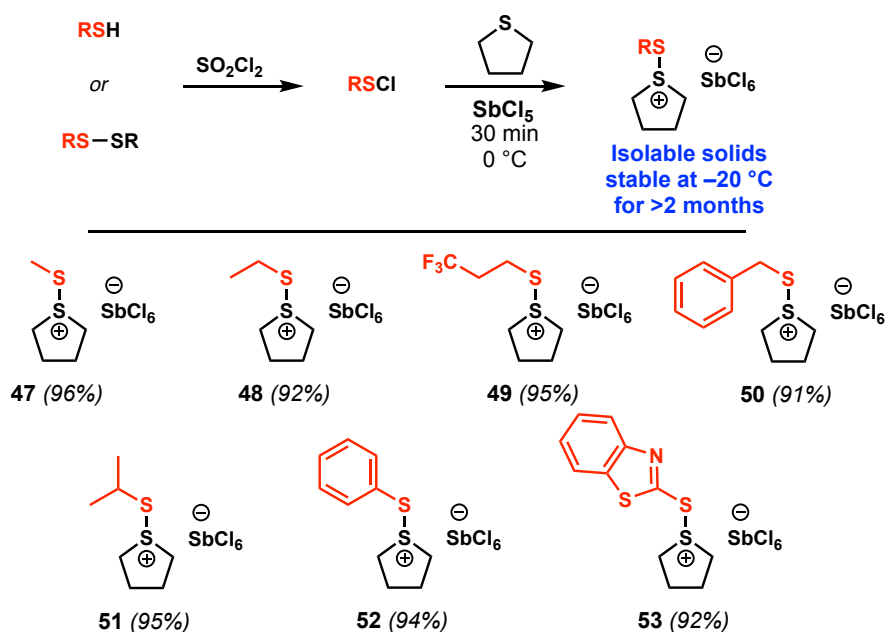
Scheme 1.5. (a) Alkyl disulfanium salts synthesized previously and the proposed mechanism for their formation; (b) Chiral disulfanium salts which served as key inspiration for developed method.

appear to be competent at performing monocyclizations, and second, these reagents were limited to three variants (**36-38**). As such, we set out to design a set of electrophilic sulfur transfer reagents that proved more potent than those of type **31**, while simultaneously pursuing a convenient preparatory method that would allow modular access to a much broader variety of corresponding alkyl and even aryl thioethers.

1.2 Modular Preparation of Novel Alkyl and Aryl Disulfanium Salts

Taking note of the impact of our group's previous contribution in this area, while remaining conscious of the clear limitations, we decided to design a modular route to a new class of disulfanium salts. In this regard, we turned our attention to the work of Pasquato and co-workers (Scheme 1.5b).¹⁴ Here, the authors prepared a highly reactive chiral disulfanium salt through the reaction of disulfide **43** with methanesulfonyl chloride and SbCl₅ which, when combined with 3-hexene (**45**) in aqueous acetonitrile at -78 °C, promoted an enantioselective thioamidation of the central alkene to provide **46** in 80% yield. Using these results, as well as preliminary work by previous group members on the use of tetrahydrothiophene to generate a potent source of electrophilic halides,¹⁵ we designed the following modular route to a variety of disulfanium salts. In our optimized procedure, the chosen sulfonyl chloride, prepared either from the commercially available thiol or analogous disulfide using SO₂Cl₂, is combined with tetrahydrothiophene and SbCl₅ at 0 °C for 30 min to generate the corresponding disulfanium salt as an isolable solid. As shown in Scheme 1.6, such a procedure has led to the preparation of a variety of alkyl, both linear and branched, and aryl disulfanium salts (**47-53**), all in yields >90%. Unfortunately, all of these species demonstrated great instability when dissolved in a variety of organic solvents and several attempts to grow crystals suitable for X-ray analysis simply resulted in decomposition. As such, structural characterization is based on

stoichiometry as well as similarly precedented sulfanium salts. Interestingly, despite their observed instability



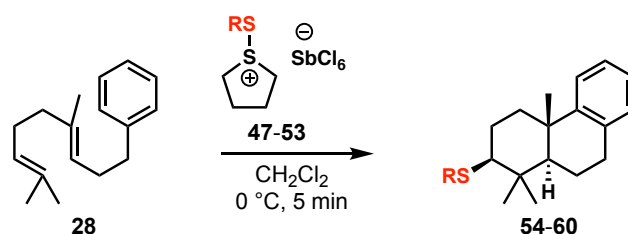
Scheme 1.6. Modular preparation of disulfanium salts **47-53** from commercially available materials.

when solvolyzed, if stored as solids at -20°C these materials retain complete reactivity. In fact, **47** has been shown to provide reproducible yields even when stored at 10°C for one week.

1.3 Applications to Polyene Cyclizations and Initial Asymmetric Studies

With this new variety of sulfur transfer reagents in hand, we then sought to compare their potency, where applicable, to that of the previously reported disulfanium species, while at the same time evaluating those more novel variants. Therefore, by subjecting the commonly utilized polyene precursor **28** to all of the prepared disulfanium species (**47-53**) in CH_2Cl_2 at 0°C for 5 min, we were able to access a variety of polycyclic thioethers, **54-60**, all in moderate to good yield. Of particular interest, when comparing reagents **47-49** to those previously employed by our own group, we found yields that were higher, in the case of **47** and **48**, or commensurate, in the case of **49**, to those previously obtained. Furthermore, the slightly more hindered variants, such as **50** and **51**, have led to the synthesis of polycycles **57** and **58** in moderate yield, where previously described linear species of the form **31** only provided the

product in trace amounts. And of course, this method of preparation has also enabled access to polycyclic aryl thioethers such as **59** and **60** in good yield. It should be noted that in addition, thioether **60** now contains a handle for further functionalization in the form of a Julia-Kocienski olefination, a transformation that has been demonstrated by Denmark *et al.* in similar systems.^{11f}



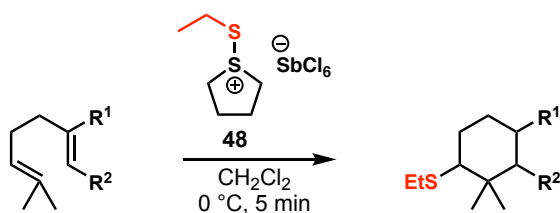
Entry	Sulfur reagent	Product	Yield (%)	Previous yield (%) from ref. 12
1	47 (R=Me)	54	55	42
2	48 (R=Et)	55	64	52
3	49 (R=CH ₂ CH ₂ CF ₃)	56	54	55
4	50 (R=Bn)	57	43	trace
5	51 (R= <i>i</i> -Pr)	58	50	trace
6	52 (R=Ph)	59	45	-
7	53 (R=heteroaryl)	60	64	-

Table 1.1. Thiiranium-promoted polyene cyclization of homogeranyl benzene (**28**) with disulfanium salts **47-53**.

An additional factor that was probed in the design of these reagents, though not extensively, was ring size. When the sulfur ring size is increased to the six-membered tetrahydrothiopyran a slight decrease in yield is observed (58% as compared to 64%, Table 1.1 entry 2). As such, we presume that the increased ring strain present in reagents of the form **48** is in part causing the observed potency of these species. At this time, the corresponding four-membered analogue has not been explored but could serve to further support or dispel this theory.

The competency of these sulfur transfer reagents was further tested by exploring the scope of compatible polyene precursors. In this effort, we elected to use **48** as the model disulfanium species, based on the rationale that this could be viewed as somewhat less reactive than other variants (such as **47** and **49**), as well as the fact that it could serve as a direct point of comparison to **37**. As can be seen in Table 1.2, **48** has been shown to promote the cyclization

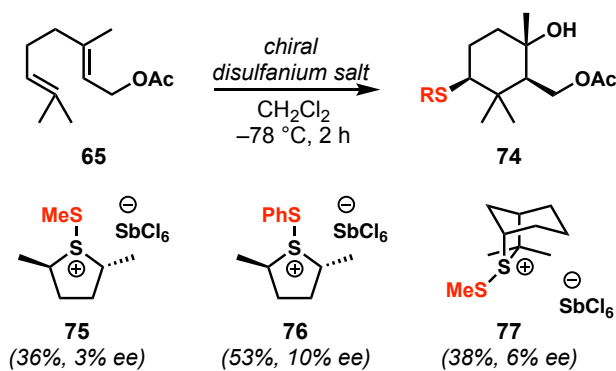
of a variety of polyene precursors. In the case of the more electron rich cyclization precursors, such as **70** and **71**, the reagent performed in commensurate yield. While in the case of a



Entry	Substrate	Product	Yield (%)	Previous yield (%) from ref. 12
1			55	0
	61	67		
2			28	0
	62	68		
3			10	52
	63	69		
4			50	50
	64	70		
5			37	29
	24	71		
6			42	35
	65	72		
7			47	20
	66	73		

Table 1.2. Scope of monoalkene and polyene cyclizations as effected by ethyl disulfanium salt **48**.

heteroatom-terminating nucleophile such as **72** and **73**, the disulfanium salt provided the desired compound in higher yield, with **73** being obtained in nearly twice the previously recorded throughput. Most notable, however, is the ability to access cyclization products **67** and **68**. These less reactive precursors gave no desired product when applying **37**, however in our case we are able to obtain yields of 55% and 28% respectively, a key result in noting the strength of these reagents. An interesting, however, unexpected result is the low yield obtained when subjecting the highly electron rich **69** to the reaction conditions. Despite the moderate yield obtained from reagent **37** (52%), the sulfur transfer species **48** gave only 10% of the desired cyclization product alongside an additional 10% of protocyclusation. At this time, it is unclear as to what causes this discrepancy in yield; however, one could presume that the more highly reactive nature of this substrate, along with the high reactivity of the reagent lends itself to undergoing a variety of decomposition pathways more readily.



Scheme 1.7. Initial exploration of chiral disulfanium salts **75-77**.

Having explored the scope of these species, our attention was focused on whether chiral variants of structure **47** could provide any asymmetric induction. As noted in the introduction to this section, the challenges in conducting asymmetric polyene cyclizations are well precedented in the literature, of which a variety of solutions have arisen, such as the chiral Lewis bases developed by the Denmark group. In the framework of tetrahydrothiophene-based sulfur transfer reagents, previous work on C_2 -symmetric species capable of inducing enantioselectivity has also been published.¹⁶

To this end, we prepared the dimethyl tetrahydrothiophene species **75** and **76**. Unfortunately, when subjecting these transfer reagents to modified reaction conditions (CH_2Cl_2 , $-78\text{ }^\circ\text{C}$, 2 h), a commensurate yield was obtained but minimal enantioselection was observed. We also considered the more sterically encumbered diphenyl and di-*tert*-butyl variants, however were unable to prepare the corresponding disulfanium species. In lieu of this we instead turned to **77**, a scaffold that has been utilized extensively by Aggarwal, among others, in the preparation of sulfur-ylides for asymmetric epoxidation and aziridination.^{16g} Unfortunately, even this highly privileged scaffold provided practically no enantioselection, thereby highlighting the inherent challenge of conducting this transformation asymmetrically.

1.4 Conclusion

Ultimately, we have developed a new set of sulfur transfer reagents in the form of disulfanium salts **47-53**. These species have been shown to engage in a variety of thiiranium-promoted polyene cyclizations, often providing the desired polycycles in higher yield than both commercial and previously developed reagents, as well as exhibiting a high tolerance for substrate variability. Furthermore, the modular route developed for the preparation of these species has allowed access not only to a variety of linear and branched alkyl thioethers, but also some aryl variants with the potential for further elaboration. Finally, initial explorations into conducting this transformation asymmetrically have been performed, utilizing both C_2 -symmetric, as well as privileged scaffolds. Unfortunately, while competent at performing the desired polyene cyclization, these particular reagents did not appear to provide any enantioselectivity.

1.5 References

1. For a recent review on cation- π cyclization chemistry, see: Snyder, S. A.; Levinson, A. M., Polyene Cyclizations. In *Comprehensive Organic Synthesis*, 2nd ed.; Knochel, P.; Molander, G. A., Eds. Elsevier: 2014; Vol. 3, pp 268 and references cited therein.
2. For a review of polyene cyclization chemistry, see: Yoder, R. A.; Johnston, J. N. *Chem. Rev.* **2005**, *105*, 4730 and references cited therein.
3. (a) Bloch, K.; Rittenberg, D. *J. Biol. Chem.* **1945**, *159*, 45; (b) Woodward, R. B.; Bloch, K. *J. Am. Chem. Soc.* **1953**, *75*, 2023.
4. (a) Stork, G.; Burgstahler, A. *J. Am. Chem. Soc.* **1955**, *77*, 5068; (b) Stadler, P.; Eschenmoser, A.; Schinz, H.; Stork, G. *Helv. Chim. Acta* **1957**, *40*, 2191; (c) Stadler, P.; Nechvatal, A.; Frey, A.; Eschenmoser, A. *Helv. Chim. Acta* **1957**, *40*, 1373.
5. (a) Gamboni, G.; Schinz, H.; Eschenmoser, A. *Helv. Chim. Acta* **1954**, *37*, 964; (b) Eschenmoser, A.; Ruzicka, L.; Jeger, O.; Arigoni, D. *Helv. Chim. Acta* **1955**, *38*, 1890; (c) Arigoni, D.; Jeger, O.; Ruzicka, L. *Helv. Chim. Acta* **1955**, *38*, 222.
6. Johnson, W. S.; Brinkmeyer, R. S.; Kapoor, V. M.; Yarnell, T. M. *J. Am. Chem. Soc.* **1977**, *99*, 8341.
7. (a) Snyder, S. A.; Treitler, D. S. *Angew. Chem. Int. Ed.* **2009**, *48*, 7899; (b) Snyder, S. A.; Treitler, D. S.; Brucks, A. P. *J. Am. Chem. Soc.* **2010**, *132*, 14303.
8. (a) Snyder, S. A.; Treitler, D. S.; Brucks, A. P.; Sattler, W. *J. Am. Chem. Soc.* **2011**, *133*, 15898; (b) Snyder, S. A.; Brucks, A. P.; Treitler, D. S.; Moga, I. *J. Am. Chem. Soc.* **2012**, *134*, 17714; (c) Zhang, Y.-A.; Yaw, N.; Snyder, S. A. *J. Am. Chem. Soc.* **2019**, *141*, 7776; (d) Taylor, C. A.; Zhang, Y.-A.; Snyder, S. A. *Chem. Sci.* **2020**, *11*, 3036.
9. For a review of DTMSF, see: (a) Adams, E. J.; Oscarson, S. *Dimethyl (methylthio) sulfonium Tetrafluoroborate (DMTSF)*. In *e-Encyclopedia of Reagents for Organic Synthesis* **2005**. For the original report, see: (b) Meerwein, H.; Zenner, K. F.; Gipp, R. *Justus Liebigs Ann. Chem.* **1965**, *688*, 67. For an earlier reagent of similar design, see: (c) Helmkamp, G. K.; Cassey, H. N.; Olsen, B. A.; Pettitt, D. J. *J. Org. Chem.* **1965**, *30*, 933; For representative examples of the application of this reagent, see: (d) Trost, B. M.; Shibata, T. *J. Am. Chem. Soc.* **1982**, *104*, 3225; (e) Trost, B. M.; Shibata, T.; Martin, S. J. *J. Am. Chem. Soc.* **1982**, *104*, 3228; (f) Caserio, M. C.; Kim, J. K. *J. Am. Chem. Soc.* **1982**, *104*, 3231; (g) Trost, B. M.; Martin, S. J. *J. Am. Chem. Soc.* **1984**, *106*, 4263; (h) O'Malley, G. J.; Cava, M. P. *Tetrahedron Lett.* **1985**, *26*, 6159.
10. (a) Edstrom, E.; Livinghouse, T. *J. Chem. Soc., Chem. Commun.* **1986**, 279; (b) Edstrom, E.; Livinghouse, T. *J. Am. Chem. Soc.* **1986**, *108*, 1334; (c) Edstrom, E. D.; Livinghouse, T. *J. Org. Chem.* **1987**, *52*, 949; (d) Haring, S. R.; Livinghouse, T. *J. Org. Chem.* **1997**, *62*, 6388; (e) Moore, J. T.; Soldi, C.; Fettinger, J. C.; Shaw, J. T. *Chem. Sci.* **2013**, *4*, 292.

11. For reviews on Lewis base catalysis see: (a) Denmark, S. E.; Beutner, G. L. *Angew. Chem. Int. Ed.* **2008**, *47*, 1560; (b) Hartmann, E.; Denmark, S. E. *Helv. Chim. Acta* **2017**, *100*, e1700158; For examples of thiiranium promoted mono- and polycyclizations see: (c) Denmark, S. E.; Kornfilt, D. J. P.; Vogler, T. *J. Am. Chem. Soc.* **2011**, *133*, 15308; (d) Denmark, S. E.; Jaunet, A. *J. Am. Chem. Soc.* **2013**, *135*, 6419; (e) Denmark, S. E.; Chi, H. M. *J. Am. Chem. Soc.* **2014**, *136*, 8915; (f) Tao, Z.; Robb, K. A.; Zhao, K.; Denmark, S. E. *J. Am. Chem. Soc.* **2018**, *140*, 3569.
12. Schevenels, F. T.; Shen, M.; Snyder, S. A. *Org. Lett.* **2016**, *19*, 2.
13. Evidence for this mechanism includes observation of **42** by crude NMR and the fact that more electron poor dithioethers would not undergo disulfanium salt formation, likely because thiiranium formation is more challenging.
14. Lucchini, V.; Modena, G.; Pasquato, L. *J. Chem. Soc., Chem. Commun.* **1994**, 1565.
15. Brucks, A. P.; Treitler, D. S.; Liu, S.-A.; Snyder, S. A. *Synthesis* **2013**, *45*, 1886.
16. For selected examples of transformations using chiral sulfonium species see: (a) Breau, L.; Ogilvie, W. W.; Durst, T. *Tetrahedron Lett.* **1990**, *31*, 35; (b) Julienne, K.; Metzner, P.; Henryon, V.; Greiner, A. *J. Org. Chem.* **1998**, *63*, 4532; (c) Julienne, K.; Metzner, P.; Henryon, V. *J. Chem. Soc., Perkin Trans. 1* **1999**, 731; (d) Zanardi, J.; Lriverend, C.; Aubert, D.; Julienne, K.; Metzner, P. *J. Org. Chem.* **2001**, *66*, 5620; (e) Zanardi, J.; Lamazure, D.; Minière, S.; Reboul, V.; Metzner, P. *J. Org. Chem.* **2002**, *67*, 9083; (f) Davoust, M.; Cantagrel, F.; Metzner, P.; Brière, J.-F. *Org. Biomol. Chem.* **2008**, *6*, 1981; (g) Illa, O.; Namutebi, M.; Saha, C.; Ostovar, M.; Chen, C. C.; Haddow, M. F.; Nocquet-Thibault, S.; Lusi, M.; McGarrigle, E. M.; Aggarwal, V. *J. Am. Chem. Soc.* **2013**, *135*, 11951.

1.6 Experimental Section

General Procedures. All reactions were carried out under an argon atmosphere with anhydrous solvents under anhydrous conditions, unless otherwise noted. Anhydrous THF, toluene, Et₂O, CH₂Cl₂, and MeCN were obtained by passing commercially available pre-dried, oxygen-free formulations through activated alumina columns. Yields refer to chromatographically and spectroscopically (¹H and ¹³C NMR) homogeneous materials, unless otherwise stated. Reagents were purchased at the highest commercial quality and used without further purification, unless otherwise stated. Reactions were magnetically stirred and monitored by TLC carried out on 0.25 mm Merck silica gel plates (60F-254) using UV light as visualizing agent, and an aqueous solution of cerium ammonium molybdate or a solution of KMnO₄ in aqueous NaHCO₃ and heat as developing agents. (2R,5R)-2,5-Dimethylthiolane, 2-benzothiazole disulfide, and all monoalkene and polyene cyclization substrates were prepared according to the procedures described in the literature. SiliCycle silica gel (60, academic grade, particle size 0.040–0.063 mm) was used for flash column chromatography. Preparative TLC separations were carried out on 0.50 mm E. Merck silica gel plates (60F-254). NMR spectra were recorded on Bruker 400 and 500 MHz instruments and calibrated using residual undeuterated solvent as an internal reference. Standard abbreviations were used to explain the multiplicities. IR spectra were recorded on a PerkinElmer 1000 series FT-IR spectrophotometer. High-resolution mass spectra (HRMS) were recorded on Agilent 6244 ToF-MS using ESI (electro-spray ionization) at the University of Chicago Mass Spectroscopy Core Facility. All *ee* values were determined by HPLC on a Daicel CHIRALCEL OD-H column.

Preparation of Disulfanium Salts; General Procedure. To a solution of the thiol or alkyl disulfide (1.0 mmol, 1.0 equiv.) in CH₂Cl₂ (1 mL) at 0 °C was added SO₂Cl₂ (0.090 mL, 1.1

mmol, 1.1equiv.) dropwise. This mixture was stirred at 0 °C for 30 min, unless otherwise specified, and subsequently transferred to a flask containing tetrahydrothiophene (0.089 mL, 1.0 mmol, 1.0 equiv.) in CH₂Cl₂ (1.0 mL) at 0 °C followed by the dropwise addition of SbCl₅ (1.0 M solution in CH₂Cl₂, 1.0 mL, 1.0 mmol, 1.0 equiv.). Upon completion, pentane (5 mL) was added and the mixture filtered to give the desired disulfanium salt as a semi-crystalline solid. The salt was dried under vacuum for 10–20 min and then immediately stored at –20 °C. Due to their instability in typical organic solvents at 23 °C, all salts were characterized by ATR-FTIR spectroscopy and melting point analysis.

Methyl Disulfanium Salt (47). Prepared from Me₂S₂ following the procedure above at –20 °C to afford **47** as a deep purple solid (0.450 g, 96%); mp 101–102 °C; IR (film): 3337, 3005, 2942, 1444, 1306, 1271, 965, 872, 687 cm⁻¹.

Ethyl Disulfanium Salt (48). Prepared from Et₂S₂ following the procedure above to afford **48** as an off-white solid (0.444 g, 92%); mp 88–89 °C; IR (film): 3006, 2954, 2870, 1445, 1302, 1269, 1249, 893, 669 cm⁻¹.

3,3,3-Trifluoropropyl Disulfanium Salt (49). Prepared from 3,3,3-trifluoropropane thiol following the procedure above to afford **49** as a grey solid (0.523 g, 95%); mp 75–78 °C; IR (film): 2996, 2947, 1309, 1240, 1139, 1094, 870, 634 cm⁻¹.

Benzyl Disulfanium Salt (50). Prepared from benzyl mercaptan following the procedure above to afford **50** as an orange-yellow solid (0.496 g, 91%); mp 64–65 °C; IR (film): 2943, 1453, 1410, 1306, 1246, 872, 696 cm⁻¹.

Isopropyl Disulfanium Salt (51). Prepared from isopropyl mercaptan following the procedure above to afford **51** as an off-white solid (0.472 g, 95%); mp 107–109 °C; IR (film): 2949, 1443, 1411, 1306, 1249, 1048, 874 cm⁻¹.

Phenyl Disulfanium Salt (52). Prepared from Ph₂S₂ following the procedure above, starting at 0 °C and slowly warming to 23 °C to afford **52** as a pale orange solid (0.500 g, 91%); mp 108–110 °C; IR (film): 2994, 2945, 1442, 1400, 1305, 1270, 1247, 862, 764, 703, 690 cm⁻¹.

2-Benzothiazole Disulfanium Salt (53). Prepared from benzothiazole disulfide following the procedure above starting at 0 °C and heating to reflux to afford **53** as a bright yellow solid (0.541 g, 92%); mp 118–119 °C; IR (film): 3064, 1427, 1312, 1237, 1005, 756, 705, 669cm⁻¹.

Chiral Phenyl Disulfanium Salt (76). Prepared from Ph₂S₂ and (2*R*,5*R*)-2,5-dimethylthiolane following the procedure above, starting at 0 °C and slowly warming to 23 °C to afford **76** as a black solid (0.453 g, 94%); mp 92–93 °C; IR (film): 2976, 2912, 1442, 1307, 1251, 999, 751, 684 cm⁻¹.

Thiiranium-Promoted Polyene Cyclizations; General Procedure. To a solution of the alkene substrate (0.1 mmol, 1.0 equiv.) in CH₂Cl₂ (2.5 mL) at 0 °C was quickly added a solution of the disulfanium salt (0.11 mmol, 1.1 equiv.) in CH₂Cl₂ (0.25 mL) in a single portion. After stirring the resultant mixture for 5 min, the reaction contents were quenched by the addition of saturated aq. NaHCO₃ (5 mL) and the aqueous layer was extracted with CH₂Cl₂ (3 × 5 mL). The organic layers were combined, dried (Na₂SO₄), and concentrated to give a crude residue, which was further purified by flash column chromatography or preparative TLC, as indicated.

Methyl(1,1,4a-trimethyl-1,2,3,4,4a,9,10,10a-octahydrophenanthren-2-yl)sulfane (54).

The crude material was purified by flash column chromatography (hexanes/CH₂Cl₂, 4:1), followed by preparative TLC (hexanes/CH₂Cl₂, 3:1) to afford **54** as a colorless oil (15.0 mg, 55%). **54**: *R_f* = 0.25 (hexanes/CH₂Cl₂, 4:1); ¹H NMR (500 MHz, CDCl₃) δ 7.24 (dd, *J* = 7.8, 1.4 Hz, 1 H), 7.13 (tdt, *J* = 7.7, 1.6, 0.8 Hz, 1 H), 7.08 (td, *J* = 7.3, 1.4 Hz, 1 H), 7.06–7.03 (m, 1 H), 3.00–2.83 (m, 2 H), 2.38 (dt, *J* = 13.1, 3.4 Hz, 1 H), 2.29 (dd, *J* = 12.7, 4.0 Hz, 1 H), 2.15 (s, 3 H), 2.12–2.06 (m, 1 H), 1.97–1.89 (m, 2 H), 1.82–1.70 (m, 1 H), 1.54–1.46 (m, 1 H), 1.39 (dd, *J* = 12.2, 2.2 Hz, 1 H), 1.22 (s, 3 H), 1.21 (s, 3 H), 0.94 (s, 3 H).

Ethyl(1,1,4a-trimethyl-1,2,3,4,4a,9,10,10a-octahydrophenanthren-2-yl)sulfane (55).

The crude material was purified by flash column chromatography (silica gel, hexanes/CH₂Cl₂, 4:1), followed by preparative TLC (silica gel, hexanes/CH₂Cl₂, 3:1) to afford **55** as a colorless oil (18 mg, 64% yield). **55**: *R_f* = 0.25 (silica gel, hexanes/CH₂Cl₂, 4:1); ¹H NMR (500 MHz, CDCl₃) δ 7.24 (dd, *J* = 7.9, 1.4 Hz, 1 H), 7.16–7.11 (m, 1 H), 7.08 (td, *J* = 7.3, 1.4 Hz, 1 H), 7.06–7.03 (m, 1 H), 2.96 (ddd, *J* = 17.2, 6.6, 1.9 Hz, 1 H), 2.87 (ddd, *J* = 17.4, 11.6, 7.2 Hz, 1 H), 2.58 (qq, *J* = 12.4, 7.4 Hz, 2 H), 2.39–2.33 (m, 2 H), 2.06 (dq, *J* = 14.0, 3.8 Hz, 1 H), 2.02–1.90 (m, 2 H), 1.82–1.70 (m, 1 H), 1.61–1.47 (m, 2 H), 1.39 (dd, *J* = 12.2, 2.2 Hz, 1 H), 1.27 (t, *J* = 7.4 Hz, 3 H), 1.22 (s, 6 H), 0.93 (s, 3 H).

(3,3,3-Trifluoropropyl)(1,1,4a-trimethyl-1,2,3,4,4a,9,10,10a-octahydrophenanthren-2-yl)sulfane (56).

The crude material was purified by flash column chromatography (silica gel, hexanes/CH₂Cl₂, 4:1), followed by preparative TLC (silica gel, hexanes/CH₂Cl₂, 3:1) to afford **56** as a colorless oil (19 mg, 54% yield). **56**: *R_f* = 0.35 (silica gel, hexanes/CH₂Cl₂, 4:1); ¹H NMR (500 MHz, CDCl₃) δ 7.23 (dd, *J* = 8.0, 1.4 Hz, 1 H), 7.13 (td, *J* = 7.5, 1.7 Hz, 1 H), 7.09

(td, $J = 7.3, 1.4$ Hz, 1 H), 7.05 (dd, $J = 7.5, 1.6$ Hz, 1 H), 2.96 (ddd, $J = 17.3, 6.7, 1.9$ Hz, 1 H), 2.91–2.84 (m, 1 H), 2.72 (qdd, $J = 12.8, 9.7, 6.5$ Hz, 2 H), 2.43–2.37 (m, 2 H), 2.36–2.33 (m, 2 H), 2.07–1.90 (m, 3 H), 1.82–1.70 (m, 1 H), 1.51 (ddd, $J = 13.0, 10.9, 4.4$ Hz, 1 H), 1.40 (dd, $J = 12.1, 2.2$ Hz, 1 H), 1.22 (s, 3 H), 1.21 (s, 3 H), 0.93 (s, 3 H).

Benzyl(1,1,4a-trimethyl-1,2,3,4,4a,9,10,10a-octahydrophenanthren-2-yl)sulfane (57). The crude material was obtained as a mixture of diastereomers (4:1), which was purified by flash column chromatography (hexanes/CH₂Cl₂, 20:1), followed by preparative TLC (hexanes/CH₂Cl₂, 3:1) to afford the major diastereomer **57** as a pale yellow oil (11.4 mg, 35%); **57**: $R_f = 0.30$ (hexanes/CH₂Cl₂, 4:1); IR (film): 3060, 3026, 2965, 2927, 1489, 1453, 1389, 756, 701 cm⁻¹; ¹H NMR (500 MHz, CDCl₃) δ 7.33–7.27 (m, 4 H), 7.21 (dd, $J = 7.7, 1.7$ Hz, 2 H), 7.11 (t, $J = 6.2$ Hz, 1 H), 7.06 (dt, $J = 7.1, 1.4$ Hz, 1 H), 7.02 (dd, $J = 7.2, 1.6$ Hz, 1 H), 3.78 (d, $J = 13.3$ Hz, 1 H), 3.72 (d, $J = 13.3$ Hz, 1 H), 2.96 (dd, $J = 16.8, 6.8$ Hz, 1 H), 2.82 (ddd, $J = 17.5, 11.6, 7.3$ Hz, 1 H), 2.31 (dt, $J = 13.1, 3.4$ Hz, 1 H), 2.27–2.20 (m, 1 H), 2.00–1.91 (m, 2 H), 1.87 (ddt, $J = 13.4, 7.3, 2.1$ Hz, 1 H), 1.72 (dtd, $J = 13.4, 11.9, 6.7$ Hz, 1 H), 1.45–1.35 (m, 1 H), 1.30–1.25 (m, 2 H), 1.20 (s, 3 H), 1.05 (s, 3 H), 0.91 (s, 3 H); ¹³C NMR (126 MHz, CDCl₃) δ 149.5, 139.0, 135.1, 129.1, 129.1, 56.4, 52.1, 39.2, 38.5, 37.9, 36.6, 30.8, 29.6, 28.0, 24.9, 19.9, 17.8; HRMS (ESI): m/z [M+H]⁺ calcd for C₂₄H₃₁S⁺ 351.2141, found 351.2142.

Isopropyl(1,1,4a-trimethyl-1,2,3,4,4a,9,10,10a-octahydrophenanthren-2-yl)sulfane (58). The crude material was purified by flash column chromatography (hexanes/CH₂Cl₂, 5:1), followed by preparative TLC (hexanes/CH₂Cl₂, 3:1) to afford **58** as a colorless oil (15.0 mg, 50%). **58**: $R_f = 0.26$ (hexanes/CH₂Cl₂, 4:1); IR (film): 3060, 2966, 2928, 2361, 1489, 1450, 1042, 758, 722 cm⁻¹; ¹H NMR (500 MHz, CDCl₃) δ 7.24 (dd, $J = 7.9, 1.4$ Hz, 1 H), 7.12 (t, $J = 7.7$ Hz, 1 H), 7.08 (td, $J = 7.3, 1.4$ Hz, 1 H), 7.04 (dd, $J = 7.6, 1.7$ Hz, 1 H), 3.00–2.83 (m, 3

H), 2.39–2.32 (m, 2 H), 2.07–1.90 (m, 3 H), 1.81–1.72 (m, 1 H), 1.51 (dt, $J = 11.1, 6.6$ Hz, 1 H), 1.40 (dd, $J = 12.2, 2.2$ Hz, 1 H), 1.29 (d, $J = 6.9$ Hz, 3 H), 1.27 (d, $J = 7.1$ Hz, 3 H), 1.21 (d, $J = 3.3$ Hz, 6 H), 0.92 (s, 3 H); ^{13}C NMR (126 MHz, CDCl_3) δ 149.6, 135.2, 129.1, 125.9, 125.5, 124.6, 56.1, 52.3, 39.5, 38.5, 37.9, 35.3, 30.9, 29.8, 29.4, 25.0, 24.13, 24.07, 20.0, 17.7; HRMS (ESI) m/z $[\text{M}+\text{H}]^+$ calcd for $\text{C}_{20}\text{H}_{31}\text{S}^+$ 303.2141, found 303.2147.

Phenyl(1,1,4a-trimethyl-1,2,3,4,4a,9,10,10a-octahydrophenanthren-2-yl)sulfane (59). The crude material was purified by flash column chromatography (hexanes/ CH_2Cl_2 , 4:1) to afford **59** as a colorless oil (15.1 mg, 45%). **59**: $R_f = 0.33$ (hexanes/ CH_2Cl_2 , 4:1); IR (film): 3070, 3057, 2965, 2935, 2360, 1456, 1437, 757, 734, 722, 691 cm^{-1} ; ^1H NMR (500 MHz, CDCl_3) δ 7.44–7.39 (m, 2 H), 7.32–7.25 (m, 2 H), 7.23–7.18 (m, 2 H), 7.11 (td, $J = 8.0, 7.5, 1.9$ Hz, 1 H), 7.08 (td, $J = 7.2, 1.5$ Hz, 1 H), 7.04 (dd, $J = 7.6, 1.8$ Hz, 1 H), 3.00–2.84 (m, 6.0 Hz, 3 H), 2.31 (dt, $J = 13.1, 3.4$ Hz, 1 H), 2.08–1.99 (m, 2 H), 1.99–1.92 (m, 1 H), 1.85–1.74 (m, 1 H), 1.51–1.47 (m, 1 H), 1.45 (dd, $J = 12.2, 2.2$ Hz, 1 H), 1.32 (s, 3 H), 1.23 (s, 3 H), 1.04 (s, 3 H); ^{13}C NMR (126 MHz, CDCl_3) δ 149.4, 137.0, 135.1, 131.5, 129.1, 129.0, 126.5, 125.9, 125.5, 124.6, 61.1, 52.4, 39.2, 38.8, 38.0, 30.9, 30.2, 28.1, 25.0, 19.9, 17.9; HRMS (ESI) m/z $[\text{M}+\text{H}]^+$ calcd for $\text{C}_{23}\text{H}_{29}\text{S}^+$ 337.1984, found 337.1983.

(2-Benzothiazole)(1,1,4a-trimethyl-1,2,3,4,4a,9,10,10a-octahydrophenanthren-2-yl)sulfane (60). The crude material was purified by flash column chromatography (hexanes/ CH_2Cl_2 , 1:1), followed by preparative TLC (hexanes/ EtOAc , 10:1) to afford **60** as a colorless oil (25.0 mg, 64%). **60**: $R_f = 0.76$ (hexanes/ EtOAc , 4:1); IR (film): 3060, 2964, 2942, 2360, 1456, 1426, 989, 755, 724 cm^{-1} ; ^1H NMR (500 MHz, CDCl_3) δ 7.83 (d, $J = 8.1$ Hz, 1 H), 7.74 (dd, $J = 8.0, 1.2$ Hz, 1 H), 7.14 (td, $J = 7.4, 1.7$ Hz, 1 H), 7.10 (td, $J = 7.3, 1.4$ Hz, 1 H), 7.06 (dd, $J = 7.5, 1.7$ Hz, 1 H), 3.95 (dd, $J = 12.8, 4.1$ Hz, 1 H), 3.03–2.86 (m, 2 H), 2.40

(dt, $J = 13.1, 3.5$ Hz, 1 H), 2.32 (dq, $J = 13.9, 3.8$ Hz, 1 H), 2.15 (qd, $J = 13.5, 3.4$ Hz, 1 H), 1.97 (ddt, $J = 13.3, 7.1, 2.1$ Hz, 1 H), 1.87–1.69 (m, 3 H), 1.61 (dd, $J = 12.2, 2.2$ Hz, 1 H), 1.28 (s, 3 H), 1.27 (s, 3 H), 1.06 (s, 3 H); ^{13}C NMR (126 MHz, CDCl_3) δ 167.6, 153.5, 149.2, 135.5, 135.0, 129.1, 126.1, 126.0, 125.7, 124.6, 124.2, 121.7, 121.0, 60.6, 52.2, 39.2, 38.8, 37.9, 30.8, 30.0, 28.4, 25.0, 20.0, 18.2; HRMS (ESI) m/z $[\text{M}+\text{H}]^+$ calcd for $\text{C}_{24}\text{H}_{28}\text{NS}_2^+$ 394.1658, found 394.1650.

(1,1-Dimethyl-1,2,3,4-tetrahydronaphthalen-2-yl)(ethyl)sulfane (67). The crude material was purified by preparative TLC (hexanes/ CH_2Cl_2 , 4:1) to afford **67** as a colorless oil (12.0 mg, 55%). **67**: $R_f = 0.31$ (hexanes/ CH_2Cl_2 , 4:1); IR (film): 3026, 2964, 2927, 2868, 1489, 1457, 1263, 1042, 758, 700 cm^{-1} ; ^1H NMR (500 MHz, CDCl_3) δ 7.30 (t, $J = 7.6$ Hz, 2 H), 7.24–7.17 (m, 2 H), 3.13 (ddd, $J = 14.2, 10.1, 4.6$ Hz, 1 H), 2.84 (s, 1 H), 2.73–2.58 (m, 2 H), 2.46 (dd, $J = 11.7, 2.3$ Hz, 1 H), 2.08–1.99 (m, 1 H), 1.66–1.59 (m, 1 H), 1.29 (t, $J = 7.5$ Hz, 3 H), 1.27 (s, 3 H), 1.15 (s, 3 H); ^{13}C NMR (126 MHz, CDCl_3) δ 142.0, 128.60, 128.59, 128.57, 128.56, 126.1, 72.8, 61.2, 34.7, 34.5, 29.0, 27.1, 25.7, 15.5; HRMS (ESI) m/z $[\text{M}+\text{H}]^+$ calcd for $\text{C}_{14}\text{H}_{21}\text{S}^+$ 221.1358, found 221.1356.

(7-Methoxy-1,1-dimethyl-1,2,3,4-tetrahydronaphthalen-2-yl)(ethyl)sulfane (68). The crude material was purified by flash column chromatography (hexanes/ CH_2Cl_2 , 2:1), followed by preparative TLC (hexanes/EtOAc, 20:1) to afford **68** as a pale yellow oil (6.8 mg, 28%). **68**: $R_f = 0.74$ (hexanes/EtOAc, 4:1); IR (film): 2965, 2931, 2870, 2833, 1610, 1504, 1251, 1186, 1076, 1046, 804 cm^{-1} ; ^1H NMR (500 MHz, CDCl_3) δ 6.96 (d, $J = 8.4$ Hz, 1 H), 6.87 (s, 1 H), 6.68 (d, $J = 8.3$ Hz, 1 H), 3.79 (s, 3 H), 2.88 (d, $J = 16.8$ Hz, 1 H), 2.82–2.72 (m, 2 H), 2.67–2.56 (m, 2 H), 2.24–2.16 (m, 1 H), 2.06–1.95 (m, 1 H), 1.51 (s, 3 H), 1.33–1.25 (m, 6 H); ^{13}C NMR (126 MHz, CDCl_3): δ 158.0, 146.8, 129.8, 127.2, 112.5, 111.6, 55.4, 54.4, 39.1, 30.0,

29.2, 27.5, 27.3, 26.3, 15.1; HRMS (ESI) m/z $[M+H]^+$ calcd for $C_{15}H_{23}OS^+$ 251.1464, found 251.1471.

(6,7-Dimethoxy-1,1-dimethyl-1,2,3,4-tetrahydronaphthalen-2-yl)(ethyl)sulfane (69). The crude material was purified by flash column chromatography (hexanes/EtOAc, 2:1) to afford **69** as a colorless oil (3.0 mg, 10%). **69**: $R_f = 0.47$ (hexanes/EtOAc, 4:1); 1H NMR (500 MHz, $CDCl_3$) δ 6.81 (s, 1 H), 6.51 (s, 1 H), 3.86 (s, 3 H), 3.83 (s, 3 H), 2.88–2.73 (m, 3 H), 2.68–2.56 (m, 2 H), 2.23–2.17 (m, 1 H), 2.05–1.97 (m, 1 H), 1.50 (s, 3 H), 1.30 (t, $J = 7.3$ Hz, 3 H), 1.28 (s, 3 H).

Ethyl(6-methoxy-1,1,4a-trimethyl-1,2,3,4,4a,9,10,10a-octahydrophenanthren-2-yl)sulfane (70). The crude material was purified by preparative TLC (hexanes/EtOAc, 6:1) to afford **70** as a colorless oil (16.0 mg, 50%). **70**: $R_f = 0.73$ (hexanes/EtOAc, 4:1); 1H NMR (500 MHz, $CDCl_3$) δ 6.97 (dd, $J = 8.4, 1.1$ Hz, 1 H), 6.78 (d, $J = 2.7$ Hz, 1 H), 6.67 (dd, $J = 8.4, 2.6$ Hz, 1 H), 3.77 (s, 3 H), 2.90 (ddd, $J = 16.7, 6.5, 1.8$ Hz, 1 H), 2.84–2.75 (m, 1 H), 2.58 (qq, $J = 12.4, 7.4$ Hz, 2 H), 2.39–2.28 (m, 2 H), 2.05 (dq, $J = 14.0, 3.8$ Hz, 1 H), 2.00–1.88 (m, 2 H), 1.80–1.68 (m, 1 H), 1.50 (td, $J = 13.2, 3.8$ Hz, 1 H), 1.37 (dd, $J = 12.1, 2.2$ Hz, 1 H), 1.26 (t, $J = 7.4$ Hz, 3 H), 1.23–1.19 (m, 6 H), 0.92 (s, 3 H).

(6,7-Dimethoxy-1,1,4a-trimethyl-1,2,3,4,4a,9,10,10a-octahydrophenanthren-2-yl)(ethyl)sulfane (71). The crude material was purified by flash column chromatography (hexanes/EtOAc, 7:1), followed by preparative TLC (hexanes/EtOAc, 4:1) to afford **71** as a colorless oil (12.8 mg, 37%). **71**: $R_f = 0.48$ (hexanes/EtOAc, 4:1); 1H NMR (500 MHz, $CDCl_3$) δ 6.73 (d, $J = 2.8$ Hz, 1 H), 6.52 (s, 1 H), 3.84 (s, 3 H), 2.82 (qd, $J = 16.8, 6.8$ Hz, 2 H), 2.66–2.50 (m, 2 H), 2.33 (ddd, $J = 28.6, 10.1, 3.5$ Hz, 2 H), 2.09–2.01 (m, 1 H), 1.93 (dt, $J = 17.5,$

9.6 Hz, 2 H), 1.73 (dt, $J = 18.6, 11.9$ Hz, 1 H), 1.49 (t, $J = 13.2$ Hz, 1 H), 1.36 (d, $J = 12.1$ Hz, 1 H), 1.26 (t, $J = 7.4$ Hz, 3 H), 1.21 (d, $J = 2.8$ Hz, 6 H), 0.91 (s, 3 H).

{6-Hydroxy-2,2,6-trimethyl-3-[(ethylthio)cyclohexyl]methyl Acetate (72)}. The crude material was purified by flash column chromatography (hexanes/EtOAc, 10:1 \rightarrow 1:1) to afford **72** as a colorless oil (11.5 mg, 42%). **72**: $R_f = 0.5$ (hexanes/EtOAc, 1:1); $^1\text{H NMR}$ (500 MHz, CDCl_3) δ 4.38 (dd, $J = 11.8, 5.4$ Hz, 1 H), 4.31 (dd, $J = 11.9, 4.9$ Hz, 1 H), 2.62–2.48 (m, 3 H), 2.34 (dd, $J = 12.5, 3.8$ Hz, 1 H), 2.06 (s, 3 H), 1.98 (dq, $J = 13.9, 3.6$ Hz, 1 H), 1.84 (dt, $J = 12.9, 3.3$ Hz, 1 H), 1.69–1.57 (m, 2 H), 1.50 (td, $J = 13.4, 3.7$ Hz, 1 H), 1.25 (t, $J = 7.4$ Hz, 3 H), 1.23 (s, 3 H), 1.21 (s, 3 H), 0.85 (s, 3 H).

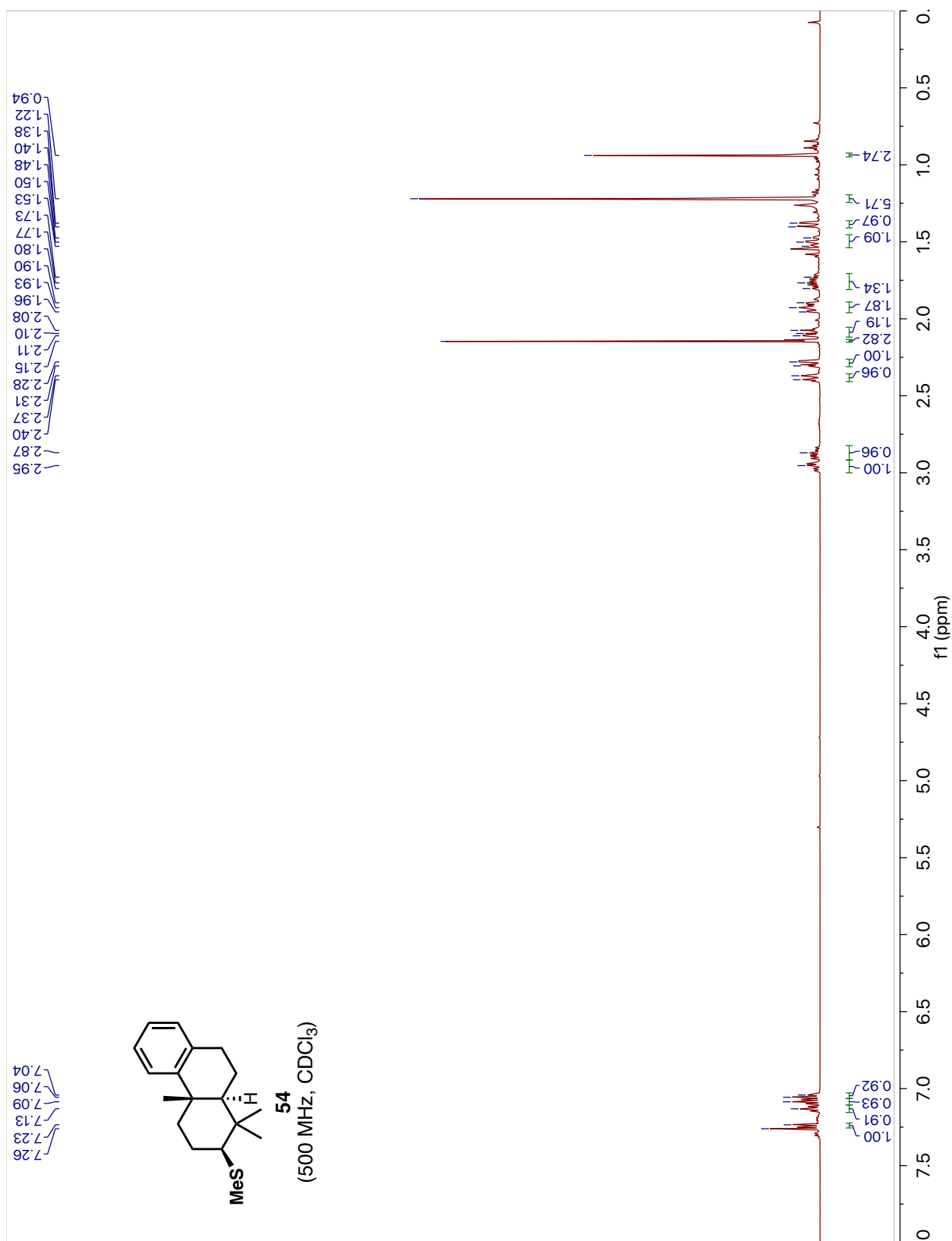
5-(Ethylthio)-4,4,7a-trimethylhexahydrobenzofuran-2(3H)-one (73)}. The crude material was purified by flash column chromatography (hexanes/EtOAc, 10:1 \rightarrow 1:1) to afford **73** as a colorless oil (11.4 mg, 47%). **73**: $R_f = 0.38$ (hexanes/EtOAc, 4:1); $^1\text{H NMR}$ (500 MHz, CDCl_3) δ 2.57 (ttd, $J = 12.4, 7.4, 5.0$ Hz, 2 H), 2.48 (dd, $J = 16.4, 14.7$ Hz, 1 H), 2.43–2.37 (m, 1 H), 2.34 (dd, $J = 16.3, 6.6$ Hz, 1 H), 2.24–2.15 (m, 1 H), 2.07–1.98 (m, 2 H), 1.74 (ddt, $J = 9.0, 7.3, 2.0$ Hz, 2 H), 1.35 (s, 3 H), 1.26 (t, $J = 7.4$ Hz, 3 H), 1.13 (s, 3 H), 0.89 (s, 3 H).

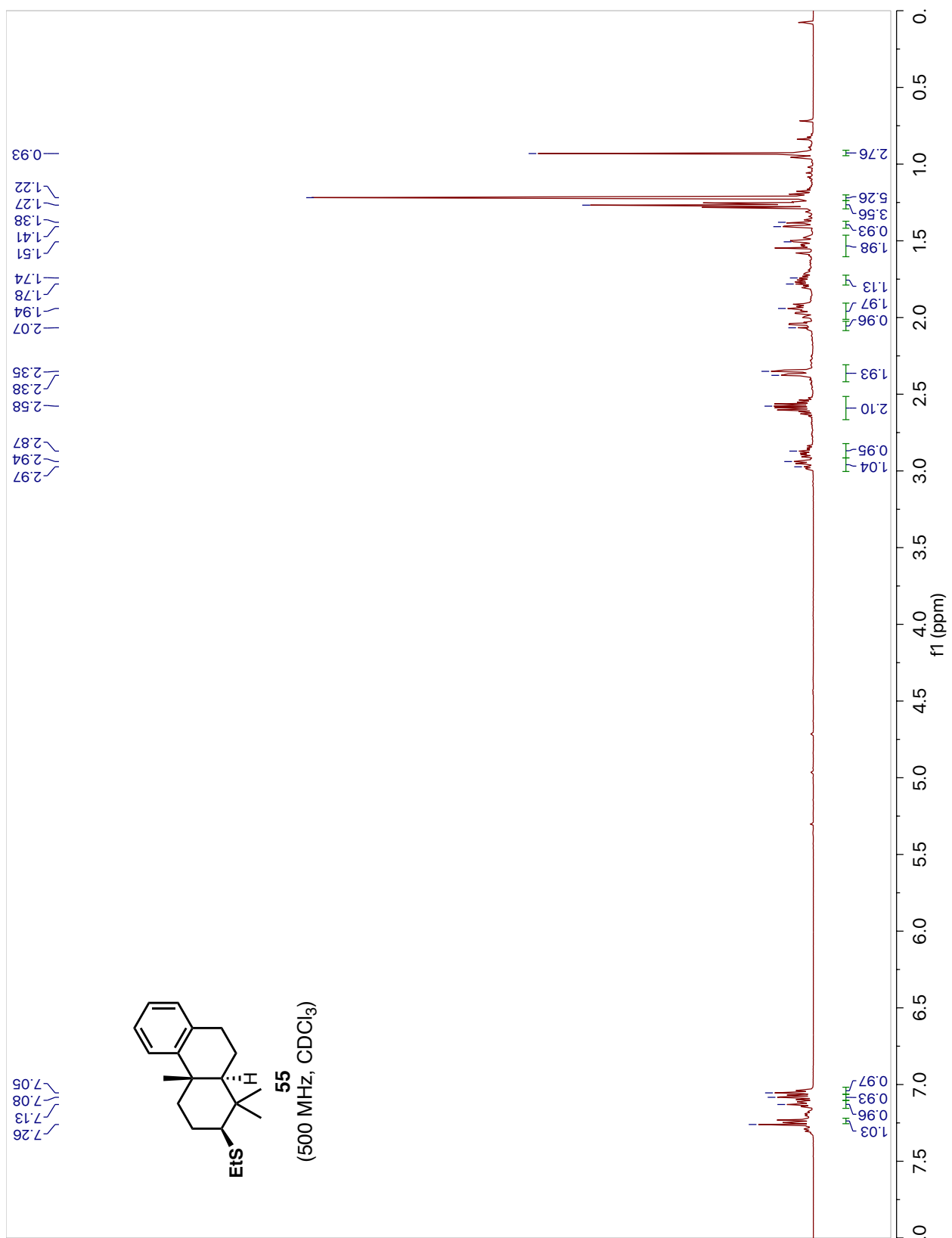
{6-Hydroxy-2,2,6-trimethyl-3-[(phenylthio)cyclohexyl]methyl Acetate (74)}. To a solution of geranyl acetate (0.021 mL, 0.1 mmol, 1.0 equiv.) in CH_2Cl_2 (2.5 mL) at -78 °C was quickly added a solution of the chiral phenyl disulfanium salt **76** (0.062 g, 0.11 mmol, 1.1 equiv.) in CH_2Cl_2 (0.25 mL) all at once. After stirring for 2 h at -78 °C, the reaction mixture was quenched with saturated aq. NaHCO_3 (5 mL), warmed to 23 °C, and the aqueous layer was extracted with CH_2Cl_2 (3×5 mL). The organic layers were combined, dried (Na_2SO_4), and concentrated to give a crude residue, which was further purified by flash column

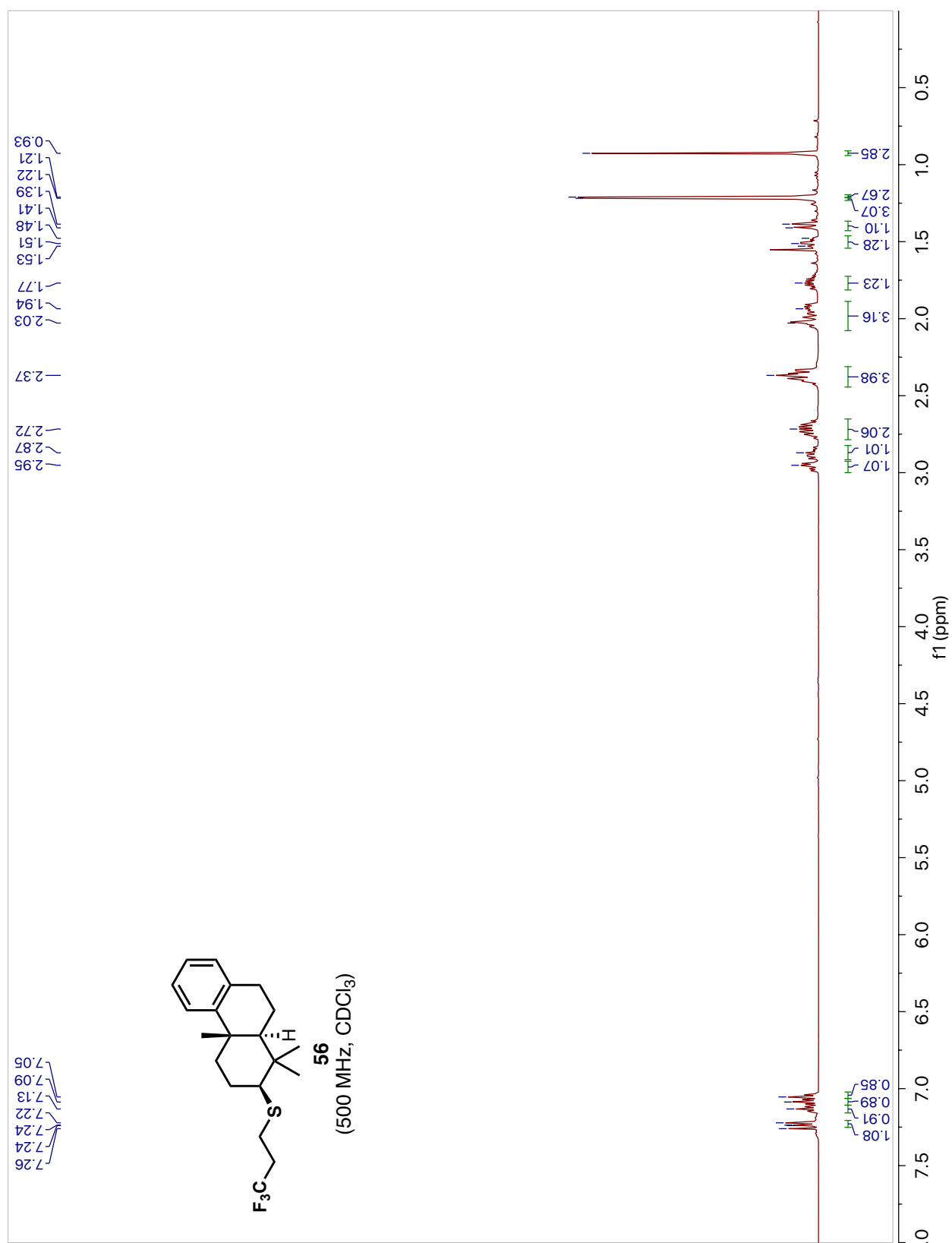
chromatography (hexanes/EtOAc, 3:1) to afford **74** as a colorless oil (17.0 mg, 53%, 10% *ee*).

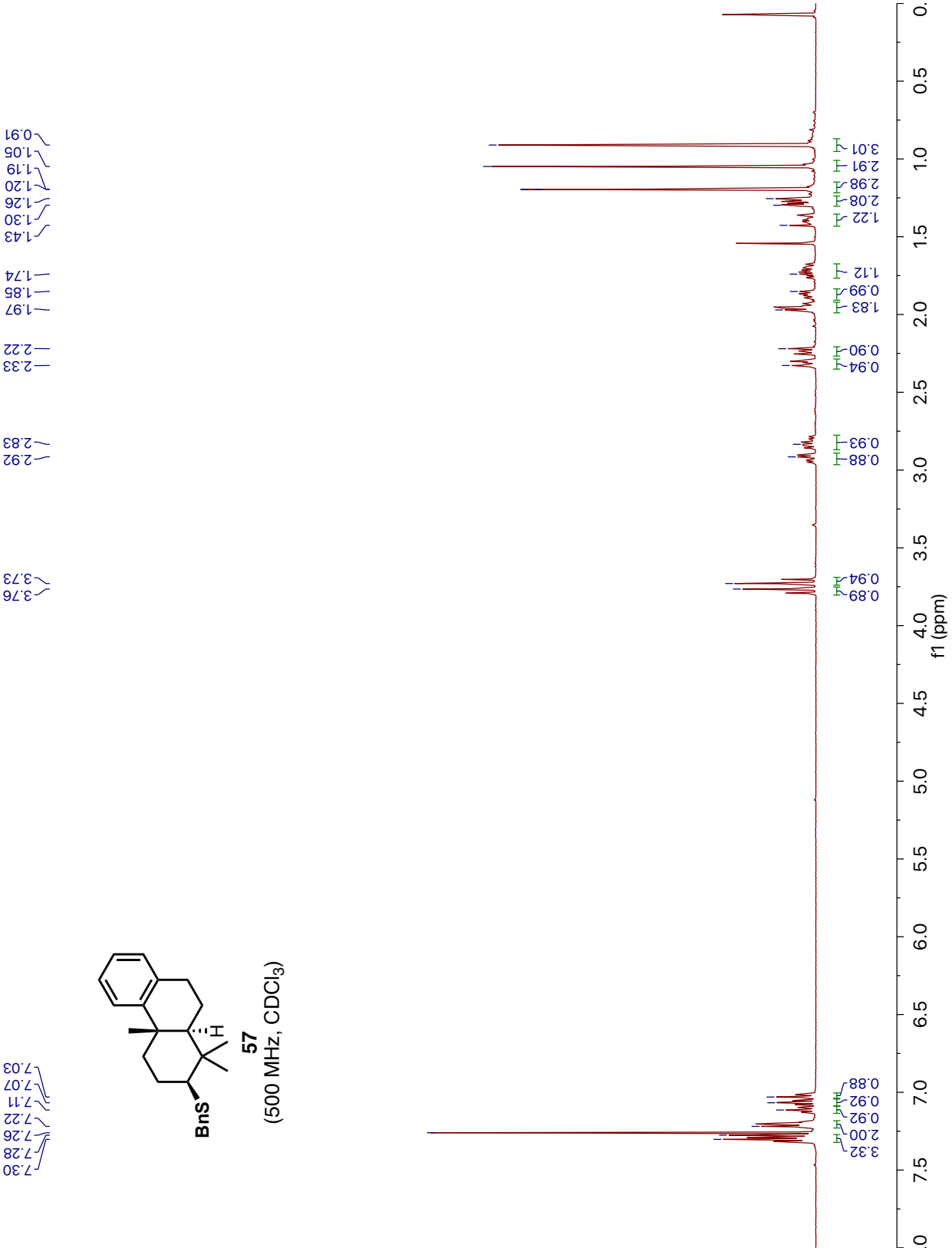
74: $R_f = 0.49$ (hexanes/EtOAc, 1:1). Note that similar reaction scales were used in the investigations with the other chiral disulfanium salts; IR (film): 3461, 3057, 2970, 2938, 2873, 1736, 1479, 1368, 1245, 1026, 740, 692 cm^{-1} ; ^1H NMR (500 MHz, CDCl_3) δ 7.44–7.38 (m, 2 H), 7.29 (t, $J = 8.4$ Hz, 2 H), 7.25–7.20 (m, 1 H), 4.42 (dd, $J = 11.8, 5.2$ Hz, 1 H), 4.33 (dd, $J = 11.8, 5.0$ Hz, 1 H), 2.88 (dd, $J = 12.5, 3.8$ Hz, 1 H), 2.07 (s, 3 H), 1.95 (dq, $J = 14.2, 3.7$ Hz, 1 H), 1.80 (dt, $J = 13.1, 3.4$ Hz, 1 H), 1.75–1.65 (m, 2 H), 1.46 (td, $J = 13.5, 4.0$ Hz, 1 H), 1.33 (s, 3 H), 1.23 (s, 3 H), 0.96 (s, 3 H); ^{13}C NMR (126 MHz, CDCl_3) δ 171.2, 136.4, 132.0, 129.1, 126.9, 72.1, 63.2, 60.7, 56.9, 42.6, 39.2, 29.9, 29.0, 23.8, 21.4, 17.6; HRMS (ESI) m/z [$\text{M}+\text{H}^+-\text{H}_2\text{O}$] calcd for $\text{C}_{18}\text{H}_{25}\text{O}_2\text{S}^+$: 305.1570, found 305.1574; The enantiomeric excess was determined by chiral HPLC using a Daicel Chiralpak OD-H column (hexanes/*i*-PrOH, 90:10, flow rate of 1.0 mL/min, 254 nm) t_R (major) = 6.37 min, t_R (minor) = 9.48 min, 10% *ee*.

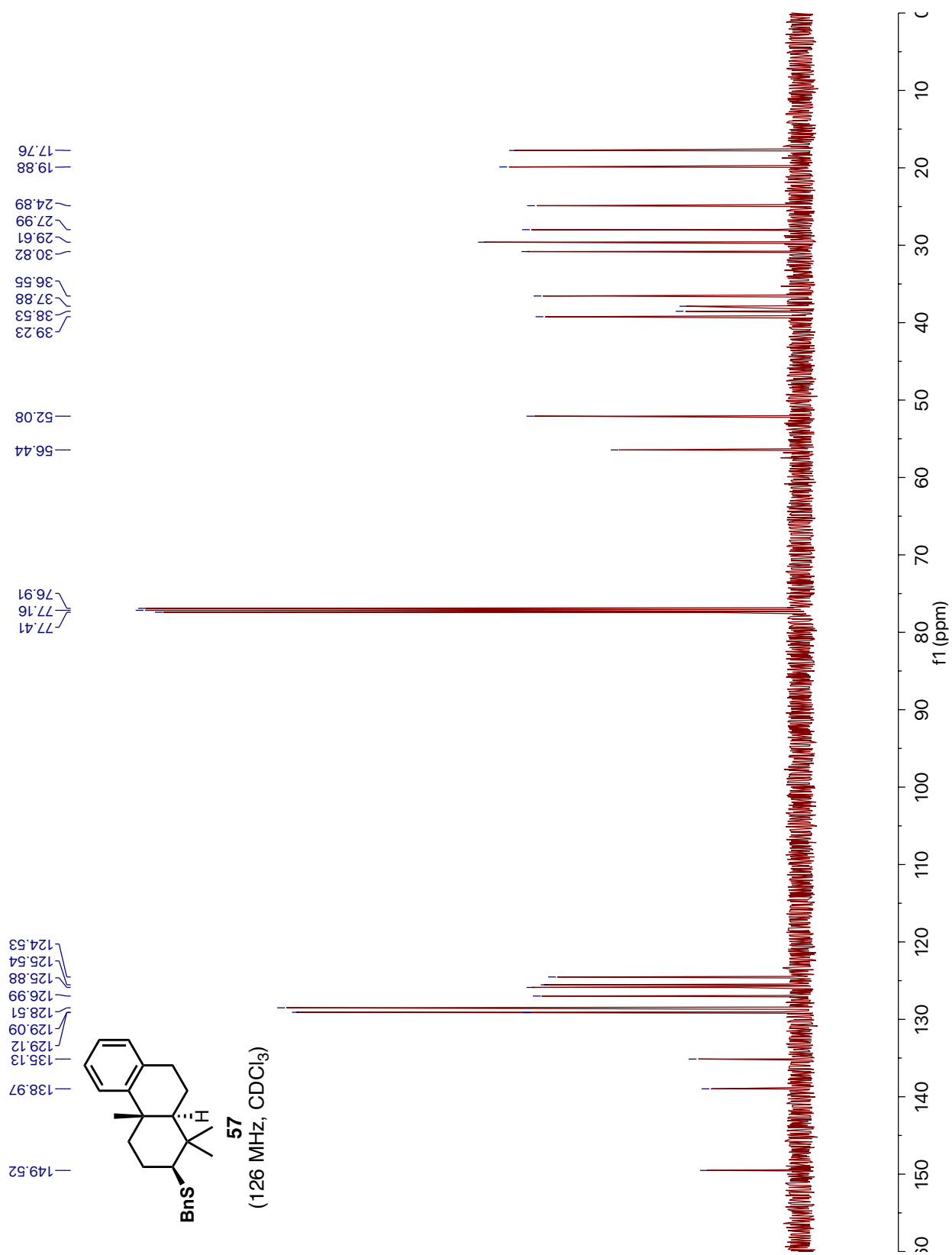
1.7 ^1H and ^{13}C NMR Data

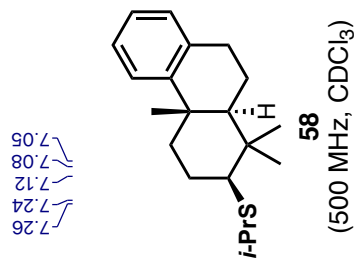






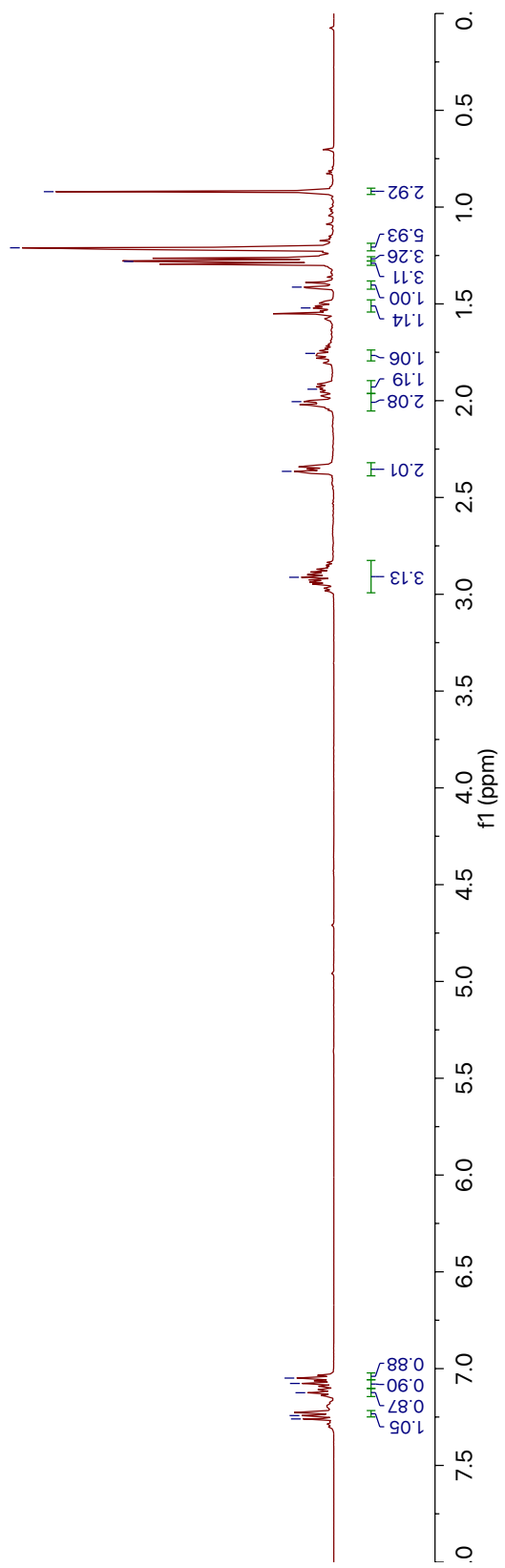


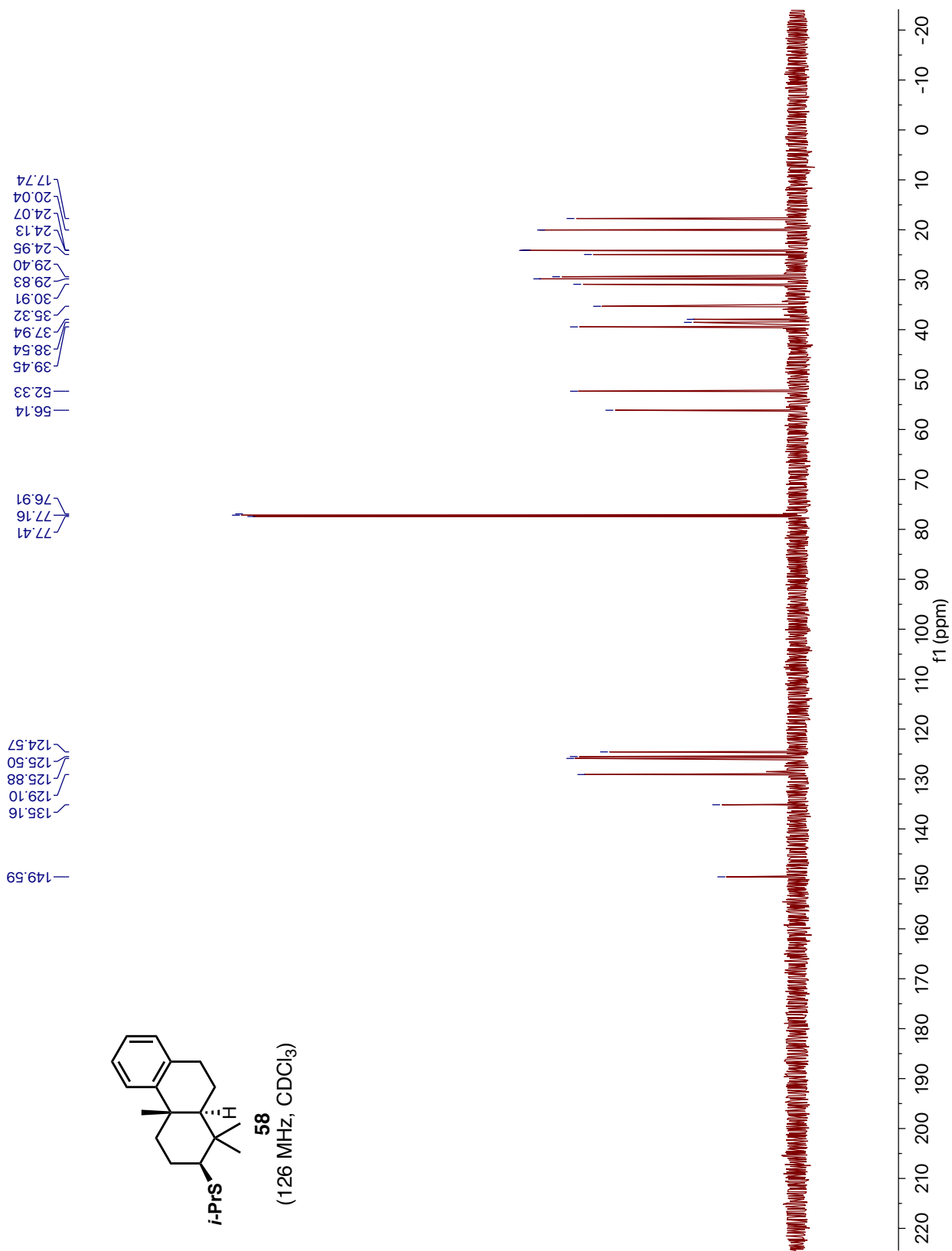
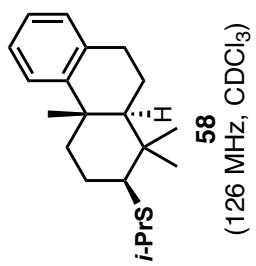


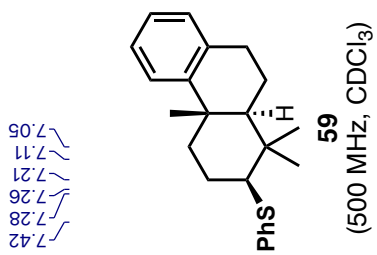


7.26
7.24
7.12
7.08
7.05

2.00
1.94
1.76
1.52
1.41
1.28
1.21
-0.92

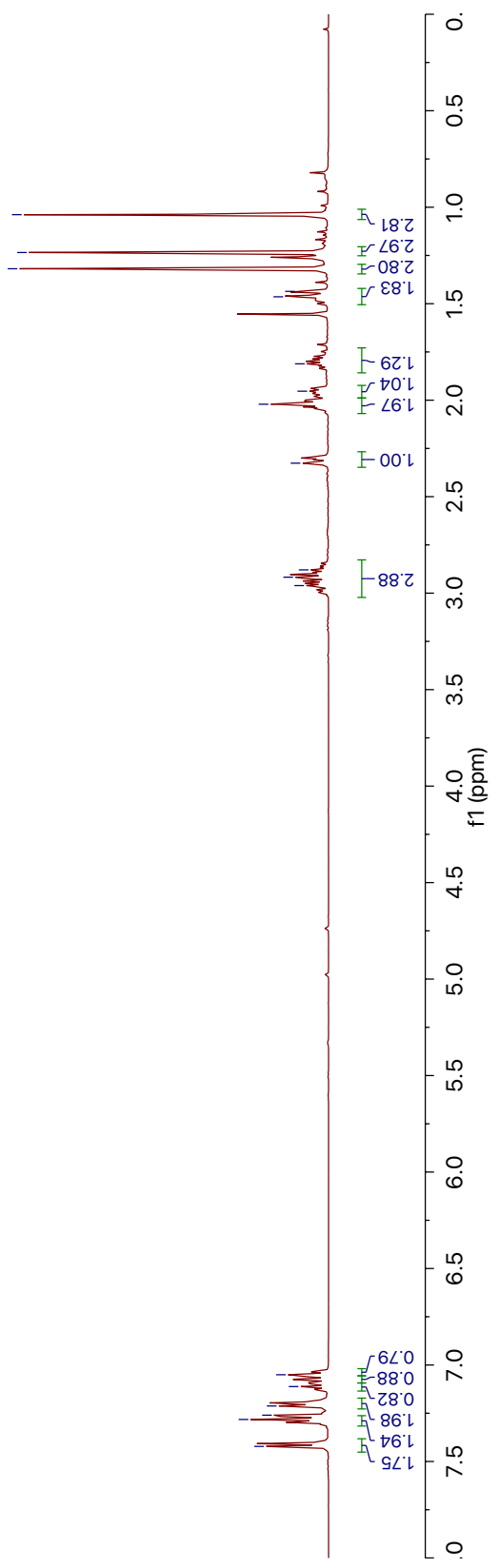


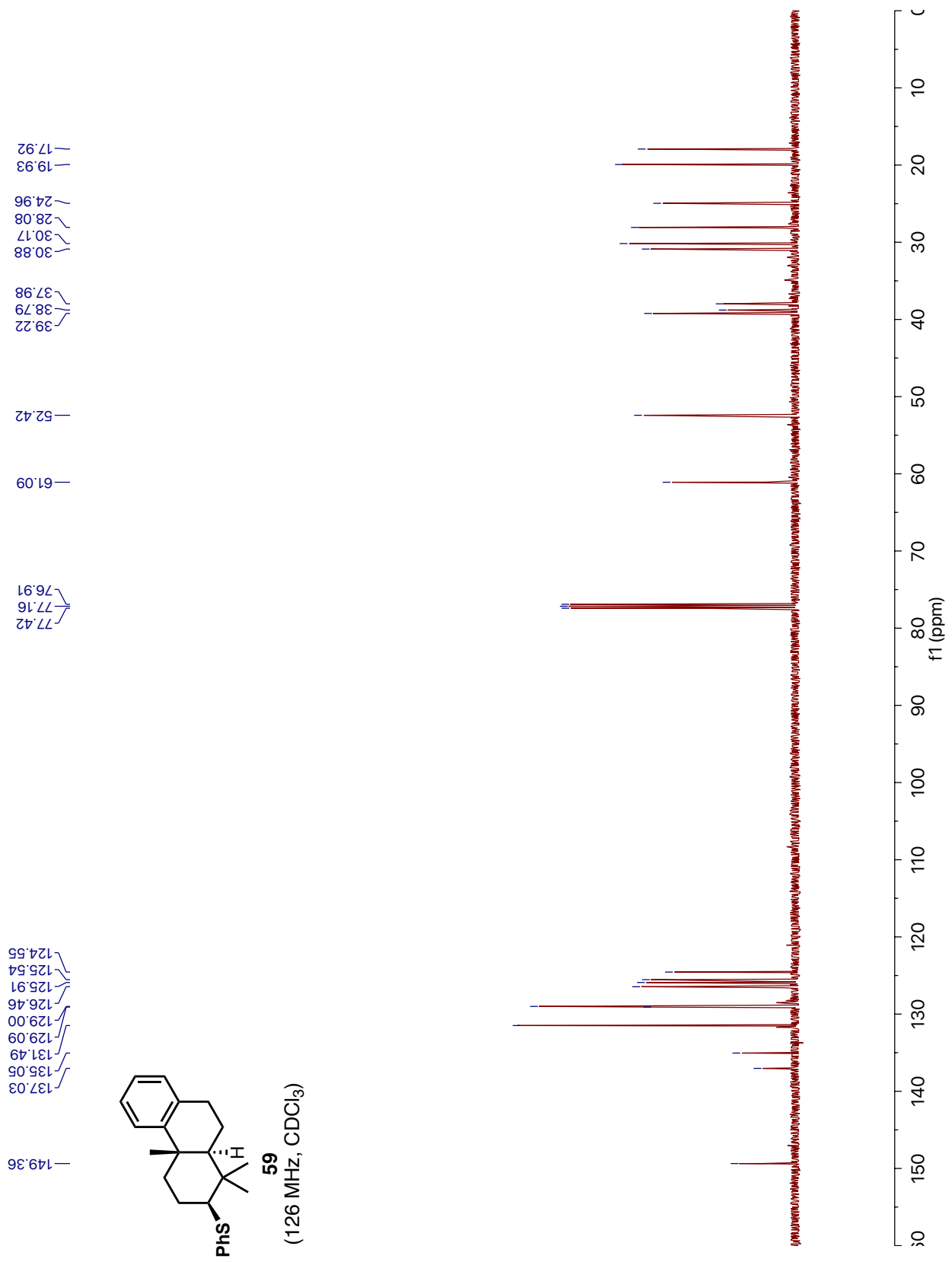


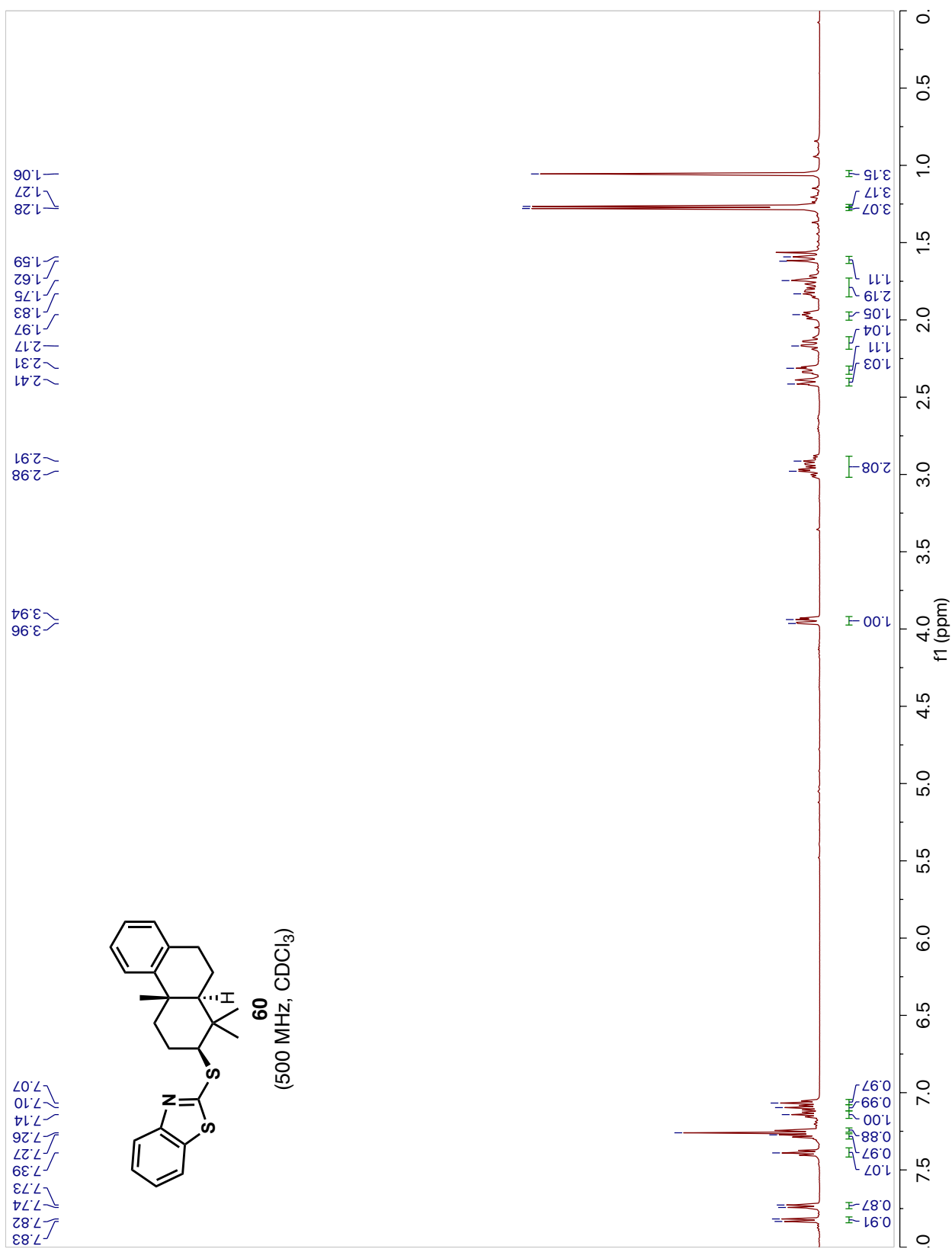


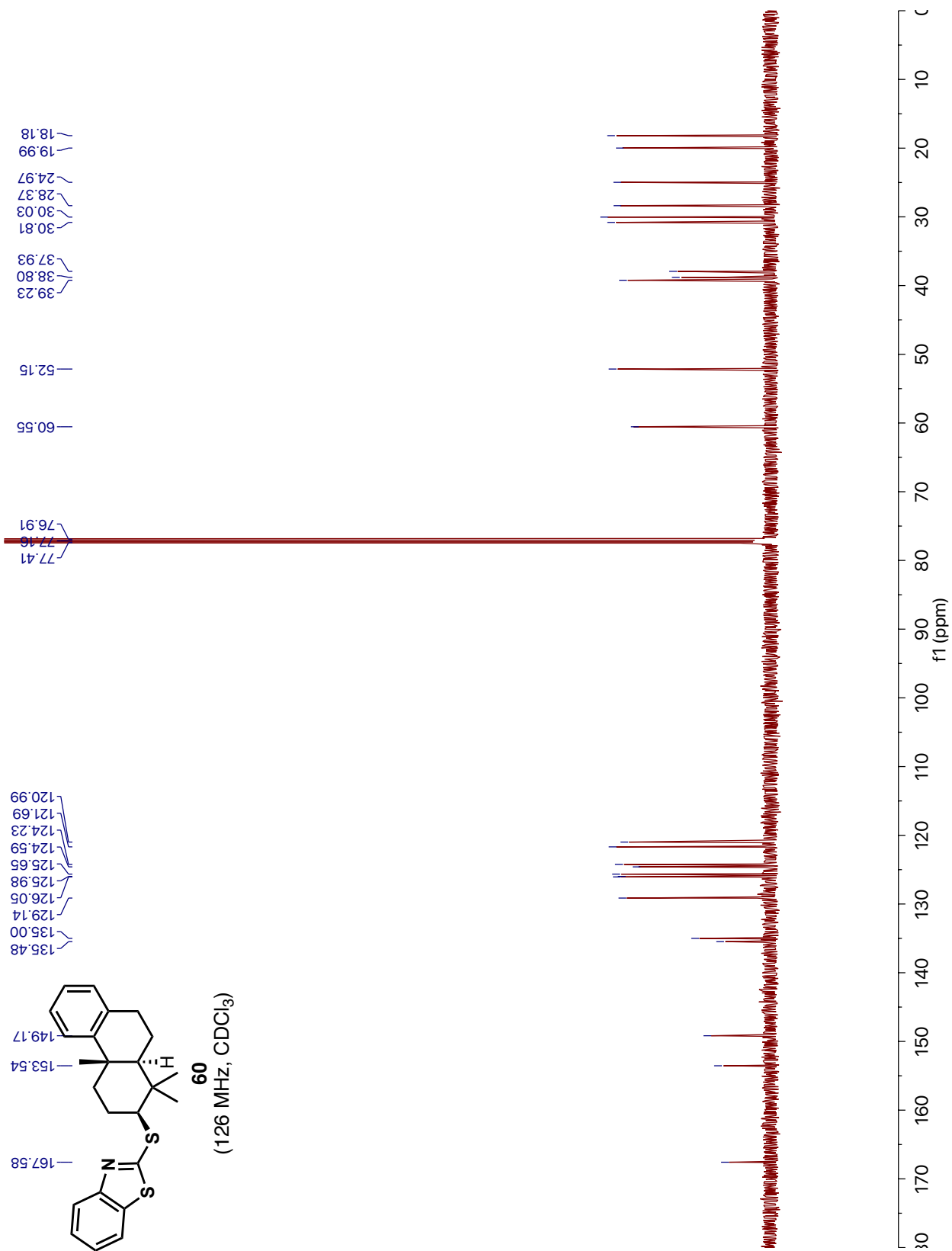
7.42
 7.28
 7.26
 7.21
 7.11
 7.05

2.96
 2.92
 2.88
 2.33
 2.02
 1.95
 1.81
 1.46
 1.44
 1.32
 1.23
 1.04

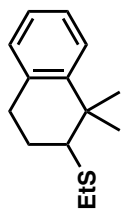






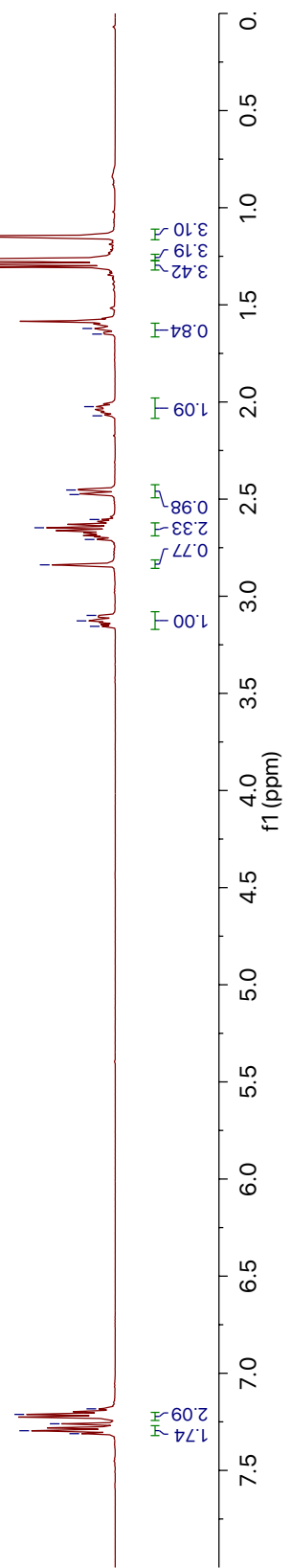


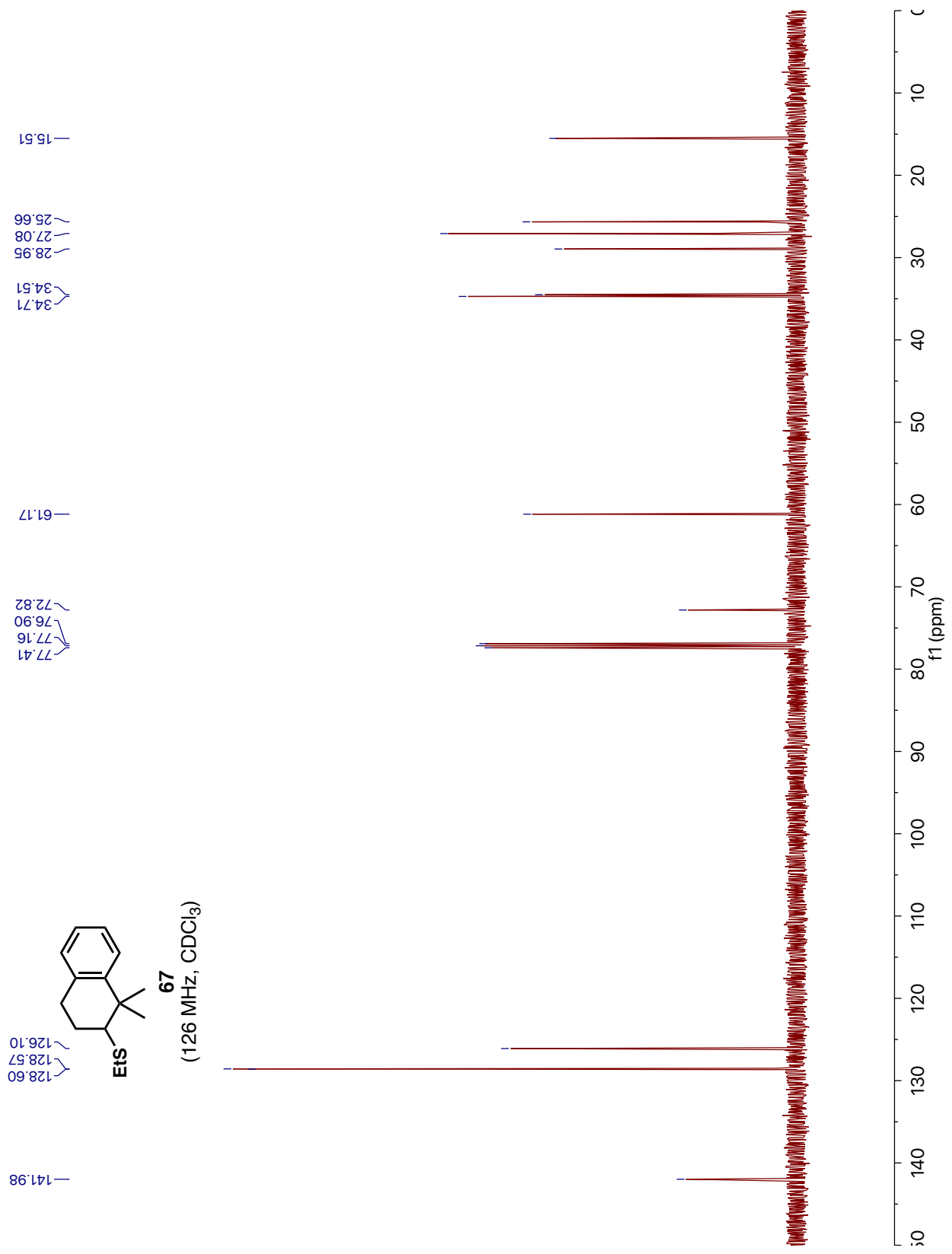
7.31
7.30
7.26
7.21
7.18

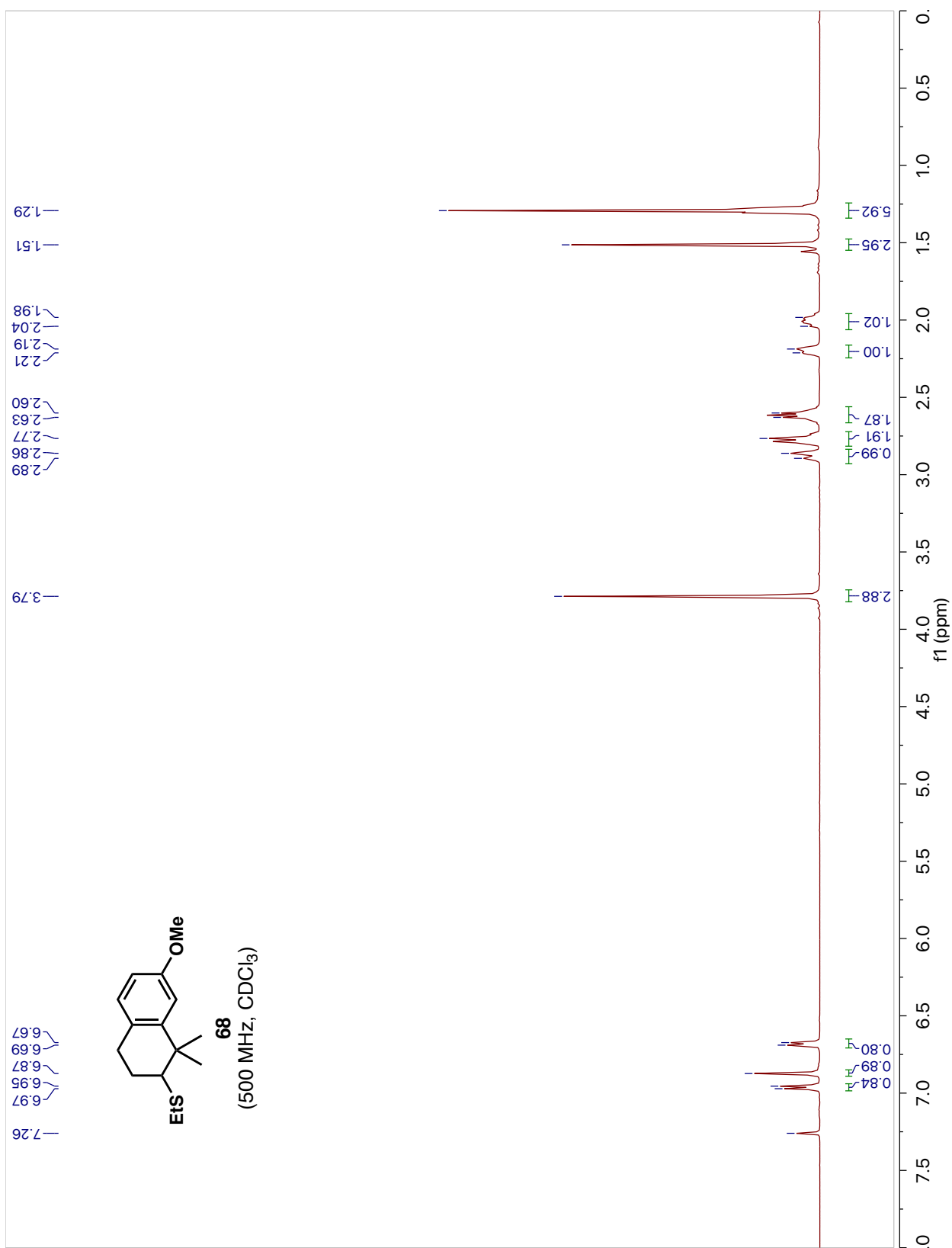


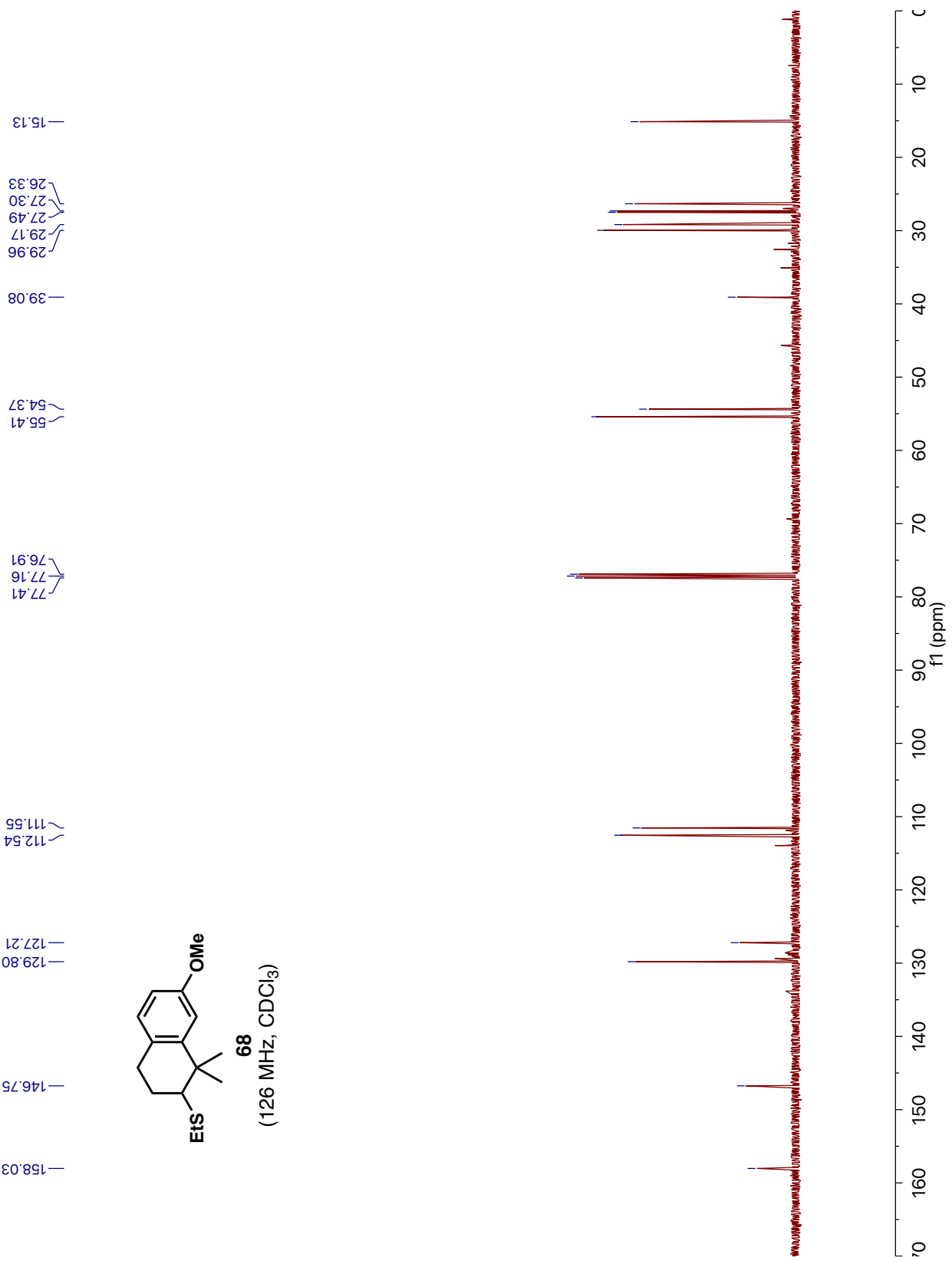
67
(500 MHz, CDCl₃)

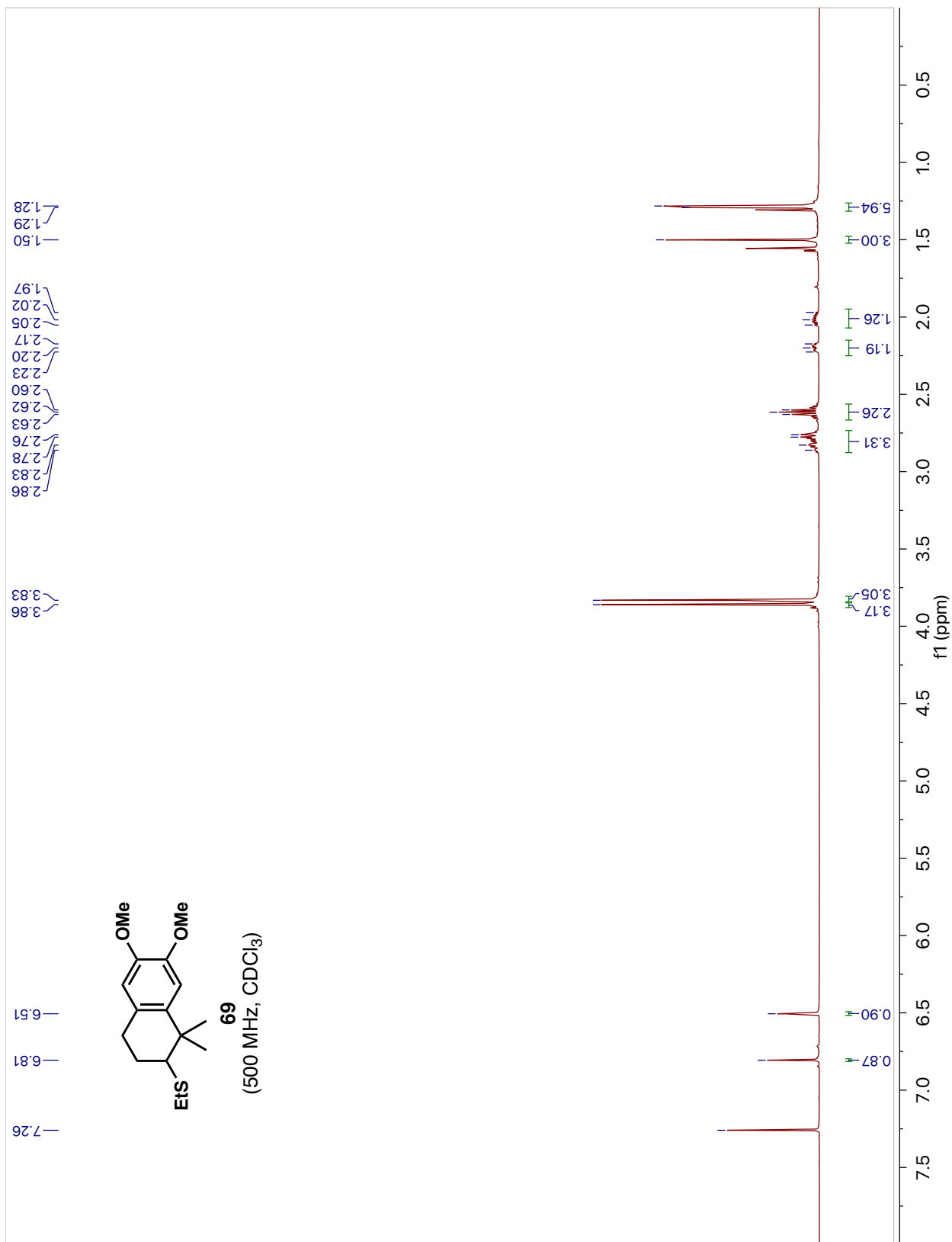
3.16
3.13
3.10
2.84
2.71
2.65
2.48
2.45
2.07
2.02
1.65
1.62
1.29
1.27
1.15

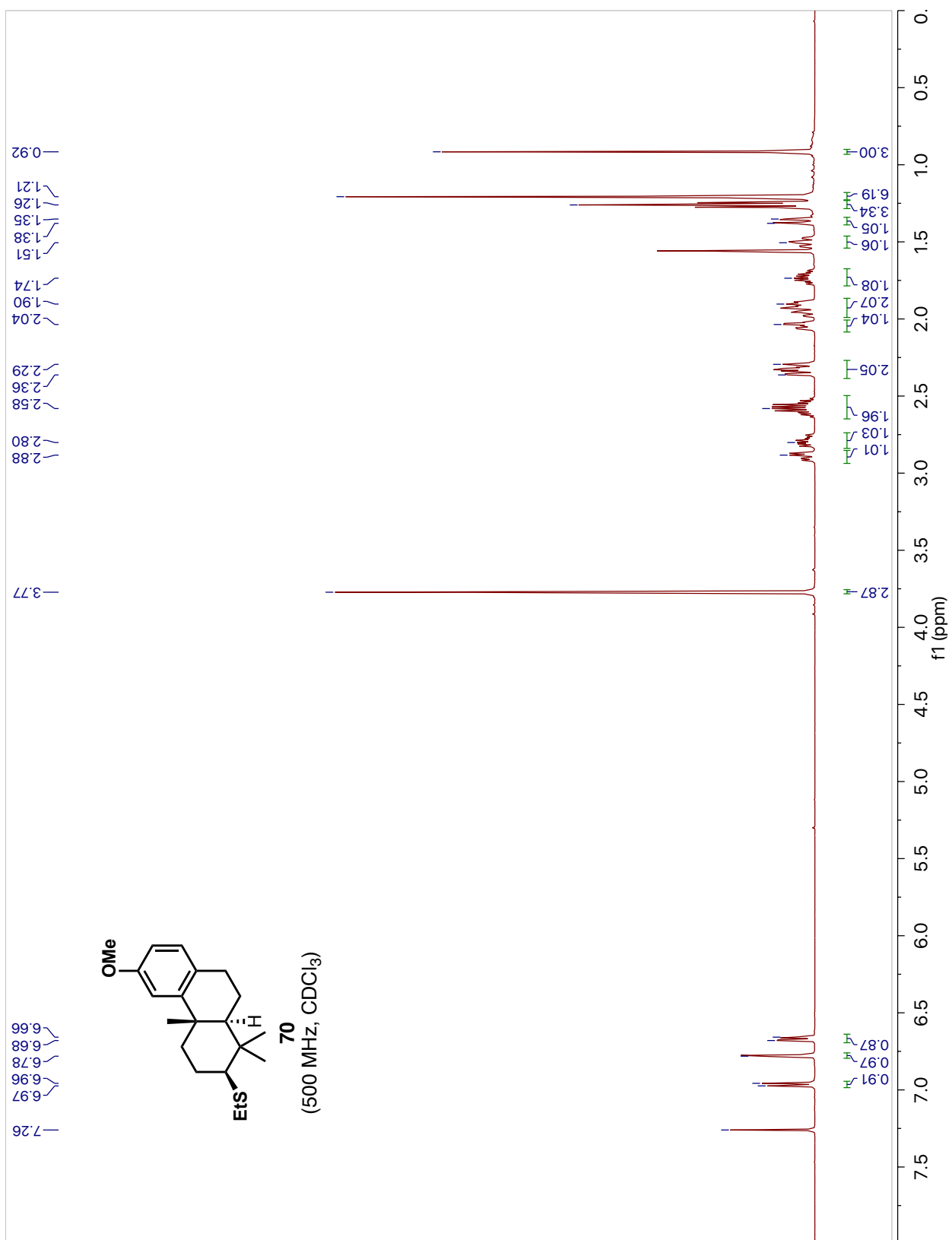


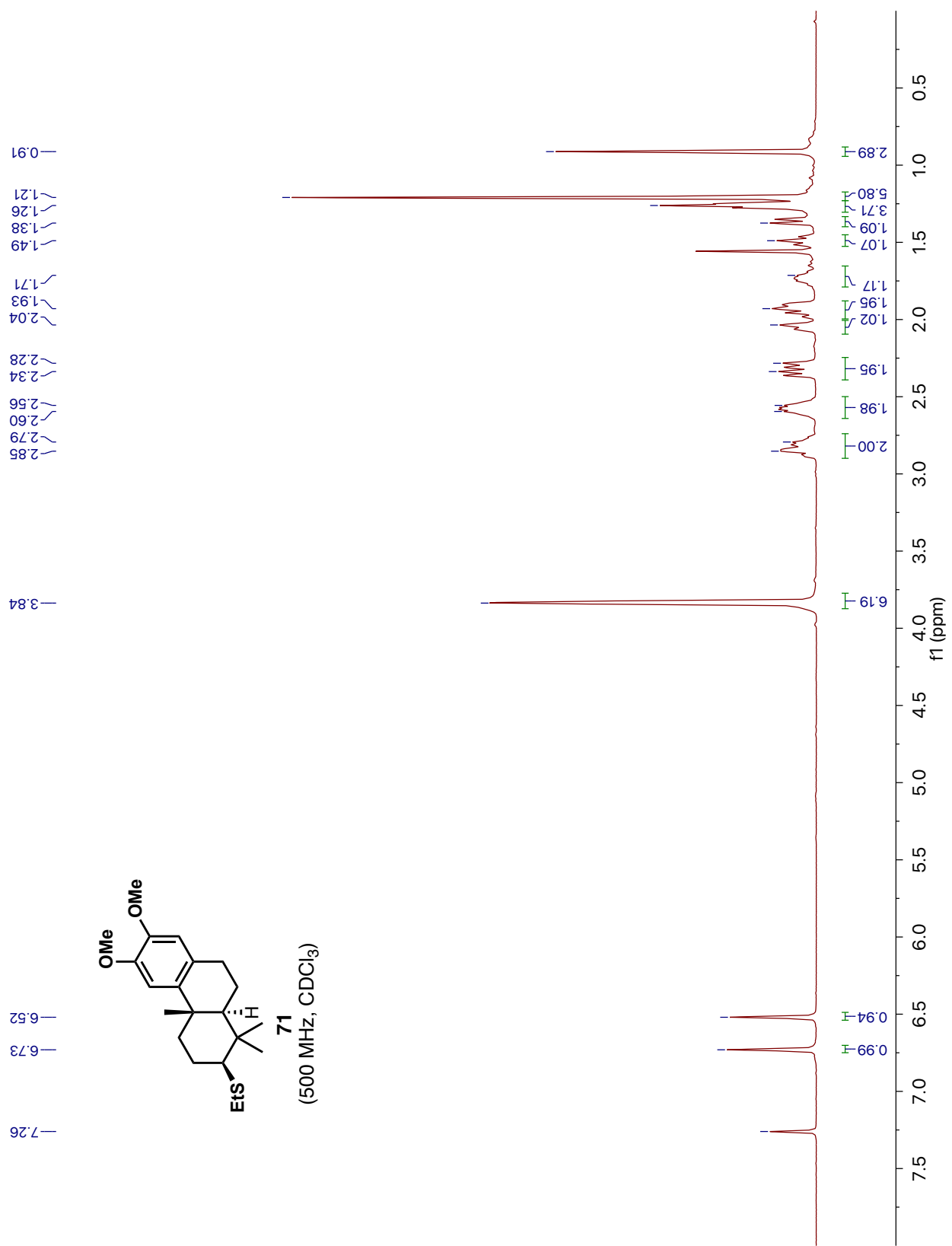


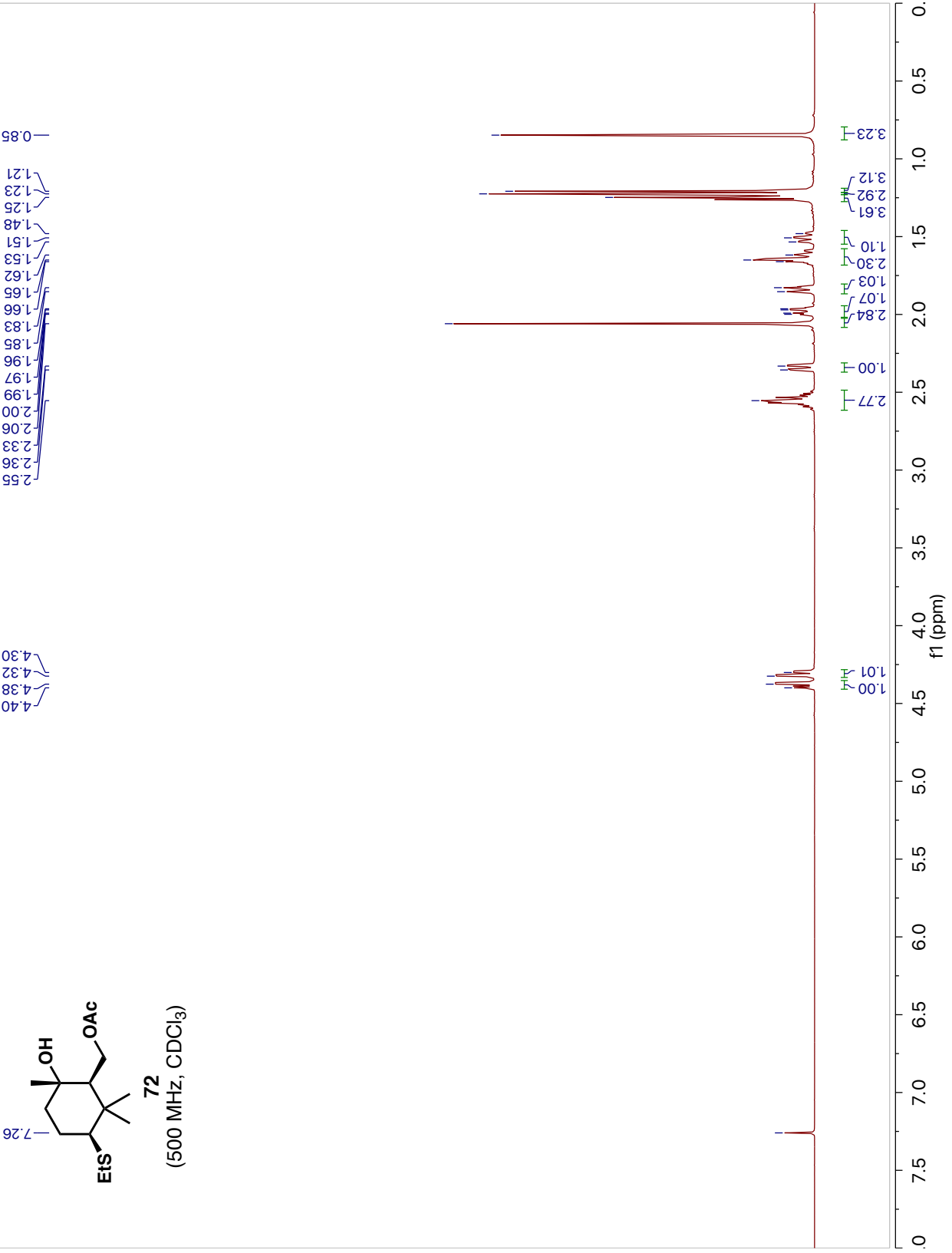
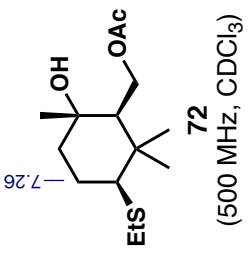


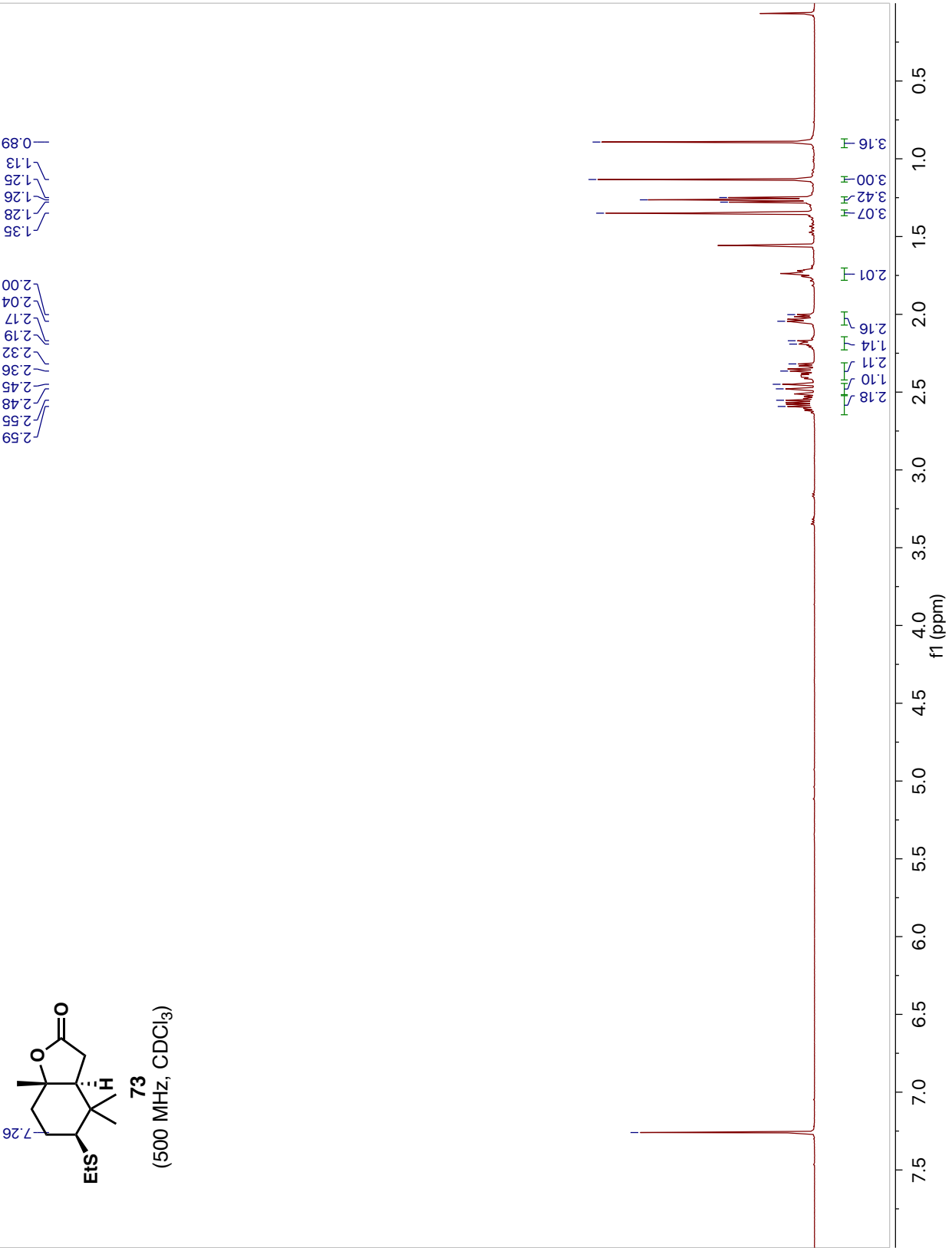
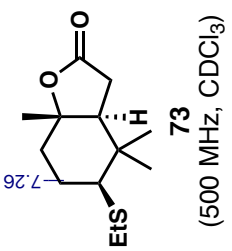


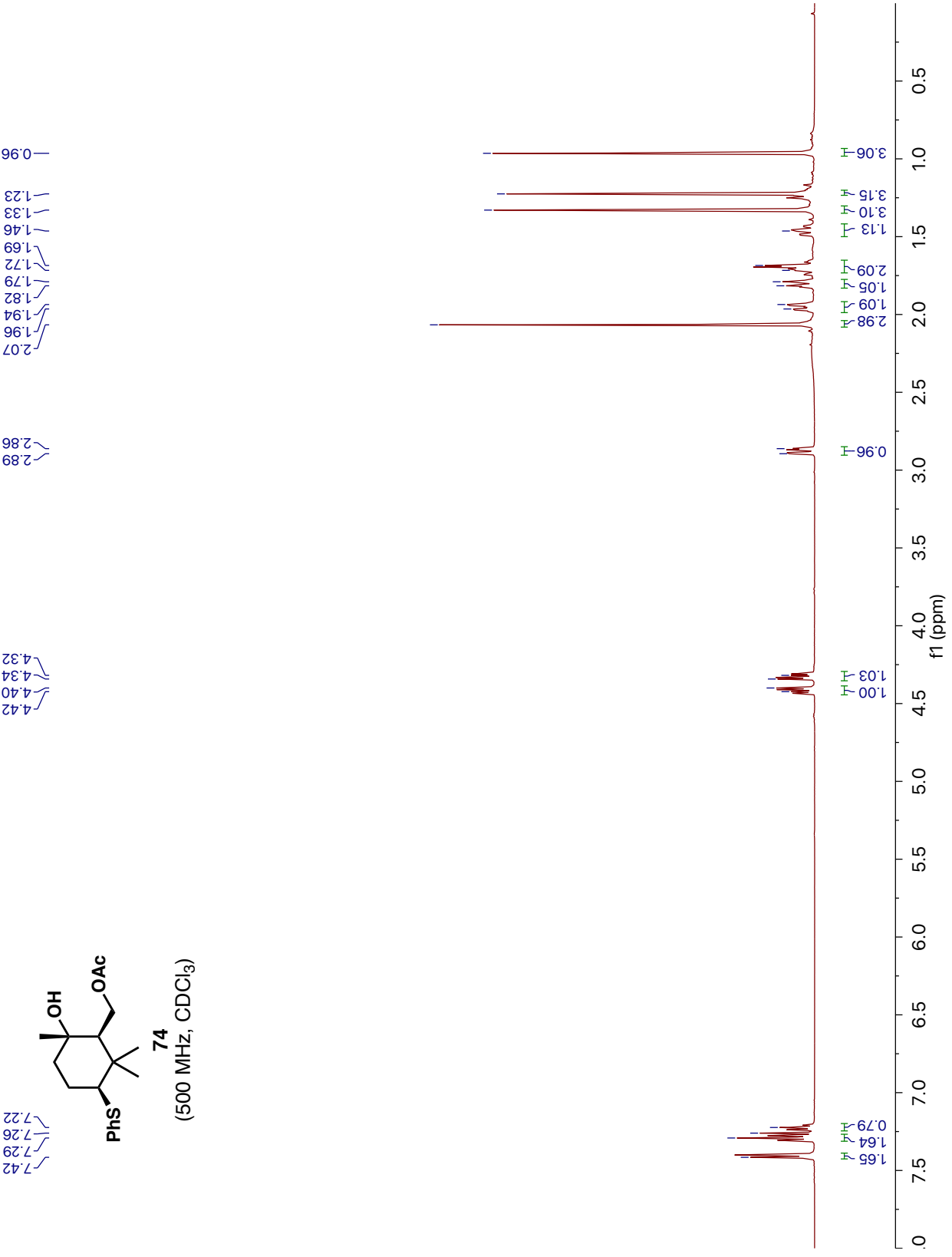
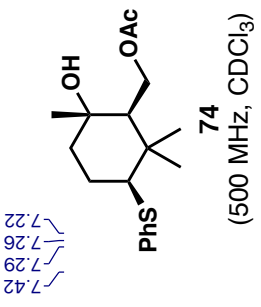


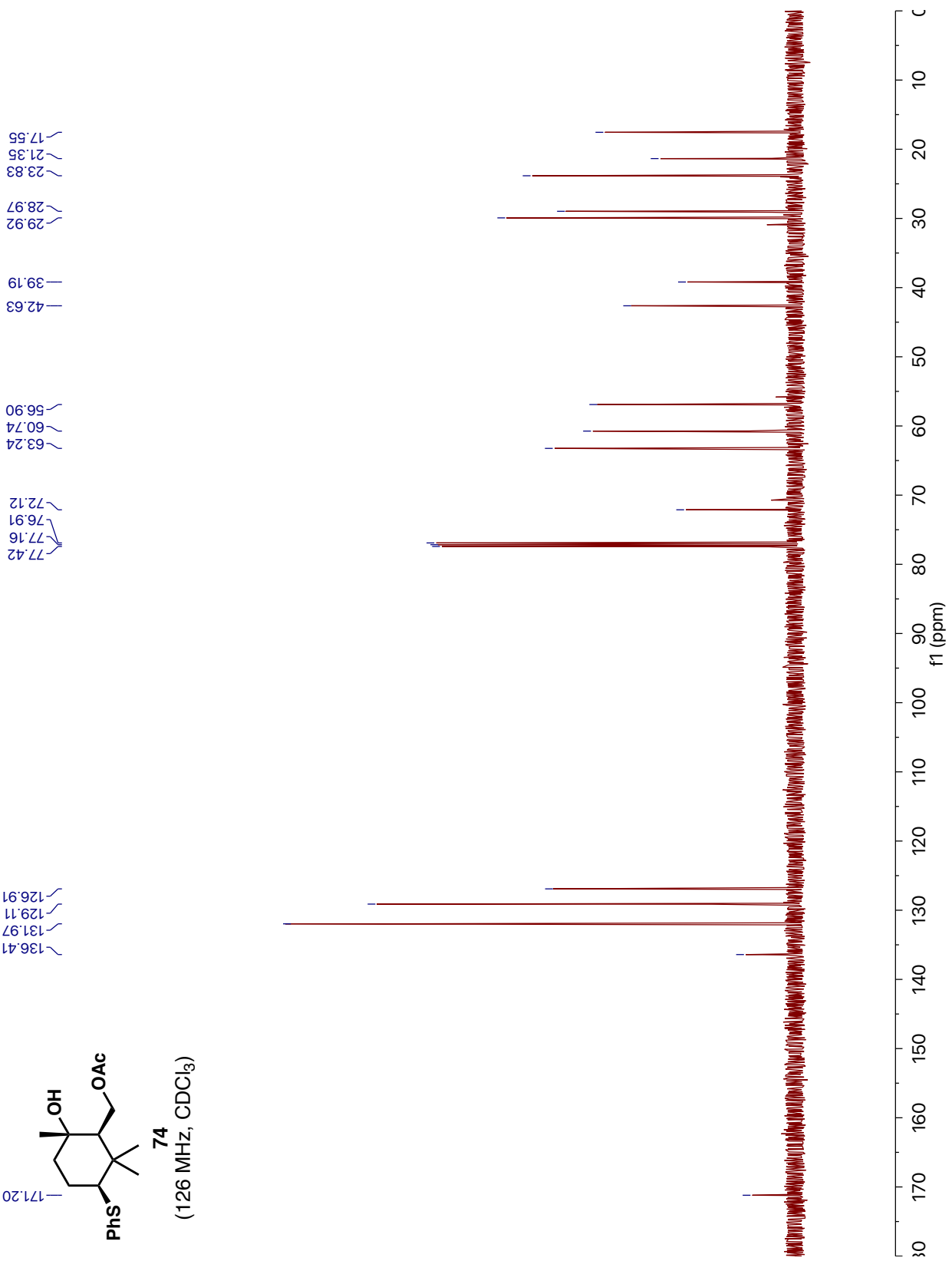
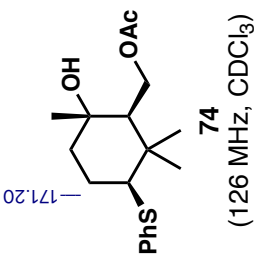






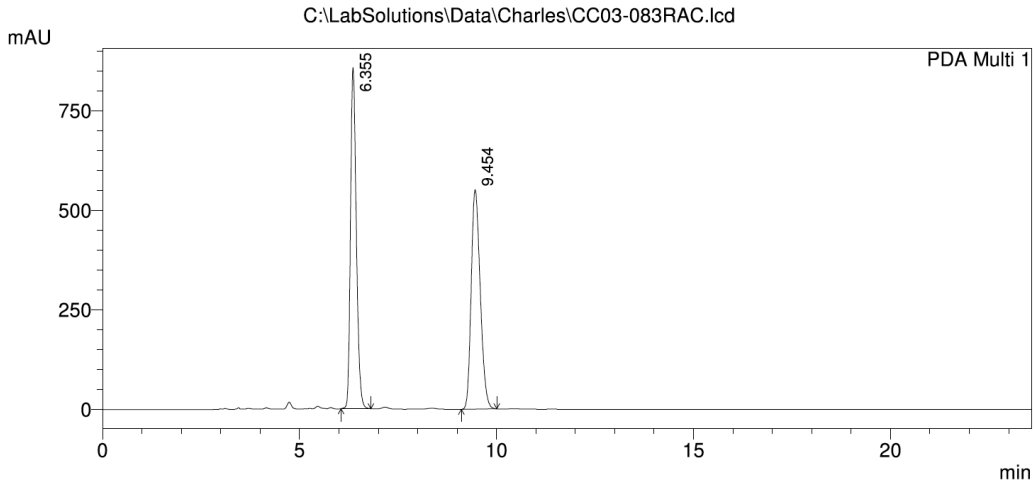






1.8 HPLC Traces

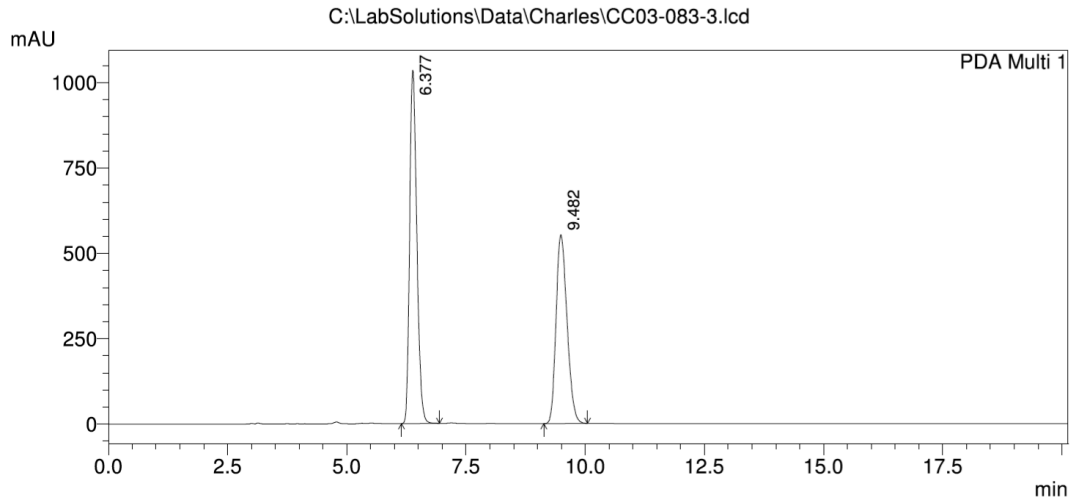
Racemic 74



PeakTable

Peak#	Ret. Time	Area	Height	Area %	Height %
1	6.355	8803273	857035	50.031	60.859
2	9.454	8792305	551194	49.969	39.141
Total		17595578	1408229	100.000	100.000

Enantioenriched 74



PeakTable

Peak#	Ret. Time	Area	Height	Area %	Height %
1	6.377	10792628	1034985	54.904	65.175
2	9.482	8864711	553030	45.096	34.825
Total		19657339	1588016	100.000	100.000

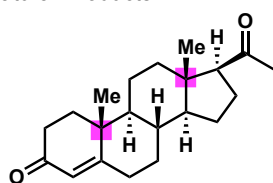
CHAPTER 2

TOTAL SYNTHESSES OF SPIROVIOLENE AND SPIROGRATERPENE A

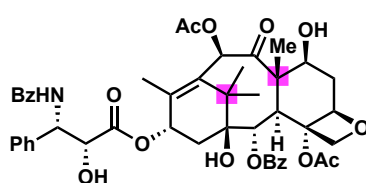
2.1 Introduction

In addition to constructing complex fused or bridged ring systems, there are certain isolated structural features that are themselves indicative of the challenges associated with accessing a particular target; one such feature is quaternary centers. These sites often serve as points of intense consideration when outlining a synthetic plan of attack, as their formation can be particularly challenging, not only from a steric perspective but also due to the fact that they are often relatively non-functionalized, thereby necessitating the installation and subsequent excision of some superfluous functionality.

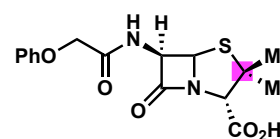
a) Natural Products



1: progesterone

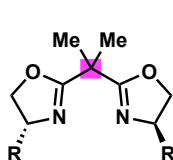


2: taxol

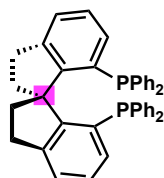


3: penicillin V

b) Ligand Design

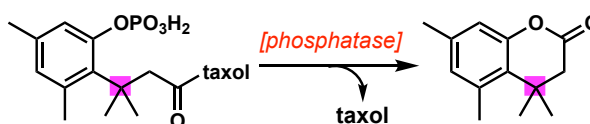


4



5

c) Medicinal Chemistry



6

7

Figure 2.1. Quaternary centers in (a) biologically relevant natural products, (b) ligands relevant to stereoselective transformations, and (c) medicinal chemistry.

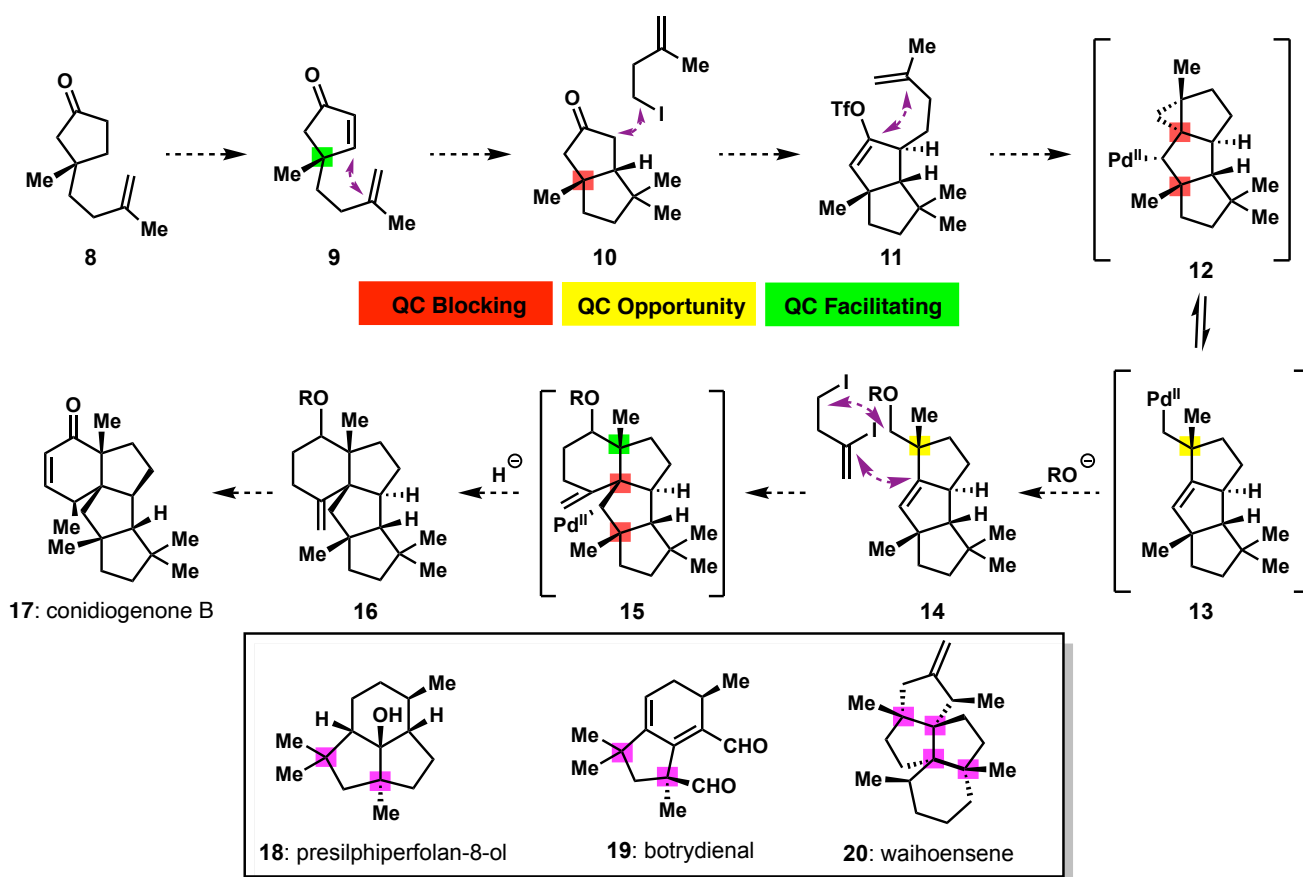
However, alongside their challenges, quaternary centers are often vitally important to molecular function and in fact have even been purposefully incorporated into several different organic structures.¹ For example, such centers can be found in many medicinally relevant natural products such as progesterone (1) and taxol (2), among others (Figure 2.1). Additionally, quaternary centers have proven integral to molecular structure as it pertains to ligand design. In bisoxazoline ligands (4), the inclusion of quaternary carbon centers not only removes the highly acidic protons that would otherwise be present on the bridging methylene but can also allow one to alter the consequent bite angle and thereby fine tune the

reactivity/selectivity of the species of interest.² Similarly, diphosphine ligands such as spirobiindane diphosphine (**5**, SDP), have shown to be superior in stereoselectivity relative to BINAP.³ Although used primarily in the realm of asymmetric hydrogenation, these quaternary center-containing diphosphines have gained broader applications in Barbier-type couplings, asymmetric allylations and hydrofunctionalizations. Essential to the efficiency of these ligands is the ability to maintain the axial chirality typical of common diphosphines, but impose a much higher degree of structural rigidity through the spirocenter.

One of the main applications of quaternary centers in synthesis, though, is through the Thorpe-Ingold effect: the ability to exponentially increase the rate of cyclization, through the compression afforded by a fully substituted carbon center within the framework of interest. This is most clearly demonstrated in the well-known example of the trimethyl lock, a common technique used within medicinal chemistry for the preparation of pro-drug derivatives (Figure 2.1c).⁴ Here, the 2-hydroxybenzene propionic acid derivative (**6**) can undergo dephosphorylation in the presence of the relevant phosphatase, at which point rapid intramolecular lactonization takes place, releasing the active drug form. In fact, the placement of methyl groups throughout the auxiliary, as depicted in **6**, provides a 10⁸-magnitude rate enhancement relative to the non-methylated variant.

Recently, our group has developed a program surrounding the consideration of quaternary centers in synthetic planning. From this perspective, quaternary centers are not viewed as challenges but as serving several key roles (Scheme 2.1); preventing undesired reactivity or selectivity (QC blocking), enabling reactivity (QC facilitating) or offering the potential for new reaction development (QC opportunity).⁵ This process has led to successful syntheses of several non-functionalized terpenes, including **17-20**, and is best illustrated with the total synthesis of the conidiogenone family of natural products.⁶

Cyclopianes such as conidiogenone B (**17**) are a family of highly strained diterpenes which contain a large number of quaternary centers relative to their overall composition. Consequently, it is when pursuing such targets synthetically that one can either view these centers as daunting challenges or as opportunities to accelerate synthetic planning and advance chemical understanding.⁷ In a forward sense, the synthesis of **17** begins from enantioenriched **8**, with the first quaternary center installed via an asymmetric 1,4-addition as developed by the Hoveyda group.⁸ This center is then viewed as facilitating the ensuing radical cyclization of **9** to **10**, through a Thorpe-Ingold like effect to establish the diquinane core (Scheme 2.1).⁹ Furthermore, this same quaternary center can now serve to promote a regioselective alkylation by introducing additional steric encumbrance at the β -position of the ketone. After forming the subsequent vinyl triflate (**11**), a Heck cyclization installs the third cyclopentane ring as well as establishes the *trans*-1,3-stereochemistry.¹⁰ It is important to note, as shown in Scheme 2.1, that the alkyl-Pd species exists in equilibrium between the neopentyl species **13** and corresponding 3-*exo*-trig product **12**. However, the positioning of quaternary centers within the structure **12**, in fact precludes any possibility of β -hydride elimination and thereby facilitates the desired nucleophilic substitution to produce **14**. The newly formed quaternary center in **14** then provided an opportunity for reaction development, in this case a diastereoselective Nozaki-Hiyama-Kishi reaction with an α -quaternary aldehyde, to install the necessary vinyl iodide sidechain.¹¹ A final reductive Heck cyclization then completes the 6/5/5/5 fused ring system of **16** where, once again, the positioning of quaternary centers in **15** precludes the possibility for β -hydride elimination. Simple functional group manipulations are then able to convert **16** to conidiogenone B in just 13 steps from commercial materials, nearly half the step count of the previously reported route.¹²

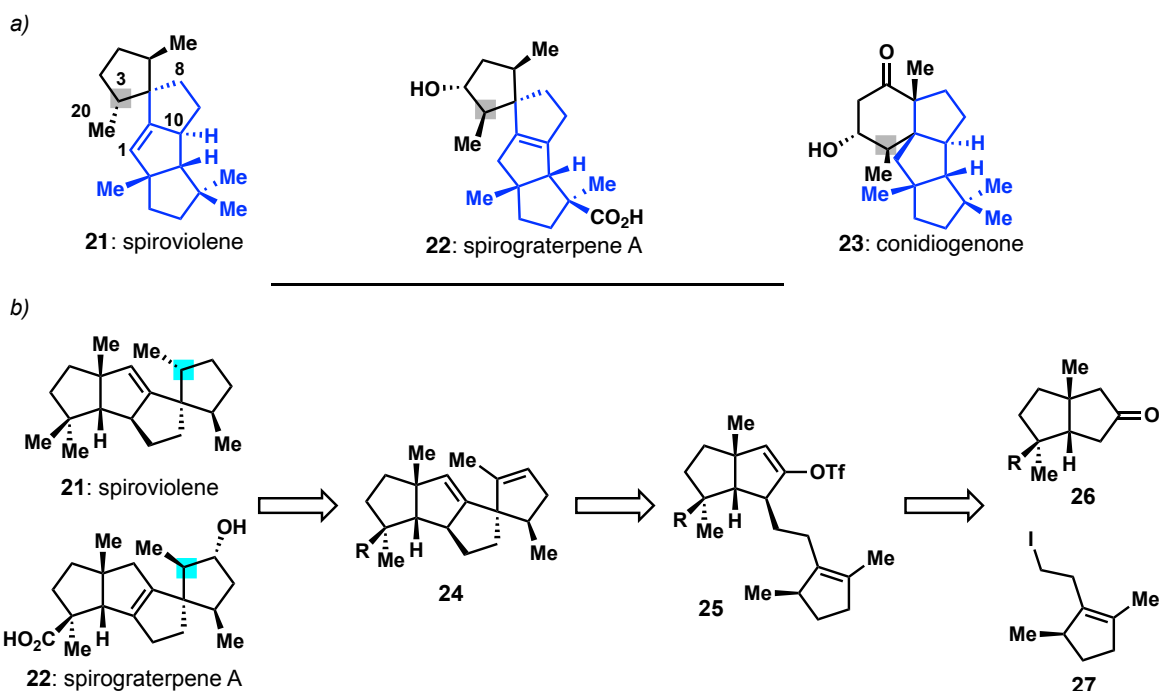


Scheme 2.1. Utilizing quaternary carbons to guide and expedite the total synthesis of non-functionalized terpenes as in **17-20**.

2.2 Pursuing New Targets

In seeking to further the number of targets pursued from the lens of quaternary center analysis, we came across two very recent isolates, spiroviolene (**21**) and spirograterpene A (**22**).^{13,14} The initial draw to these targets was not only the presence of multiple quaternary centers but the fact that much of the scaffold was shared with the conidiogenone family members, in particular the linear triquinane frame (Scheme 2.2). In fact, **22** was isolated alongside some previously characterized members of this family. In addition, we found it quite interesting that although **21** and **22** are almost identical in structure, there was a key stereochemical discrepancy between the two (highlighted in blue, Scheme 2.2b). While this may have seemed unlikely, it did not appear impossible, with **21** and **22** being isolated from bacterial and fungal terpene origins, respectively. Hence, we prepared a retrosynthetic analysis

to gain access to these targets and possibly further confirm the assignment provided (retrosynthetic analysis performed by Dr. Hyung Min Chi).

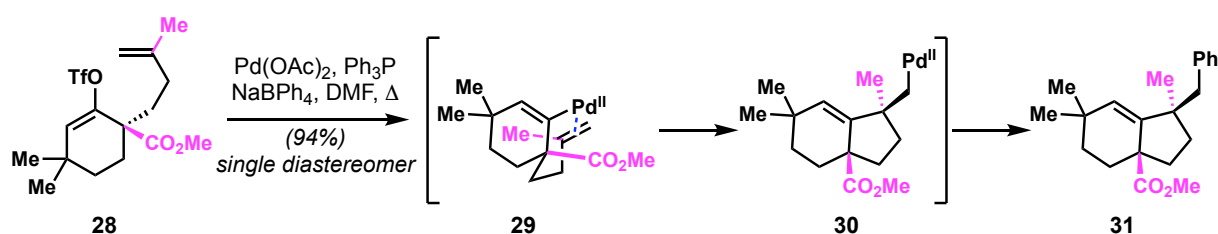


Scheme 2.2. (a) Structural similarities between non-functionalized terpenes **21**, **22** and **23**; (b) Retrosynthetic analysis of **21** and **22**.

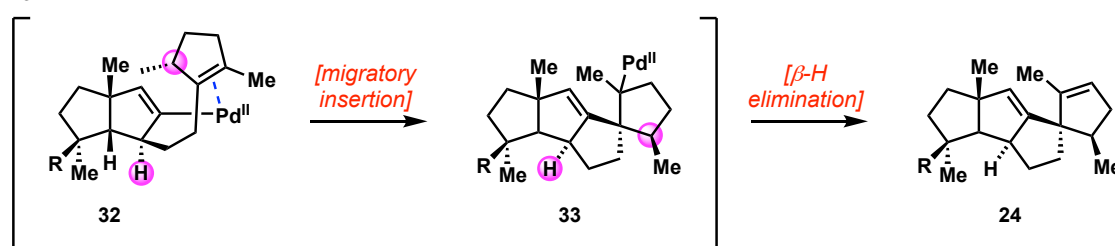
Clear to us was the fact that we wanted to access these compounds from a previously synthesized intermediate, given the structural homogeneity between spirocycles **21** and **22** and the conidiogenones. And so, we traced both targets back to triquinane **24**, whereby an olefin reduction would provide **21**, while an olefin migration and series of oxidation state manipulations would yield **22**. The spirocycle was then viewed to be established through a Heck cyclization of the corresponding vinyl triflate **25**. Worth noting, is that the Heck reaction would set the requisite *trans*-1,3 stereochemistry about the newly formed cyclopentane ring. Such stereoselectivity was first observed by Overman and co-workers in 1992 when studying Heck cascades in hydrocarbon frameworks, after which it was reported by Grigg in 1997 (Scheme 2.3a).¹⁰ Grigg and co-workers propose that the ester and methyl groups within **28** must adopt a *trans* relationship in order to accommodate the rigid four-membered palladacycle intermediate necessary for the migratory insertion. We have applied this logic to intermediate **32** in Scheme 2.3b to justify the proposed stereo-outcome. Subsequently, **25** could then be

easily obtained from bicyclic ketone **26** and alkyl iodide **27**. While a divergent synthesis that grants access to both targets would be ideal, the ability to perform selective late-stage oxidations on an intermediate such as **24**, was already considered implausible in our group's synthesis of the conidiogenones.⁵ Unfortunately, the only functional handle that could provide any form of directed reactivity, the secondary alcohol in **22**, is by no means sufficiently proximal to afford the necessary selectivity. While on the other hand, any C–H oxidation process would likely favor any one of the four tertiary C–H bonds found within the target.¹⁵ Therefore, we decided instead to approach **21** and **22** in a modular fashion, with the synthesis of **21** proceeding from an intermediate in the synthesis of conidiogenone B (**17**) and the synthesis of **22** proceeding from an intermediate in the synthesis of conidiogenone C (**38**).

a) Grigg, 1997



b) This work

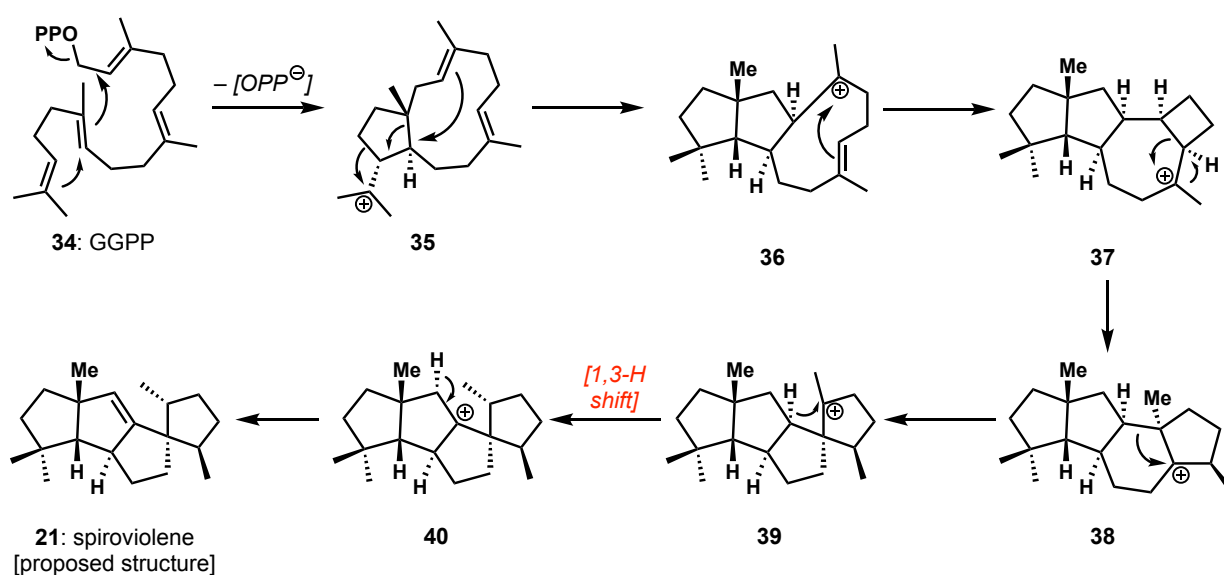


Scheme 2.3. (a) Literature precedent for the 1,3-*trans*-stereochemistry as set by the Heck cyclization; (b) Stereo-determining step of the Heck cyclization to afford **24**.

2.3 Proposed Biosyntheses of Spiroviolene and Spirograterpene A

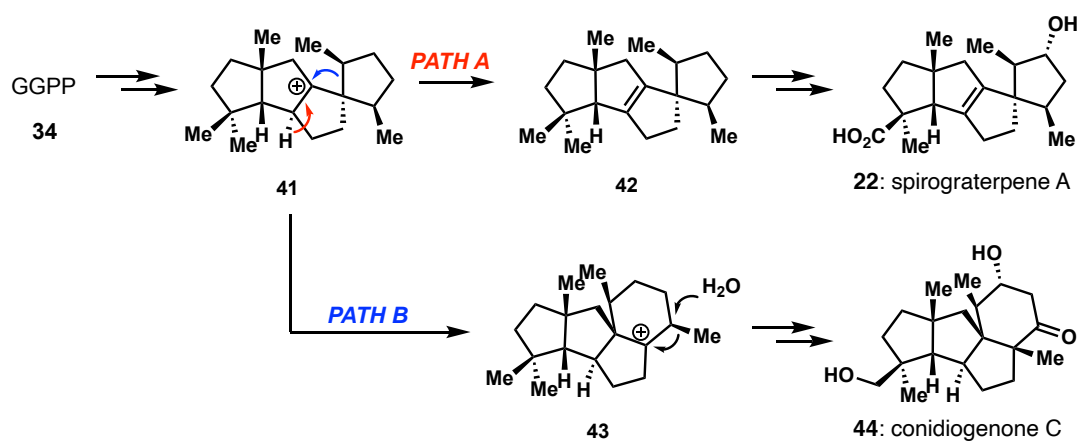
Spiroviolene (**21**) was first isolated by Dickschat *et al.* in 2017 while studying novel bacterial diterpene cyclases.¹³ After expressing the terpene cyclase gene from *Streptomyces violens* NRRL ISP-5597, the resultant recombinant protein was fed several common

biosynthetic terpene precursors. While geranyl diphosphate (GPP) and farnesyl diphosphate (FPP) showed no conversion, geranyl geranyl diphosphate (GGPP) was converted to diterpene **21**. Due to the interesting spirocyclic motif found within this product, the compound was named spiroviolene, and the corresponding cyclase named spiroviolene synthase (SvS). The structure of this compound was determined by 1D and 2D NMR spectroscopy, with HMBC correlations used to identify bond connections and NOE interactions used to assign relative stereochemistry where possible. In addition to characterizing this product, the Dickschat group proceeded to conduct a number of isotopic labelling and fragmentation studies in an effort to elucidate the biosynthetic pathway from GGPP to **21**. The proposed pathway is as follows; first, a 1,11-10,14 cyclization converts GGPP into macrocycle **35**, two 1,2-alkyl shifts then establish the cyclopentane ring containing the *gem*-dimethyl group and a subsequent cyclization forms requisite diquinane **36**.¹⁶ From here, a second cyclization constructs the fused 7/4 ring system **37**, which can undergo a dyotropic rearrangement, followed by a ring contraction to form spirocycle **39**.¹⁷ A subsequent facially selective 1,3-hydride shift to the tertiary carbocation in **39** then forms the last stereocenter, and a simple elimination to form the trisubstituted olefin produces **21**.¹⁸



Scheme 2.4. Proposed biosynthesis of **21** from GGPP (**34**).

Not long after **21** was isolated and characterized, a report from Yang and co-workers presented the isolation and characterization of a novel diterpene **22**, alongside two previously known members of the conidiogenone family, conidiogenone C and conidiogenone I.¹⁴ From the large-scale fermentation of *Penicillium granulatum* MCCC 3A00475 they were able to obtain 10.5 mg of **22**. Once again, the interesting spirocyclic motif led to this compound being named spirograterpene A. And similar to the previous isolate **21**, the structure was deduced primarily by NMR spectroscopy. However, in this case, Mosher ester analysis was used to assign the absolute stereochemistry. Taking note of the proposed biosynthetic pathway of **21**

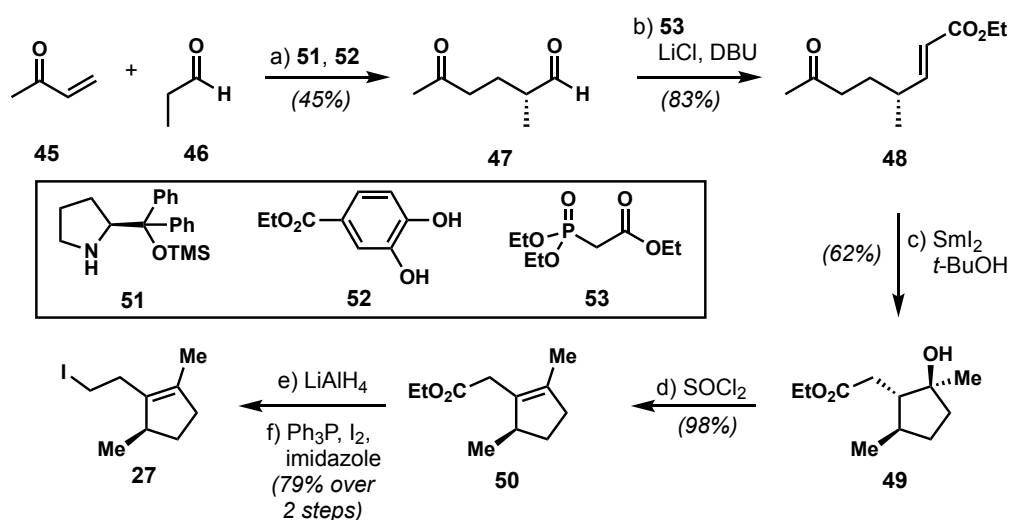


Scheme 2.5. Proposed biosynthesis of **22** and **44** from GGPP.

as presented by Dickschat, the Yang group posited that GGPP was similarly the necessary biosynthetic precursor leading to an almost identical intermediate **41**. However, Yang believed that the stereochemistry about C-3 was opposite to that proposed for **21**. Such a stereochemical disposition was certainly supported by the fact that **22** was isolated alongside **44** and so, assuming a unified biogenesis for these two products, it would only be expected that the stereochemistry about the analogous methyl group in **44** was identical to that proposed in **22**. From here, intermediate **41** could either undergo an elimination to introduce the tetrasubstituted olefin of **42** (**PATH A**), or a ring expansion of the spirocycle to produce hydrindane **43** (**PATH B**). After a series of oxidative manipulations, **42** and **43** could then lead to **22** and **44** respectively.

2.4 Total Synthesis of Spiroviolene

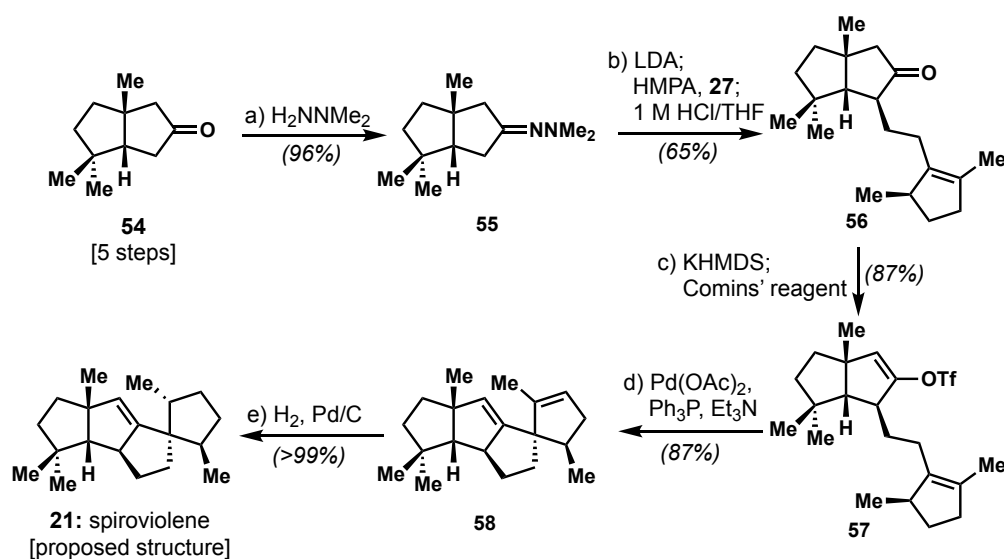
With a route to **26** already developed from our group's previous synthesis of the conidiogenones, the first task was the construction of the appropriate side chain (design and preparation of **27** was first conducted by Dr. Hyung Min Chi). The proposed alkyl iodide **27** was viewed as accessible from the corresponding β,γ -unsaturated ester, itself accessed from the tertiary alcohol via a simple elimination reaction. Quite pleasingly, the desired compound **49** not only had a previous synthetic route but was also prepared in an asymmetric fashion by Piva and co-workers.¹⁹ And so, starting from methyl vinyl ketone (**45**) and propionaldehyde (**46**), the asymmetric Michael addition proceeded as described in the literature, utilizing the Jørgensen-Hayashi catalyst **51** and catechol **52** to afford keto-aldehyde **47**. Utilizing the identical Horner-Wadsworth-Emmons reaction conditions and a subsequent SmI_2 mediated ketyl radical cyclization, we were able to access tertiary alcohol **49**. From this point an elimination promoted by SOCl_2 at elevated temperature provided enoate **50** in near quantitative yield. Interestingly, not only did these conditions provide the tetra-substituted olefin as expected, but there was no observation of olefin migration to the corresponding α,β -



Scheme 2.6. Asymmetric preparation of sidechain **27**: (a) **51** (5 mol%), **52** (20 mol%), neat, 0 °C, 24 h, 45%; (b) **53** (1.2 equiv.), LiCl (1.2 equiv.), DBU (1.0 equiv.), MeCN, 23 °C, 6 h, 83%; (c) SmI_2 (4 equiv.), *t*-BuOH (4 equiv.), THF, 25 °C, 6 h, 62%; (d) pyridine (1.2 equiv.), CH_2Cl_2 , then SOCl_2 (1.1 equiv.), 0 °C to 40 °C, 12 h, 98%; (e) LiAlH_4 (2.0 equiv.), Et_2O , 0 °C, then **50**, Et_2O , 0 °C to 23 °C, 30 min; (f) Ph_3P (1.2 equiv.), imidazole (1.5 equiv.), CH_2Cl_2 , 23 °C, 5 min, then I_2 (1.2 equiv.), 0 °C to 23 °C, 1 h, 79% over 2 steps.

unsaturated ester. Reduction of **50** to the homoallylic alcohol with LiAlH_4 and subsequent Appel reaction afforded the desired homoallylic iodide **27**.

With the side chain in hand, efforts were refocused to the target at hand (total synthesis of **21** was conducted by Dr. Hyung Min Chi, Scheme 2.7). At this stage, conditions for the alkylation of bicyclic ketone **54** were probed. The alkylation via the hydrazone (**55**), similar to that developed for our group's synthesis of conidiogenone B, proved to be most ideal, providing the regio- and diastereoselective alkylation product **56** in 65% yield after hydrolysis.²⁰ Formation of vinyl triflate **57**, via deprotonation with KHMDS and treatment with Comins' reagent gave rise to the key Heck cyclization precursor.



Scheme 2.7. Total synthesis of spiroviolene (**21**) starting from known intermediate **54**: (a) H_2NNMe_2 (5.0 equiv.), 23 °C, 12 h, 96%; (b) LDA (1.3 equiv.), THF, -78 °C, 15 min, then **55**, THF, 0 °C, 2 h, then HMPA (1.3 equiv.), -78 °C, 10 min, then **27** (1.2 equiv.), THF, -78 °C to 23 °C, 15 h, then 1 M HCl/THF (1 : 1), 23 °C, 12 h, 65%; (c) KHMDS (1.3 equiv.), THF, -78 °C to 0 °C, 2 h, then Comins' reagent (1.1 equiv.), THF, -78 °C, 1 h, 87%; (g) $\text{Pd}(\text{OAc})_2$ (10 mol%), Ph_3P (20 mol%), toluene, 23 °C, then Et_3N (2.0 equiv.), 90 °C, 20 h, 88%; (h) H_2 (balloon pressure), Pd/C (10 wt%), EtOH, 23 °C, 30 min, >99%.

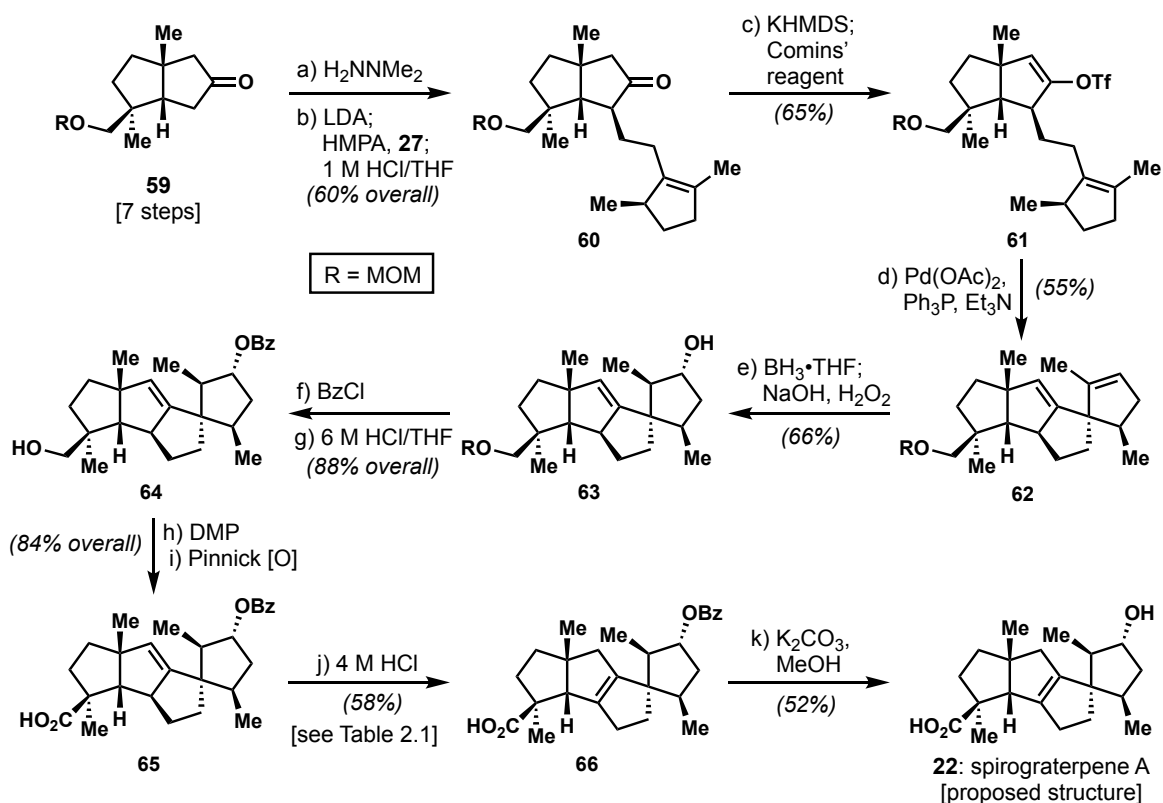
Using standard Heck cyclization conditions, spirocycle **58** was accessed in high yield as the desired *trans*-1,3-diastereomer.¹⁰ From here, selective olefin reduction is all that remained to complete the target. Chemoselectivity was not as much of a concern, simply due to the steric hindrance about the internal olefin likely preventing any reactivity. The larger concern was the facial selectivity when reducing the desired olefin. Based on simple models it appeared as

though hydrogenation would afford the undesired diastereomer, and as a result initial efforts focused on the use of hydrogen-atom-transfer processes, whereby an invertible radical, generated upon reduction of the alkene, might grant access to the desired diastereomer.²¹ Unfortunately, such conditions never provided any desired product and so the reaction was conducted under standard hydrogenation conditions. Surprisingly, these conditions yielded a single product, near quantitatively, whose spectral data and optical rotation fully matched that of the isolation team. This result then piqued our interest into the true identity of the chiral center in question. However, despite several attempts we were never able to grow crystals of suitable quality for X-ray crystallographic analysis. As such our attention turned instead to the goal of synthesizing the structural homologue spirograterpene A (**22**).

2.5 Total Synthesis of Spirograterpene A

As indicated in the retrosynthetic analysis of **21** and **22**, it was clear that a similar sequence of transformations would lead us to both targets, simply requiring additional oxidative manipulations in the case of **22**. The first goal was accessing the requisite spirocycle **62**. Through a similar alkylation of the dimethyl hydrazone of **59** with alkyl iodide **27** and subsequent hydrolysis, we could obtain bicyclic ketone **60** in 60% yield. Regioselective formation of vinyl triflate **61**, followed by the Heck cyclization under identical conditions afforded, once again, the desired spirocycle with the requisite *trans*-1,3-stereochemistry.¹⁰ At this stage, a facially selective hydroboration/oxidation sequence was performed to provide the desired secondary alcohol as a single diastereomer, setting two more key chiral centers.

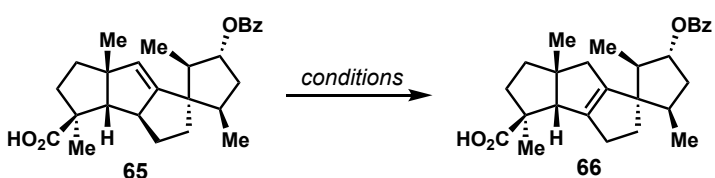
From this point, all that remained was olefin migration and a few oxidation state manipulations. Initially, we sought to perform a selective oxidation of the neopentyl alcohol to the corresponding carboxylic acid in the presence of the secondary alcohol using various oxoammonium salts in the presence of different additives, but unfortunately such trials were



Scheme 2.8. Total synthesis of spirograterpene A (**22**) starting from known intermediate **59**: (a) H_2NNMe_2 (3.0 equiv.), 23 °C, 12 h, 96%; (b) LDA (1.5 equiv.), THF, -78 °C, 15 min, then **59**, THF, 0 °C, 2 h, then HMPA (1.5 equiv.), -78 °C, 30 min, then **27** (1.2 equiv.), THF, -78 °C to 23 °C, 15 h, then 1 M HCl, 23 °C, 12 h, 63%; (c) KHMDS (1.3 equiv.), THF, -78 °C to 0 °C, 2 h, then Comins' reagent (1.1 equiv.), THF, -78 °C, 1 h, 65%; (d) $\text{Pd}(\text{OAc})_2$ (20 mol%), Ph_3P (40 mol%), Et_3N (3.0 equiv.), toluene, 23 °C, then **61**, toluene, 23 °C to 90 °C, 16 h, 55%; (e) $\text{BH}_3\cdot\text{THF}$ (1.0 equiv.), THF, 0 °C, 5 h, then $\text{NaOH}/\text{H}_2\text{O}_2$ (1 : 1), 23 °C, 1 h, 66%; (f) BzCl (3.0 equiv.), Et_3N (4.0 equiv.), 4-DMAP (1.0 equiv.), CH_2Cl_2 , 23 °C, 2 h, 96%; (g) 6 M HCl/THF (1 : 2), 50 °C, 4 h, 92%; (h) Dess–Martin periodinane (1.5 equiv.), NaHCO_3 (5.0 equiv.), CH_2Cl_2 , 23 °C, 1 h, 85%; (i) 2-methyl-2-butene (10 equiv.), *t*-BuOH, then NaClO_2 (35 equiv.), NaH_2PO_4 (50 equiv.), H_2O , 23 °C, 1 h, 96%; (j) HCl (4 M in 1,4-dioxane), 80 °C, 48 h, 58%; (k) K_2CO_3 (3.0 equiv.), MeOH, 55 °C, 15 h, 52%.

unsuccessful.²² In addition, efforts to effect olefin migration with an unprotected secondary alcohol proved challenging, often resulting in decomposition of the starting material. As such, we chose instead to first protect the secondary alcohol as the corresponding benzoate and deprotect the MOM group with 6M HCl/THF to afford **64**. Oxidation of the primary alcohol to the corresponding carboxylic acid **65** then set the stage to investigate appropriate conditions for olefin isomerization. As shown in Table 2.1, even with this arguably more stable material, the olefin migration remained a formidable challenge. In fact, despite attempting several different reaction formats (i.e. transition metal, photochemical and organic acid-mediated conditions) the starting material was only ever recovered unchanged.²³ Only when subjected to 4M HCl in 1,4-dioxane at 55 °C did we see even partial conversion to the desired

tetrasubstituted olefin. By increasing both the temperature (80 °C) and the reaction time (72 h) we observed complete conversion to the desired product. Of particular note here, it was necessary to use strictly anhydrous HCl in dioxane, as the presence of even trace water caused partial hydrolysis of the benzoate, resulting in measurable amounts of benzoic acid that proved challenging to remove. Finally, methanolysis of the benzoate under standard conditions produced the desired target (**22**), which matched the spectral data provided by Yang and co-workers.



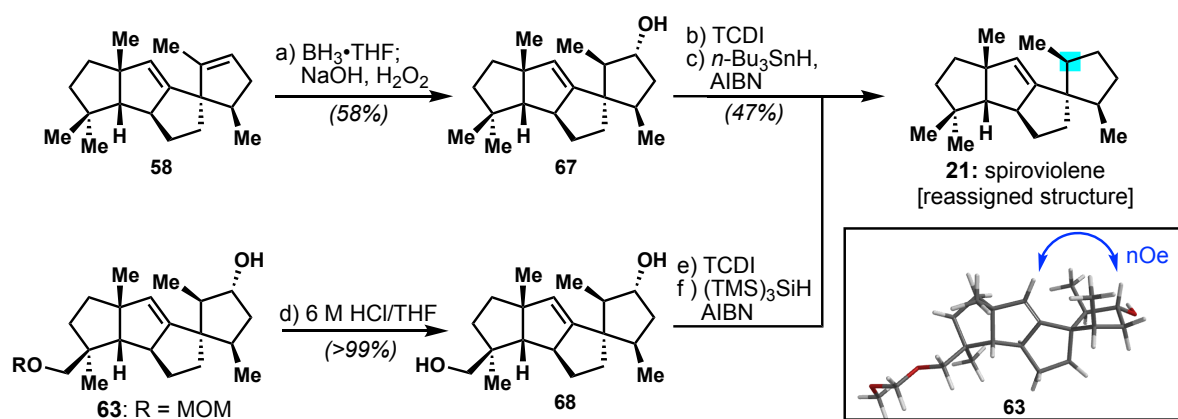
Entry	Conditions	Result
1	[Pd(CH ₃ CN) ₄](BF ₄) ₂ , CH ₃ CN, 23 °C, 12 h	no reaction
2	[Pd(CH ₃ CN) ₄](BF ₄) ₂ , CH ₃ CN, 80 °C, 12 h	no reaction
3	UV (<365 nm), Et ₂ O, 23 °C, 1 h	no reaction
4	UV (<365 nm), Et ₂ O, 23 °C, 12 h	decomposition
5	<i>p</i> -TsOH, toluene, 100 °C, 12 h	no reaction
6	<i>p</i> -TsOH, 1,4-dioxane, 100 °C, 12 h	no reaction
7	TfOH, 1,4-dioxane, 100 °C, 12 h	no reaction
8	HCl (4 M in 1,4-dioxane), 23 °C, 12 h	no reaction
9	HCl (4 M in 1,4-dioxane), 55 °C, 12 h	< 15% conversion
10	HCl (4 M in 1,4-dioxane), 80 °C, 72 h	full conversion (58% yield)

Table 2.1. Conditions screened to effect olefin isomerization to **66**.

Central to both of these routes was the fact the chirality at C-3 was set by a completely facially selective olefin functionalization. This led us to believe that the stereochemistry should be consistent in these two targets and therefore, that one of them had been misassigned. Unfortunately, despite the use of several different crystallization techniques with a number of solvent combinations and a variety of intermediates, and derivatives thereof, we were never able to obtain a crystal of suitable quality for X-ray analysis to definitively confirm the proposed misassignment.

2.6 Evidence for the Structural Reassignment of 21

Without crystallographic evidence to confirm the proposed structural reassignment we instead turned to experimental, spectral and computational data. Initially, we sought to prove that the stereochemistry about C-3 is conserved between these structures. To ensure that there was no unexpected difference in the facial selectivity between hydroboration and hydrogenation, we employed a series of transformations more similar to that of spirograterpene A in order to prepare spiroviolene. To this end, intermediate **58** was subjected to an identical hydroboration/oxidation sequence to afford secondary alcohol **67**. Following treatment with TCDI to introduce the necessary thiocarbamate moiety, subsection of the substrate to typical Barton-McCombie deoxygenation conditions afforded a compound with identical spectral properties to that of **21**. In a similar manner, MOM-ether **63** was deprotected to give diol **68**, after which a double Barton-McCombie deoxygenation once again provided material with ¹H and ¹³C NMR data identical to **21**.²⁴ These important results demonstrate that the C-3 stereochemistry must be consistent between the two targets. This then begs the question, what is that stereochemistry?



Scheme 2.9. Synthetic and NMR support for the structural reassignment of spiroviolene (**21**): (a) $\text{BH}_3 \cdot \text{THF}$ (1.0 equiv.), THF, 0 °C, 5 h, then $\text{NaOH}/\text{H}_2\text{O}_2$ (1:1), 23 °C, 1 h, 58%; (b) TCDI (3.0 equiv.), 4-DMAP (0.5 equiv.), $\text{CH}_2\text{Cl}_2/\text{pyridine}$ (1:1), 23 °C, 12 h; (c) $n\text{-Bu}_3\text{SnH}$ (2.0 equiv.), AIBN (0.15 equiv.), toluene, 110 °C, 10 min, 47%; (d) 6 M HCl/THF (1:2), 50 °C, 4 h, >99%; (e) TCDI (4.0 equiv.), 4-DMAP (0.5 equiv.), $\text{CH}_2\text{Cl}_2/\text{pyridine}$ (1:1), 23 °C, 12 h; (f) $(\text{TMS})_3\text{SiH}$ (4.0 equiv.), AIBN (0.2 equiv.), toluene, 110 °C, 30 min.

This was answered in part through computational analysis. Seeing that the key chemical transformations which set the stereogenic centers of interest were both facially selective, we

decided to investigate this transformation using DFT transition state analysis (work performed by Cooper Taylor). For the purposes of this analysis, we used a simplified version of **62** as shown in Figure 2.2 and studied the hydroboration of this substrate. As can be seen, there is an ~ 8.2 kcal mol⁻¹ difference favoring approach from the α -face of the substrate. This difference in energy can even be observed in the facial approach of borane, where the β -face approach itself is 9.14 kcal mol⁻¹ higher in energy. This data therefore supports the stereochemistry presented in the proposed structure of spirograterpene A (**22**).

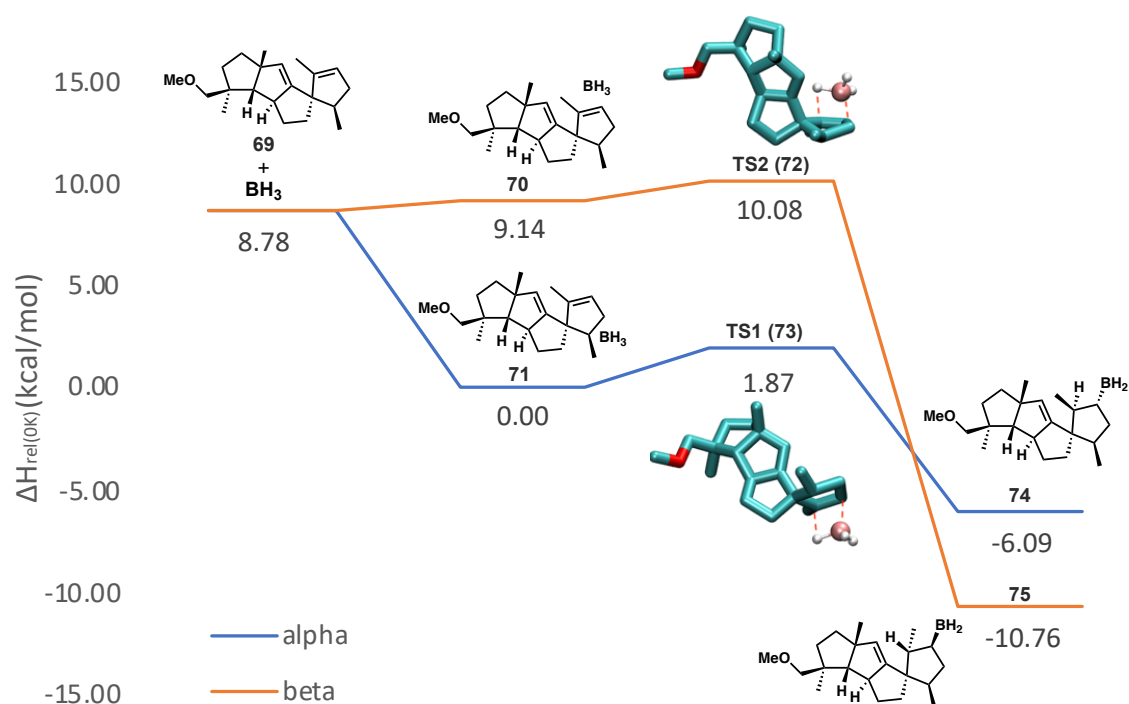


Figure 2.2. Potential Energy Surface for both α - and β -face hydroboration of simplified substrate **69**, indicating a kinetic preference via TS1. Calculated at the B3LYP/aug-cc-pvDZ level of theory in the gas phase, values are relative, zero-point energy corrected total energies [$\Delta H_{rel}(0K)$ (kcal/mol)].

Finally, a look at NMR data, our own and that of both isolation teams, provided further evidence. As shown in Scheme 2.9, we observed a key NOE interaction in **63** between the vinylic proton and the proton geminal to the hydroxyl group, an interaction that could only be observed had the hydroboration exhibited the predicted facial selectivity. This result was further supported by Mosher ester analysis as conducted by the spirograterpene A isolation team, which indicated that the absolute stereochemistry about the carbinol carbon is as drawn

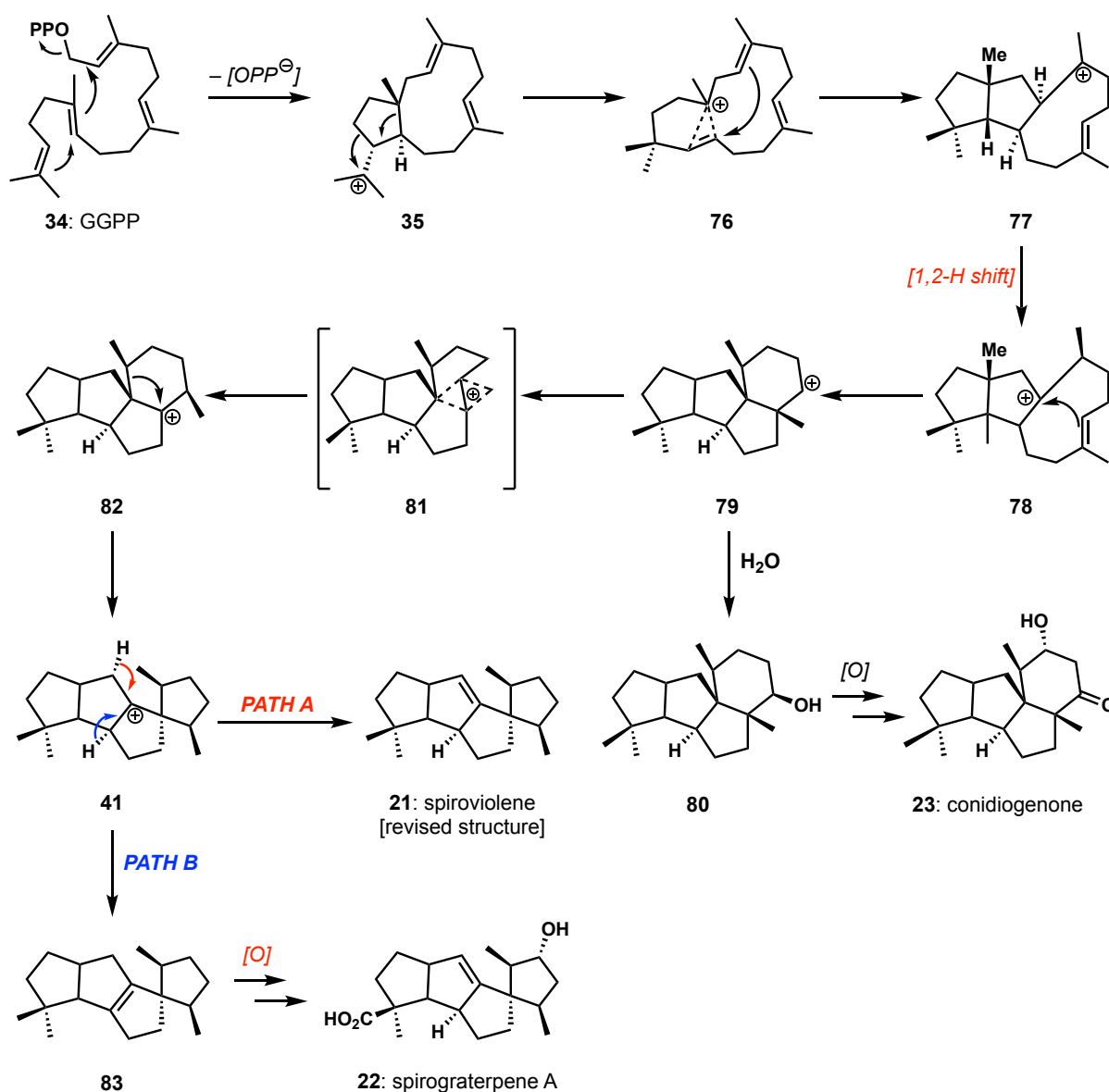
in **22**. Separate consideration of the spectral data provided by the Dickschat group also provided notable NOE interactions (see Scheme 2.2a for positional numbering). In particular, C-20 exhibits NOE interactions with both H-10 and H-8 α , which would appear to support either of the proposed structures. More importantly however, is an observed correlation, although quite weak, between the vinylic proton (H-1) and methyl group (C-20), suggesting that the chirality of this center should be revised to match that of spirograterpene A.

With all of the information described above, even in the absence of X-ray crystallographic data, we believe that the structure of **21** should be reassigned, wherein the stereochemistry about C-3 would now match that of **22**. Noteworthy is that the stereochemistry about this position was integral to the originally proposed biosynthetic pathway, indicating that this proposal may also require revision. And while a unified pathway between **21**, **22** and the conidiogenones would in fact seem likely, it is not necessary given that **21** and **22** are isolated from bacteria and fungi, respectively.

2.7 Revised Biosynthesis of Spiroviolene

With the compiled evidence in hand, we reached out to the original isolation team of **21** to share our proposed structural reassignment. It is worth noting that this seemingly inconsequential change has significant implications on the originally proposed biosynthetic pathway. As discussed previously, the stereochemistry about C-3 was believed to arise from a facially selective 1,3-hydride shift (**39**→**40**, Scheme 2.4) that can account for the originally proposed structure but not the reassigned one.¹³ Taking the provided data into account, Dickschat and co-workers proceeded to conduct a series of labelling and fragmentation studies resulting in a revised biosynthetic pathway, which offers a unified path between the bacterial SvS and the fungal cyclopiane-type diterpene synthase.²⁵

In this proposed pathway, a 1,11–10,14 cyclization of GGPP provides **35** (similar to the originally proposed pathway), then, following ring expansion of the cyclopentane in **35**, they propose a “highly asynchronous ring-opening/ring closing process that accomplishes the same net result as a 1,2-alkyl shift”, the mechanism of which was first proposed by Tantillo *et al.* in their computational study of the biosynthesis of variediene (Scheme 2.10).²⁶ A subsequent cyclization and 1,2-hydride shift provides **78**, thereby setting the stereochemistry of the center in question. Following a third cyclization, the secondary carbocation in structure **79** can then



Scheme 2.10. Revised biosynthesis for the formation of **21** that also provides reasonable access to **22** and **23**.

be trapped by water and after further oxidative manipulations provide access to the conidiogenones.²⁷ Alternatively, a 1,2-methyl migration via a non-classical carbocation and subsequent ring contraction to form the spirocenter, provides an intermediate which can serve as a precursor to both **21** and **83** via alternate deprotonation events, with **83** being converted to **22** following a series of oxidations.

2.8 Conclusion

Hence, we have successfully achieved the first total syntheses of **21** and **22** in 10 and 18 steps respectively, further advancing the idea of quaternary center-guided synthesis, particularly as it relates to non-functionalized terpenes. In addition, we were able to provide compelling experimental, spectral and computational evidence for the structural reassignment of **21** at C-3. This data has separately led the isolation team to propose a new and unified route which, starting from GGPP, would provide access to both **21** and **22**, as well as several members of the conidiogenone family of natural products.

2.9 References

1. For selected reviews, see: (a) Christoffers, J.; Baro, A. *Quaternary stereocenters: Challenges and Solutions for Organic Synthesis*. Wiley-VCH: 2005; (b) Mehta, G.; Srikrishna, A. *Chem. Rev.* **1997**, *97*, 671; (c) Quasdorf, K. W.; Overman, L. E. *Nature* **2014**, *516*, 181; (d) Bueschleb, M.; Dorich, S.; Hanessian, S.; Tao, D.; Schenthal, K. B.; Overman, L. E. *Angew. Chem. Int. Ed.* **2016**, *55*, 4156.
2. Desimoni, G.; Faita, G.; Jørgensen, K. A. *Chem. Rev.* **2006**, *106*, 3561.
3. Xie, J.-H.; Zhou, Q.-L. *Acc. Chem. Res.* **2008**, *41*, 581.
4. (a) Jung, M. E.; Piizzi, G. *Chem. Rev.* **2005**, *105*, 1735; (b) Levine, M. N.; Raines, R. T. *Chem. Sci.* **2012**, *3*, 2412; (c) Talele, T. T. *J. Med. Chem.* **2017**, *61*, 2166; (d) Okoh, O. A.; Klahn, P. *ChemBioChem* **2018**, *19*, 1668.
5. Hu, P.; Chi, H. M.; DeBacker, K. C.; Gong, X.; Keim, J. H.; Hsu, I. T.; Snyder, S. A. *Nature* **2019**, *569*, 703.
6. For examples of of quaternary center guided synthesis from our own group, see: (a) Snyder, S. A.; Wespe, D. A.; von Hof, J. M. *J. Am. Chem. Soc.* **2011**, *133*, 8850; (b) Hu, P.; Snyder, S. A. *J. Am. Chem. Soc.* **2017**, *139*, 5007; (c) Peng, C.; Arya, P.; Zhou, Z.; Snyder, S. A. *Angew. Chem. Int. Ed.* **2020**, *59*, 13521. For an example of reaction development see: (d) Yi, H.; Hu, P.; Snyder, S. A. *Angew. Chem. Int. Ed.* **2020**, *59*, 2674.
7. For selected examples, see: (a) Mendoza, A.; Ishihara, Y.; Baran, P. S. *Nat. Chem.* **2012**, *4*, 21; (b) Pronin, S. V.; Shenvi, R. A. *Nat. Chem.* **2012**, *4*, 915; (c) Hong, A. Y.; Stoltz, B. M. *Angew. Chem. Int. Ed.* **2012**, *51*, 9674; (d) Zhang, Q.; Tiefenbacher, K. *Nat. Chem.* **2015**, *7*, 197; (e) Zhang, Q.; Rinkel, J.; Goldfuss, B.; Dickschat, J. S.; Tiefenbacher, K. *Nat. Catal.* **2018**, *1*, 609; (f) Syntrivanis, L.-D.; Némethová, I.; Schmid, D.; Levi, S.; Prescimone, A.; Bissegger, F.; Major, D. T.; Tiefenbacher, K. *J. Am. Chem. Soc.* **2020**, *142*, 5894.
8. (a) Brown, M. K.; Hoveyda, A. H. *J. Am. Chem. Soc.* **2008**, *130*, 12904; (b) May, T. L.; Brown, M. K.; Hoveyda, A. H. *Angew. Chem. Int. Ed.* **2008**, *47*, 7358.
9. Lo, J. C.; Yabe, Y.; Baran, P. S. *J. Am. Chem. Soc.* **2014**, *136*, 1304.
10. (a) Overman, L. E.; Abelman, M. M.; Kucera, D. J.; Tran, V. D.; Ricca, D. J. *Pure Appl. Chem.* **1992**, *64*, 1813; (b) Grigg, R.; Sansano, J.; Santhakumar, V.; Sridharan, V.; Thangavelanthum, R.; Thornton-Pett, M.; Wilson, D. *Tetrahedron* **1997**, *53*, 11803; (c) Grigg, R.; Sridharan, V. *J. Organomet. Chem.* **1999**, *576*, 65.
11. Tian, Q.; Zhang, G. *Synthesis* **2016**, *48*, 4038.
12. Hou, S. H.; Tu, Y. Q.; Wang, S. H.; Xi, C. C.; Zhang, F. M.; Wang, S. H.; Li, Y. T.; Liu, L. *Angew. Chem. Int. Ed.* **2016**, *55*, 4456.

13. Rabe, P.; Rinkel, J.; Dolja, E.; Schmitz, T.; Nubbemeyer, B.; Luu, T. H.; Dickschat, J. S. *Angew. Chem. Int. Ed.* **2017**, *56*, 2776.
14. Niu, S.; Fan, Z.-W.; Xie, C.-L.; Liu, Q.; Luo, Z.-H.; Liu, G.; Yang, X.-W. *J. Nat. Prod.* **2017**, *80*, 2174.
15. Sun, C.-L.; Li, B.-J.; Shi, Z.-J. *Chem. Rev.* **2011**, *111*, 1293.
16. (a) Cane, D. E.; Oliver, J. S.; Harrison, P. H.; Abell, C.; Hubbard, B. R.; Kane, C. T.; Lattman, R. *J. Am. Chem. Soc.* **1990**, *112*, 4513; (b) Wang, C.-M.; Hopson, R.; Lin, X.; Cane, D. E. *J. Am. Chem. Soc.* **2009**, *131*, 8360.
17. Gutta, P.; Tantillo, D. J. *J. Am. Chem. Soc.* **2006**, *128*, 6172.
18. For reviews on the biosynthesis of similar terpene frameworks, see: (a) Dickschat, J. S. *Nat. Prod. Rep.* **2016**, *33*, 87; (b) Rabe, P.; Rinkel, J.; Klapschinski, T. A.; Barra, L.; Dickschat, J. S. *Org. Biomol. Chem.* **2016**, *14*, 158; (c) Rinkel, J.; Rabe, P.; Garbeva, P.; Dickschat, J. S. *Angew. Chem. Int. Ed.* **2016**, *55*, 13593; (d) Dickschat, J. S. *Angew. Chem. Int. Ed.* **2019**, *58*, 15964-15976.
19. Feuillastre, S.; Pelotier, B.; Piva, O. *Eur. J. Org. Chem.* **2014**, *2014*, 1753.
20. Corey, E.; Enders, D. *Tetrahedron Lett.* **1976**, *17*, 3.
21. (a) Iwasaki, K.; Wan, K. K.; Oppedisano, A.; Crossley, S. W.; Shenvi, R. A. *J. Am. Chem. Soc.* **2014**, *136*, 1300. For a review of metal-mediated HAT processes in synthesis see: (b) Crossley, S. W.; Obradors, C.; Martinez, R. M.; Shenvi, R. A. *Chem. Rev.* **2016**, *116*, 8912; (c) Bosch, C.; Fiser, B.; Gómez-Bengoa, E.; Bradshaw, B.; Bonjoch, J. *Org. Lett.* **2015**, *17*, 5084; (d) Ruider, S. A.; Sandmeier, T.; Carreira, E. M. *Angew. Chem. Int. Ed.* **2015**, *54*, 2378; (e) Lu, H.-H.; Pronin, S. V.; Antonova-Koch, Y.; Meister, S.; Winzeler, E. A.; Shenvi, R. A. *J. Am. Chem. Soc.* **2016**, *138*, 7268.
22. For some of the procedures attempted to selectively oxidize the primary alcohol, see: (a) Lucio Anelli, P.; Biffi, C.; Montanari, F.; Quici, S. *J. Org. Chem.* **1987**, *52*, 2559; (b) Epp, J. B.; Widlanski, T. S. *J. Org. Chem.* **1999**, *64*, 293; (c) Zhao, M.; Li, J.; Mano, E.; Song, Z.; Tschaen, D. M.; Grabowski, E. J.; Reider, P. J. *J. Org. Chem.* **1999**, *64*, 2564; (d) Zhao, M. M.; Li, J.; Mano, E.; Song, Z. J.; Tschaen, D. M. *Org. Synth.* **2003**, *81*, 195; (e) Shibuya, M.; Sato, T.; Tomizawa, M.; Iwabuchi, Y. *Chem. Commun.* **2009**, 1739.
23. For examples of metal mediated olefin isomerization, see: (a) Grieco, P. A.; Nishizawa, M.; Marinovic, N.; Ehmann, W. J. *J. Am. Chem. Soc.* **1976**, *98*, 7102; (b) Andrieux, J.; Barton, D. H.; Patin, H. *J. Chem. Soc., Perkin Trans. 1* **1977**, 359; (c) Paquette, L. A.; Fristad, W. E.; Dime, D. S.; Bailey, T. R. *J. Org. Chem.* **1980**, *45*, 3017; (d) Sen, A.; Lai, T. W. *Inorg. Chem.* **1984**, *23*, 3257; (e) Sen, A.; Lai, T.-W.; Thomas, R. R. *J. Organomet. Chem.* **1988**, *358*, 567.
24. For the original report, see: (a) Barton, D. H.; McCombie, S. W. *J. Chem. Soc., Perkin Trans. 1* **1975**, 1574. For an example of application in synthesis see: (b) Liu, W.-C.; Liao, C.-C. *Chem. Commun.* **1999**, 117.

25. Xu, H.; Dickschat, J. S. *ChemBioChem* **2021**, *22*, 850.
26. Hong, Y. J.; Tantillo, D. J. *Aust. J. Chem.* **2017**, *70*, 362.
27. (a) Roncal, T.; Cordobés, S.; Ugalde, U.; He, Y.; Sterner, O. *Tetrahedron Lett.* **2002**, *43*, 6799; (b) Mitsuhashi, T.; Kikuchi, T.; Hoshino, S.; Ozeki, M.; Awakawa, T.; Shi, S.-P.; Fujita, M.; Abe, I. *Org. Lett.* **2018**, *20*, 5606.

2.10 Experimental Section

General Procedures. All reactions were carried out under an argon atmosphere with dry solvents under anhydrous conditions, unless otherwise noted. Dry tetrahydrofuran (THF), toluene, diethyl ether (Et₂O), dichloromethane (CH₂Cl₂), and acetonitrile (CH₃CN) were obtained by passing commercially available pre-dried, oxygen-free formulations through activated alumina columns. Yields refer to chromatographically and spectroscopically (¹H and ¹³C NMR) homogeneous materials, unless otherwise stated. Reagents were purchased at the highest commercial quality and used without further purification, unless otherwise stated. Reactions were magnetically stirred and monitored by thin-layer chromatography (TLC) carried out on 0.25 mm E. Merck silica gel plates (60F-254) using UV light as visualizing agent, and an ethanolic solution of phosphomolybdic acid and cerium sulfate or a solution of KMnO₄ in aq. NaHCO₃ and heat as developing agents. SiliCycle silica gel (60, academic grade, particle size 0.040–0.063 mm) was used for flash column chromatography. Preparative thin-layer chromatography separations were carried out on 0.50 mm E. Merck silica gel plates (60F-254). NMR spectra were recorded on Bruker 400 and 500 MHz instruments and calibrated using residual undeuterated solvent as an internal reference. The following abbreviations were used to explain the multiplicities: s = singlet, d = doublet, t = triplet, q = quartet, br = broad, app = apparent. IR spectra were recorded on a Perkin-Elmer 1000 series FT-IR spectrometer. High-resolution mass spectra (HRMS) were recorded on Agilent 6244 ToF-MS using ESI (Electrospray Ionization) at the University of Chicago Mass Spectroscopy Core Facility. All *ee* values were determined by HPLC on Daicel Chiralcel or Chiralpak columns.

Alkyl Iodide 27. To a flame-dried, 250 mL flask was added **49**¹⁹ (1.67 g, 8.35 mmol, 1.0 equiv.), pyridine (0.805 mL, 10.0 mmol, 1.2 equiv.) and CH₂Cl₂ (40 mL). A reflux condenser was attached and the system was purged with Ar. The reaction mixture was cooled to 0 °C and

SOCl₂ (0.670 mL, 9.19 mmol, 1.1 equiv.) was added dropwise. The contents of the flask were then immersed into a preheated oil bath at 40 °C and heated at that temperature for 12 h. Upon completion, the mixture was poured over crushed ice and further diluted with CH₂Cl₂ (20 mL). The layers were separated and the aqueous layer was extracted with CH₂Cl₂ (3 × 20 mL). The organic layers were combined, dried (Na₂SO₄) and concentrated *in vacuo* at 5 °C, to give a brown oil. This crude product was further purified by flash column chromatography (silica gel, pentanes/Et₂O, 9/1) to give the desired volatile alkene **50** (1.50 g, 98% yield) as a pale brown oil. Pressing forward without any additional purification, to a flame-dried 250 mL flask was added LiAlH₄ (0.63 g, 16.7 mmol, 2.0 equiv.) and Et₂O (60 mL) and the suspension was cooled to 0 °C. A solution of **50** (1.50 g, 8.23 mmol, 1.0 equiv.) in Et₂O (20 mL) was then added dropwise. The reaction contents were then warmed to 23 °C and stirred for 30 min. Upon completion, the reaction was quenched by the careful addition of H₂O (0.5 mL), followed by NaOH (1.0 mL, 2 N aqueous) and H₂O (1.5 mL). The resultant slurry was stirred for 30 min at 23 °C after which it was filtered through Celite, washing the pad with Et₂O (3 × 50 mL). The filtrate was then concentrated *in vacuo* at 5 °C and the crude alcohol (1.36 g) was taken to the next step without any further purification. Next, to a flame-dried 25 mL flask was added Ph₃P (0.472 g, 1.80 mmol, 1.2 equiv.), imidazole (0.153 g, 2.25 mmol, 1.5 equiv.), a portion of the crude alcohol (0.210 g, 1.50 mmol, 1.0 equiv.) and CH₂Cl₂ (3 mL). This mixture was stirred for 5 min at 23 °C and then cooled to 0 °C at which time I₂ (0.457 g, 1.80 mmol, 1.2 equiv.) was added slowly, portion-wise. The mixture was then warmed to 23 °C and stirred for 1 h. Upon completion, the reaction was quenched by the addition of pentanes (5 mL) and stirred at 23 °C for 1 h. The contents of the flask were then filtered through a plug of silica gel eluting using pentanes and the eluted material was concentrated *in vacuo* at 5 °C to give an orange oil. This crude material was further purified by flash column chromatography (silica gel, pentanes/Et₂O, 20/1) to give alkyl iodide **27** (0.298 g, 79% yield) as a colorless oil. **27**: *R*_f =

0.81 (silica gel, hexanes/EtOAc, 4/1); $[\alpha]_{\text{D}}^{20} = +2.4^{\circ}$ ($c = 1.0$, CHCl_3); IR (film) ν_{max} 2952, 2925, 2864, 2839, 1454, 1435, 1165, 742, 696 cm^{-1} ; ^1H NMR (500 MHz, CDCl_3) δ 3.19 (td, $J = 9.5, 5.0$ Hz, 1 H), 3.05 (td, $J = 9.4, 7.5$ Hz, 1 H), 2.68 (ddd, $J = 13.9, 9.6, 7.5$ Hz, 2 H), 2.62–2.53 (m, 1 H), 2.28–2.12 (m, 2 H), 2.08–2.00 (m, 1 H), 1.62 (dd, $J = 2.0, 1.1$ Hz, 3 H), 1.31 (ddt, $J = 12.7, 9.0, 6.4$ Hz, 1 H), 0.98 (d, $J = 6.9$ Hz, 3 H); ^{13}C NMR (126 MHz, CDCl_3) δ 138.25, 134.72, 41.14, 36.80, 31.34, 31.27, 19.71, 14.43, 4.56.

Bicyclic Ketone 56. To a flask containing **54**⁵ (0.166 g, 1.00 mmol, 1.0 equiv.) was added *N,N*-dimethyl hydrazine (0.380 mL, 5.00 mmol, 5.0 equiv.) and the resultant mixture stirred at 23 °C for 12 h. Upon completion the reaction was quenched with NH_4Cl (2 mL) and extracted with Et_2O (3×2 mL). The combined organic layers were then washed with H_2O (1 mL), brine (1 mL), dried (Na_2SO_4), and concentrated to give the desired hydrazone **55** (0.200 g, 96% yield) as a yellow oil. To a flame-dried 30-mL Schlenk flask was added solid LDA (0.070 g, 0.65 mmol, 1.3 equiv., used to exclude any incorporation of hexanes) in a glove box at 23 °C. The flask was capped with a septum and transferred from the glove box to a Schlenk manifold and place under positive pressure of N_2 . The flask was cooled to -78 °C and THF (2.5 mL) was added. Once all solids had dissolved, a solution of a portion of hydrazone **55** (0.104 g, 0.50 mmol, 1.0 equiv.) in THF (2.5 mL) was added dropwise over the course of 5 min, and the resulting pale yellow solution was stirred at 0 °C for 2 h. The reaction mixture was then recooled to -78 °C and HMPA (0.113 mL, 0.65 mmol, 1.3 equiv.) was added dropwise. After stirring for 10 min, a solution of alkyl iodide **27** (0.150 g, 0.60 mmol, 1.2 equiv.) in THF (0.6 mL) was added at -78 °C slowly over the course of 5 min. The yellow solution was stirred at -78 °C for 15 h, where temperature gradually warmed to room temperature. The reaction mixture was quenched with saturated aqueous NH_4Cl (5 mL) and extracted with Et_2O (3×5 mL). The combined organic layers were dried (Na_2SO_4), filtered, and concentrated to afford

the crude product as a pale yellow oil. The crude oil was then further purified by flash column chromatography (silica gel, hexanes/EtOAc, 4/1) to give the alkylated hydrazone (0.118 g, 71% yield) as a pale yellow oil. $R_f = 0.36$ (hexanes/EtOAc, 4/1). Pressing forward, to a 25-mL round bottomed flask was added the alkylated hydrazone (0.118 g, 0.36 mmol, 1.0 equiv.), THF (5 mL), and 1 M aqueous HCl (5 mL) at 23 °C. The reaction mixture was then vigorously stirred at 23 °C for 12 h. Upon completion, the resulting mixture was extracted with Et₂O (5 × 10 mL), and the combined organic layers were dried (Na₂SO₄), filtered, and concentrated to afford a yellow oil. The crude oil was purified by filtration through a short silica gel plug (hexanes/EtOAc, 4/1) to afford alkylated ketone **56** (0.094 g, 92% yield) as a pale yellow oil. **56**: $R_f = 0.69$ (silica gel, hexanes/EtOAc, 4/1); $[\alpha]_D^{20} = -2.3^\circ$ ($c = 1.0$, CHCl₃); IR (film) ν_{\max} 2950, 2864, 1738, 1457, 1410, 1385, 1376, 1367, 1351, 1333, 1261, 1169, 1092, 1018, 995, 805 cm⁻¹; ¹H NMR (500 MHz, CDCl₃) δ 2.68–2.59 (m, 1 H), 2.31 (d, $J = 18.1$ Hz, 1 H), 2.18–2.10 (m, 4 H), 2.03–1.90 (m, 2 H), 1.81–1.63 (m, 3 H), 1.61 (s, 3 H), 1.59–1.52 (m, 4 H), 1.33–1.20 (m, 2 H), 1.19 (s, 3 H), 1.08 (s, 3 H), 0.97 (d, $J = 6.9$ Hz, 3 H), 0.89 (s, 3 H); ¹³C NMR (125 MHz, CDCl₃) δ 138.98, 131.92, 63.96, 53.51, 50.64, 44.93, 42.31, 41.62, 41.36, 40.13, 36.73, 31.65, 31.42, 31.24, 30.56, 29.85, 24.86, 24.53, 19.78, 14.22. [Note: Despite efforts to obtain HRMS data no successful ionization was achieved with either ESI or CI].

Triflate 57. To a flame-dried 10 mL Schlenk flask was added a solution of ketone **56** (57.7 mg, 0.20 mmol, 1.0 equiv.) in THF (2 mL). The resulting yellow solution was cooled to –78 °C and a solution of KHMDS (0.260 mL, 1.0 M in THF, 0.26 mmol, 1.3 equiv.) was added. The reaction mixture was stirred at 0 °C for 2 h. Subsequently, the reaction mixture was cooled to –78 °C and a solution of Comins' reagent (86.4 mg, 0.22 mmol, 1.1 equiv.) in THF (0.37 mL) was added dropwise via syringe. After stirring for 1 h at –78 °C, the yellow solution was diluted with hexanes (5 mL). This mixture was subjected directly to purification by flash

column chromatography (silica gel, hexanes/Et₃N, 99/1) to give triflate **57** (73.2 mg, 87% yield) as a colorless oil. **57**: R_f = 0.86 (silica gel, hexanes/EtOAc, 4/1), 0.31 (silica gel, hexanes); [α]_D²⁰ = -8.6° (c = 1.0, CHCl₃); IR (film) ν_{max} 2952, 2864, 1655, 1457, 1423, 1249, 1211, 1144, 1054, 915, 873 cm⁻¹; ¹H NMR (500 MHz, CDCl₃) δ 5.42 (d, J = 1.1 Hz, 1 H), 2.68–2.60 (m, 2 H), 2.29–2.21 (m, 1 H), 2.19–2.11 (m, 2 H), 2.01 (ddd, J = 13.0, 8.3, 4.2 Hz, 1 H), 1.87 (t, J = 12.7 Hz, 1 H), 1.78 (ddt, J = 14.6, 10.3, 5.0 Hz, 1 H), 1.69–1.63 (m, 2 H), 1.62 (s, 3 H), 1.54 (d, J = 2.4 Hz, 1 H), 1.45 (td, J = 6.9, 3.9 Hz, 2 H), 1.30 (ddd, J = 12.5, 6.2, 2.8 Hz, 1 H), 1.25 (s, 3 H), 1.20–1.12 (m, 1 H), 1.05 (s, 3 H), 0.98 (s, 3 H), 0.96 (s, 3 H); ¹³C NMR (125 MHz, CDCl₃) δ 149.19, 138.85, 131.65, 124.98, 118.7 (q, J = 320.7 Hz), 63.49, 52.62, 45.83, 42.37, 41.88, 40.33, 37.42, 36.75, 32.93, 31.43, 30.09, 29.92, 24.56, 24.26, 19.78, 14.12; HRMS (ESI) calcd for C₂₁H₃₂F₃O₃S⁺ [M+H]⁺ 421.2024, found 421.2019.

Diene 58. To a flame-dried 4 mL scintillation vial was added triflate **57** (30.0 mg, 0.071 mmol), Ph₃P (3.7 mg, 0.014 mmol, 0.2 equiv.), Pd(OAc)₂ (1.6 mg, 0.0071 mmol, 0.1 equiv.), and toluene (1.2 mL). After sparging the reaction mixture with Ar for 30 min at 23 °C, Et₃N (0.0195 mL, 0.14 mmol, 2.0 equiv.) was added via syringe, and the vial was sealed with a Teflon-lined cap. The reaction mixture was heated at 90 °C for 20 h. The yellowish-black mixture was cooled to 23 °C and diluted with hexanes (1 mL). The reaction mixture was subjected directly to purification by flash column chromatography (silica gel, hexanes/Et₃N, 99/1) to give diene **58** (16.9 mg, 88% yield) as a colorless oil. **58**: R_f = 0.72 (silica gel, hexanes); [α]_D²⁰ = +54.2° (c = 1.0, C₆D₆); IR (film) ν_{max} 3035, 2942, 2864, 1458, 1383, 1371, 1013, 856 cm⁻¹; ¹H NMR (500 MHz, CDCl₃) δ 5.32 (s, 1 H), 4.86 (d, J = 2.9 Hz, 1 H), 2.80 (dtd, J = 9.6, 6.6, 3.1 Hz, 1 H), 2.30–2.14 (m, 3 H), 1.97–1.90 (m, 1 H), 1.74–1.61 (m, 3 H), 1.66 (s, 3 H), 1.56–1.48 (m, 3 H), 1.39 (dd, J = 10.8, 5.9 Hz, 1 H), 1.29 (s, 3 H), 1.09 (dt, J = 12.0, 4.8 Hz, 1 H), 1.03 (s, 3 H), 1.02 (d, J = 6.9 Hz, 3 H), 1.00 (s, 3 H); ¹³C NMR (125 MHz, CDCl₃) δ 151.43, 147.37,

128.06, 123.21, 66.29, 63.72, 58.95, 56.85, 47.16, 41.30, 41.06, 40.72, 38.97, 37.89, 32.54, 32.36, 29.21, 26.06, 16.46, 14.36. [Note: Despite efforts to obtain HRMS data no successful ionization was achieved with either ESI or CI].

(–)-Spiroviolene (21). To a 4 mL scintillation vial at 23 °C was added diene **58** (9.0 mg, 0.033 mmol, 1.0 equiv.), Pd/C (20.0 mg, 10 wt %, reduced dry powder), and EtOH (0.33 mL). The vial was sealed with a septum and the reaction mixture was sparged with hydrogen for 5 min at 23 °C. The reaction mixture was then stirred for 30 min at 23 °C. Upon completion, the black mixture was filtered through a short plug of Celite and silica gel, rinsing with hexanes (3 × 2 mL). The filtrate was evaporated and purified via flash column chromatography (silica gel, hexanes) to afford (–)-spiroviolene (**21**, 9.1 mg, >99% yield) as a colorless oil. **21**: $R_f = 0.84$ (silica gel, hexanes); $[\alpha]_D^{20} = -5.4^\circ$ ($c = 0.2$, C_6D_6); IR (film) ν_{max} 3032, 2943, 2866, 2361, 1463, 1370, 1260, 853, 808 cm^{-1} ; 1H NMR (500 MHz, C_6D_6) δ 4.82 (d, $J = 2.9$ Hz, 1 H), 2.78 (dddd, $J = 12.3, 6.4, 6.2, 2.9$ Hz, 1 H), 1.93 (ddd, $J = 12.7, 12.7, 6.9$ Hz, 1 H), 1.86–1.63 (m, 7 H), 1.64–1.55 (m, 3 H), 1.48–1.35 (m, 3 H), 1.35 (s, 3 H), 1.14–1.07 (m, 1 H), 1.05 (s, 3 H), 1.04 (s, 3 H), 0.98 (d, $J = 6.7$ Hz, 3 H), 0.95 (d, $J = 6.7$ Hz, 3 H); ^{13}C NMR (125 MHz, C_6D_6) δ 148.96, 128.98, 66.13, 63.70, 59.42, 53.79, 46.64, 44.76, 41.27, 40.83, 39.58, 38.60, 33.06, 32.37, 31.32, 30.70, 29.16, 26.10, 15.17, 15.09. [Note: Despite efforts to obtain HRMS data no successful ionization was achieved with either ESI or CI]. All NMR spectral data matched that reported in the literature; see comparison in Table 2.2. Literature $[\alpha]_D^{21} = -5.6^\circ$ ($c = 0.2$, C_6D_6).

Table 2.2. Comparison of 1H NMR data of spiroviolene (**21**) between our synthetic sample and the natural isolate.¹³

Synthetic 21 (500 MHz)	Natural 21 (500 MHz)
4.82 (d, $J = 2.9$ Hz, 1 H)	4.81 (d, $J = 2.9$ Hz, 1 H)

Table 2.2. *continued.*

2.78 (dddd, $J = 12.3, 6.4, 6.2, 2.9$ Hz, 1 H)	2.77 (dddd, $J = 12.5, 6.4, 6.4, 2.9$ Hz, 1 H)
1.93 (ddd, $J = 12.7, 12.7, 6.9$ Hz, 1 H)	1.92 (ddd, $J = 12.7, 6.9, 6.9$ Hz, 1 H)
1.86–1.63 (m, 7 H)	1.81 (m, 1 H)
	1.79 (m, 1 H)
	1.74 (m, 1 H)
	1.73 (m, 1 H)
	1.72 (m, 1 H)
	1.69 (m, 1 H)
	1.67 (m, 1 H)
1.64–1.55 (m, 3 H)	1.60 (m, 1 H)
	1.59 (m, 1 H)
	1.58 (m, 1 H)
1.48–1.35 (m, 3 H)	1.43 (dddd, $J = 11.8, 6.6, 1.5, 1.5$ Hz, 1 H)
	1.38 (m, 1 H)
	1.33 (m, 1 H)
1.35 (s, 3 H)	1.34 (s, 3 H)
1.14–1.07 (m, 1 H)	1.09 (dddd, $J = 12.2, 12.2, 11.3, 7.6$ Hz, 1 H)
1.05 (s, 3 H)	1.04 (s, 3 H)
1.04 (s, 3 H)	1.03 (s, 3 H)
0.98 (d, $J = 6.7$ Hz, 3 H)	0.97 (d, $J = 6.7$ Hz, 3 H)
0.95 (d, $J = 6.7$ Hz, 3 H)	0.94 (d, $J = 6.7$ Hz, 3 H)
7.16 (s, C ₆ D ₆)	7.16 (s, C ₆ D ₆)

Table 2.3. Comparison of ^{13}C NMR data of spiroviolene (**21**) between our synthetic sample and the natural isolate.¹³

Synthetic 21 (500 MHz)	Natural 21 (500 MHz)
148.96	148.9
128.98	128.9
66.13	66.0
63.70	63.7
59.42	59.4
53.79	53.8
46.64	46.6
44.83	44.7
41.27	41.3
40.83	40.8
39.58	39.5
38.60	38.6
33.06	33.1
32.37	32.4
31.32	31.3
30.70	30.7
29.16	29.1
26.10	26.1
15.17	15.2
15.09	15.1
128.06 (s, C_6D_6)	128.06 (s, C_6D_6)

Bicyclic Ketone 60. To a flask containing **59**⁵ (1.37 g, 6.05 mmol, 1.0 equiv.) was added *N,N*-dimethyl hydrazine (1.38 mL, 18.15 mmol, 3.0 equiv.) and the resultant mixture stirred at 23 °C for 12 h. Upon completion, the reaction contents were quenched with NH₄Cl (5 mL) and diluted with Et₂O (5 mL). After stirring for 30 min, the resultant mixture was transferred to a separatory funnel and further diluted with NH₄Cl (30 mL) and Et₂O (50 mL). The organic layer was separated and further washed with NH₄Cl (2 × 30 mL), H₂O (30 mL), brine (30 mL), dried (Na₂SO₄) and concentrated to give the hydrazone (1.56 g, 96% yield) as a yellow oil. Pressing forward without any further purification, to a flame-dried, 250 mL Schlenk flask was added solid LDA in a glovebox at 23 °C. The flask was then transferred from the glovebox, attached to a Schlenk manifold, and placed under positive pressure of N₂. THF (35 mL) was then added, and the flask was cooled to -78 °C. After all solids had dissolved, freshly prepared hydrazone was added as a solution in THF (20 mL) slowly over the course of 5 min. Once that addition was complete, the flask was then warmed to 0 °C and the contents were stirred for 2 h. The reaction contents were then re-cooled to -78 °C and HMPA (1.51 mL, 8.70 mmol, 1.5 equiv.) was added dropwise. After stirring at -78 °C for 30 min, a solution of alkyl iodide **27** (1.74 g, 7.00 mmol, 1.2 equiv.) in THF (5 mL) was added over the course of 5 min. The reaction contents were then allowed to slowly warm to 23 °C over the course of 5 h and were stirred at 23 °C for an additional 10 h. Upon completion, the reaction contents were quenched by the addition of 1 N HCl (50 mL) and stirred under a N₂ atmosphere for an additional 12 h. The reaction mixture was diluted with Et₂O (50 mL) and transferred to a separatory funnel. After separating the resultant layers, the aqueous layer was extracted with Et₂O (2 × 50 mL). The combined organic layers were washed with saturated aqueous NaHCO₃ (30 mL), H₂O (2 × 30 mL) and brine (30 mL), dried (Na₂SO₄) and concentrated. Purification of the resultant yellow oil via flash column chromatography (silica gel, hexanes/EtOAc, 4/1) gave alkylated product **60** (1.43 g, 63% yield) as a pale yellow oil. **60**: R_f = 0.50 (silica gel, hexanes/EtOAc, 4/1); [α]_D²⁰

= +0.9° (*c* = 0.75, CHCl₃); IR (film) ν_{\max} 2948, 2865, 1737, 1454, 1148, 1110, 1048 cm⁻¹; ¹H NMR (500 MHz, CDCl₃) δ 4.63 (s, 2 H), 3.36 (s, 3 H), 3.35–3.29 (m, 2 H), 2.68–2.58 (m, 1 H), 2.33 (dd, *J* = 18.1, 1.8 Hz, 1 H), 2.22 (q, *J* = 6.6 Hz, 3 H), 2.19–2.09 (m, 1 H), 1.98 (ddt, *J* = 12.0, 7.3, 3.6 Hz, 2 H), 1.81–1.76 (m, 3 H), 1.67 (td, *J* = 6.3, 2.5 Hz, 2 H), 1.61 (dd, *J* = 2.1, 1.1 Hz, 3 H), 1.49 (dt, *J* = 12.6, 6.3 Hz, 1 H), 1.33–1.23 (m, 4 H), 1.18 (s, 3 H), 0.96 (d, *J* = 6.9 Hz, 3 H), 0.95 (s, 3 H); ¹³C NMR (126 MHz, CDCl₃) δ 221.52, 138.97, 131.92, 96.85, 76.66, 59.24, 55.32, 52.98, 50.46, 46.33, 45.13, 41.54, 39.28, 36.86, 36.71, 31.39, 31.19, 30.86, 24.29, 21.21, 19.77, 14.22; HRMS (ESI) calcd for C₂₂H₃₆O₃⁺ [M]⁺ 348.2700, found 348.2694.

Diene 62. To a flame-dried, 50 mL flask was added ketone **60** (0.593 g, 1.70 mmol, 1.0 equiv.) and THF (17 mL) at 23 °C. The flask was cooled to –78 °C and KHMDS (4.42 mL, 0.5 M in toluene, 2.2 mmol, 1.3 equiv.) was added dropwise. The reaction contents were warmed to 0 °C and stirred for 2 h. The reaction mixture was re-cooled to –78 °C and a solution of Comins' reagent (0.734 g, 1.87 mmol, 1.1 equiv.) in THF (3 mL) was added over the course of 10 min. The reaction was maintained at –78 °C for 20 min before being warmed to 23 °C and stirred for 1 h. Upon completion the reaction was quenched with saturated aqueous NaHCO₃ (5 mL) and diluted with Et₂O (20 mL) and H₂O (10 mL). The mixture was then transferred to a separatory funnel and the aqueous layer was extracted with Et₂O (2 × 15 mL). The combined organic layers were washed with H₂O (2 × 25 mL) and brine (25 mL), dried (Na₂SO₄), and concentrated. The resultant yellow oil was further purified by flash column chromatography (silica gel, hexanes/EtOAc, 20/1) to give **61** (0.531 g, 65% yield) as a colorless oil. Next, to a flame-dried, 20 mL pressure vessel at 23 °C were added Pd(OAc)₂ (49.4 mg, 0.22 mmol, 0.2 equiv.), Ph₃P (0.115 g, 0.44 mmol, 0.4 equiv.) and Et₃N (0.460 mL, 3.3 mmol, 3.0 equiv.). The contents of the flask were suspended in toluene (8 mL) and Ar was bubbled through the reaction mixture for 15 min. A solution of triflate **61** (0.528 g, 1.1 mmol, 1.0 equiv.) in toluene (3 mL)

was then added at 23 °C and the reaction mixture was heated to 90 °C for 16 h. Upon completion, the reaction contents were diluted with hexanes (5 mL) and directly purified via flash column chromatography (silica gel, hexanes/EtOAc, 20/1) to give the desired cyclization product **62** (0.200 g, 55% yield) as a pale yellow oil. **62**: $R_f = 0.68$ (silica gel, hexanes/EtOAc, 9/1); $[\alpha]_D^{20} = +23.6^\circ$ ($c = 0.33$, CHCl_3); IR (film) ν_{max} 3034, 2928, 2863, 1449, 1373, 1110, 1049 cm^{-1} ; ^1H NMR (500 MHz, CDCl_3) δ 5.32 (p, $J = 1.7$ Hz, 1 H), 4.89 (dd, $J = 3.0, 0.7$ Hz, 1 H), 4.64 (s, 2 H), 3.38 (s, 3 H), 3.36 (q, $J = 9.0$ Hz, 2 H), 2.89 (dtd, $J = 12.3, 6.6, 3.0$ Hz, 1 H), 2.27 (dddd, $J = 13.3, 7.5, 2.4, 1.3$ Hz, 1 H), 2.24–2.15 (m, 2 H), 1.94 (ddt, $J = 14.9, 8.3, 2.3$ Hz, 1 H), 1.78 (d, $J = 6.7$ Hz, 1 H), 1.76–1.65 (m, 6 H), 1.55–1.40 (m, 2 H), 1.25 (s, 3 H), 1.07 (s, 3 H), 1.02 (d, $J = 6.9$ Hz, 3 H); ^{13}C NMR (126 MHz, CDCl_3) δ 151.63, 147.25, 127.80, 123.32, 96.88, 75.35, 63.67, 61.65, 58.03, 56.83, 55.26, 47.16, 45.33, 41.19, 38.93, 37.35, 36.96, 32.48, 31.66, 21.70, 16.45, 14.40; HRMS (ESI) calcd for $\text{C}_{22}\text{H}_{34}\text{O}_2^+ [\text{M}]^+$ 330.2559, found 330.2557.

Secondary Alcohol 63. To a flame-dried 5 mL pressure vessel at 23 °C was added **62** (129.0 mg, 0.39 mmol, 1.0 equiv.) and THF (2 mL). The contents of the vessel were then cooled to 0 °C and $\text{BH}_3 \cdot \text{THF}$ (0.390 mL, 1.0 M in THF, 0.39 mmol, 1.0 equiv.) was added. The reaction was maintained at 0 °C with stirring and after 5 h, NaOH (0.33 mL, 6 M aqueous) and H_2O_2 (0.33 mL, 30% w/w) were added simultaneously. The reaction mixture was then warmed to 23 °C and stirred for 1 h, after which time it was diluted with Et_2O (10 mL) and H_2O (10 mL). The layers were separated and the aqueous layer was further extracted with Et_2O (2×10 mL). The combined organic layers were washed with brine (15 mL), dried (Na_2SO_4), and concentrated to give a yellow oil. This crude material was further purified by flash column chromatography (silica gel, hexanes/EtOAc, 6/1) to give alcohol **63** (89.7 mg, 66% yield) as a

colorless oil. **63**: $R_f = 0.33$ (silica gel, hexanes/EtOAc, 4/1); $[\alpha]_D^{20} = -6.7^\circ$ ($c = 0.67$, CHCl_3); IR (film) ν_{max} 3362, 3030, 2931, 2869, 1456, 1371, 1111, 1050 cm^{-1} ; ^1H NMR (500 MHz, CDCl_3) δ 4.80 (d, $J = 2.9$ Hz, 1 H), 4.64 (s, 2 H), 3.85 (td, $J = 8.8, 3.8$ Hz, 1 H), 3.37 (s, 3 H), 3.34 (d, $J = 12.4$ Hz, 2 H), 2.76 (dtd, $J = 12.7, 6.5, 2.9$ Hz, 1 H), 2.14 (ddq, $J = 13.5, 10.4, 6.7$ Hz, 1 H), 1.95 (td, $J = 12.9, 7.0$ Hz, 1 H), 1.86–1.62 (m, 8 H), 1.61–1.53 (m, 2 H), 1.52–1.42 (m, 2 H), 1.24 (s, 3 H), 1.05 (s, 3 H), 0.99 (d, $J = 6.8$ Hz, 3 H), 0.87 (d, $J = 6.8$ Hz, 3 H); ^{13}C NMR (126 MHz, CDCl_3) δ 148.98, 128.77, 96.87, 78.55, 75.17, 63.48, 61.14, 58.28, 55.26, 53.20, 53.10, 45.55, 43.11, 41.12, 39.65, 37.77, 36.73, 32.52, 31.57, 21.60, 14.80, 12.62; HRMS (ESI) calcd for $\text{C}_{22}\text{H}_{36}\text{O}_3^+ [\text{M}]^+$ 348.2664, found 348.2664.

Benzoate 64. To a flame-dried, 4 mL vial at 23 °C was added **63** (19.8 mg, 0.057 mmol, 1.0 equiv.) and CH_2Cl_2 (0.6 mL). To this solution was then added BzCl (0.020 mL, 0.17 mmol, 3.0 equiv.), Et_3N (0.032 mL, 0.228 mmol, 4.0 equiv.) and 4-DMAP (7.0 mg, 0.057 mmol, 1.0 equiv.). The reaction mixture was stirred at 23 °C for 2 h. Upon completion, the reaction contents were quenched with saturated aqueous NH_4Cl (1 mL) and diluted with CH_2Cl_2 (5 mL) and H_2O (5 mL). The layers were separated, and the aqueous layer was extracted with CH_2Cl_2 (3 · 5 mL). The combined organic layers were dried (Na_2SO_4) and concentrated to give an orange oil. Purification of this crude material by flash column chromatography (silica gel, hexanes/EtOAc, 10/1) gave the desired benzoate (24.7 mg, 96% yield) as a pale yellow oil. $R_f = 0.73$ (silica gel, hexanes/EtOAc, 4/1); $[\alpha]_D^{20} = -44.3^\circ$ ($c = 0.28$, CHCl_3); IR (film) ν_{max} 2927, 2871, 1718, 1279, 1113, 1047, 712 cm^{-1} ; ^1H NMR (500 MHz, CDCl_3) δ 8.04 (d, $J = 7.9$ Hz, 2 H), 7.55 (t, $J = 7.2$ Hz, 1 H), 7.44 (t, $J = 7.5$ Hz, 2 H), 5.01–4.93 (m, 2 H), 4.65 (s, 2 H), 3.38 (s, 3 H), 3.35 (d, $J = 11.6$ Hz, 2 H), 2.79 (dd, $J = 12.8, 6.7$ Hz, 1 H), 2.23–2.14 (m, 1 H), 2.03 (qd, $J = 13.3, 12.4, 8.6$ Hz, 3 H), 1.89–1.66 (m, 6 H), 1.59–1.46 (m, 3 H), 1.26 (s, 3 H), 1.06

(s, 3 H), 1.03 (d, $J = 6.8$ Hz, 3 H), 0.92 (d, $J = 6.7$ Hz, 3 H); ^{13}C NMR (126 MHz, CDCl_3) δ 166.98, 148.31, 132.85, 129.69, 129.21, 128.43, 96.93, 81.37, 75.28, 63.68, 61.26, 58.34, 55.27, 52.57, 49.91, 45.56, 43.54, 39.63, 38.74, 37.72, 36.83, 32.53, 31.53, 29.85, 21.65, 14.59, 12.72; HRMS (ESI) calcd for $\text{C}_{29}\text{H}_{40}\text{O}_4^+ [\text{M}]^+$ 452.2927, found 452.2943. To a 4-mL vial at 23 °C containing a solution of MOM ether (57.0 mg, 0.126 mmol, 1.0 equiv.) in THF (2.5 mL) was added 6 M HCl (1.5 mL) dropwise. The reaction mixture was then heated to 50 °C for 4 h. Upon completion, the reaction contents were cooled to 23 °C and diluted with brine (5 mL). The resultant layers were separated, and the aqueous layer was then extracted with Et_2O (3×5 mL). The combined organic layers were then dried (Na_2SO_4) and concentrated. Purification of the resultant residue by flash column chromatography (silica gel, hexanes/ EtOAc , 5/1) gave alcohol **64** (47.5 mg, 92% yield) as a colorless oil. **64**: $R_f = 0.29$ (silica gel, hexanes/ EtOAc , 4/1); $[\alpha]_D^{20} = -17.5^\circ$ ($c = 0.35$, MeOH); IR (film) ν_{max} 3417, 2952, 2923, 2870, 1718, 1704, 1452, 1281, 1115, 712 cm^{-1} ; ^1H NMR (500 MHz, CDCl_3) δ 8.04 (d, $J = 7.2$ Hz, 2 H), 7.55 (t, $J = 7.4$ Hz, 1 H), 7.43 (t, $J = 7.7$ Hz, 2 H), 4.98 (d, $J = 2.9$ Hz, 1 H), 4.98–4.94 (m, 1 H), 3.51 (d, $J = 10.6$ Hz, 1 H), 3.41 (d, $J = 10.6$ Hz, 1 H), 2.80 (dtd, $J = 12.7, 6.5, 2.8$ Hz, 1 H), 2.23–2.15 (m, 1 H), 2.08–1.97 (m, 3 H), 1.89–1.77 (m, 2 H), 1.76–1.63 (m, 5 H), 1.53–1.43 (m, 2 H), 1.26 (s, 3 H), 1.04 (s, 3 H), 1.03 (d, $J = 6.7$ Hz, 3 H), 0.92 (d, $J = 6.7$ Hz, 3 H); ^{13}C NMR (126 MHz, CDCl_3) δ 166.98, 148.34, 132.86, 129.67, 129.10, 128.42, 81.33, 70.26, 63.72, 60.97, 58.30, 52.55, 49.84, 46.65, 43.50, 39.58, 38.69, 37.56, 36.30, 32.48, 31.38, 21.00, 14.58, 12.69; HRMS (ESI) calcd for $\text{C}_{54}\text{H}_{69}\text{O}_4^+ [2\text{M}+\text{H}]^+$ 845.4992, found 845.4984.

Carboxylic Acid 65. To a flame-dried, 4 mL vial at 23 °C was added **64** (42.8 mg, 0.105 mmol, 1.0 equiv.), NaHCO_3 (44.1 mg, 0.525 mmol, 5.0 equiv.) and CH_2Cl_2 (2 mL). To this suspension was added Dess–Martin periodinane (66.8 mg, 0.158 mmol, 1.5 equiv.). After stirring the

resultant mixture at 23 °C for 1 h, the reaction contents were quenched with a 1:1 mixture of saturated aqueous NaHCO₃ (2.5 mL) and Na₂S₂O₃ (2.5 mL). The resultant biphasic mixture was then stirred vigorously for 30 min after which time the resultant layers were separated, and the aqueous layer was extracted with Et₂O (3 × 5 mL). The combined organic layers were then dried (Na₂SO₄) and concentrated to give a yellow oil which was further purified by flash column chromatography (silica gel, hexanes/EtOAc, 20/1) to give the aldehyde (35.8 mg, 85% yield) as a colorless oil. Next, to a 4 mL vial at 23 °C containing a solution of aldehyde (35.8 mg, 0.088 mol, 1.0 equiv.) and 2-methyl-2-butene (0.932 mL, 0.88 mmol, 10.0 equiv.) in *t*-BuOH (1 mL) was added a solution of NaClO₂ (294.0 mg, 3.26 mmol, 35.0 equiv.) and NaH₂PO₄ (528.0 mg, 4.40 mmol, 50.0 equiv.) in H₂O (2 mL). The reaction mixture was stirred at 23 °C for 1 h after which time the reaction mixture was diluted with H₂O (5 mL) and EtOAc (5 mL). The layers were separated, and the aqueous layer was extracted with EtOAc (3 × 5 mL). The combined organic layers were dried (Na₂SO₄) and concentrated to give pale yellow residue. Purification of that crude material by flash column chromatography (silica gel, hexanes/EtOAc, 5/1) gave carboxylic acid **65** (35.0 mg, 96% yield) as a pale yellow oil. **65**: *R*_f = 0.32 (silica gel, hexanes/EtOAc, 6/1); [α]_D²⁰ = -20.4° (*c* = 0.46, MeOH); IR (film) ν_{max} 2953, 2932, 2869, 1717, 1698, 1452, 1280, 1114, 713 cm⁻¹; ¹H NMR (500 MHz, CDCl₃) δ 8.04 (d, *J* = 7.3 Hz, 2 H), 7.55 (t, *J* = 7.4 Hz, 1 H), 7.44 (t, *J* = 7.7 Hz, 2 H), 5.02 (d, *J* = 2.7 Hz, 1 H), 4.96 (td, *J* = 9.1, 3.5 Hz, 1 H), 2.73 (dtd, *J* = 12.7, 6.6, 2.8 Hz, 1 H), 2.47 (dd, *J* = 6.5, 1.4 Hz, 1 H), 2.30 (ddd, *J* = 13.8, 7.0, 3.9 Hz, 1 H), 2.23–2.14 (m, 1 H), 2.03 (tdd, *J* = 13.2, 8.5, 4.8 Hz, 3 H), 1.92–1.66 (m, 4 H), 1.61–1.43 (m, 3 H), 1.31 (s, 3 H), 1.21 (s, 3 H), 1.03 (d, *J* = 6.8 Hz, 3 H), 0.92 (d, *J* = 6.7 Hz, 3 H); ¹³C NMR (126 MHz, CDCl₃) δ 184.45, 166.98, 148.13, 132.89, 129.67, 129.26, 128.43, 81.25, 63.38, 61.72, 58.33, 52.49, 52.22, 49.81, 43.51, 39.74, 38.68, 38.35, 36.85, 32.39, 31.33, 30.37, 21.77, 14.59, 12.68; HRMS (ESI) calcd for C₅₄H₇₀O₂⁺ [2M–H₂O]⁺ 798.5223, found 798.5219.

Tetrasubstituted Alkene 66. To a flame-dried 4 mL vial at 23 °C was added carboxylic acid **65** (19.9 mg, 0.047 mmol, 1.0 equiv.) and HCl (1 mL, 4 M in dioxane). The reaction mixture was then heated to 80 °C for 48 h. Upon completion, the mixture was diluted with H₂O (5 mL) and EtOAc (5 mL). The layers were then separated, and the aqueous layer was extracted with EtOAc (3 × 5 mL). The combined organic layers were dried (Na₂SO₄) and concentrated to give a brown oil. Purification of that residue by flash column chromatography (silica gel, hexanes/EtOAc, 5/1) gave the desired isomerized product **66** (11.5 mg, 58% yield) as a pale yellow oil. **66**: R_f = 0.55 (silica gel, hexanes/EtOAc, 2/1); [α]_D²⁰ = -8.5° (c = 0.15, MeOH); IR (film) ν_{max} 2953, 2929, 2869, 1717, 1695, 1279, 1113 cm⁻¹; ¹H NMR (500 MHz, CDCl₃) δ 8.05 (d, J = 8.4 Hz, 2 H), 7.55 (t, J = 7.4 Hz, 1 H), 7.44 (t, J = 7.7 Hz, 2 H), 5.00 (td, J = 9.1, 3.7 Hz, 1 H), 2.83 (d, J = 2.3 Hz, 1 H), 2.32–1.81 (m, 11 H), 1.71–1.54 (m, 3 H), 1.23 (s, 3 H), 1.18 (s, 3 H), 1.00 (d, J = 6.9 Hz, 3 H), 0.87 (d, J = 6.8 Hz, 3 H); ¹³C NMR (126 MHz, CDCl₃) δ 183.90, 166.94, 147.96, 145.95, 132.89, 130.90, 129.69, 128.44, 80.96, 61.95, 59.48, 56.97, 52.85, 50.53, 47.40, 43.11, 39.63, 39.40, 38.59, 38.38, 30.10, 29.70, 20.94, 14.44, 13.34; HRMS (ESI) calcd for C₂₇H₃₄O₄Na⁺ [M+Na]⁺ 445.2354, found 445.2344.

Spirograterpene A (22). To a solution of **66** (11.5 mg, 0.027 mmol, 1.0 equiv.) in MeOH (0.25 mL) in a 4-mL vial was added K₂CO₃ (11.2 mg, 0.081 mmol, 3.0 equiv.). The vial was sealed and the reaction contents heated to 55 °C. After 15 h, the reaction was quenched by the addition of NH₄Cl (1 mL). The aqueous layer was extracted with Et₂O (3 × 2 mL), dried (Na₂SO₄) and concentrated to give a yellow oil. This crude material was further purified by flash column chromatography (silica gel, hexanes/EtOAc, 2/1) to give **22** (4.7 mg, 52% yield). **22**: R_f = 0.29 (silica gel, hexanes/EtOAc, 2/1); [α]_D²⁰ = -18.0° (c = 0.11, MeOH); IR (film) ν_{max} 3400, 3313, 3203, 2960, 2925, 2855, 1698, 1373, 1260, 1028, 800, 668 cm⁻¹; ¹H NMR (500 MHz, CD₃OD)

δ 3.78 (dt, $J = 8.4, 6.8$ Hz, 1 H), 2.80 (d, $J = 2.6$ Hz, 1 H), 2.30–2.21 (m, 1 H), 2.20–2.11 (m, 5 H), 2.10–2.04 (m, 1 H), 2.03–1.97 (m, 1 H), 1.73 (dd, $J = 10.4, 6.8$ Hz, 2 H), 1.69–1.60 (m, 2 H), 1.59–1.50 (m, 2 H), 1.19 (s, 3 H), 1.15 (s, 3 H), 0.98 (d, $J = 6.9$ Hz, 4 H), 0.85 (d, $J = 6.9$ Hz, 3 H); ^{13}C NMR (126 MHz, CD_3OD) δ 182.54, 149.20, 147.25, 78.54, 63.08, 61.00, 57.72, 54.87, 54.37, 48.60, 44.02, 42.59, 40.65, 39.49, 30.64, 30.41, 21.79, 14.93, 13.53; HRMS (ESI) calcd for $\text{C}_{20}\text{H}_{30}\text{O}_3^+ [\text{M}]^+$ 318.2915, found 318.2194. All NMR spectral data matched that reported in the literature; see comparison in Table 2.3. Literature $[\alpha]_{\text{D}}^{25} = -22.2^\circ$ ($c = 0.35$, MeOH).

Table 2.4. Comparison of ^1H NMR data of spirograterpene A (**22**) between our synthetic sample and the natural isolate.¹⁴

Synthetic 22 (500 MHz)	Natural 22 (600 MHz)
3.80 (dt, $J = 8.4, 6.8$ Hz, 1 H)	3.80 (dt, $J = 8.1, 7.0$ Hz, 1 H)
2.82 (d, $J = 2.6$, Hz 1 H)	2.81 (d, $J = 1.8$, Hz 1 H)
2.30–2.21 (m, 1 H)	2.28 (m, 1 H)
2.20–2.11 (m, 5 H)	2.17 (m, 1 H)
	2.16 (m, 1 H)
	2.14–2.19 (m, 2 H)
	2.12 (m, 1 H)
2.10–2.04 (m, 1 H)	2.06 (m, 1 H)
2.03–1.97 (m, 1 H)	2.00 (dt, $J = 16.1, 2.5$ Hz, 1 H)
1.73 (dd, $J = 10.4, 6.8$ Hz, 2 H)	1.74–1.76 (m, 2 H)
1.69–1.60 (m, 2 H)	1.68 (m, 1 H)
	1.65 (m, 1 H)

Table 2.4. *continued.*

1.59–1.50 (m, 2 H)	1.57 (m, 1 H)
	1.57 (m, 1 H)
1.21 (s, 3 H)	1.22 (s, 3 H)
1.17 (s, 3 H)	1.17 (s, 3 H)
1.00 (d, $J = 6.9$, Hz 3 H)	1.00 (d, $J = 6.9$, Hz 3 H)
0.87 (d, $J = 6.9$, Hz 3 H)	0.87 (d, $J = 6.9$, Hz 3 H)
3.33 (p, CD ₃ OD)	3.33 (p, CD ₃ OD)

Table 2.5. Comparison of ¹³C NMR data of spirograterpene A (**22**) between our synthetic sample and the natural isolate.¹⁴

Synthetic 22 (500 MHz)	Natural 22 (600 MHz)
182.54	182.30
149.20	149.07
147.25	147.33
78.54	78.51
63.08	63.02
61.00	60.98
57.72	57.72
54.87	54.83
54.37	54.23
48.60	48.57
44.02	44.01
42.59	42.56
40.65	40.61

Table 2.5. *continued.*

39.49	39.46
30.64	30.62
30.41	30.40
21.79	21.72
14.93	14.95
13.53	13.54
49.00 (p, CD ₃ OD)	49.00 (p, CD ₃ OD)

Alcohol 67. To a flame-dried 10 mL vial was added diene **58** (14.0 mg, 0.05 mmol, 1.0 equiv.) and THF (0.25 mL). The reaction mixture was cooled to 0 °C and BH₃•THF (0.05 mL, 0.05 mmol, 1.0 equiv., 1.0 M in THF) was added. The reaction was stirred at this temperature for 4 h, after which NaOH (0.05 mL, 6 M aqueous) and H₂O₂ (0.05 mL, 30% w/w) were added simultaneously. The reaction mixture was warmed to 23 °C and stirred for 1 h, after which it was diluted with Et₂O (1 mL) and H₂O (1 mL). The layers were separated, and the aqueous layer was further extracted with Et₂O (3 × 1 mL). The combined organic layers were washed with brine (1 mL), dried (Na₂SO₄) and concentrated to give a yellow oil. The crude material was further purified by preparative TLC (silica gel, hexanes/EtOAc, 4/1) to give alcohol **67** (7.7 mg, 54% yield) as a colorless oil. **67**: R_f = 0.20 (silica gel, hexanes/EtOAc, 4/1); ¹H NMR (500 MHz, CDCl₃) δ 4.77 (d, *J* = 2.7 Hz, 1 H), 3.85 (td, *J* = 9.4, 8.9, 3.6 Hz, 1 H), 2.68 (dtd, *J* = 12.5, 6.4, 2.8 Hz, 1H), 2.21–2.09 (m, 1 H), 1.99–1.90 (m, 1 H), 1.85–1.74 (m, 2 H), 1.72–1.64 (m, 2 H), 1.62 (td, *J* = 4.2, 1.6 Hz, 1 H), 1.60–1.56 (m, 1 H), 1.55–1.50 (m, 3 H), 1.44 (d, *J* = 11.0 Hz, 1 H), 1.41–1.37 (m, 1 H), 1.28 (d, *J* = 1.6 Hz, 3 H), 1.02 (d, *J* = 1.5 Hz, 3 H), 1.00–0.97 (m, 6 H), 0.87 (d, *J* = 6.8 Hz, 3 H).

Barton Deoxygenation to Spiroviolene (21). To a 4 mL scintillation vial at 23 °C was added alcohol **67** (7.7 mg, 0.027 mmol, 1.0 equiv.), 1,1'-thiocarbonyldiimidazole (14.4 mg, 0.081 mmol, 3.0 equiv.) and 4-DMAP (1.7 mg, 0.0135 mmol, 0.5 equiv.). This mixture was dissolved in CH₂Cl₂/pyridine (0.6 mL, 1:1) and the solution was then stirred for 12 h at 23 °C. Once complete, the contents were directly purified by column chromatography (silica gel, hexanes/EtOAc, 19/1) to afford the desired thionoimidazolide intermediate (10.6 mg, 98% yield) as a colorless oil. Next, to a 4 mL scintillation vial at 23 °C was added the resulting thionoimidazole (10.6 mg, 0.027 mmol, 1.0 equiv.) and toluene (0.6 mL). To this solution was then added tri-*n*-butyltin hydride (0.015 mL, 0.054 mmol, 2.0 equiv.) and AIBN (0.7 mg, 0.0041 mmol, 0.15 equiv.). The resultant mixture was heated to 110 °C for 10 min. Upon completion, the reaction contents were cooled to 23 °C, the reaction mixture was concentrated directly, and then purified by flash column chromatography (silica gel, hexanes) to afford deoxygenated product **21** (3.6 mg, 47% yield) whose spectral data matched that of natural spiroviolene (see Figures 2.3 and 2.4).

Figure 2.3. ^1H NMR comparison of the Barton product (top) to synthetic **21** (bottom).

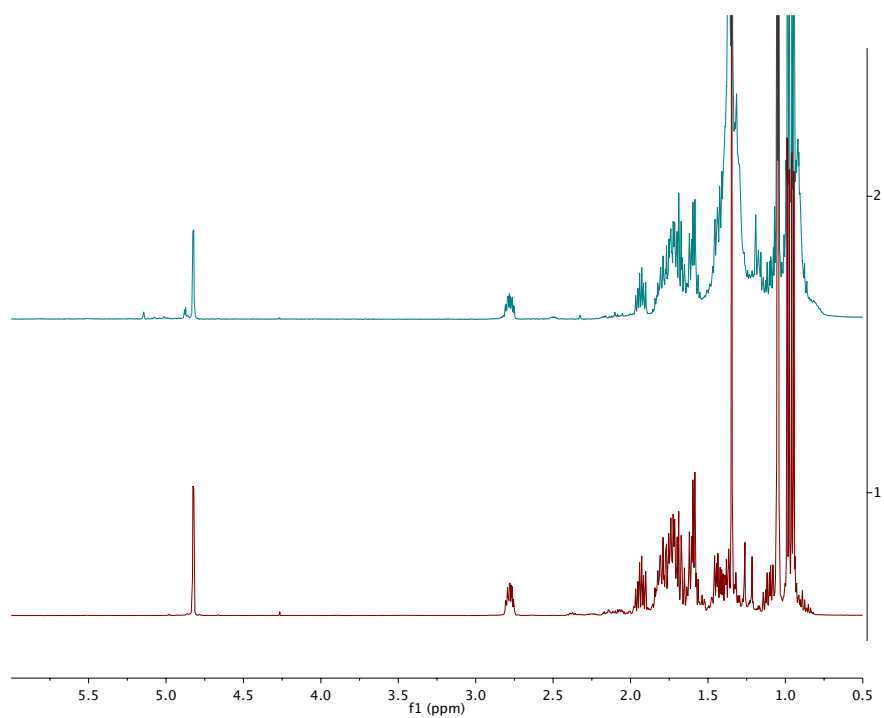
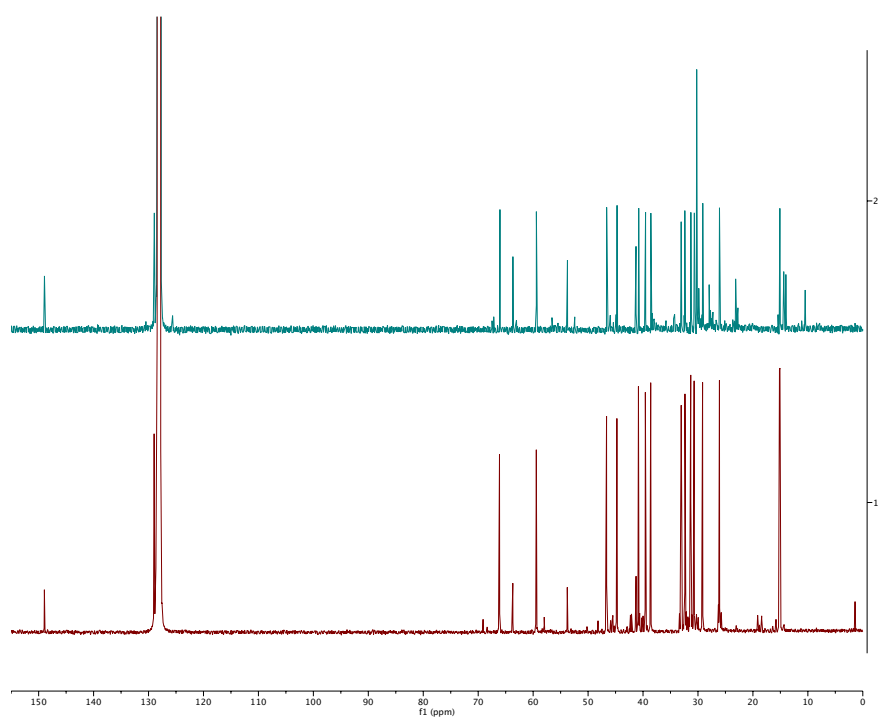


Figure 2.4. ^{13}C NMR comparison of the Barton product (top) to synthetic **21** (bottom).



Diol 68. To a 4 mL vial at 23 °C containing a solution of MOM ether **63** (12.0 mg, 0.034 mmol, 1.0 equiv.) in THF (0.7 mL) was added 6 M HCl (0.3 mL) dropwise. The reaction mixture was then heated to 50 °C for 4 h. Upon completion, the reaction contents were cooled to 23 °C and diluted with brine (5 mL). The resultant layers were separated, and the aqueous layer was then extracted with Et₂O (3 × 5 mL). The combined organic layers were then dried (Na₂SO₄) and concentrated. Purification of the resultant residue by flash column chromatography (silica gel, hexanes/EtOAc, 2/1) gave alcohol **68** (10.1 mg, 97% yield) as a colorless oil. **68**: R_f = 0.12 (silica gel, hexanes/EtOAc, 4/1); ¹H NMR (400 MHz, CDCl₃) δ 4.81 (d, *J* = 2.9 Hz, 1 H), 3.85 (td, *J* = 8.7, 3.9 Hz, 1 H), 3.50 (d, *J* = 10.6 Hz, 1 H), 3.40 (d, *J* = 10.7 Hz, 1 H), 2.76 (dtd, *J* = 12.5, 6.4, 2.8 Hz, 1 H), 2.22–2.08 (m, 1 H), 1.95 (td, *J* = 12.9, 7.0 Hz, 1 H), 1.86–1.75 (m, 2 H), 1.75–1.63 (m, 5 H), 1.63–1.57 (m, 1 H), 1.53–1.41 (m, 3 H), 1.23 (s, 3 H), 1.03 (s, 3 H), 0.99 (d, *J* = 6.7 Hz, 3 H), 0.87 (d, *J* = 6.8 Hz, 3 H).

Double Barton Deoxygenation to Spiroviolene (21). To a 4 mL scintillation vial at 23 °C was added alcohol **68** (5.3 mg, 0.017 mmol, 1.0 equiv.), 1,1'-thiocarbonyldiimidazole (12.4 mg, 0.070 mmol, 4.0 equiv.) and 4-DMAP (1.1 mg, 0.009 mmol, 0.5 equiv.). This mixture was dissolved in CH₂Cl₂/pyridine (0.6 mL, 1:1) and the solution was then stirred for 18 h at 23 °C. Once complete, the contents were directly purified by column chromatography (silica gel, hexanes/EtOAc, 3/2) to afford the desired thionoimidazolide intermediate (4.3 mg, 52% yield) as a pale yellow oil. Next, to a 4 mL scintillation vial at 23 °C was added the resulting bis-thionoimidazole (4.3 mg, 0.009 mmol, 1.0 equiv.) and toluene (0.2 mL). To this solution was then added tris(trimethyl)silane (0.010 mL, 0.033 mmol, 4.0 equiv.) and AIBN (0.3 mg, 0.002 mmol, 0.2 equiv.). The resultant mixture was heated to 110 °C for 1 h. Upon completion, the reaction contents were cooled to 23 °C, the reaction mixture was concentrated directly, and then purified by flash column chromatography (silica gel, hexanes) to afford deoxygenated product **4** whose spectral data matched that of natural spiroviolene (see Figures 2.5 and 2.6).

Figure 2.5. ^1H NMR comparison of the Double Barton product (top) to synthetic **21**(bottom).

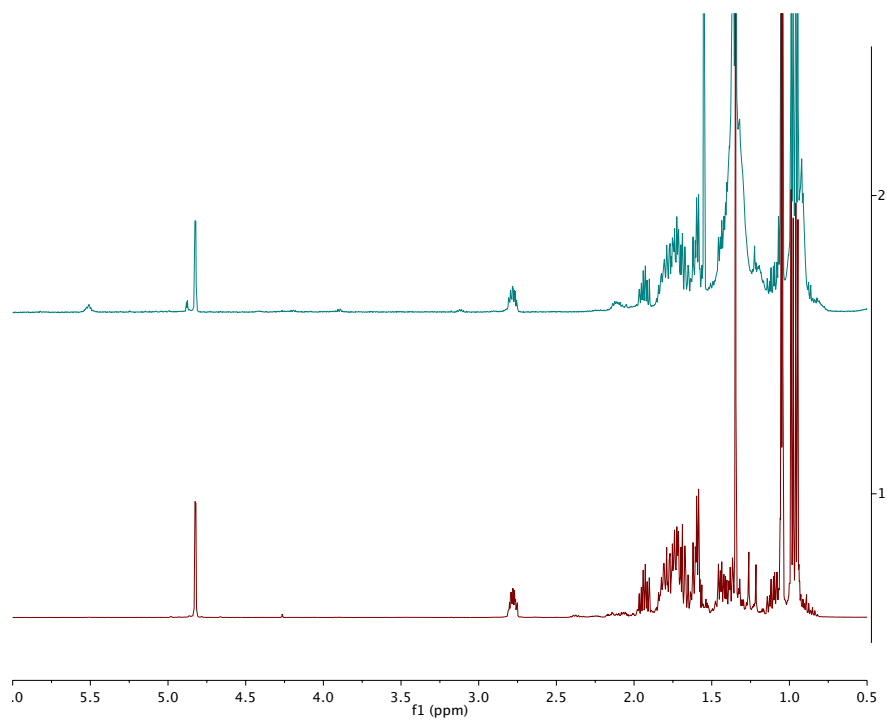
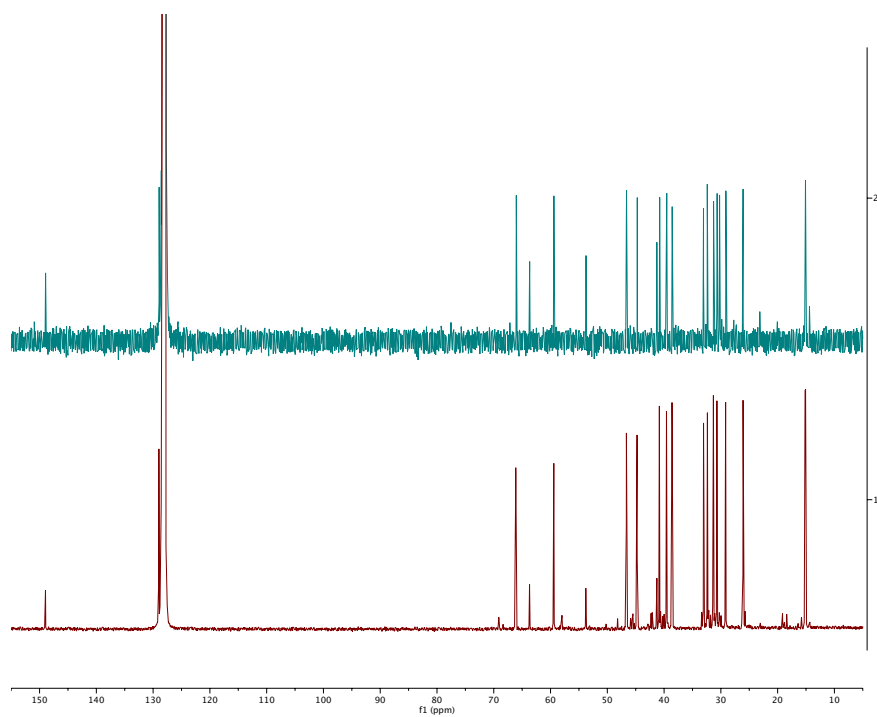
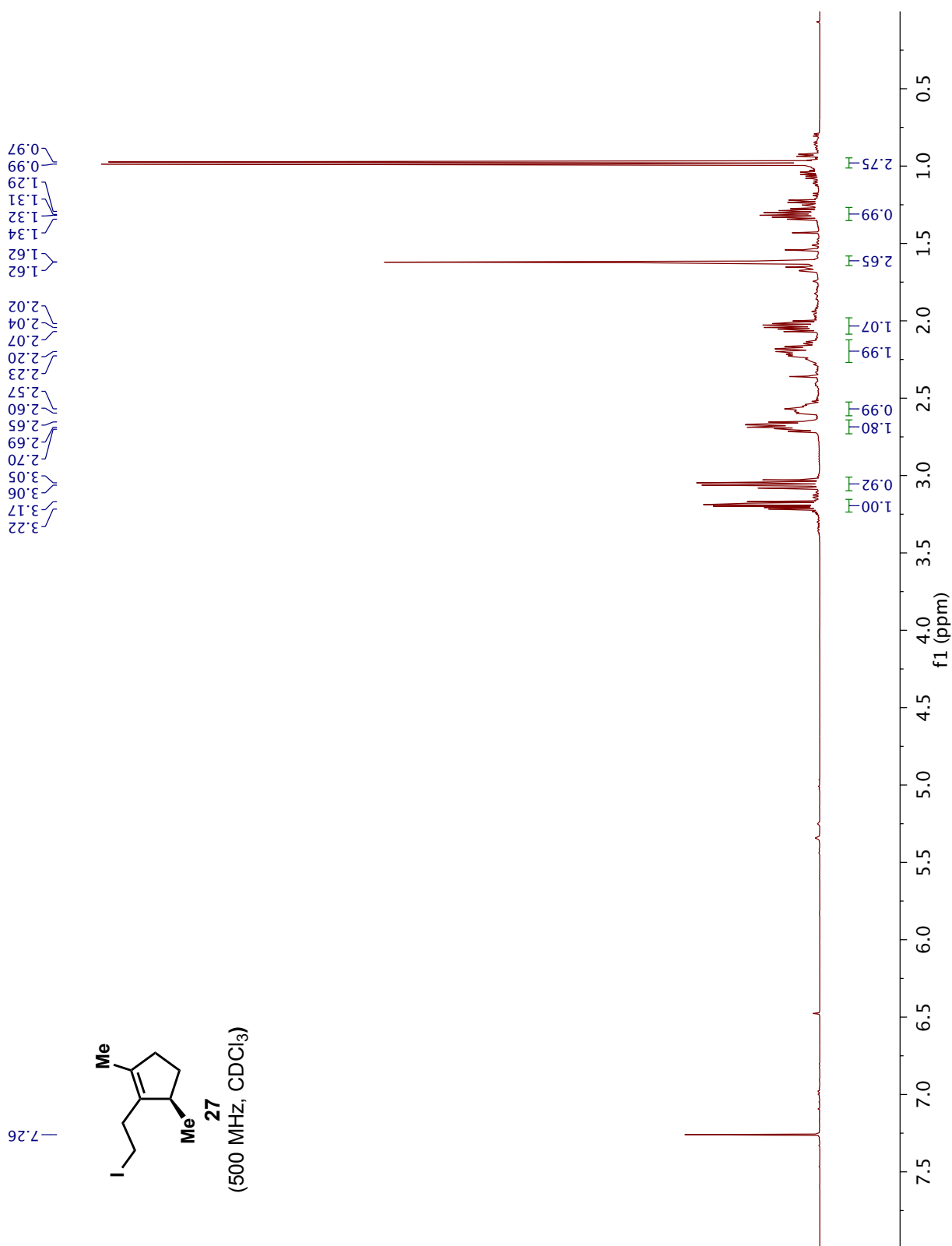
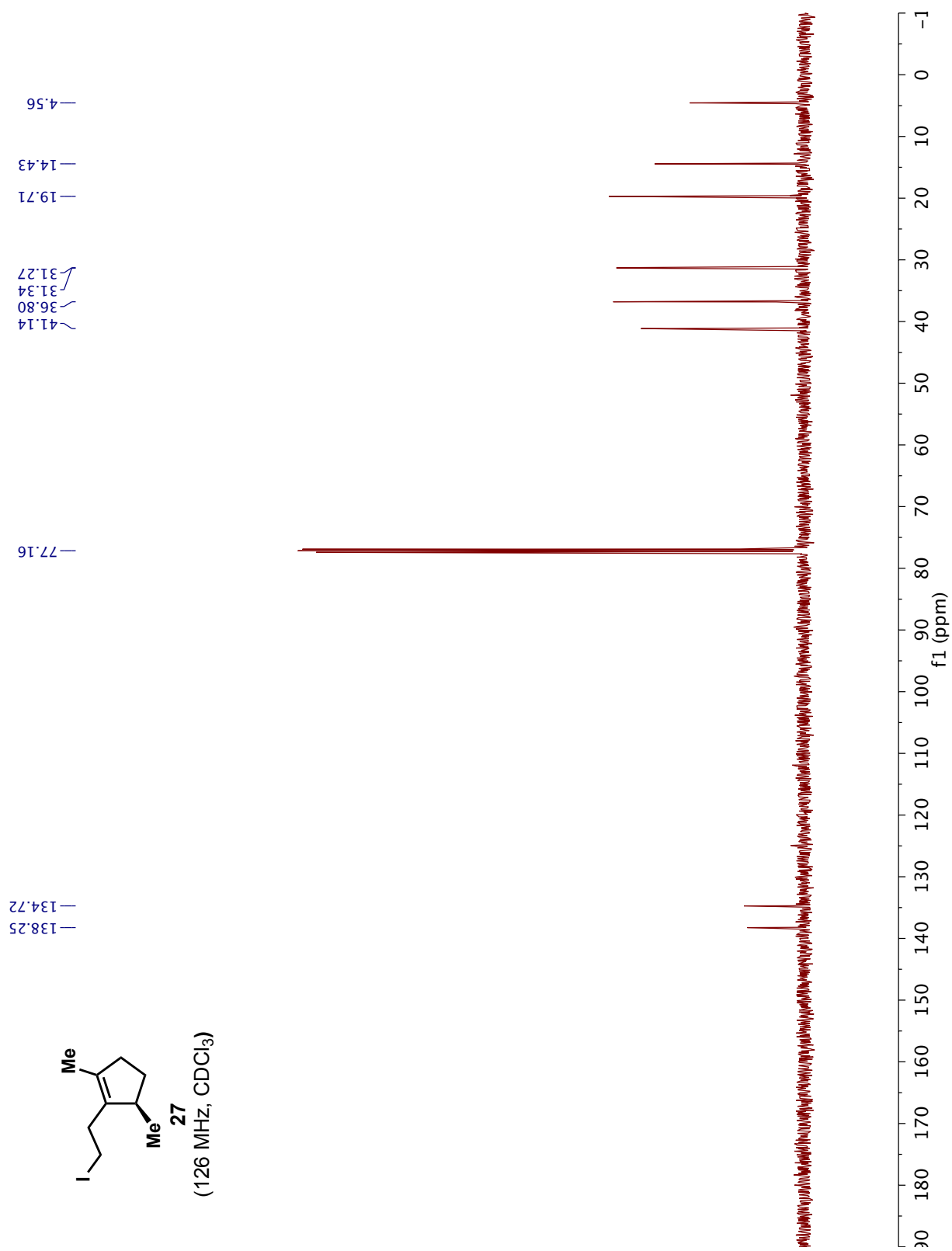


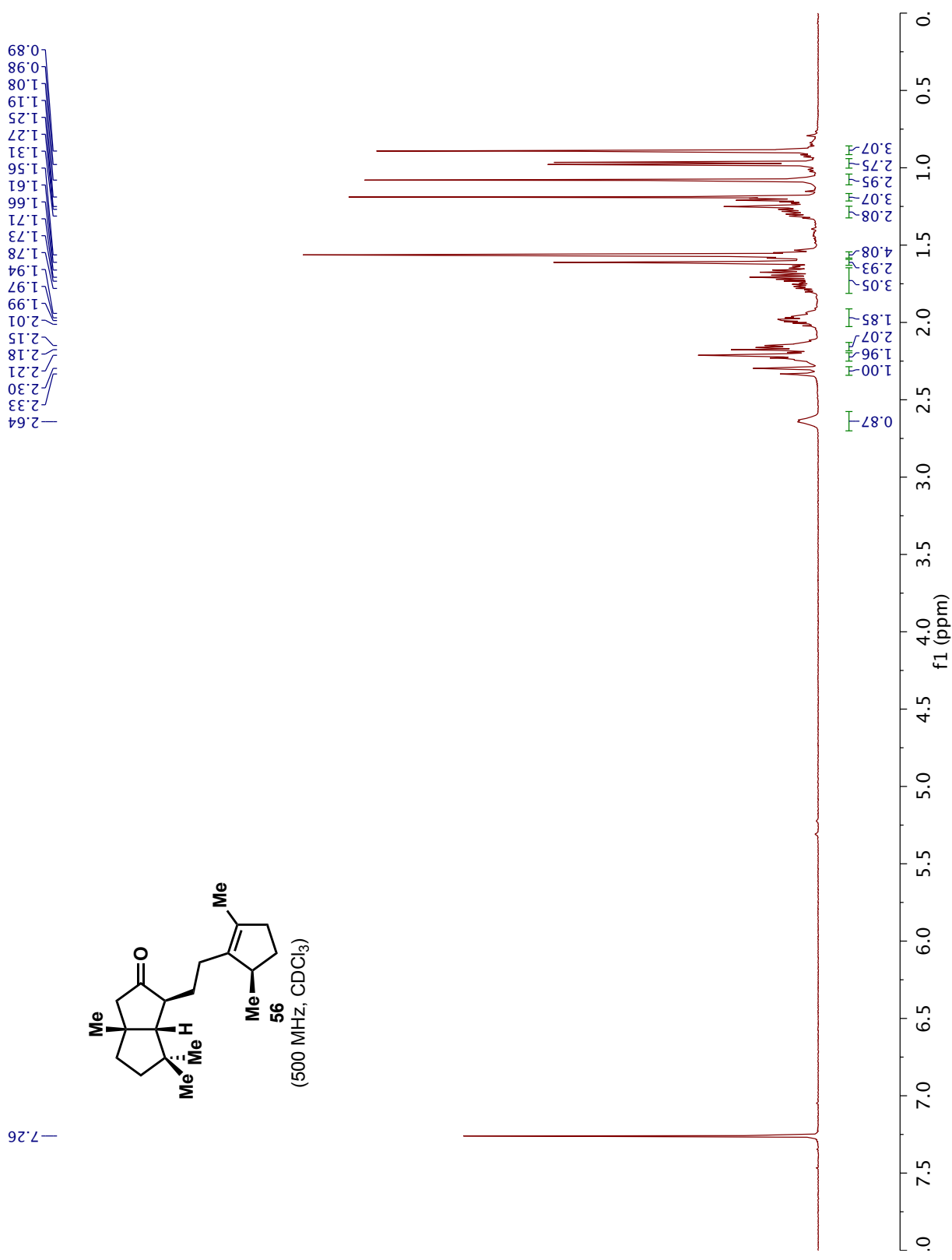
Figure 2.6. ^{13}C NMR comparison of the Double Barton product (top) to synthetic **21** (bottom).

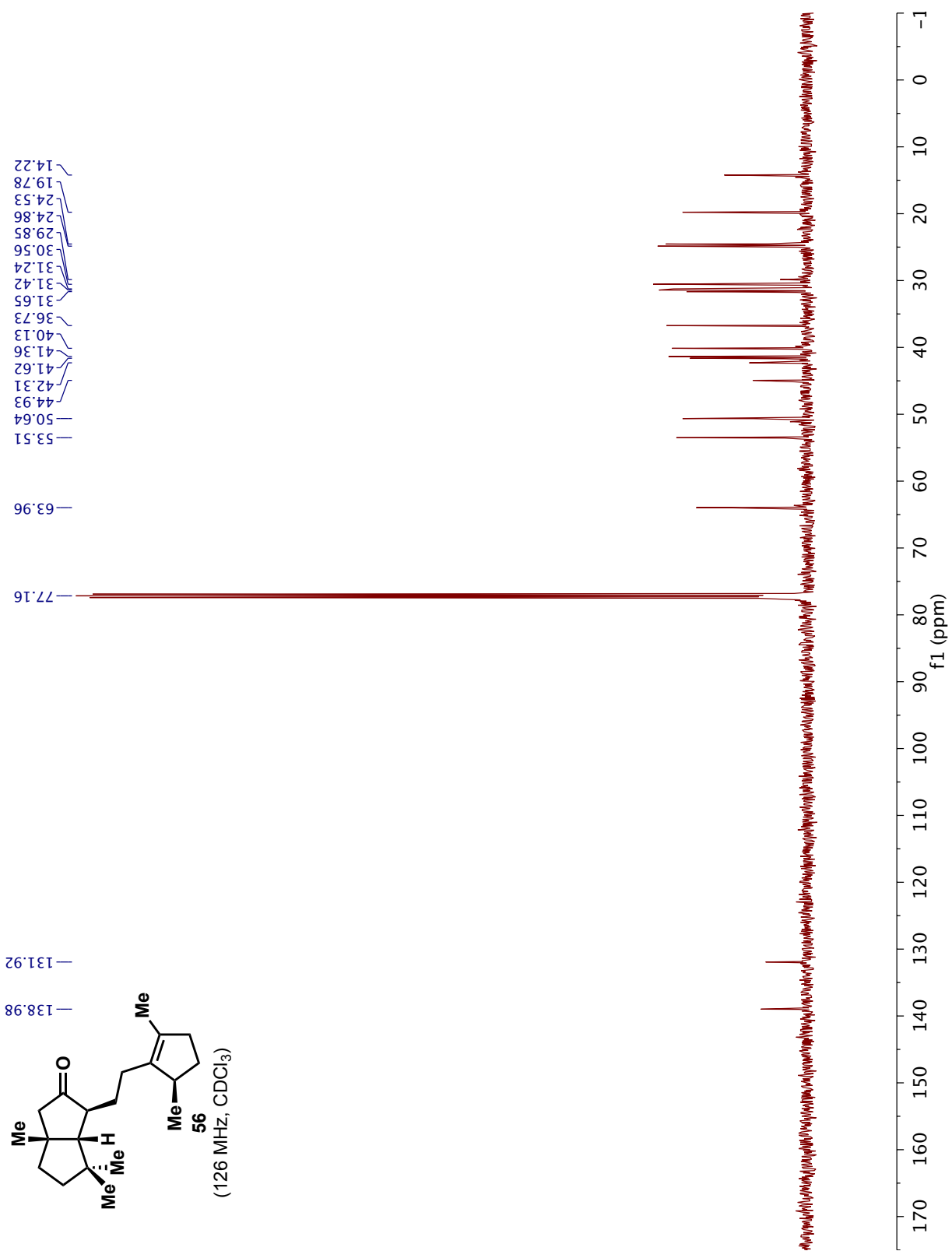


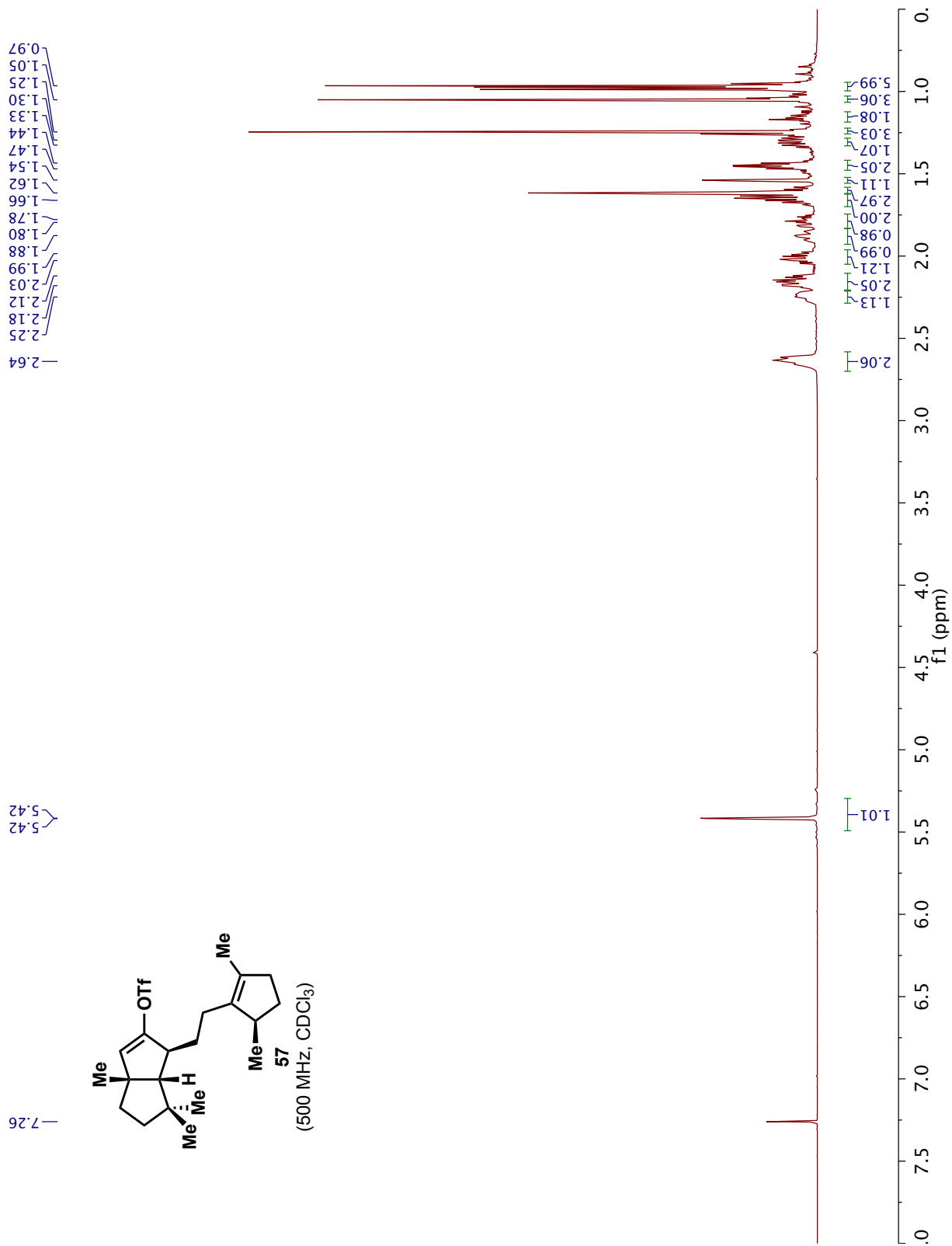
2.11 ^1H and ^{13}C NMR Data

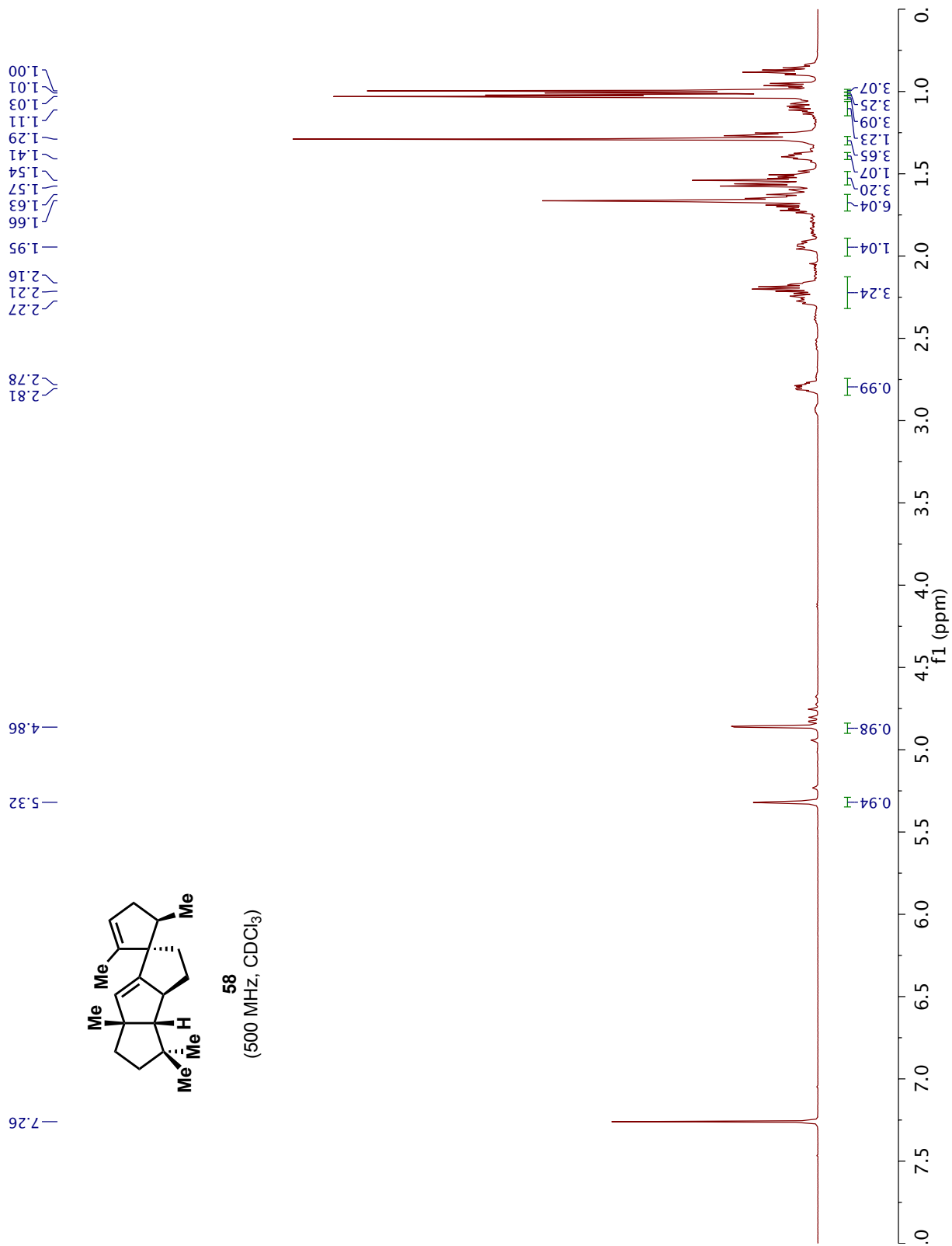


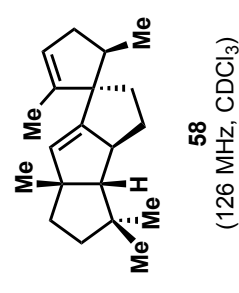
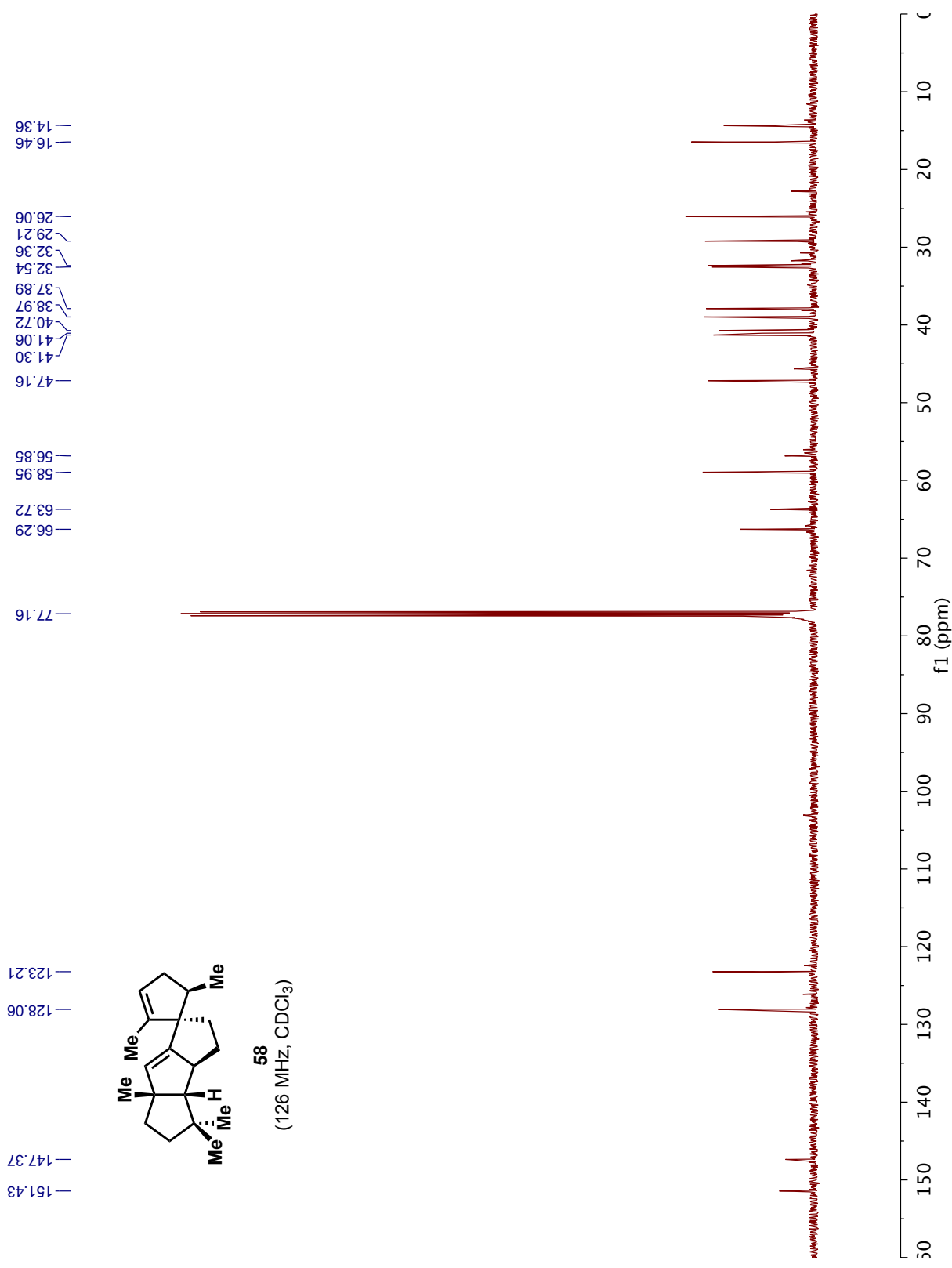


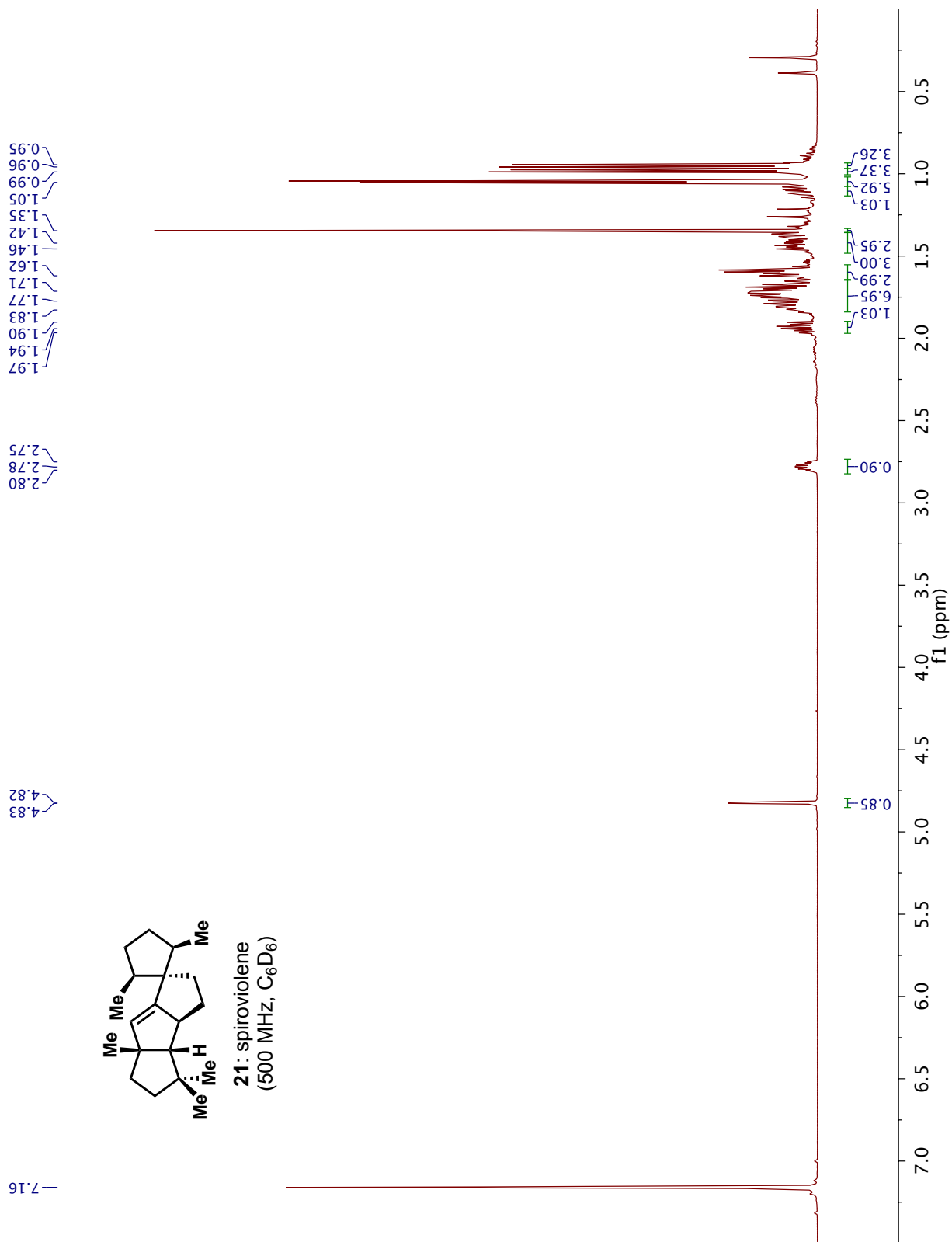


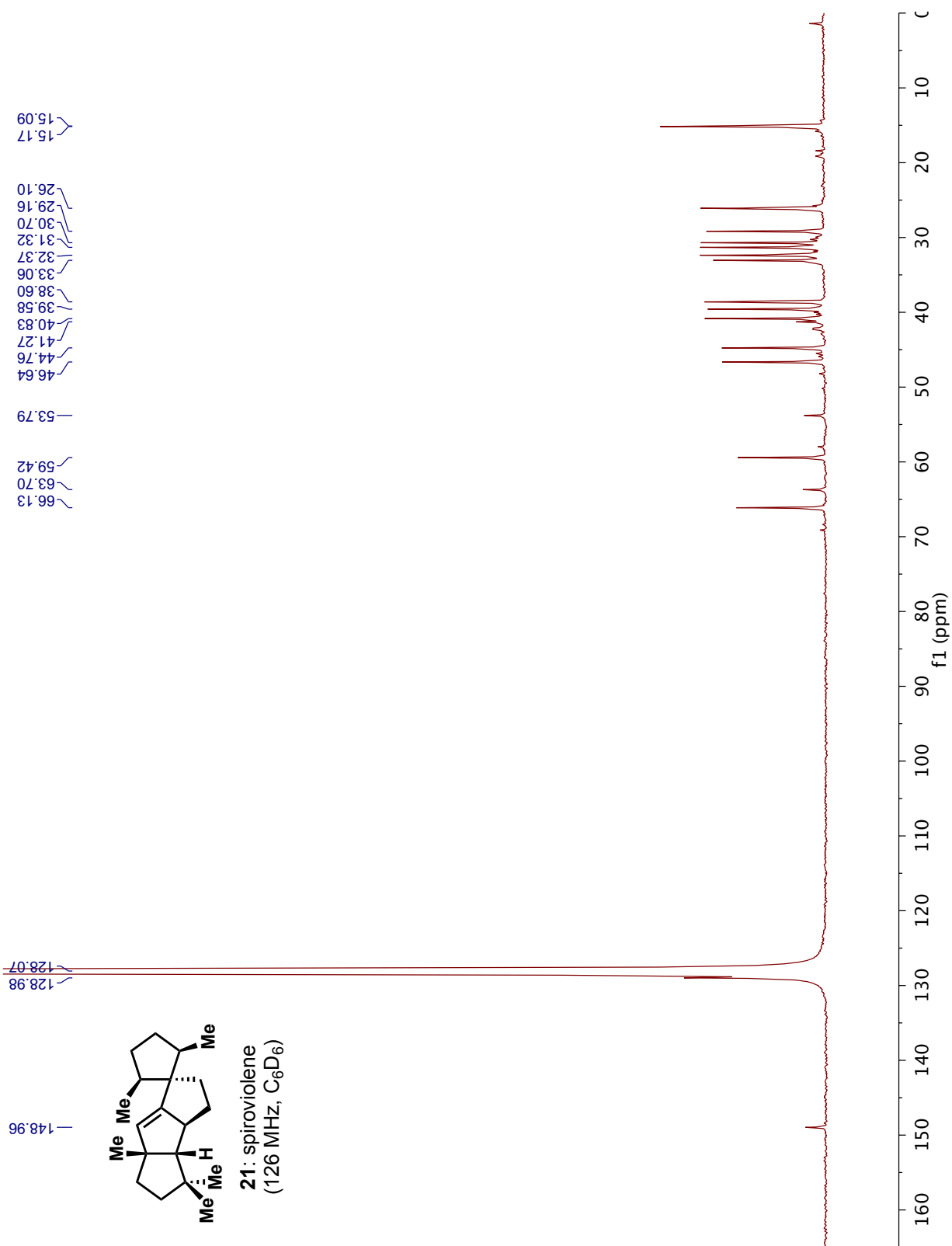


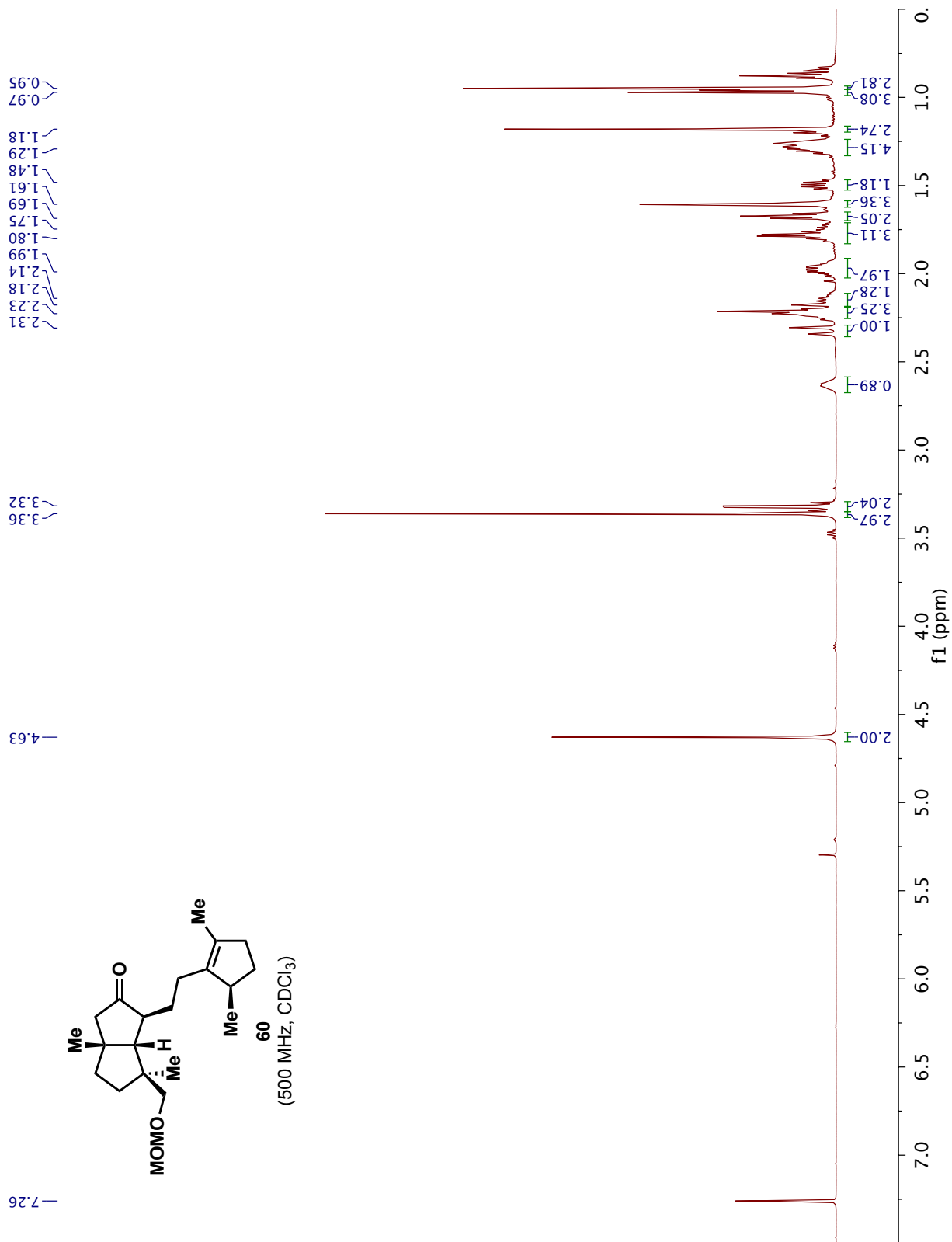


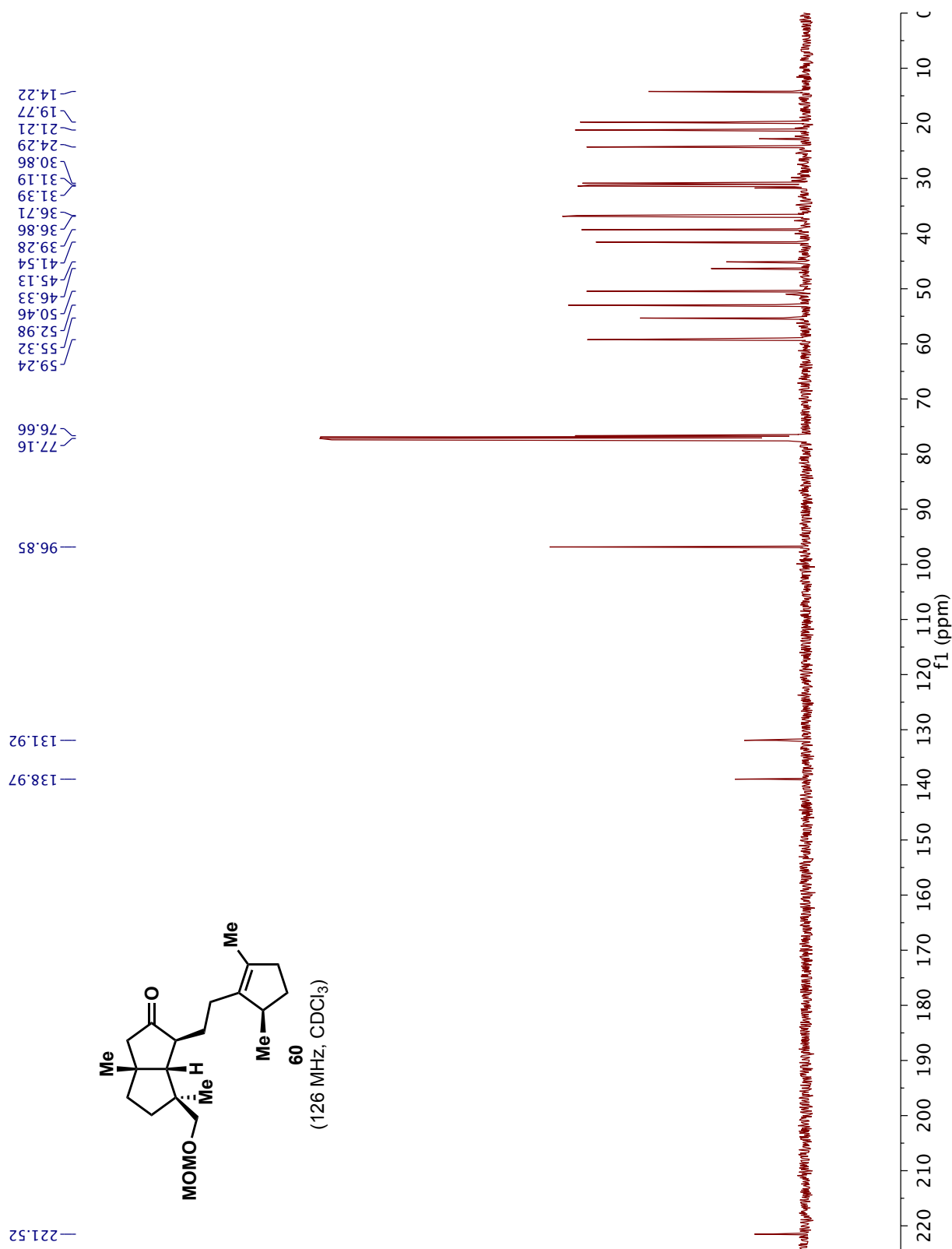


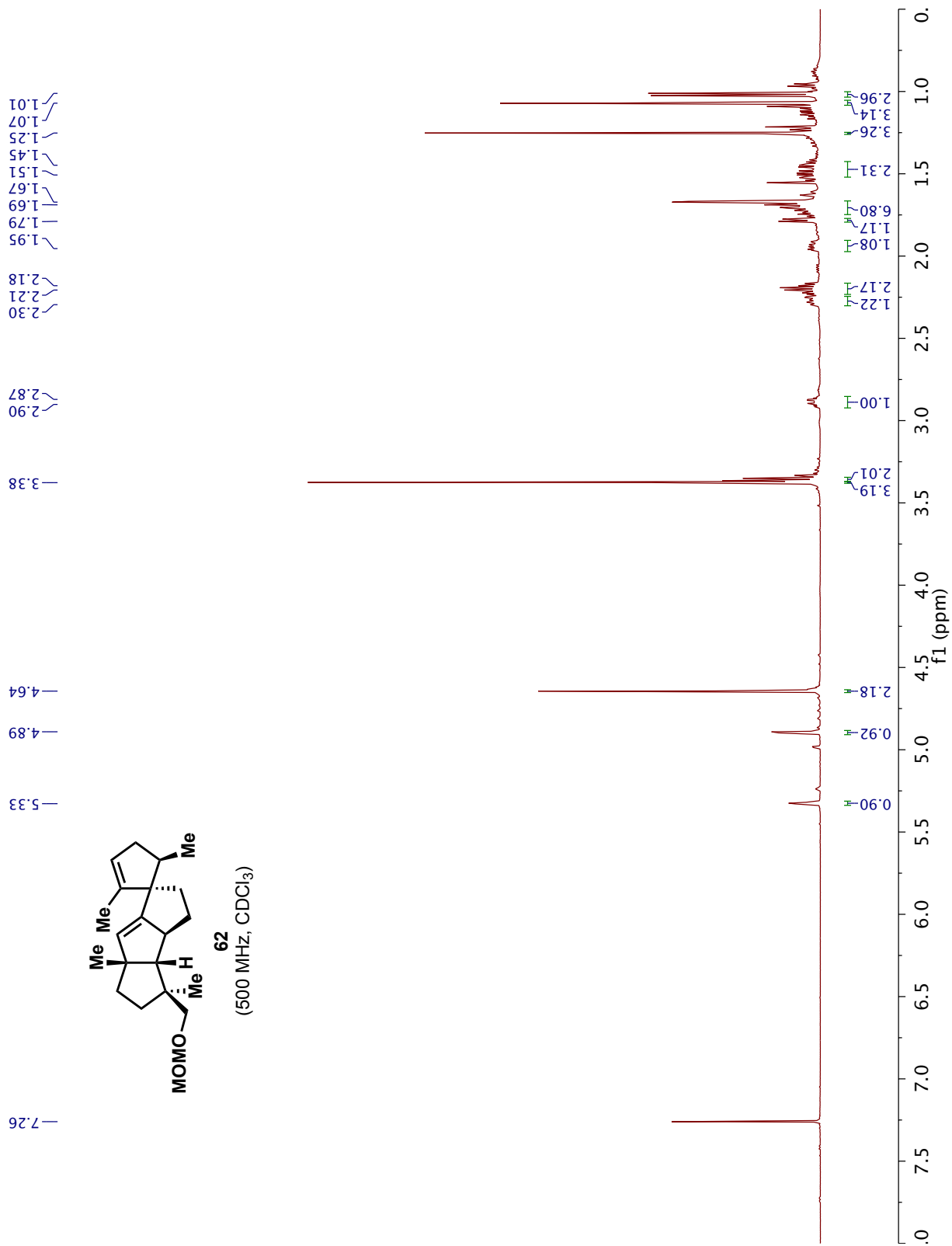


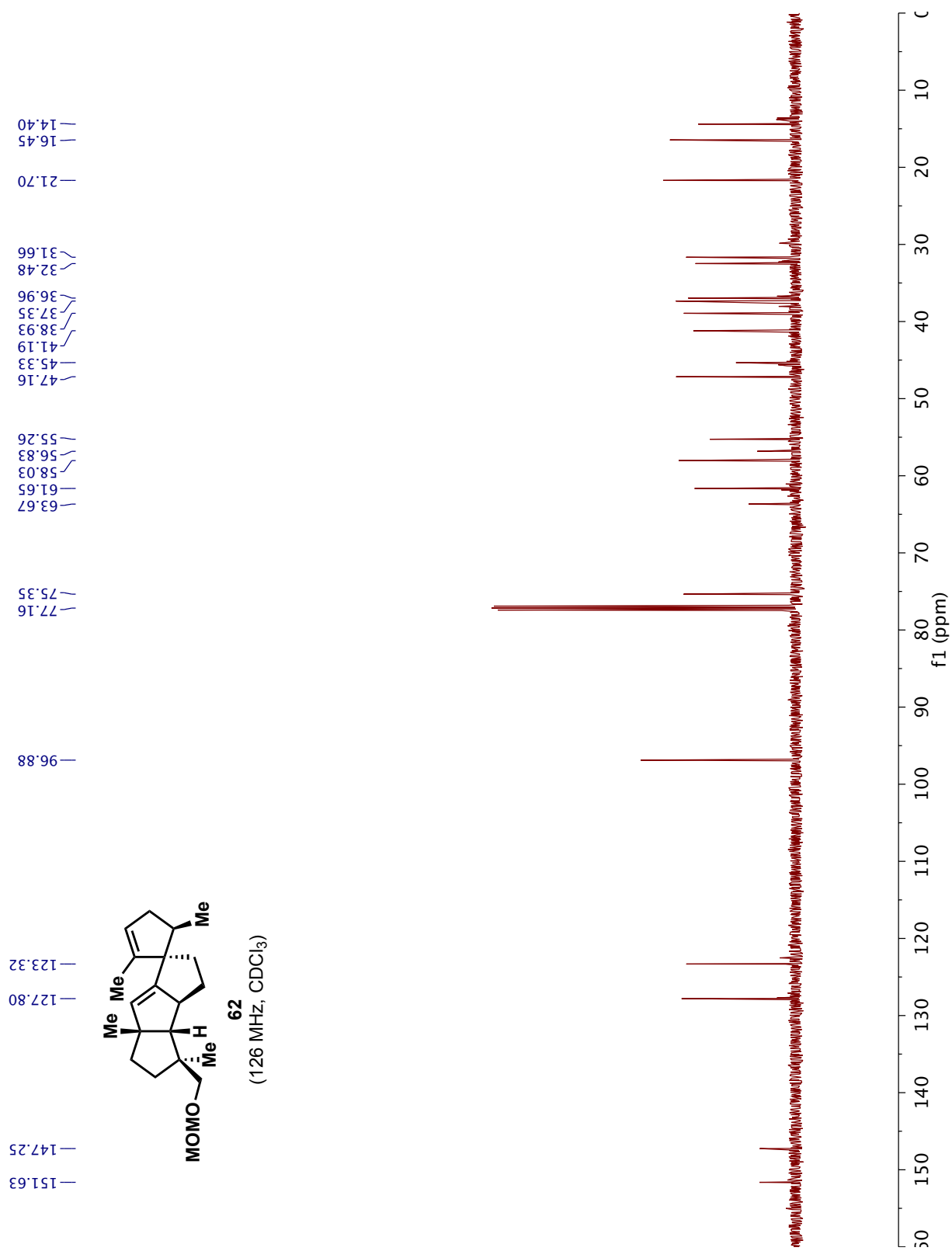


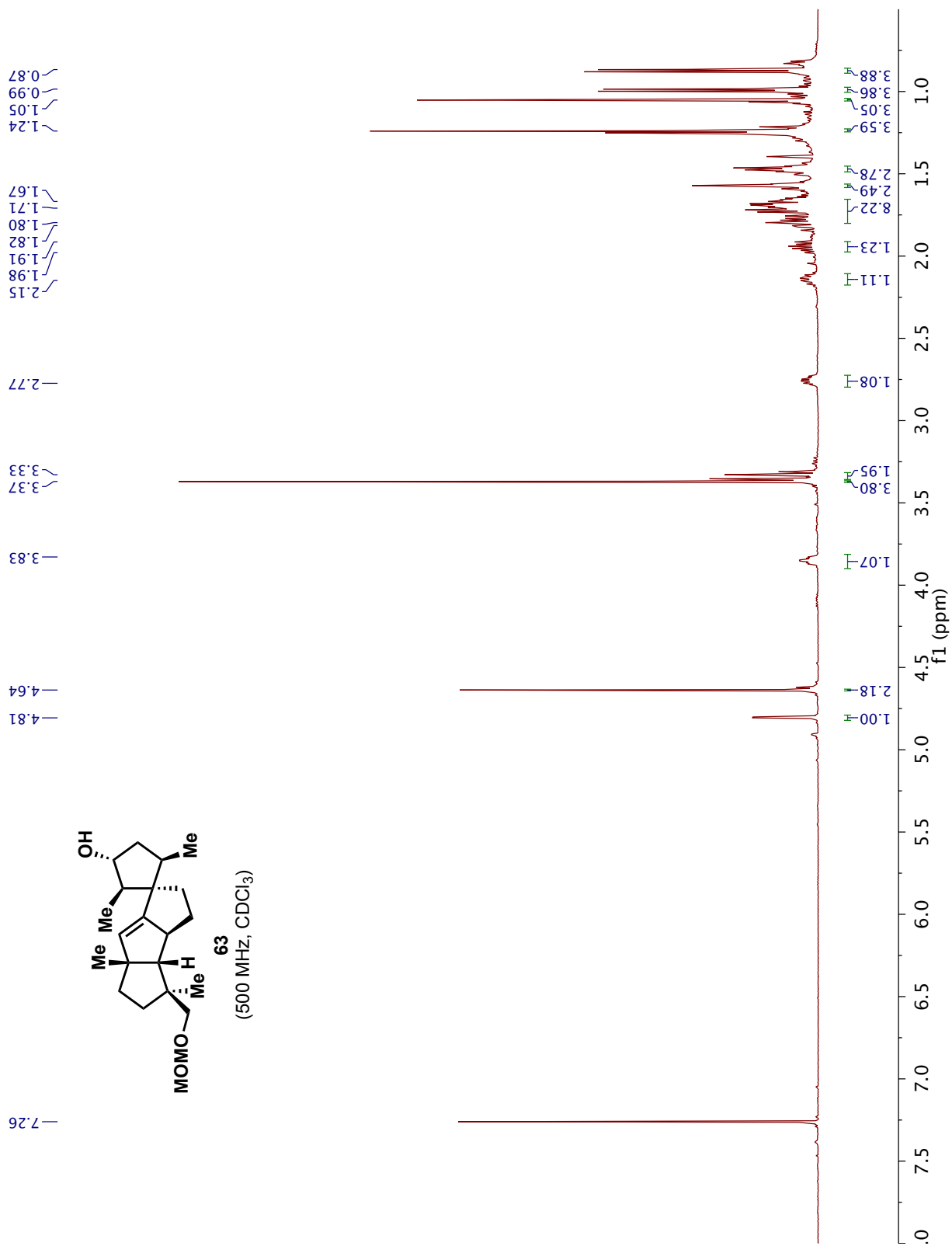


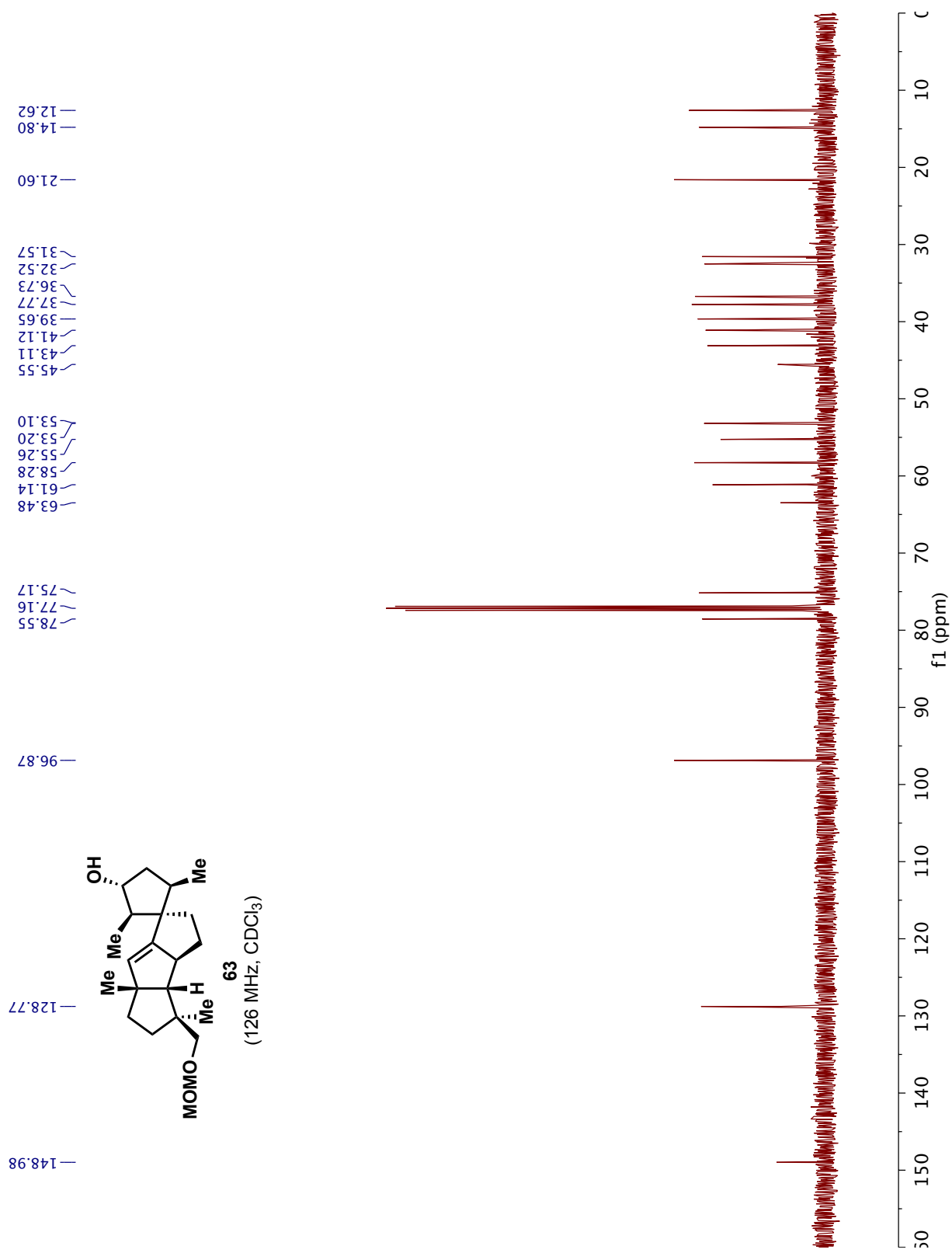


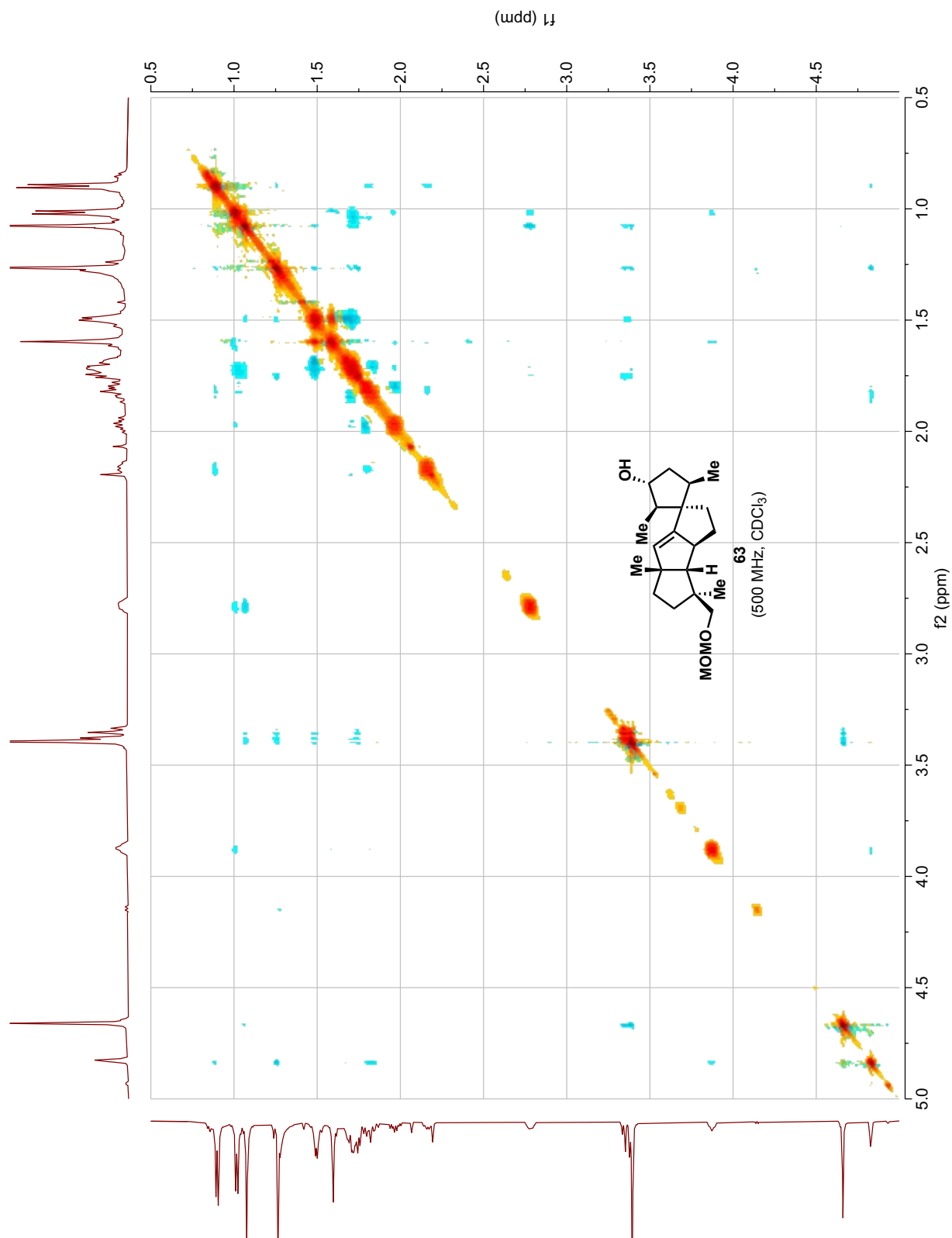


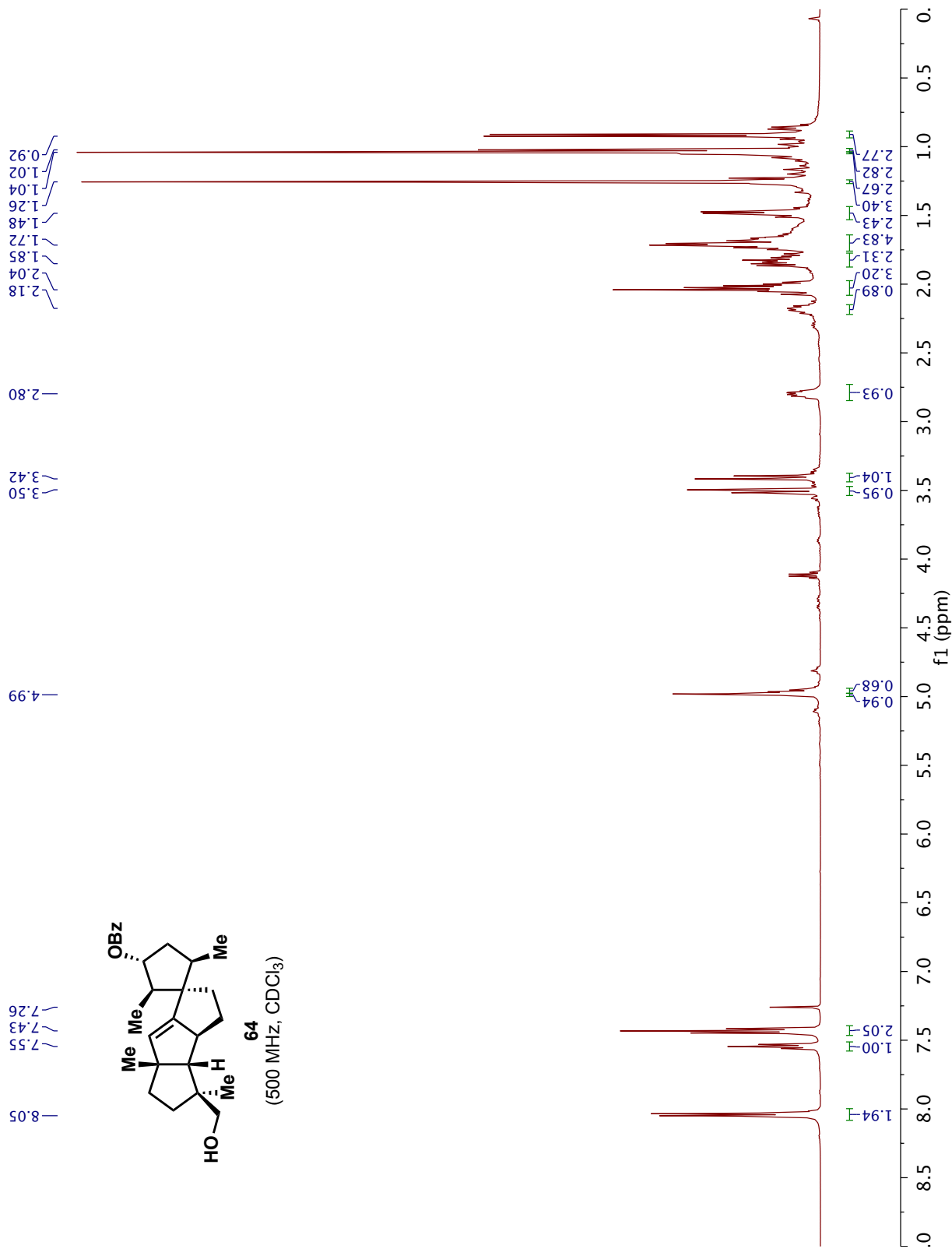


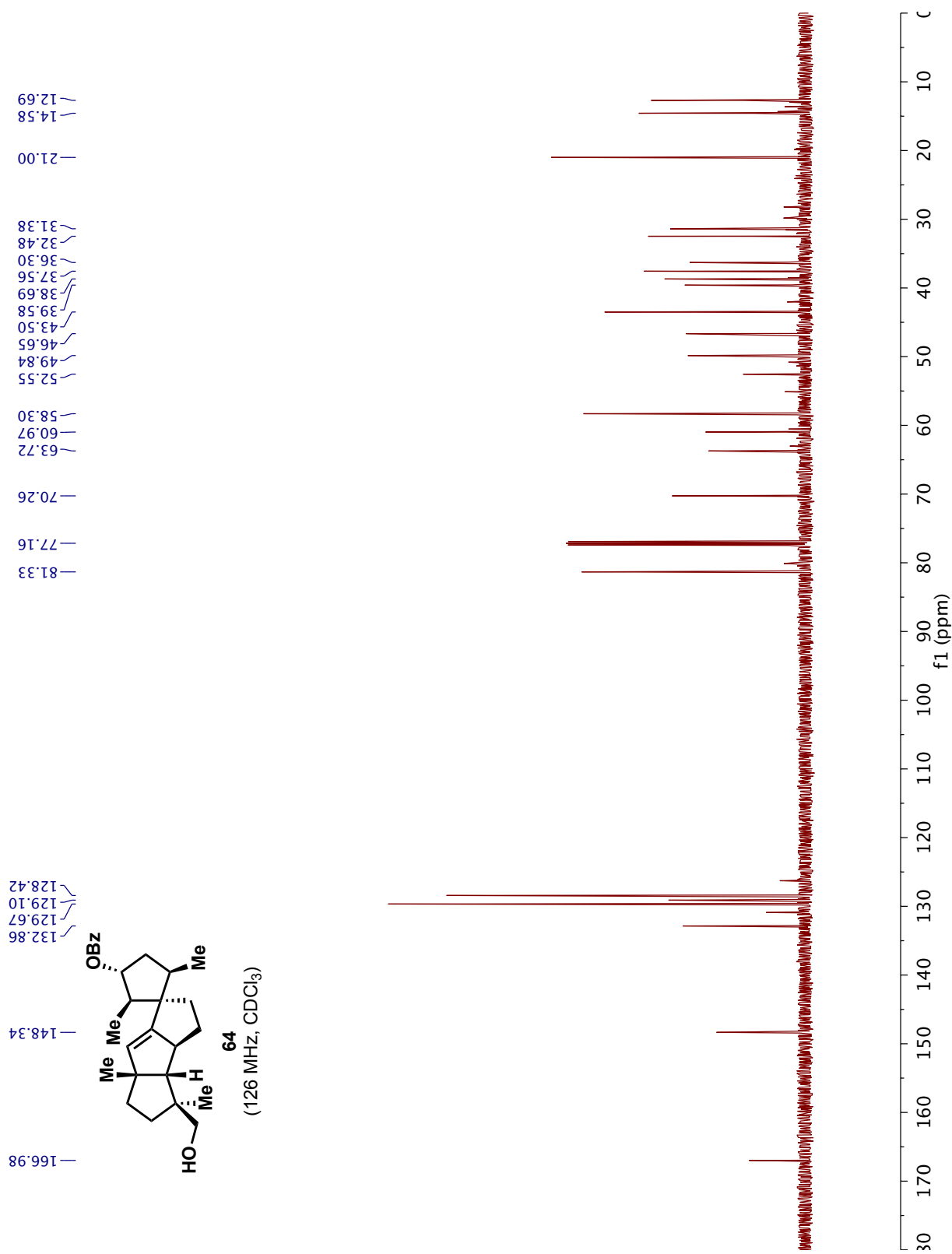


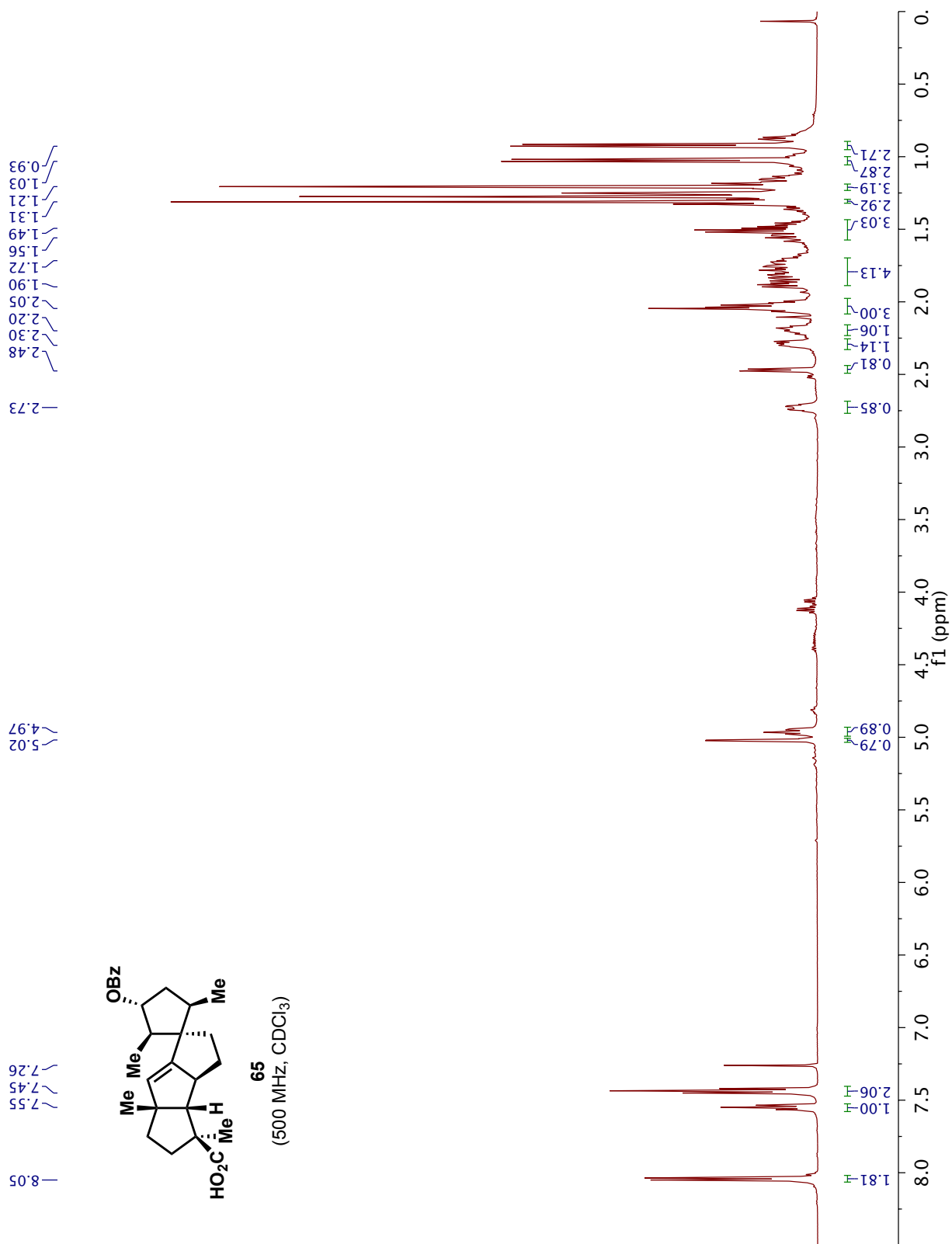


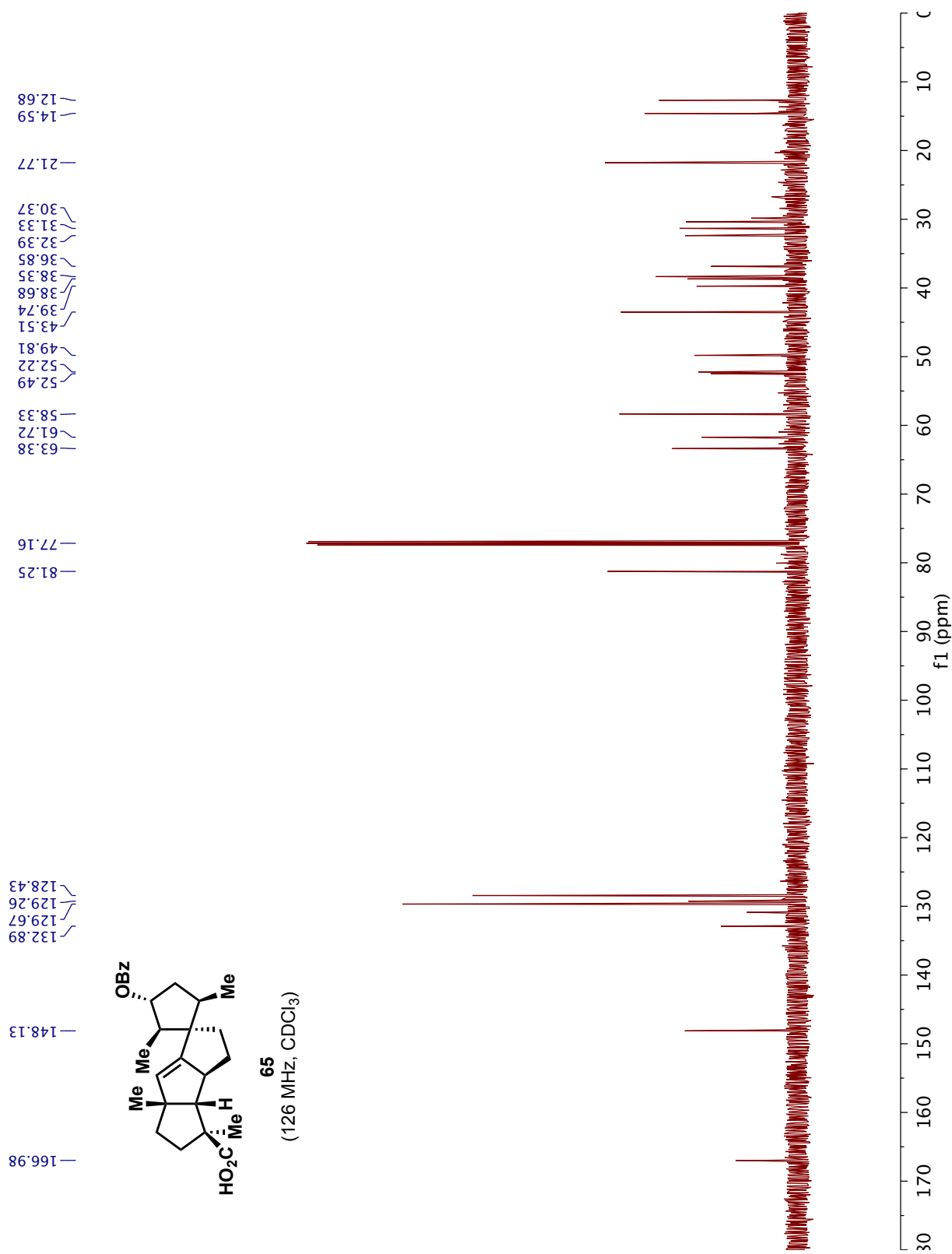


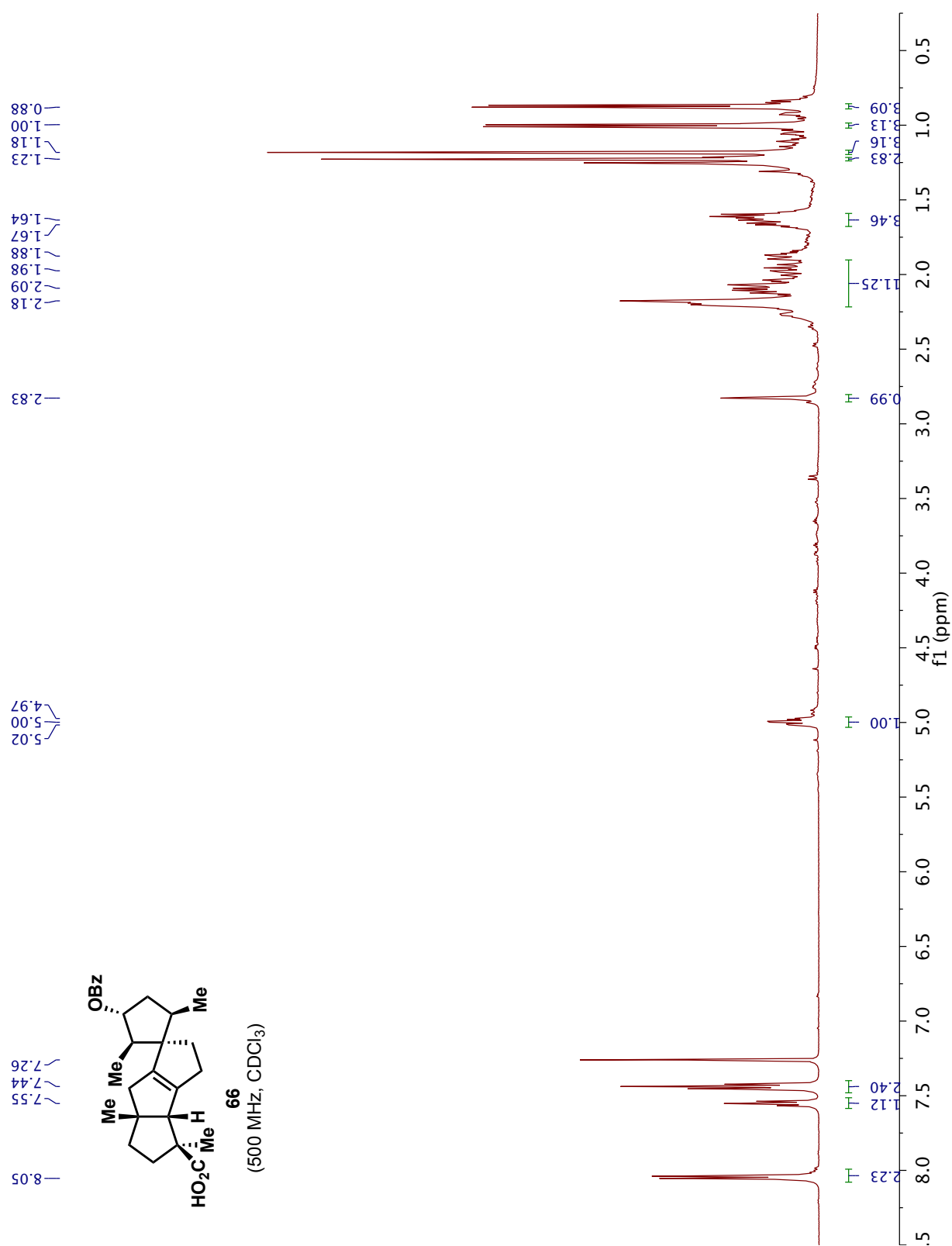


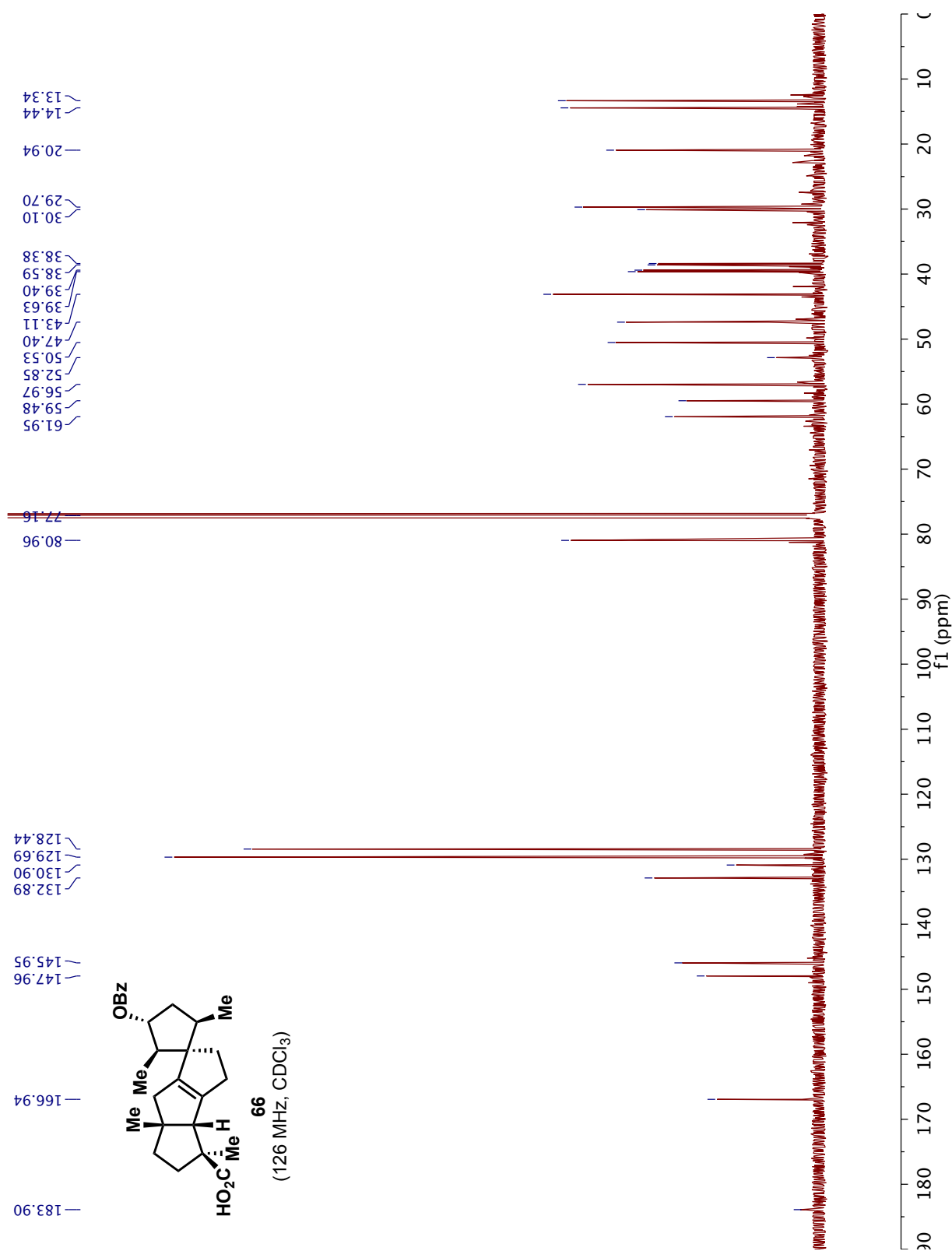


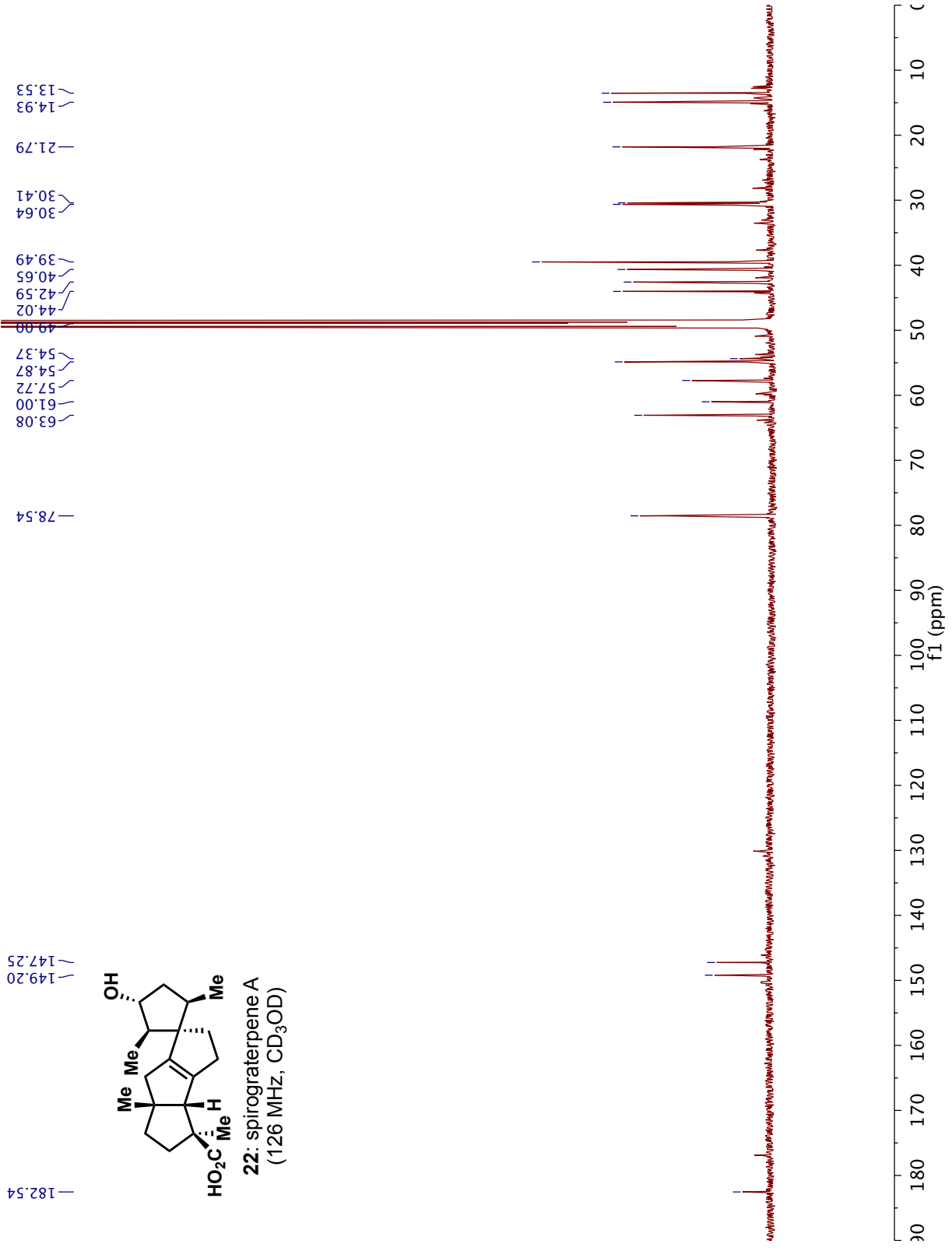


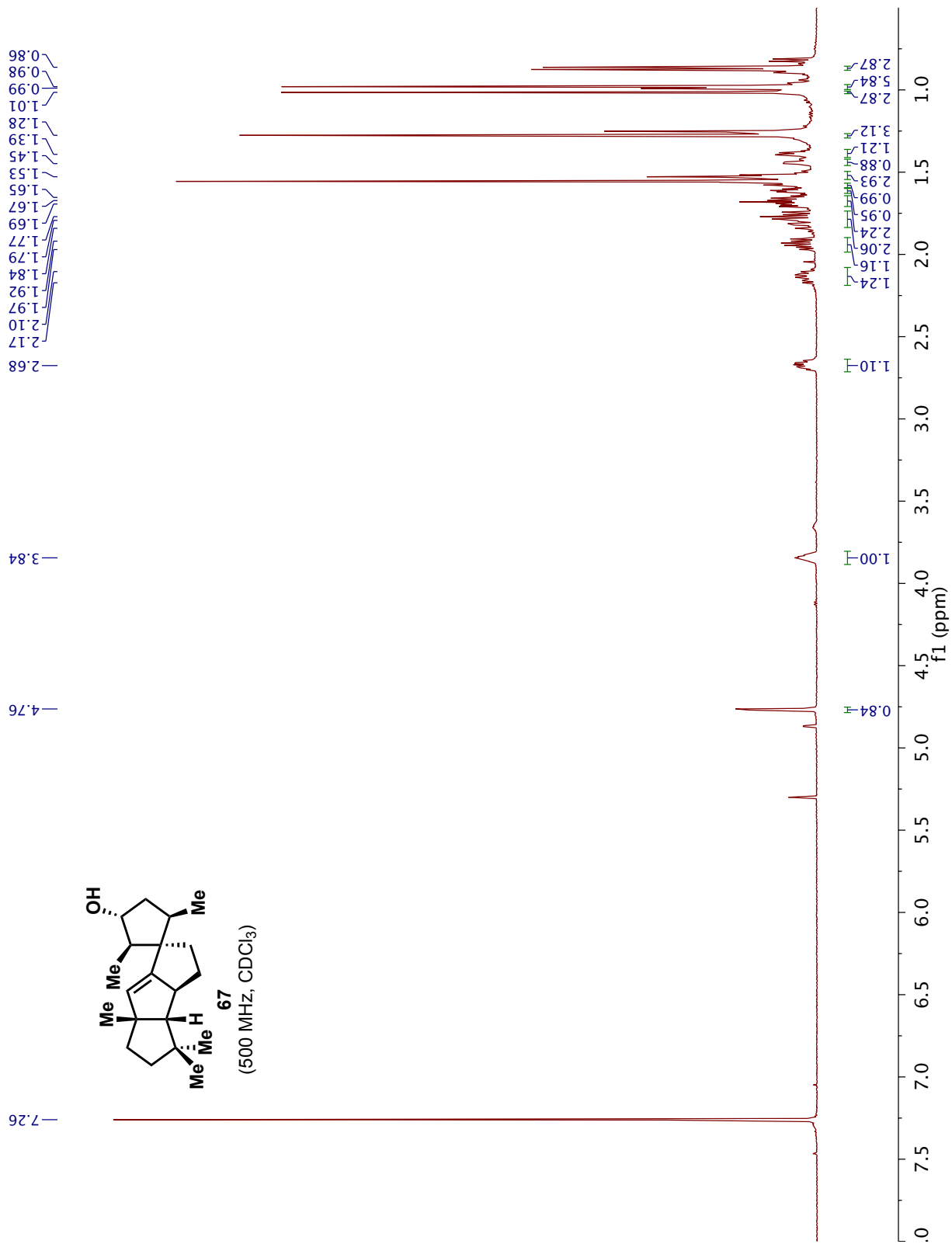


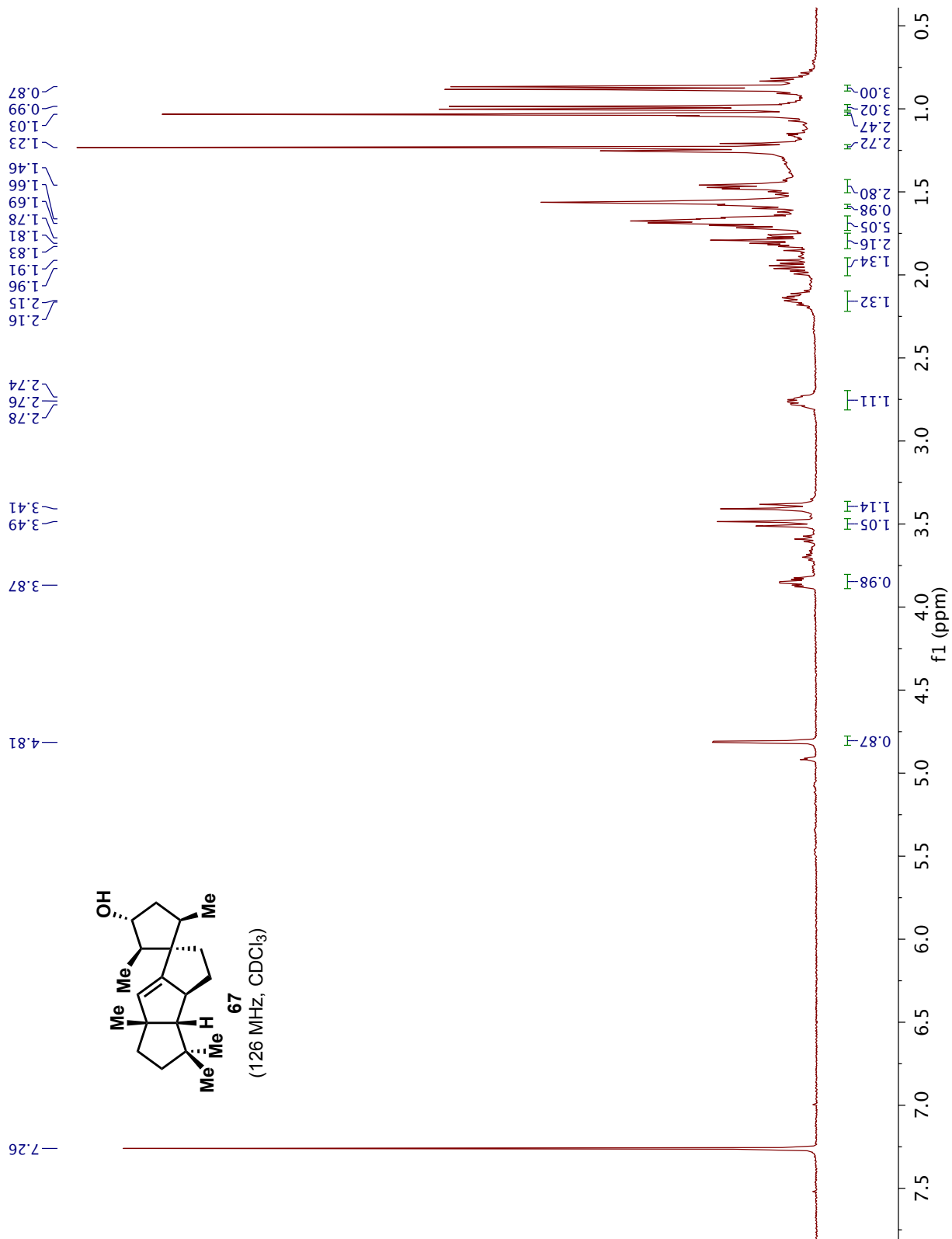


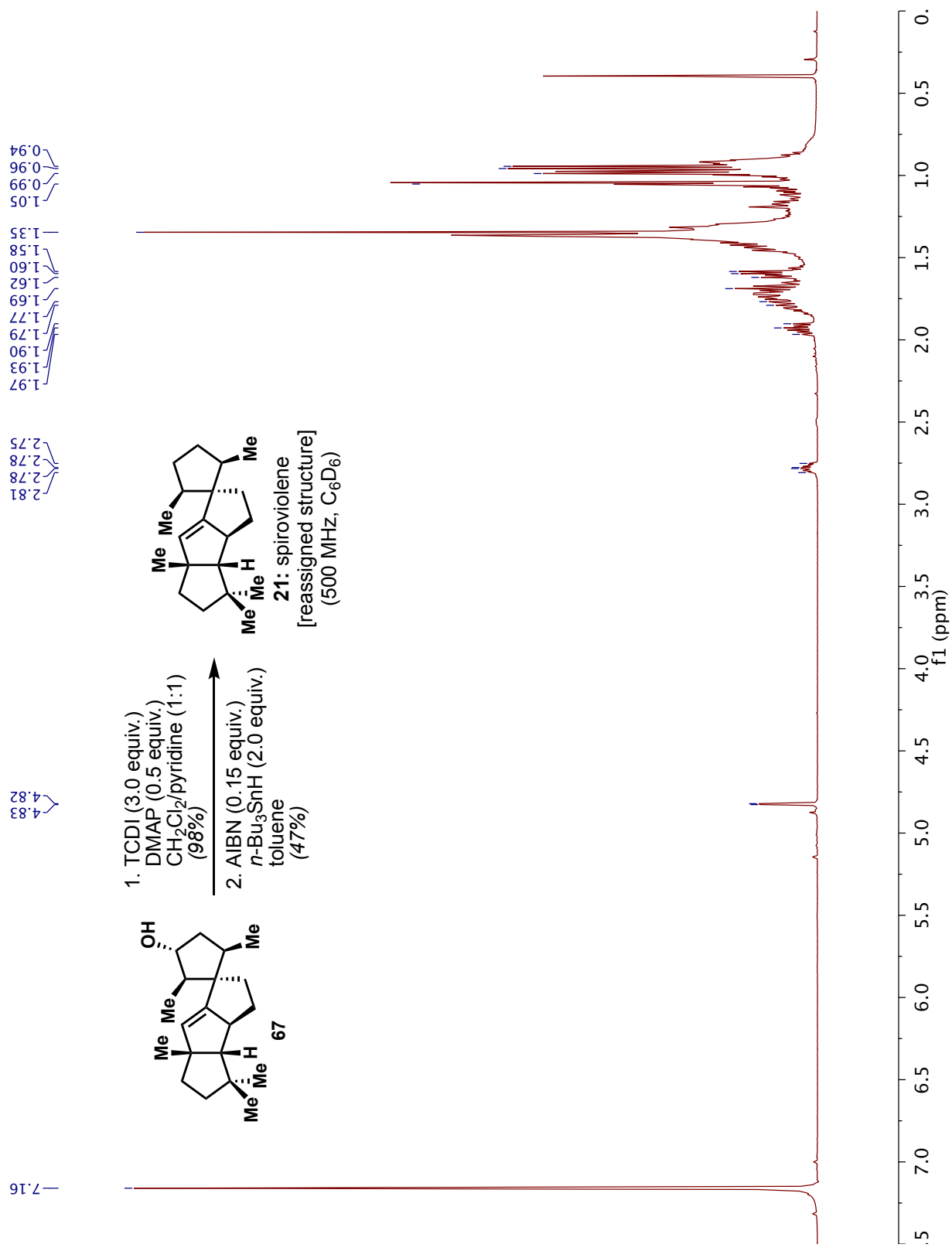






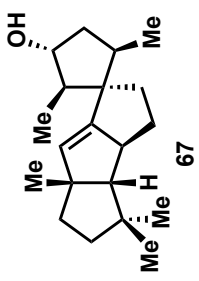


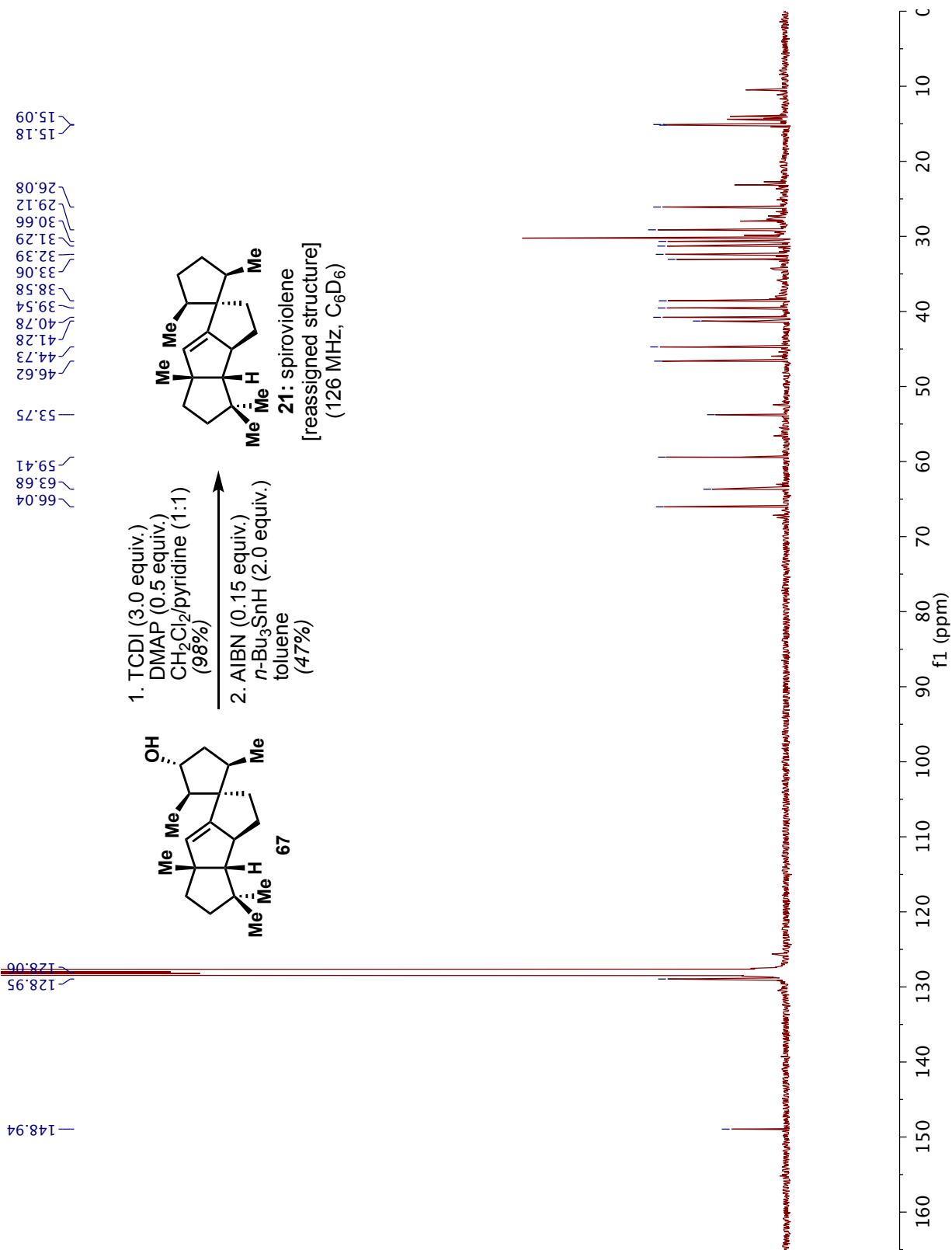


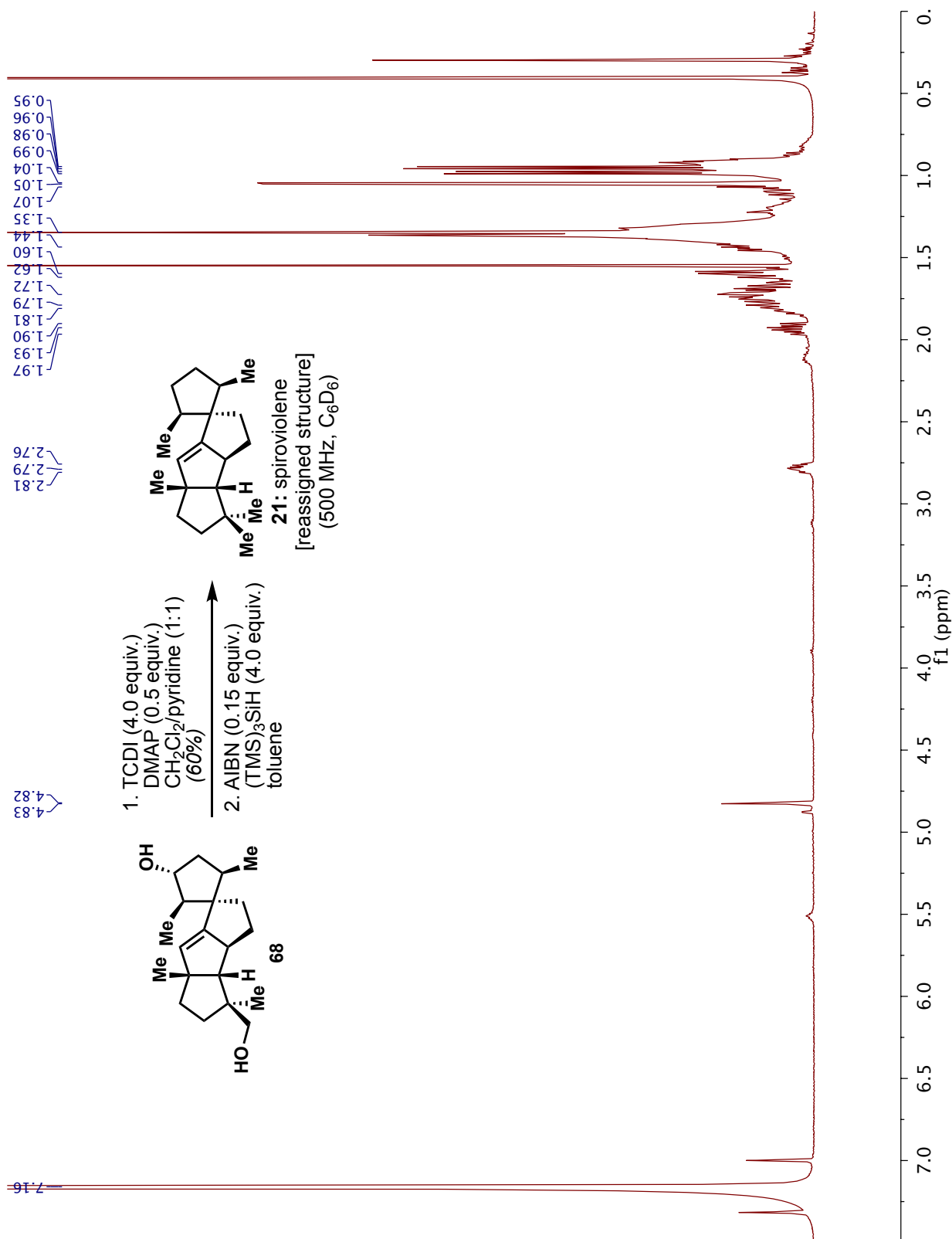


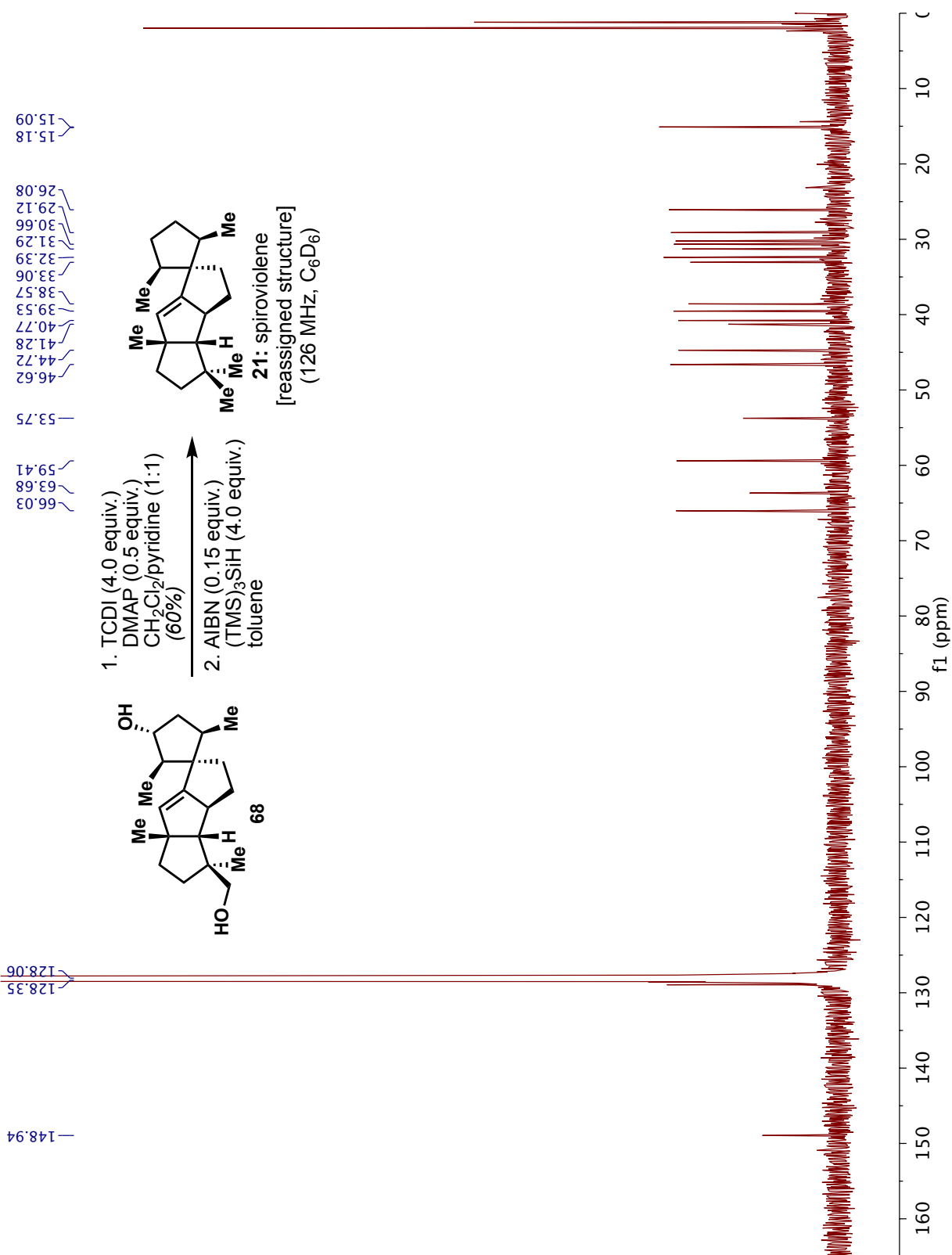
1. TCDI (3.0 equiv.)
 DMAP (0.5 equiv.)
 $\text{CH}_2\text{Cl}_2/\text{pyridine}$ (1:1)
 (98%)

2. AIBN (0.15 equiv.)
n-Bu₃SnH (2.0 equiv.)
 toluene
 (47%)







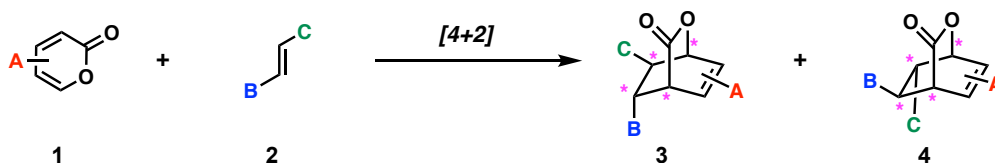


CHAPTER 3

DEVELOPMENT OF AN ASYMMETRIC PYRONE DIELS–ALDER REACTION MEDIATED BY DIENAMINE CATALYSIS

3.1 Introduction

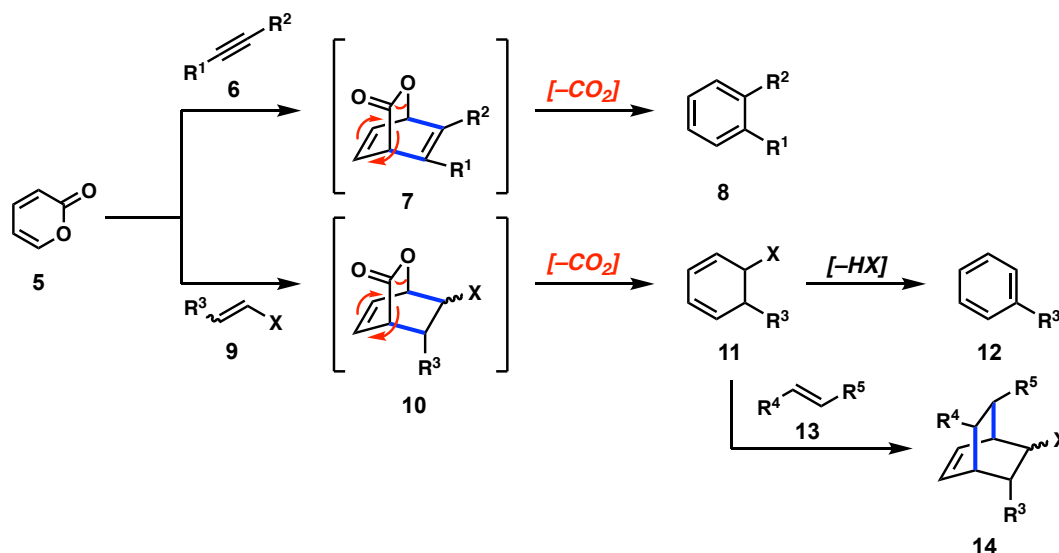
There are a number of chemical transformations that have stood the test of time, which, despite their early discovery, remain a constant in the realm of target molecule synthesis. Of these, the Diels–Alder reaction is arguably one of the most synthetically useful and commonly employed transformations.¹ Unsurprisingly, there have been many variations on the traditional [4+2] cycloaddition, developed as a means to access scaffolds with a high degree of functionalization and structural complexity. One such variation is the use of 2-pyrones as dienes to afford bicyclic lactone adducts (Scheme 3.1).² In fact, the use of these heterocycles as competent dienes was first reported by the reaction’s own namesakes, Otto Diels and Kurt Alder, shortly after their original report.³ With the cycloadducts obtained from this reaction, one not only gains the wealth of relative stereochemical information imparted in the standard [4+2] cycloaddition, but an additional bridged lactone moiety which serves as an important point of derivatization for these heterocycles, either through ring opening of the lactone itself or the loss of CO₂ via the retro [4+2] pathway to access arene-based structures.⁴



Scheme 3.1. Pyrone Diels–Alder reaction.

Of particular note, these heterocycles can often require quite harsh reaction conditions to promote the desired cycloaddition, a result of their inherent aromatic nature. What this meant, as it related to early examples employing 2-pyrones, is that the more complex and stereochemically rich lactone intermediates simply could not survive the conditions used to promote the desired [4+2] cycloaddition and rapidly underwent the subsequent retro-Diels–Alder reaction, extruding CO₂ and providing to the corresponding benzene (**8**) or dihydrobenzene (**11**) species (Scheme 3.2).^{2b} While the products of alkynyl dienophiles, bridged cyclohexadiene **7**, possess too much strain and are themselves not isolable, it was

certainly understood that cycloadducts of the form **10** would be very useful to synthetic chemists. Later examples of pyrone Diels–Alder reactions focused on the use of electronic matching of reaction partners in an effort to lower the HOMO-LUMO energy gap and thereby permit the reaction to take place under milder conditions.



Scheme 3.2. Pyrone Diels–Alder reactions as a means to access arene and bridged frameworks.

3.2 The Pyrone Diels–Alder Reaction in Total Synthesis

Overall, pyrone Diels–Alder reactions have served as the key transformation in a number of total syntheses to date (Figure 3.1), either through the construction of a [2.2.2]-bicyclic lactone or some derivative thereof. Scheme 3.3 presents three examples of the common uses of pyrone Diels–Alder reactions in synthesis: 1) to install the bicyclic lactone as found in the target,⁵ 2) to perform a Diels–Alder/retro-Diels–Alder sequence to access arene frameworks⁶ or provide a new diene for further functionalization,⁷ and 3) to install important relative stereochemistry about the core cyclohexane ring.^{21–33} In the case of chatancin (**17**, Scheme 3.3a), the Maimone group viewed the lactol motif found in the target as coming from an intramolecular pyrone Diels–Alder reaction. Pyrone **23**, accessed in 5 steps from (*l*)-dihydrofarnesol, underwent a thermally promoted intramolecular [4+2] cycloaddition to form

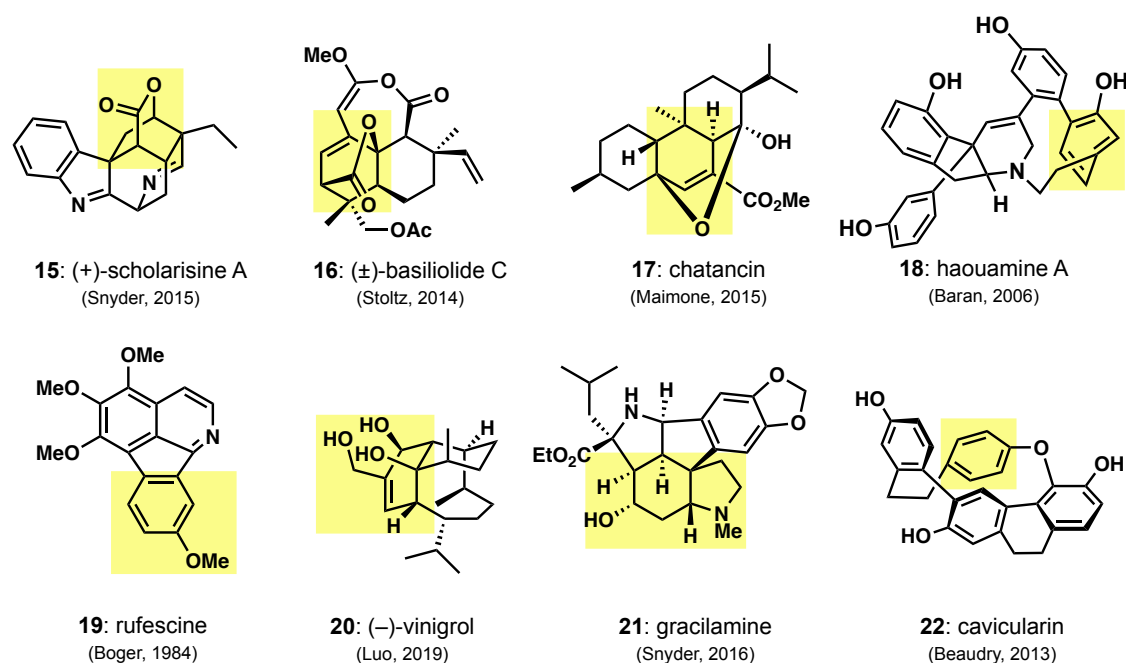
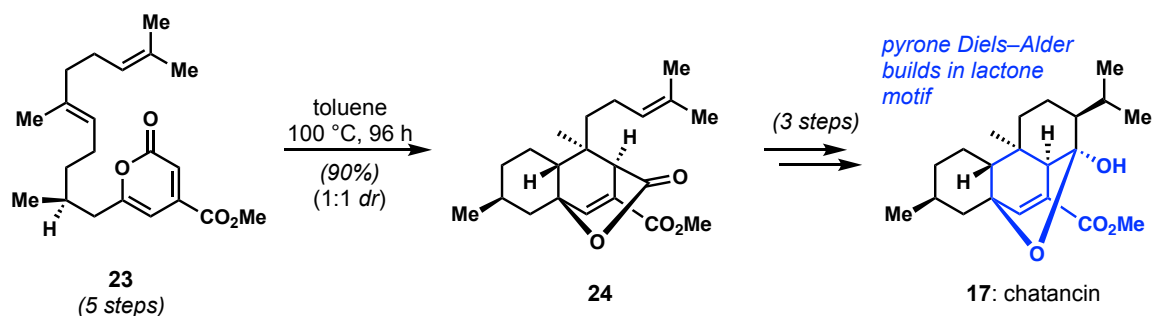


Figure 3.1. Natural products accessed via key pyrone Diels–Alder reactions.

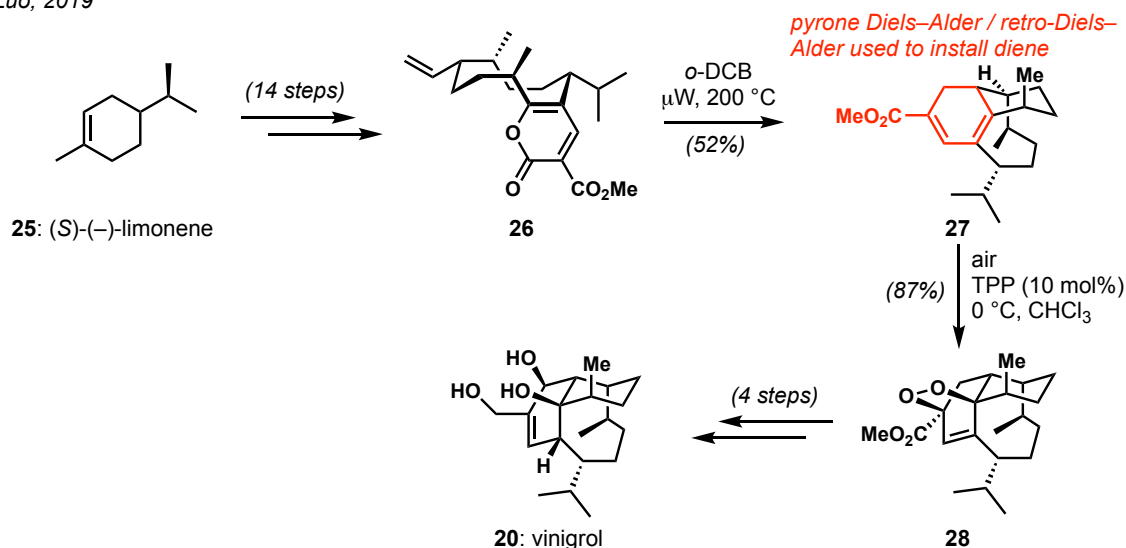
decalin **24** in a 1:1 *dr*.^{5d} From here, three additional steps were needed to introduce the Diels–Alder reaction served to construct much of the carbocyclic frame of the target as well as establish the bicyclic lactone, making this transformation integral to the brevity of this approach. Such a strategy has also been applied in the total synthesis of the basiliolide/transtaganolide family of natural products by the Stoltz group.^{5a,5c} A more common use of this transformation, especially in earlier examples, is the sequential Diels–Alder/retro-Diels–Alder process, which can either be used to construct arene motifs or to form a diene that can serve as a point of further elaboration. The latter was the tactic employed by the Luo group in their synthesis of vinigrol (**20**).^{7b} Starting from chiral pool materials, Luo *et al.* were able to access 3-carbomethoxy-2-pyrone derivative **26** in 14 steps. Under microwave conditions, the macrocycle performs a transannular Diels–Alder reaction to establish the bicyclic lactone, which extrudes CO₂ to produce electron poor diene **27**. The newly formed diene serves a vital role by providing a functional handle through which to introduce the bridgehead alcohol, in this case via a Diels–Alder reaction with singlet oxygen to form *endo*-peroxide **28**. And so, by using the 2-pyrone derivative (**26**) as a competent diene partner, Luo and co-workers were able

to access vinigrol (**20**) in a concise and scalable manner (20 steps from commercial materials), with the last step of the sequence conducted on gram-scale.

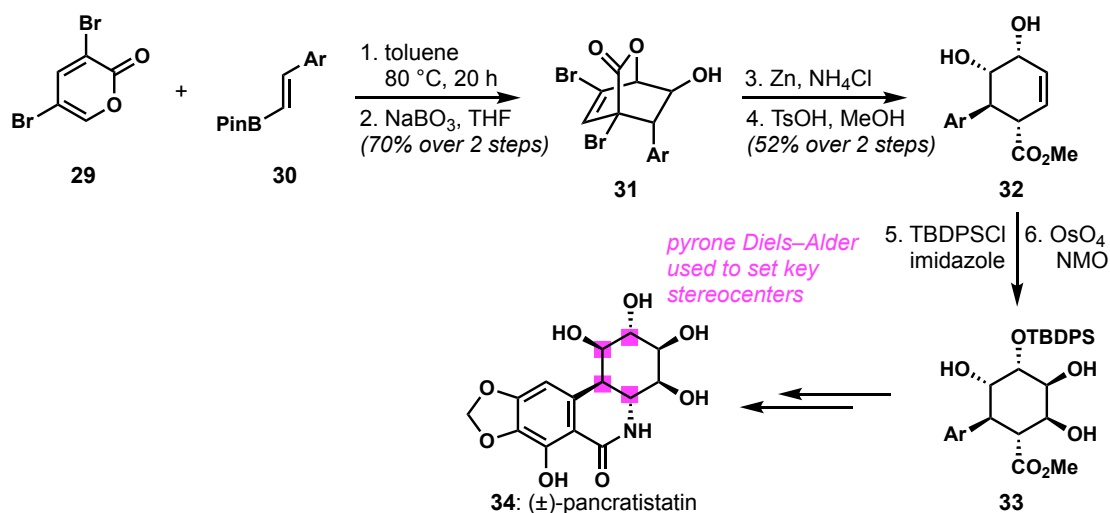
a) Maimone, 2015



b) Luo, 2019



c) Cho, 2013

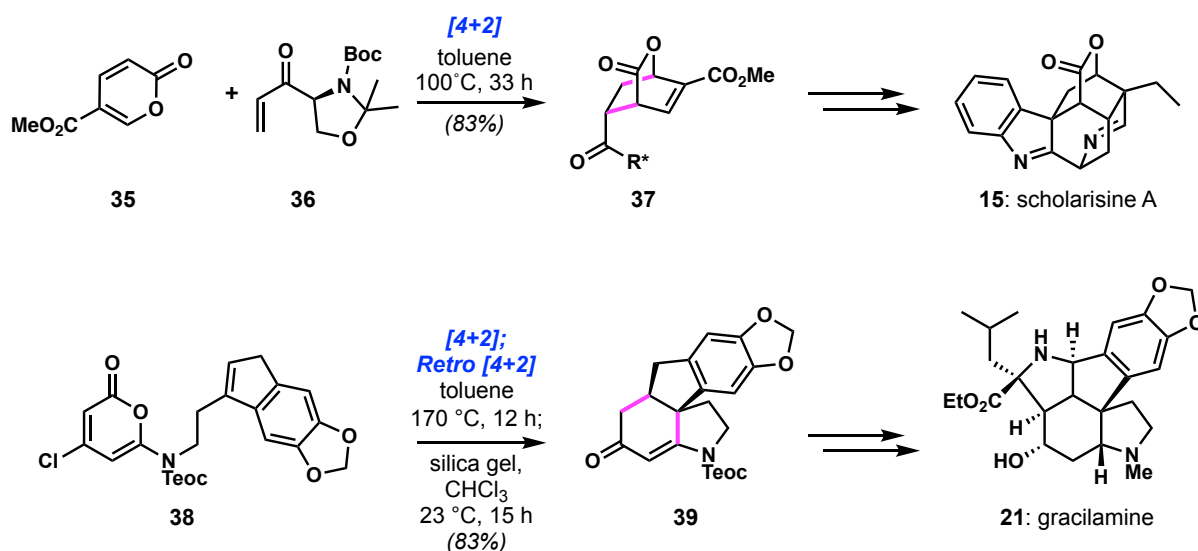


Scheme 3.3. Pyrone Diels-Alder reactions used in total synthesis to (a) install a bicyclic lactone, (b) form a diene for further functionalization and (c) set key relative stereochemistry.

An alternate use of this reaction is to take advantage of the wealth of relative stereochemistry obtained. While this may be true of all [4+2] cycloadditions, the use of a 2-pyrone species as the diene has the added advantage of the newly formed lactone as a further functional handle. This strategy has granted access to several members of the *Amaryllidaceae* alkaloids and represents a large part of the research program developed by Cheon-Gyu Cho.^{8,9} A representative example is the synthesis of (±)-pancratistatin (**34**) and (±)-*epi*-pancratistatin from 3,5-dibromopyrone (**29**).^{8g} It should be mentioned that **29** is an ambident diene, reacting efficiently with both electron rich and electron poor dienophiles.¹⁰ A Diels–Alder cycloaddition of **29** with styrenyl borane **30**, followed by oxidation of the alkyl borane with NaBO₃ provides lactone **31**. Reduction of both the vinyl and bridgehead bromide atoms and subsequent acid catalyzed lactone opening produces **32**. At this stage the pyrone Diels–Alder reaction had set four of the six stereocenters found within the target, one of which would then be used to introduce the remaining two. Protection of the allylic alcohol as the TBDPS ether then forces the Upjohn dihydroxylation to take place stereospecifically to afford *cis*-diol **33**. Additional transformations, including inversion of one of the carbinol centers, a Curtius rearrangement, and lactam formation, then provides pancratistatin (**34**) in a racemic fashion (Scheme 3.3). This example elegantly illustrates the benefit of using the 2-pyrone diene to introduce relative stereochemistry, whereby many of the necessary centers were introduced in the opening steps, while the remaining ones were formed using existing stereocenters. At the same time, many of the requisite functional groups, such as the methyl ester for the Curtius rearrangement, the olefin necessary for dihydroxylation, and the hydroxyl groups, were all fashioned by the opening cycloaddition.

Our group has also made significant contributions to the field of pyrone Diels–Alder reactions. The first of two examples is the total synthesis of scholarisine A (**15**), which utilized a pyrone Diels–Alder reaction as one of the opening steps, in order to install the bicyclic lactone

core of the natural product.^{5b} Here, the dienophile (**36**) was prepared from a chiral amino acid precursor in order to render the reaction diastereoselective (3:1 *dr*). Of note, despite the lack of electronic matching between the diene and dienophile, the reaction proceeds under comparatively mild conditions (100 °C, 33 h). Lactone **37** then served as the core around which



Challenges:

- often require high temperature or pressure
- avoiding Retro [4+2] products
- enantioselectivity

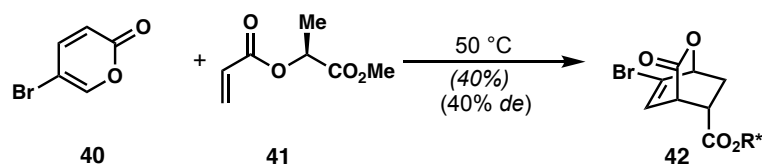
Scheme 3.4. Previous work from the Snyder group in pyrone Diels–Alder chemistry.

the remainder of the molecule was constructed, thereby granting access to **15**. In addition to this synthesis, our group has developed a method utilizing a one-pot pyrone Diels–Alder/retro-Diels–Alder sequence to prepare indoline and hydroindoline scaffolds.^{7a} Scheme 3.4 demonstrates this approach with pyrone **38**. Here an intramolecular pyrone Diels–Alder reaction, wherein the dienophile is tethered through an amine linkage, provides the bicyclic lactone under forcing conditions (170 °C, 12 h), which undergoes a subsequent retro-[4+2] process to afford the intermediate vinyl chloride species. This is then hydrolyzed in one-pot to the corresponding enone **39**. Having prepared half of the central rings in a single step, **39** could then be carried forward to gracilamine (**21**) in 14 steps.

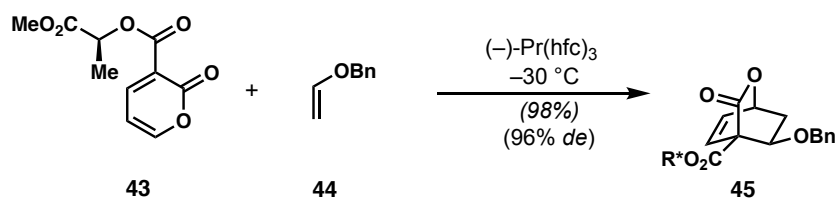
While these examples demonstrate the clear utility of the pyrone Diels–Alder reaction, they also present common challenges. More specifically; 1) both transformations require elevated temperatures for a prolonged period of time to promote the desired reaction, 2) although not observed in these examples, as mentioned above, such conditions often result in the retro-Diels–Alder process, and 3) in both cases enantioselectivity was a challenge. In the synthesis of **15**, a chiral center, which was later ablated, had to be installed in the dienophile to effect a diastereoselective reaction, while in the case of gracilamine (**21**), the developed method was completely racemic (though conceptually, the placement of some chiral center along the tether might afford stereocontrol). Based on this, we sought to develop a pyrone Diels–Alder reaction which would not only take place under mild conditions, but could be conducted in a catalytic, asymmetric fashion. We also hoped that the method would allow access to lactone structures distinct from those already found in the literature.

3.3 Asymmetric Pyrone Diels–Alder Reactions

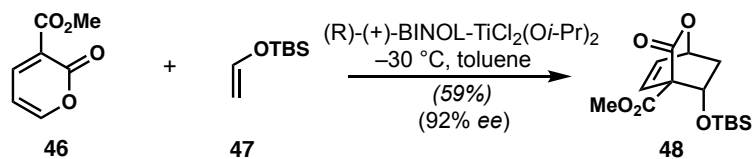
Posner, 1992



Posner, 1992

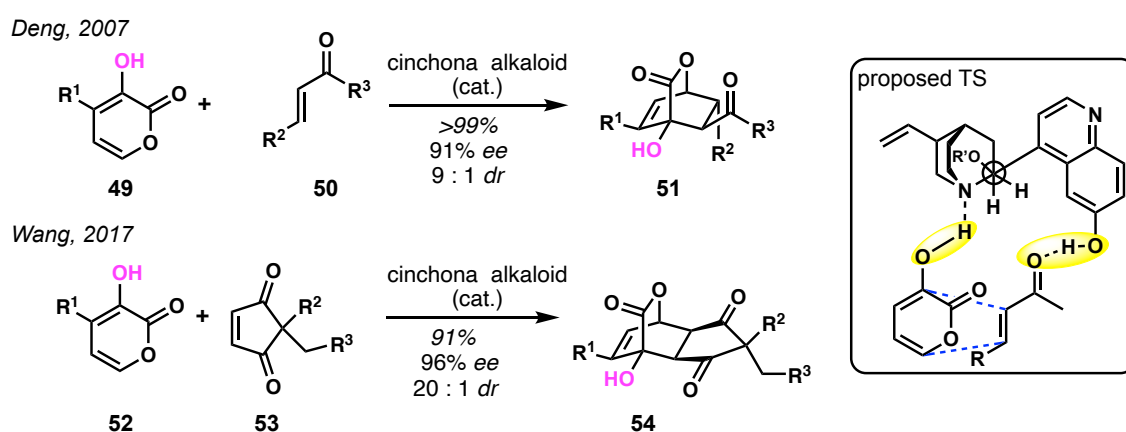


Posner, 1994



Scheme 3.5. Initial approaches to controlling absolute stereochemistry in the pyrone Diels–Alder reaction.

Asymmetric pyrone Diels–Alder reaction are known in the literature, however examples are quite limited. Initial work from Posner focused on the use of chiral auxiliaries placed on either the diene or dienophile to afford several bicyclic lactone products in moderate to good diastereoselectivity (Scheme 3.5).¹¹ One of the first catalytic asymmetric variants, also from the Posner group, used electron poor pyrone **46** and TBS vinyl ether (**47**) to produce cycloadduct **48**.¹² Although this served an important role in the asymmetric synthesis of the vitamin D precursor calcitriol, the scope was extremely limited with only modest enantioselectivity.¹³ Much later the Deng group was able to develop a more general asymmetric normal electron-demand pyrone Diels–Alder reaction. Building off of previous work published by the Okamura group,^{11c,14} Li Deng demonstrated that 3-hydroxypyrone derivatives (**49**) can undergo [4+2] cycloadditions with electron poor dienophiles (**50**) in an asymmetric fashion (Scheme 3.6).¹⁵ Here, the asymmetry is induced via dual hydrogen bonding activation of the diene and dienophile by a cinchona alkaloid derivative. This work was furthered by the Wang group, who employed a similar cinchona alkaloid-based catalyst in the desymmetrization of cyclopentadienones (**53**).¹⁶

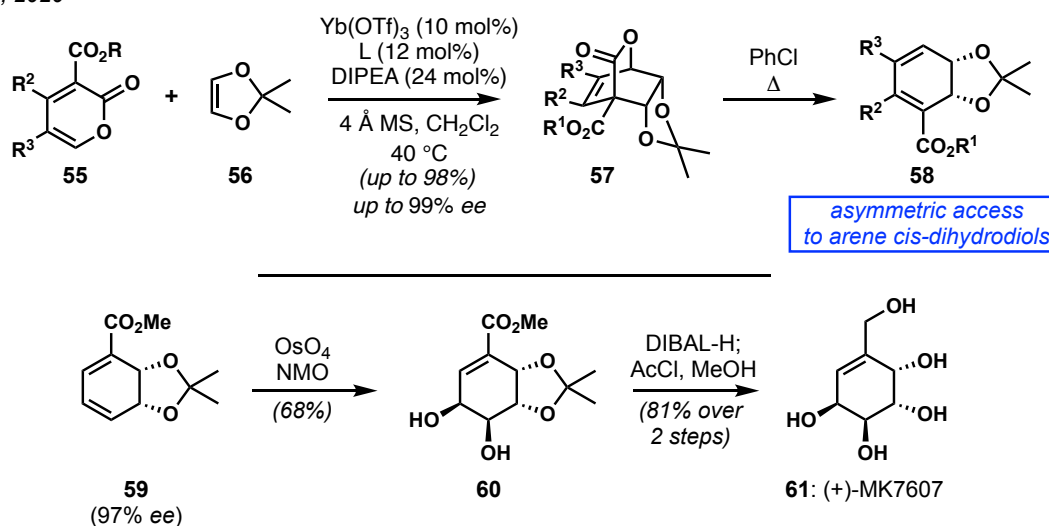


Scheme 3.6. Literature-precedented normal electron-demand asymmetric pyrone Diels–Alder reaction.

Following this report and during our own studies, an asymmetric inverse electron-demand pyrone Diels–Alder reaction was published by Cai and co-workers (Scheme 3.7).¹⁷ In this approach, following the seminal work of Posner and Markó,¹² 3-carbomethoxy pyrone

derivatives (**55**) were shown to achieve [4+2] cycloadditions with acetonide **56** asymmetrically, with the use of Lewis acid $\text{Yb}(\text{OTf})_3$ and an electron poor BINOL derivative. Quite importantly, it was demonstrated that the resultant lactone could undergo the subsequent retro-Diels–Alder reaction (in some cases in a one-pot transformation) to grant asymmetric access to a variety of arene *cis*-dihydrodiols, highly valuable synthetic precursors. As a testament to the value of this method, the authors show that retro-Diels–Alder product **59** can be easily converted in short sequence to the bioactive natural product (+)-MK7607 (**61**).

Cai, 2020

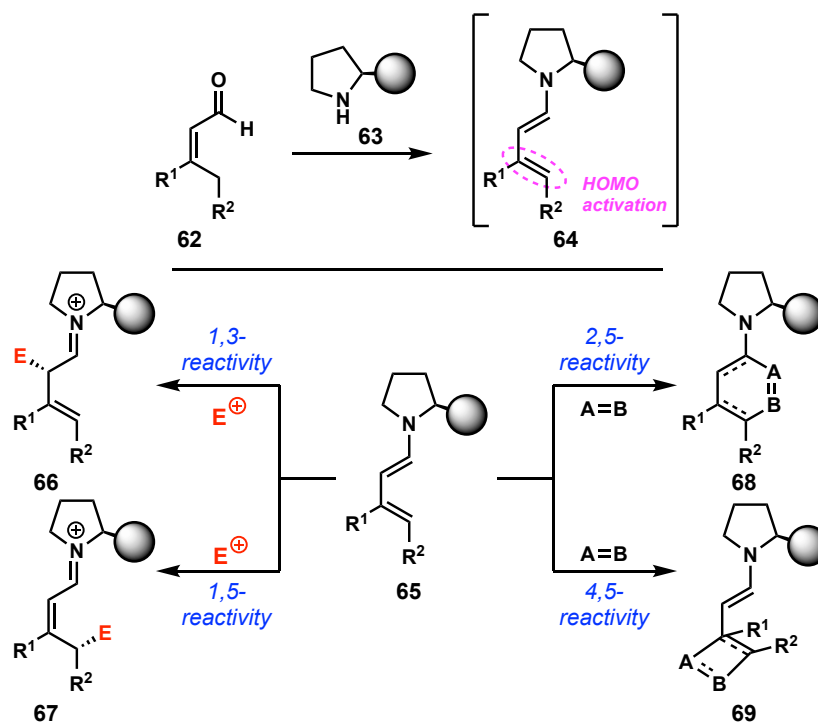


Scheme 3.7. Literature-precedented inverse electron-demand pyrone Diels–Alder reaction and the application to the synthesis of (+)-MK7607.

Although the methods presented above are significant in and of their own right, they do have one important factor in common: they rely on activation of the pyrone partner in order to promote reactivity and induce enantioselectivity. This, in turn, means that there are requisite functionalities that must be placed on the pyrone partner, a hydroxyl group for the Deng approach and a methyl ester for the Cai approach, coincidentally both at the 3-position. As such, we wondered whether it would be possible to develop an approach towards this reaction that would rely solely on the activation of the dienophile, thereby removing any base structural requirements on the pyrone, other than the necessary electronic considerations. Having this in mind, we looked to dienamine catalysis.

3.4 Dienamine Catalysis and the Diels–Alder Reaction

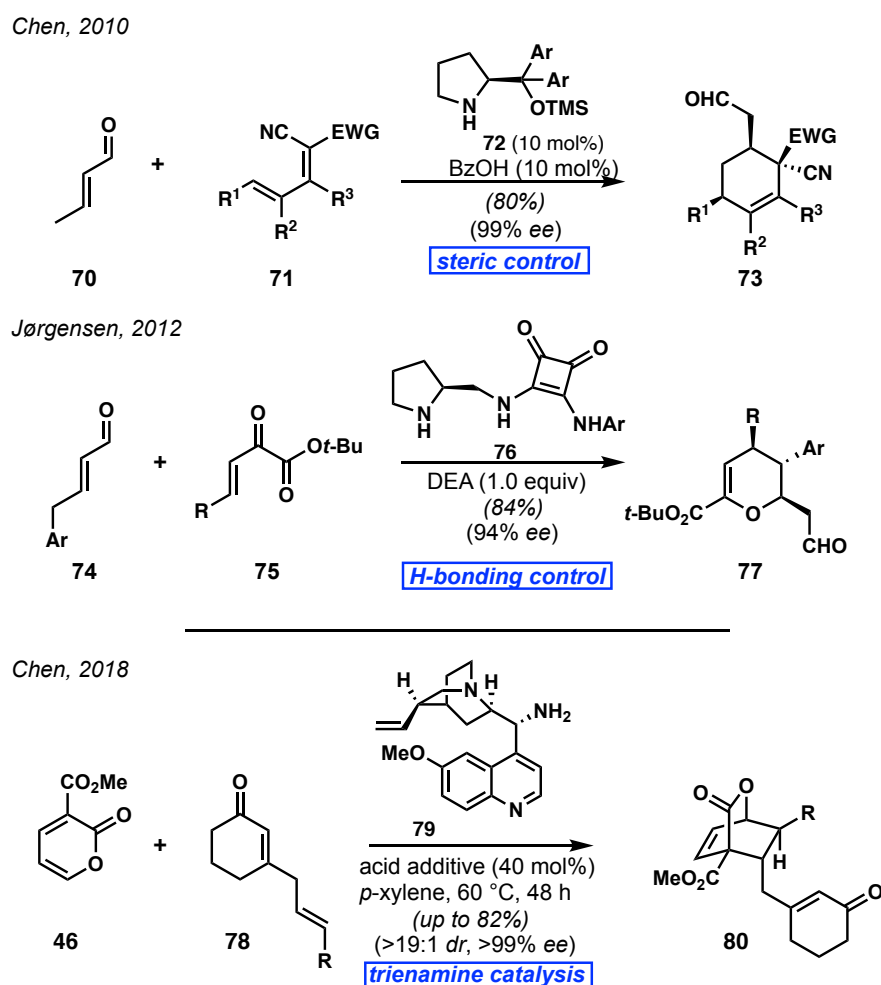
In a general sense, dienamine catalysis is the condensation of some, typically secondary, amine onto an α,β -unsaturated aldehyde (Scheme 3.8). The resulting species contains a highly activated HOMO, turning the traditionally electrophilic enal into a quite potent nucleophile. Dienamines demonstrate four main categories of reactivity: 1,3-reactivity or α -functionalization, 1,5-reactivity or γ -functionalization, 2,5-reactivity where the species itself acts as a diene, and 4,5-reactivity where the terminal olefin behaves as a dienophile, dipolarophile etc. It is this last mode of reactivity that we were particularly interested in, more specifically the ability of these species to partake in [4+2] cycloadditions.^{18,19}



Scheme 3.8. Reactivity patterns common to dienamine catalysis.

Examples of such reactivity do exist within the literature, as shown in Scheme 3.9. While nearly every example utilizes some functionalized pyrrolidine core, they can be placed into two distinct categories based on the asymmetry-inducing motif. The more common of these is the diarylprolinol (72), where the fully substituted carbon of the tertiary alcohol effectively prevents approach from a single face.²⁰ One of the first examples comes from the

Chen group, in which decorated cyclohexenes are obtained enantioselectively through a dienamine-catalyzed Diels–Alder reaction of crotonaldehyde with the highly electron poor diene, **71**.²¹ Less common but still well studied, is the placement of some hydrogen bonding handle, typically in the form of a thiourea or squaramide, onto the prolinamine ring (**76**).²² Such species provide activation of both the dienophile, through formation of the dienamine, and the diene via favorable hydrogen bonding interactions which also guide enantioselectivity. One example is presented from the Jørgensen group, where a hetero-Diels–Alder reaction between enal **74** and α - ketoester **75** provide asymmetric access to a variety of dihydropyrans, in this case catalyzed by squaramide **76**.

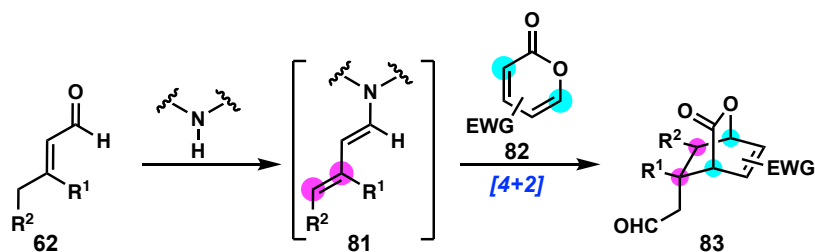


Scheme 3.9. Literature precedent for dienamine- and trienamine-catalyzed Diels–Alder reactions.

While conducting our own studies on these systems as applied to 2-pyrones, an interesting example was published by the Chen group.²³ In this event, trienamine catalysis was

employed to promote the asymmetric Diels–Alder reaction between 2-pyrone **46** and the skipped dienone **78**. While this certainly represents an important contribution, there were still some unresolved challenges. In particular, the reaction required harsh conditions relative to other dienamine catalyzed [4+2] reactions (40 mol% acid additive, 60 °C, 48 h) and the substrate scope was greatly limited, with the only compatible pyrone being **46** and only variations at the terminal position of **78** being tolerated.

With all of these preceding results in mind, we then set out to make our own contribution to this field. We hoped that under dienamine catalysis we could efficiently and stereoselectively conduct a Diels–Alder reaction with a variety of electron poor pyrone species. We hoped that by relying on activation of the dienophile partner we would afford fewer functional restrictions on the pyrone and potentially access alternative frameworks to those already in the literature.



Scheme 3.10. Generic proposal for dienamine-catalyzed pyrone Diels–Alder reaction.

3.5 Initial Discovery and Reaction Optimization

We first sought to establish a base system of reactivity using the conditions previously employed by the Chen group in their own studies on dienamine-catalyzed inverse electron-demand Diels–Alder reactions.^{21a} When using methyl coumalate (**35**, 1 equiv.)²⁴ as the diene and crotonaldehyde (**70**, 3 equiv.), as the dienamine precursor, we were able to obtain the desired bicyclic lactone product (**85**) in good yield (87%) as a 1.5:1 mixture of diastereomers, slightly favoring the *endo* species (Table 3.1). Knowing that substituent patterning along the aldehyde partner can have a significant impact on the stereoselectivity in these systems, a trend

observed by the Chen group themselves,^{21b} we then probed the placement of methyl groups along the enal. When placing a methyl group at the α -position we observed a complete loss of reactivity, with both reaction partners recovered unchanged. On the other hand, the placement of a second methyl substituent at the β -position not only restored reactivity to the levels previously observed, but to our surprise, increased the enantiomeric excess of the products from ~5% to 75%, with the diastereoselectivity essentially unchanged.

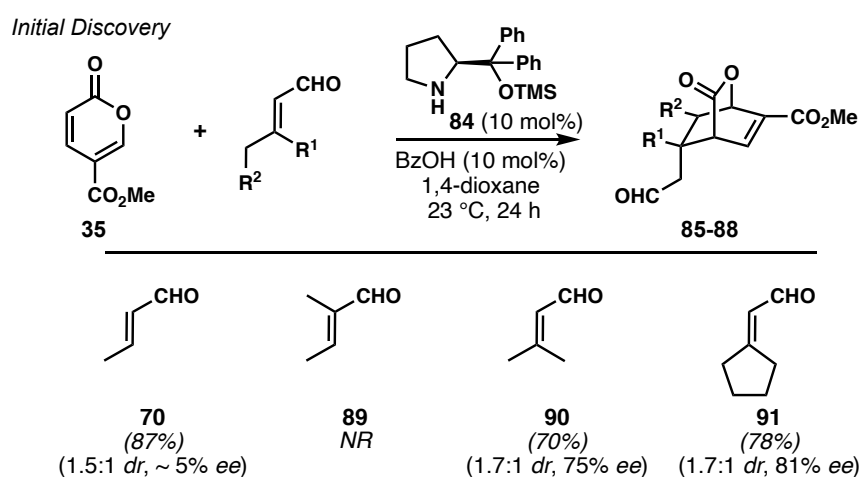
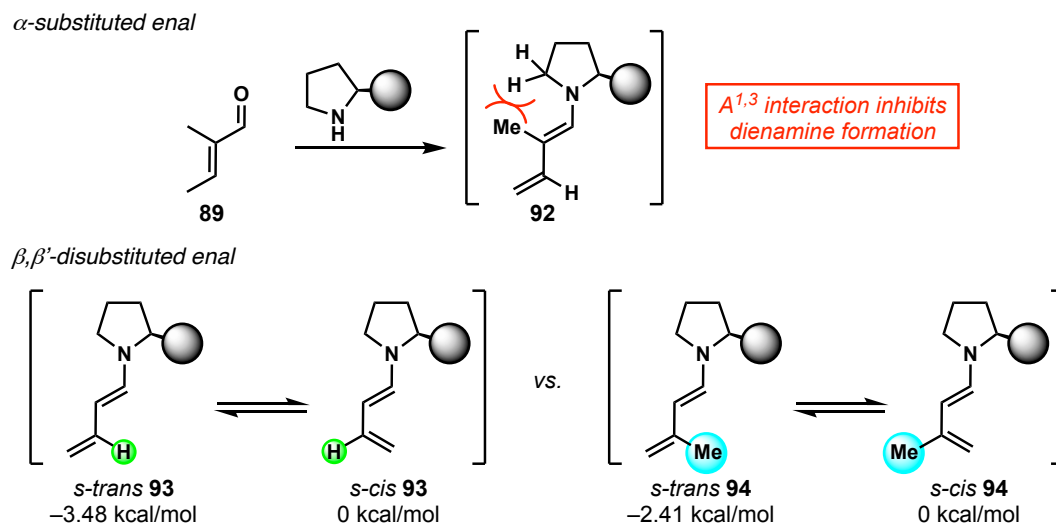


Table 3.1. Initial reaction discovery and substrate screening.

As shown in Scheme 3.11, we have tried to rationalize this observed difference in reactivity and stereoselectivity. In the case of **89**, it could be presumed that the challenge is the formation of dienamine **92**. If one were to condense pyrrolidine onto **89**, the resulting methyl group at the α -position of the enamine would demonstrate a significant $A^{1,3}$ strain with the methylene adjacent to the nitrogen atom. This would likely inhibit the formation of the requisite dienamine, thereby preventing the desired reaction from taking place. The reason for the sizeable impact of the additional β -substituent on stereoselectivity, however, is less clear. One possible rationale is the ratio of *s-cis* to *s-trans* diene conformers. Although the *s-trans* conformation is undoubtedly favored, as shown with simple ground state calculations (work performed by Cooper Taylor), we posit that the placement of an additional β -substituent produces $A^{1,3}$ strain in the *s-trans* species that reduces the extent to which this structure is favored. If the *s-cis* species was in fact favored, the reactive site would then be brought much

closer to the asymmetry-inducing steric handle, thereby improving the enantioselectivity of this transformation. It must be said that this reasoning would not seem to account for the drastic difference in stereoselectivity observed and there may be a myriad of other unidentified factors at work to produce this outcome.



Scheme 3.11. Accounting for observed substrate trends initial screening (B3LYP/cc-pVDZ Ground State Energy Calculations).

Having noted the observed trend, we decided to pursue cyclic α,β -unsaturated aldehydes, as not only do they contain the seemingly requisite β - β' -substitution pattern but the products themselves would offer a degree of complexity not previously observed in forms, such as the bridged hydrindane product of **88**, and containing a newly formed quaternary center (structure confirmed by X-ray crystallographic analysis). Pleasingly, enal **91** gave the desired product in good yield (78%) and a slightly higher enantiomeric excess (81% *ee*). With these results in hand, we then went through the process of optimizing other factors including solvent, temperature, concentration and catalyst loading. Most notable of these, however, was the fact that the reaction performed best without any additional additive. Dienamine-mediated transformations are often improved by the inclusion of acid additives, which promote the condensation of the amine catalyst onto the enal partner and as such, it is quite surprising that our system performs better in their absence.²⁵ Furthermore, catalyst loading can be reduced to as little as 5 mol%, this too is significant as typical loadings are in the realm of 10-40 mol%.

With all other parameters optimized, we wanted to explore the importance of catalyst structure as it pertained to the reaction. Under the manifold of dienamine catalysis broadly, we wanted to survey two things: 1) the degree of substitution of the amine, and 2) the handle used to induce asymmetry (steric control vs. hydrogen bonding). As can be seen in Table 3.2, of the

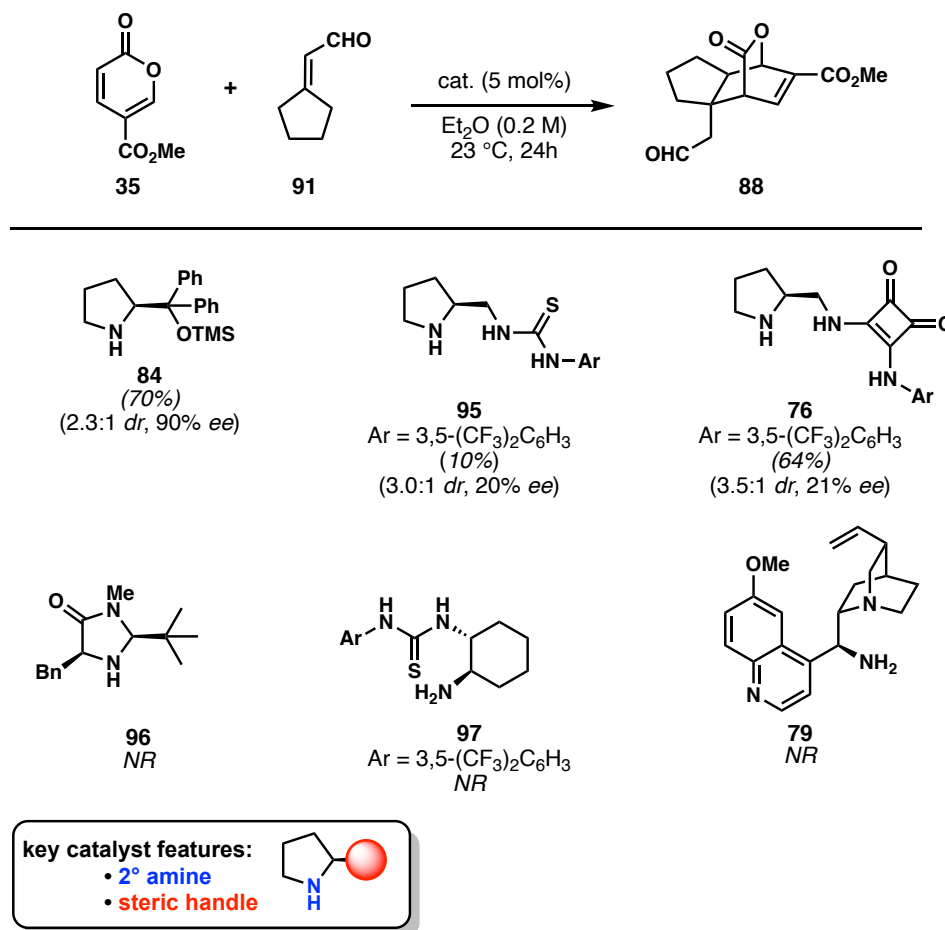


Table 3.2. Exploration of various catalyst scaffolds to promote the pyrone Diels–Alder reaction.

various catalyst types surveyed, secondary amines were required to promote reactivity, with structures such as **79** and **97** showing no desired product. On the other hand, good enantioselectivity was only observed when a steric handle was placed on the pyrrolidine ring (**84**) as opposed to a hydrogen bond donor (**95** and **76**).^{20c,22, 26}

This led us to further explore catalysts similar in structure to **84**. As shown in Table 3.3, after varying the aryl group as well as the protecting group on the tertiary alcohol, optimum

results were obtained using the Jørgensen-Hayashi catalyst **72**.²⁰ We then took these as the optimized reaction conditions with which to study the substrate scope of the reaction.

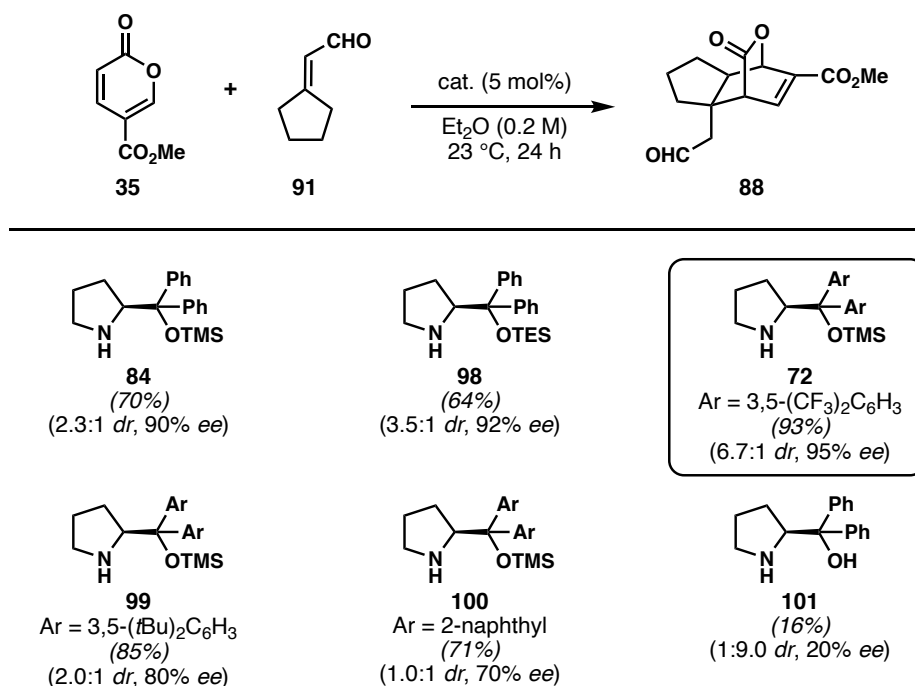


Table 3.3. Exploration of diarylprolinol scaffolds to promote the Diels–Alder reaction.

3.6 Exploring and Understanding the Reaction Scope

With the reaction conditions optimized, we set out to survey the scope of the reaction. Pleasingly, we could increase the ring size of the enal partner to include six-, seven- and eight-membered cycloalkylidene aldehydes, to produce the corresponding fused ring systems in good yield and enantioselectivity. Noteworthy, is that the fused twelve-membered ring analogue **105** could be accessed in good yield and high diastereoselectivity, albeit with low enantioselectivity. The complexity of the products could also be extended to the tricyclic benzo-fused species **106-109**, all in good yield and enantioselectivity. Further, we were able to demonstrate that although the cycloalkylidene based aldehydes offered a wealth of structural complexity in the products, they were not strictly required for the success of the reaction as seen in compounds **110-115**, which arise from the β -aryl substituted crotonaldehyde starting materials. The reaction showed tolerance for electron rich (**111**) and electron poor (**112**)

systems, as well as a variety of heterocycle substituted species (**113-115**). Of note, we believe that the comparably lower yield observed in the case of **114** is a result of the furan moiety itself possibly serving as a competent diene partner in the reaction, thereby promoting undesired reaction pathways.

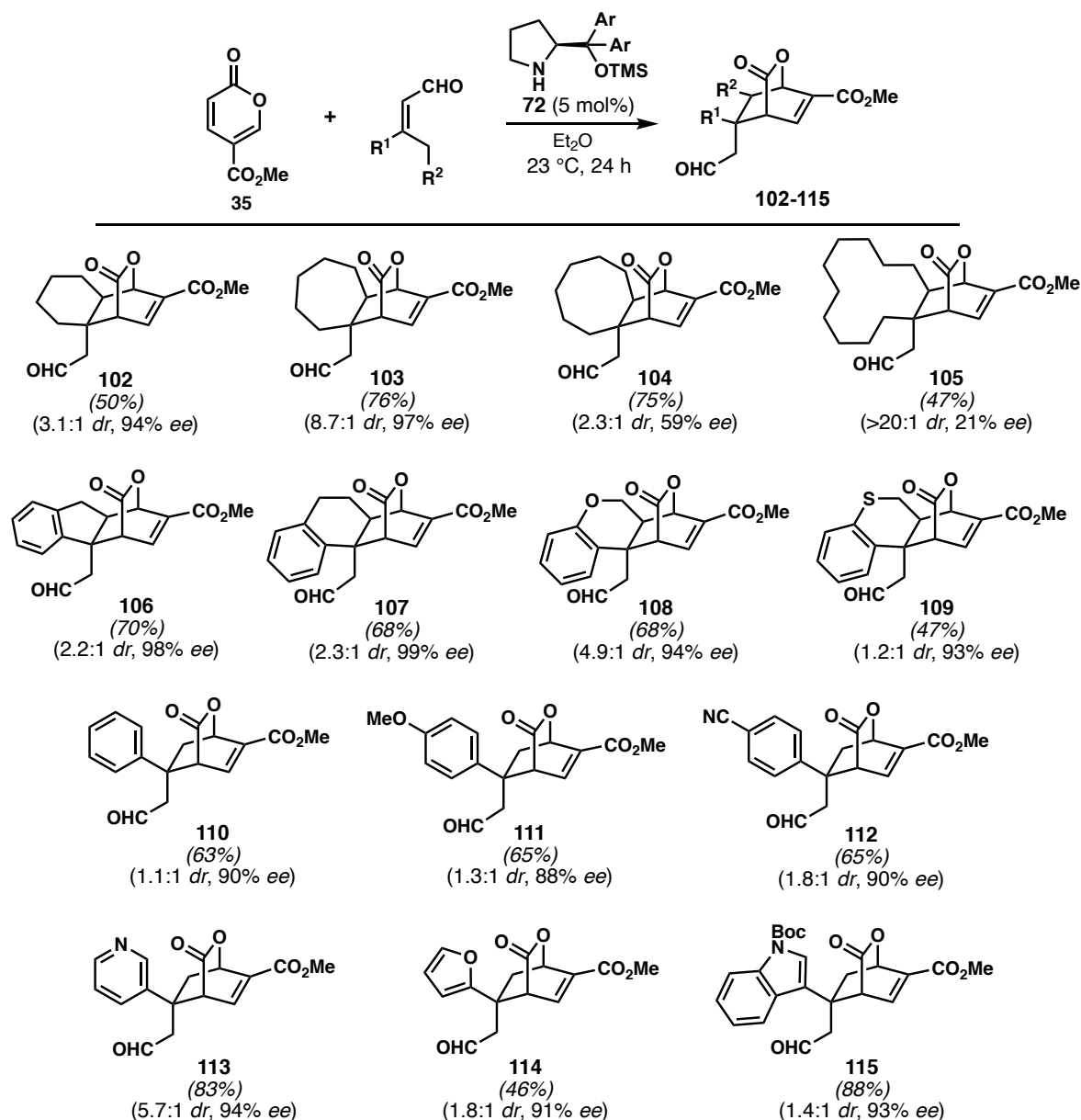
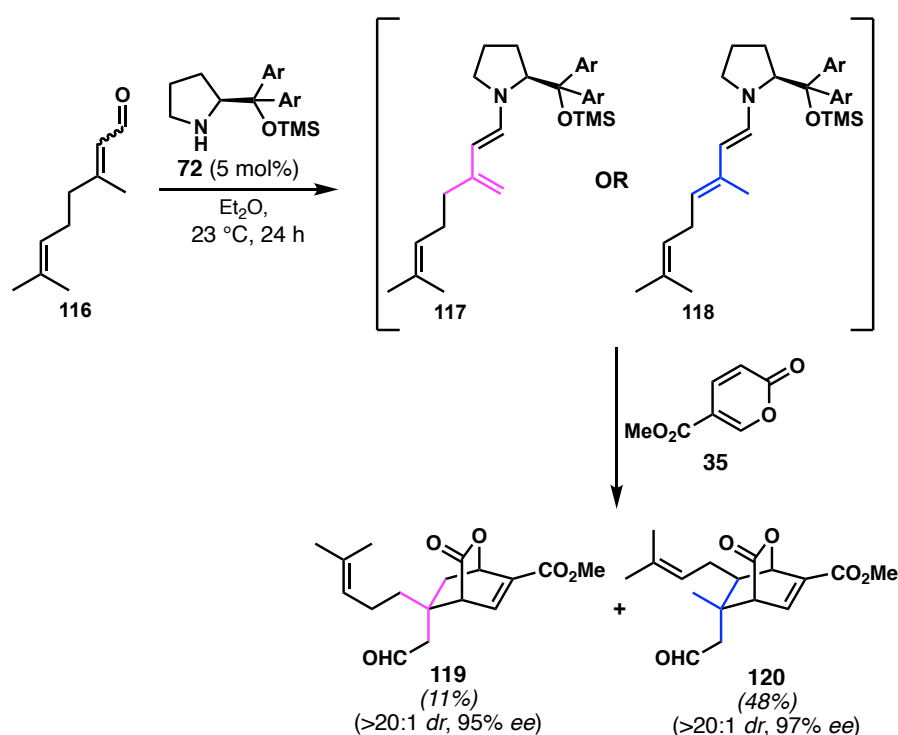


Table 3.4. Exploring the scope of compatible enal partners.

Having completed the scope of dienophile partners, we noticed that in all cases presented thus far there is only one possible site for gamma deprotonation on the α,β -unsaturated aldehyde, thus there is only one possible regioisomer of the proposed dienamine intermediate.

But what would the reaction outcome be if multiple regioisomers of the active dienamine existed in solution? To study this, we turned to citral (**116**, Scheme 3.12). Upon condensation of **116** with **72**, one can form either the “kinetic” regioisomer **117** or the “thermodynamic” regioisomer **118**, both of which would be competent in performing the desired reaction. Interestingly, in our system we obtain ~5:1 *rr* favoring the product of the dienamine **118**, indicating that there is some possibility of equilibration of these species to the more thermodynamically stable intermediate prior to the cycloaddition taking place. It should be noted that both products in this case are obtained in excellent diastereo- and enantioselectivity.



Scheme 3.12. Studying the regioisomeric outcome from the reaction of **35** with citral (**116**).

After probing the scope of α,β -unsaturated aldehydes, we moved our focus to the corresponding pyrone counterpart. Initially, we wanted to study how the placement of the methyl ester substituent along the diene impacted the system. While the product of the 3-carbomethoxy pyrone (**123**) could be obtained in good yield and moderate enantioselectivity, placing the ester functionality at any other position along the diene resulted in no observed

reactivity. In line with our own observations, such a trend was observed by the Zu group in their studies of electron poor pyrones participating in Rauhut-Currier type reactions.²⁷

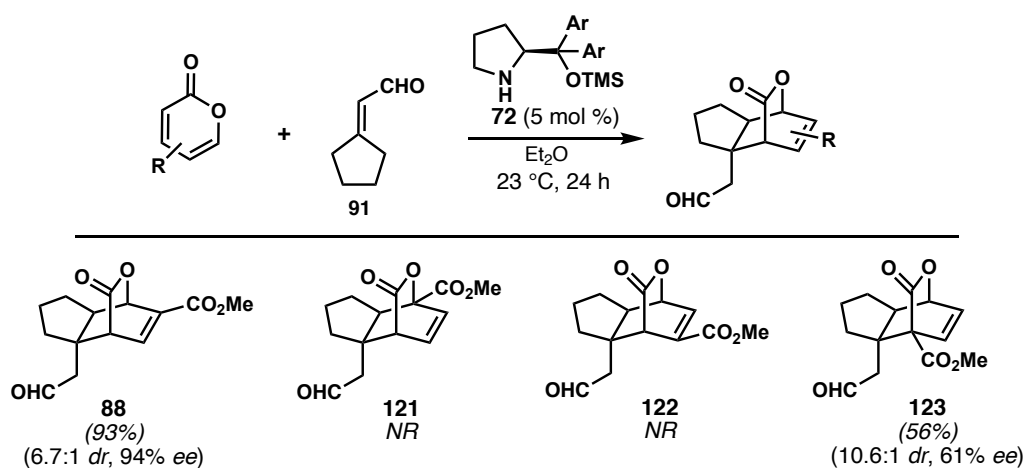


Table 3.5. Exploring the effect of ester positioning on the reactivity of the pyrone partner.

With this important data point in mind, we studied the scope of compatible pyrones, varying the identity of the electron withdrawing group. Here, the methyl ester could be replaced by the phenyl ketone (**124**) or carbonitrile (**125**) functionality while maintaining good reactivity and stereoselectivity (Table 3.6). In addition, the more electron poor diester variant **126** could also be obtained, albeit with a greatly reduced diastereoselectivity. What we found particularly interesting was that a bromine atom could be placed at the 3-position of the pyrone starting material without hindering reactivity or stereoselectivity. This is significant, not only because the resulting bridgehead bromide could be viewed as a point of further elaboration, but more importantly that we are able to construct two vicinal fully substituted carbon atoms in an asymmetric manner and in a single step, from materials that themselves are completely achiral, truly demonstrating the power of this reaction.²⁸ Despite having surveyed a variety of dienes and dienophiles, there remained one more observation that we thought important to pursue. As can be seen in Tables 3.4 and 3.6, in cases where the enal contains aliphatic substituents at both the β and β' positions, *dr* levels are on the order of \sim 3:1 to as high as $>20:1$. However, when one of the β -substituents is replaced with an aryl group, there is an immediate decrease in the diastereoselectivity of the reaction to \sim 1:1. This then led us to consider whether there were any

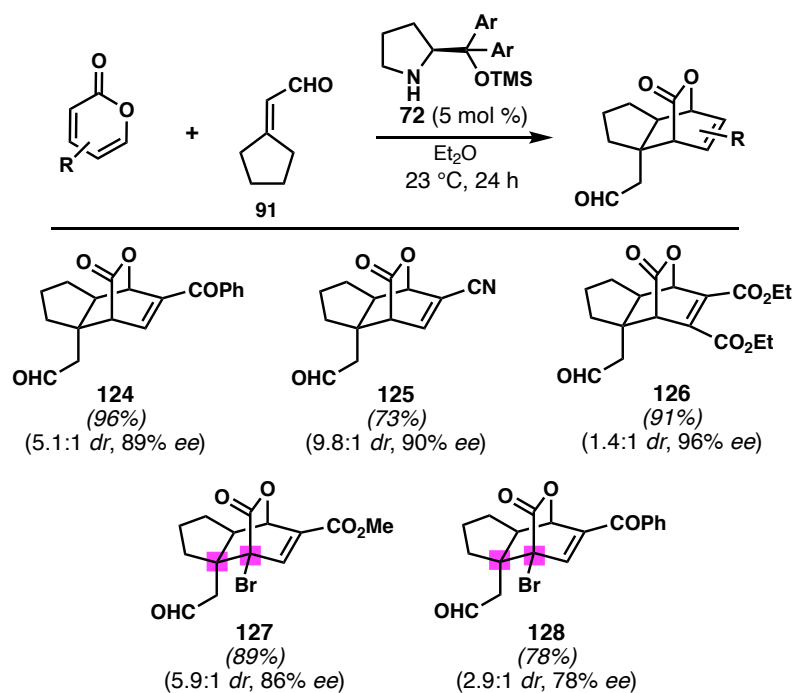


Table 3.6. Exploring the scope of 2-pyrone as dienes.

possible substrate effects on the transition states that could account for this fact. As can be seen in Figure 3.2, when R = alkyl, favorable secondary orbital overlap between the 4,5-position of the pyrone and the internal olefin of the dienamine would favor the *endo* transition state, as would be expected. However, when an aryl group is placed at the β -position of the dienamine, we believe that there is a competing interaction. Here, favorable orbital overlap between the oxygen atom of the ester and the π -system of the aryl ring can stabilize the *exo* transition state and thereby erase any diastereoselectivity. In order to overcome this effect, one would essentially have to remove this competing interaction. We envisioned that this might be possible if the ester group was replaced with the related nitrile. From this perspective, one retains the electronic nature of the pyrone, but the *sp*-hybridized geometry of the nitrile should prevent any effective overlap between that and the aryl π -system. In fact, we were able to synthesize two cycloadducts from 5-carbonitrile-2-pyrone, **132** and **133** (Figure 3.2). These products showed *dr*'s of 5.5:1 and 8.9:1, while those from the corresponding 5-carbomethoxy-2-pyrone showed *dr*'s of 1.1:1 and 2.3:1, respectively, in effect supporting our hypothesis.

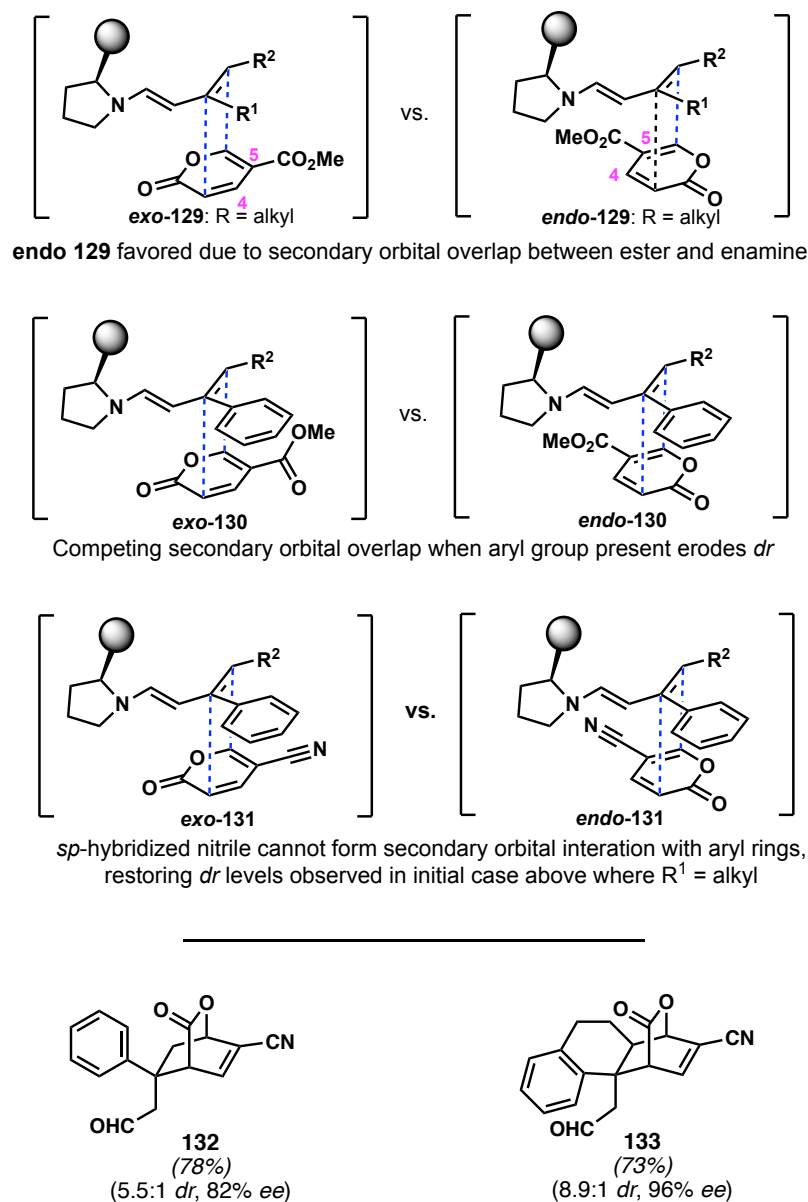
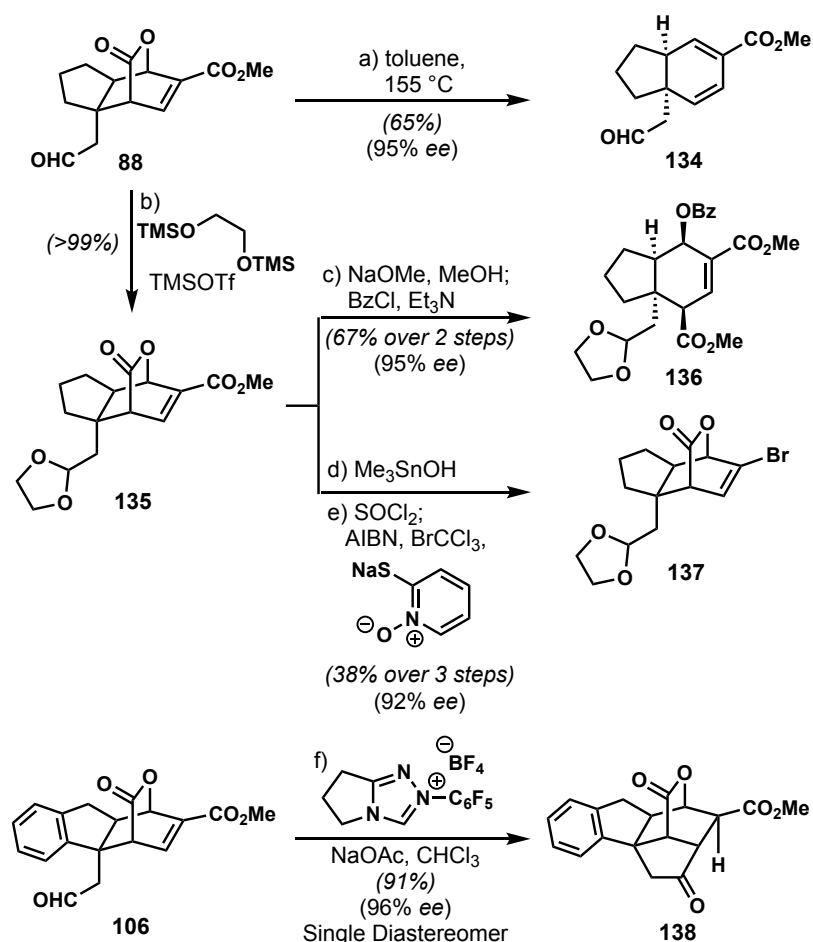


Figure 3.2. Transition state analysis to account for *dr* outcomes.

3.7 Derivatization of Bicyclic Lactone Products

In order to demonstrate the utility of the structures synthesized in this chapter, we wanted to perform additional transformations. As shown in Scheme 3.13, the first of these was the traditional retro-Diels–Alder reaction. Upon heating cycloadduct **88** in toluene at 155 °C for 24 h we were able to obtain the corresponding decarboxylated product, which could potentially serve as a point of further elaboration through a second [4+2] pathway. In fact, a report by the Albrecht group demonstrated that such a transformation could be performed intramolecularly

to build a subsequent [2.2.2]-bicycle containing a fused cyclobutane ring.²⁹ Separately, the pendant aldehyde could be protected as the corresponding acetal (**135**), following which the lactone could be opened using NaOMe/MeOH and protected as the corresponding benzoate (**136**). This then provides access to a highly substituted *cis*-hydrindane core in an asymmetric fashion. Alternatively, if one desired to functionalize the ester handle while keeping the lactone intact, treatment with Me₃SnOH at elevated temperature, followed by a Barton decarboxylation reaction using BrCCl₃ as a bromide radical source, provides vinyl bromide **137**.^{30,31} Not only does this species provide a point for further transformations through traditional cross coupling



Scheme 3.13. Selected derivatization of Diels–Alder products: (a) toluene, 155 °C, 24 h, sealed tube, 67%, 95% ee; (b) 1,2-bis(trimethoxysilyl)ethane (2.0 equiv.), TMSOTf (0.1 equiv.), 0 °C, 1 h, 98%; (c) NaOMe (2.0 equiv.), MeOH, 0 °C, 2 h; BzCl (2.0 equiv.), Et₃N (2.0 equiv.), 4-DMAP (2.0 equiv.), CH₂Cl₂, 23 °C, 1 h, 67% over two steps, 95% ee; (d) Me₃SnOH (3.0 equiv.), 1,2-DCE, 80 °C, 16 h; (e) SOCl₂ (5.0 equiv.), toluene, 23 °C, 24 h; AIBN (0.1 equiv.), mercaptopyridine *N*-oxide sodium salt (1.1 equiv.), BrCCl₃, 100 °C, 1 h, 38% over three steps, 92% ee; (f) NHC (20 mol%), NaOAc (1.2 equiv.), CHCl₃, 40 °C, 30 min, 91%, 95% ee.

chemistry, but it also represents the product of a Diels–Alder reaction using 5-bromopyrone, a system which is difficult to engage in a racemic fashion, far less asymmetrically, as has been done here in a formal sense.^{11d} However, one of the more fascinating transformations is the Stetter reaction, converting **106** to **138** as a single diastereomer about the α -carbon of the ester. This example clearly illustrates the degree of structural complexity and steric congestion that can be built into this system: two bridged bicycles as well as the fused tricyclic motif. In particular, we have been able to set every stereocenter about the central cyclohexane ring in an almost fully stereoselective manner starting from completely achiral materials in just two short steps, thereby demonstrating the true utility of these structures, as well as the preceding cycloaddition.

3.8 Initial Studies Towards the Gardmutine Alkaloids

As a means of illustrating the potential of our newly developed reaction, we looked to apply this method to natural product total synthesis. In searching for a target that would be best suited to the framework obtained from our reaction, we came across the gardmutine alkaloids.³² The gardmutines (**139-142**, Figure 3.3a) are a series of 7*S*-oxindole alkaloids isolated from *Gardneria multiflora*. These compounds are interesting not only structurally, as they are the only members of the gardmutine family to contain a 7*S* center, but also biologically, with gardmutines D and E showing moderate cytotoxicity towards HeLa, breast, and colon cancer cell lines (IC₅₀ 1.4–8.1 μ M).³² In applying our dienamine catalyzed pyrone Diels–Alder we hoped, in particular, to take advantage of the relative stereochemistry imparted by this reaction, as well as the variety of functional groups introduced in this key step. As can be seen in Figure 3.3a, the overall framework of the gardmutines overlays quite well with the generic cycloadduct. The pendant aldehyde could serve as a point of introduction for the amine, while the lactone provides the necessary primary alcohol as well as a secondary alcohol handle,

through which to introduce that second C–N bond. Further, the α,β -unsaturated ester could act as a precursor to the spirooxindole moiety. There is, however, still one major difference: the ring size of the core. We sought to solve this problem through a ring expansion approach as presented in Figure 3.3b. Using the olefin afforded by the pyrone Diels–Alder reaction, we sought to introduce a *gem*-dihalocyclopropane (**143**). In the presence of Ag(I), such species would undergo a disrotatory $2-\pi$ electrocyclic ring opening process to generate an allylic carbocation which, although typically trapped via an external nucleophile (e.g. H₂O), could be trapped intramolecularly via the secondary amine to form the requisite azabicycle **145**.³³

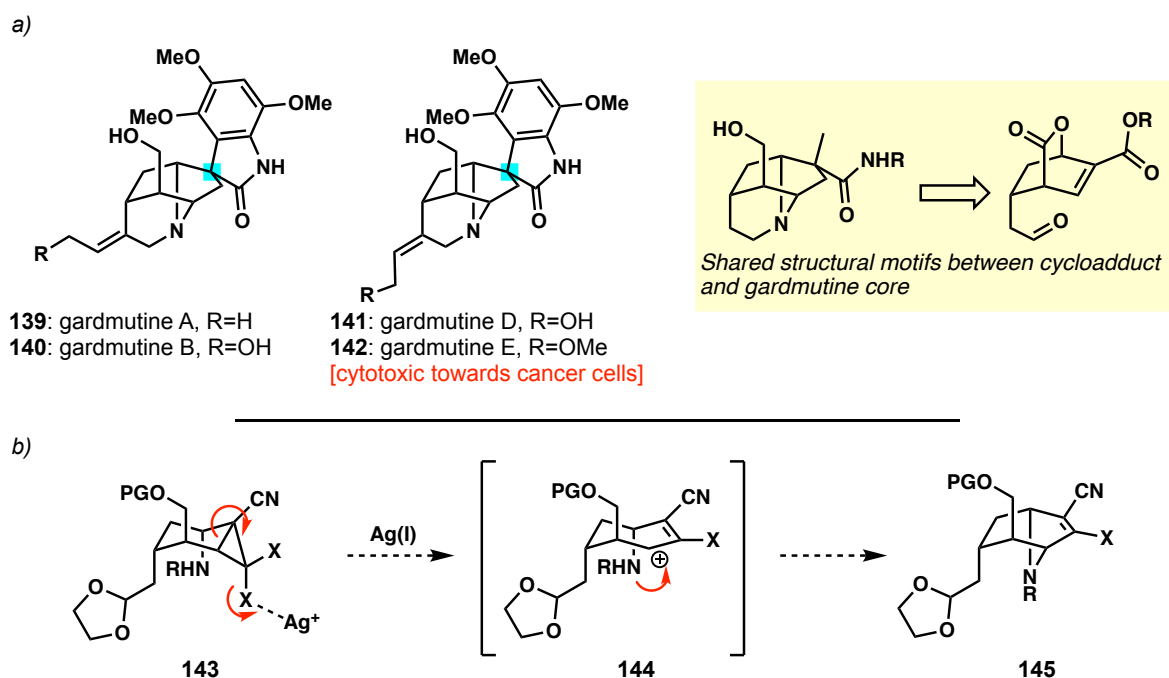
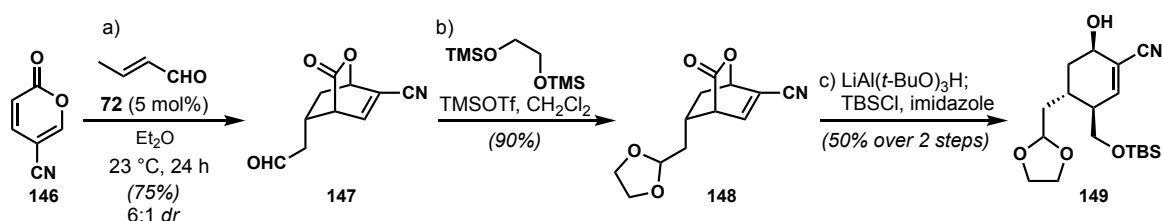


Figure 3.3. (a) Gardmutine alkaloids and shared structural framework with pyrone Diels–Alder product. (b) Proposed key ring expansion to form core azabicycle **145**.

In practice, our first goal was to access some variant of the lactone-opened product from which we could attempt formation of the *gem*-dihalocyclopropane. Starting from 5-cyanopyrone **146**, the dienamine-catalyzed Diels–Alder reaction with crotonaldehyde provided desired *endo*-cycloadduct **147** in good yield and decent diastereoselectivity (Scheme 3.14). Here, we decided to use the nitrile functional handle as opposed to the ester group, such that there was greater differentiation between that position and the bridged lactone in later steps.

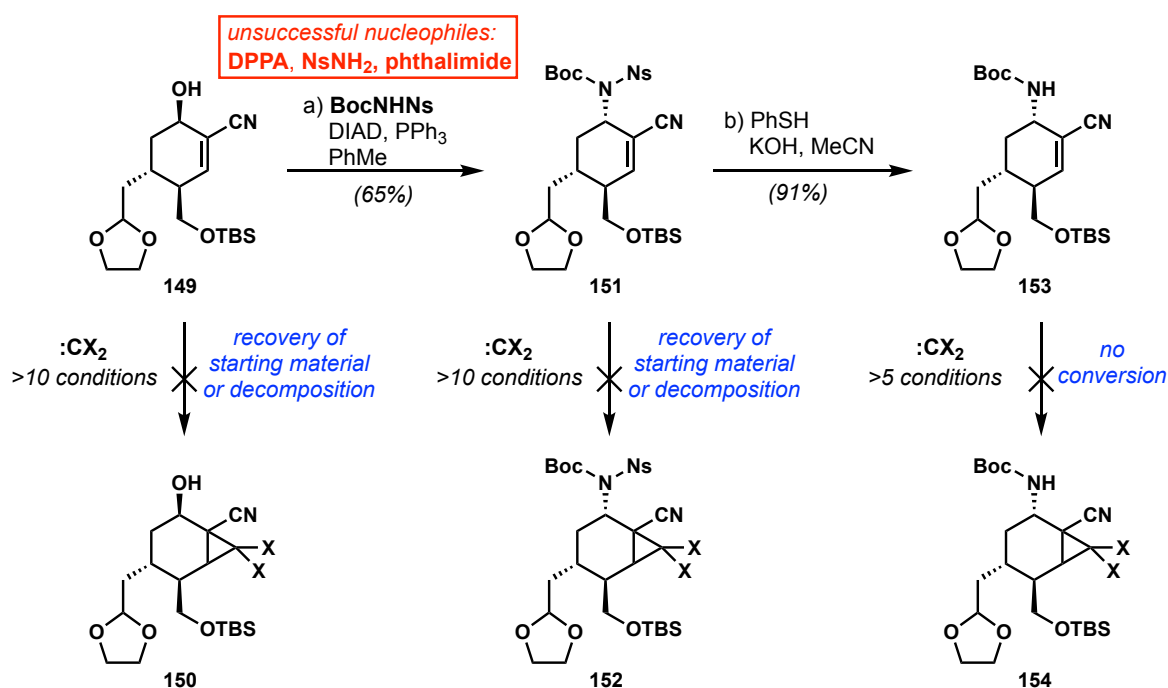
Knowing the reactivity of the newly formed aldehyde, in particular the potential for a retro-Michael reaction and resultant undesired reaction pathways, we protected this species as the corresponding acetal which could be revealed later in the route as needed. Lactone **148** was then reduced with $\text{LiAl}(t\text{-BuO})_3\text{H}$ to afford the desired diol, in which the primary alcohol could be selectively protected as the corresponding TBS ether (**149**). Other reductants such as LiAlH_4 or LiBH_4 led to complex mixtures and lower yields of the desired diol.



Scheme 3.14. Conversion of cyanopyrone **146** to protected diol **149**: (a) **72** (5 mol%), **70** (3.0 equiv.), Et_2O , 23 °C, 36 h, 75%; (b) 1,2-bis(trimethoxysilyl)ethane (2.0 equiv.), TMSOTf (0.1 equiv.), 0 °C, 1 h, 90%; (c) $\text{LiAl}(t\text{-BuO})_3\text{H}$ (1.0 equiv.), THF, then TBSCl (1.2 equiv.), imidazole (2.9 equiv.), DMF, 50% over 2 steps.

At this stage, we attempted to introduce the nitrogen atom via a Mitsunobu reaction, fearing that such a transformation might be sterically challenging after introducing the *gem*-dihalocyclopropane ring. Of the variety of nitrogen-based nucleophiles attempted, only BocNHNs proved capable of performing the desired substitution to afford **151** (Scheme 3.15). At this point, a number of conditions were screened to introduce the desired cyclopropane system, including dihalo carbenes, in both organic solvents and phase-transfer systems, as well as nucleophilic haloform anions that could add in a 1,4-fashion.³³ Under more forcing conditions, decomposition pathways began to take over. At first, we attributed this to the fact that we had both a highly electron poor amine, as well as a labile protecting group in the form of *o*-nosyl. After removing this group under standard conditions, we once again attempted a similar series of conditions to introduce the requisite cyclopropane, but no desired reaction took place. It was then thought that by first performing the Mitsunobu reaction, the central cyclohexane was too sterically encumbered for the desired reaction to take place, with large groups residing on both faces of the ring. With this in mind, we also tried a series of similar transformations on the secondary alcohol **149**, as well as a number of protected variants of this

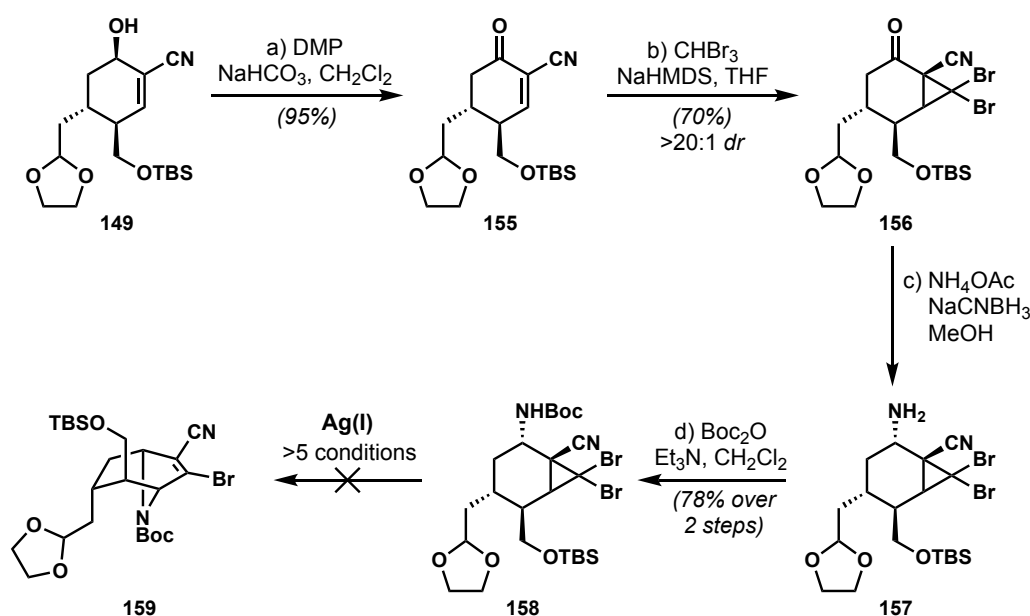
compound and bicyclic lactone **148**. But unfortunately, we were never successful in installing the ring at this stage.³³



Scheme 3.15. Early attempts at forming the gem-dihalocyclopropane: (a) BocNHNs (1.0 equiv.), Ph₃P (1.2 equiv.), DIAD (1.2 equiv.), toluene, 23 °C, 2 h, 65%; (b) PhSH (4.0 equiv.), KOH (2.0 equiv.), MeCN, 23 °C, 30 min, 91%.

We then wondered whether it was instead a problem of electronics rather than strictly sterics.³⁴ Knowing that we required the nitrile, or some electron poor variant thereof, as a precursor to the spirooxindole, we did not think it efficient to remove this handle simply to reinstall it later in the sequence. Instead, we proposed to increase the reactivity of the Michael acceptor. From this perspective, although reactions involving dihalocarbenes might be more challenging, those involving haloform anions might have a greater chance of success. Based on this strategy we then oxidized secondary alcohol **149** to the corresponding ketone **155** (Scheme 3.16). This now, highly reactive, Michael acceptor smoothly underwent cyclopropane formation in an almost completely diastereoselective manner to afford **156**.³⁵ Although unclear from the spectra obtained, it is almost certain that the newly formed ring sits *trans* to the neighboring TBS ether. This ketone could then be easily converted into the desired amine through a reductive amination with NH₄OAc and NaCNBH₃, which could then be Boc-

protected to provide **158**. Here, we believe that the stereoselectivity of the reduction is a result of the *endo*-bromide atom on the cyclopropane ring effectively preventing hydride approach from the *si*-face. We then faced a different challenge: opening the dibromocyclopropane ring. Despite trying a number of Ag(I), salts we never observed any conversion of the starting material.³³ We then attempted ring opening with several intermediates, including ketone **156**, in these cases using an aqueous biphasic mixture to attempt external nucleophile capture of the resulting carbocation. However, despite several attempts we could never successfully open the cyclopropane ring within species such as **158**. It is possible that the *endo*-bromide atom, the one that is abstracted in the concerted ring opening process, was too hindered and the resulting allylic carbocation, with a neighboring electron withdrawing group, was too unstable, leaving no driving force for the reaction to take place. With this transformation being key to the

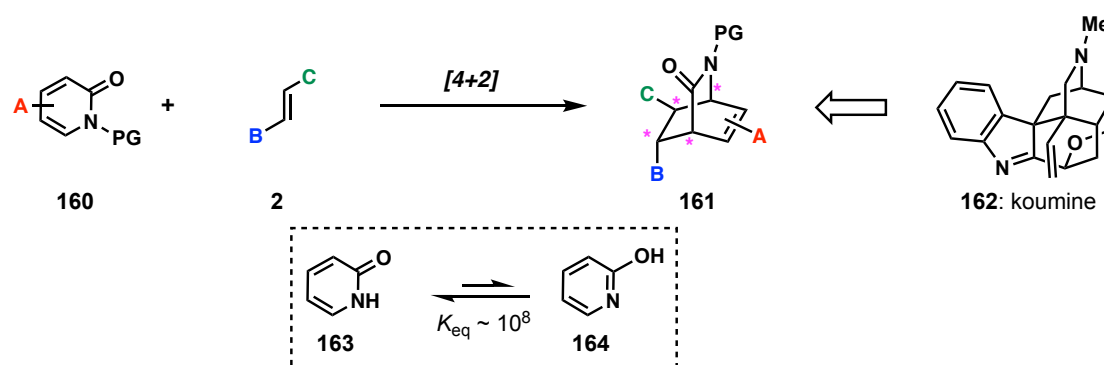


Scheme 3.16. Installation of gem-dibromocyclopropane and attempts at Ag-promoted ring opening: (a) DMP (3.0 equiv.), NaHCO₃ (5.0 equiv.), CH₂Cl₂, 0 °C, 1 h, 95%; (b) CHBr₃ (5.0 equiv.), NaHMDS (1.3 equiv.), THF, -78 °C, 1 h, 70%, >20:1 *dr*; (c) NH₄OAc (15.0 equiv.), NaCNBH₃ (5.0 equiv.), MeOH, 50 °C, 2 h; (d) Boc₂O (2.5 equiv.), Et₃N (3.0 equiv.), DMAP (1.0 equiv.), CH₂Cl₂, 1 h, 23 °C, 78%.

formation of the requisite seven-membered core of the gardmutines and no clear alternative in sight, this route was abandoned. It is worth noting that despite this unsuccessful approach, key lessons were learned in regard to the ability to functionalize the stereochemically rich core obtained from our dienamine-catalyzed pyrone Diels–Alder reaction.

3.9 Application to the Pyridone Diels–Alder Reaction

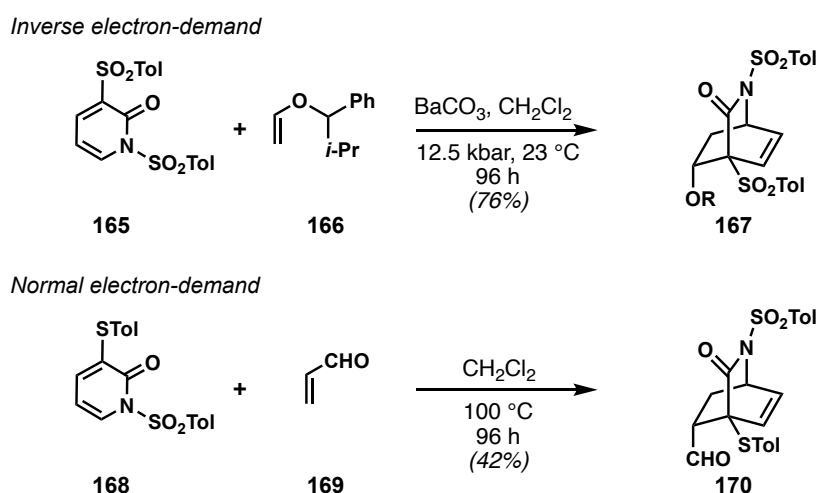
Analogous to the pyrone Diels–Alder, although less studied, is the pyridone Diels–Alder reaction.^{2b} Owing to the substrate's greater aromatic nature, in the form of a fully aromatic tautomer (**164**), such reactions are far more challenging than the analogous 2-pyrone variant.³⁶ However, the potential of this transformation is quite apparent. As shown in Scheme 3.17, the overall structure of the products is almost identical to that of the pyrone Diels–Alder reaction, with the key difference being the formation of the *aza*-bicycle, a scaffold that is featured in alkaloid natural products, such as koumine (**162**).



Scheme 3.17. Pyridone Diels–Alder reaction.

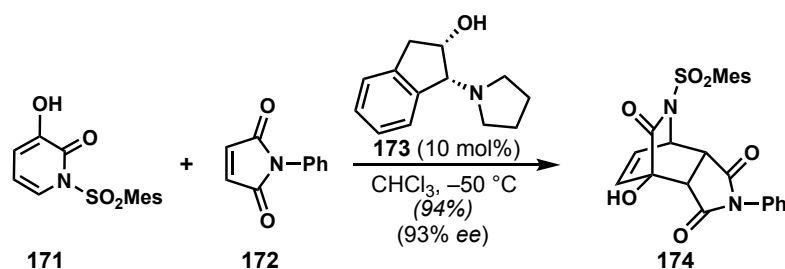
When studying the reaction variant with 2-pyridones, the substituents placed along the ring become extremely important, with the most significant being the group placed on the nitrogen atom. While there are examples of these pyridone Diels–Alder reactions where the nitrogen atom is protected with an alkyl group, it is much more typical to use a highly electron withdrawing group as a means to reduce the delocalization of the nitrogen lone pair into the ring and thereby decrease the aromatic character of the species. In this regard, *N*-sulfonyl groups are the most commonly employed. While it is possible to prepare the *N*-acyl or *N*-carbamate variants, these species can undergo rapid *N,O*-rearrangement at low temperature to afford the corresponding *O*-protected 2-pyridinols.³⁷ Although the use of such electron poor protecting groups is necessary, there is an adverse effect on the reactivity of the resultant pyridone. For example, if one places a sulfonyl group on the nitrogen atom, according to

standard frontier MO theory, the HOMO of the diene will be lowered, resulting in a larger energy gap between the diene and dienophile in the case of a normal demand reaction. Conversely, the presence of this electron withdrawing group has relatively little impact on the energy level of the LUMO and as a result the corresponding inverse electron-demand process. Therefore, most examples using 2-pyridones as dienes often place highly electron donating or withdrawing substituents along the ring in order to promote the desired reaction, often still requiring quite harsh conditions to promote the cycloaddition (Scheme 3.18).³⁸



Scheme 3.18. Examples of normal and inverse electron-demand pyridone Diels–Alder reactions.

The first example of a catalytic asymmetric pyridone Diels–Alder reaction, reported by Tan and co-workers in 2009, follows a similar strategy to that of the Deng group. As seen in Scheme 3.19, aminoindanol **173**, like the cinchona alkaloid derivative **79**, is used to induce a hydrogen bonding mode of catalysis that both activates 3-hydroxypyridone **171** and maleimide **172**, while at the same time inducing asymmetry.³⁹



Scheme 3.19. First example of a catalytic asymmetric pyridone Diels–Alder Reaction.

Our hope was that by preparing a sufficiently electron poor 2-pyridone, we might be able to engage the substrate in a similar dienamine catalyzed [4+2] cycloaddition in an asymmetric fashion. In practice this proved more difficult than a simple transposition of reaction conditions onto this new system. First, in terms of substitution on the pyridone ring, the only substrate which proved capable of engaging in the desired Diels–Alder reaction was the highly electron poor 3-bromo-5-carbomethoxy-2-pyridone (**175**). Following this, we screened a variety of protecting groups, finding that most sulfonyl groups were tolerated in the reaction. It should be noted that while the dinitrophenylsulfonyl group (DNs) was sufficiently electron withdrawing, conversion was often low as a result of the secondary amine catalyst promoting the deprotection of **176** back to the corresponding pyridinol. After settling on the nitrosulfonyl group (*p*-Ns), due to its ease of removal after the Diels–Alder reaction, we moved on to look at substrate scope. Unfortunately, many substrates showed limited consumption of the starting pyridone alongside complex reaction mixtures. As shown in Table 3.7, we attempted this reaction with several substrates that had performed well in the 2-pyrone variant, however only moderate conversion was ever obtained. We believe the greatest challenge is the electronic matching of the diene and dienophile. While we have placed two electron withdrawing groups on the ring, as well as the highly electron withdrawing *p*-Ns group on the nitrogen atom, the pyridone does not appear to be sufficiently electron poor to undergo the desired cycloaddition. In this case, where a competent diene partner is not present, it is thought that the dienamine itself can begin to react with the excess α,β -unsaturated aldehyde in solution, and not strictly in a [4+2] sense, thereby leading to the complex mixtures observed. Hence, any efforts going forward, will likely focus on the electronic properties of the pyridone partner in hopes of narrowing the diene-dienophile energy gap.

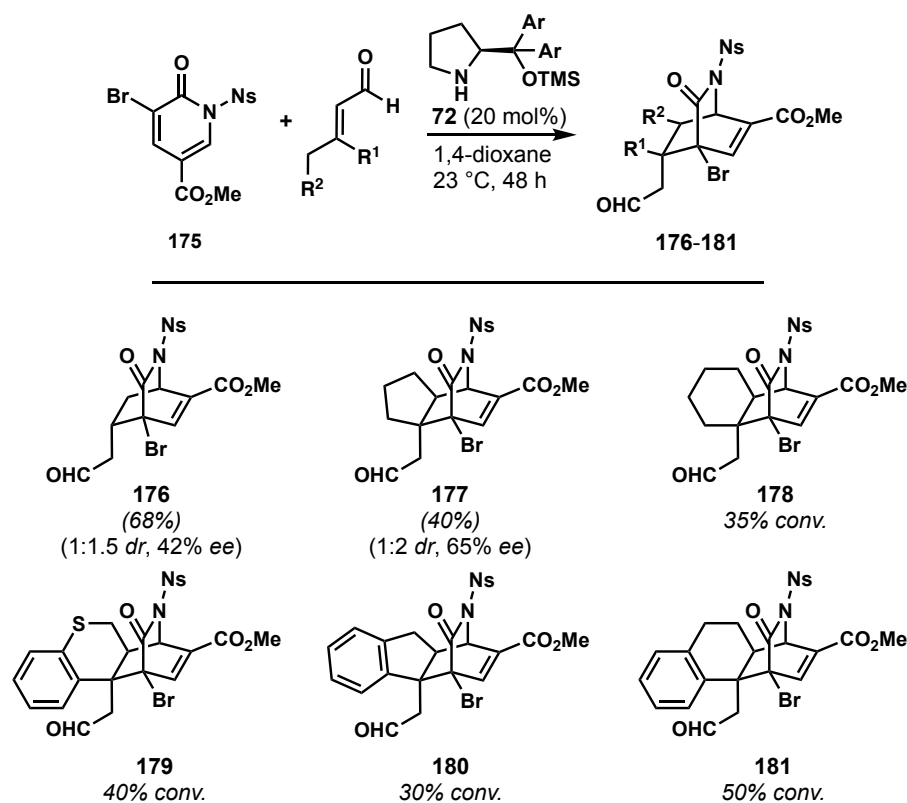


Table 3.7. Initial substrate screen for the dienamine catalyzed pyridone Diels–Alder Reaction.

3.10 Conclusion

This chapter presents our group's most recent contribution to the field of pyrone Diels–Alder reactions. By approaching this problem from the frame of dienophile activation, we have been able to access bicyclic lactone frameworks distinct from those accessible via previous methods. Further insight into the overall stereoselectivity of this reaction has been offered through the consideration of potential transition states. After exploring the substrate scope of this transformation, as well as derivatization of the products, we have shown initial forays into the application of this approach to the pyridone Diels–Alder reaction as well as to the study of the gardmutine alkaloids. It is our hope that the chemistry presented herein will prove useful to those within the field and aid in target-oriented synthesis where possible.

3.11 References

1. For selected reviews of the Diels–Alder reaction, see: (a) Corey, E. J. *Angew. Chem. Int. Ed.* **2002**, *41*, 1650; (b) Nicolaou, K. C.; Snyder, S. A.; Montagnon, T.; Vassilikogiannakis, G. *Angew. Chem. Int. Ed.* **2002**, *41*, 1668.
2. For reviews on the pyrone Diels–Alder reaction, see: (a) Afarinkia, K.; Vinader, V.; Nelson, T. D.; Posner, G. H. *Tetrahedron* **1992**, *48*, 9111; (b) Woodard, B. T.; Posner, G. H. *Adv. Cycloadd.* **1999**, *5*, 47; (c) Cai, Q. *Chin. J. Chem.* **2019**, *37*, 946.
3. Diels, O.; Alder, K.; Beckmann, S. *Ann.* **1931**, *486*, 191.
4. Goldstein, M.; Thayer Jr, G. *J. Am. Chem. Soc.* **1965**, *87*, 1925.
5. For selected examples where a pyrone Diels–Alder reaction is used to install a lactone, see: (a) Nelson, H. M.; Murakami, K.; Virgil, S. C.; Stoltz, B. M. *Angew. Chem. Int. Ed.* **2011**, *50*, 3688; (b) Smith, M. W.; Snyder, S. A. *J. Am. Chem. Soc.* **2013**, *135*, 12964; (c) Gordon, J. R.; Nelson, H. M.; Virgil, S. C.; Stoltz, B. M. *J. Org. Chem.* **2014**, *79*, 9740; (d) Zhao, Y. M.; Maimone, T. J. *Angew. Chem. Int. Ed.* **2015**, *54*, 1223; (e) Liang, X.; Zhou, L.; Min, L.; Ye, W.; Bao, W.; Ma, W.; Yang, Q.; Qiao, F.; Zhang, X.; Lee, C.-S. *J. Org. Chem.* **2017**, *82*, 3463.
6. For selected examples employing a pyrone Diels–Alder/retro-Diels–Alder sequence in total synthesis, see: (a) Boger, D. L.; Brotherton, C. E. *J. Org. Chem.* **1984**, *49*, 4050; (b) Boger, D. L.; Takahashi, K. *J. Am. Chem. Soc.* **1995**, *117*, 12452; (c) Baran, P. S.; Burns, N. Z. *J. Am. Chem. Soc.* **2006**, *128*, 3908; (d) Zhao, P.; Beaudry, C. M. *Org. Lett.* **2013**, *15*, 402; (e) Zhao, P.; Beaudry, C. M. *Angew. Chem. Int. Ed.* **2014**, *53*, 10500; (f) Zhao, P.; Beaudry, C. M. *Synlett* **2015**, *26*, 1923.
7. (a) Gan, P.; Smith, M. W.; Braffman, N. R.; Snyder, S. A. *Angew. Chem. Int. Ed.* **2016**, *55*, 3625; (b) Yu, X.; Xiao, L.; Wang, Z.; Luo, T. *J. Am. Chem. Soc.* **2019**, *141*, 3440.
8. For selected examples using the relative stereochemistry imparted through a key pyrone Diels–Alder reaction, see: (a) Posner, G. H.; Wettlaufer, D. G. *J. Am. Chem. Soc.* **1986**, *108*, 7373; (b) Posner, G. H.; Kinter, C. M. *J. Org. Chem.* **1990**, *55*, 3967; (c) Shin, I. J.; Choi, E. S.; Cho, C. G. *Angew. Chem. Int. Ed.* **2007**, *46*, 2303; (d) Tam, N. T.; Chang, J.; Jung, E.-J.; Cho, C.-G. *J. Org. Chem.* **2008**, *73*, 6258; (e) Chang, J. H.; Kang, H.-U.; Jung, I.-H.; Cho, C.-G. *Org. Lett.* **2010**, *12*, 2016; (f) Jung, Y.-G.; Lee, S.-C.; Cho, H.-K.; Darvatkar, N. B.; Song, J.-Y.; Cho, C.-G. *Org. Lett.* **2012**, *15*, 132; (g) Cho, H.-K.; Lim, H.-Y.; Cho, C.-G. *Org. Lett.* **2013**, *15*, 5806; (h) Lee, J.-H.; Cho, C.-G. *Org. Lett.* **2016**, *18*, 5126.
9. Jung, Y.-G.; Lee, S.-C.; Cho, H.-K.; Darvatkar, N. B.; Song, J.-Y.; Cho, C.-G. *Org. Lett.* **2013**, *15*, 132.
10. Cho, C.-G.; Kim, Y.-W.; Lim, Y.-K.; Park, J.-S.; Lee, H.; Koo, S. *J. Org. Chem.* **2002**, *67*, 290.

11. For examples of pyrone Diels–Alder reactions involving chiral auxiliaries, see: (a) Posner, G. H.; Wettlaufer, D. G. *Tetrahedron Lett.* **1986**, *27*, 667; (b) Markó, I. E.; Evans, G. R. *Tetrahedron Lett.* **1994**, *35*, 2767; (c) Okamura, H.; Morishige, K.; Iwagawa, T.; Nakatani, M. *Tetrahedron Lett.* **1998**, *39*, 1211; (d) Afarinkia, K.; Posner, G. H. *Tetrahedron Lett.* **1992**, *33*, 7839.
12. For early catalytic asymmetric examples, see: (a) Markó, I. E.; Evans, G. R.; Declercq, J.-P. *Tetrahedron* **1994**, *50*, 4557; (b) Posner, G. H.; Dai, H.; Bull, D. S.; Lee, J.-K.; Eydoux, F.; Ishihara, Y.; Welsh, W.; Pryor, N.; Petr, S. *J. Org. Chem.* **1996**, *61*, 671; (c) Markó, I. E.; Chellé-Regnaut, I.; Leroy, B.; Warriner, S. L. *Tetrahedron Lett.* **1997**, *38*, 4269; (d) Hashimoto, Y.; Abe, R.; Morita, N.; Tamura, O. *Org. Biomol. Chem.* **2018**, *16*, 8913.
13. (a) Posner, G. H.; Carry, J. C.; Anjeh, T. E.; French, A. N. *J. Org. Chem.* **1992**, *57*, 7012; (b) Posner, G. H.; Dai, H.; Afarinkia, K.; Murthy, N. N.; Guyton, K. Z.; Kensler, T. W. *J. Org. Chem.* **1993**, *58*, 7209; (c) Posner, G. H.; Eydoux, F.; Lee, J.; Bull, D. S. *Tetrahedron Lett.* **1994**, *35*, 7541; (d) Posner, G. H.; Ishihara, Y. *Tetrahedron Lett.* **1994**, *35*, 7545.
14. (a) Okamura, H.; Nakamura, Y.; Iwagawa, T.; Nakatani, M. *Chem. Lett.* **1996**, *25*, 193; (b) Okamura, H.; Shimizu, H.; Nakamura, Y.; Iwagawa, T.; Nakatani, M. *Tetrahedron Lett.* **2000**, *41*, 4147; (c) Shimizu, H.; Okamura, H.; Yamashita, N.; Iwagawa, T.; Nakatani, M. *Tetrahedron Lett.* **2001**, *42*, 8649; (d) Shimizu, H.; Okamura, H.; Iwagawa, T.; Nakatani, M. *Tetrahedron* **2001**, *57*, 1903.
15. (a) Wang, Y.; Li, H.; Wang, Y.-Q.; Liu, Y.; Foxman, B. M.; Deng, L. *J. Am. Chem. Soc.* **2007**, *129*, 6364; (b) Singh, R. P.; Bartelson, K.; Wang, Y.; Su, H.; Lu, X.; Deng, L. *J. Am. Chem. Soc.* **2008**, *130*, 2422.
16. Shi, L.-M.; Dong, W.-W.; Tao, H.-Y.; Dong, X.-Q.; Wang, C.-J. *Org. Lett.* **2017**, *19*, 4532.
17. (a) Liang, X. W.; Zhao, Y.; Si, X. G.; Xu, M. M.; Tan, J. H.; Zhang, Z. M.; Zheng, C. G.; Zheng, C.; Cai, Q. *Angew. Chem. Int. Ed.* **2019**, *58*, 14562; (b) Si, X. G.; Zhang, Z. M.; Zheng, C. G.; Li, Z. T.; Cai, Q. *Angew. Chem. Int. Ed.* **2020**, *59*, 18412.
18. (a) Mukherjee, S.; Yang, J. W.; Hoffmann, S.; List, B. *Chem. Rev.* **2007**, *107*, 5471; (b) Moyano, A.; Rios, R. *Chem. Rev.* **2011**, *111*, 4703; (c) Li, J.-L.; Liu, T.-Y.; Chen, Y.-C. *Acc. Chem. Res.* **2012**, *45*, 1491; (d) Arceo, E.; Melchiorre, P. *Angew. Chem. Int. Ed.* **2012**, *51*, 5290; (e) Ramachary, D. B.; Reddy, Y. V. *Eur. J. Org. Chem.* **2012**, 865; (f) Jurberg, I. D.; Chatterjee, I.; Tannert, R.; Melchiorre, P. *Chem. Commun.* **2013**, *49*, 4869; (g) Jiang, X.; Wang, R. *Chem. Rev.* **2013**, *113*, 5515; (h) Marcos, V.; Alemán, J. *Chem. Soc. Rev.* **2016**, *45*, 6812; (i) Held, F. E.; Tsogoeva, S. B. *Catal. Sci. Technol.* **2016**, *6*, 645; (j) Klier, L.; Tur, F.; Poulsen, P. H.; Jørgensen, K. A. *Chem. Soc. Rev.* **2017**, *46*, 1080.
19. For reviews on computational studies of dienamine catalyzed reactions, see: (a) Halskov, K. S.; Donslund, B. S.; Paz, B. M.; Jørgensen, K. A. *Acc. Chem. Res.* **2016**, *49*, 974; (b) Renzi, P.; Hioe, J.; Gschwind, R. M. *Acc. Chem. Res.* **2017**, *50*, 2936.

20. (a) Hayashi, Y.; Gotoh, H.; Hayashi, T.; Shoji, M. *Angew. Chem. Int. Ed.* **2005**, *44*, 4212; (b) Franzén, J.; Marigo, M.; Fielenbach, D.; Wabnitz, T. C.; Kjærsgaard, A.; Jørgensen, K. A. *J. Am. Chem. Soc.* **2005**, *127*, 18296; (c) Mielgo, A. *Chem. Asian J.* **2008**, *3*, 922; (d) Palomo, C.; Mielgo, A. *Angew. Chem. Int. Ed.* **2006**, *45*, 7876; (e) Jensen, K. L.; Dickmeiss, G.; Jiang, H.; Albrecht, Ł.; Jørgensen, K. A. *Acc. Chem. Res.* **2012**, *45*, 248; (f) Donslund, B. S.; Monleón, A.; Larsen, J.; Ibsen, L.; Jørgensen, K. A. *Chem. Commun.* **2015**, *51*, 13666; (g) Reyes-Rodríguez, G. J.; Rezayee, N. M.; Vidal-Albalat, A.; Jørgensen, K. A. *Chem. Rev.* **2019**, *119*, 4221.
21. (a) Li, J. L.; Kang, T. R.; Zhou, S. L.; Li, R.; Wu, L.; Chen, Y. C. *Angew. Chem. Int. Ed.* **2010**, *49*, 6148; (b) Li, J.-L.; Zhou, S.-L.; Chen, P.-Q.; Dong, L.; Liu, T.-Y.; Chen, Y.-C. *Chem. Sci.* **2012**, *3*, 1879.
22. (a) Albrecht, Ł.; Dickmeiss, G.; Weise, C. F.; Rodríguez-Escrich, C.; Jørgensen, K. A. *Angew. Chem. Int. Ed.* **2012**, *51*, 13109; (b) Weise, C. F.; Lauridsen, V. H.; Rambo, R. S.; Iversen, E. H.; Olsen, M.-L.; Jørgensen, K. A. *J. Org. Chem.* **2014**, *79*, 3537.
23. Zhou, Y.; Zhou, Z.; Du, W.; Chen, Y. *Acta Chim. Sin.* **2018**, *76*, 382.
24. (a) Imagawa, T.; Sueda, N.; Kawanisi, M. *Tetrahedron* **1974**, *30*, 2227; (b) Jung, M. E.; Street, L. J.; Usui, Y. *J. Am. Chem. Soc.* **1986**, *108*, 6810; (c) Markó, I. E.; Evans, G. R. *Tetrahedron Lett.* **1993**, *34*, 7309; (d) Kraus, G. A.; Pollock III, G. R.; Beck, C. L.; Palmer, K.; Winter, A. H. *RSC Adv.* **2013**, *3*, 12721; (e) Yu, H.; Kraus, G. A. *Tetrahedron Lett.* **2018**, *59*, 4008.
25. For a review on the importance of additives in these systems see: Hong, L.; Sun, W.; Yang, D.; Li, G.; Wang, R. *Chem. Rev.* **2016**, *116*, 4006.
26. Bertelsen, S.; Marigo, M.; Brandes, S.; Diner, P.; Jørgensen, K. A. *J. Am. Chem. Soc.* **2006**, *128*, 12973.
27. Liu, Q.; Zu, L. *Angew. Chem. Int. Ed.* **2018**, *57*, 9505.
28. Posner, G. H.; Nelson, T. D.; Kinter, C. M.; Afarinkia, K. *Tetrahedron Lett.* **1991**, *32*, 5295.
29. Saktura, M.; Grzelak, P.; Dybowska, J.; Albrecht, Ł. *Org. Lett.* **2020**, *22*, 1813.
30. Nicolaou, K.; Estrada, A. A.; Zak, M.; Lee, S. H.; Safina, B. S. *Angew. Chem. Int. Ed.* **2005**, *44*, 1378.
31. Barton, D. H.; Crich, D.; Motherwell, W. B. *Tetrahedron* **1985**, *41*, 3901.
32. Zhong, X.-H.; Xiao, L.; Wang, Q.; Zhang, B.-J.; Bao, M.-F.; Cai, X.-H.; Peng, L. *Phytochem. Lett.* **2014**, *10*, 55.
33. For selected reviews on the preparation of *gem*-dihalocyclopropanes and subsequent ring opening, see: (a) Banwell, M. G.; Harvey, J. E.; Hockless, D. C.; Wu, A. W. *J. Org. Chem.* **2000**, *65*, 4241; (b) Banwell, M.; Edwards, A.; Harvey, J.; Hockless, D.;

- Willis, A. *J. Chem. Soc., Perkin Trans. 1* **2000**, 2175; (c) Matveenko, M.; Kokas, O. J.; Banwell, M. G.; Willis, A. C. *Org. Lett.* **2007**, *9*, 3683.
34. For an example of *gem*-dibromocyclopropane ring formation on a similar system, see: Banwell, M. G.; Forman, G. S.; Hockless, D. C. *Acta Crystal. Sec. C: Cryst. Struct. Commun.* **1996**, *52*, 1804.
35. Kats-Kagan, R.; Herzon, S. B. *Org. Lett.* **2015**, *17*, 2030.
36. (a) Thyagarajan, B.; Rajagopalan, K. *Tetrahedron* **1963**, *19*, 1483; (b) Beak, P. *Acc. Chem. Res.* **1977**, *10*, 186; (c) Bird, C. *Tetrahedron* **1986**, *42*, 89.
37. (a) Mckillop, A.; Zelesko, M. J.; Taylor, E. C. *Tetrahedron Lett.* **1968**, *9*, 4945; (b) Curtin, D. Y.; Engelmann, J. H. *Tetrahedron Lett.* **1968**, *9*, 3911.
38. (a) Posner, G. H.; Switzer, C. *J. Org. Chem.* **1987**, *52*, 1642; (b) Herdeis, C.; Hartke, C. *Heterocycles* **1989**, *29*, 287; (c) Herdeis, C.; Hartke-Karger, C. *Liebigs Ann. Chem.* **1991**, *99*, 10.
39. Soh, J. Y.-T.; Tan, C.-H. *J. Am. Chem. Soc.* **2009**, *131*, 6904.

3.12 Experimental Section

General Procedures. All reactions were carried out under an argon atmosphere with dry solvents under anhydrous conditions, unless otherwise noted. Dry tetrahydrofuran (THF), toluene, diethyl ether (Et₂O), dichloromethane (CH₂Cl₂), and acetonitrile (CH₃CN) were obtained by passing commercially available pre-dried, oxygen-free formulations through activated alumina columns. Yields refer to chromatographically and spectroscopically (¹H and ¹³C NMR) homogeneous materials, unless otherwise stated. Reagents were purchased at the highest commercial quality and used without further purification, unless otherwise stated. Reactions were magnetically stirred and monitored by thin-layer chromatography (TLC) carried out on 0.25 mm E. Merck silica gel plates (60F-254) using UV light as visualizing agent, and an ethanolic solution of phosphomolybdic acid and cerium sulfate or a solution of KMnO₄ in aq. NaHCO₃ and heat as developing agents. SiliCycle silica gel (60, academic grade, particle size 0.040–0.063 mm) was used for flash column chromatography. Preparative thin-layer chromatography separations were carried out on 0.50 mm E. Merck silica gel plates (60F-254). NMR spectra were recorded on Bruker 400 and 500 MHz instruments and calibrated using residual undeuterated solvent as an internal reference. The following abbreviations were used to explain the multiplicities: s = singlet, d = doublet, t = triplet, q = quartet, br = broad, app = apparent. IR spectra were recorded on a Perkin-Elmer 1000 series FT-IR spectrometer. High-resolution mass spectra (HRMS) were recorded on Agilent 6244 ToF-MS using ESI (Electrospray Ionization) at the University of Chicago Mass Spectroscopy Core Facility. All *ee* values were determined by HPLC on Daicel Chiralcel or Chiralpak columns.

General Procedure for Dienamine Catalyzed Cycloaddition. To a 1 dram screw-capped vial was added the pyrone substrate (0.30 mmol, 1.0 equiv.), (*S*)- α,α -bis[3,5-bis(trifluoromethyl)phenyl]-2-pyrrolidinemethanol trimethylsilyl ether (9.0 mg, 0.015 mmol,

0.05 equiv.), the α,β -unsaturated aldehyde (0.15 mmol, 3.0 equiv.) and Et₂O (1.5 mL). The reaction contents were stirred at 23 °C for 24 h. Upon completion, the reaction mixture was subjected directly to flash column chromatography to give the desired cycloadducts. In order to determine enantiomeric excess, all aldehydes were converted into the corresponding α,β -unsaturated methyl ester as follows: to a 1 dram screw-capped vial containing a solution of the cycloadduct (0.1 mmol, 1.0 equiv.) in CH₂Cl₂ (1.0 mL) at 23 °C was added methyl (triphenylphosphoranylidene)acetate (0.100 g, 0.3 mmol, 3.0 equiv.) and the reaction mixture stirred at 23 °C for 1 h. Upon completion, the crude reaction mixture was subjected directly to preparative TLC (silica gel, hexanes/EtOAc, 3:1) to afford the desired product that was subsequently analyzed by chiral phase HPLC.

Methyl(3a*R*,4*R*,7*R*,7a*R*)-8-oxo-7a-(2-oxoethyl)-2,3,3a,4,7,7a-hexahydro-1*H*-4,7-(epoxy methano)indene-5-carboxylate (*Endo*-88). Prepared following the general procedure described above, the crude material was purified by flash column chromatography (silica gel, hexanes/EtOAc, 3:1) to afford the desired product (73.0 mg combined, 93% combined yield; 62.3 mg, 80% yield *Endo*-88; 10.7 mg, 13% yield *Exo*-88) as a pale yellow oil. The *dr* was 6:1 as determined by crude ¹H NMR. *Endo*-88: R_f = 0.13 (silica gel, hexanes/EtOAc, 2:1); [α]_D²³ = -6.00° (*c* = 1.0 in CHCl₃); IR (thin film) 2955, 2870, 1759, 1718, 1258 cm⁻¹; ¹H NMR (500 MHz, CDCl₃) δ 9.71 (d, *J* = 1.8 Hz, 1 H), 7.28 (dd, *J* = 6.4, 2.1 Hz, 1 H), 5.45 (d, *J* = 1.9 Hz, 1 H), 3.80 (s, 3 H), 3.77 (d, *J* = 6.4 Hz, 1 H), 2.52 (dd, *J* = 16.7, 1.6 Hz, 1 H), 2.41 (dd, *J* = 16.6, 2.2 Hz, 1 H), 2.04–1.98 (m, 2 H), 1.88–1.74 (m, 5 H); ¹³C NMR (126 MHz, CDCl₃) δ 199.94, 171.54, 162.69, 140.98, 137.55, 77.55, 53.15, 51.40, 49.63, 48.15, 36.05, 28.57, 27.27; HRMS (ESI) calcd for C₁₄H₁₅O₄⁺ [M+H-H₂O]⁺ 247.0965, found: 247.0966. The enantiomeric excess was determined by chiral HPLC using a Daicel Chiralpak IA column (hexanes/*i*-PrOH,

85:15, flow rate of 1.0 mL/min, 254 nm) $t_R = 8.83$ min (minor), $t_R = 11.42$ min (major), 94% *ee*.

Exo-88: $R_f = 0.16$ (silica gel, hexanes/EtOAc, 2:1); $[\alpha]_D^{23} = +2.42$ ($c = 1.0$ in CHCl_3). IR (thin film) 2955, 2872, 1759, 1718, 1258 cm^{-1} ; ^1H NMR (500 MHz, CDCl_3) δ 9.78 (t, $J = 1.2$ Hz, 1 H), 7.34 (dd, $J = 6.6, 2.4$ Hz, 1 H), 5.54 (dd, $J = 4.3, 2.4$ Hz, 1 H), 4.01 (d, $J = 6.6$ Hz, 1 H), 3.83 (s, 3 H), 2.75 (dd, $J = 17.9, 1.4$ Hz, 1 H), 2.71–2.63 (m, 1 H), 2.53 (ddd, $J = 8.8, 7.0, 4.2$ Hz, 1 H), 2.00 (dq, $J = 13.8, 6.8$ Hz, 1 H), 1.83 (dt, $J = 12.4, 5.6$ Hz, 1 H), 1.66–1.60 (m, 2 H), 1.51 (dt, $J = 13.6, 8.2$ Hz, 1 H), 1.11 (dq, $J = 14.0, 7.8$ Hz, 1 H); ^{13}C NMR (126 MHz, CDCl_3) δ 199.51, 171.88, 163.34, 141.30, 136.76, 76.96, 53.42, 52.51, 52.11, 50.31, 47.72, 36.47, 28.74, 27.01; HRMS (ESI) calcd for $\text{C}_{14}\text{H}_{17}\text{O}_5^+$ $[\text{M}+\text{H}]^+$ 265.1071, found 265.1060. The enantiomeric excess was determined by chiral HPLC using a Daicel Chiralpak IA column (hexanes/*i*PrOH, 95:5, flow rate of 1.0 mL/min, 254 nm) $t_R = 15.30$ min (major), $t_R = 19.32$ min (minor), 85% *ee*.

Methyl(1*R*,4*R*,4*aR*,8*aR*)-9-oxo-4a-(2-oxoethyl)-1,4,4a,5,6,7,8,8a-octahydro-1,4-(epoxy methano)naphthalene-2-carboxylate (Endo-102). Prepared following the general procedure described above, the crude material was purified by flash column chromatography (silica gel, hexanes/EtOAc, 3:1) to afford the desired product (41.0 mg combined, 50% combined yield; 28.7 mg, 35% yield **Endo-102**; 12.3 mg, 15% yield **Exo-102**) as a colorless oil. The *dr* was 3:1 as determined by crude ^1H NMR. **Endo-102:** $R_f = 0.17$ (silica gel, hexanes/EtOAc, 2:1); $[\alpha]_D^{21} = -33.96^\circ$ ($c = 1.0$ in CHCl_3); IR (thin film) 2951, 2871, 1759, 1717, 1633, 1261 cm^{-1} ; ^1H NMR (500 MHz, CDCl_3) δ 9.73 (t, $J = 2.2$ Hz, 1 H), 7.25 (dd, $J = 5.9, 1.7$ Hz, 1 H), 5.35–5.33 (m, 1 H), 3.80 (s, 4 H), 2.57 (dd, $J = 16.0, 2.2$ Hz, 1 H), 2.11 (dt, $J = 16.0, 2.1$ Hz, 1 H), 1.89–1.73 (m, 3 H), 1.72–1.53 (m, 3 H), 1.52–1.43 (m, 1 H), 1.40–1.28 (m, 2 H); ^{13}C NMR (126 MHz, CDCl_3) δ 199.93, 171.38, 162.62, 139.20, 136.81, 77.33, 52.43, 51.51, 50.68, 44.20,

37.86, 27.39, 22.61, 18.69, 16.70; HRMS (ESI) calcd for $C_{15}H_{17}O_4^+$ $[M+H-H_2O]^+$ 261.1121, found 261.1123. The enantiomeric excess was determined by chiral HPLC using a Daicel Chiralpak IA column (hexanes/*i*-PrOH, 95:5, flow rate of 1.0 mL/min, 254 nm) $t_R = 19.75$ min (minor), $t_R = 26.89$ min (major), 94% *ee*.

Exo-102: $R_f = 0.25$ (silica gel, hexanes/EtOAc, 2:1); $[\alpha]_D^{21} = +7.30^\circ$ ($c = 1.0$ in $CHCl_3$); IR (thin film) 2936, 2868, 1759, 1719, 1638, 1257 cm^{-1} ; 1H NMR (500 MHz, $CDCl_3$) δ 9.79 (dd, $J = 2.6, 1.1$ Hz, 1 H), 7.32 (dd, $J = 6.6, 2.3$ Hz, 1 H), 5.44 (dd, $J = 3.6, 2.2$ Hz, 1 H), 3.95 (d, $J = 6.6$ Hz, 1 H), 3.81 (s, 3 H), 2.74 (dd, $J = 17.1, 2.5$ Hz, 1 H), 2.44 (dt, $J = 17.3, 1.4$ Hz, 1 H), 1.86 (ddd, $J = 12.9, 5.3, 3.6$ Hz, 1 H), 1.79–1.45 (m, 4 H), 1.37–1.22 (m, 1 H), 1.16 (dddd, $J = 14.3, 12.9, 7.3, 1.9$ Hz, 1 H), 0.71 (qd, $J = 13.3, 3.7$ Hz, 1 H); ^{13}C NMR (126 MHz, $CDCl_3$) δ 199.55, 171.39, 163.13, 140.73, 135.03, 77.14, 52.45, 51.62, 50.87, 46.07, 38.86, 26.06, 23.24, 18.57, 16.38; HRMS (ESI) calcd for $C_{15}H_{18}O_5^+$ $[M]^+$ 278.1154, found 278.1151. The enantiomeric excess was determined by chiral HPLC using a Daicel Chiralpak IA column (hexanes/*i*PrOH, 95:5, flow rate of 1.0 mL/min, 254 nm) $t_R = 24.05$ min (major), $t_R = 27.30$ min (minor), 73% *ee*.

Methyl(1*R*,4*R*,4*aR*,9*aR*)-10-oxo-4*a*-(2-oxoethyl)-4,4*a*,5,6,7,8,9,9*a*-octahydro-1*H*-1,4-(epoxymethano)benzo[7]annulene-2-carboxylate (Endo-103). Prepared following the general procedure described above, the crude material was purified by flash column chromatography (silica gel, hexanes/EtOAc, 3:1) to afford the desired product (68.0 mg combined, 76% combined yield; 62.3 mg, 70 % yield **Endo-103**; 5.7 mg, 6% yield **Exo-103**) as a colorless oil. The *dr* was 10:1 as determined by crude 1H NMR. **Endo-103:** $R_f = 0.20$ (silica gel, hexanes/EtOAc, 2:1); $[\alpha]_D^{21} = -31.76^\circ$ ($c = 1.0$ in $CHCl_3$); IR (thin film) 2927, 2856, 1758, 1717, 1637, 1258, 752 cm^{-1} ; 1H NMR (500 MHz, $CDCl_3$) δ 9.72 (d, $J = 2.0$ Hz, 1 H), 7.29 (d, $J = 6.4$ Hz, 1 H), 5.25 (d, $J = 1.6$ Hz, 1 H), 3.79 (d, $J = 1.5$ Hz, 3 H), 3.71 (dd, $J = 6.4, 1.3$ Hz,

1 H), 2.86 (dt, $J = 16.2, 1.6$ Hz, 1 H), 2.15 (dd, $J = 16.2, 1.9$ Hz, 1 H), 2.06–1.91 (m, 3 H), 1.83 (d, $J = 13.2$ Hz, 2 H), 1.76–1.65 (m, 1 H), 1.62–1.41 (m, 3 H), 1.33–1.14 (m, 2 H); ^{13}C NMR (126 MHz, CDCl_3) δ 199.83, 171.30, 162.70, 140.41, 136.86, 79.49, 53.51, 52.39, 51.70, 49.46, 42.13, 34.42, 31.17, 30.66, 28.21, 24.76; HRMS (ESI) calcd for $\text{C}_{16}\text{H}_{21}\text{O}_5^+$ $[\text{M}+\text{H}]^+$ 293.1384, found 293.1392. The enantiomeric excess was determined by chiral HPLC using a Daicel Chiralpak IA column (hexanes/*i*-PrOH, 95:5, flow rate of 1.0 mL/min, 254 nm) $t_R = 19.49$ min (minor), $t_R = 28.49$ min (major), 97% *ee*.

2-((1*R*,4*R*,4*aR*,10*aR*)-2-((methylperoxy)methyl)-11-oxo1,5,6,7,8,9,10,10a octahydro-1,4-epoxymethano)benzo[8]annulen-4*a*(4*H*)-yl)acet aldehyde (*Endo*-104). Prepared following the general procedure described above, the crude material was purified by flash column chromatography (silica gel, hexanes/EtOAc, 3:1) to afford the desired product (66.8 mg combined, 75% combined yield; 45.0 mg, 51% yield *Endo*-104; 21.8 mg, 24% yield *Exo*-104) as a pale yellow oil. The *dr* was 2:1 as determined by crude ^1H NMR. ***Endo*-104:** $R_f = 0.14$ (silica gel, hexanes/EtOAc, 2:1); $[\alpha]_{\text{D}}^{21} = -1.90^\circ$ ($c = 1.0$ in CHCl_3); IR (thin film) 2927, 2855, 1757, 1717, 1643, 1263 cm^{-1} ; ^1H NMR (500 MHz, CDCl_3) δ 9.74 (d, $J = 1.7$ Hz, 1 H), 7.29 (dt, $J = 6.5, 1.7$ Hz, 1 H), 5.36 (d, $J = 2.0$ Hz, 1 H), 3.81 (d, $J = 1.3$ Hz, 3 H), 3.76 (d, $J = 6.4$ Hz, 1 H), 2.97 (d, $J = 17.0$ Hz, 1 H), 2.15 (d, $J = 17.0$ Hz, 1 H), 2.09 (dd, $J = 15.5, 5.1$ Hz, 1 H), 2.01–1.90 (m, 1 H), 1.83–1.12 (m, 11 H); ^{13}C NMR (126 MHz, CDCl_3) δ 199.69, 171.46, 162.79, 141.40, 135.69, 81.85, 55.04, 52.41, 50.73, 46.76, 42.33, 33.77, 29.41, 28.42, 26.39, 26.36, 25.58. HRMS (ESI) calcd for $\text{C}_{17}\text{H}_{23}\text{O}_5^+$ $[\text{M}+\text{H}]^+$ 307.1540, found 307.1545. The enantiomeric excess was determined by chiral HPLC using a Daicel Chiralpak AD-H column (hexanes/*i*-PrOH, 98:2, flow rate of 1.0 mL/min, 254 nm) $t_R = 24.05$ min (major), $t_R = 27.30$ min (minor), 73% *ee*.

Exo-104: $R_f = 0.25$ (silica gel, hexanes/EtOAc, 2:1); $[\alpha]_D^{21} = -32.56^\circ$ ($c = 1.0$ in CHCl_3); IR (thin film) 2928, 2855, 1759, 1717, 1636, 1258 cm^{-1} ; ^1H NMR (500 MHz, CDCl_3) δ 9.78 (d, $J = 1.7$ Hz, 1 H), 7.30 (dd, $J = 6.6, 2.3$ Hz, 1 H), 5.39 (dd, $J = 4.0, 2.3$ Hz, 1 H), 3.98 (d, $J = 6.7$ Hz, 1 H), 3.81 (s, 3 H), 3.16 (dd, $J = 18.3, 1.8$ Hz, 1 H), 2.48 (d, $J = 18.3$ Hz, 1 H), 2.03 (ddd, $J = 15.1, 5.9, 2.5$ Hz, 1 H), 1.75 (dd, $J = 9.7, 3.9$ Hz, 1 H), 1.73–1.58 (m, 3 H), 1.53–1.37 (m, 4 H), 1.31–1.08 (m, 4 H); ^{13}C NMR (126 MHz, CDCl_3) δ 199.11, 171.87, 163.14, 140.25, 135.82, 79.11, 53.92, 52.43, 52.27, 49.28, 43.23, 33.16, 29.12, 26.30, 25.97, 25.76, 25.34; HRMS (ESI) calcd for $\text{C}_{17}\text{H}_{23}\text{O}_5^+ [\text{M}+\text{H}]^+$ 307.1540, found 307.1532. The enantiomeric excess was determined by chiral HPLC using a Daicel Chiralpak AD-H column (hexanes/*i*-PrOH, 95:5, flow rate of 1.0 mL/min, 254 nm) $t_R = 18.88$ min (minor), $t_R = 30.12$ min (major), 2% *ee*.

Methyl(1*R*,4*R*,4*aR*,14*aR*)-15-oxo-4a-(2-oxoethyl)-1,4,4a,5,6,7,8,9,10,11,12,13,14,14a-tetra decahydro-1,4-(epoxymethano)benzo[12] annulene-2-carboxylate (Endo-105). Prepared following the general procedure described above, the crude material was purified by flash column chromatography (silica gel, hexanes/EtOAc, 3:1) to afford the desired product (47.1 mg, 47% yield **Endo-105**) as a colorless oil. The *dr* was >20:1 as determined by crude ^1H NMR. **Endo-105:** $R_f = 0.37$ (silica gel, hexanes/EtOAc, 2:1); $[\alpha]_D^{21} = -6.86^\circ$ ($c = 1.0$ in CHCl_3); IR (thin film) 2931, 2861, 1763, 1719, 1639, 1258 cm^{-1} ; ^1H NMR (500 MHz, CDCl_3) δ 9.84 (d, $J = 2.1$ Hz, 1 H), 7.18 (dd, $J = 6.5, 2.3$ Hz, 1 H), 5.42 (d, $J = 2.3$ Hz, 1 H), 3.96 (d, $J = 6.5$ Hz, 1 H), 3.83 (s, 3 H), 2.70 (dd, $J = 17.2, 2.2$ Hz, 1 H), 2.45 (d, $J = 17.1$ Hz, 1 H), 1.84–1.75 (m, 1 H), 1.72 (dd, $J = 9.6, 3.4$ Hz, 1 H), 1.65–1.54 (m, 3 H), 1.43–1.21 (m, 11 H), 1.19–1.06 (m, 5 H); ^{13}C NMR (126 MHz, CDCl_3) δ 199.97, 171.95, 162.61, 138.50, 136.98, 77.22, 52.41, 51.28, 46.91, 43.56, 40.32, 37.64, 28.23, 26.54, 25.72, 24.77, 24.09, 24.06, 23.97, 23.92, 22.54; HRMS (ESI) calcd for $\text{C}_{21}\text{H}_{31}\text{O}_5^+ [\text{M}+\text{H}]^+$ 363.2166, found 363.2174. The enantiomeric excess

was determined by chiral HPLC using a Daicel Chiralpak AD-H column (hexanes/*i*-PrOH, 90:10, flow rate of 1.0 mL/min, 254 nm) $t_R = 8.76$ min (minor), $t_R = 10.59$ min (major), 21% *ee*.

Methyl(1*R*,4*R*,4*aS*,9*aR*)-10-oxo-4*a*-(2-oxoethyl)-4,4*a*,9,9*a*-tetrahydro-1*H*-1,4-(epoxy methano)fluorene-2-carboxylate (*Endo*-106). Prepared following the general procedure described above, the crude material was purified by flash column chromatography (silica gel, hexanes/EtOAc, 3:1) to afford the desired product (65.5 mg combined, 70% combined yield; 42.6 mg, 46% yield *Endo*-106; 22.9 mg, 24% yield *Exo*-106) as a pale yellow oil. The *dr* was 2:1 as determined by crude ^1H NMR. ***Endo*-106:** $R_f = 0.12$ (silica gel, hexanes/EtOAc, 2:1); $[\alpha]_D^{21} = -119.50^\circ$ ($c = 1.0$ in CHCl_3); IR (thin film) 2953, 2851, 1762, 1720, 1634, 1254, 758 cm^{-1} ; ^1H NMR (500 MHz, CDCl_3) δ 9.41 (s, 1 H), 7.36 (dd, $J = 6.3, 2.1$ Hz, 1 H), 7.25 (t, $J = 4.4$ Hz, 3 H), 7.20 (q, $J = 4.2$ Hz, 1 H), 5.62 (d, $J = 2.1$ Hz, 1 H), 3.91 (d, $J = 6.3$ Hz, 1 H), 3.84 (s, 3 H), 3.49 (dd, $J = 17.1, 10.1$ Hz, 1 H), 3.15 (dd, $J = 17.1, 3.1$ Hz, 1 H), 3.00 (dd, $J = 16.0, 1.5$ Hz, 1 H), 2.65 (dt, $J = 10.1, 2.5$ Hz, 1 H), 2.60 (dd, $J = 16.1, 2.4$ Hz, 1 H); ^{13}C NMR (126 MHz, CDCl_3) δ 199.49, 169.80, 162.51, 143.14, 141.75, 139.48, 137.16, 129.35, 127.84, 125.69, 123.26, 78.24, 53.68, 53.31, 53.19, 52.55, 46.56, 34.58; HRMS (ESI) calcd for $\text{C}_{18}\text{H}_{15}\text{NO}_4^+$ $[\text{M}+\text{H}-\text{H}_2\text{O}]^+$ 295.0965, found 295.0972. The enantiomeric excess was determined by chiral HPLC using a Daicel Chiralpak AD-H column (hexanes/*i*-PrOH, 90:10, flow rate of 1.0 mL/min, 254 nm) $t_R = 21.19$ min (major), $t_R = 25.69$ min (minor), 98% *ee*.

***Exo*-106:** $R_f = 0.27$ (silica gel, hexanes/EtOAc, 2:1); $[\alpha]_D^{21} = -77.24^\circ$ ($c = 1.0$ in CHCl_3); IR (thin film) 2953, 2852, 1759, 1719, 1636, 1259, 755 cm^{-1} ; ^1H NMR (500 MHz, CDCl_3) δ 9.47 (d, $J = 1.6$ Hz, 1 H), 7.18 (dd, $J = 5.8, 3.1$ Hz, 2 H), 7.16–7.10 (m, 1 H), 7.10–7.05 (m, 1 H), 6.83 (dd, $J = 6.5, 2.3$ Hz, 1 H), 5.70 (dd, $J = 4.4, 2.3$ Hz, 1 H), 3.92 (d, $J = 6.5$ Hz, 1 H), 3.71 (s, 3 H), 3.37 (dd, $J = 17.3, 10.2$ Hz, 1 H), 3.22 (dd, $J = 17.1, 1.4$ Hz, 1 H), 3.14

(ddd, $J = 10.2, 4.4, 3.2$ Hz, 1 H), 2.88 (dd, $J = 17.1, 1.8$ Hz, 1 H), 2.55 (dd, $J = 17.4, 3.2$ Hz, 1 H); ^{13}C NMR (126 MHz, CDCl_3) δ 198.72, 171.03, 163.36, 143.09, 142.35, 140.89, 134.12, 128.87, 127.73, 125.27, 122.18, 76.77, 53.21, 52.74, 52.52, 52.41, 46.97, 33.42; HRMS (ESI) calcd for $\text{C}_{18}\text{H}_{15}\text{NO}_4^+$ $[\text{M}+\text{H}-\text{H}_2\text{O}]^+$ 295.0965, found 295.0974. The enantiomeric excess was determined by chiral HPLC using a Daicel Chiralpak IA column (hexanes/*i*-PrOH, 95:5, flow rate of 1.0 mL/min, 254 nm) $t_R = 15.33$ min (minor), $t_R = 17.69$ min (major), 72% *ee*.

Methyl(1*R*,4*R*,4*aS*,10*aR*)-11-oxo-4*a*-(2-oxoethyl)-1,4,4*a*,9,10,10*a*-hexahydro-1,4-(epoxy methano)phenanthrene-2-carboxylate (*Endo*-107). Prepared following the general procedure described above, the crude material was purified by flash column chromatography (silica gel, hexanes/EtOAc, 3:1) to afford the desired product (66.0 mg combined, 68% combined yield; 45.5 mg, 47% yield *Endo*-107; 20.5 mg, 21% yield *Exo*-107) as a colorless oil. The *dr* was 2:1 as determined by crude ^1H NMR. *Endo*-107: $R_f = 0.10$ (silica gel, hexanes/EtOAc, 2:1); $[\alpha]_D^{21} = -86.98^\circ$ ($c = 1.0$ in CHCl_3); IR (thin film) 2950, 2852, 1763, 1719, 1638, 1254 cm^{-1} ; ^1H NMR (500 MHz, CDCl_3) δ 9.30 (s, 1 H), 7.49 (dd, $J = 8.0, 1.2$ Hz, 1 H), 7.38 (dd, $J = 6.5, 2.3$ Hz, 1 H), 7.28 (td, $J = 7.6, 1.8$ Hz, 1 H), 7.22–7.13 (m, 2 H), 5.50 (dd, $J = 2.3, 1.1$ Hz, 1 H), 4.23 (d, $J = 6.4$ Hz, 1 H), 3.84 (s, 3 H), 2.87 (ddd, $J = 15.7, 6.9, 3.9$ Hz, 1 H), 2.70 (dd, $J = 14.2, 2.4$ Hz, 1 H), 2.68–2.61 (m, 1 H), 2.44 (dd, $J = 14.2, 3.1$ Hz, 1 H), 2.24–2.10 (m, 2 H), 1.91–1.82 (m, 1 H); ^{13}C NMR (126 MHz, CDCl_3) δ 200.46, 169.86, 162.44, 139.06, 138.97, 137.95, 136.11, 129.48, 127.79, 127.58, 126.53, 78.47, 55.84, 52.52, 52.14, 44.39, 40.78, 28.37, 26.56; HRMS (ESI) calcd for $\text{C}_{19}\text{H}_{17}\text{O}_4^+$ $[\text{M}+\text{H}-\text{H}_2\text{O}]^+$ 309.1121, found 309.1130. The enantiomeric excess was determined by chiral HPLC using a Daicel Chiralpak IA column (hexanes/*i*-PrOH, 90:10, flow rate of 1.0 mL/min, 254 nm) $t_R = 20.27$ min (major), $t_R = 23.07$ min (minor), 99% *ee*.

Exo-107: $R_f = 0.20$ (silica gel, hexanes/EtOAc, 2:1); $[\alpha]_D^{21} = -44.28^\circ$ ($c = 1.0$ in CHCl_3); IR (thin film) 2950, 2854, 1761, 1719, 1637, 1254 cm^{-1} ; ^1H NMR (500 MHz, CDCl_3) δ 9.36 (dd, $J = 3.3, 1.7$ Hz, 1 H), 7.38 (dd, $J = 7.9, 1.4$ Hz, 1 H), 7.29–7.23 (m, 1 H), 7.17 (td, $J = 7.4, 1.3$ Hz, 1 H), 7.06 (td, $J = 7.0, 1.8$ Hz, 2 H), 5.58 (dd, $J = 3.2, 2.3$ Hz, 1 H), 4.35 (d, $J = 6.4$ Hz, 1 H), 3.73 (s, 3 H), 3.00 (dd, $J = 15.0, 1.7$ Hz, 1 H), 2.74 (ddd, $J = 9.6, 6.8, 3.2$ Hz, 1 H), 2.64 (dd, $J = 15.0, 3.3$ Hz, 1 H), 2.58 (td, $J = 10.5, 10.0, 5.0$ Hz, 1 H), 2.48 (ddd, $J = 15.8, 6.8, 4.3$ Hz, 1 H), 2.22 (dtd, $J = 13.6, 6.8, 4.4$ Hz, 1 H), 1.18 (dtd, $J = 13.7, 9.7, 4.3$ Hz, 1 H); ^{13}C NMR (126 MHz, CDCl_3) δ 199.38, 171.26, 163.05, 140.44, 138.25, 136.69, 136.02, 129.32, 127.66, 127.51, 125.60, 77.48, 56.97, 52.44, 52.42, 45.92, 41.51, 27.97, 25.43; HRMS (ESI) calcd for $\text{C}_{19}\text{H}_{19}\text{O}_5^+$ $[\text{M}+\text{H}]^+$ 327.1227, found 327.1235. The enantiomeric excess was determined by chiral HPLC using a Daicel Chiralpak IA column (hexanes/*i*-PrOH, 90:10, flow rate of 1.0 mL/min, 254 nm) $t_R = 15.96$ min (minor), $t_R = 18.04$ min (major), 96% *ee*.

Methyl(6a*S*,7*R*,10*R*,10a*S*)-11-oxo-10a-(2-oxoethyl)-6a,7,10,10a-tetrahydro-6*H*-7,10-(epoxymethano)benzo[*c*]chromene-8-carboxylate (Endo-108). Prepared following the general procedure described above, the crude material was purified by flash column chromatography (silica gel, hexanes/EtOAc, 3:1) to afford the desired product (60.1 mg combined, 68% combined yield; 52.6 mg, 60% yield **Endo-108**; 7.5 mg, 8% yield **Exo-108**) as an amorphous pale yellow solid. The *dr* was 6:1 as determined by crude ^1H NMR. **Endo-108:** $R_f = 0.07$ (silica gel, hexanes/EtOAc, 2:1); $[\alpha]_D^{21} = -80.60^\circ$ ($c = 1.0$ in CHCl_3); IR (thin film) 2954, 2853, 1767, 1720, 1490, 1253, 758 cm^{-1} ; ^1H NMR (500 MHz, CDCl_3) δ 9.47 (dd, $J = 2.8, 1.8$ Hz, 1 H), 7.41 (dd, $J = 7.9, 1.6$ Hz, 1 H), 7.37 (dd, $J = 6.4, 2.1$ Hz, 1 H), 7.21 (ddd, $J = 8.4, 7.4, 1.6$ Hz, 1 H), 7.06 (td, $J = 7.5, 1.3$ Hz, 1 H), 6.95 (dd, $J = 8.1, 1.3$ Hz, 1 H), 5.62 (dd, $J = 2.3, 1.2$ Hz, 1 H), 4.45 (dd, $J = 11.7, 5.6$ Hz, 1 H), 4.19 (dd, $J = 11.7, 6.0$ Hz, 1 H), 4.03 (d, $J = 6.4$ Hz, 1 H), 3.85 (s, 3 H), 2.97 (dd, $J = 15.1, 1.8$ Hz, 1 H), 2.48 (dd, $J = 15.1, 2.8$

Hz, 1 H), 2.35 (td, $J = 5.8, 1.2$ Hz, 1 H); ^{13}C NMR (126 MHz, CDCl_3) δ 199.71, 162.20, 156.00, 138.95, 137.65, 129.61, 126.53, 124.97, 123.33, 118.70, 76.45, 67.69, 54.77, 53.44, 52.69, 44.53, 37.94; HRMS (ESI) calcd for $\text{C}_{18}\text{H}_{15}\text{O}_5^+$ $[\text{M}+\text{H}-\text{H}_2\text{O}]^+$ 311.0914, found 311.0920. The enantiomeric excess was determined by chiral HPLC using a Daicel Chiralcel OD-H column (hexanes/*i*-PrOH, 90:10, flow rate of 1.0 mL/min, 205 nm) $t_R = 34.71$ min (major), $t_R = 49.92$ min (minor), 94% *ee*.

Exo-108: $R_f = 0.20$ (silica gel, hexanes/EtOAc, 2:1); $[\alpha]_{\text{D}}^{21} = -74.88^\circ$ ($c = 1.0$ in CHCl_3); IR (thin film) 2954, 2852, 1757, 1720, 1489, 1290 cm^{-1} ; ^1H NMR (500 MHz, CDCl_3) δ 9.64 (t, $J = 1.5$ Hz, 1 H), 7.27 (dd, $J = 7.8, 1.6$ Hz, 1 H), 7.13 (ddd, $J = 8.2, 7.3, 1.6$ Hz, 1 H), 6.98 (td, $J = 7.5, 1.3$ Hz, 1 H), 6.78 (dd, $J = 8.1, 1.3$ Hz, 1 H), 6.67 (dd, $J = 6.4, 2.2$ Hz, 1 H), 5.71 (dd, $J = 3.2, 2.1$ Hz, 1 H), 4.28 (dd, $J = 12.0, 4.1$ Hz, 1 H), 4.23 (dd, $J = 12.0, 1.5$ Hz, 1 H), 3.77 (s, 3 H), 3.68–3.61 (m, 2 H), 2.79–2.71 (m, 2 H); ^{13}C NMR (126 MHz, CDCl_3) δ 198.61, 170.81, 162.65, 155.37, 138.38, 135.94, 129.00, 125.17, 125.08, 122.93, 118.55, 77.36, 64.61, 54.88, 54.05, 52.42, 47.18, 38.60; HRMS (ESI) calcd for $\text{C}_{18}\text{H}_{15}\text{O}_5^+$ $[\text{M}+\text{H}-\text{H}_2\text{O}]^+$ 311.0914, found 311.0923. The enantiomeric excess was determined by chiral HPLC using a Daicel Chiralpak AD-H column (hexanes/*i*-PrOH, 90:10, flow rate of 1.0 mL/min, 254 nm) $t_R = 30.56$ min (major), $t_R = 38.12$ min (minor), 98% *ee*.

Methyl(6a*R*,7*R*,10*R*,10a*R*)-11-oxo-10a-(2-oxoethyl)-6a,7,10,10a-tetrahydro-6*H*-7,10 (epoxymethano)benzo[*c*]thiochromene-8-carboxylate (Endo-109). Prepared following the general procedure described above, the crude material was purified by flash column chromatography (silica gel, hexanes/EtOAc, 1:1) to afford the desired product (48.2 mg combined, 47% combined yield; 27.0 mg, 26% yield **Endo-109**; 21.2 mg, 21% yield **Exo-109**) as a pale yellow oil. The *dr* was 1:1 as determined by crude ^1H NMR. **Endo-109:** $R_f = 0.17$ (silica gel, hexanes/EtOAc, 2:1); $[\alpha]_{\text{D}}^{21} = +16.10^\circ$ ($c = 1.0$ in CHCl_3); IR (thin film) 2952,

1762, 1717, 1268, 751 cm^{-1} ; ^1H NMR (500 MHz, CDCl_3) δ 9.20 (dd, $J = 3.0, 2.1$ Hz, 1 H), 7.63 (dd, $J = 8.1, 1.4$ Hz, 1 H), 7.42 (ddd, $J = 6.6, 3.2, 1.9$ Hz, 2 H), 7.22 (dtd, $J = 25.2, 7.4, 1.6$ Hz, 2 H), 5.47 (dd, $J = 2.4, 1.1$ Hz, 1 H), 4.70 (d, $J = 6.7$ Hz, 1 H), 3.86 (s, 3 H), 3.11 (dd, $J = 13.0, 5.7$ Hz, 1 H), 2.95 (dd, $J = 14.5, 2.2$ Hz, 1 H), 2.75 (t, $J = 13.0$ Hz, 1 H), 2.46 (ddd, $J = 12.9, 5.7, 1.1$ Hz, 1 H), 2.26 (dd, $J = 14.4, 3.1$ Hz, 1 H); ^{13}C NMR (126 MHz, CDCl_3) δ 200.06, 169.43, 162.25, 138.94, 137.88, 137.39, 136.52, 130.93, 128.22, 127.87, 127.15, 76.53, 54.74, 52.67, 51.24, 48.20, 42.56, 31.82; HRMS (ESI) calcd for $\text{C}_{18}\text{H}_{15}\text{O}_4\text{S}^+$ $[\text{M}+\text{H}]^+$ 327.0695, found 327.0694. The enantiomeric excess was determined by chiral HPLC using a Daicel Chiralpak AD-H column (hexanes/*i*-PrOH, 95:5, flow rate of 1.0 mL/min, 254 nm) $t_R = 44.35$ min (minor), $t_R = 51.25$ min (major), 93% *ee*.

Exo-109: $R_f = 0.23$ (silica gel, hexanes/EtOAc, 2:1); $[\alpha]_{\text{D}}^{21} = -10.60^\circ$ ($c = 1.0$ in CHCl_3); IR (thin film) 2952, 2851, 1762, 1718, 1260, 753 cm^{-1} ; ^1H NMR (500 MHz, CDCl_3) δ 9.45 (t, $J = 1.9$ Hz, 1 H), 7.42 (dd, $J = 8.0, 1.5$ Hz, 1 H), 7.27–7.24 (m, 1 H), 7.21 (td, $J = 7.7, 1.7$ Hz, 1 H), 7.15 (td, $J = 7.5, 1.4$ Hz, 1 H), 7.07 (dd, $J = 6.4, 2.2$ Hz, 1 H), 5.57 (t, $J = 2.5$ Hz, 1 H), 4.42 (d, $J = 6.3$ Hz, 1 H), 3.75 (s, 3 H), 3.28 (dd, $J = 13.4, 5.2$ Hz, 1 H), 3.06–2.99 (m, 2 H), 2.96 (dd, $J = 16.3, 2.3$ Hz, 1 H), 2.30 (dd, $J = 13.3, 9.3$ Hz, 1 H); ^{13}C NMR (126 MHz, CDCl_3) δ 198.46, 170.81, 162.86, 139.02, 136.51, 135.55, 130.30, 127.54, 127.19, 127.08, 76.60, 55.81, 52.48, 51.57, 51.12, 42.71, 29.76; HRMS (ESI) calcd for $\text{C}_{18}\text{H}_{15}\text{O}_4\text{S}^+$ $[\text{M}+\text{H}]^+$ 327.0695, found 327.0696. The enantiomeric excess was determined by chiral HPLC using a Daicel Chiralpak AD-H column (hexanes/*i*-PrOH, 95:5, flow rate of 1.0 mL/min, 254 nm) $t_R = 37.16$ min (minor), $t_R = 46.02$ min (major), 93% *ee*.

Methyl(1*R*,4*R*,8*R*)-3-oxo-8-(2-oxoethyl)-8-phenyl-2-oxabicyclo[2.2.2]oct-5-ene-6-carboxylate (Endo-110). Prepared following the general procedure described above, the crude material was purified by flash column chromatography (silica gel, hexanes/EtOAc, 3:1) to

afford the desired product (56.8 mg combined, 63% combined yield; 29.5 mg, 33% yield **Endo-110**; 27.3 mg, 30% yield **Exo-110**) as a colorless oil. The *dr* was 1:1 as determined by crude ¹H NMR. **Endo-110**: $R_f = 0.13$ (silica gel, hexanes/EtOAc, 2:1); $[\alpha]_D^{21} = -45.90^\circ$ ($c = 1.0$ in CHCl₃); IR (thin film) 2954, 2852, 1761, 1718, 1637, 1438, 1264 cm⁻¹; ¹H NMR (500 MHz, CDCl₃) δ 9.36 (t, $J = 2.0$ Hz, 1 H), 7.48–7.41 (m, 3 H), 7.37 (t, $J = 7.9$ Hz, 2 H), 7.30–7.23 (m, 1 H), 5.75 (dt, $J = 4.0, 1.9$ Hz, 1 H), 4.26 (d, $J = 6.6$ Hz, 1 H), 3.85 (s, 3 H), 3.05 (dd, $J = 14.2, 4.1$ Hz, 1 H), 2.79 (dd, $J = 15.8, 2.6$ Hz, 1 H), 2.72 (dd, $J = 15.8, 1.7$ Hz, 1 H), 2.07 (dd, $J = 14.2, 1.6$ Hz, 1 H); ¹³C NMR (126 MHz, CDCl₃) δ 199.81, 170.26, 162.45, 142.34, 140.17, 137.24, 129.24, 127.86, 126.83, 73.64, 55.13, 52.57, 50.82, 43.07, 39.82; HRMS (ESI) calcd for C₁₇H₁₅O₅⁺ [M+H–H₂O]⁺ 283.0965, found 283.0966. The enantiomeric excess was determined by chiral HPLC using a Daicel Chiralpak IA column (hexanes/*i*-PrOH, 90:10, flow rate of 1.0 mL/min, 254 nm) $t_R = 20.97$ min (minor), $t_R = 29.31$ min (major), 90% *ee*.

Exo-110: $R_f = 0.25$ (silica gel, hexanes/EtOAc, 2:1); $[\alpha]_D^{21} = -25.00^\circ$ ($c = 1.0$ in CHCl₃); IR (thin film) 2953, 2851, 1763, 1718, 1636, 1261, 753 cm⁻¹; ¹H NMR (500 MHz, CDCl₃) δ 9.45 (s, 1 H), 7.33 (d, $J = 1.1$ Hz, 2 H), 7.28–7.20 (m, 3 H), 7.14 (dd, $J = 6.3, 2.2$ Hz, 1 H), 5.77–5.74 (m, 1 H), 4.33 (d, $J = 6.3$ Hz, 1 H), 3.74 (s, 3 H), 3.11 (dd, $J = 16.9, 1.6$ Hz, 1 H), 2.91 (dd, $J = 16.9, 1.7$ Hz, 1 H), 2.59–2.54 (m, 2 H); ¹³C NMR (126 MHz, CDCl₃) δ 198.59, 171.42, 162.46, 142.36, 140.17, 136.20, 129.18, 127.55, 126.64, 73.71, 56.43, 52.39, 51.51, 42.69, 39.11; HRMS (ESI) calcd for C₁₇H₁₅O₅⁺ [M+H–H₂O]⁺ 283.0965, found 283.0973. The enantiomeric excess was determined by chiral HPLC using a Daicel Chiralpak IA column (hexanes/*i*-PrOH, 95:5, flow rate of 1.0 mL/min, 254 nm) $t_R = 30.48$ min (minor), $t_R = 34.23$ min (major), 72% *ee*.

Methyl(1*R*,4*R*,8*R*)-8-(4-methoxyphenyl)-3-oxo-8-(2-oxoethyl)-2oxabicyclo[2.2.2]oct-5-ene-6-carboxylate (Endo-111). Prepared following the general procedure described above, the

crude material was purified by flash column chromatography (silica gel, hexanes/EtOAc, 3:1) to afford the desired product (64.2 mg combined, 65% combined yield; 33.4 mg, 34% yield **Endo-111**; 30.8 mg, 31% yield **Exo-111**) as a colorless oil. The *dr* was 1:1 as determined by crude ¹H NMR. **Endo-111**: *R_f* = 0.16 (silica gel, hexanes/EtOAc, 2:1); [α]_D²¹ = -73.70° (*c* = 1.0 in CHCl₃); IR (thin film) 2954, 2839, 760, 1720, 1516, 1253 cm⁻¹; ¹H NMR (500 MHz, CDCl₃) δ 9.37 (dd, *J* = 2.5, 1.7 Hz, 1 H), 7.41 (dd, *J* = 6.5, 2.4 Hz, 1 H), 7.35 (d, *J* = 8.9 Hz, 2 H), 6.89 (d, *J* = 8.9 Hz, 2 H), 5.74 (dt, *J* = 4.1, 1.8 Hz, 1 H), 4.19 (d, *J* = 6.6 Hz, 1 H), 3.84 (s, 3 H), 3.78 (s, 3 H), 3.02 (dd, *J* = 14.2, 4.1 Hz, 1 H), 2.76 (dd, *J* = 15.7, 2.6 Hz, 1 H), 2.67 (dd, *J* = 15.7, 1.8 Hz, 1 H), 2.04 (dd, *J* = 14.3, 1.7 Hz, 1 H); ¹³C NMR (126 MHz, CDCl₃) δ 200.08, 170.36, 162.47, 158.92, 140.13, 137.14, 134.12, 128.01, 114.53, 73.65, 55.39, 55.15, 52.55, 51.31, 42.50, 39.66; HRMS (ESI) calcd for C₁₈H₁₉O₆⁺ [M+H]⁺ 331.1176, found 331.1173. The enantiomeric excess was determined by chiral HPLC using a Daicel Chiralpak IA column (hexanes/*i*-PrOH, 90:10, flow rate of 1.0 mL/min, 240 nm) *t_R* = 30.15 min (minor), *t_R* = 33.32 min (major), 88% *ee*.

Exo-111: *R_f* = 0.26 (silica gel, hexanes/EtOAc, 2:1); [α]_D²¹ = -51.70° (*c* = 1.0 in CHCl₃); IR (thin film) 2954, 2839, 1760, 1719, 1636, 1515, 1259 cm⁻¹; ¹H NMR (500 MHz, CDCl₃) δ 9.45 (t, *J* = 1.7 Hz, 1 H), 7.12 (m, 3 H), 6.84 (d, *J* = 8.9 Hz, 2 H), 5.74 (q, *J* = 2.6 Hz, 1 H), 4.26 (d, *J* = 6.3 Hz, 1 H), 3.77 (s, 3 H), 3.74 (s, 3 H), 3.08 (dd, *J* = 16.8, 1.7 Hz, 1 H), 2.85 (dd, *J* = 16.8, 1.8 Hz, 1 H), 2.56–2.52 (m, 2 H); ¹³C NMR (126 MHz, CDCl₃) δ 198.90, 171.46, 162.51, 158.70, 140.29, 135.98, 134.09, 127.72, 114.44, 73.75, 56.44, 55.38, 52.37, 51.93, 42.10, 38.93. HRMS (ESI) calcd for C₁₈H₁₉O₆⁺ [M+H]⁺ 331.1176, found 331.1172. The enantiomeric excess was determined by chiral HPLC using a Daicel Chiralpak AD-H column (hexanes/*i*-PrOH, 90:10, flow rate of 1.0 mL/min, 215 nm) *t_R* = 20.39 min (minor), *t_R* = 23.54 min (major), 55% *ee*.

Methyl(1*R*,4*R*,8*R*)-8-(4-cyanophenyl)-3-oxo-8-(2-oxoethyl)-2oxabicyclo[2.2.2]oct-5-ene-6-carboxylate (*Endo*-112). Prepared following the general procedure described above, the crude material was purified by flash column chromatography (silica gel, hexanes/EtOAc, 1:1) to afford the desired product (62.4 mg combined, 65% combined yield; 41.2 mg, 43% yield *Endo*-112; 21.2 mg, 22% yield *Exo*-112) as a yellow oil. The *dr* was 2:1 as determined by crude ¹H NMR. ***Endo*-112:** *R_f* = 0.07 (silica gel, hexanes/EtOAc, 2:1); [α]_D²¹ = -73.72° (*c* = 1.0 in CHCl₃); IR (thin film) 2955, 2851, 2292, 1761, 1719, 1639, 1269, 752 cm⁻¹; ¹H NMR (500 MHz, CDCl₃) δ 9.41 (t, *J* = 1.3 Hz, 1 H), 7.67 (d, *J* = 8.6 Hz, 2 H), 7.60 (d, *J* = 8.6 Hz, 2 H), 7.42 (dd, *J* = 6.6, 2.3 Hz, 1 H), 5.81–5.74 (m, 1 H), 4.33 (d, *J* = 6.6 Hz, 1 H), 3.87 (s, 3 H), 3.00 (dd, *J* = 14.4, 4.1 Hz, 1 H), 2.97–2.91 (m, 1 H), 2.85 (d, *J* = 17.2 Hz, 1 H), 2.09 (dd, *J* = 14.4, 1.7 Hz, 1 H); ¹³C NMR (126 MHz, CDCl₃) δ 198.12, 169.78, 162.19, 147.97, 139.47, 137.60, 132.74, 127.89, 118.20, 111.81, 73.44, 54.88, 52.65, 50.27, 43.09, 39.99. HRMS (ESI) calcd for C₁₈H₁₄NO₄⁺ [M+H-H₂O]⁺ 308.0917, found 308.0917. The enantiomeric excess was determined by chiral HPLC using a Daicel Chiralpak IA column (hexanes/*i*-PrOH, 90:10, flow rate of 1.0 mL/min, 240 nm) *t_R* = 78.37 min (minor), *t_R* = 87.08 min (major), 90% *ee*.

***Exo*-112:** *R_f* = 0.17 (silica gel, hexanes/EtOAc, 2:1); [α]_D²¹ = -51.92° (*c* = 1.0 in CHCl₃). IR (thin film) 2954, 2920, 2851, 2228, 1761, 1719, 1638, 1261 cm⁻¹; ¹H NMR (500 MHz, CDCl₃) δ 9.48 (s, 1 H), 7.62 (d, *J* = 8.6 Hz, 2 H), 7.36 (d, *J* = 8.6 Hz, 2 H), 7.11 (dd, *J* = 6.3, 2.2 Hz, 1 H), 5.75 (dt, *J* = 3.6, 2.1 Hz, 1 H), 4.35 (d, *J* = 6.2 Hz, 1 H), 3.75 (s, 3 H), 3.20 (d, *J* = 18.2 Hz, 1 H), 3.05 (d, *J* = 18.2 Hz, 1 H), 2.55 (dd, *J* = 6.3, 2.8 Hz, 2 H); ¹³C NMR (126 MHz, CDCl₃) δ 197.34, 170.73, 162.18, 148.08, 139.37, 136.86, 132.73, 127.74, 118.13, 111.63, 73.43, 56.28, 52.53, 50.74, 42.84, 39.51. HRMS (ESI) calcd for C₁₈H₁₄NO₄⁺ [M+H-H₂O]⁺ 308.0917, found 308.0920. The enantiomeric excess was determined by chiral HPLC using a Daicel Chiralpak IA column (hexanes/*i*-PrOH, 90:10, flow rate of 1.0 mL/min, 240 nm) *t_R* = 59.99 min (major), *t_R* = 65.51 min (minor), 90% *ee*.

Methyl(1*R*,4*R*,8*R*)-3-oxo-8-(2-oxoethyl)-8-(pyridin-3-yl)-2-oxabi cyclo[2.2.2]oct-5-ene-6-carboxylate (*Endo*-113). Prepared following the general procedure described above, the crude material was purified by flash column chromatography (silica gel, hexanes/EtOAc, 2:1) to afford the desired product (75.0 mg combined, 83% combined yield; 64.3 mg, 71% yield *Endo*-113; 10.7 mg, 12% yield *Exo*-113) as a pale yellow oil. The *dr* was 6:1 as determined by crude ¹H NMR. ***Endo*-113:** $R_f = 0.17$ (silica gel, hexanes/EtOAc, 2:1); $[\alpha]_D^{21} = -12.18^\circ$ ($c = 1.0$ in CHCl₃); IR (thin film) 2955, 2853, 1759, 1721, 1279, 755 cm⁻¹; ¹H NMR (500 MHz, CDCl₃) δ 9.42 (s, 1 H), 8.70 (d, $J = 2.6$ Hz, 1 H), 8.50 (dd, $J = 4.8, 1.5$ Hz, 1 H), 7.85 (ddd, $J = 8.2, 2.7, 1.5$ Hz, 1 H), 7.41 (dd, $J = 6.6, 2.4$ Hz, 1 H), 7.30 (dd, $J = 8.1, 4.8$ Hz, 1 H), 5.76 (dt, $J = 4.1, 1.9$ Hz, 1 H), 4.36 (d, $J = 6.5$ Hz, 1 H), 3.85 (s, 3 H), 3.02 (dd, $J = 14.4, 4.0$ Hz, 1 H), 2.92 (dd, $J = 17.2, 1.6$ Hz, 1 H), 2.84 (dd, $J = 17.2, 1.2$ Hz, 1 H), 2.08 (dd, $J = 14.3, 1.6$ Hz, 1 H); ¹³C NMR (126 MHz, CDCl₃) δ 198.37, 169.84, 162.26, 148.80, 148.70, 139.54, 138.51, 137.52, 134.58, 123.52, 73.47, 55.02, 52.64, 50.15, 41.52, 39.86; HRMS (ESI) calcd for C₁₆H₁₆NO₅⁺ [M+H]⁺ 302.1023, found 302.1024. The enantiomeric excess was determined by chiral HPLC using a Daicel Chiralpak AD-H column (hexanes/*i*-PrOH, 95:5, flow rate of 1.0 mL/min, 254 nm) $t_R = 34.54$ min (major), $t_R = 40.94$ min (minor), 94% *ee*.

***Exo*-113:** $R_f = 0.27$ (silica gel, hexanes/EtOAc, 2:1); $[\alpha]_D^{21} = -23.16^\circ$ ($c = 1.0$ in CHCl₃); IR (thin film) 2954, 2853, 1760, 1719, 1638, 1262 cm⁻¹; ¹H NMR (500 MHz, CDCl₃) δ 9.50 (s, 1 H), 8.54 (d, $J = 2.7$ Hz, 1 H), 8.47 (dd, $J = 4.8, 1.5$ Hz, 1 H), 7.57 (ddd, $J = 8.2, 2.7, 1.5$ Hz, 1 H), 7.29–7.24 (m, 1 H), 7.12 (dd, $J = 6.3, 2.2$ Hz, 1 H), 5.78–5.74 (m, 1 H), 4.36 (d, $J = 6.3$ Hz, 1 H), 3.75 (s, 3 H), 3.26–3.20 (m, 1 H), 3.04 (dd, $J = 18.2, 1.0$ Hz, 1 H), 2.57 (t, $J = 2.4$ Hz, 2 H); ¹³C NMR (126 MHz, CDCl₃) δ 197.52, 170.83, 162.24, 148.63, 148.30, 139.52, 138.31, 136.77, 134.63, 123.56, 73.50, 56.26, 52.51, 50.84, 41.23, 38.97; HRMS (ESI) calcd for C₁₆H₁₄NO₄⁺ [M+H–H₂O]⁺ 284.0917, found 284.0913. The enantiomeric excess was

determined by chiral HPLC using a Daicel Chiralpak OD-H column (hexanes/*i*-PrOH, 80:20, flow rate of 1.0 mL/min, 254 nm) $t_R = 20.89$ min (minor), $t_R = 26.04$ min (major), 55% *ee*.

Methyl(1*R*,4*R*,8*R*)-8-(furan-2-yl)-3-oxo-8-(2-oxoethyl)-2-oxabicyclo[2.2.2]oct-5-ene-6 carboxylate (Endo-114). Prepared following the general procedure described above, the crude material was purified by flash column chromatography (silica gel, hexanes/EtOAc, 3:1) to afford the desired product (40.4 mg combined, 46% combined yield; 25.9 mg, 29% yield **Endo-114**; 14.5 mg, 17% yield **Exo-114**) as a yellow oil. The *dr* was 2:1 as determined by crude ^1H NMR. **Endo-114**: $R_f = 0.10$ (silica gel, hexanes/EtOAc, 2:1); $[\alpha]_{\text{D}}^{21} = -95.32^\circ$ ($c = 1.0$ in CHCl_3); IR (thin film) 2955, 1764, 1720, 1635, 1274, 751 cm^{-1} ; ^1H NMR (500 MHz, CDCl_3) δ 9.55 (s, 1 H), 7.31 (dd, $J = 1.8, 0.9$ Hz, 1 H), 7.03 (dd, $J = 6.5, 2.2$ Hz, 1 H), 6.25 (dd, $J = 3.3, 1.9$ Hz, 1 H), 5.99 (dd, $J = 3.4, 0.9$ Hz, 1 H), 5.76 (dd, $J = 3.7, 1.9$ Hz, 1 H), 4.01 (d, $J = 6.4$ Hz, 1 H), 3.79 (s, 3 H), 3.24 (dd, $J = 16.8, 1.6$ Hz, 1 H), 2.73 (dd, $J = 16.7, 1.9$ Hz, 1 H), 2.46 (dd, $J = 14.5, 3.7$ Hz, 1 H), 2.38 (dd, $J = 14.5, 1.8$ Hz, 1 H); ^{13}C NMR (126 MHz, CDCl_3) δ 198.37, 170.51, 162.55, 154.52, 142.52, 139.80, 136.23, 110.69, 107.71, 73.88, 52.96, 52.46, 51.74, 39.03, 37.50; HRMS (ESI) calcd for $\text{C}_{15}\text{H}_{15}\text{O}_6^+$ $[\text{M}+\text{H}]^+$ 291.0863, found: 291.0868. The enantiomeric excess was determined by chiral HPLC using a Daicel Chiralpak AD-H column (hexanes/*i*-PrOH, 95:5, flow rate of 1.0 mL/min, 254 nm) $t_R = 38.01$ min (minor), $t_R = 81.61$ min (major), 91% *ee*.

Exo-114: $R_f = 0.20$ (silica gel, hexanes/EtOAc, 2:1); $[\alpha]_{\text{D}}^{21} = -17.82^\circ$ ($c = 1.0$ in CHCl_3); IR (thin film) 2955, 2852, 1761, 1721, 1638, 1261, 751 cm^{-1} ; ^1H NMR (500 MHz, CDCl_3) δ 9.51 (t, $J = 2.1$ Hz, 1 H), 7.38 (dd, $J = 1.8, 0.9$ Hz, 1 H), 7.35 (dd, $J = 6.5, 2.3$ Hz, 1 H), 6.32–6.30 (m, 2 H), 5.77–5.71 (m, 1 H), 4.00 (d, $J = 6.5$ Hz, 1 H), 3.84 (s, 3 H), 2.93–2.88 (m, 2 H), 2.59 (dd, $J = 15.7, 2.2$ Hz, 1 H), 1.93 (dd, $J = 14.3, 1.6$ Hz, 1 H); ^{13}C NMR (126 MHz, CDCl_3) δ 199.16, 169.82, 162.34, 154.60, 143.15, 139.02, 137.45, 110.80, 107.93, 73.16,

52.60, 51.85, 51.65, 39.56, 37.13; HRMS (ESI) calcd for $C_{15}H_{15}O_6^+$ $[M+H]^+$ 291.0863, found 291.0872. The enantiomeric excess was determined by chiral HPLC using a Daicel Chiralcel OD-H column (hexanes/*i*-PrOH, 95:5, flow rate of 1.0 mL/min, 254 nm) $t_R = 41.58$ min (minor), $t_R = 44.78$ min (major), 18% *ee*.

***tert*-Butyl3-((1*R*,4*R*,5*R*)-7-(methoxycarbonyl)-3-oxo-5-(2-oxoethyl)-2oxabicyclo[2.2.2]**

oct-7-en-5-yl)-1*H*-indole-1-carboxylate (*Endo*-115). Prepared following the general procedure described above, the crude material was purified by flash column chromatography (silica gel, hexanes/EtOAc, 2:1) to afford the desired product (77.0 mg combined, 89% combined yield; 39.3 mg, 45% yield *Endo*-115; 37.7 mg, 44% yield *Exo*-115) as a yellow oil. The *dr* was 1:1 as determined by crude 1H NMR. ***Endo*-115:** $R_f = 0.10$ (silica gel, hexanes/EtOAc, 2:1); $[\alpha]_D^{21} = -28.68^\circ$ ($c = 1.0$ in $CHCl_3$); IR (thin film) 2979, 1762, 1723, 1636, 1374, 1157, 750 cm^{-1} ; 1H NMR (500 MHz, $CDCl_3$) δ 9.36 (s, 1 H), 8.23 (d, $J = 8.4$ Hz, 1 H), 7.71 (s, 1 H), 7.52 (d, $J = 7.9$ Hz, 1 H), 7.46 (dd, $J = 6.6, 2.3$ Hz, 1 H), 7.36 (ddd, $J = 8.3, 7.2, 1.2$ Hz, 1 H), 7.30–7.24 (m, 1 H), 5.75 (dt, $J = 3.9, 1.9$ Hz, 1 H), 4.42 (d, $J = 6.6$ Hz, 1 H), 3.86 (s, 3 H), 3.08 (dd, $J = 15.2, 1.8$ Hz, 1 H), 2.95 (dd, $J = 13.9, 3.9$ Hz, 1 H), 2.63 (dd, $J = 15.1, 3.1$ Hz, 1 H), 2.12 (dd, $J = 13.9, 1.8$ Hz, 1 H), 1.67 (s, 9 H); ^{13}C NMR (126 MHz, $CDCl_3$) δ 200.14, 170.55, 162.44, 149.32, 139.78, 137.10, 136.50, 127.92, 125.04, 123.60, 122.93, 121.49, 119.98, 116.24, 84.47, 73.52, 52.56, 51.23, 49.69, 39.47, 38.59, 28.26; HRMS (ESI) calcd for $C_{24}H_{24}NO_6^+$ $[M+H-H_2O]^+$ 422.1598, found 422.1605. The enantiomeric excess was determined by chiral HPLC using a Daicel Chiralpak OD-H column (hexanes/*i*-PrOH, 90:10, flow rate of 1.0 mL/min, 254 nm) $t_R = 19.43$ min (major), $t_R = 23.22$ min (minor), 93% *ee*.

***Exo*-115:** $R_f = 0.20$ (silica gel, hexanes/EtOAc, 2:1); $[\alpha]_D^{21} = -5.84^\circ$ ($c = 1.0$ in $CHCl_3$); IR (thin film) 2979, 2852, 1763, 1724, 1374, 1156, 750 cm^{-1} ; 1H NMR (500 MHz, $CDCl_3$) δ 9.48 (t, $J = 1.9$ Hz, 1 H), 8.20–8.07 (m, 1 H), 7.60 (d, $J = 7.9$ Hz, 1 H), 7.38–7.31 (m, 2 H),

7.30–7.24 (m, 1 H), 7.18 (dd, $J = 6.5, 2.2$ Hz, 1 H), 5.77 (dt, $J = 3.9, 1.9$ Hz, 1 H), 4.54 (d, $J = 6.5$ Hz, 1 H), 3.75 (s, 3 H), 3.19 (d, $J = 16.4$ Hz, 1 H), 3.05 (dd, $J = 16.5, 2.2$ Hz, 1 H), 2.61 (dd, $J = 14.1, 3.9$ Hz, 1 H), 2.45 (dd, $J = 14.0, 1.8$ Hz, 1 H), 1.68 (s, 9 H); ^{13}C NMR (126 MHz, CDCl_3) δ 198.68, 170.86, 162.49, 149.46, 140.08, 136.39, 135.74, 127.42, 125.25, 123.59, 123.09, 121.52, 119.85, 116.24, 84.86, 73.62, 52.85, 52.40, 50.60, 38.72, 38.50, 28.35; HRMS (ESI) calcd for $\text{C}_{24}\text{H}_{24}\text{NO}_6^+$ $[\text{M}+\text{H}-\text{H}_2\text{O}]^+$ 422.1598, found 422.1604. The enantiomeric excess was determined by chiral HPLC using a Daicel Chiralpak AD-H column (hexanes/*i*-PrOH, 90:10, flow rate of 1.0 mL/min, 254 nm) $t_R = 9.07$ min (minor), $t_R = 11.91$ min (major), 16% *ee*.

Methyl(1*R*,4*R*,8*S*)-8-(4-methylpent-3-en-1-yl)-3-oxo-8-(2-oxoethyl)-2-oxabicyclo[2.2.2]oct-5-ene-6-carboxylate (*Endo*-119). Prepared following the general procedure described above, the crude material was purified by flash column chromatography (silica gel, hexanes/EtOAc, 3:1) to afford the desired product (12.8 mg, 11% yield *Endo*-119) as a colorless oil. The *dr* was >20:1 as determined by crude ^1H NMR. ***Endo*-119**: $R_f = 0.20$ (silica gel, hexanes/EtOAc, 2:1); $[\alpha]_D^{21} = -36.94^\circ$ ($c = 1.0$ in CHCl_3); IR (thin film) 2923, 2857, 1761, 1719, 1636, 1266, 1007 cm^{-1} ; ^1H NMR (500 MHz, CDCl_3) δ 9.72 (t, $J = 1.8$ Hz, 1 H), 7.30 (dd, $J = 6.5, 2.3$ Hz, 1 H), 5.63 (dd, $J = 4.0, 1.9$ Hz, 1 H), 5.03 (tdd, $J = 5.7, 2.9, 1.4$ Hz, 1 H), 3.81 (s, 3 H), 3.77 (d, $J = 6.5$ Hz, 1 H), 2.45 (dd, $J = 16.6, 1.8$ Hz, 1 H), 2.40 (dd, $J = 16.6, 2.0$ Hz, 1 H), 2.17 (dd, $J = 14.1, 4.0$ Hz, 1 H), 2.16–2.06 (m, 1 H), 1.95 (tt, $J = 13.6, 6.5$ Hz, 1 H), 1.72–1.67 (m, 3 H), 1.66 (s, 3 H), 1.58 (d, $J = 1.3$ Hz, 3 H); ^{13}C NMR (126 MHz, CDCl_3) δ 199.55, 170.97, 162.51, 140.35, 136.74, 133.11, 122.62, 73.69, 52.46, 51.13, 49.56, 39.46, 39.03, 38.71, 25.73, 23.29, 17.76; HRMS (ESI) calcd for $\text{C}_{17}\text{H}_{23}\text{O}_5^+$ $[\text{M}+\text{H}]^+$ 307.1540, found 307.1550. The enantiomeric excess was determined by chiral HPLC using a Daicel Chiralpak

AD-H column (hexanes/*i*-PrOH, 95:5, flow rate of 1.0 mL/min, 254 nm) $t_R = 16.25$ min (minor), $t_R = 27.18$ min (major), 95% *ee*.

Methyl(1*R*,4*R*,7*R*,8*R*)-8-methyl-7-(3-methylbut-2-en-1-yl)-3-oxo-8-(2-oxoethyl)-2-oxa bicyclo[2.2.2]oct-5-ene-6-carboxylate (*Endo*-120). Prepared following the general procedure described above, the crude material was purified by flash column chromatography (silica gel, hexanes/EtOAc, 3:1) to afford the desired product (58.0 mg, 48% yield *Endo*-120) as a colorless oil. The *dr* was >20:1 as determined by crude ^1H NMR. ***Endo*-120:** $R_f = 0.10$ (silica gel, hexanes/EtOAc, 2:1); $[\alpha]_D^{21} = -32.10^\circ$ ($c = 1.0$ in CHCl_3); IR (thin film) 2970, 2855, 1761, 1721, 1439, 1258 cm^{-1} ; ^1H NMR (500 MHz, CDCl_3) δ 9.72 (t, $J = 1.8$ Hz, 1 H), 7.24 (dd, $J = 6.4, 2.3$ Hz, 1 H), 5.43 (dd, $J = 2.3, 1.1$ Hz, 1 H), 5.12 (dddd, $J = 7.4, 6.0, 3.0, 1.6$ Hz, 1 H), 3.80 (s, 3 H), 3.45 (d, $J = 6.3$ Hz, 1 H), 2.40 (dd, $J = 16.3, 1.8$ Hz, 1 H), 2.37–2.30 (m, 2 H), 2.19 (ddd, $J = 14.3, 11.2, 8.5$ Hz, 1 H), 1.76 (s, 3 H), 1.66 (s, 3 H), 1.51 (ddd, $J = 11.2, 4.5, 1.1$ Hz, 1 H), 1.28 (s, 3 H); ^{13}C NMR (126 MHz, CDCl_3) δ 199.73, 171.34, 162.54, 139.24, 137.43, 135.73, 121.10, 76.15, 55.56, 54.37, 52.42, 45.92, 37.09, 26.65, 25.99, 22.22, 18.08; HRMS (ESI) calcd for $\text{C}_{17}\text{H}_{23}\text{O}_5^+$ $[\text{M}+\text{H}]^+$ 307.1540, found 307.1530. The enantiomeric excess was determined by chiral HPLC using a Daicel Chiralpak AD-H column (hexanes/*i*-PrOH, 97:3, flow rate of 1.0 mL/min, 254 nm) $t_R = 18.17$ min (minor), $t_R = 20.97$ min (major), 97% *ee*.

Methyl(3*aR*,4*S*,7*R*,7*aR*)-8-oxo-7*a*-(2-oxoethyl)-1,2,3,3*a*,4,7*a*-hexahydro-7*H*-4,7-(epoxy methano)indene-7-carboxylate (*Endo*-123). Prepared following the general procedure described above, the crude material was purified by flash column chromatography (silica gel, hexanes/EtOAc, 2:1) to afford the desired product (32.7 mg combined, 56% combined yield; 31.5 mg, 51% yield *Endo*-123; 1.5 mg, 5% yield *Exo*-123) as a colorless oil. The *dr* was 10.6:1 as determined by crude ^1H NMR. ***Endo*-123:** $R_f = 0.43$ (silica gel, hexanes/EtOAc, 3:2); $[\alpha]_D^{21}$

= +5.72° (*c* = 1.0 in CHCl₃); IR (thin film) 3086, 2957, 2875, 2749, 2256, 1754, 1741, 1621, 1278, 1083 cm⁻¹; ¹H NMR (500 MHz, CDCl₃) δ 9.71 (t, *J* = 3.1 Hz, 1H), 6.72 (dd, *J* = 7.8, 1.9 Hz, 1H), 6.62 (dd, *J* = 7.8, 5.0 Hz, 1H), 4.99 (d, *J* = 5.2 Hz, 1H), 3.88 (s, 3H), 2.55 (dd, *J* = 14.0, 3.3 Hz, 1H), 2.39 (dd, *J* = 13.9, 2.8 Hz, 1H), 2.30 (t, *J* = 7.6 Hz, 1H), 2.19 – 2.11 (m, 1H), 2.11 – 1.95 (m, 2H), 1.91 (dh, *J* = 13.3, 3.0 Hz, 1H), 1.80 – 1.65 (m, 2H); ¹³C NMR (126 MHz, CDCl₃) δ 200.79, 169.48, 168.16, 132.80, 132.18, 78.11, 63.43, 53.15, 51.85, 51.30, 50.36, 36.47, 28.51, 27.61; HRMS (ESI) calcd for C₁₄H₁₅O₄⁺ [M+H–H₂O]⁺ 247.0971, found 247.0973. The enantiomeric excess of its homologated methyl ester was determined by chiral HPLC using a Daicel Chiralpak AD-H column (hexanes/*i*-PrOH, 95:5, flow rate of 1.0 mL/min, 240 nm) *t*_R = 22.45 min (minor), *t*_R = 25.49 min (major), 61% *ee*.

2-((3*aR*,4*R*,7*R*,7*aR*)-5-benzoyl-8-oxo-1,2,3,3*a*,4,7-hexahydro-7*aH*-4,7(epoxymethano)inden-7*a*-yl)acetaldehyde (*Endo*-124). Prepared following the general procedure described above, the crude material was further purified by flash column chromatography (silica gel, hexanes/EtOAc, 3:1) to afford the desired product (89.0 mg combined, 96% combined yield; 72.8 mg, 78% yield *Endo*-124; 16.2 mg, 18% yield *Exo*-124) as an off-white amorphous solid. The *dr* was 5:1 as determined by crude ¹H NMR. *Endo*-124: *R*_f = 0.21 (silica gel, hexanes/EtOAc, 2:1); [α]_D²³ = –9.70° (*c* = 1.0 in CHCl₃); IR (thin film) 2957, 2873, 1758, 1721, 1644, 1258 cm⁻¹; ¹H NMR (500 MHz, CDCl₃) δ 9.71 (s, 1 H), 7.74 (d, *J* = 7.7 Hz, 2 H), 7.61 (t, *J* = 7.4 Hz, 1 H), 7.49 (t, *J* = 7.6 Hz, 3 H), 6.98 (dd, *J* = 6.3, 2.1 Hz, 1 H), 5.61 (d, *J* = 1.8 Hz, 1 H), 3.84 (d, *J* = 6.3 Hz, 1 H), 2.55 (d, *J* = 16.5 Hz, 1 H), 2.36 (dd, *J* = 16.5, 2.3 Hz, 1 H), 2.09 (m, 2 H), 1.96–1.81 (m, 5 H); ¹³C NMR (126 MHz, CDCl₃) δ 199.98, 190.84, 171.80, 141.25, 133.45, 130.32, 129.41, 128.89, 128.63, 78.38, 53.31, 51.47, 50.03, 49.00, 36.24, 28.66, 27.35; HRMS (ESI) calcd for C₁₉H₁₇O₃⁺ [M+H]⁺ 293.1183, found 293.1183. The enantiomeric excess was determined by chiral HPLC using a Daicel Chiralpak IA column

(hexanes/*i*-PrOH, 97:3, flow rate of 1.0 mL/min, 254 nm) $t_R = 38.55$ min (minor), $t_R = 52.30$ min (major), 89% *ee*.

(3a*R*,4*R*,7*R*,7a*R*)-8-oxo-7a-(2-oxoethyl)-2,3,3a,4,7,7a-hexahydro-1*H*-4,7(epoxymethano)indene-5-carbonitrile (*Endo*-125). Prepared following the general procedure described above, the crude material was purified by flash column chromatography (silica gel, hexanes/EtOAc, 3:1) to afford the desired product (50.6 mg combined, 73% combined yield; 47.1 mg, 68% yield *Endo*-125; 3.5 mg, 5% yield *Exo*-125) as a white amorphous solid. The *dr* was 9:1 as determined by crude ¹H NMR. ***Endo*-125:** $R_f = 0.14$ (silica gel, hexanes/EtOAc, 2:1); $[\alpha]_D^{24} = -7.53^\circ$ ($c = 1.0$ in CHCl₃); IR (thin film) 2960, 2873, 2224, 1762, 1720, 1655, 1588 cm⁻¹; ¹H NMR (500 MHz, CDCl₃) δ 9.72 (d, $J = 1.6$ Hz, 1 H), 7.24 (dd, $J = 6.4, 2.1$ Hz, 1 H), 5.13 (t, $J = 1.7$ Hz, 1 H), 3.90 (d, $J = 6.4$ Hz, 1 H), 2.61 (d, 17.3 Hz, 1 H), 2.44 (dd, $J = 17.2, 1.8$ Hz, 1 H), 2.13–2.05 (m, 1 H), 1.91–1.72 (m, 6 H); ¹³C NMR (126 MHz, CDCl₃) δ 199.30, 146.95, 118.98, 113.96, 78.54, 52.84, 51.29, 49.55, 48.03, 36.06, 28.45, 27.19; HRMS (ESI) calcd for C₁₃H₁₁NO₄⁺ [M+H]⁺ 214.0862, found 214.0860. The enantiomeric excess was determined by chiral HPLC using a Daicel Chiralpak IA column (hexanes/*i*-PrOH, 88:12, flow rate of 1.0 mL/min, 254 nm) $t_R = 14.19$ min (major), $t_R = 17.85$ min (minor), 89% *ee*.

Diethyl(3a*R*,4*R*,7*S*,7a*R*)-8-oxo-7a-(2-oxoethyl)-2,3,3a,4,7,7a-hexahydro-1*H*-4,7(epoxy methano)indene-5,6-dicarboxylate (126). Prepared following the general procedure described above, the crude material was purified by flash column chromatography (silica gel, hexanes/EtOAc, 3:1) to afford the desired product (96.6 mg combined, 92% combined yield) as a colorless oil which was characterized as a 1:1 mixture of diastereomers. The *dr* was 1:1 as determined by crude ¹H NMR. **126:** $R_f = 0.23$ (silica gel, hexanes/EtOAc, 2:1); $[\alpha]_D^{21} = +0.24^\circ$ ($c = 1.0$ in CHCl₃); IR (thin film) 2962, 2873, 2738, 1766, 1721, 1649, 1277 cm⁻¹; ¹H NMR

(500 MHz, CDCl₃) δ 9.77 (d, *J* = 1.4 Hz, 1 H), 9.70 (d, *J* = 1.2 Hz, 1 H), 5.42 (d, *J* = 4.3 Hz, 1 H), 5.39 (d, *J* = 1.3 Hz, 1 H), 4.36–4.22 (m, 8 H), 4.06 (s, 1 H), 4.02 (s, 1 H), 2.76–2.69 (m, 2 H), 2.69–2.63 (m, 2 H), 2.61–2.51 (m, 2 H), 2.01 (td, *J* = 9.5, 8.5, 4.1 Hz, 2 H), 1.89–1.53 (m, 10 H), 1.38–1.23 (m, 12 H); ¹³C NMR (126 MHz, CDCl₃) δ 199.38, 199.20, 170.59, 170.30, 164.60, 164.18, 162.91, 162.12, 140.95, 139.68, 136.14, 136.05, 78.03, 77.51, 62.43, 62.40, 62.17, 62.09, 53.21, 52.74, 52.19, 51.46, 51.45, 49.82, 47.58, 47.19, 36.13, 35.75, 28.42, 27.23, 26.84, 14.09, 14.07, 14.02; HRMS (ESI) calcd for C₁₈H₂₀O₆⁺ [M+H–H₂O]⁺ 333.1333, found 333.1323. The enantiomeric excess was determined by chiral HPLC using a Daicel Chiralcel OD-H column (hexanes/*i*-PrOH, 90:10, flow rate of 1.0 mL/min, 254 nm) *t*_R = 12.66 min (minor), *t*_R = 13.43 min (major), 96% *ee*. *t*_R = 9.85 min (minor), *t*_R = 16.33 min (major), 87% *ee*.

Methyl(3a*R*,4*R*,7*S*,7a*R*)-7-bromo-8-oxo-7a-(2-oxoethyl)-2,3,3a,4,7,7a-hexahydro-1*H*-4,7-(epoxymethano)indene-5-carboxylate (*Endo*-127). Prepared following the general procedure described above, the crude material was purified by flash column chromatography (silica gel, hexanes/EtOAc, 3:1) to afford the desired product (86.8 mg combined, 89% combined yield; 74.5 mg, 76% yield *Endo*-127; 12.3 mg, 13% yield *Exo*-127) as a colorless oil. The *dr* was 6:1 as determined by crude ¹H NMR. *Endo*-127: *R*_f = 0.30 (silica gel, hexanes/EtOAc, 2:1); [α]_D²⁴ = –3.24° (*c* = 1.0 in CHCl₃); IR (thin film) 2955, 2877, 1772, 1722, 1630, 1280, 1255 cm^{–1}; ¹H NMR (500 MHz, CDCl₃) δ 9.79 (t, *J* = 2.2 Hz, 1 H), 7.26 (d, *J* = 2.1 Hz, 1 H), 5.47 (t, *J* = 2.0 Hz, 1 H), 3.82 (s, 3 H), 3.05 (dd, *J* = 15.9, 2.4 Hz, 1 H), 2.54–2.43 (m, 2 H), 2.27 (ddt, *J* = 12.8, 9.0, 7.5 Hz, 1 H), 2.00–1.69 (m, 5 H); ¹³C NMR (126 MHz, CDCl₃) δ 199.75, 166.85, 161.58, 145.19, 136.64, 77.09, 69.93, 55.50, 52.85, 49.28, 35.43, 30.24, 26.64; HRMS (ESI) calcd for C₁₄H₁₄BrO₄⁺ [M+H–H₂O]⁺ 325.0070, found 325.0063. The enantiomeric excess was

determined by chiral HPLC using a Daicel Chiralpak AD-H column (hexanes/*i*-PrOH, 95:5, flow rate of 1.0 mL/min, 254 nm) $t_R = 13.60$ min (major), $t_R = 15.23$ min (minor), 86% *ee*.

2-((3a*R*,4*R*,7*S*,7a*R*)-5-benzoyl-7-bromo-8-oxo-1,2,3,3a,4,7-hexahydro-7a*H*-4,7(epoxy methano)inden-7a-yl) acetaldehyde (*Endo*-128). Prepared following the general procedure described above, the crude material was purified by flash column chromatography (silica gel, hexanes/EtOAc, 3:1) to afford the desired product (76.0 mg combined, 65% combined yield; 57.1 mg, 49% yield *Endo*-128; 18.9 mg, 16% yield *Exo*-128) as an off-white amorphous solid. The *dr* was 4:1 as determined by crude ^1H NMR. *Endo*-128: $R_f = 0.38$ (silica gel, hexanes/EtOAc, 2:1); $[\alpha]_D^{24} = -9.70^\circ$ ($c = 1.0$ in CHCl_3); IR (thin film) 2926, 2871, 1768, 1721, 1649, 1254 cm^{-1} ; ^1H NMR (500 MHz, CDCl_3) δ 9.79 (t, $J = 2.2$ Hz, 1 H), 7.78–7.71 (m, 2 H), 7.67–7.60 (m, 1 H), 7.52 (t, $J = 7.8$ Hz, 2 H), 6.92 (d, $J = 2.0$ Hz, 1 H), 5.61 (t, $J = 2.0$ Hz, 1 H), 3.02 (dd, $J = 15.8, 2.5$ Hz, 1 H), 2.58 (ddd, $J = 8.9, 4.8, 1.8$ Hz, 1 H), 2.49 (dd, $J = 15.8, 2.1$ Hz, 1 H), 2.33 (ddd, $J = 13.3, 8.9, 7.4$ Hz, 1 H), 2.07–1.74 (m, 5 H); ^{13}C NMR (126 MHz, CDCl_3) δ 199.61, 189.51, 167.09, 144.78, 142.89, 135.41, 133.84, 129.38, 129.08, 77.93, 70.06, 56.22, 53.00, 49.81, 35.63, 30.36, 26.65; HRMS (ESI) calcd for $\text{C}_{19}\text{H}_{16}\text{BrO}_3^+ [\text{M}+\text{H}-\text{H}_2\text{O}]^+$ 371.0277, found 371.0278. The enantiomeric excess was determined by chiral HPLC using a Daicel Chiralpak AD-H column (hexanes/*i*-PrOH, 95:5, flow rate of 1.0 mL/min, 254 nm) $t_R = 27.80$ min (minor), $t_R = 31.79$ min (major), 78% *ee*.

(1*R*,4*R*,8*R*)-3-oxo-8-(2-oxoethyl)-8-phenyl-2-oxabicyclo[2.2.2]oct-5-ene-6-carbonitrile (*Endo*-132). Prepared following the general procedure described above, the crude material was purified by flash column chromatography (silica gel, hexanes/EtOAc, 3:1) to afford the desired product (62.4 mg combined, 78% combined yield; 53.0 mg, 66% yield *Endo*-132; 9.4 mg, 12% yield *Exo*-132) as a colorless oil. The *dr* was 6:1 as determined by crude ^1H NMR. *Endo*-132:

$R_f = 0.20$ (silica gel, hexanes/EtOAc, 2:1); $[\alpha]_D^{21} = -48.90^\circ$ ($c = 0.2$ in CHCl_3); IR (thin film) 2925, 2853, 2225, 1766, 1721, 1585, 1367, 1010 cm^{-1} ; ^1H NMR (500 MHz, CDCl_3) δ 9.37 (t, $J = 1.8$ Hz, 1 H), 7.43–7.36 (m, 5 H), 7.32–7.28 (m, 1 H), 5.41 (dt, $J = 4.1, 2.0$ Hz, 1 H), 4.37 (d, $J = 6.7$ Hz, 1 H), 3.08 (dd, $J = 14.4, 4.0$ Hz, 1 H), 2.83 (dd, $J = 15.9, 1.6$ Hz, 1 H), 2.77 (dd, $J = 15.9, 2.3$ Hz, 1 H), 2.17 (dd, $J = 14.4, 1.7$ Hz, 1 H); ^{13}C NMR (126 MHz, CDCl_3) δ 199.23, 168.28, 146.27, 141.56, 129.40, 128.18, 126.68, 118.60, 113.70, 74.68, 54.91, 50.55, 42.94, 39.73; HRMS (ESI) calcd for $\text{C}_{16}\text{H}_{15}\text{NO}_3\text{Na}_3^+$ $[\text{M}+3\text{Na}]^+$ 112.0196, found 112.0202. The enantiomeric excess was determined by chiral HPLC using a Daicel Chiralpak IA column (hexanes/*i*-PrOH, 90:10, flow rate of 1.0 mL/min, 254 nm) $t_R = 20.43$ min (minor), $t_R = 25.78$ min (major), 82% *ee*.

(1*R*,4*R*,4*aS*,10*aR*)-11-oxo-4a-(2-oxoethyl)-1,4,4*a*,9,10,10*a*-hexahydro-1,4-(epoxy methano)phenanthrene-2-carbonitrile (*Endo*-133). Prepared following the general procedure described above, the crude material was purified by flash column chromatography (silica gel, hexanes/EtOAc, 2:1) to afford the desired product (43.0 mg combined, 75% combined yield; 38.7 mg, 68% yield *Endo*-133; 4.3 mg, 7% yield *Exo*-133) as a pale yellow oil. The *dr* was 9:1 as determined by crude ^1H NMR. ***Endo*-133:** $R_f = 0.20$ (silica gel, hexanes/EtOAc, 2:1); $[\alpha]_D^{21} = -117.48^\circ$ ($c = 1.0$ in CHCl_3); IR (thin film) 2941, 2853, 2224, 1769, 1720, 1657, 1588, 736 cm^{-1} ; ^1H NMR (500 MHz, CDCl_3) δ 9.32 (d, $J = 2.5$ Hz, 1 H), 7.44 (d, $J = 7.9$ Hz, 1 H), 7.33 (dd, $J = 6.6, 2.3$ Hz, 1 H), 7.31–7.26 (m, 1 H), 7.22 (t, $J = 7.4$ Hz, 1 H), 7.18 (d, $J = 7.5$ Hz, 1 H), 5.15 (d, $J = 2.3$ Hz, 1 H), 4.32 (d, $J = 6.4$ Hz, 1 H), 2.87 (ddd, $J = 15.7, 6.7, 3.9$ Hz, 1 H), 2.73–2.63 (m, 2 H), 2.50 (dd, $J = 14.3, 2.7$ Hz, 1 H), 2.29–2.18 (m, 2 H), 1.82 (qd, $J = 11.8, 11.3, 7.8$ Hz, 1 H); ^{13}C NMR (126 MHz, CDCl_3) δ 199.92, 167.92, 145.09, 138.80, 135.32, 129.63, 128.11, 127.74, 126.38, 119.19, 113.76, 79.36, 55.35, 51.86, 44.43, 40.58, 28.18, 26.32; HRMS (ESI) calcd for $\text{C}_{54}\text{H}_{45}\text{N}_3\text{O}_9^+$ $[3\text{M}]^+$ 879.3156, found

879.3154. The enantiomeric excess was determined by chiral HPLC using a Daicel Chiralpak IA column (hexanes/*i*-PrOH, 90:10, flow rate of 1.0 mL/min, 254 nm) $t_R = 17.53$ min (minor), $t_R = 21.06$ min (major), 97% *ee*.

Methyl (3a*S*, 7a*S*)-7a-(2-oxoethyl)-2, 3, 3a, 7a-tetrahydro-1*H*-indene-5-carboxylate (134).

A solution of **Endo-88** (20 mg, 0.075 mmol, 1.0 equiv.) in toluene (1.5 mL) was heated to 155 °C for 24 h. Upon completion, the reaction mixture was cooled to 23 °C and concentrated *in vacuo* to give the crude product which was further purified by column chromatography (silica gel, hexanes/EtOAc 3:1) to give the desired product as a yellow oil (5.5 mg, 67% yield). Following the general procedure above, the aldehyde was converted into the corresponding α , β -unsaturated ester for HPLC analysis. **134**: $R_f = 0.78$ (silica gel, hexanes/EtOAc, 2:1); $[\alpha]_D^{23} = +52.6^\circ$ ($c = 1.0$ in CHCl_3); IR (thin film) 2951, 2928, 2869, 2862, 1719, 1654, 1263, 1090 cm^{-1} ; ^1H NMR (500 MHz, CDCl_3) δ 9.61 (t, $J = 2.8$ Hz, 1 H), 7.02 (d, $J = 5.6$ Hz, 1 H), 6.38 (dd, $J = 9.9, 1.5$ Hz, 1 H), 5.67 (d, $J = 9.8$ Hz, 1 H), 3.77 (s, 3 H), 2.50 (td, $J = 8.5, 7.9, 5.5$ Hz, 1 H), 2.39 (d, $J = 2.9$ Hz, 2 H), 2.19–2.06 (m, 1 H), 1.94–1.78 (m, 2 H), 1.56–1.43 (m, 3 H); ^{13}C NMR (126 MHz, CDCl_3) δ 202.15, 166.31, 139.99, 133.22, 125.38, 119.96, 54.92, 51.93, 44.51, 41.37, 34.55, 29.86, 22.80. HRMS (ESI) calcd for $\text{C}_{13}\text{H}_{17}\text{O}_3^+$ $[\text{M}+\text{H}]^+$ 221.1172, found 221.1163. The enantiomeric excess was determined by chiral HPLC using a Daicel Chiralpak OJ-H column (hexanes/*i*-PrOH, 95:5, flow rate of 1.0 mL/min, 254 nm) $t_R = 14.70$ min (minor), $t_R = 17.68$ min (major), 95% *ee*.

Methyl (3a*R*,4*R*,7*R*,7a*R*)-7a-((1,3-dioxolan-2-yl)methyl)-8-oxo-2,3,3a,4,7,7a-hexahydro-1*H*-4,7-(epoxymethano)indene-5-carboxylate (135). To a solution of **Endo-135** (20 mg, 0.075 mmol, 1.0 equiv.) in CH_2Cl_2 (1.5 mL) at 0 °C was added bis(trimethylsiloxy)ethane (0.037 mL, 0.15 mmol, 2.0 equiv.) and TMSOTf (0.002 mL, 0.0075 mmol, 0.1 equiv.). The

solution was stirred at 0 °C for 1 hour after which it was quenched with H₂O (1 mL), the organic layer separated, and the aqueous layer extracted with CH₂Cl₂ (2 × 2 mL). The organic layers were combined, dried over Na₂SO₄ and concentrated *in vacuo* to give the crude product as an orange oil. This residue was further purified using a silica plug (silica gel, hexanes/EtOAc, 1:1) to afford the desired acetal as a colourless oil (23 mg, 98% yield) **135**: R_f = 0.19 (silica gel, hexanes/EtOAc, 2:1); [α]_D²³ = -26.92° (c = 1.0 in CHCl₃). IR (thin film) 2954, 2888, 1761, 1717, 1631, 1252 cm⁻¹; ¹H NMR (500 MHz, CDCl₃) δ 7.35 (dd, J = 6.4, 2.1 Hz, 1 H), 5.43 (s, 1 H), 4.83 (dd, J = 6.9, 2.5 Hz, 1 H), 3.99 (q, J = 6.5 Hz, 1 H), 3.96–3.89 (m, 1 H), 3.89–3.83 (m, 1 H), 3.81–3.77 (m, 2 H), 3.80 (s, 3 H), 2.00–1.58 (m, 7 H), 1.53 (dd, J = 14.4, 6.9 Hz, 1 H); ¹³C NMR (126 MHz, CDCl₃) δ 172.83, 163.08, 142.74, 136.10, 102.26, 77.57, 65.25, 64.47, 52.29, 51.59, 50.55, 47.99, 43.91, 35.39, 28.32, 27.33. HRMS (ESI) calcd for C₃₂H₄₁O₁₂⁺ [2M+H]⁺ 617.2598, found 617.2607.

Dimethyl (3aR,4R,7R,7aR)-3a-((1,3-dioxolan-2-yl)methyl)-7-(benzoyloxy)-2,3,3a,4,7, 7a-hexahydro-1H-indene-4,6-dicarboxylate (136). Acetal **135** (10mg, 0.03 mmol, 1.0 equiv.) was dissolved in MeOH/CH₂Cl₂ (0.3 mL, 4:1) and cooled to 0 °C. To this was added sodium methoxide (0.5 M in MeOH, 0.12 mL, 0.06 mmol, 2.0 equiv.) dropwise. The reaction mixture was stirred at 0 °C for 2 h. Upon completion, the reaction was quenched with sat. NH₄Cl, and the aqueous layer extracted with EtOAc (3 × 5 mL). The organic layers were combined, dried over Na₂SO₄ and concentrated *in vacuo*. The crude material was then placed in a flask and dissolved in CH₂Cl₂ (0.4 mL). To this solution was added DMAP (4.4 mg, 0.036 mmol, 2.0 equiv.), Et₃N (0.005 mL, 0.036 mmol, 2.0 equiv.) and benzoyl chloride (0.005 mL, 0.036 mmol, 2.0 equiv.) and the mixture stirred for 1 h. Upon completion, the reaction mixture was directly purified by preparative TLC (silica gel, hexanes/EtOAc, 3:1) to give the desired product (8.9 mg, 67% yield) as a colourless oil. **136**: R_f = 0.42 (silica gel, hexanes/EtOAc, 2:1);

$[\alpha]_D^{23} = -22.48^\circ$ ($c = 0.5$ in CHCl_3); IR (thin film) 2952, 2885, 1807, 1715, 1243 cm^{-1} ; ^1H NMR (500 MHz, CDCl_3) δ 8.18–8.09 (m, 1 H), 7.67–7.61 (m, 1 H), 7.53–7.47 (m, 2 H), 6.97 (d, $J = 3.9$ Hz, 1 H), 4.89 (dd, $J = 6.9, 2.8$ Hz, 1 H), 4.83 (dd, $J = 4.0, 1.2$ Hz, 1 H), 3.95–3.88 (m, 2 H), 3.85–3.72 (m, 5 H), 3.50 (s, 3 H), 3.30 (d, $J = 4.1$ Hz, 1 H), 2.79 (d, $J = 8.4$ Hz, 1 H), 2.73–2.64 (m, 1 H), 2.20 (dd, $J = 14.9, 7.0$ Hz, 1 H), 2.13–2.03 (m, 1 H), 1.83 (dd, $J = 14.9, 2.9$ Hz, 1 H), 1.78–1.70 (m, 1 H), 1.64 (dt, $J = 5.5, 2.9$ Hz, 3 H); ^{13}C NMR (126 MHz, CDCl_3) δ 167.08, 166.97, 162.36, 147.30, 134.43, 130.73, 128.90, 103.02, 77.36, 73.65, 65.01, 64.57, 60.01, 52.02, 51.26, 45.81, 42.78, 42.27, 35.54, 31.22, 23.54; HRMS (ESI) calcd for $\text{C}_{24}\text{H}_{24}\text{O}_6^+$ $[\text{M}-2\text{H}_2\text{O}]^+$ 213.0839, found 213.0840. The enantiomeric excess was determined by chiral HPLC using a Daicel Chiralpak AD-H column (hexanes/*i*-PrOH, 97:3, flow rate of 1.0 mL/min, 240 nm) $t_R = 13.57$ min (minor), $t_R = 15.17$ min (major), 95% *ee*.

(3aR,4R,7R,7aR)-7a-((1,3-dioxolan-2-yl)methyl)-5-Bromo-2,3,3a,4,7,7a-hexahydro-1H-4,7-(epoxymethano)inden-8-one (137). To a solution of **135** (10 mg, 0.03 mmol, 1.0 equiv.) in DCE (0.75 mL) was added trimethyltin hydroxide (17.5 mg, 0.09 mmol, 3.0 equiv.). The reaction mixture was heated to 80 °C for 16h and once complete was concentrated *in vacuo*. This crude residue was dissolved in toluene (0.35 mL) followed by the addition of thionyl chloride (0.015 mL, 0.17 mmol, 5.0 equiv.) and the reaction mixture stirred at 23 °C for 24 h. The solvent and excess reagent was removed *in vacuo*. The crude residue was then dissolved in bromotrichloromethane (0.3 mL) to which was added AIBN (0.6 mg, 0.0034 mmol, 0.1 equiv.). This mixture was added over 30 min via syringe pump to a solution of 2-mercaptopyridine *N*-oxide sodium salt (5.6 mg, 0.037 mmol, 1.1 equiv.) in bromotrichloromethane (0.3 mL) at 100 °C. Upon completion, the reaction was cooled to 23 °C, concentrated *in vacuo* and subjected directly to purification by flash column chromatography (silica gel, hexanes/EtOAc, 3:2) to give the desired vinyl bromide (4.3 mg,

38% yield) as a colourless oil. **137**: $R_f = 0.35$ (silica gel, hexanes/EtOAc, 2:1); $[\alpha]_D^{23} = -53.20^\circ$ ($c = 0.1$ in CHCl_3); $^1\text{H NMR}$ (500 MHz, CDCl_3) δ 6.57 (dd, $J = 6.6, 2.4$ Hz, 1 H), 4.88–4.79 (m, 2 H), 4.03–3.89 (m, 2 H), 3.89–3.75 (m, 2 H), 3.63 (d, $J = 6.6$ Hz, 1 H), 2.09–2.03 (m, 1 H), 1.96–1.90 (m, 1 H), 1.81 (ddt, $J = 14.8, 9.9, 3.7$ Hz, 3 H), 1.77–1.63 (m, 4 H); $^{13}\text{C NMR}$ (126 MHz, CDCl_3) δ 131.49, 121.18, 102.37, 84.74, 65.22, 64.50, 52.51, 50.58, 48.07, 43.59, 35.05, 29.85, 28.33, 27.43; HRMS (ESI) calcd for $\text{C}_{28}\text{H}_{34}\text{Br}_2\text{O}_8\text{Na}^+ [2\text{M}+\text{Na}]^+$ 679.0518, found 679.0515. The enantiomeric excess was determined by chiral HPLC using a Daicel Chiralpak AS-H column (hexanes/*i*-PrOH, 90:10, flow rate of 1.0 mL/min, 215 nm) $t_R = 34.66$ min (major), $t_R = 39.10$ min (minor), 92% *ee*.

***tert*-Butyl-3-(8-(methoxycarbonyl)-1,6-dioxohexahydro-3,7-methanocyclopenta[*c*]pyran-4a(1*H*)-yl)-1*H*-indole-1-carboxylate (138)**. To a solution of ***Endo*-106** (10.0 mg, 0.023 mmol, 1.0 equiv) in CHCl_3 (1.0 mL) was added 6,7-dihydro-2-pentafluorophenyl-5*H*-pyrrolo[2,1-*c*]-1,2,4-triazolium tetrafluoroborate (1.7 mg, 0.0046 mmol, 0.2 equiv) and NaOAc (2.3 mg, 0.028 mmol, 1.2 equiv) at 23 °C. The reaction mixture was warmed to 40 °C and stirred for 30 min. The reaction mixture was then subjected directly to flash column chromatography (silica gel, hexanes/EtOAc, 2:1) to afford the desired product (9.1 mg, 91% yield) as a yellow oil. **138**: $R_f = 0.45$ (silica gel, hexanes/EtOAc, 2:1); $[\alpha]_D^{23} = -96.80^\circ$ ($c = 0.5$ in CHCl_3); IR (thin film) 2922, 2850, 1754, 1171 cm^{-1} ; $^1\text{H NMR}$ (500 MHz, CDCl_3) δ 7.30–7.25 (m, 2 H), 7.26–7.21 (m, 2 H), 5.08 (t, $J = 2.2$ Hz, 1 H), 3.79 (s, 3 H), 3.50 (d, $J = 5.3$ Hz, 1 H), 3.37 (dd, $J = 17.1, 10.5$ Hz, 1 H), 3.26 (d, $J = 5.4$ Hz, 2 H), 3.26 (d, $J = 17.0, 5.9$ Hz, 2 H), 2.93–2.90 (m, 1 H), 2.85 (dd, $J = 18.3, 1.5$ Hz, 1 H), 2.63 (d, $J = 18.3$ Hz, 1 H), 2.62–2.59 (m, 1 H). $^{13}\text{C NMR}$ (126 MHz, CDCl_3) δ 213.78, 170.25, 169.42, 141.76, 140.40, 129.17, 127.93, 125.53, 123.02, 77.85, 56.05, 53.37, 51.66, 49.78, 48.13, 48.11, 47.32, 34.07. HRMS (ESI) calcd for $\text{C}_{36}\text{H}_{33}\text{O}_{10}^+ [2\text{M}+\text{H}]^+$ 625.2069, found 625.206. The enantiomeric excess was determined by chiral HPLC

using a Daicel Chiralpak OD-H column (hexanes/*i*-PrOH, 85:15, flow rate of 1.0 mL/min, 205 nm) $t_R = 49.45$ min (major), $t_R = 74.00$ min (minor), 96% *ee*.

Lactone 147. **72** (0.195 g, 0.6 mmol, 0.05 equiv.) and **146** (1.45 g, 12.0 mmol, 1.0 equiv.) were dissolved in Et₂O (60 mL). To this solution was added **70** (3.0 mL, 36.0 mmol, 3.0 equiv.) and the mixture stirred for 36 h. Upon completion, the reaction was quenched by the addition of saturated aq. NH₄Cl (20 mL). The layers were separated and the aqueous layer was extracted with EtOAc (2 × 20 mL). The organic layers were combined, dried over Na₂SO₄ and concentrated *in vacuo*. The crude material was purified by flash column chromatography (silica gel, hexanes/EtOAc, 4:1) to afford the desired product (1.72 g, 75% yield) as a yellow oil. The *dr* was 6:1 as determined by crude ¹H NMR. **Endo-147:** ¹H NMR (500 MHz, CDCl₃) δ 9.73 (s, 1 H), 7.19 (dd, *J* = 6.5, 2.2 Hz, 1 H), 5.32 (dt, *J* = 3.9, 1.9 Hz, 1 H), 3.76 (dd, *J* = 6.4, 2.5 Hz, 1 H), 2.88 – 2.78 (m, 1 H), 2.78 – 2.66 (m, 1 H), 2.58 – 2.51 (m, 1 H), 2.49 – 2.43 (m, 1 H), 1.35 (ddd, *J* = 14.0, 3.9, 1.5 Hz, 1 H).

Acetal 148. To a flask containing a solution of **147** (660.0 mg, 3.45 mmol, 1.0 equiv.) in CH₂Cl₂ (60 mL) at 0 °C was added (TMSOCH₂)₂ (1.70 mL, 6.90 mmol, 2.0 equiv.) and TMSOTf (0.07 mL, 0.345 mmol, 0.1 equiv.). After 30 mins the reaction was quenched by the addition of saturated aq. NaHCO₃ (30 mL) and the layers separated. The aqueous layer was extracted with CH₂Cl₂ (2 × 20 mL) and the organic layers were combined, dried over Na₂SO₄ and concentrated *in vacuo*. The crude residue was purified by flash column chromatography (silica gel, hexanes/EtOAc, 4:1) to afford the desired product (730 mg, 90% yield) as a pale yellow oil. **148:** ¹H NMR (500 MHz, CDCl₃) δ 7.22 (dd, *J* = 6.5, 2.2 Hz, 1 H), 5.29 (ddt, *J* = 5.8, 3.8, 2.0 Hz, 1 H), 4.84 (dd, *J* = 5.0, 3.3 Hz, 1 H), 3.96 (ddd, *J* = 11.1, 5.3, 3.1 Hz, 2 H),

3.92 – 3.79 (m, 2 H), 2.61 – 2.49 (m, 2 H), 1.99 – 1.78 (m, 1 H), 1.70 (ddd, $J = 14.3, 6.3, 3.4$ Hz, 1 H), 1.56 (dq, $J = 14.1, 4.8$ Hz, 1 H), 1.50 – 1.44 (m, 1 H).

Alcohol 149. To a flame-dried flask was added a solution of **148** (455.0 mg, 1.93 mmol, 1.0 equiv.) in THF (20 mL). The reaction mixture was cooled to 0 °C and LiAl(*t*-BuO)₃H (1.0 M solution in THF, 1.9 mL, 1.93 mmol, 1.0 equiv.) was added dropwise. After 2 h, the reaction was quenched by the addition of saturated aq. Rochelle's Salt (20 mL). After stirring for 1 h, the layers were separated and the aqueous layer was extracted with EtOAc (3 × 15 mL). The organic layers were combined, dried over Na₂SO₄ and concentrated *in vacuo*. The crude product was carried forward without further purification.

To a solution of the crude diol (233.2 mg) in DMF (20 mL) was added TBSCl (175.0 mg, 1.16 mmol, 1.2 equiv.) and imidazole (191.5 mg, 2.8 mmol, 2.9 equiv.). The reaction was stirred at 23 °C for 6 h after which it was diluted with H₂O (20 mL) and EtOAc (15 mL). The layers were separated and the aqueous layer extracted with EtOAc (5 × 10 mL). The combined organic layers were washed with H₂O (5 × 10 mL), dried over Na₂SO₄ and concentrated *in vacuo*. The crude product was purified by flash column chromatography (silica gel, hexanes/EtOAc, 2:1) to afford the desired product (300 mg, 89% yield) as a colorless oil. **149**: ¹H NMR (500 MHz, CDCl₃) δ 6.76 (d, $J = 2.8$ Hz, 1 H), 4.90 (d, $J = 5.0$ Hz, 1 H), 4.31 (d, $J = 4.7$ Hz, 1 H), 3.96 (q, $J = 6.9$ Hz, 2 H), 3.89 – 3.76 (m, 2 H), 3.52 (dd, $J = 9.9, 7.2$ Hz, 1 H), 2.20 (d, $J = 6.7$ Hz, 1 H), 2.08 (dt, $J = 14.0, 3.6$ Hz, 1 H), 1.98 (d, $J = 9.4$ Hz, 1 H), 1.89 – 1.80 (m, 1 H), 1.67 – 1.57 (m, 2 H), 0.89 (s, 9 H), 0.06 (s, 6 H).

Sulfonamide 151. To a flame-dried flask containing **149** (266.0 mg, 0.75 mmol, 1.0 equiv.), BocNHNs (226.9 mg, 0.75 mmol, 1.0 equiv.) and Ph₃P (236.0 mg, 0.90 mmol, 1.2 equiv.) was added toluene (7.5 mL). To this mixture was added DIAD (0.18 mL, 0.90 mmol, 1.2 equiv.)

dropwise and the mixture stirred at 23 °C for 2 h. The reaction mixture was directly purified by flash column chromatography (silica gel, toluene/acetone, 19:1) to afford the desired product as white amorphous solid (252 mg, 65% yield). **151**: ¹H NMR (500 MHz, CDCl₃) δ 8.44 (dd, *J* = 6.9, 2.9 Hz, 1 H), 7.86 – 7.72 (m, 3 H), 6.72 (d, *J* = 2.7 Hz, 1 H), 5.08 – 4.87 (m, 5 H), 4.02 – 3.93 (m, 2 H), 3.87 – 3.79 (m, 2 H), 3.48 – 3.43 (m, 1 H), 2.39 (dd, *J* = 10.3, 5.9 Hz, 1 H), 2.20 (s, 1 H), 2.13 (q, *J* = 12.2 Hz, 1 H), 1.90 (dd, *J* = 12.4, 5.0 Hz, 2 H), 1.43 (d, *J* = 2.1 Hz, 9 H), 0.89 (d, *J* = 2.1 Hz, 9 H), 0.06 (d, *J* = 2.4 Hz, 6 H).

Carbamate 153. To a solution of **151** (25.0 mg, 0.039 mmol, 1.0 equiv.) in MeCN (0.25 mL) at 0 °C was added PhSH (0.016 mL, 0.156 mmol, 4.0 equiv.) and KOH (5.0 M aq., 0.015 mL, 0.078 mmol, 2.0 equiv.). After 30 mins, the reaction was diluted with EtOAc (2 mL) and H₂O (2 mL). The layers were separated and the aqueous layer was extracted with EtOAc (3 × 3 mL). The combined organic layers were dried over Na₂SO₄ and concentrated *in vacuo*. The crude residue was further purified by flash column chromatography (silica gel, hexanes/EtOAc, 3:1) to afford the desired product as a pale yellow oil (16.0 mg, 91% yield). **153**: ¹H NMR (500 MHz, CDCl₃) δ 6.69 (s, 1H), 4.86 (d, *J* = 4.8 Hz, 1 H), 4.63 (d, *J* = 9.6 Hz, 1 H), 4.34 (s, 1 H), 3.95 (h, *J* = 5.9 Hz, 2 H), 3.88 – 3.74 (m, 3 H), 3.46 (dd, *J* = 10.0, 7.1 Hz, 1 H), 2.36 – 2.29 (m, 1 H), 2.19 – 2.11 (m, 1 H), 1.90 – 1.75 (m, 2 H), 1.46 (s, 9 H), 1.30 (d, *J* = 12.0 Hz, 1 H), 0.87 (d, *J* = 2.0 Hz, 9 H), 0.04 (s, 6 H).

Enone 155. To a flask containing **149** (300.0 mg, 0.85 mmol, 1.0 equiv.) was added CH₂Cl₂ (15 mL) and NaHCO₃ (357.0 mg, 4.25 mmol, 5.0 equiv.). The reaction was cooled to 0 °C and DMP (1.06 g, 2.5 mmol, 3.0 equiv.) in a single portion. The reaction was warmed to 23 °C and stirred at this temperature for 1 h. Upon completion the reaction was quenched with mixture of NaHCO₃ and NaHSO₃ (15 mL, 1:1 v/v) and the layers separated. The aqueous layer was further

extracted with CH₂Cl₂ (3 × 10 mL) and the combined organic layers dried over Na₂SO₄ and concentrated *in vacuo*. The crude material was further purified by flash column chromatography (silica gel, hexanes/EtOAc, 3:2) to afford the desired product as a pale yellow oil (206.0 mg, 70% yield). **155**: ¹H NMR (500 MHz, CDCl₃) δ 7.69 (d, *J* = 3.0 Hz, 1 H), 4.88 (t, *J* = 4.7 Hz, 1 H), 3.99 – 3.88 (m, 3 H), 3.84 (p, *J* = 6.7 Hz, 2 H), 3.69 (dd, *J* = 10.2, 6.3 Hz, 1 H), 2.94 – 2.84 (m, 1 H), 2.64 (d, *J* = 6.7 Hz, 1 H), 2.43 – 2.32 (m, 2 H), 1.89 (dt, *J* = 14.5, 4.2 Hz, 1 H), 1.76 – 1.67 (m, 1 H), 0.88 (s, 9 H), 0.07 (s, 6 H).

Dibromide 156. To a flame-dried flask was added CHBr₃ (0.21 mL, 2.42 mmol, 5.0 equiv.) and THF (2.5 mL). The mixture was cooled to –78 °C and NaHMDS (1.0 M solution in THF, 0.62 ml, 0.62 mmol, 1.3 equiv.) was added dropwise. After 15 mins, a solution of 155 (170.0 mg, 0.48 mmol, 1.0 equiv.) in THF (2.5 mL) dropwise. After stirring at this temperature for 1 h, the reaction was quenched by the addition of saturated aq. NH₄Cl (10 mL). The reaction was diluted with EtOAc (5 mL) and the layers separated. The aqueous layer was further extracted with EtOAc (3 × 5 mL). The organic layers were combined, dried over Na₂SO₄ and concentrated *in vacuo*. The crude product was further purified by flash column chromatography (silica gel, hexanes/EtOAc, 3:2) to afford the desired product as a yellow oil (170.0 mg, 68% yield). **156**: ¹H NMR (500 MHz, CDCl₃) δ 4.83 (d, *J* = 4.9 Hz, 1 H), 4.01 – 3.90 (m, 2 H), 3.82 (qd, *J* = 10.8, 5.3 Hz, 3 H), 2.85 (t, *J* = 2.9 Hz, 1 H), 2.73 (d, *J* = 15.4 Hz, 1 H), 2.34 – 2.21 (m, 2 H), 1.97 – 1.84 (m, 2 H), 1.59 (dd, *J* = 13.6, 6.1 Hz, 1 H), 0.93 (d, *J* = 2.1 Hz, 9 H), 0.12 (dd, *J* = 6.1, 2.0 Hz, 6 H).

Amine 158. To a solution of **156** (5.0 mg, 0.0096 mmol, 1.0 equiv.) and NH₄OAc (11.0 mg, 0.144 mmol, 15.0 equiv.) in MeOH (0.15 mL) was added NaCNBH₃ (1.0 M solution in THF, 0.05 mL, 0.048 mmol, 5.0 equiv.). The reaction temperature was increased to 50 °C and stirred for 2 h. Upon completion, the reaction was quenched with H₂O (2 mL) and diluted with EtOAc

(2 mL). The aqueous layer was extracted with EtOAc (2 × 2 mL), the organic layers combined, dried over Na₂SO₄ and concentrated *in vacuo*. The crude amine was carried forward without any further purification.

To a solution of the crude amine (3.0 mg) in CH₂Cl₂ (0.1 mL) was added Et₃N (0.003 mL, 0.021 mmol, 3.0 equiv.), DMAP (0.7 mg, 0.006 mmol, 1.0 equiv.) and Boc₂O (2.5 mg, 0.0114 mmol, 2.5 equiv.). After 1 h the reaction was purified directly by column (silica gel, hexanes/EtOAc, 2:3) to afford the desired product (2.8 mg, 78% yield). **158**: ¹H NMR (500 MHz, CDCl₃) δ 5.47 (t, *J* = 8.8 Hz, 1 H), 4.83 (t, *J* = 4.8 Hz, 1 H), 3.98 – 3.86 (m, 3 H), 3.86 – 3.77 (m, 2 H), 3.69 (dd, *J* = 10.3, 4.5 Hz, 1 H), 2.55 (d, *J* = 2.0 Hz, 1 H), 2.16 (dd, *J* = 10.8, 7.2 Hz, 1 H), 1.83 – 1.75 (m, 1 H), 1.74 – 1.60 (m, 3 H), 1.52 (d, *J* = 5.3 Hz, 9 H), 0.91 (s, 9 H), 0.09 (d, *J* = 5.9 Hz, 6 H).

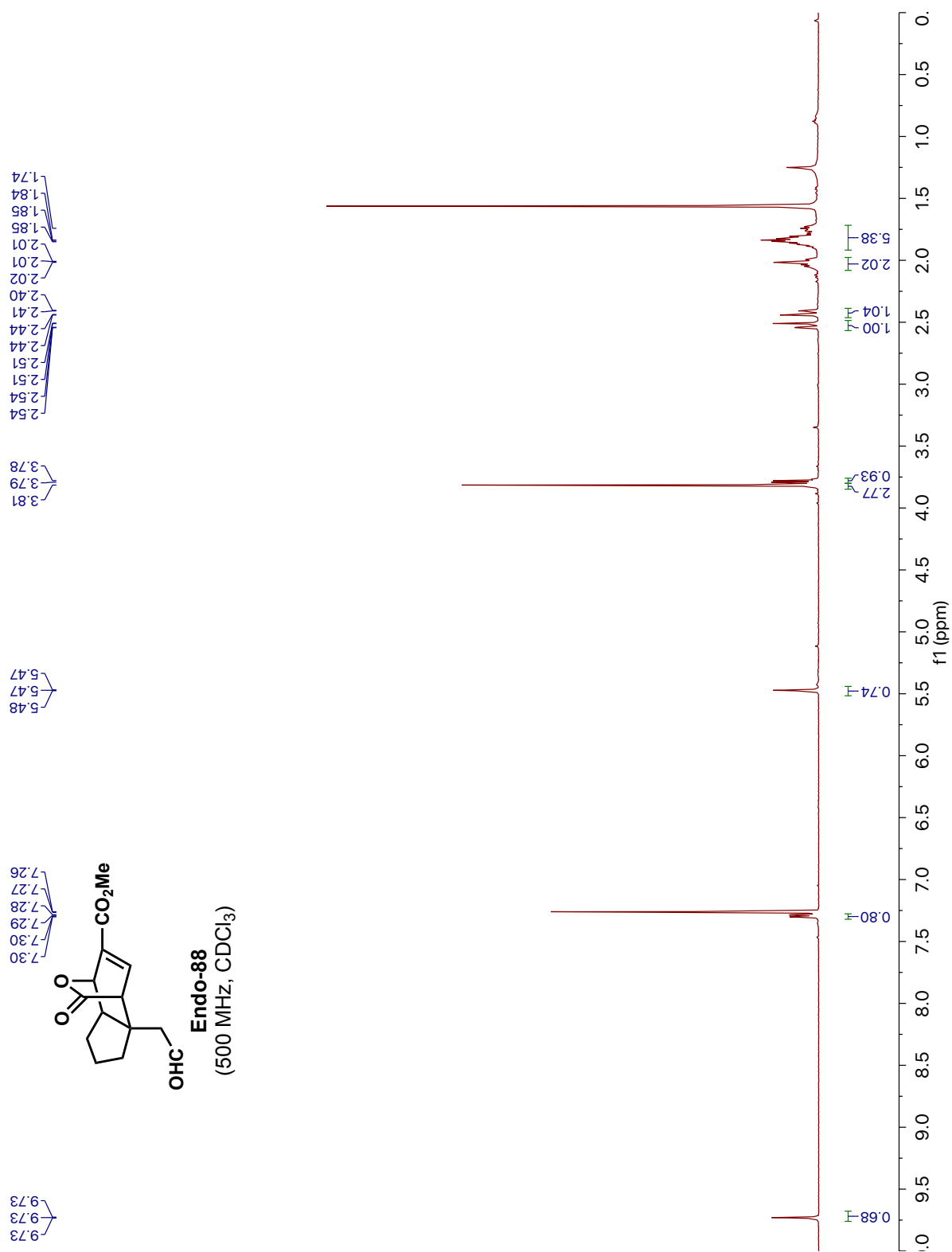
Pyridone 175. To a solution of 3-bromo-5-carbomethoxy-2-hydroxypyridine (100 mg, 0.43 mmol, 1.0 equiv.) in CH₂Cl₂ (10 mL) at 0 °C was added NaH (60% in mineral oil, 37.9 mg, 0.95 mmol, 2.2 equiv.) portionwise. After stirring for 30 min, *p*-NsCl (172.9 mg, 0.78 mmol, 1.8 equiv.) was added and the reaction warmed to 23 °C. Upon completion, the reaction was quenched by the addition of saturated aq. NH₄Cl (10 mL), the layers separated, and the aqueous layer extracted with CH₂Cl₂ (2 × 10 mL). The combined organic layers were dried over Na₂SO₄ and concentrated *in vacuo*. The crude solid was further purified by flash column chromatography (silica gel, hexanes/EtOAc, 4:1) to afford the desired pyridone as a white crystalline solid (80 mg, 53% yield). **175**: ¹H NMR (500 MHz, CDCl₃) δ 8.90 (d, *J* = 2.2 Hz, 1 H), 8.43 (d, *J* = 8.8 Hz, 2 H), 8.37 (d, *J* = 9.2 Hz, 1 H), 8.29 (d, *J* = 2.2 Hz, 1 H), 3.94 (s, 3 H).

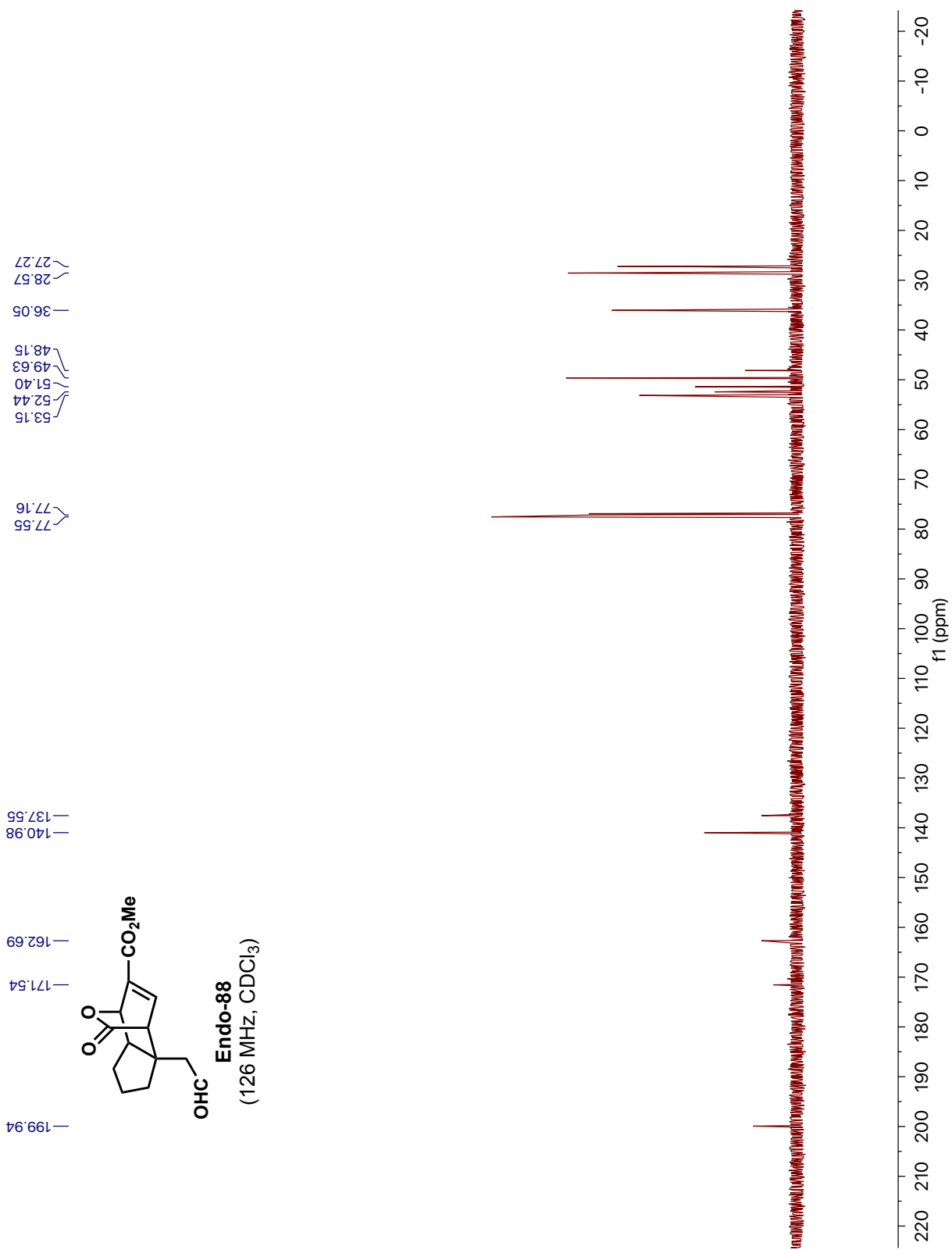
Lactam 176. To a 4 mL scintillation vial containing **175** (100 mg, 0.24 mmol, 1.0 equiv.) and **72** (5.9 mg, 0.048 mmol, 0.2 equiv.) was added 1,4-dioxane (1.2 mL). Crotonaldehyde (0.06 mL, 0.72 mmol, 3.0 equiv.) was added to the solution and the reaction stirred for 48 h at 23 °C.

Following this, the reaction was quenched by the addition of saturated aq. NH_4Cl (3 mL) and diluted with EtOAc (3 mL). The layers were separated and the aqueous layer extracted with EtOAc (2×5 mL). The combined organic layers were dried over Na_2SO_4 and concentrated *in vacuo*. The crude residue was further purified by flash column chromatography (silica gel, hexanes/EtOAc, 4:1) to afford the desired product (71 mg combined, 74% combined yield; 39 mg, 41% yield **Endo-176**; 32 mg, 33% yield **Exo-176**) as a colorless oil. The *dr* was 1:1.1 as determined by crude ^1H NMR. **Endo-176**: ^1H NMR (500 MHz, CDCl_3) δ 9.73 (s, 1 H), 8.35 (d, $J = 8.8$ Hz, 1 H), 8.18 (d, $J = 8.8$ Hz, 2 H), 7.09 – 7.02 (m, 1 H), 5.86 (dt, $J = 4.1, 2.1$ Hz, 1 H), 3.84 (s, 3 H), 3.28 – 3.21 (m, 1 H), 2.79 (ddt, $J = 11.2, 7.0, 3.4$ Hz, 1 H), 2.71 (ddd, $J = 13.0, 9.0, 3.7$ Hz, 1 H), 2.40 – 2.27 (m, 1 H), 1.43 (ddd, $J = 13.4, 4.1, 2.2$ Hz, 1 H).

Exo-176: ^1H NMR (500 MHz, CDCl_3) δ 9.77 (s, 1 H), 8.35 (d, $J = 8.9$ Hz, 2 H), 8.17 (d, $J = 9.0$ Hz, 2 H), 7.20 (d, $J = 2.1$ Hz, 1 H), 5.94 – 5.85 (m, 1 H), 3.84 (s, 3 H), 3.26 – 3.19 (m, 1 H), 2.82 – 2.72 (m, 1 H), 2.36 – 2.26 (m, 2 H), 1.88 (dt, $J = 13.6, 3.9$ Hz, 1 H).

3.13 ^1H and ^{13}C NMR Data



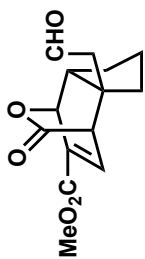


1.08
 1.12
 1.50
 1.61
 1.81
 1.83
 1.99
 2.01
 2.50
 2.53
 2.54
 2.64
 2.68
 2.68
 2.68
 2.73
 2.73
 2.76
 2.76
 3.83
 3.83
 4.00
 4.01

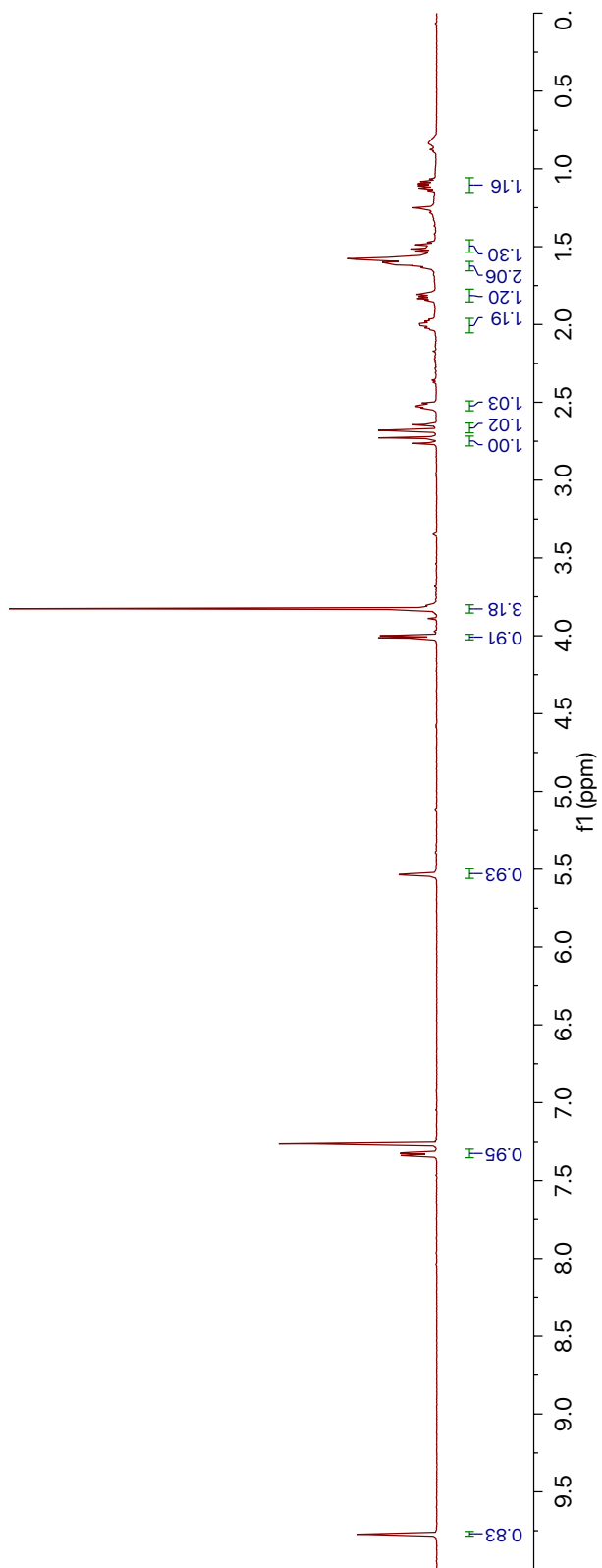
5.53
 5.53
 5.54
 5.54

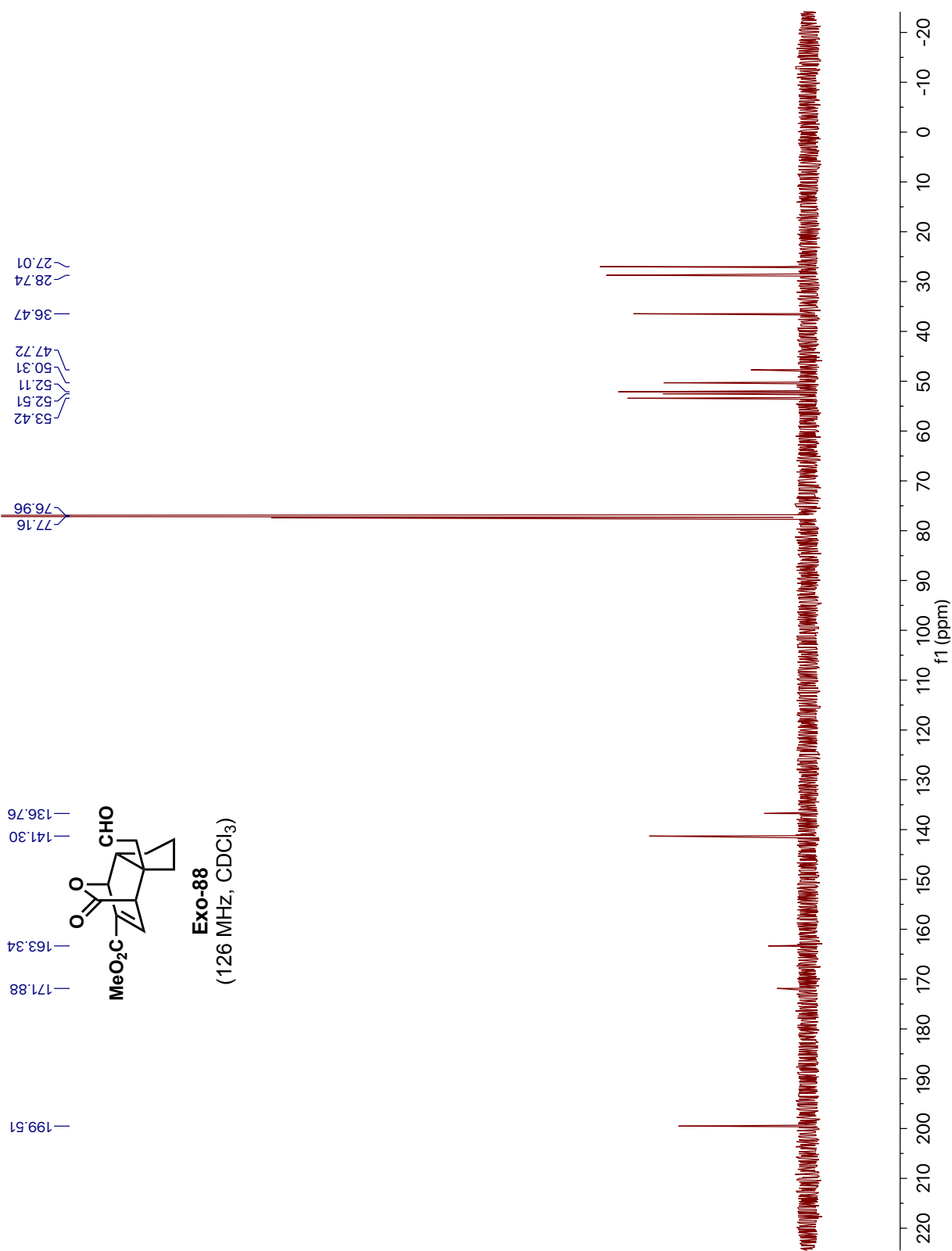
7.26
 7.32
 7.32
 7.33
 7.34
 7.34

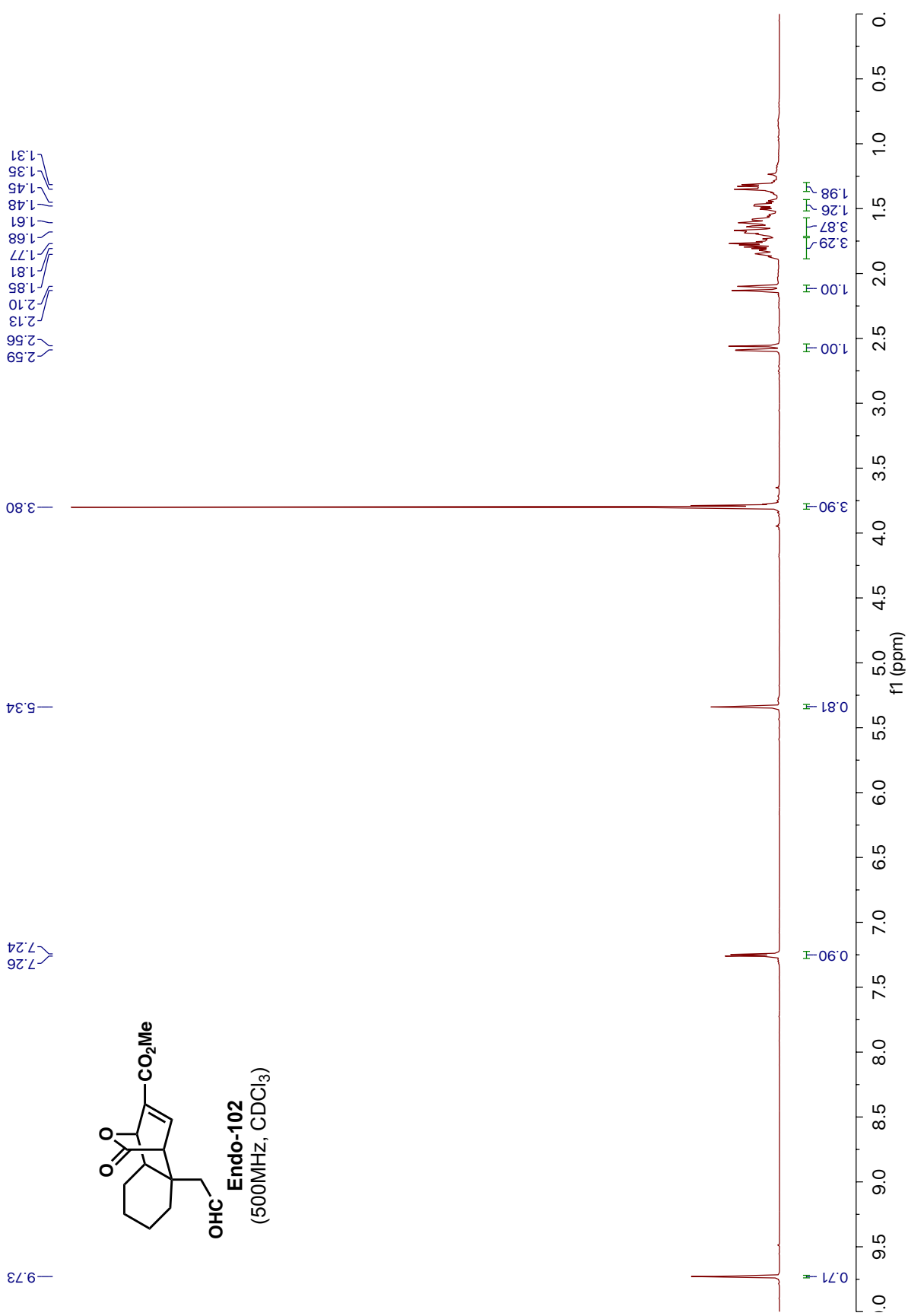
9.77
 9.77
 9.78

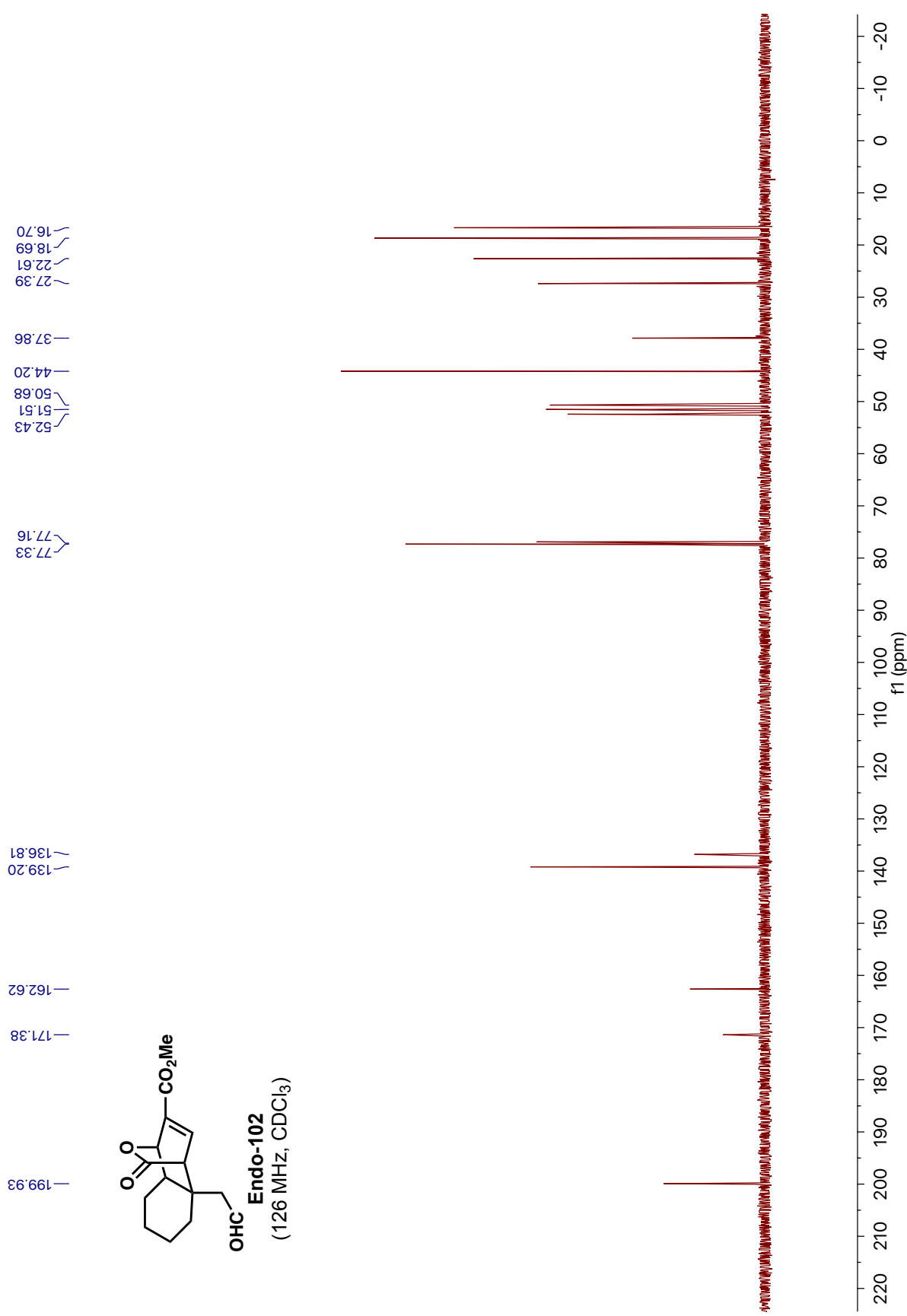


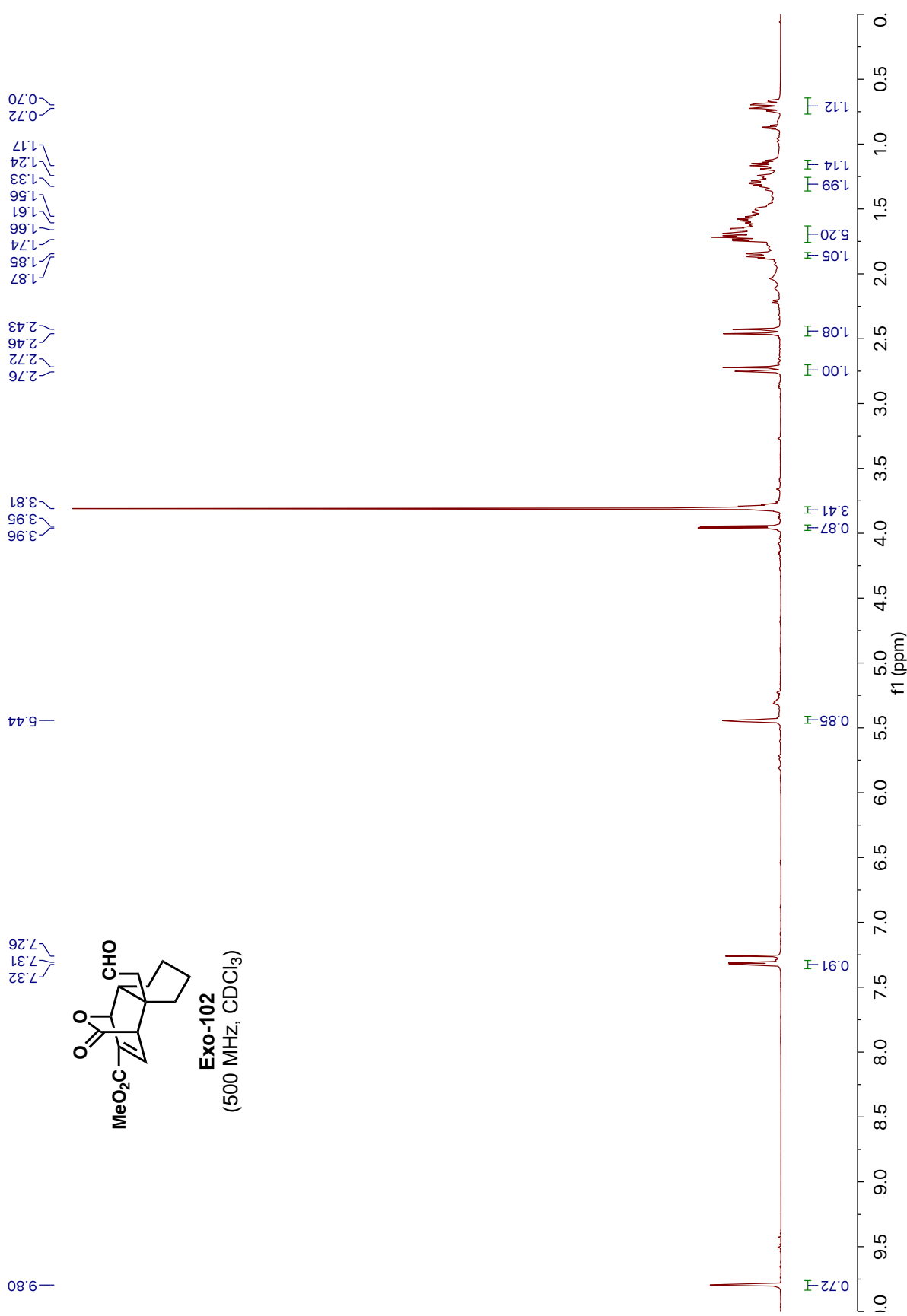
Exo-88
 (500 MHz, CDCl₃)

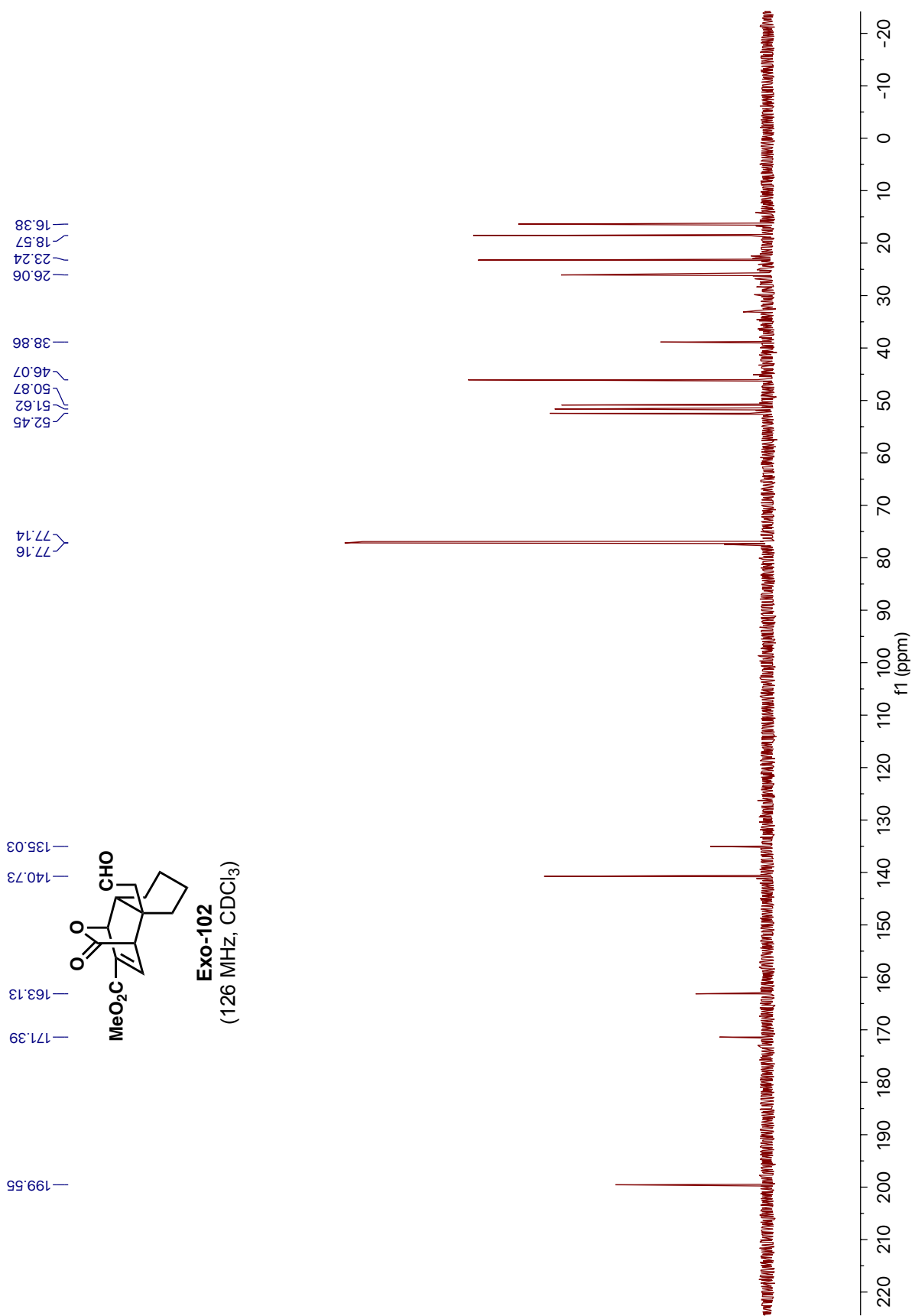


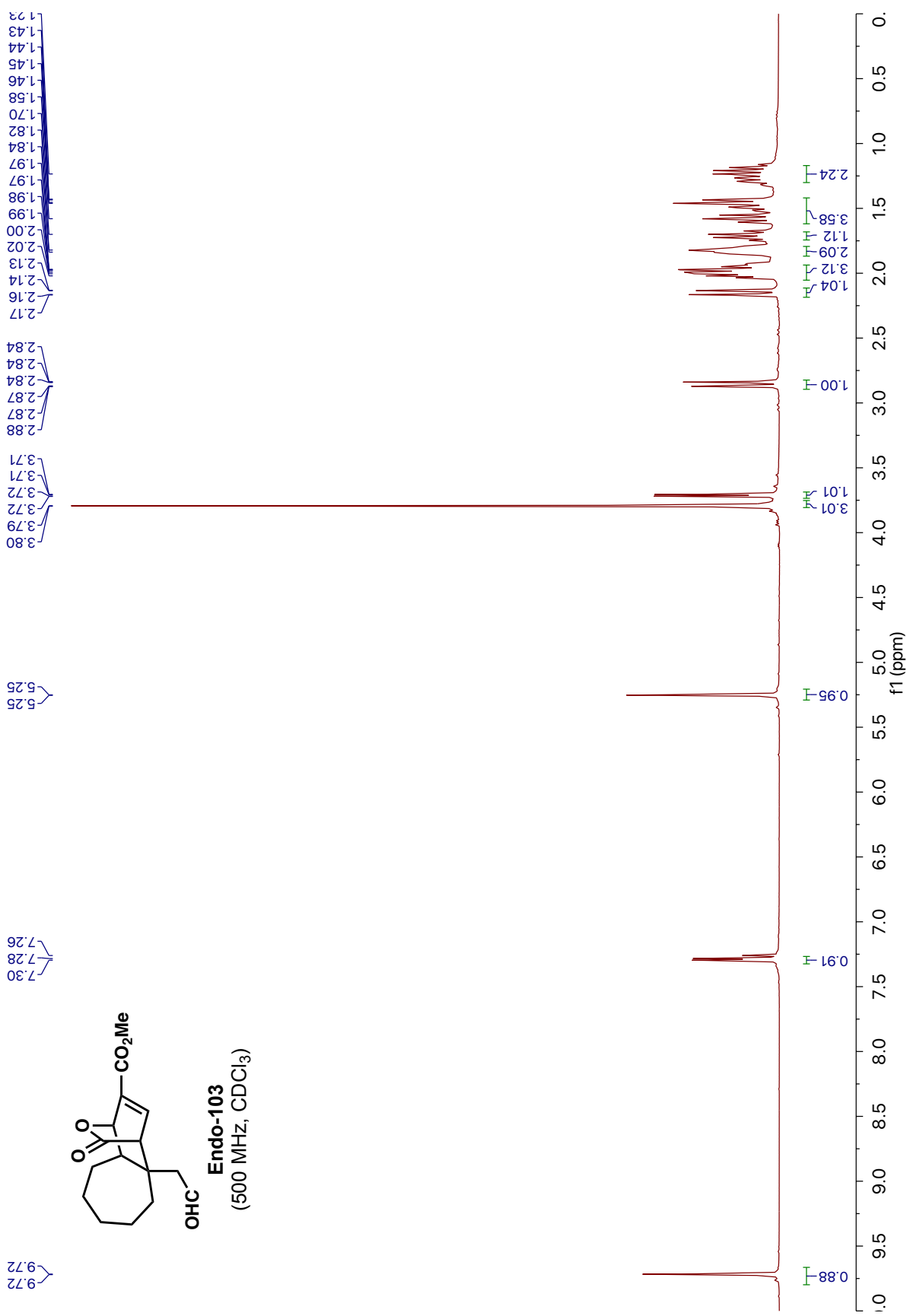


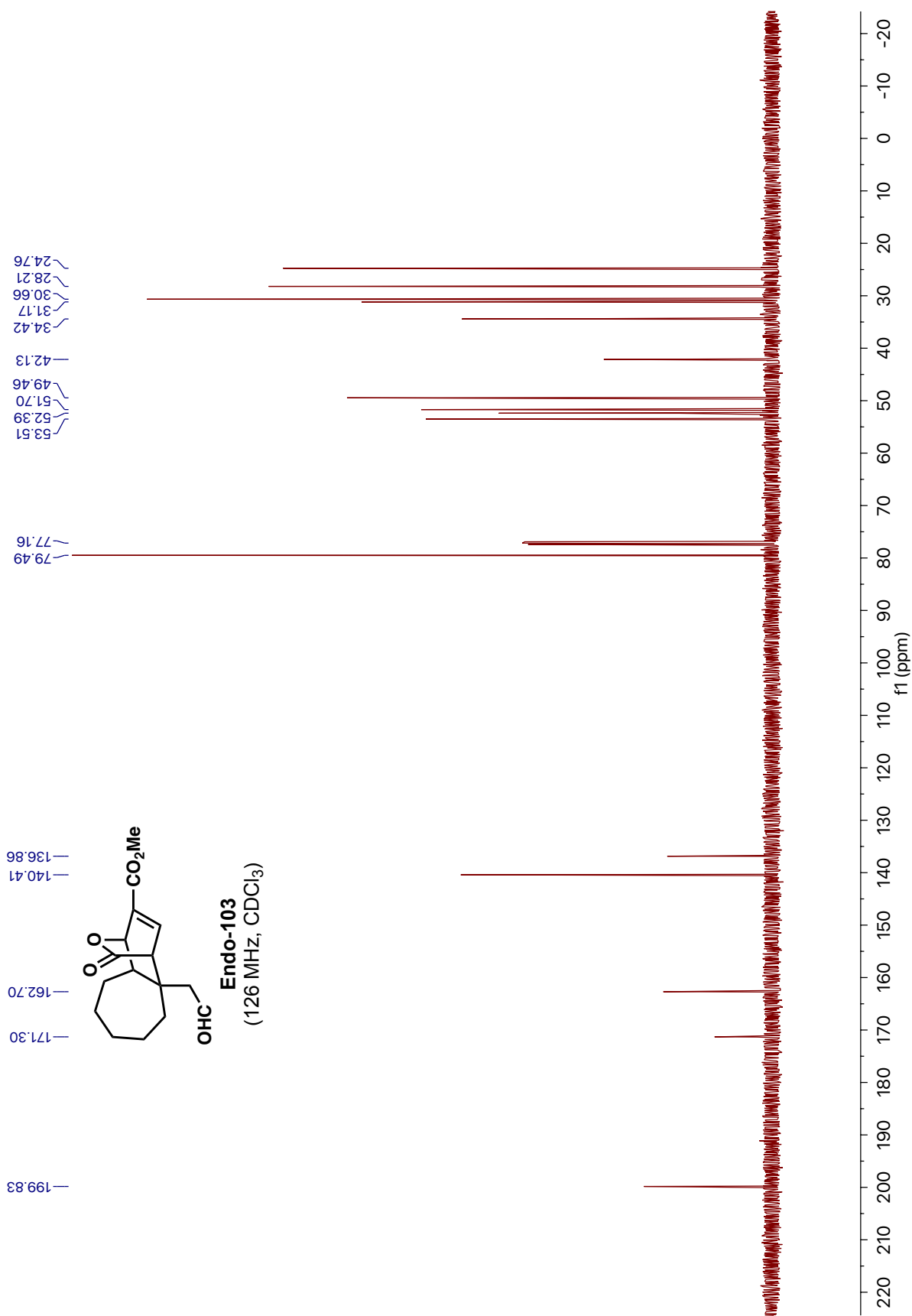


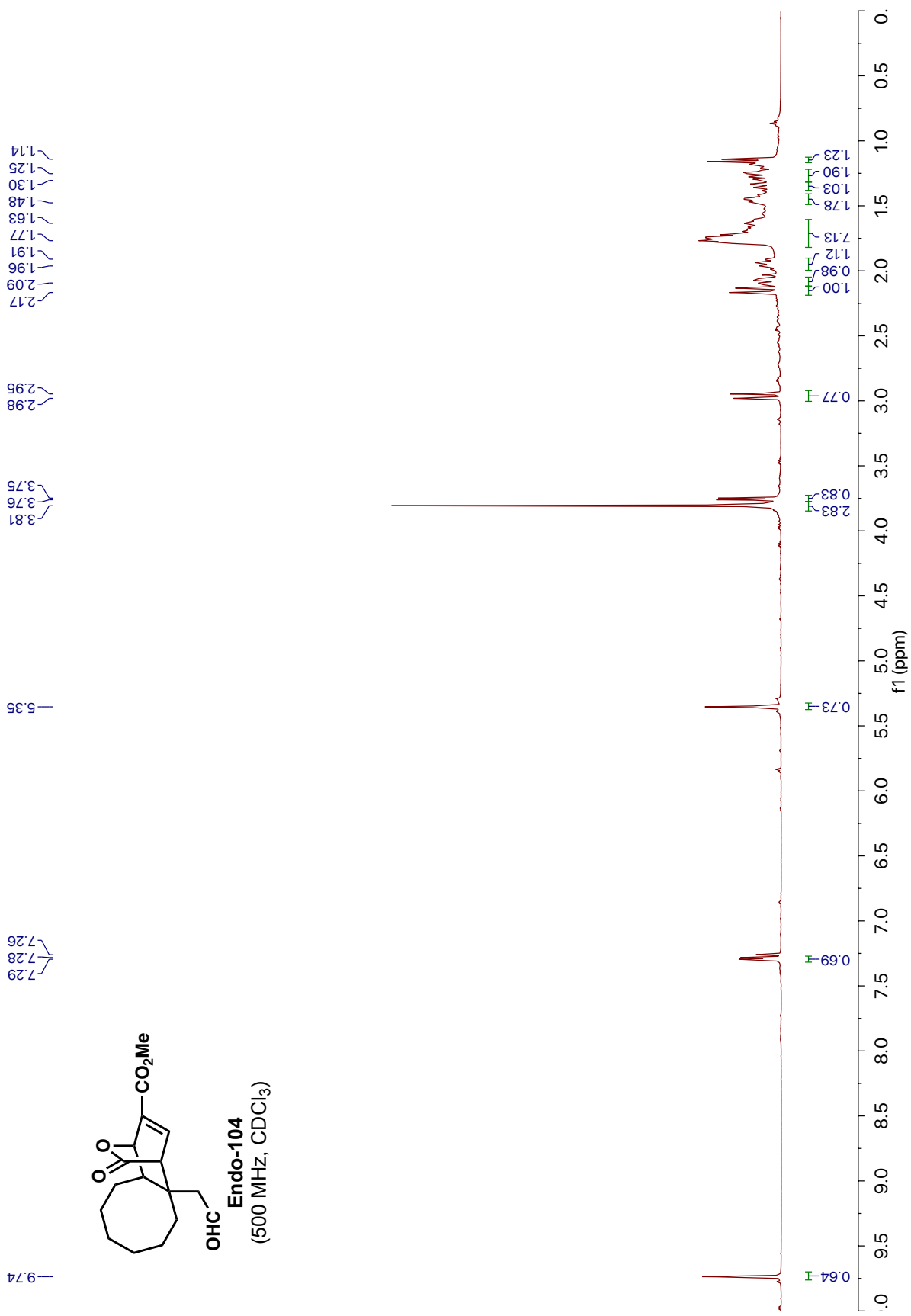


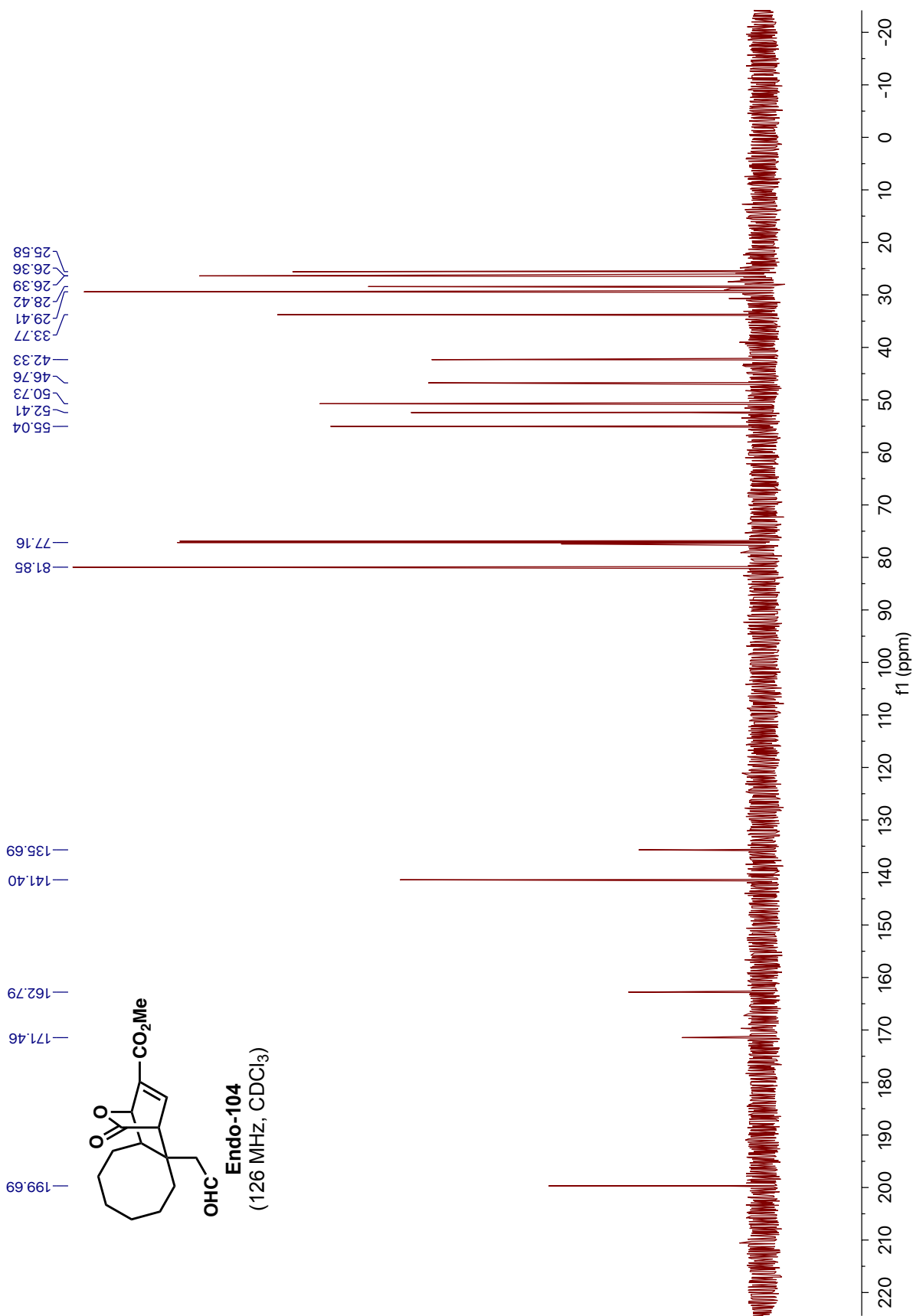


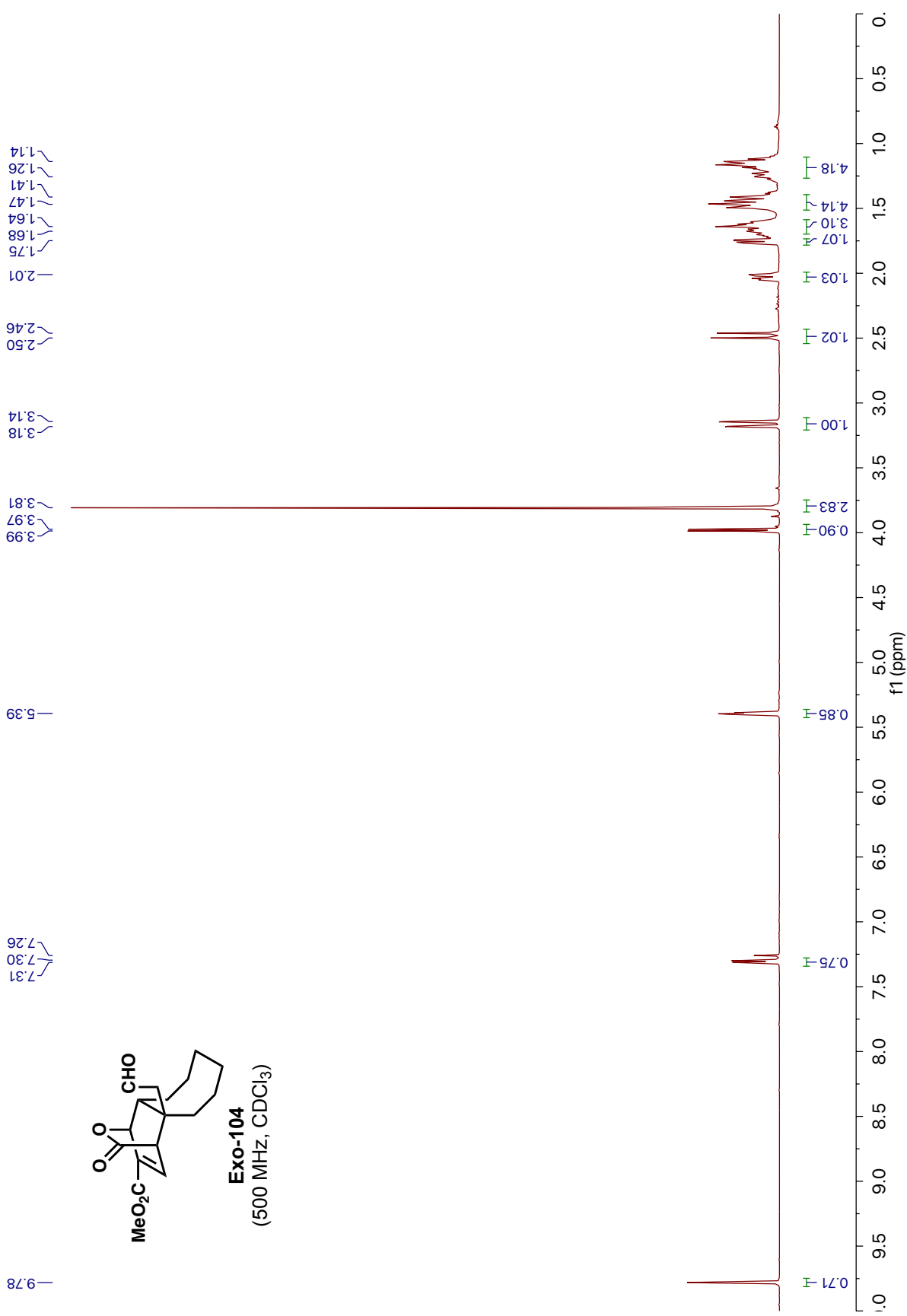


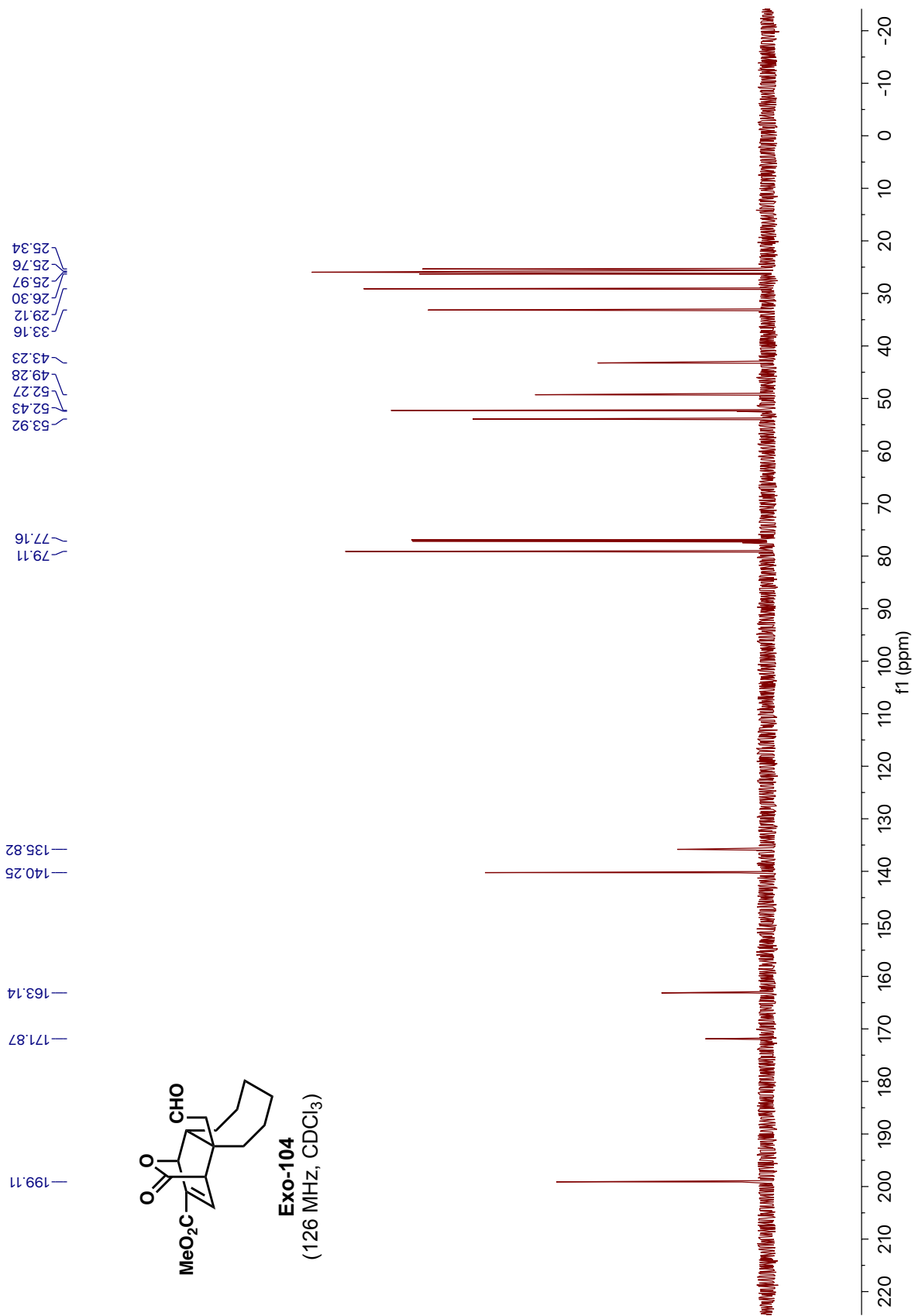


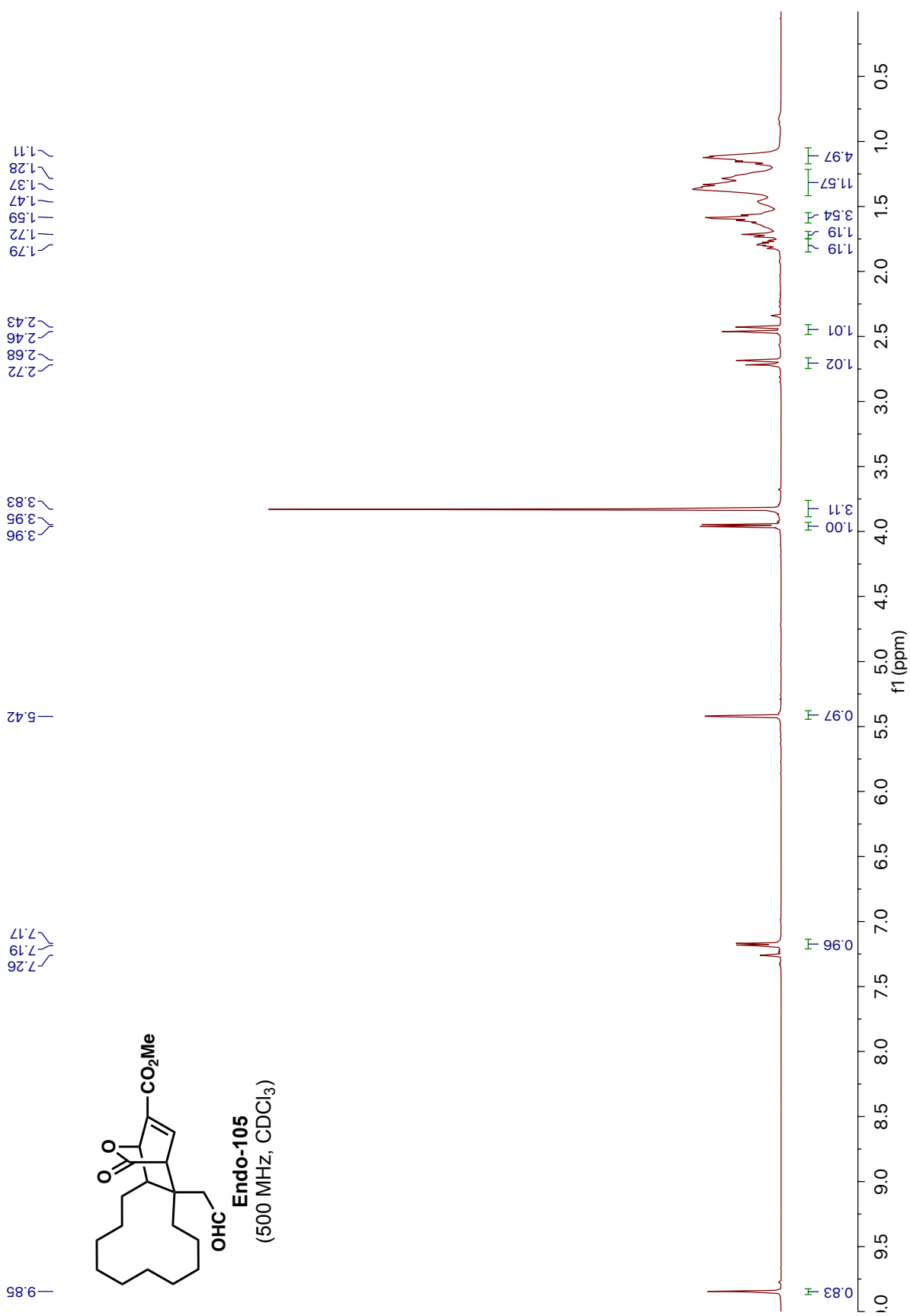


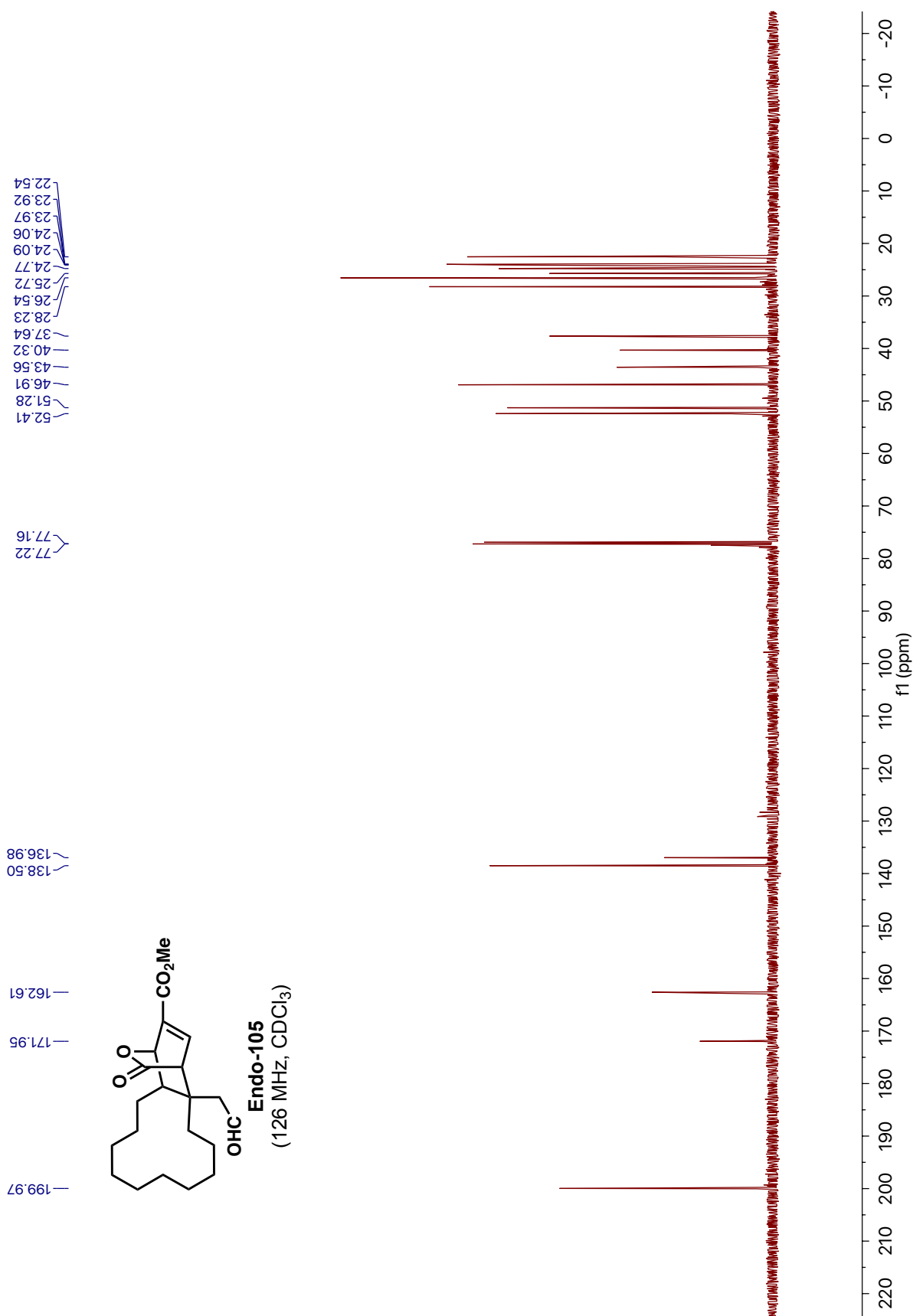


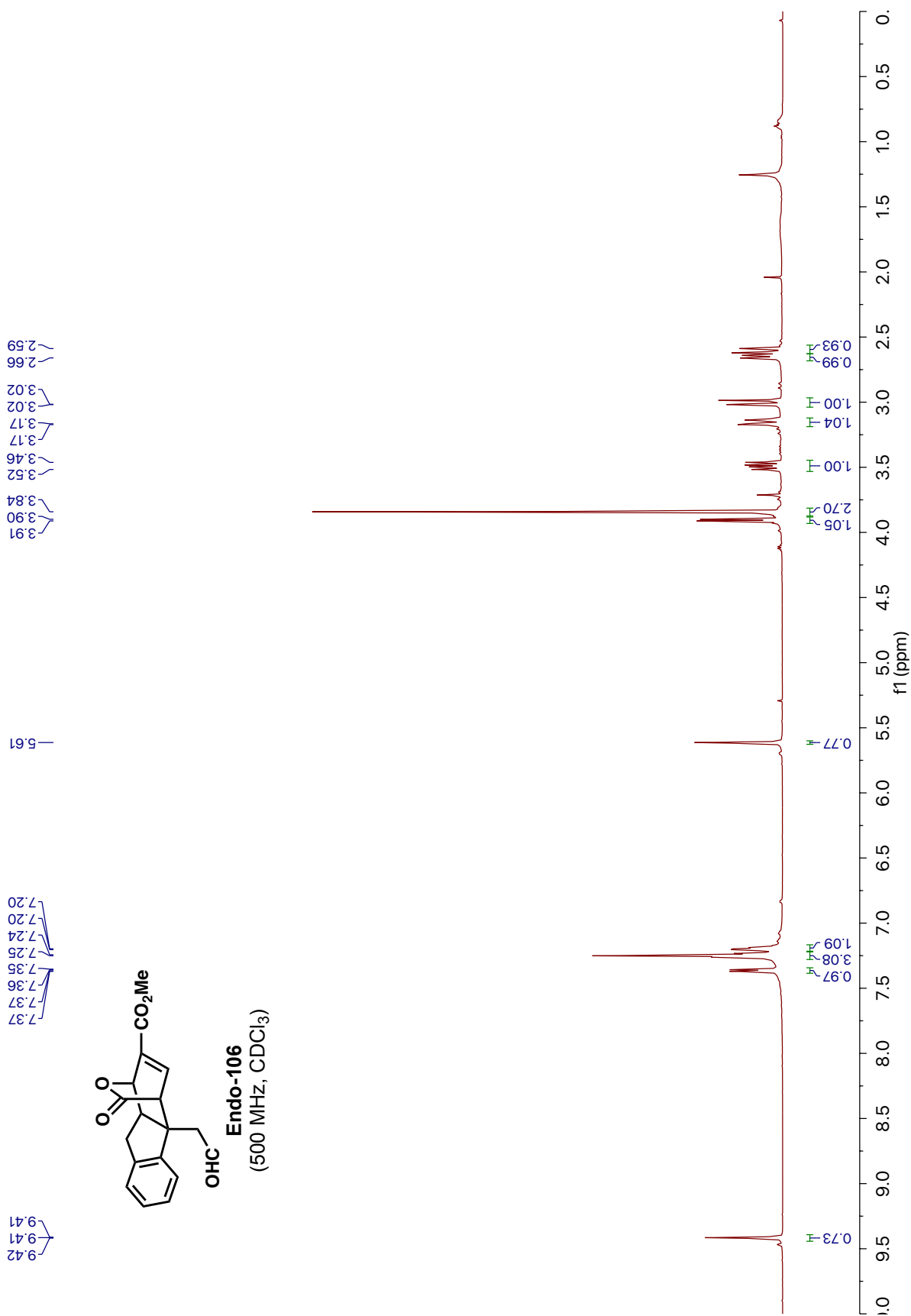


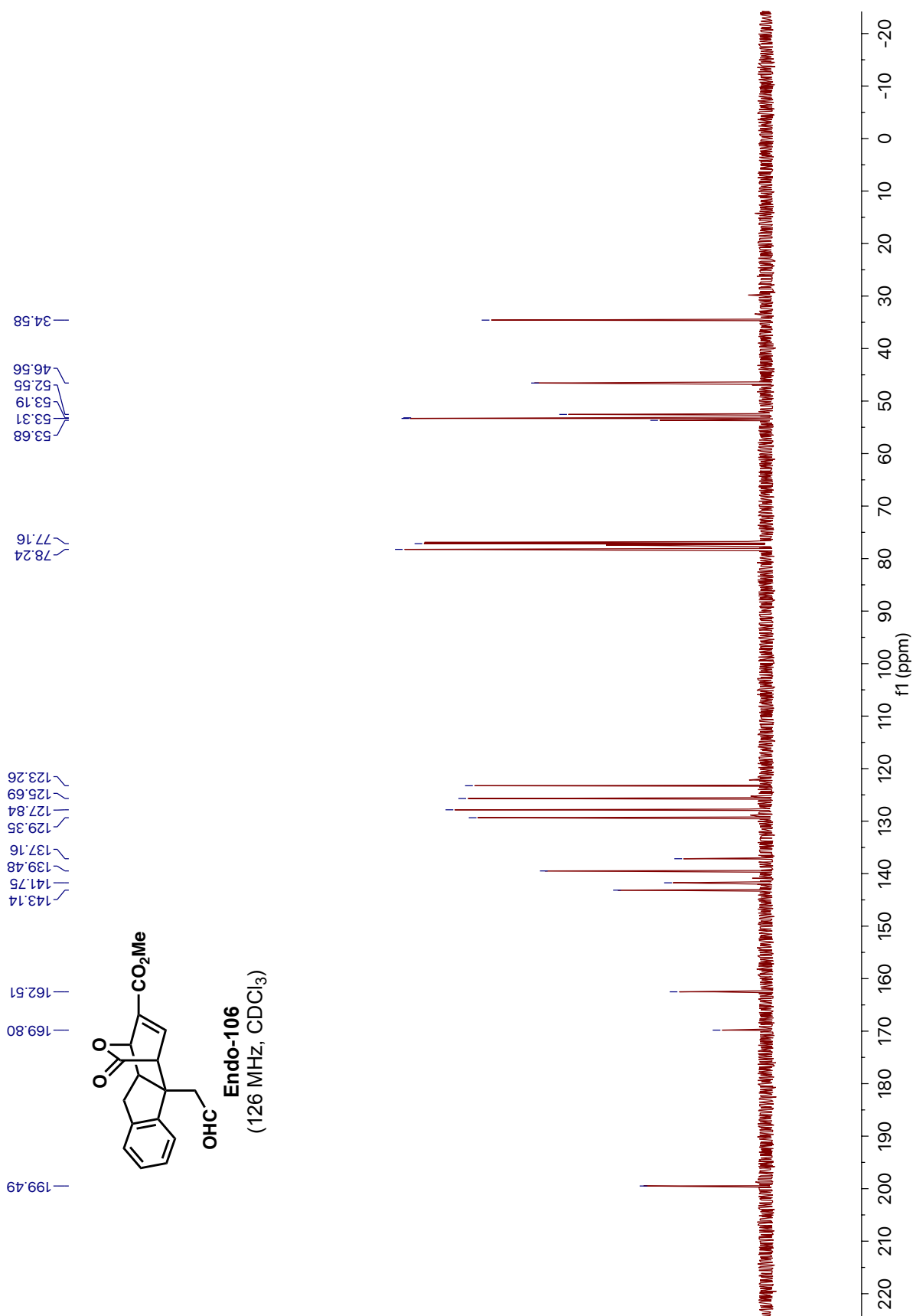


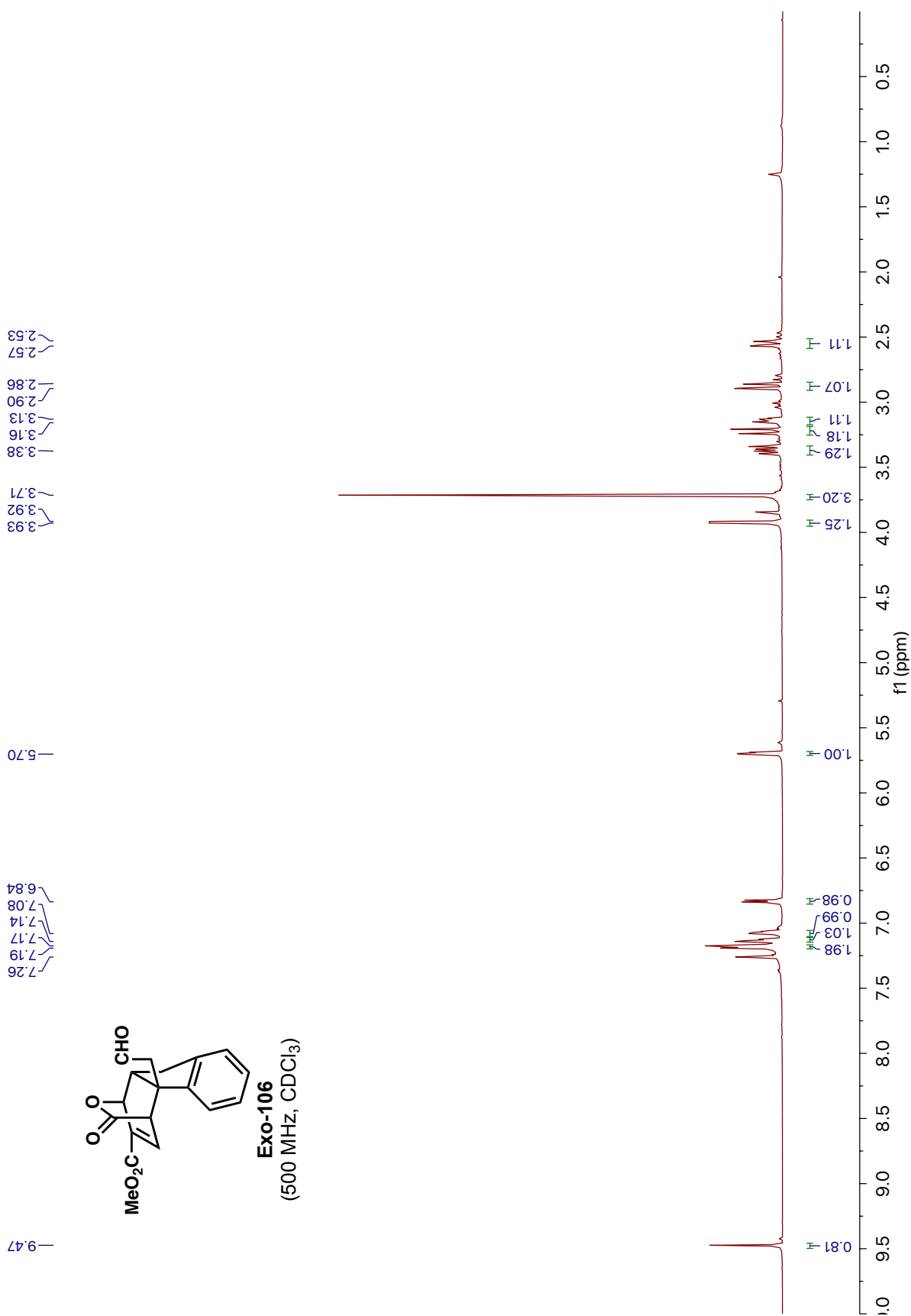


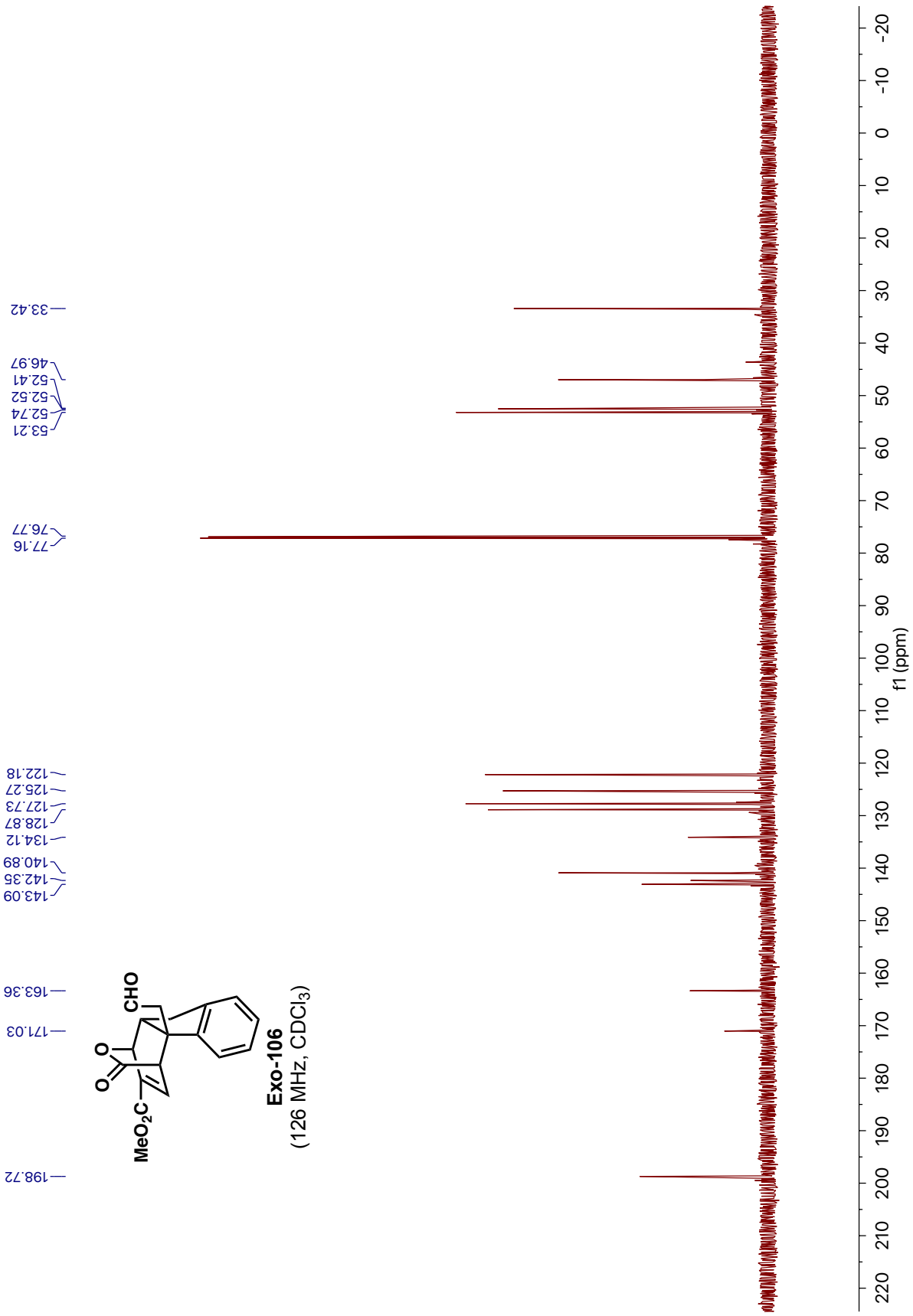


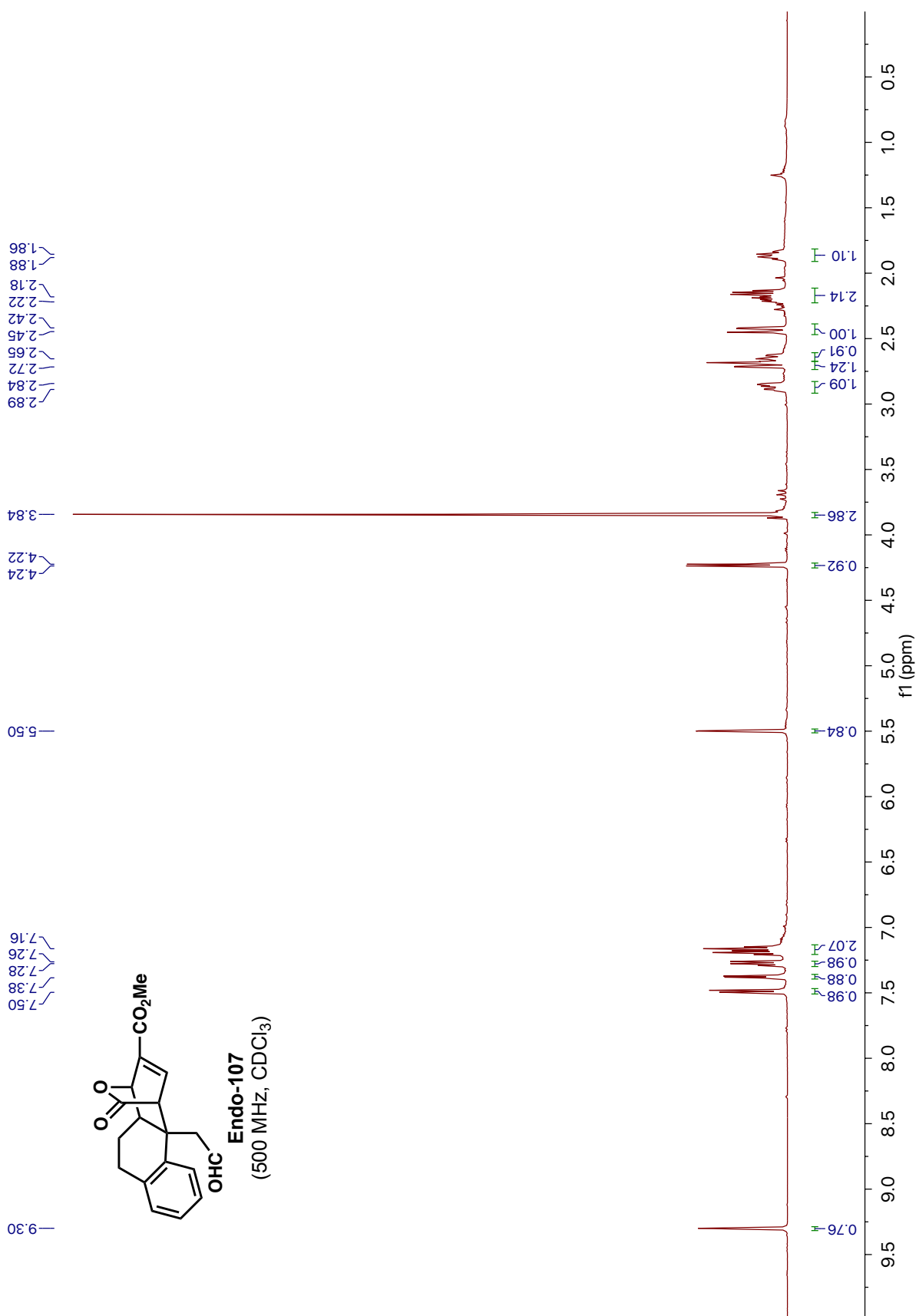


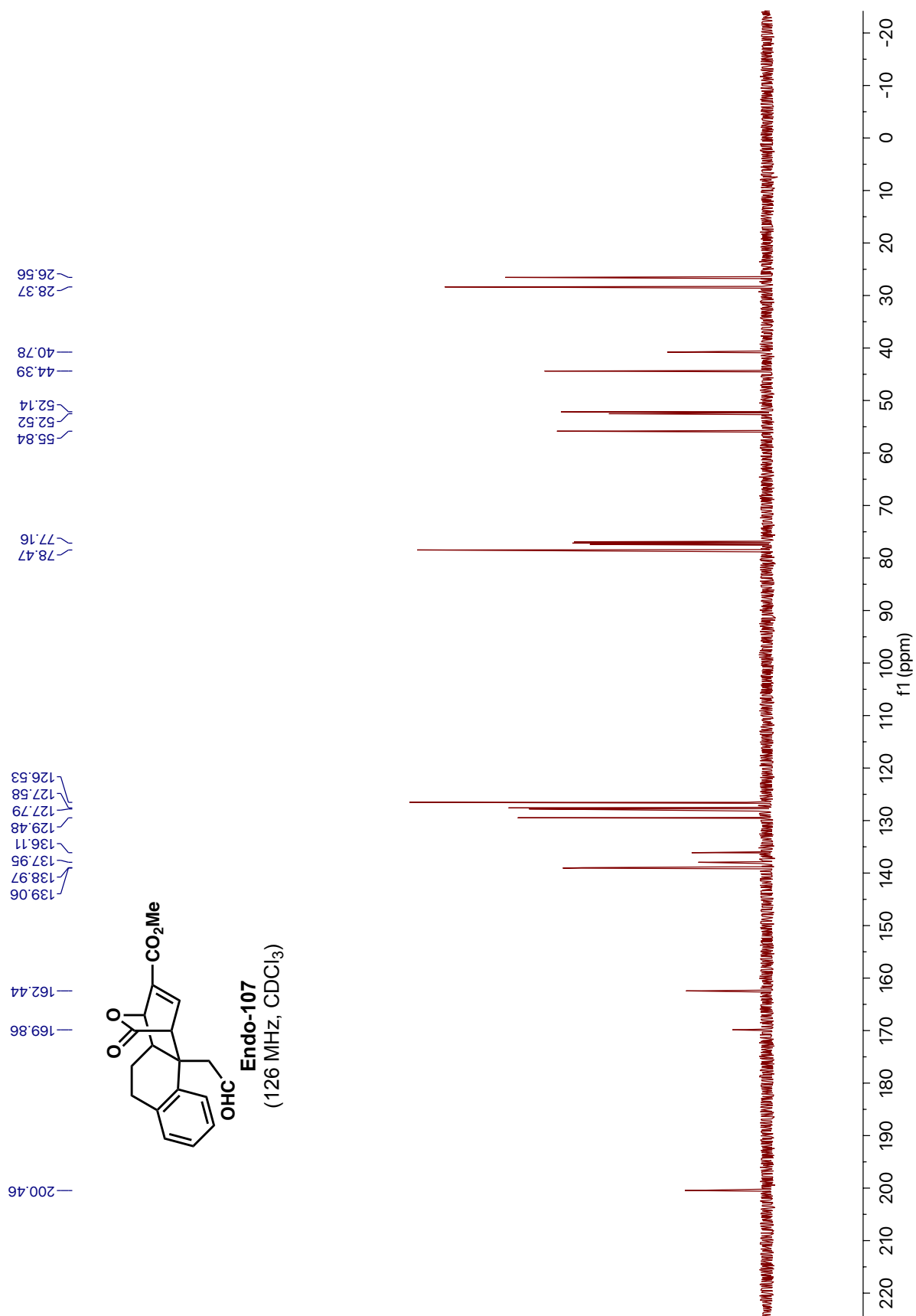


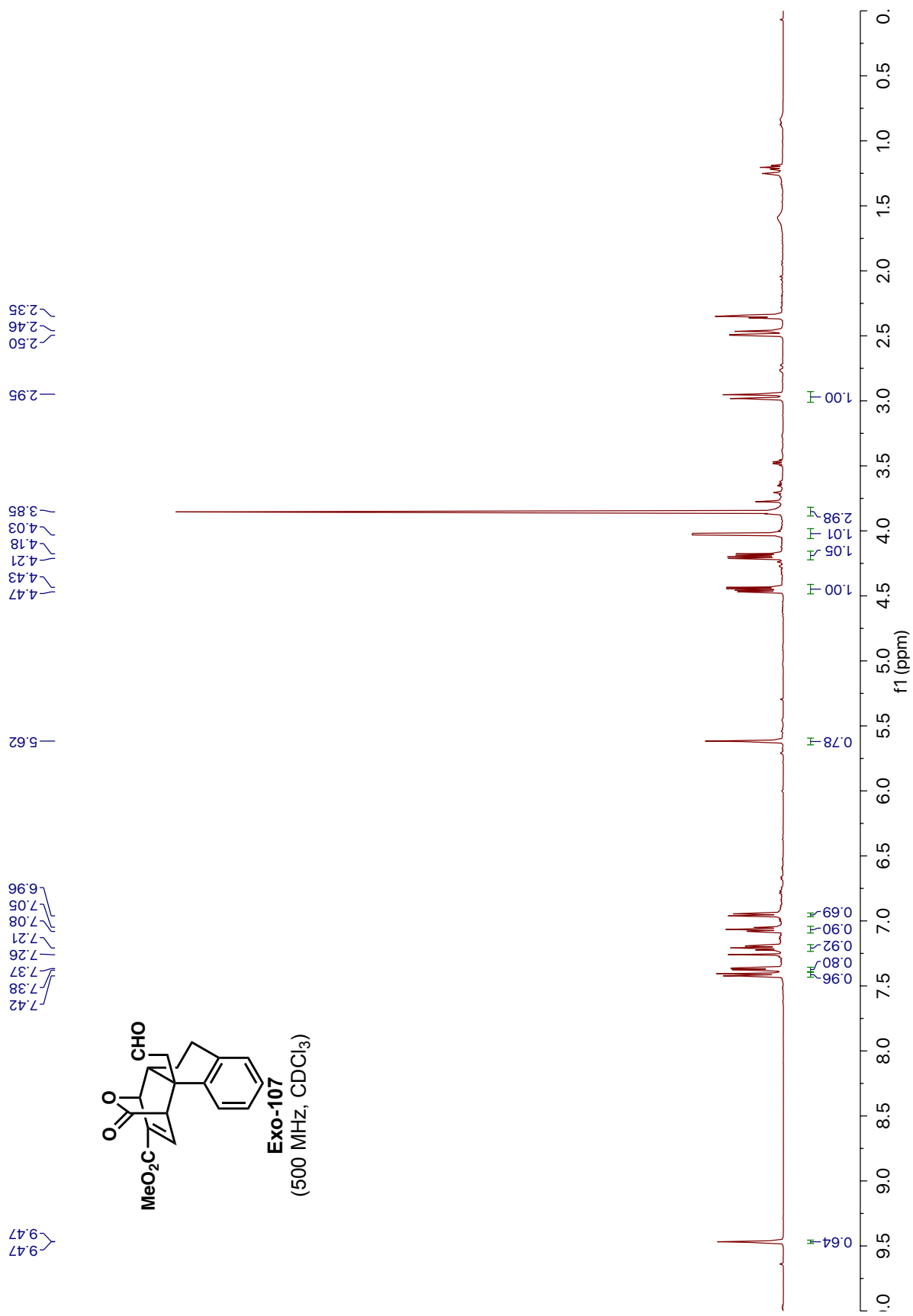


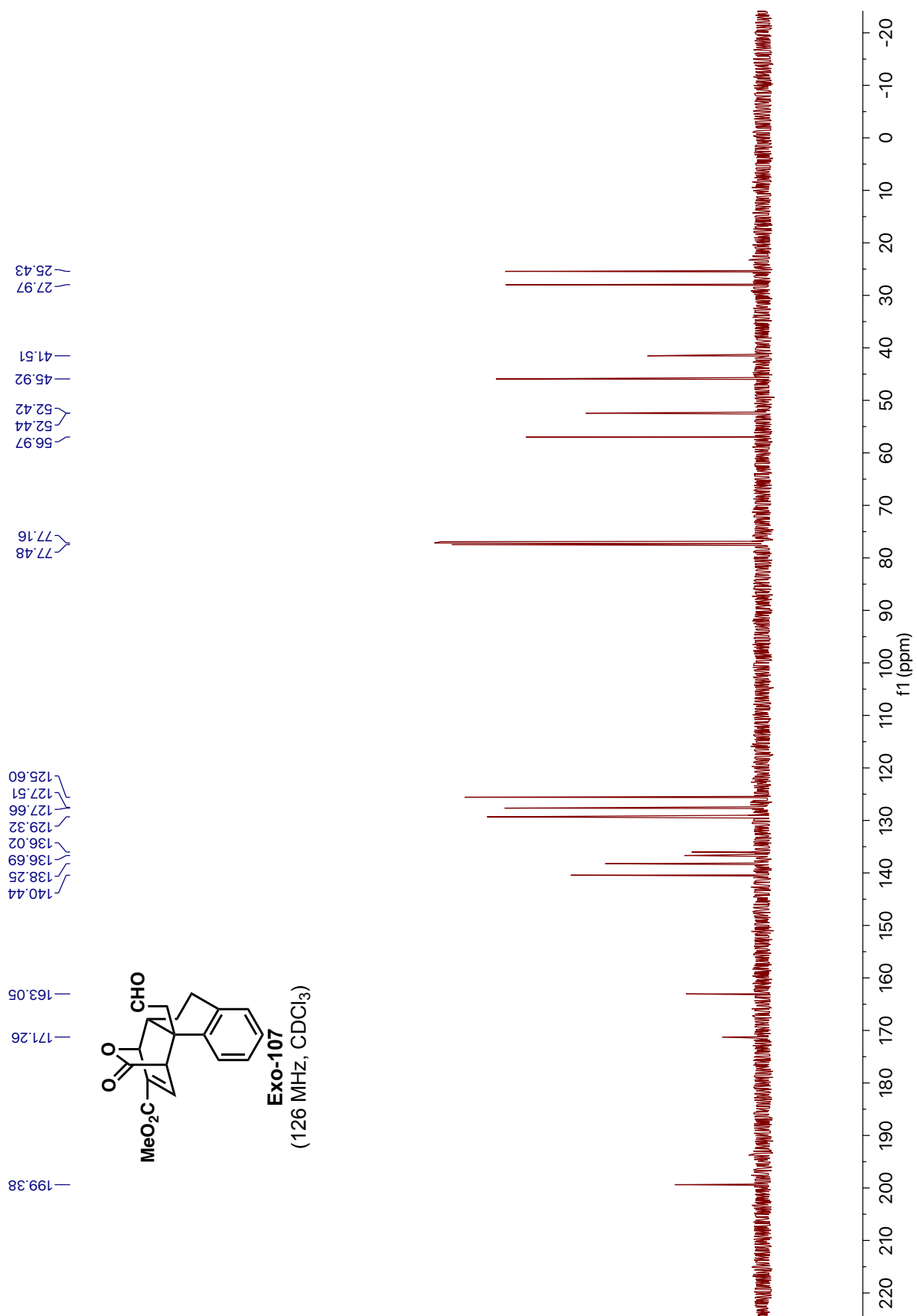


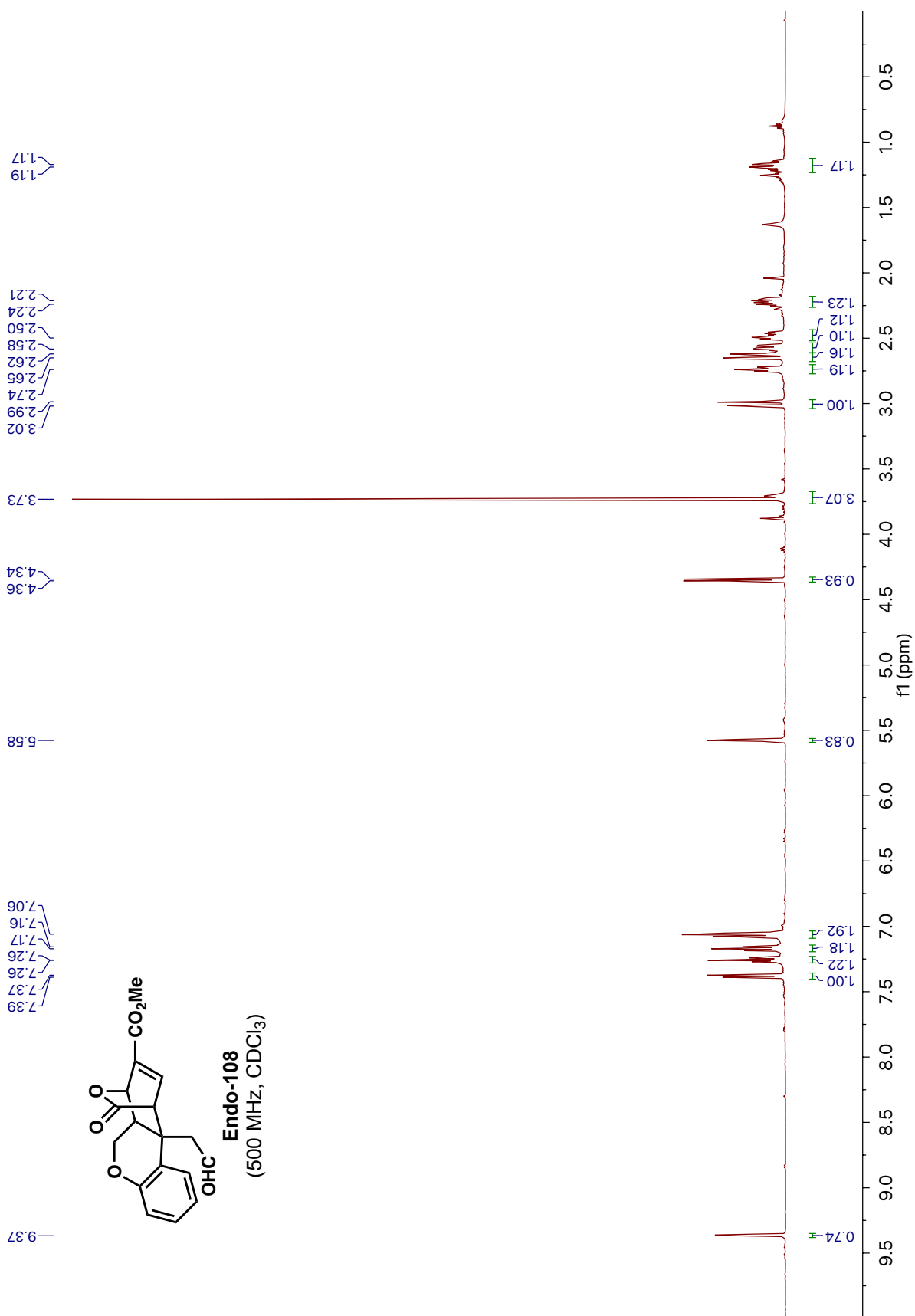


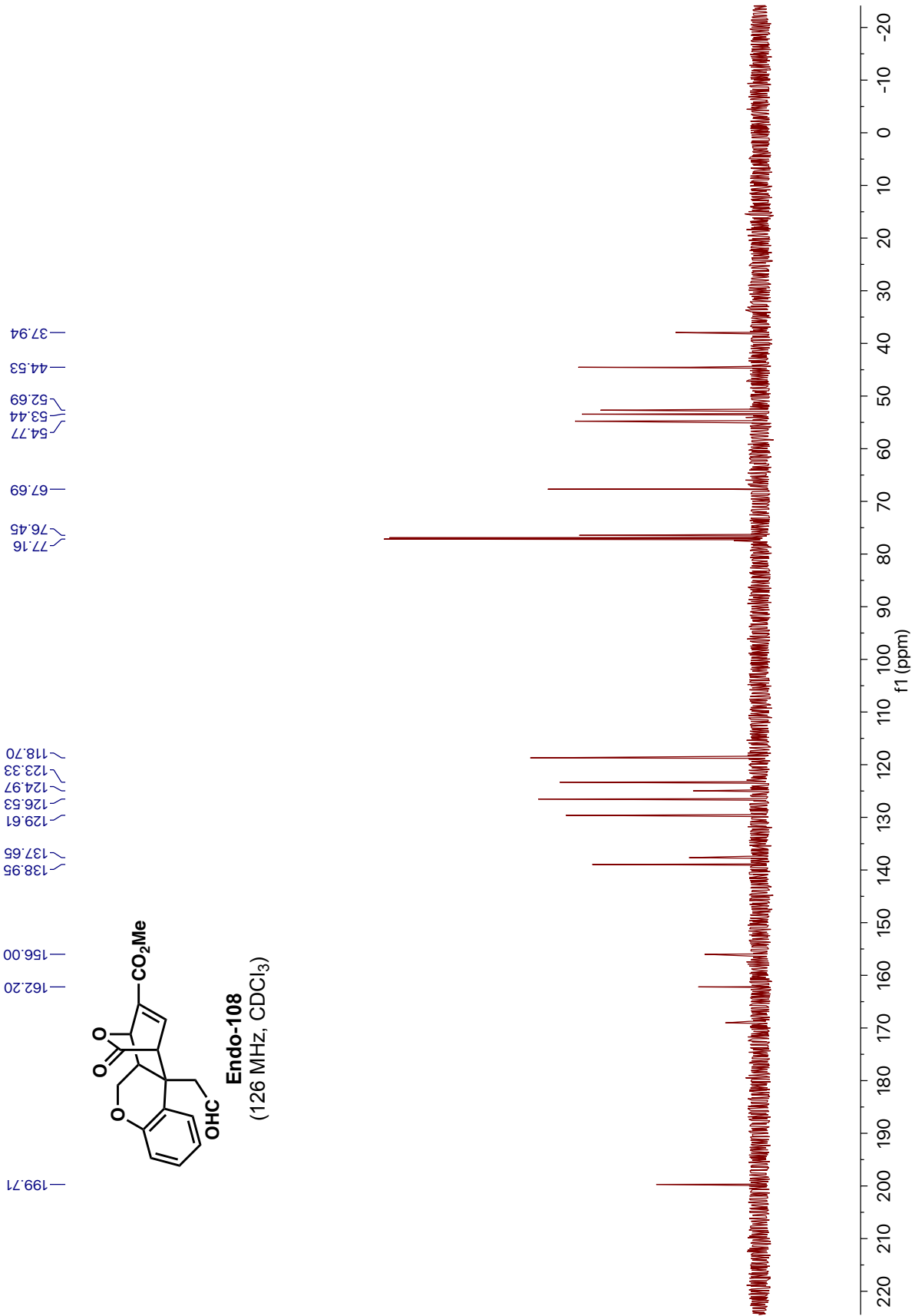


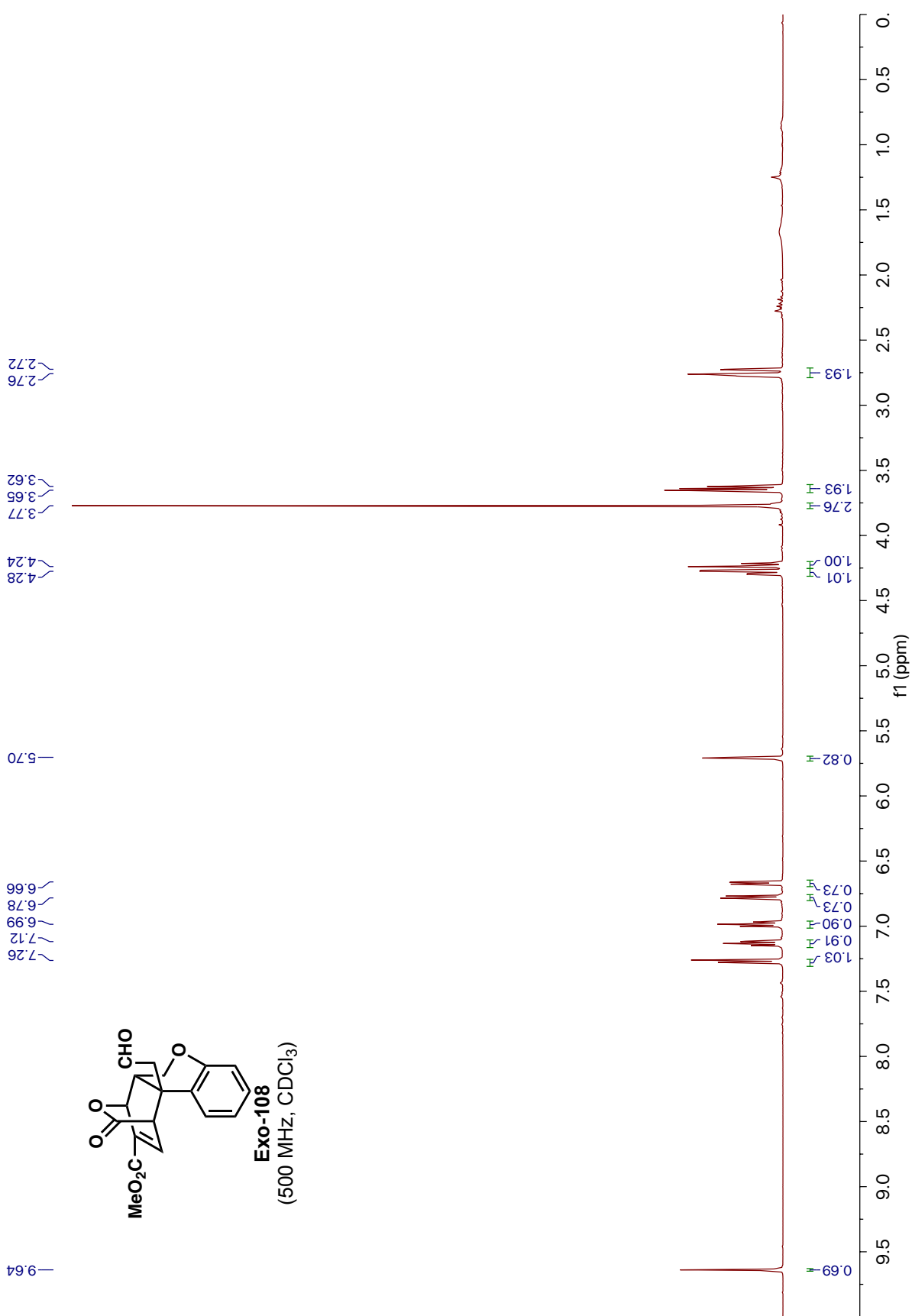


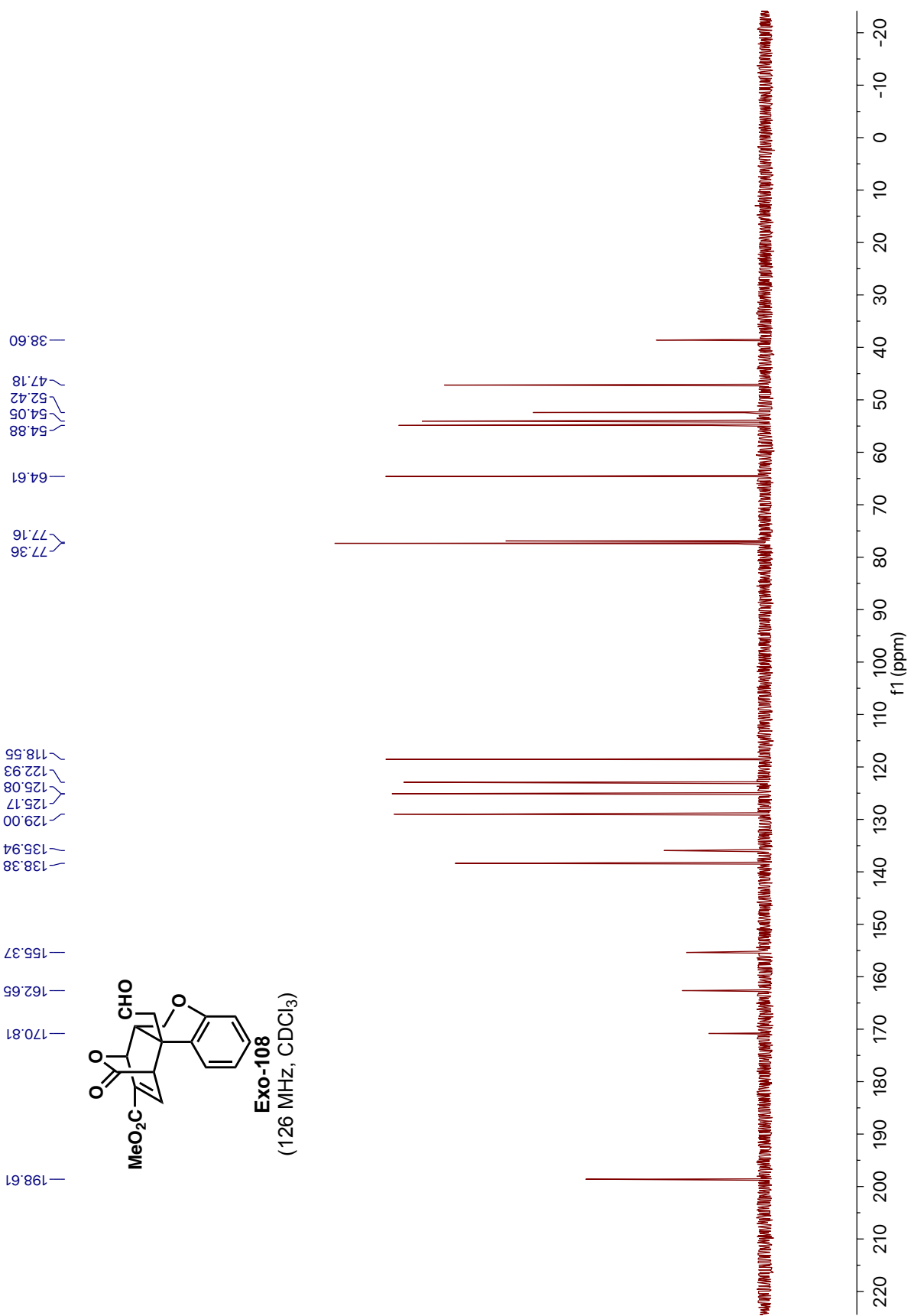


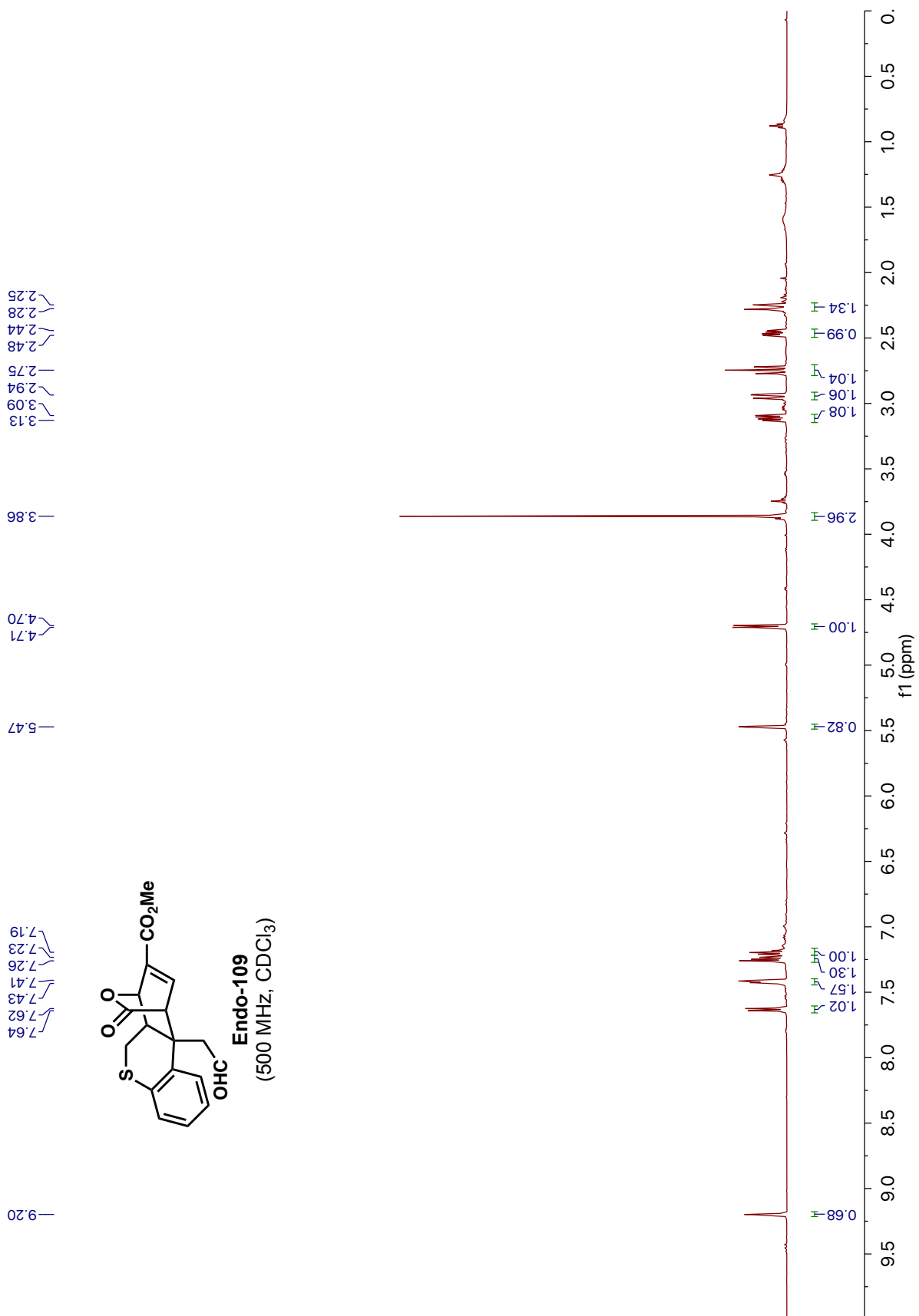


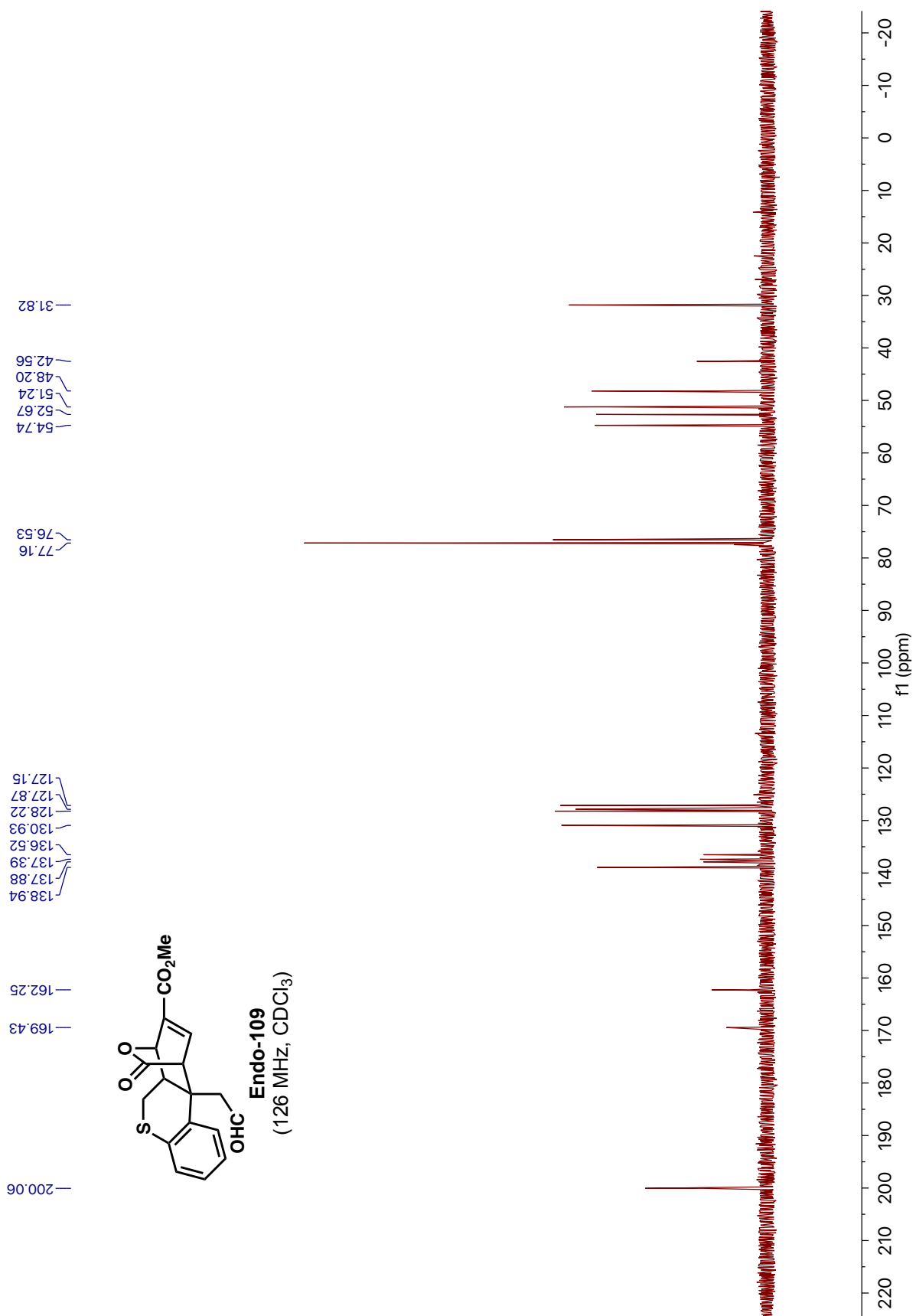


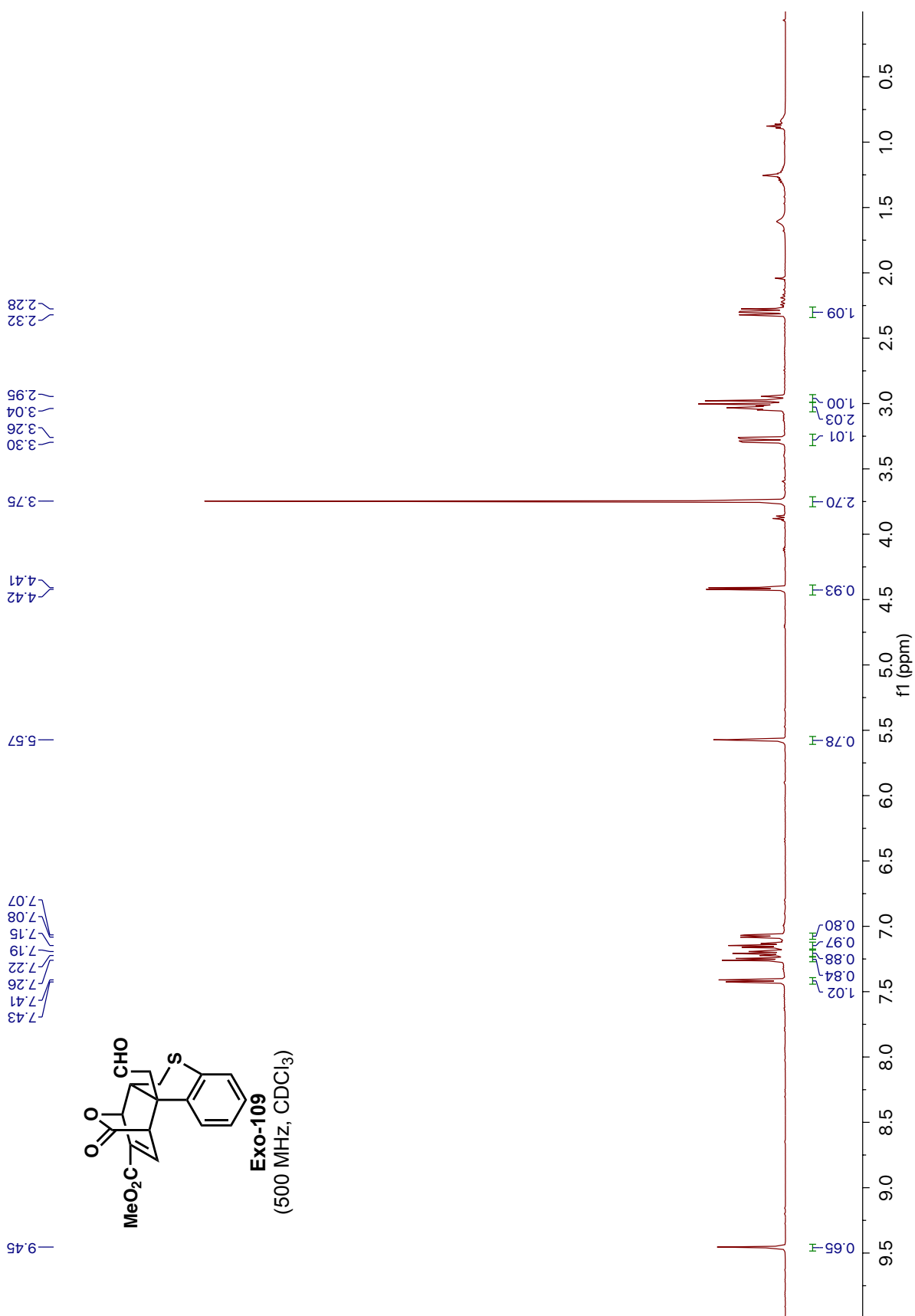


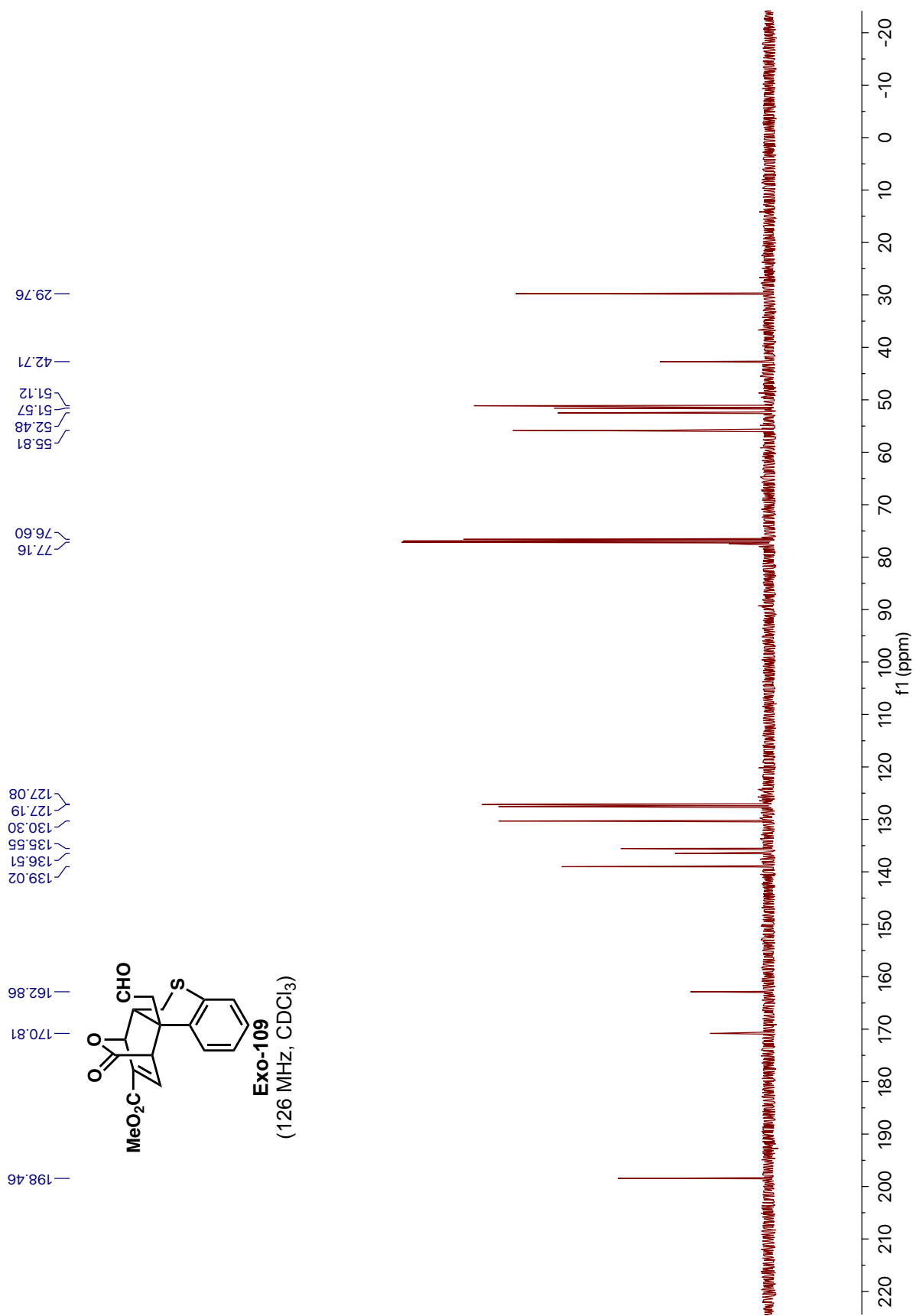


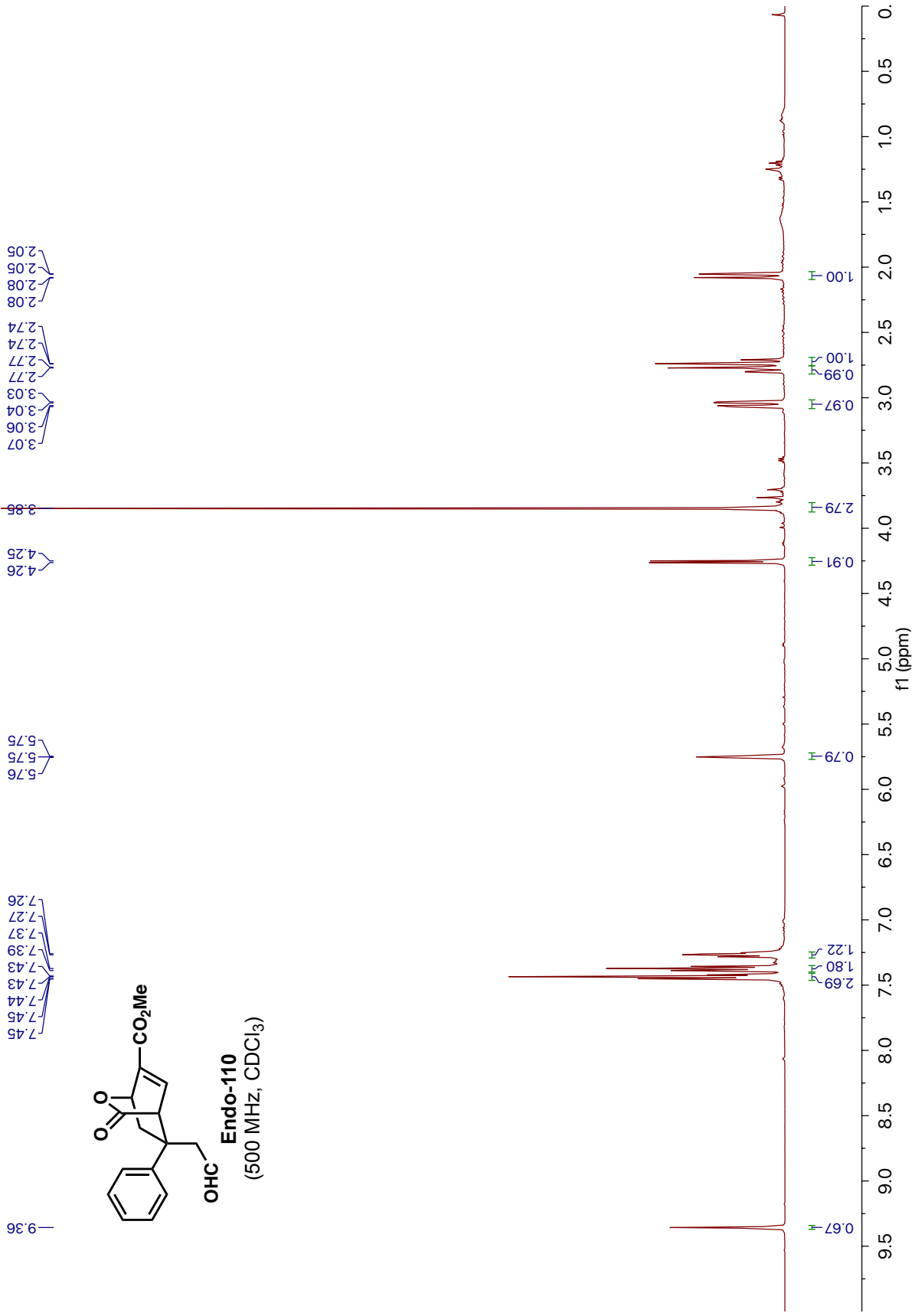


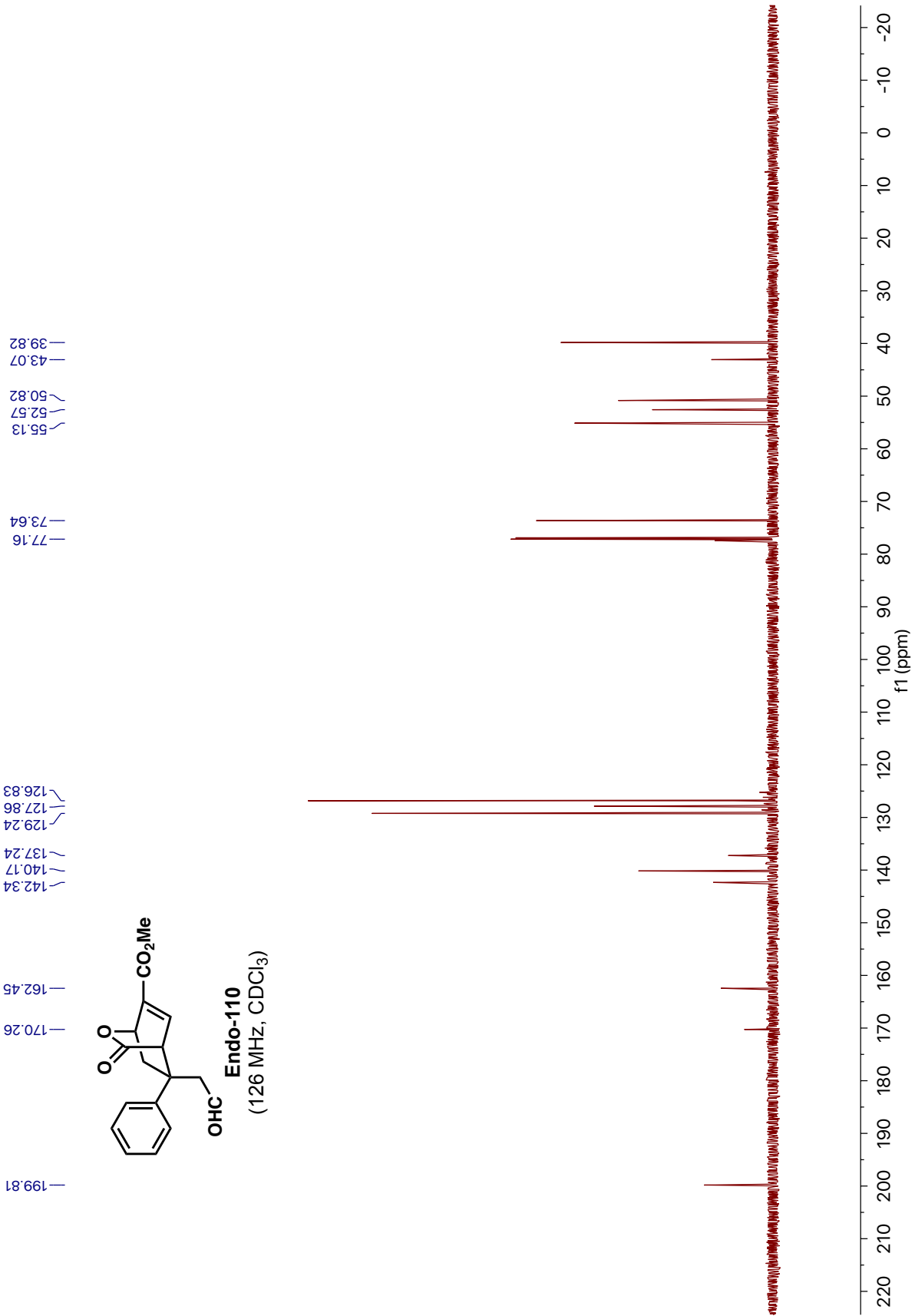


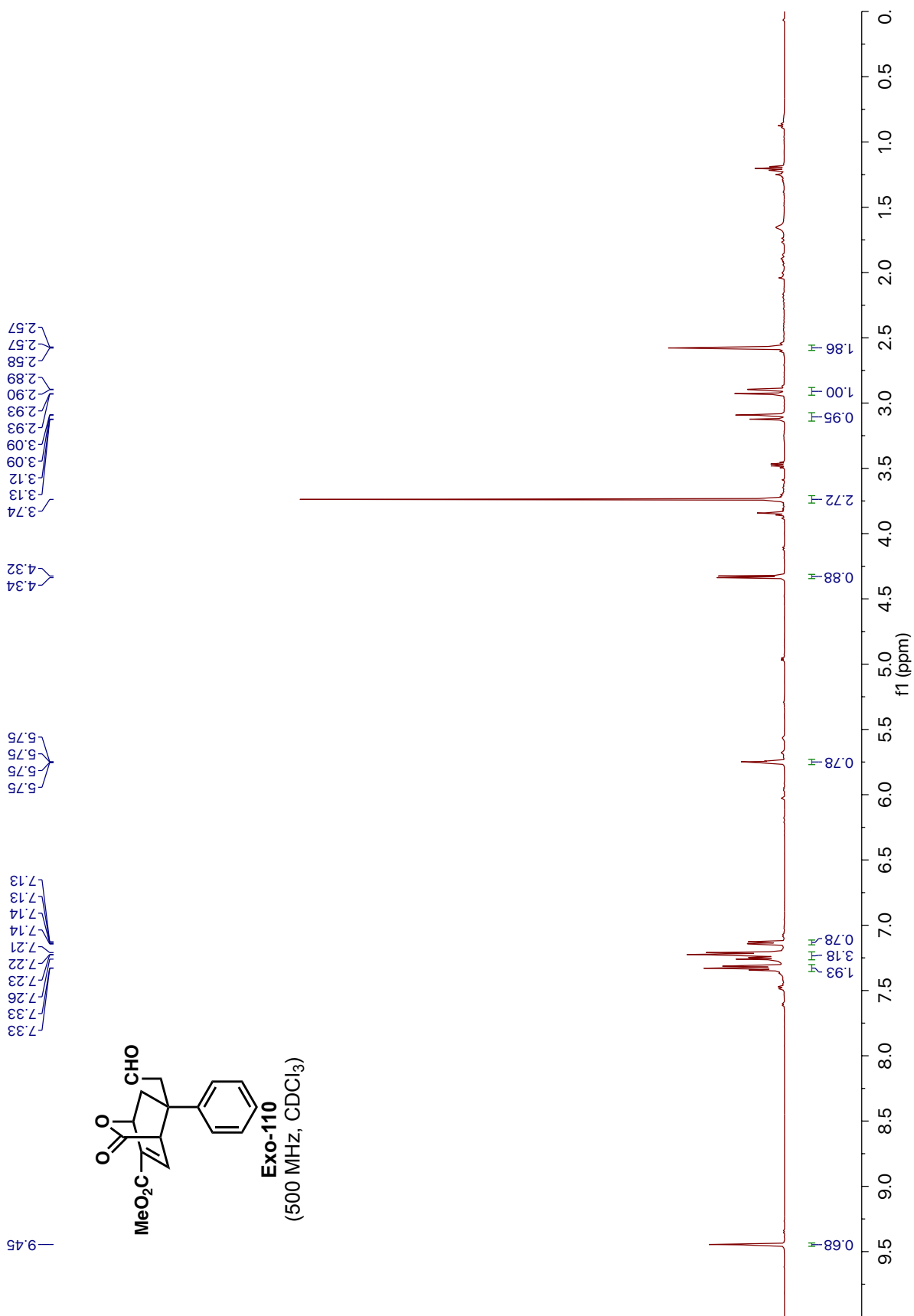


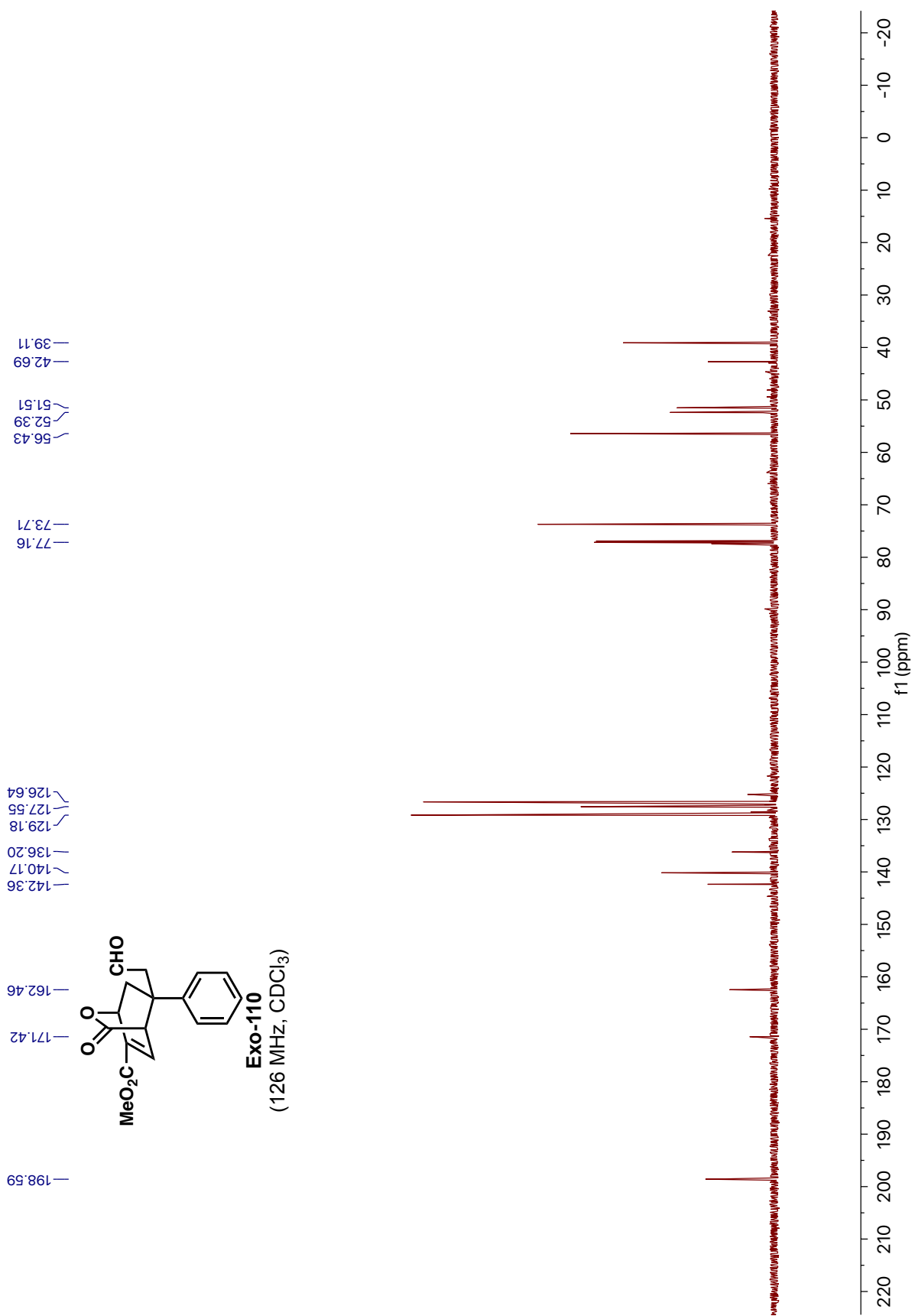


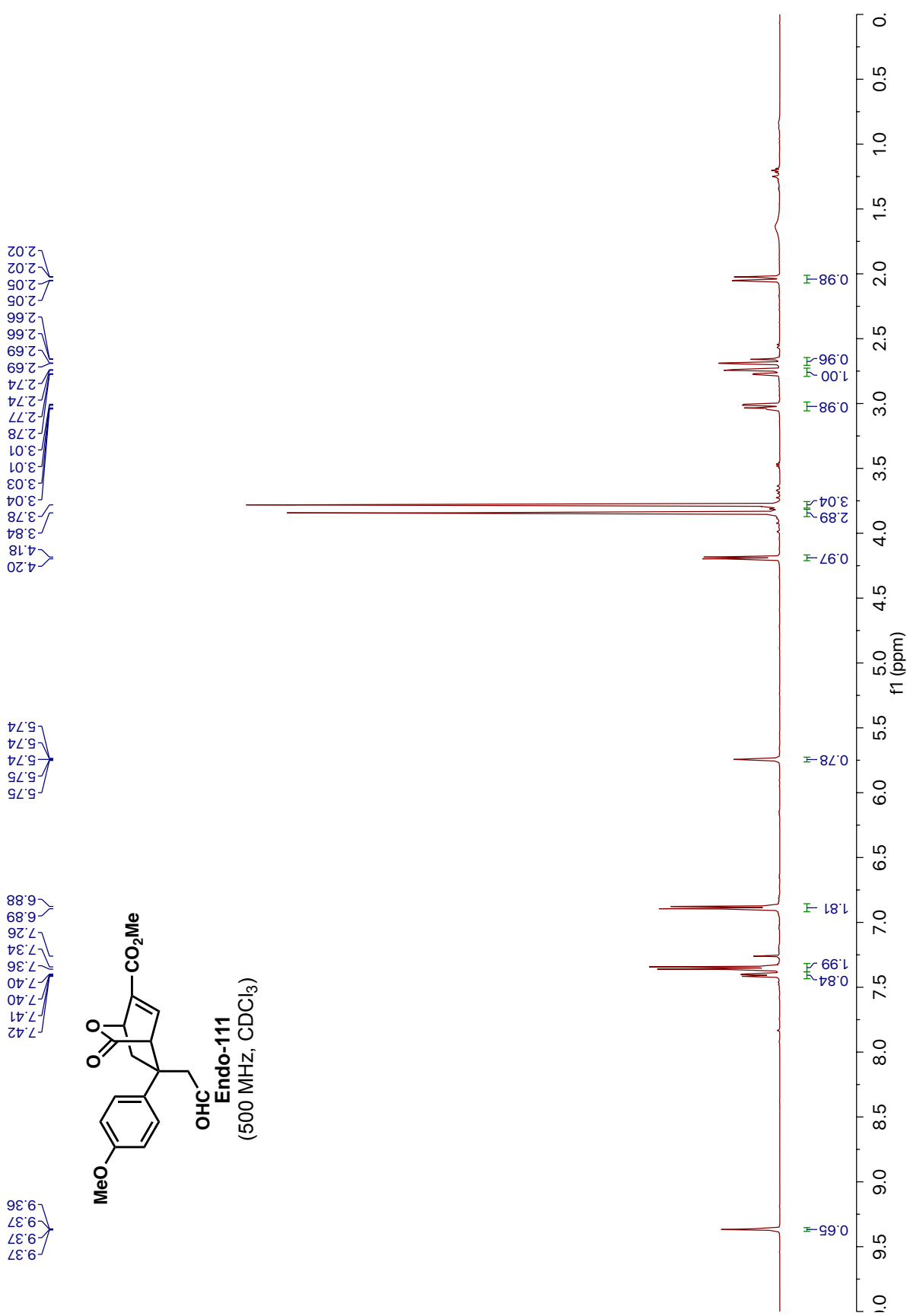


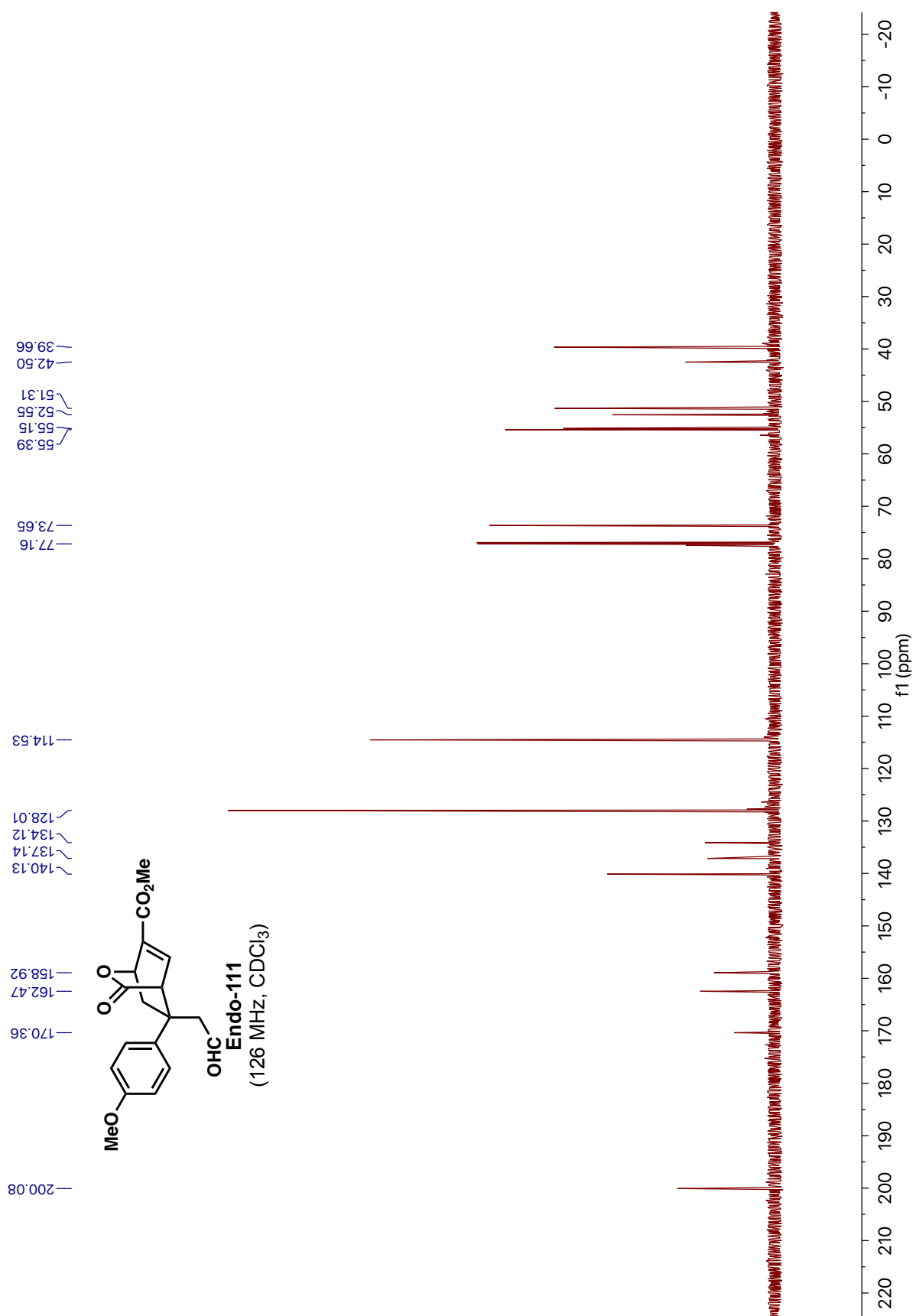


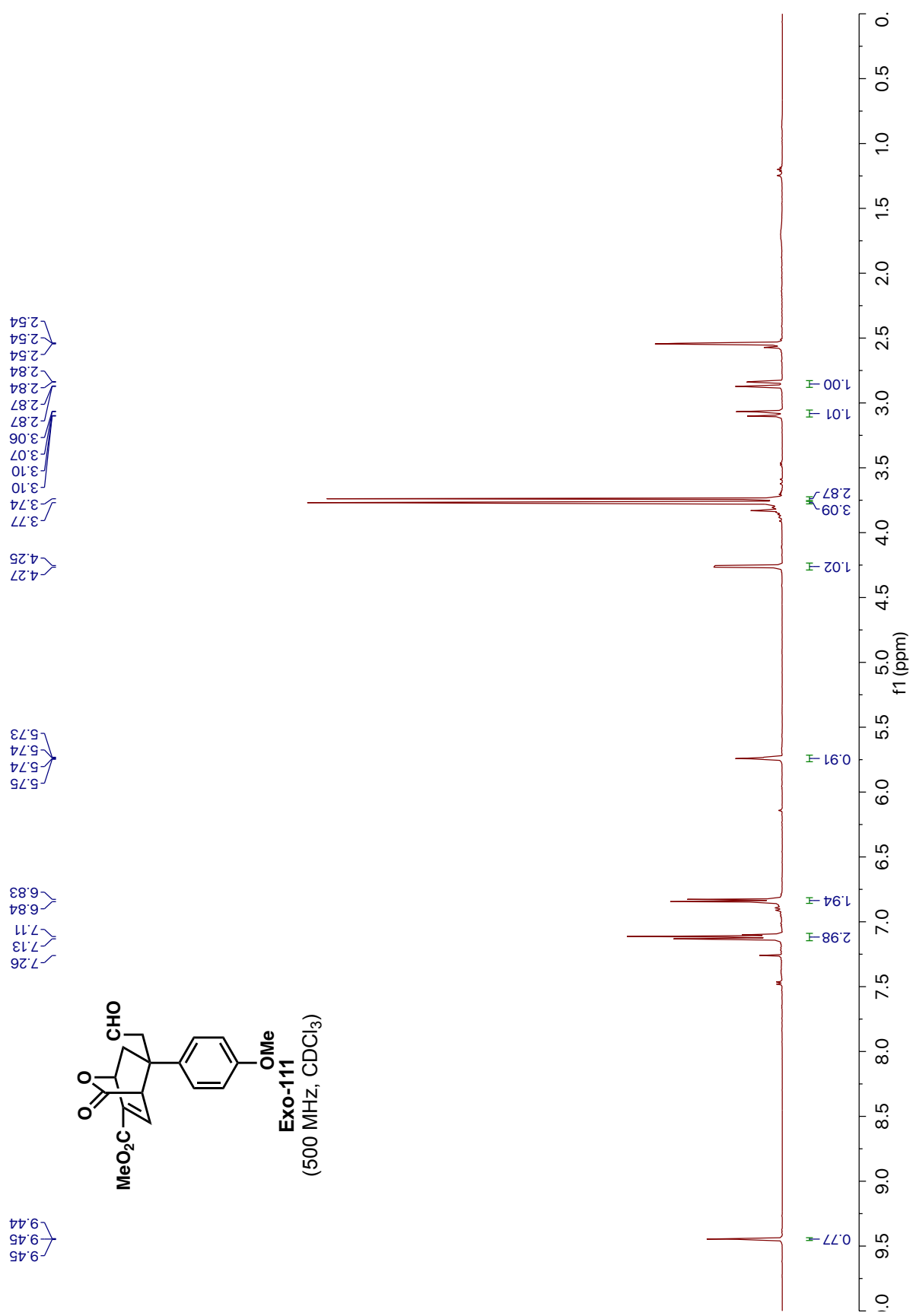


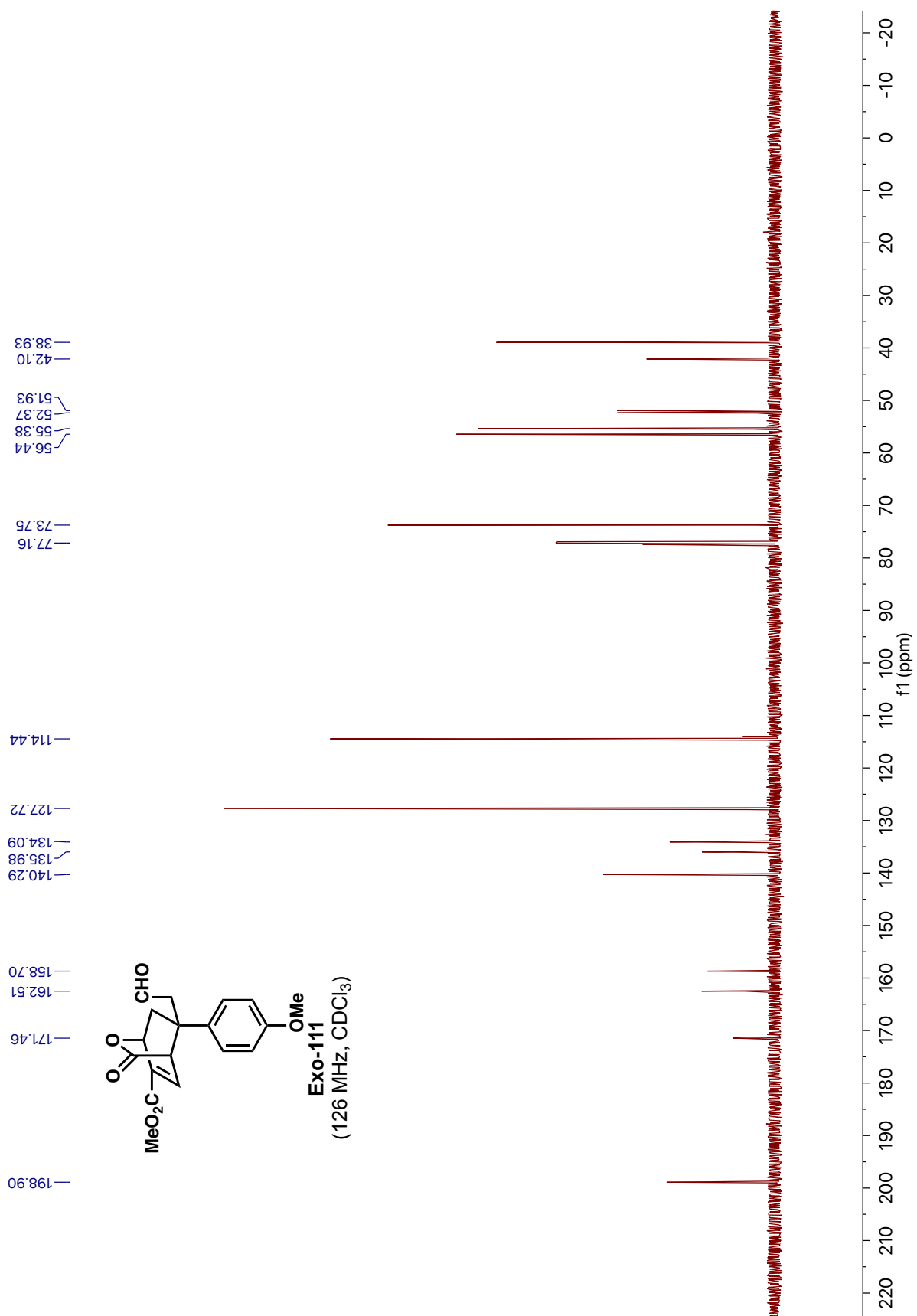


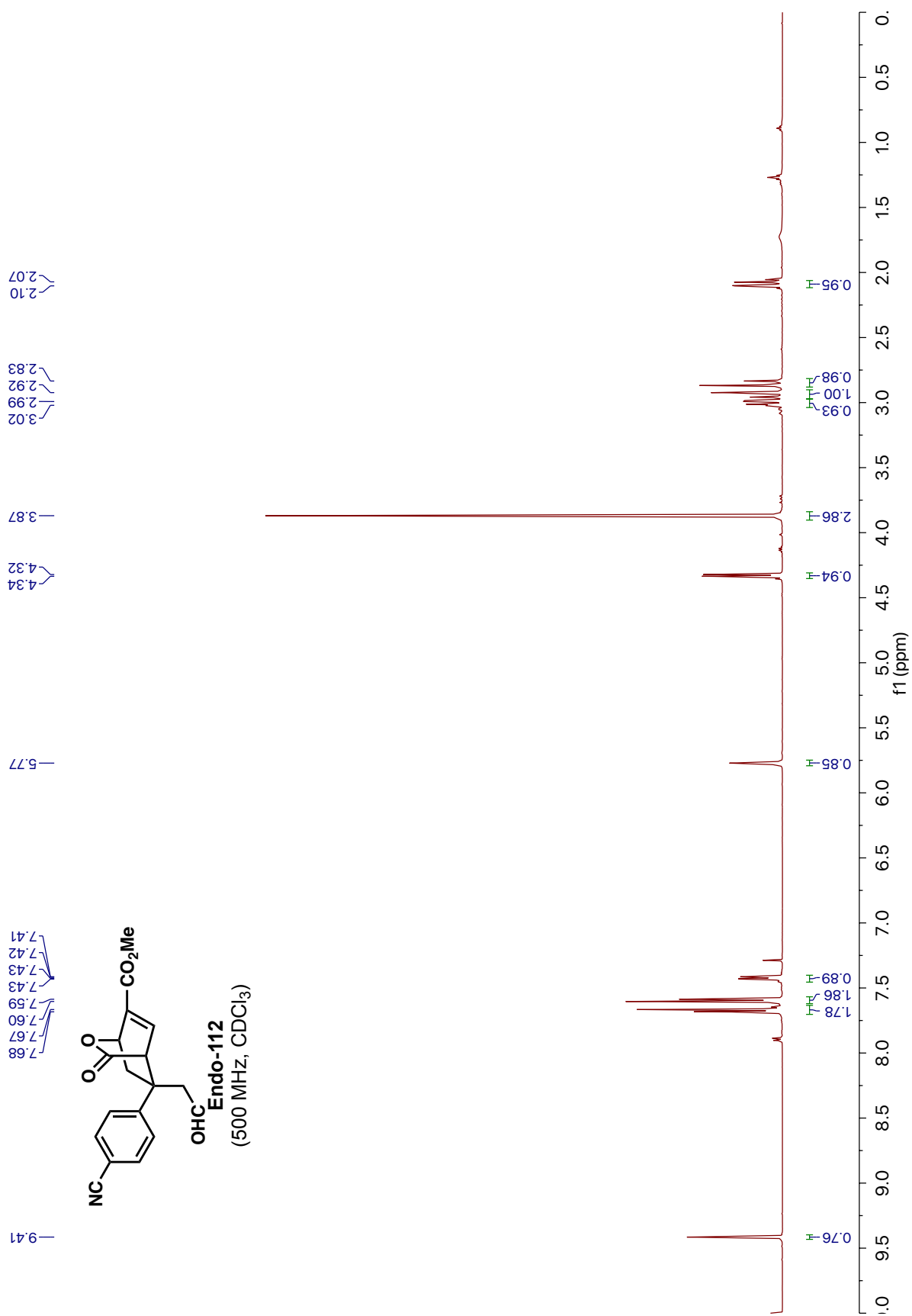


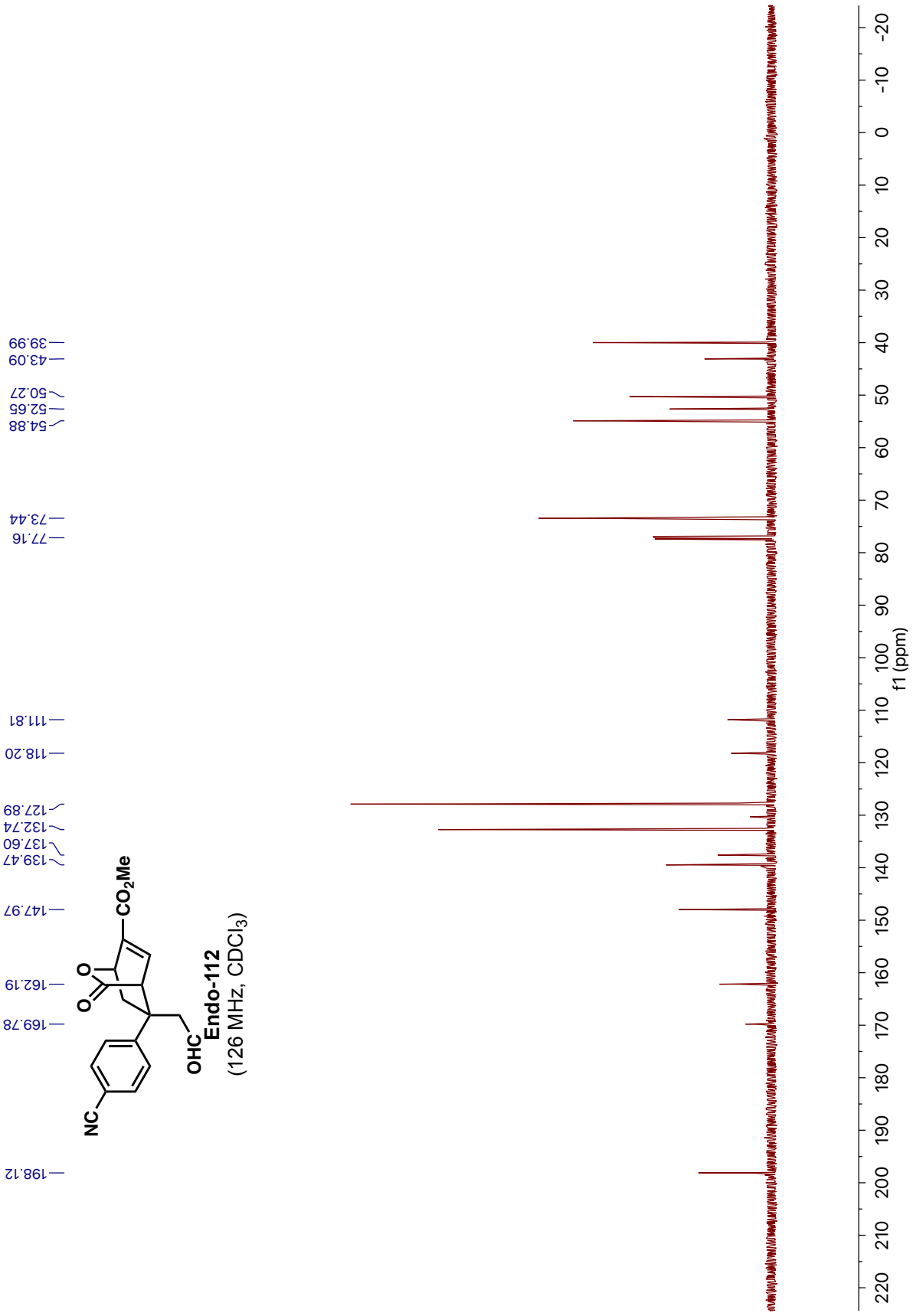


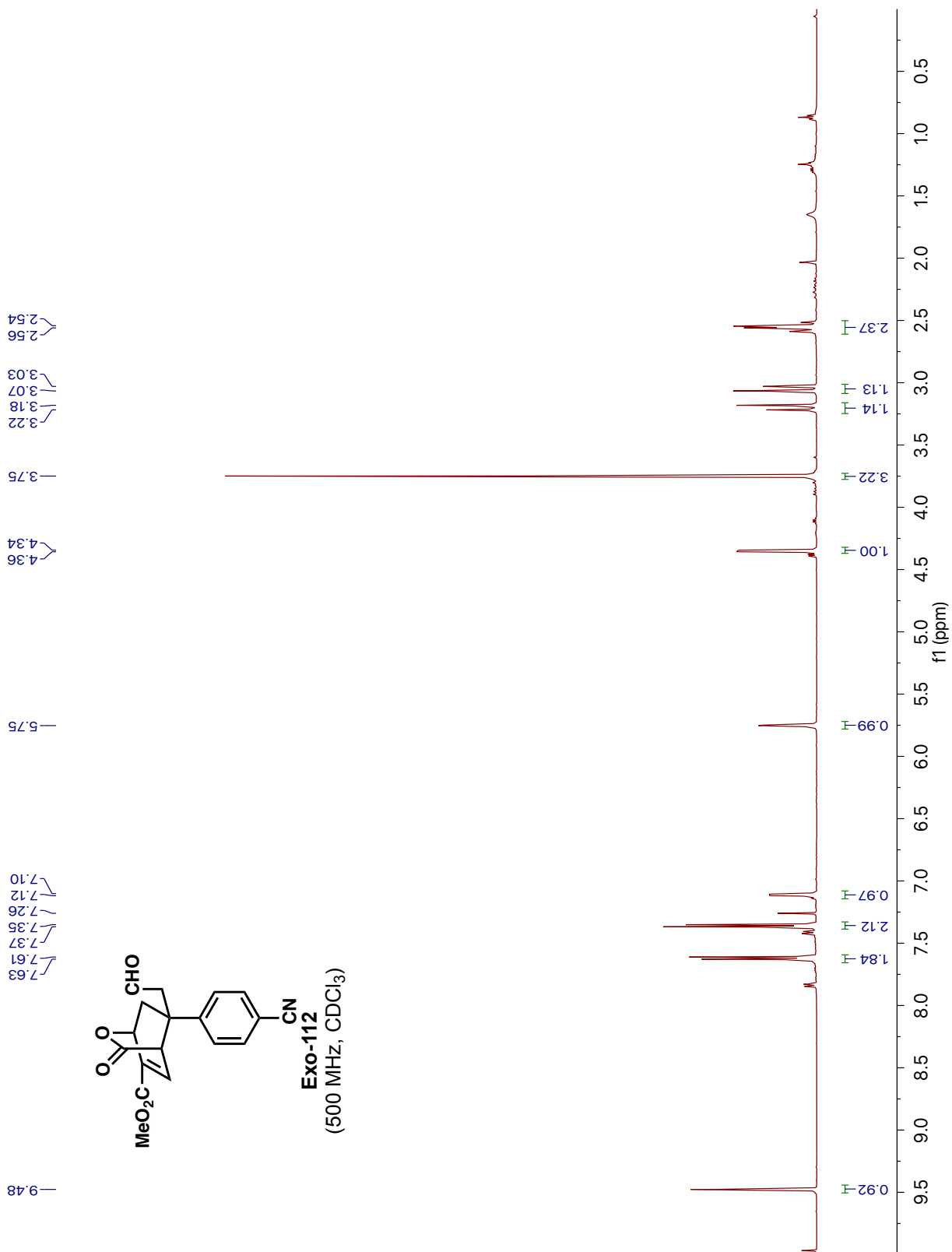


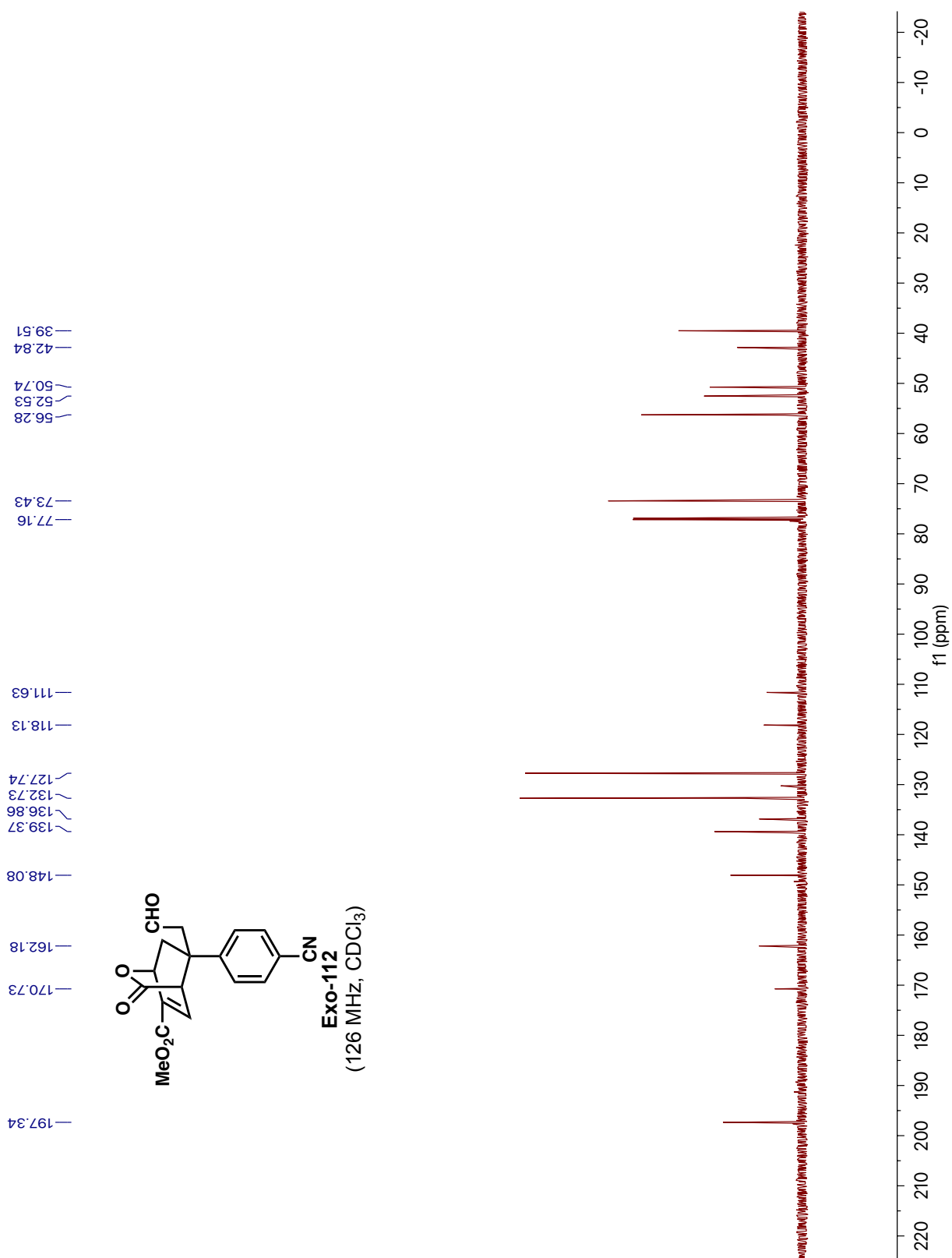


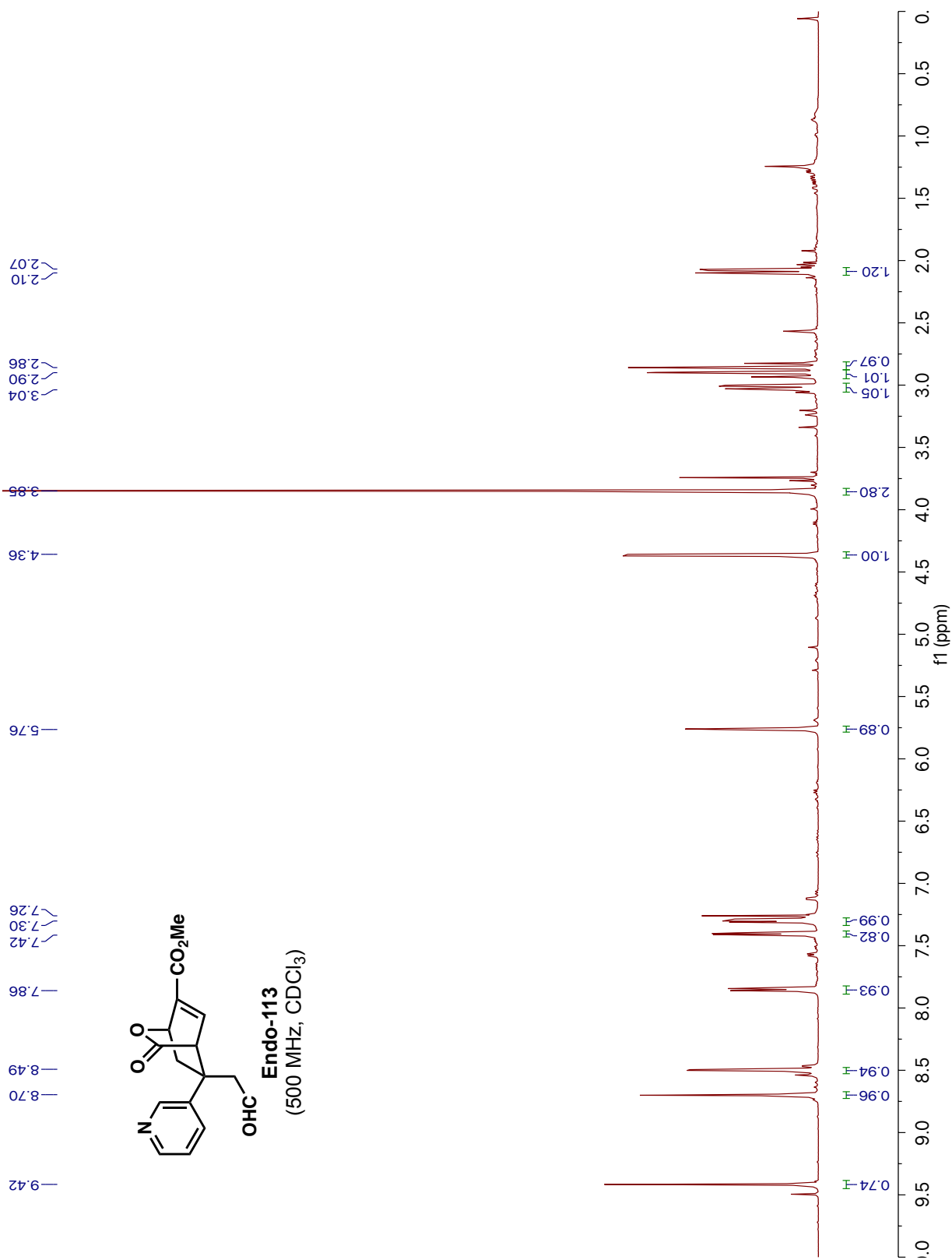


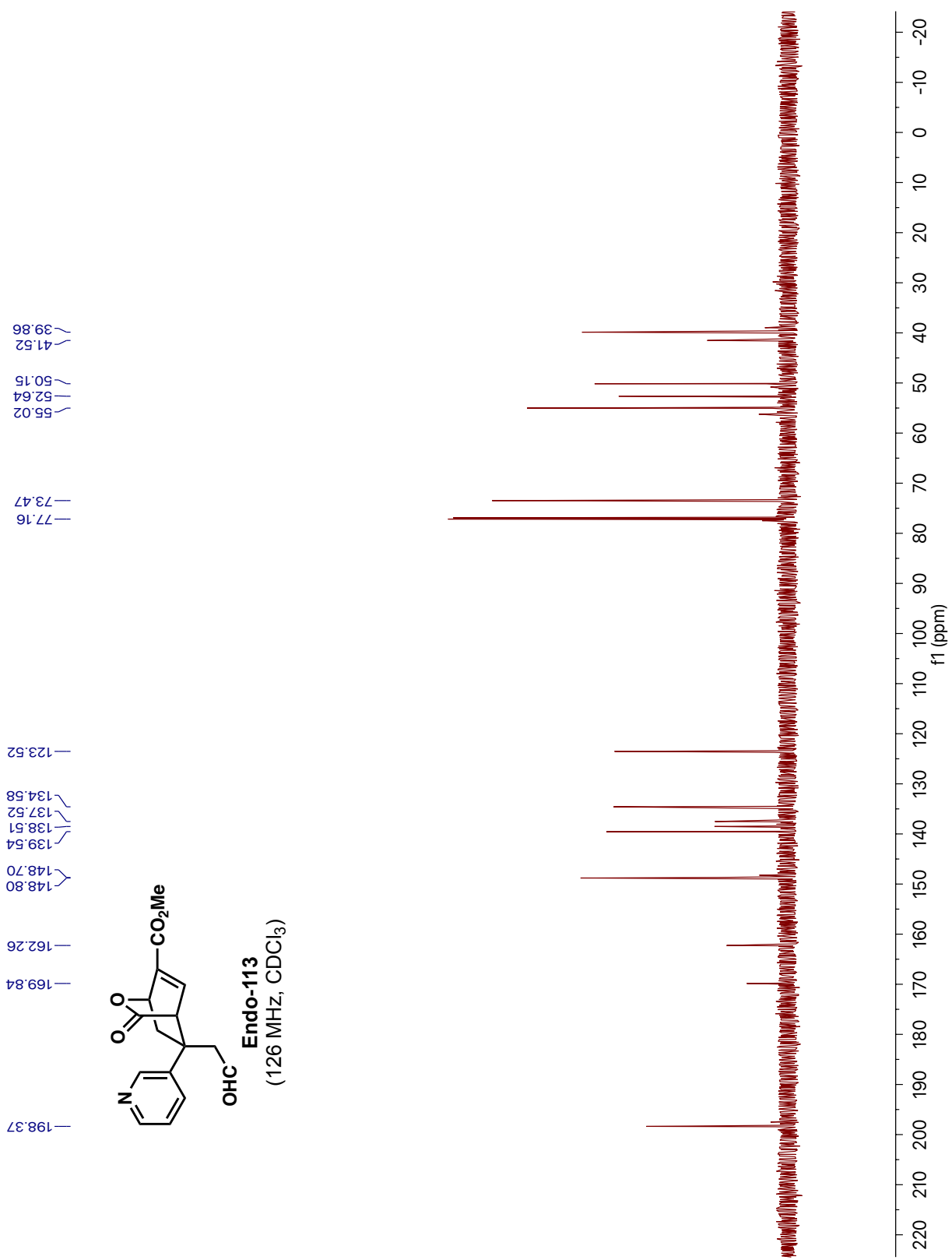


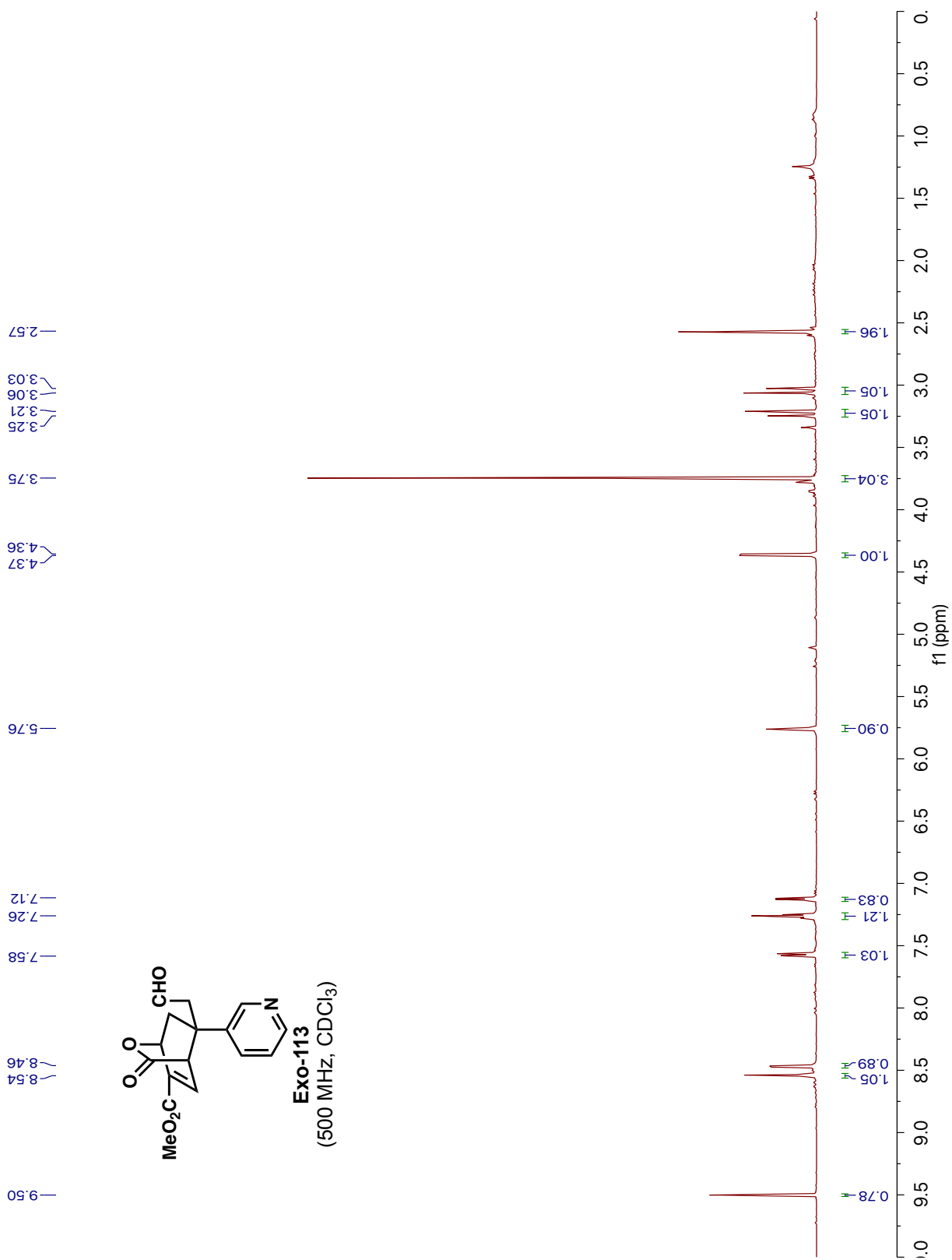


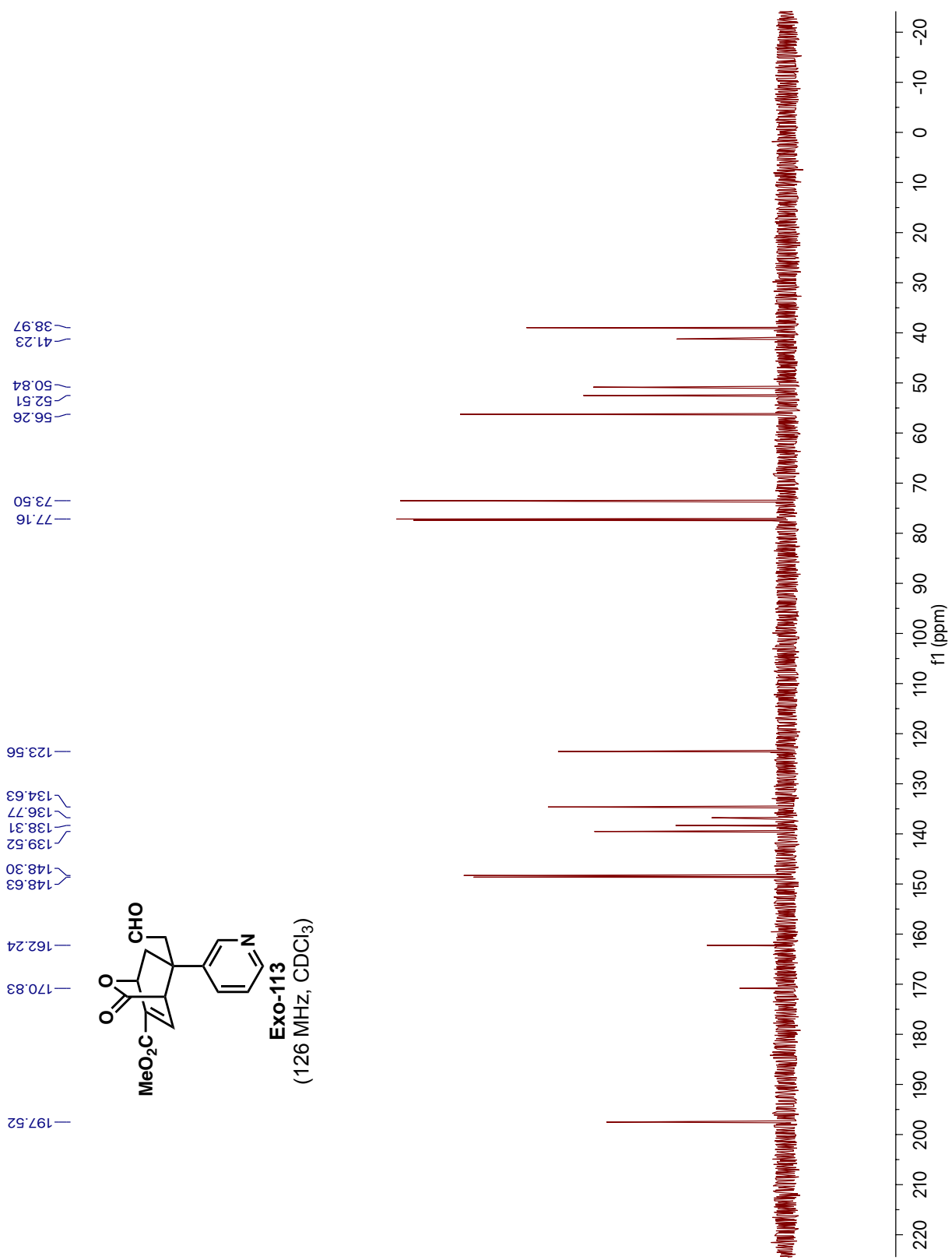


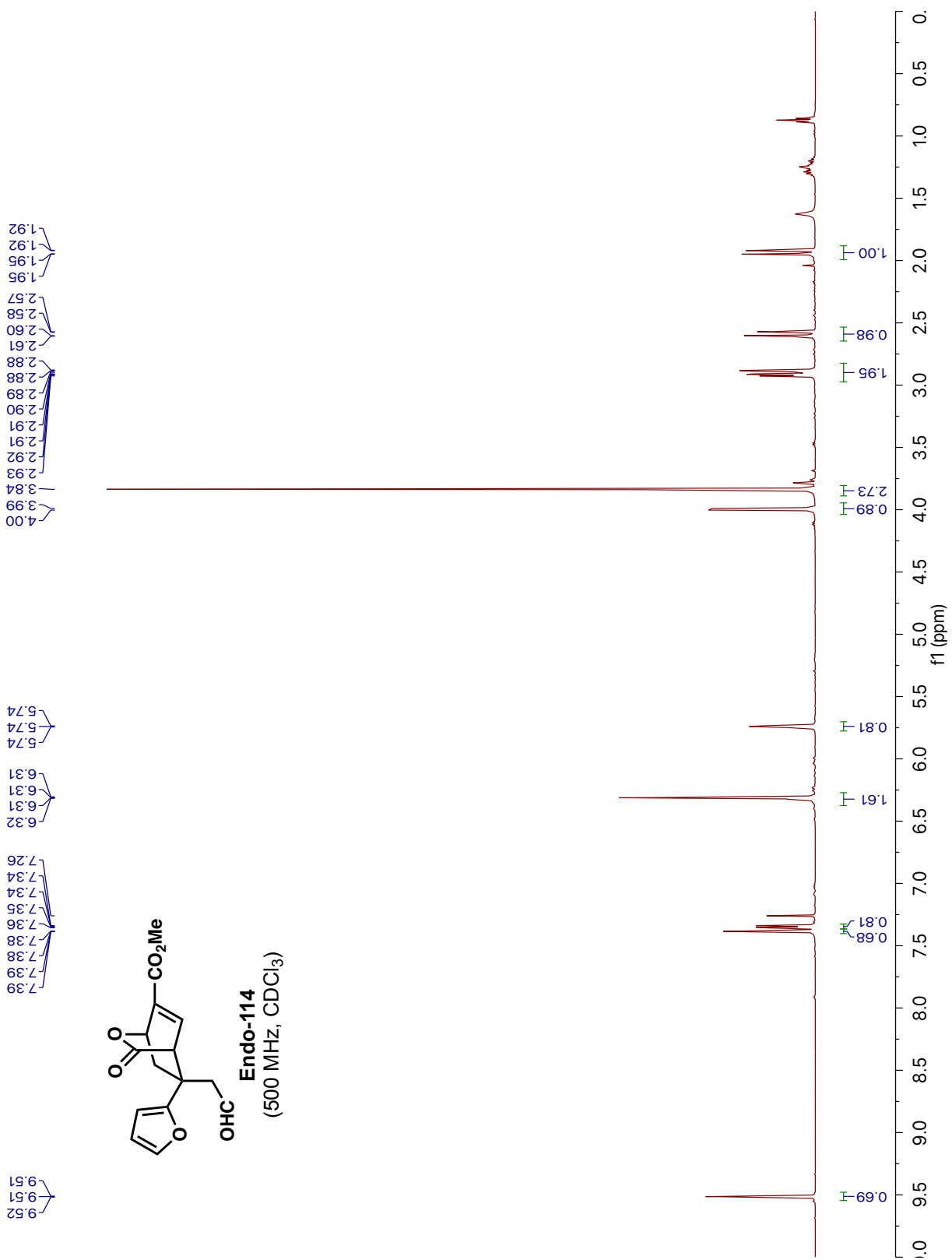


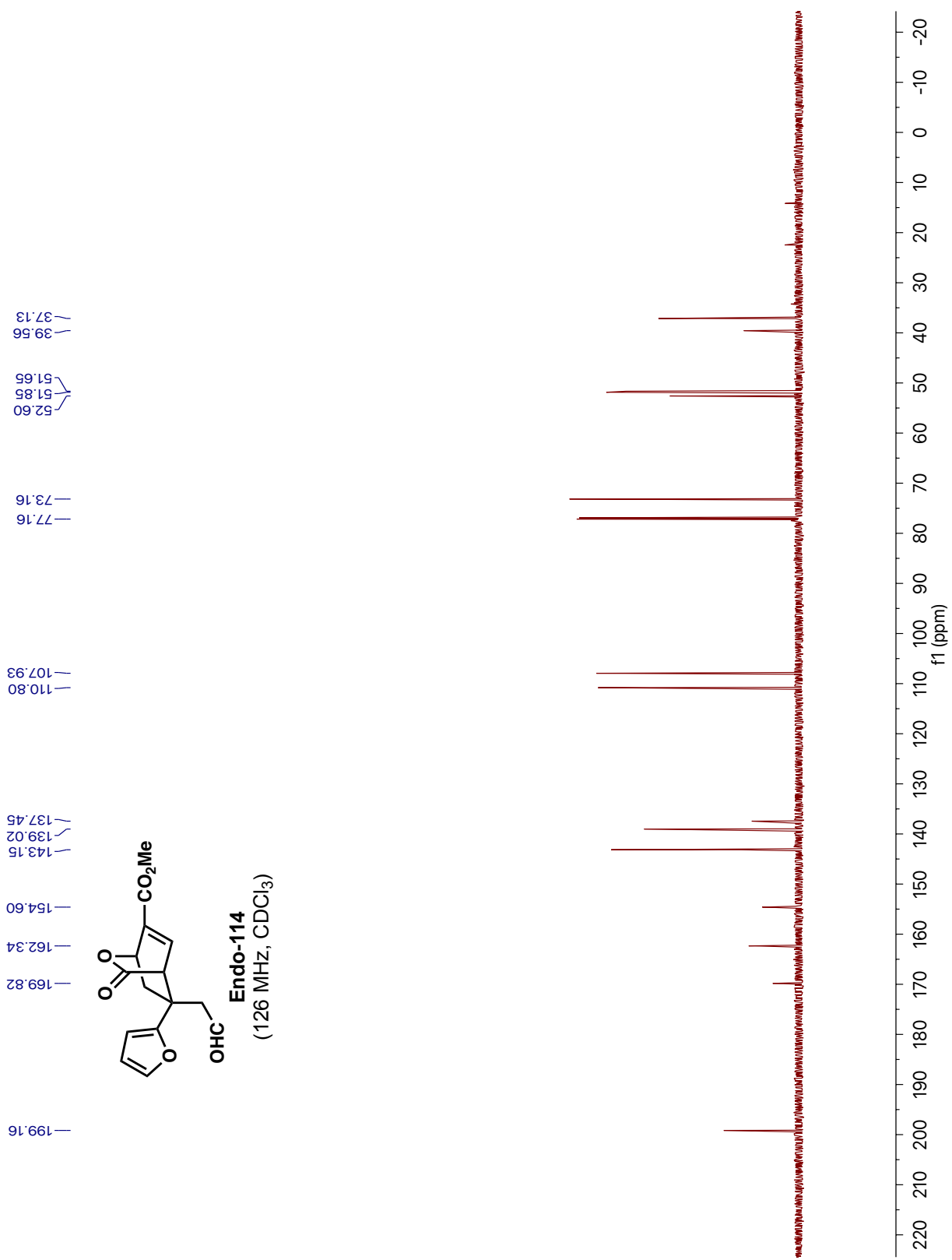


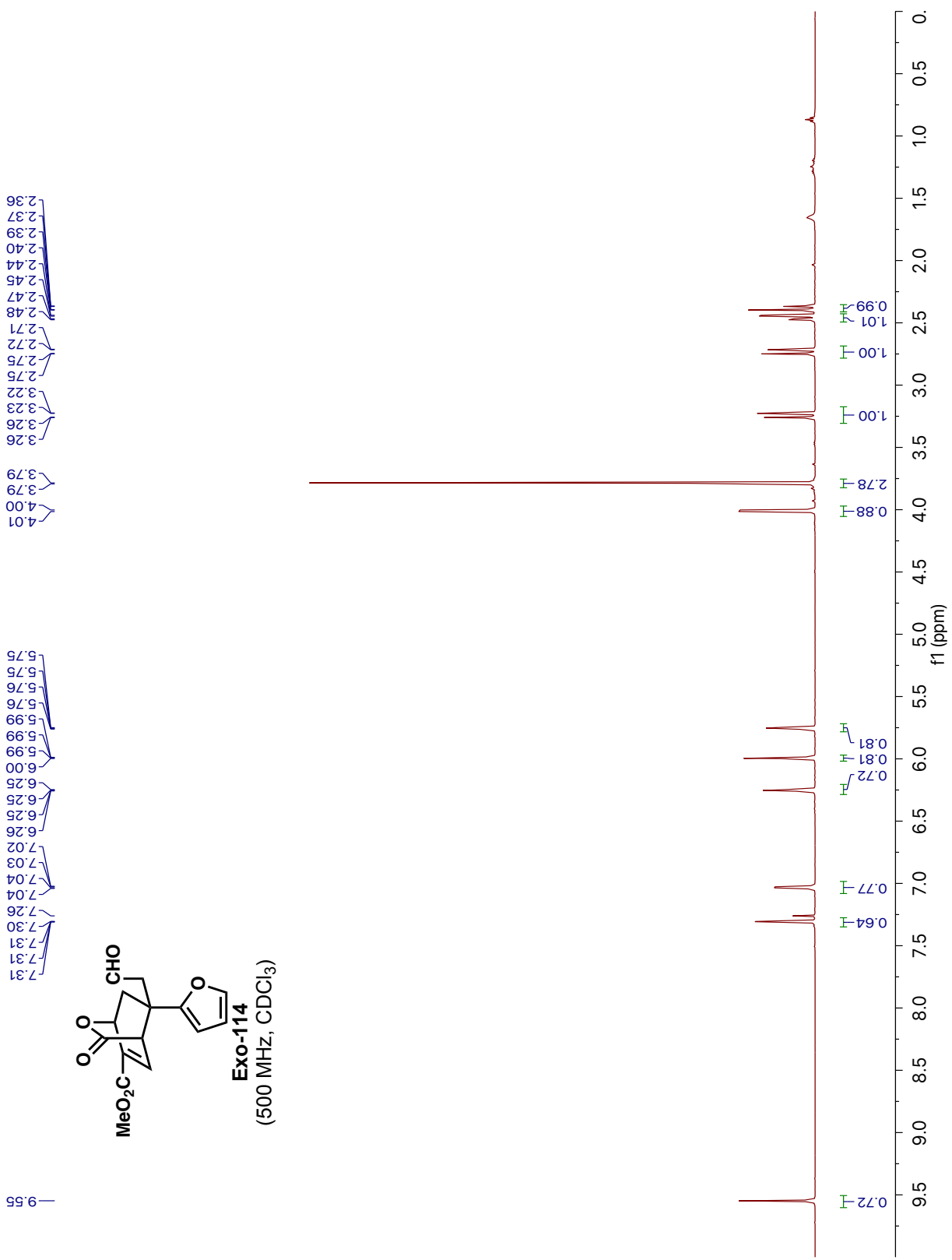


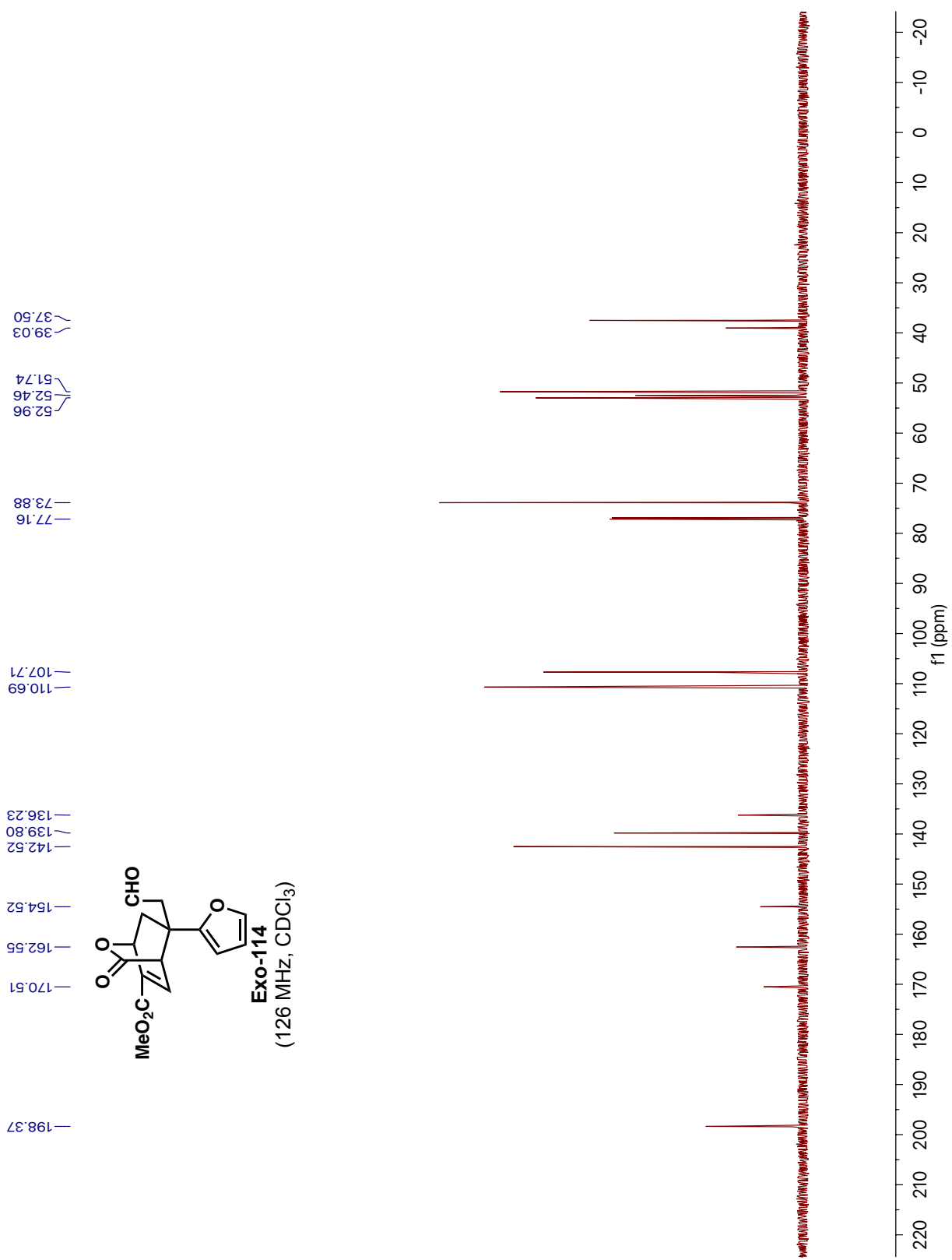


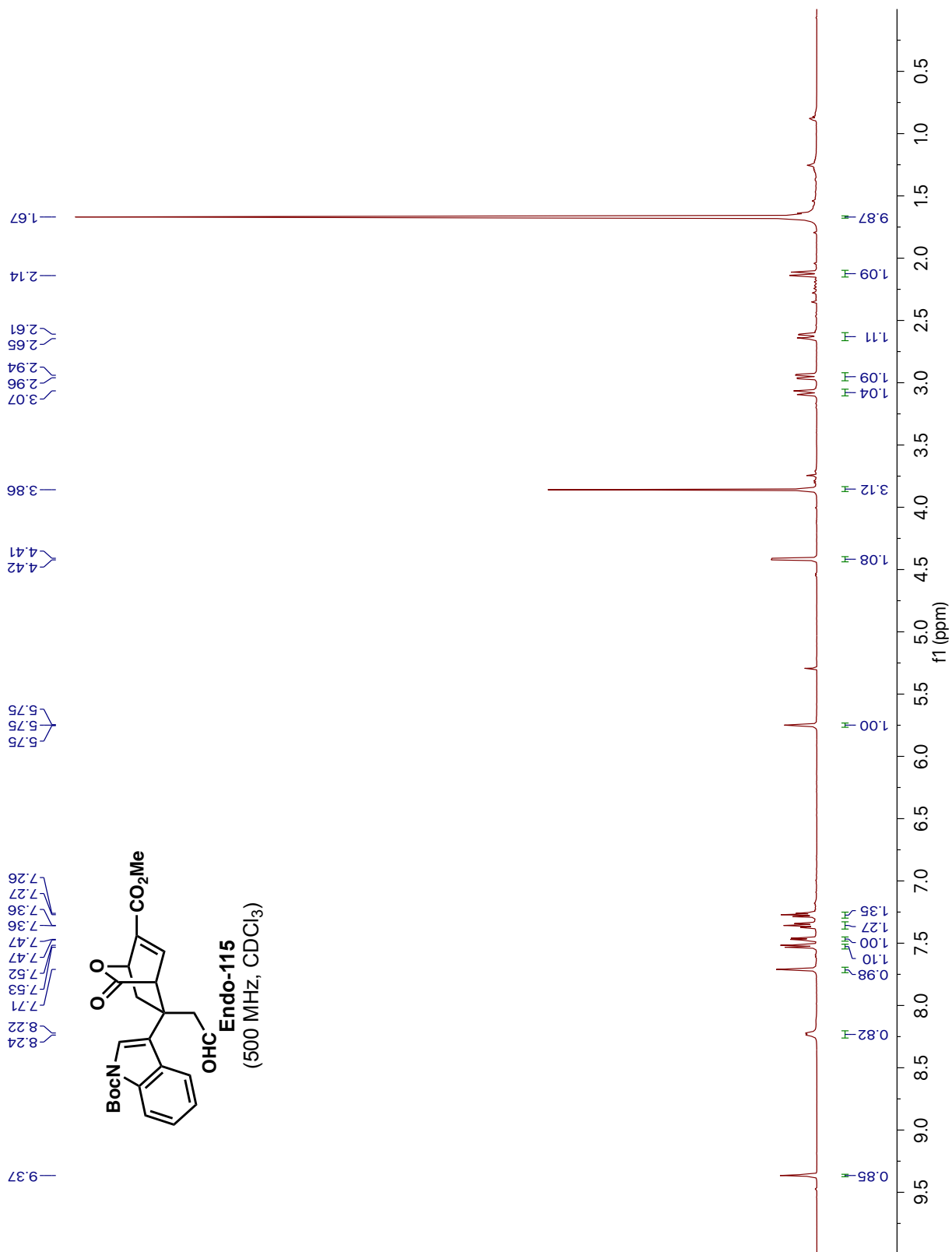


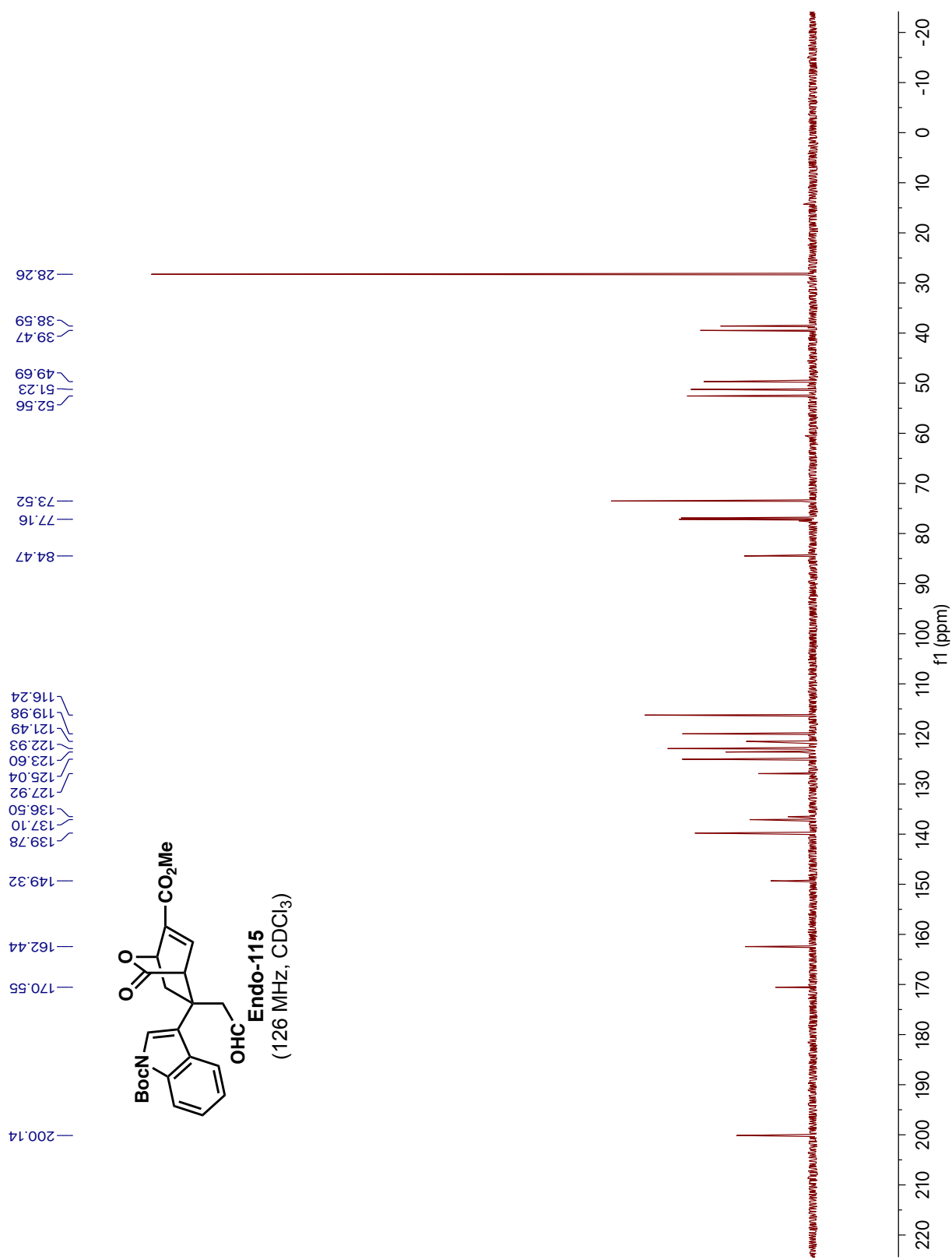


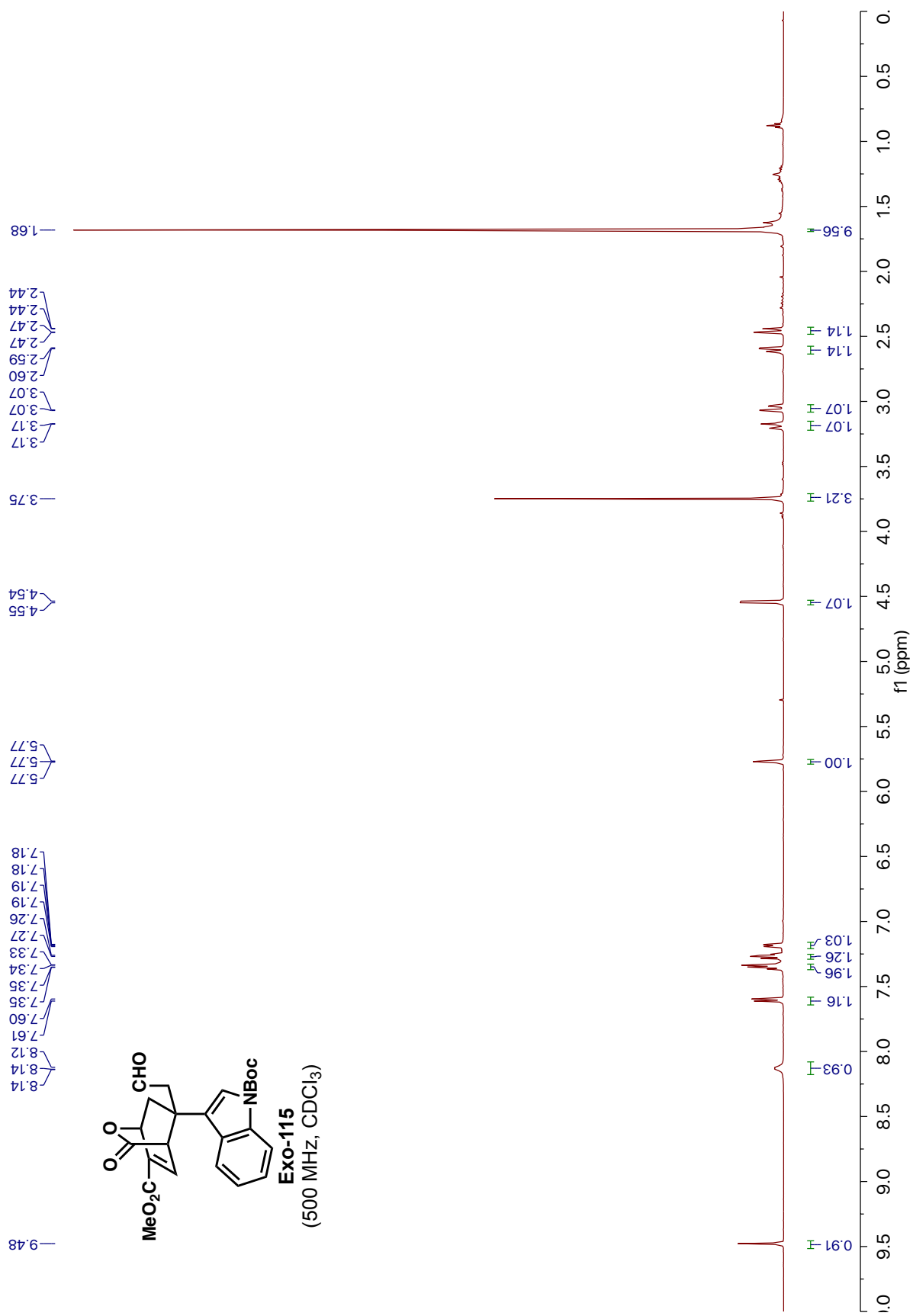


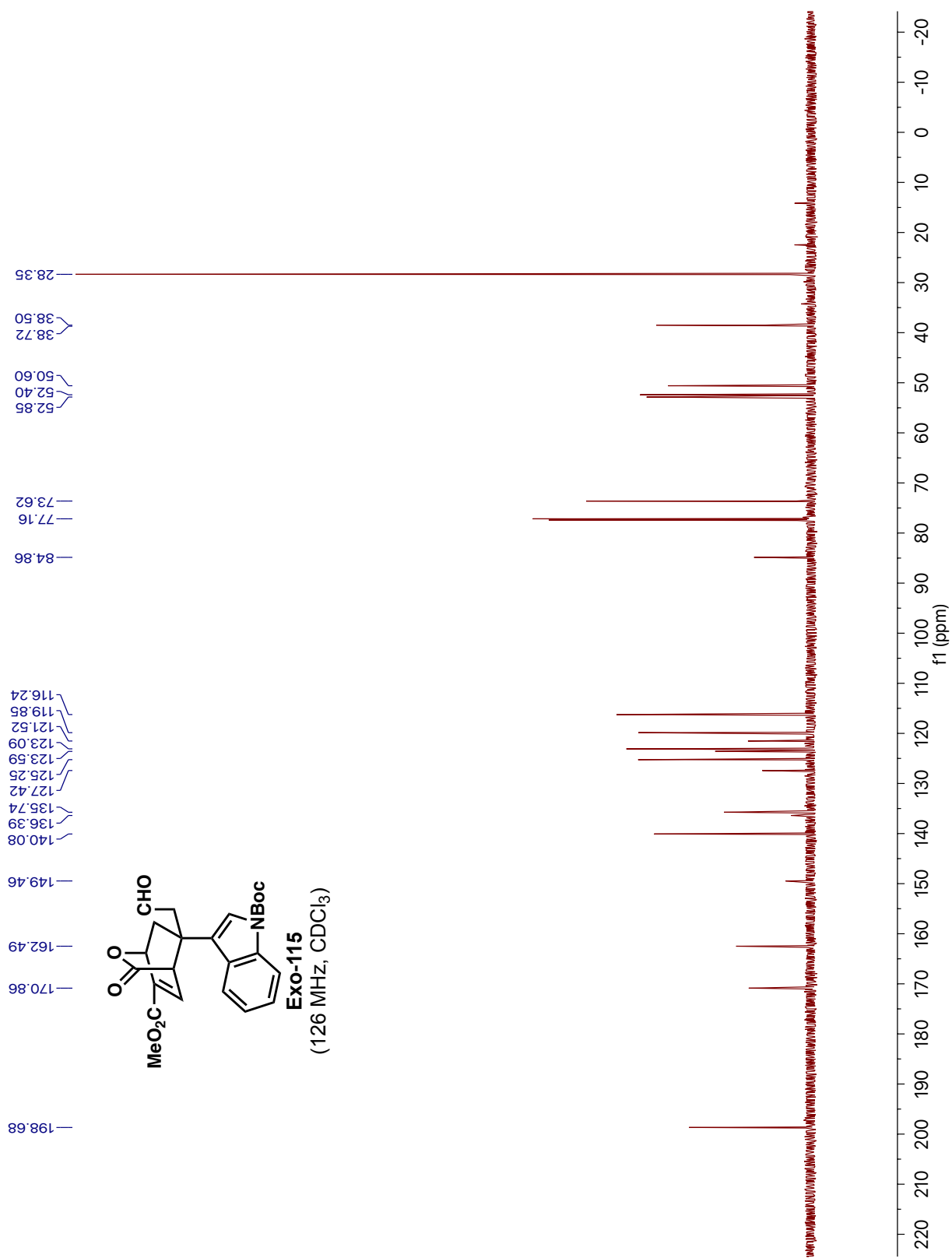


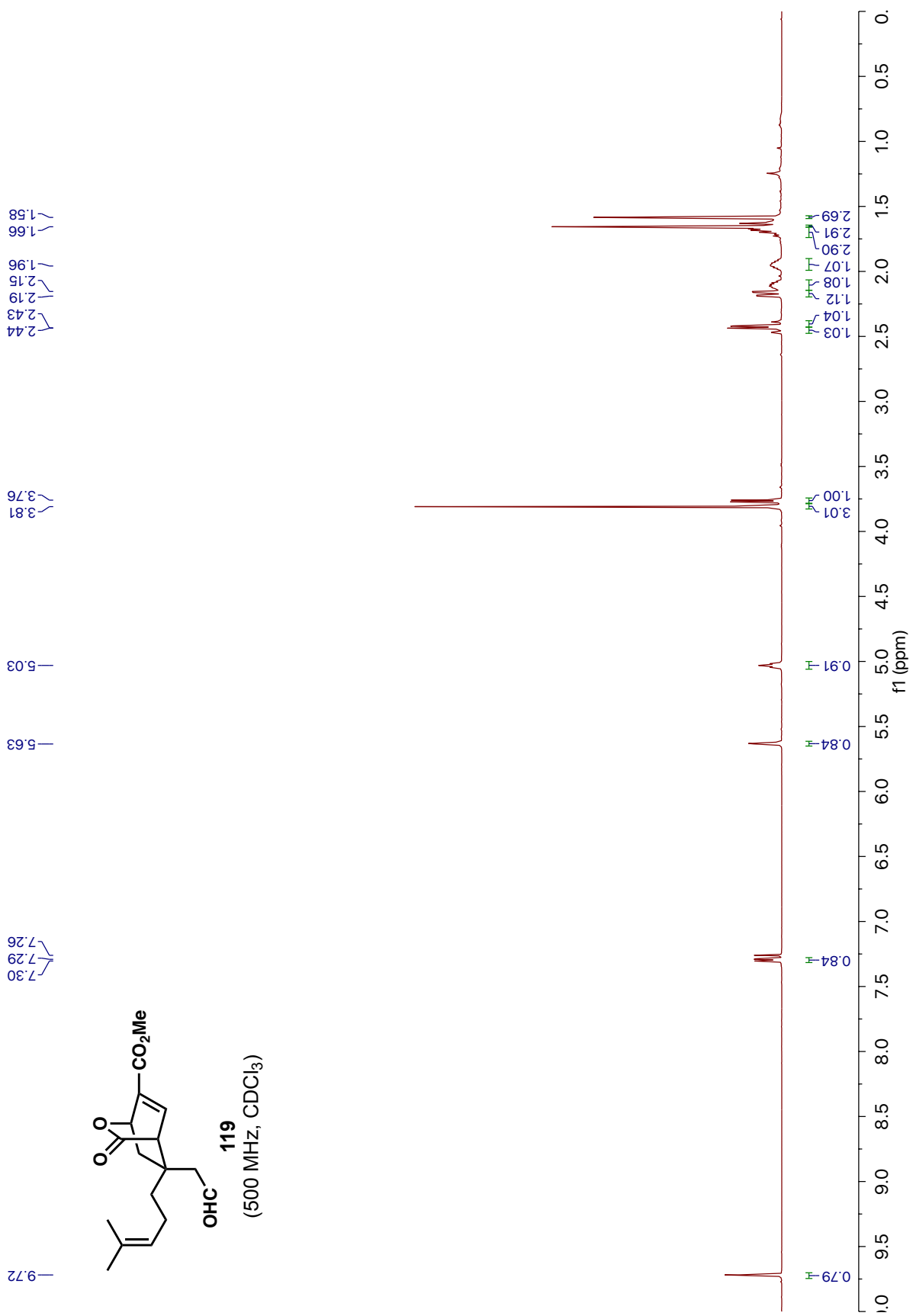


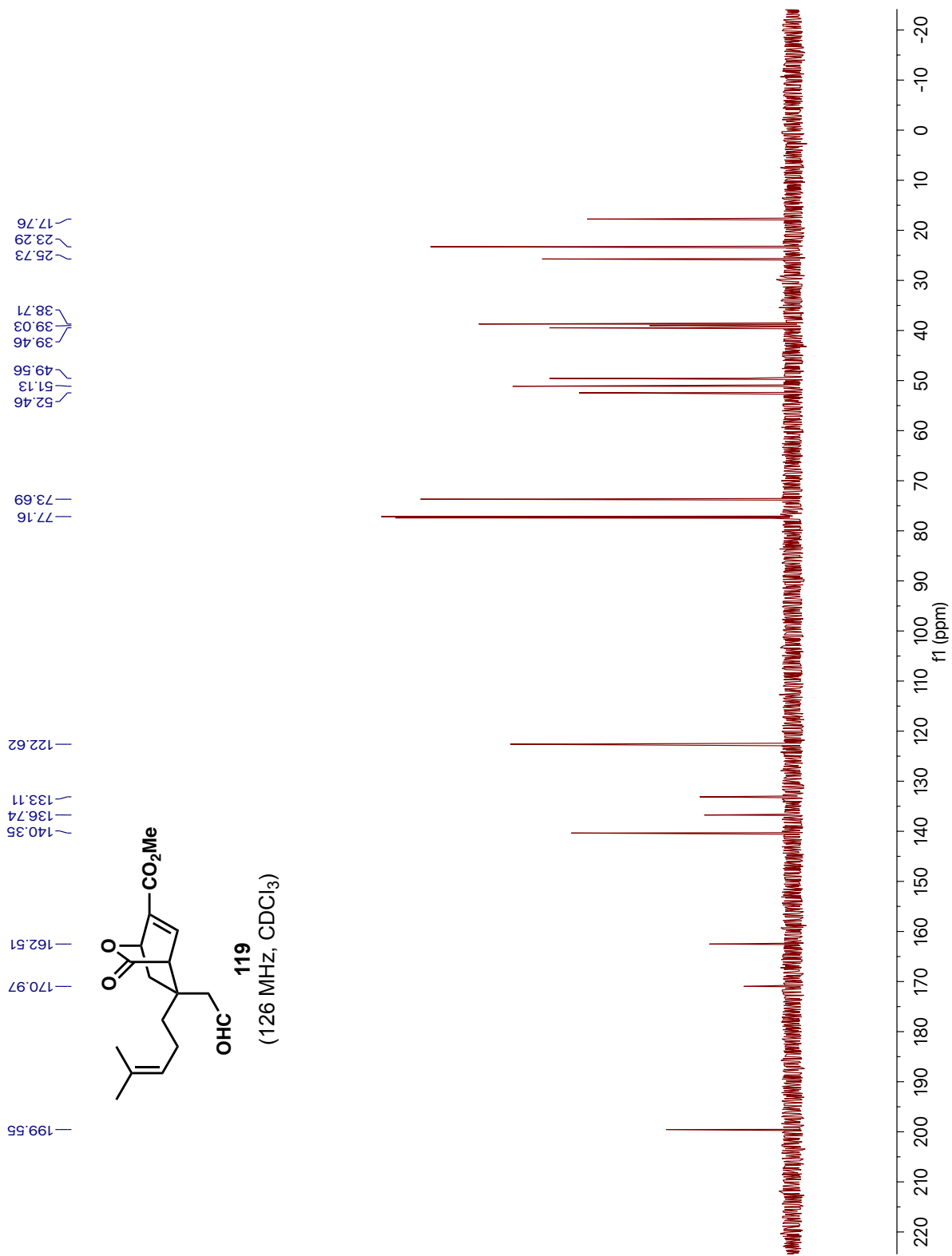


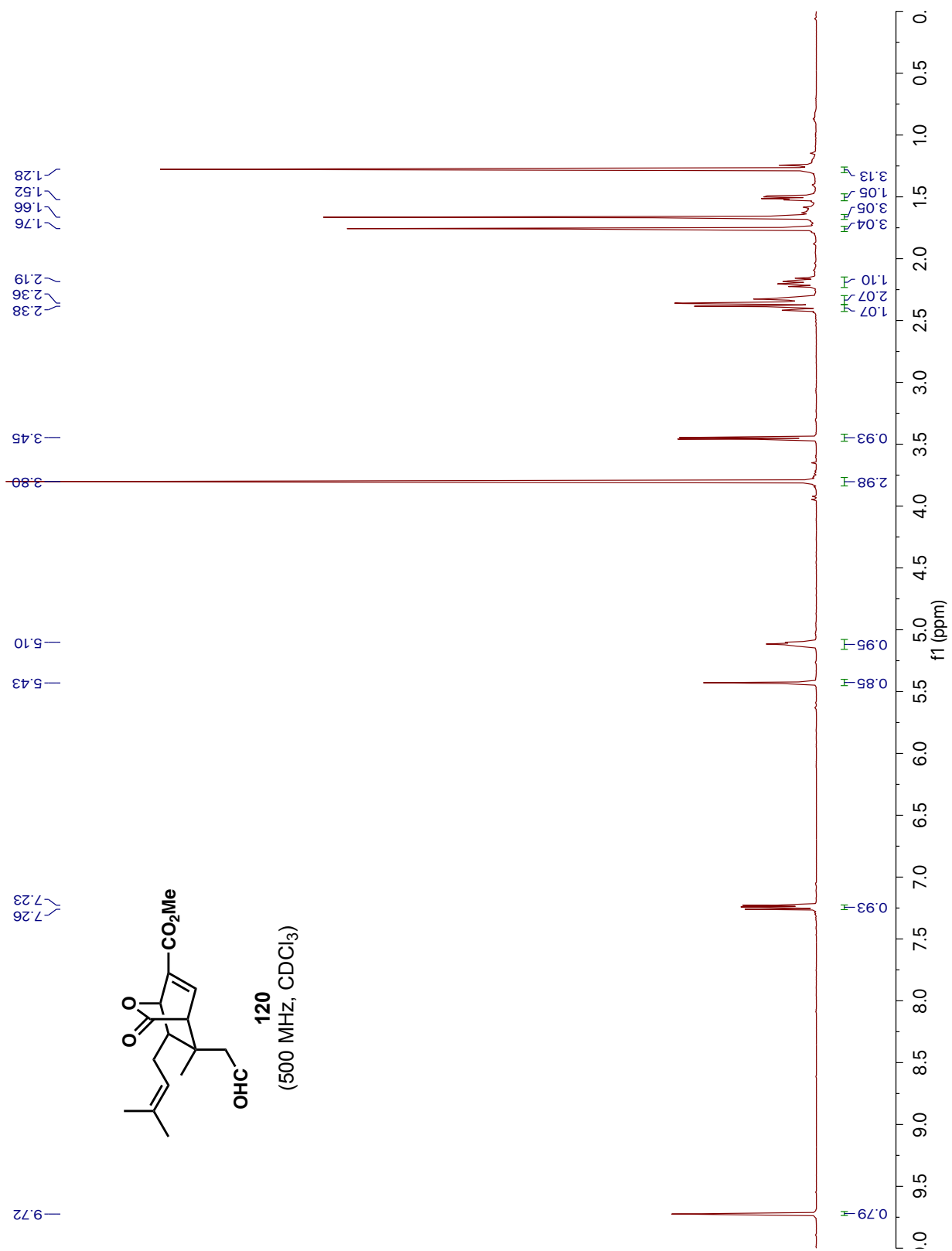


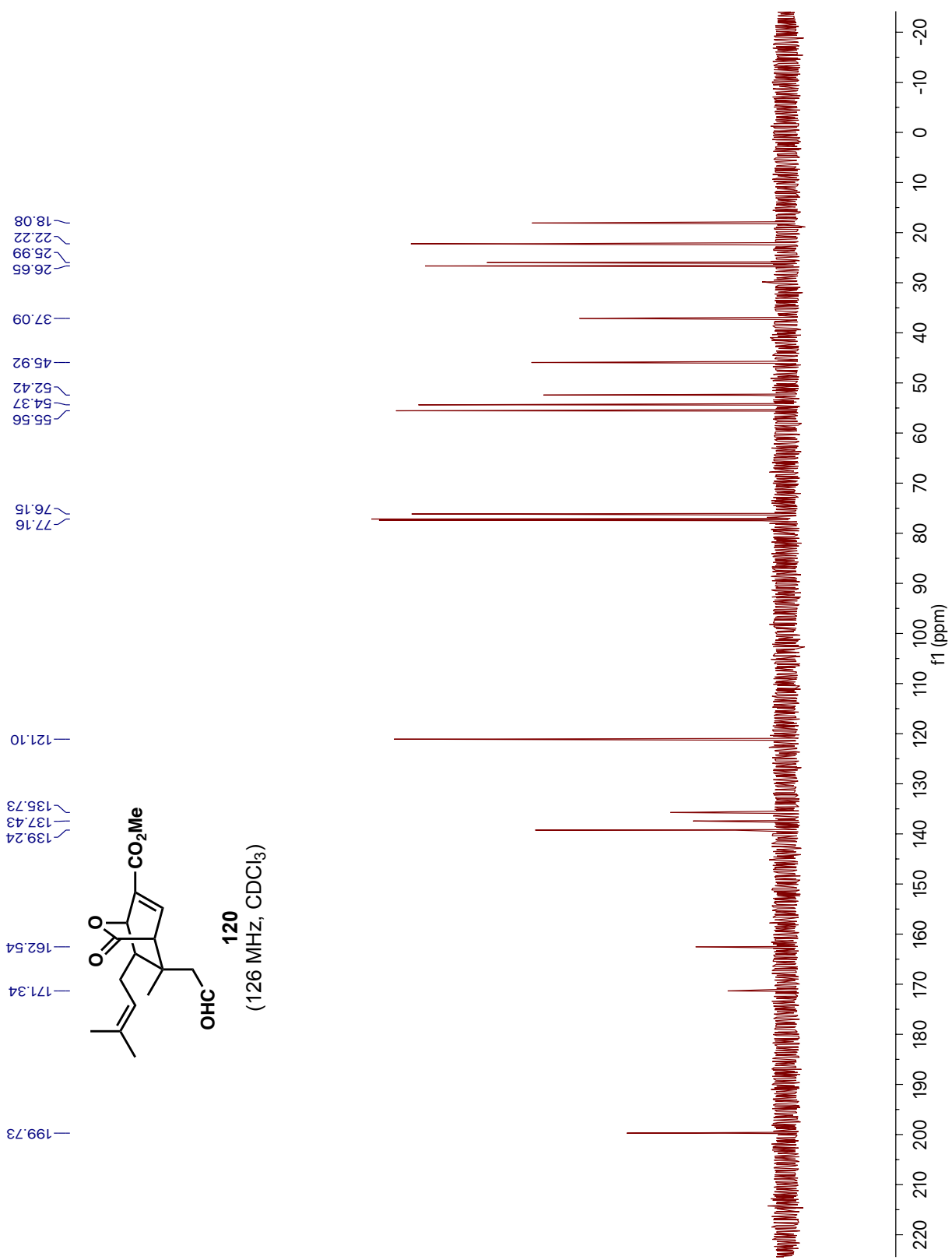


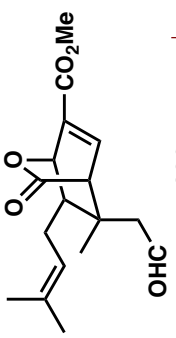




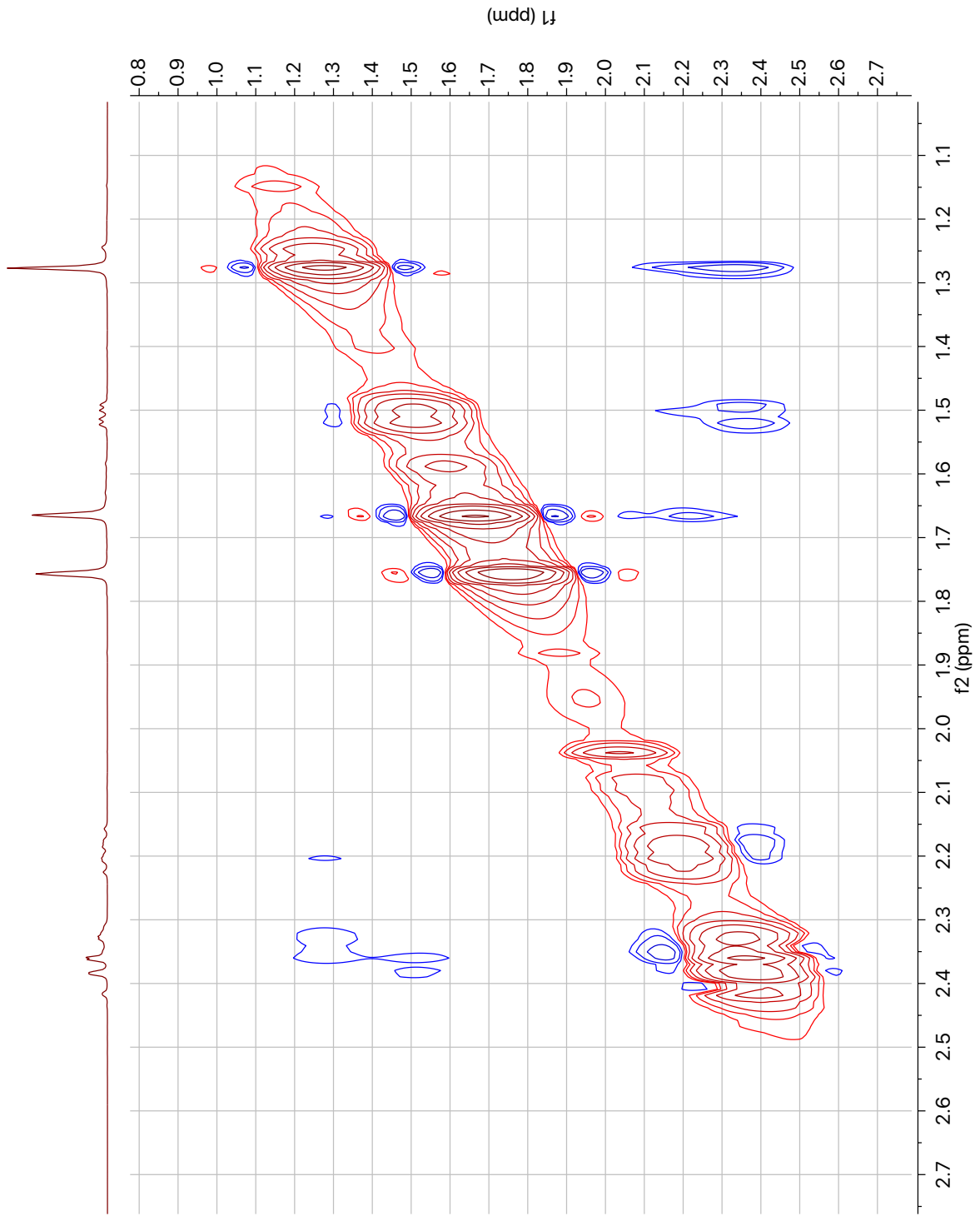


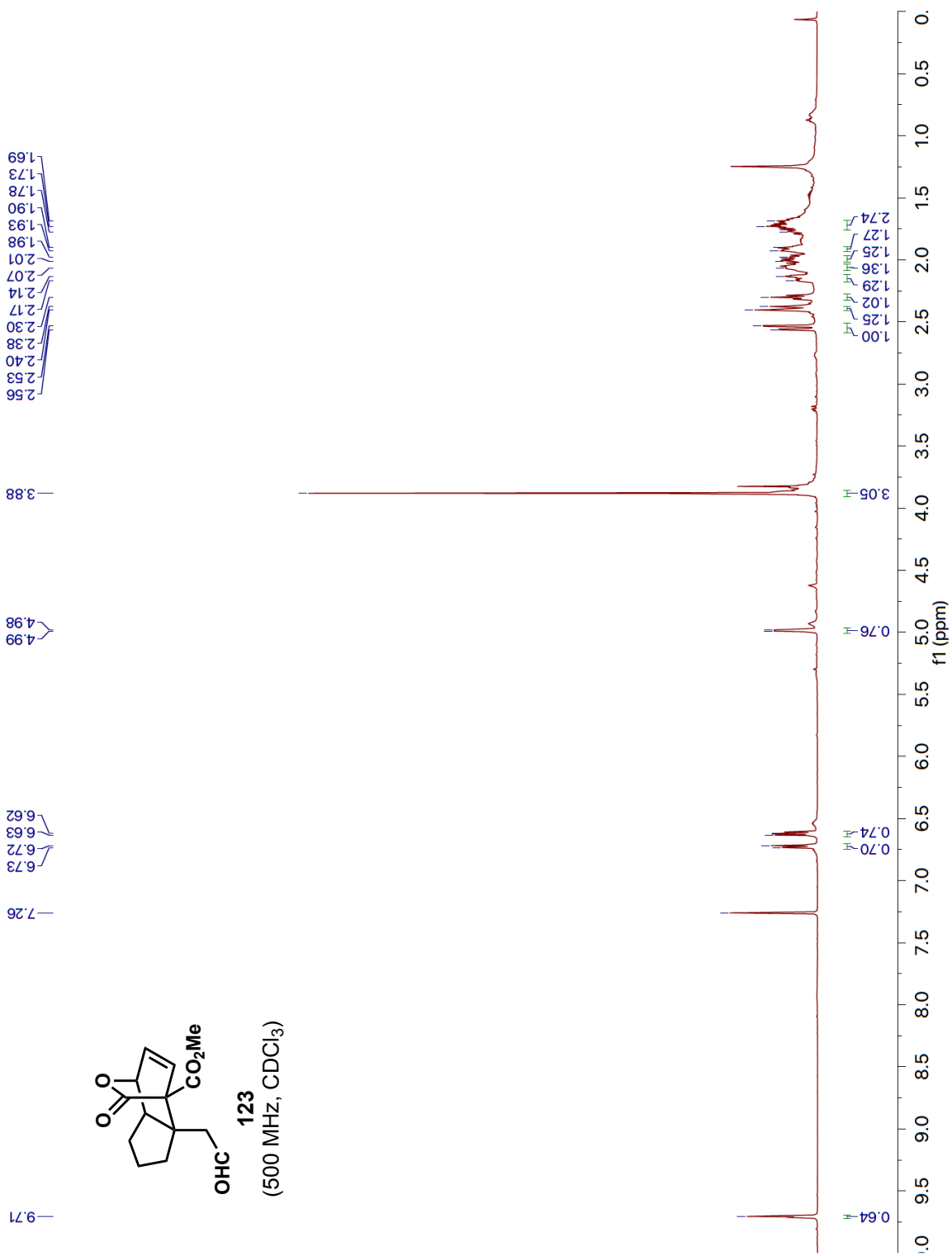


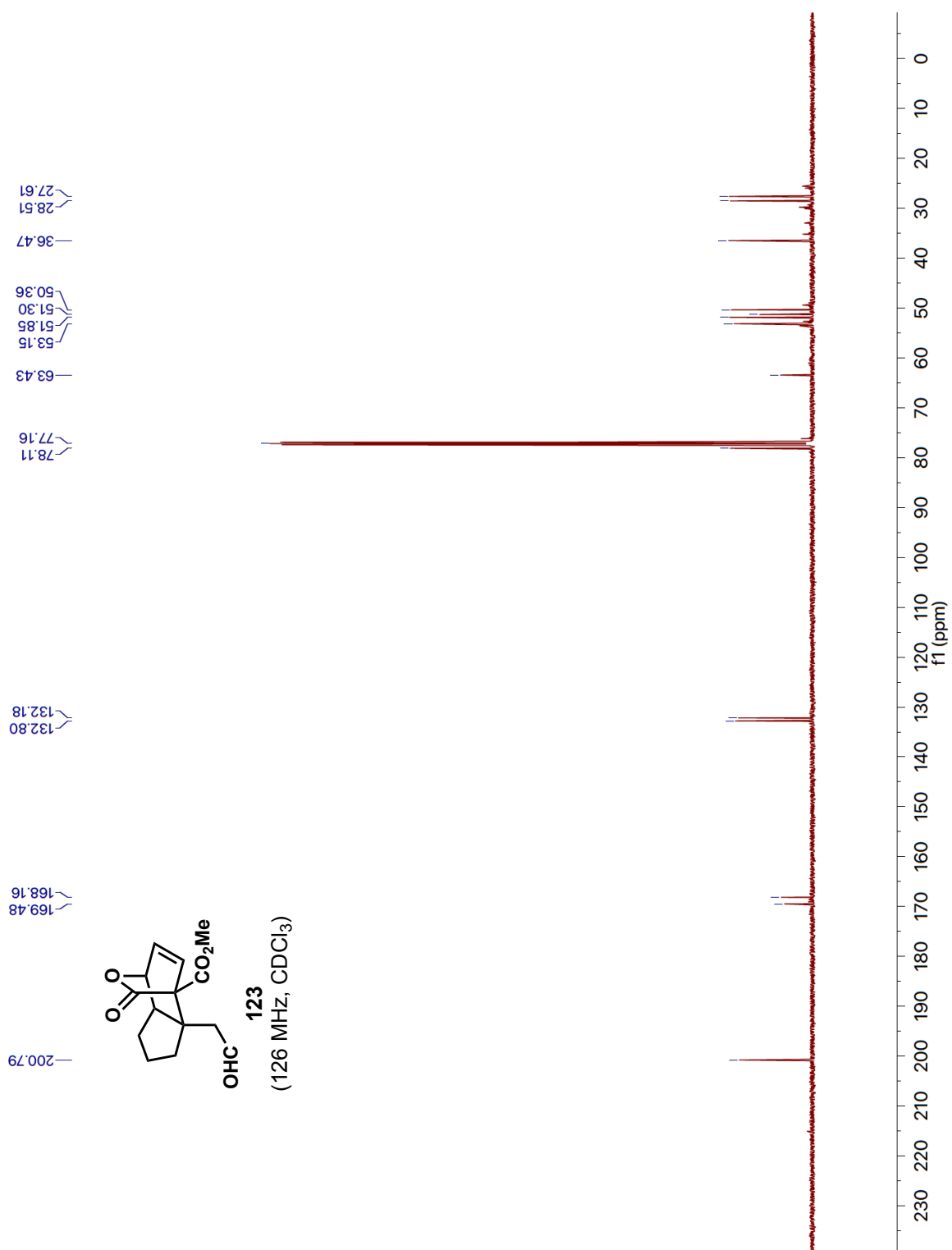


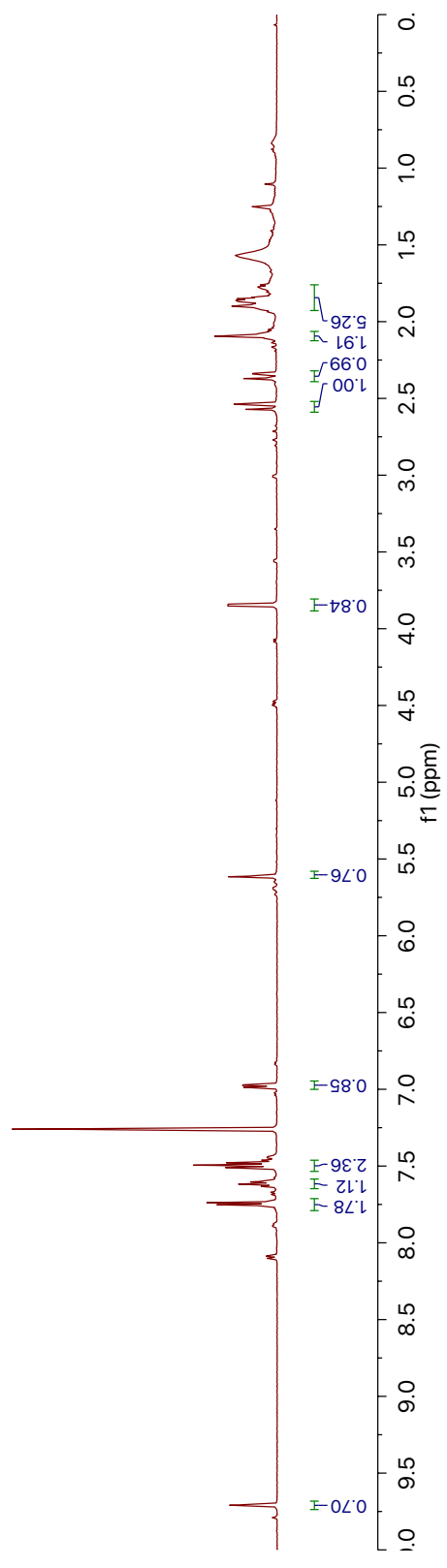
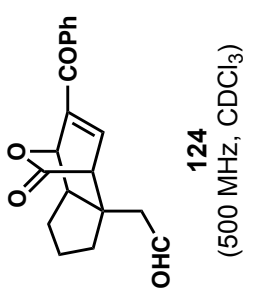
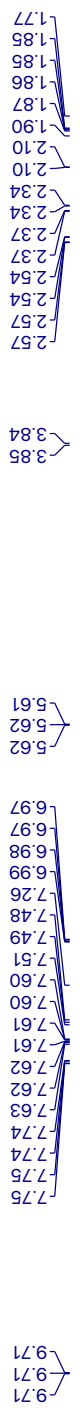


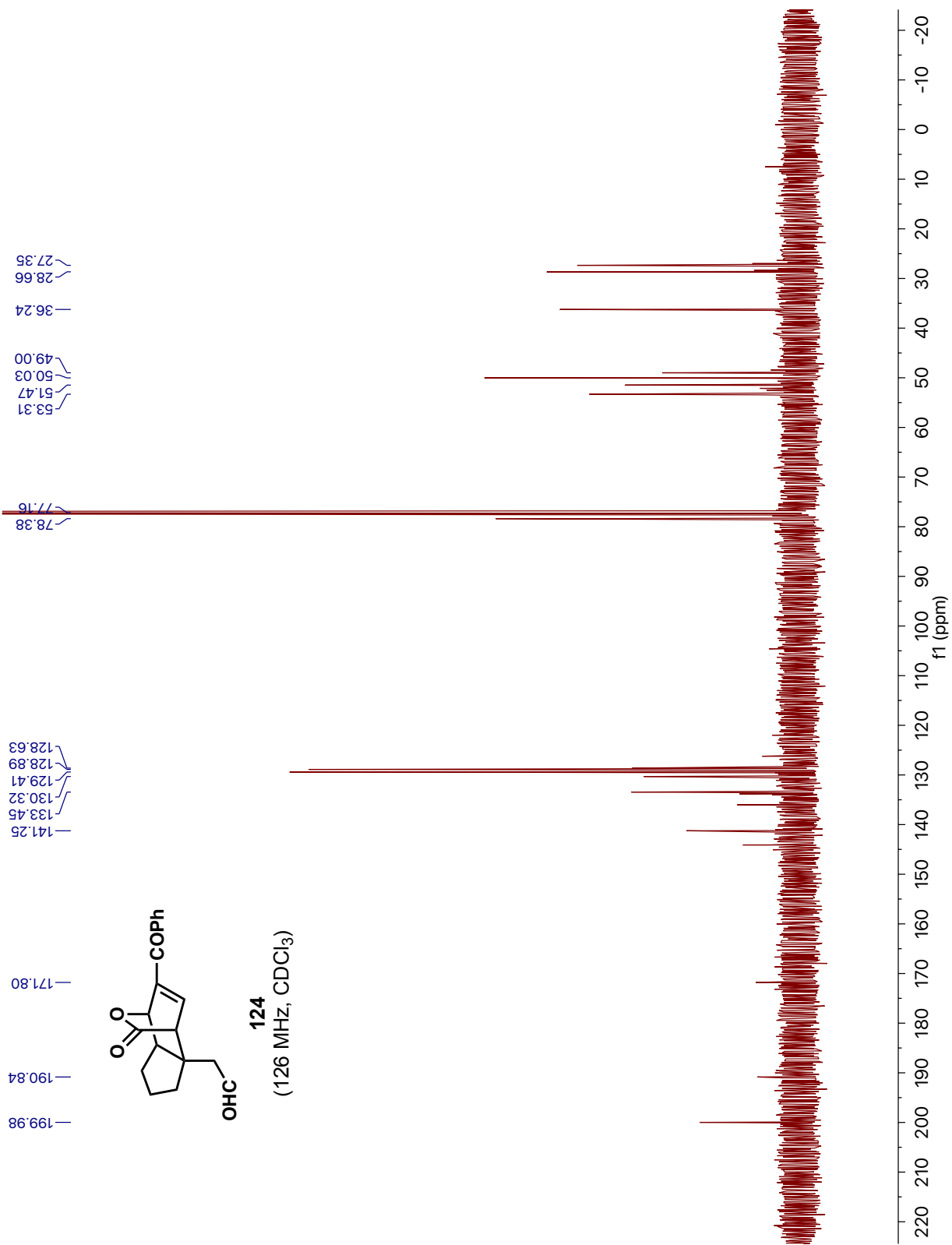
120
(500 MHz, CDCl₃)

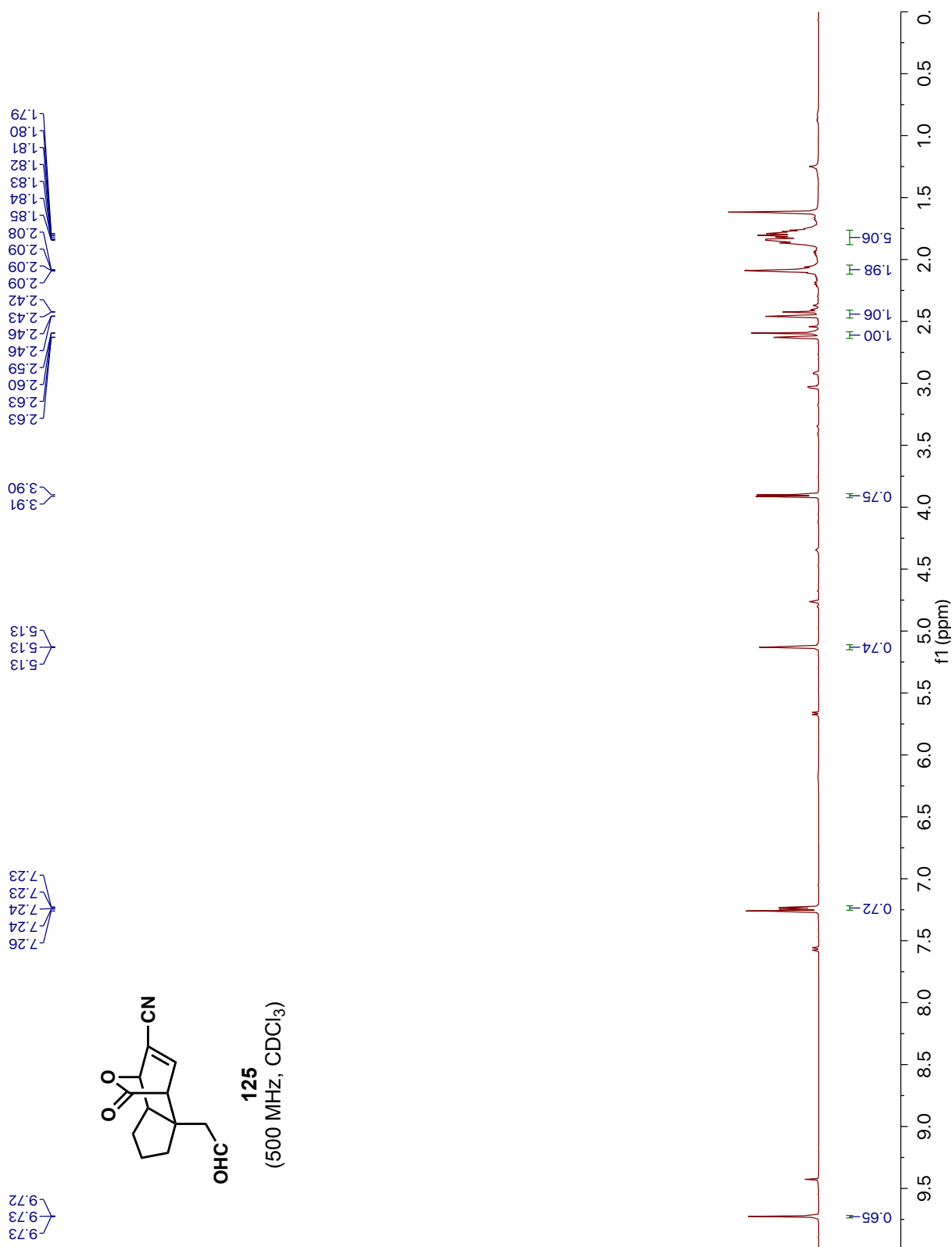


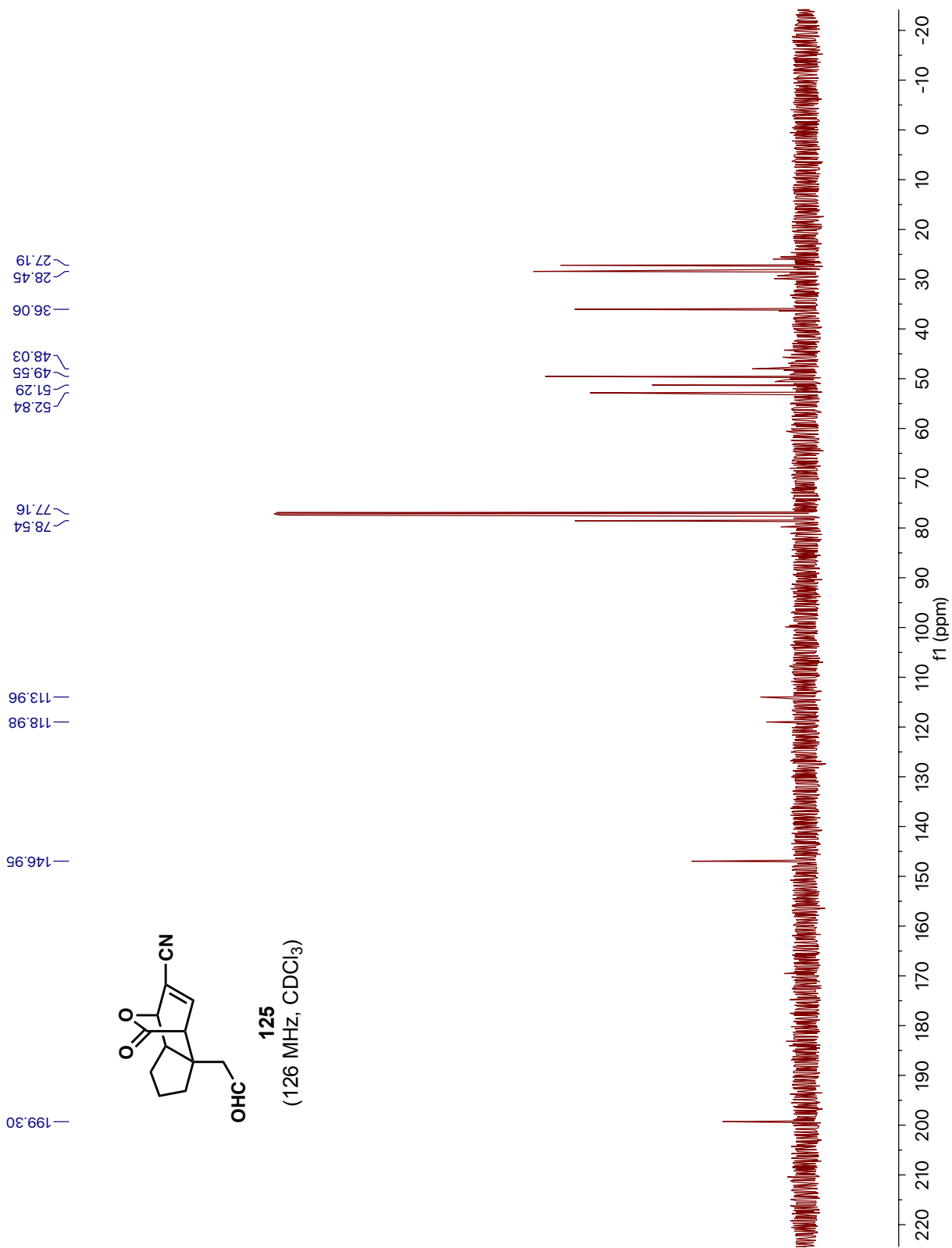


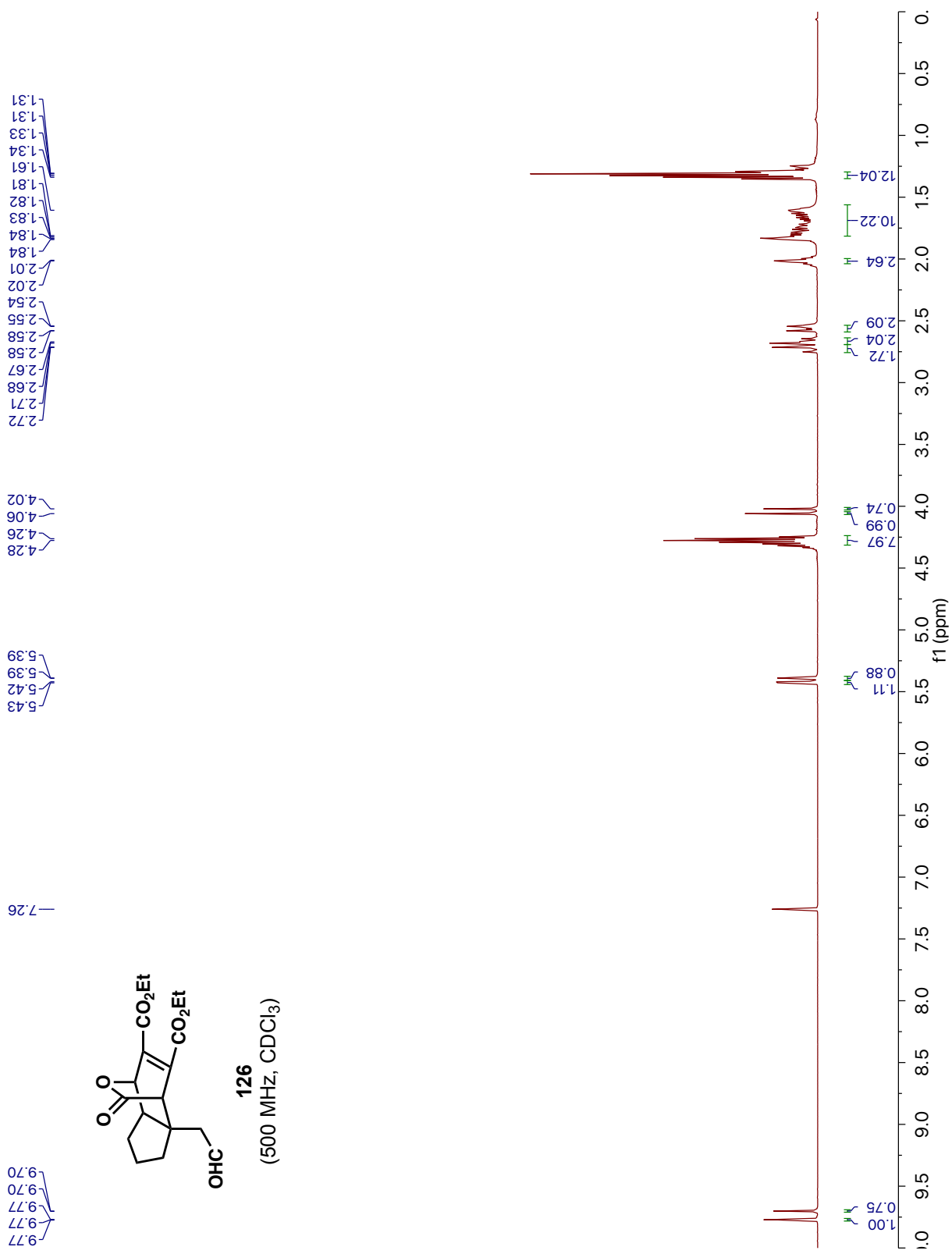


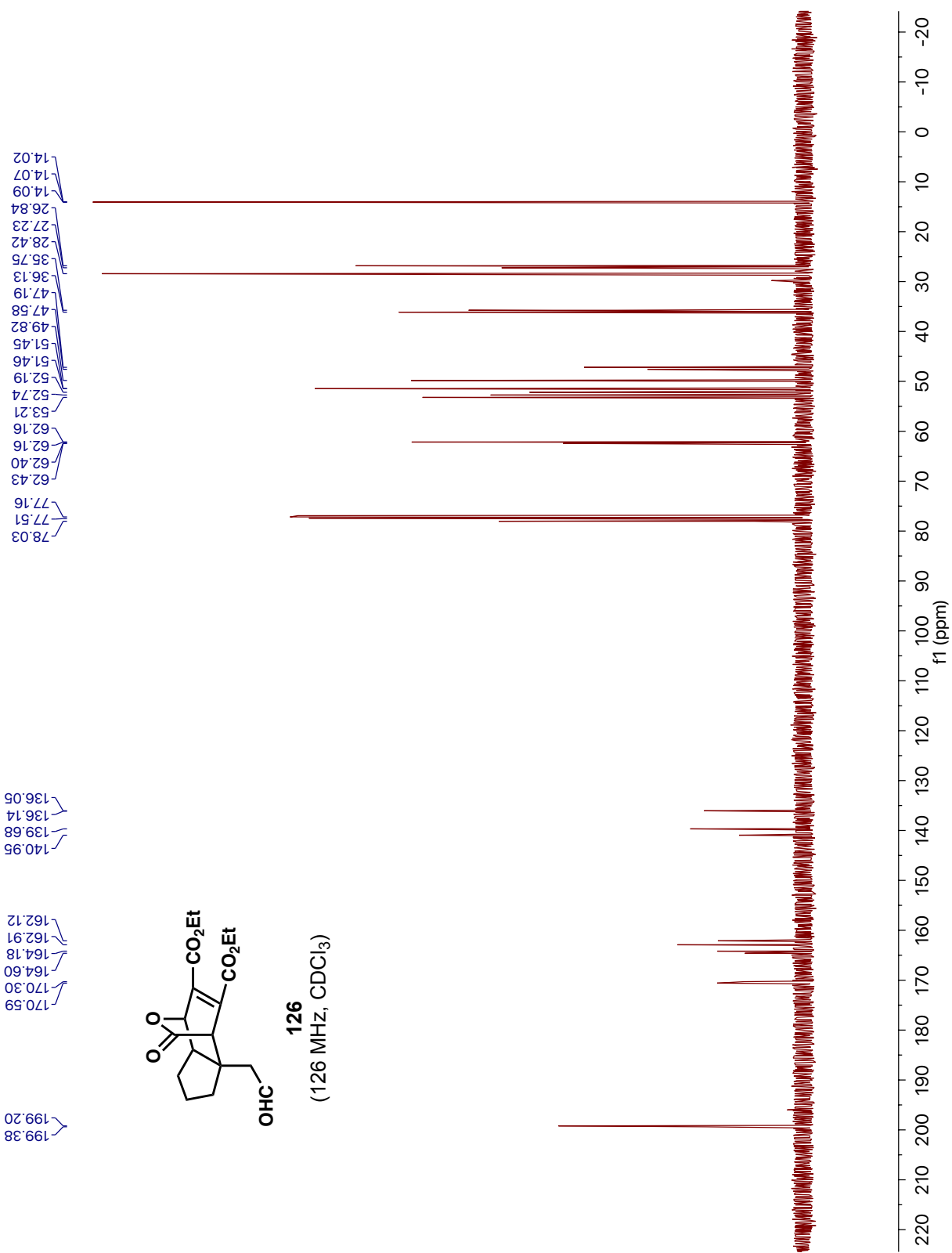


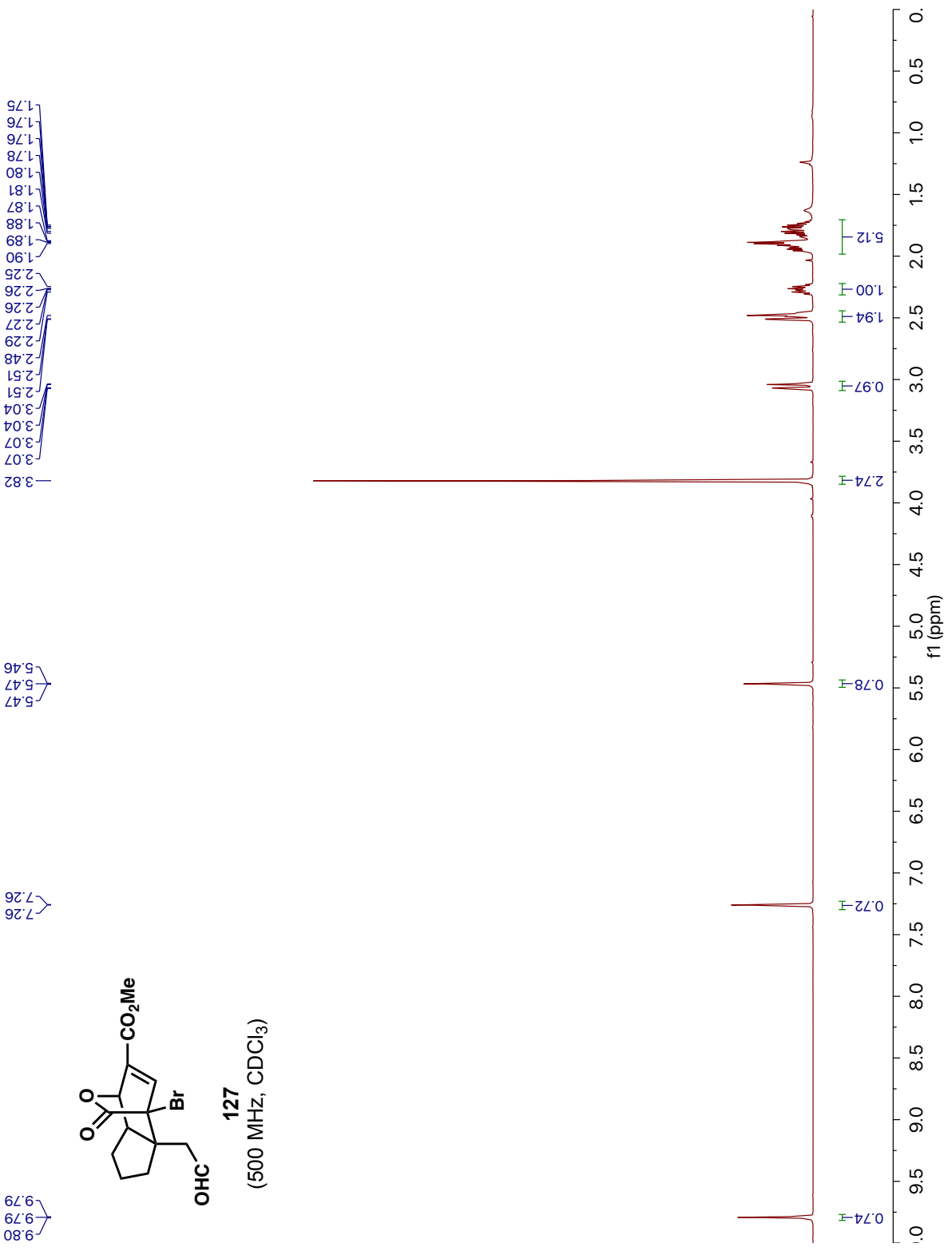


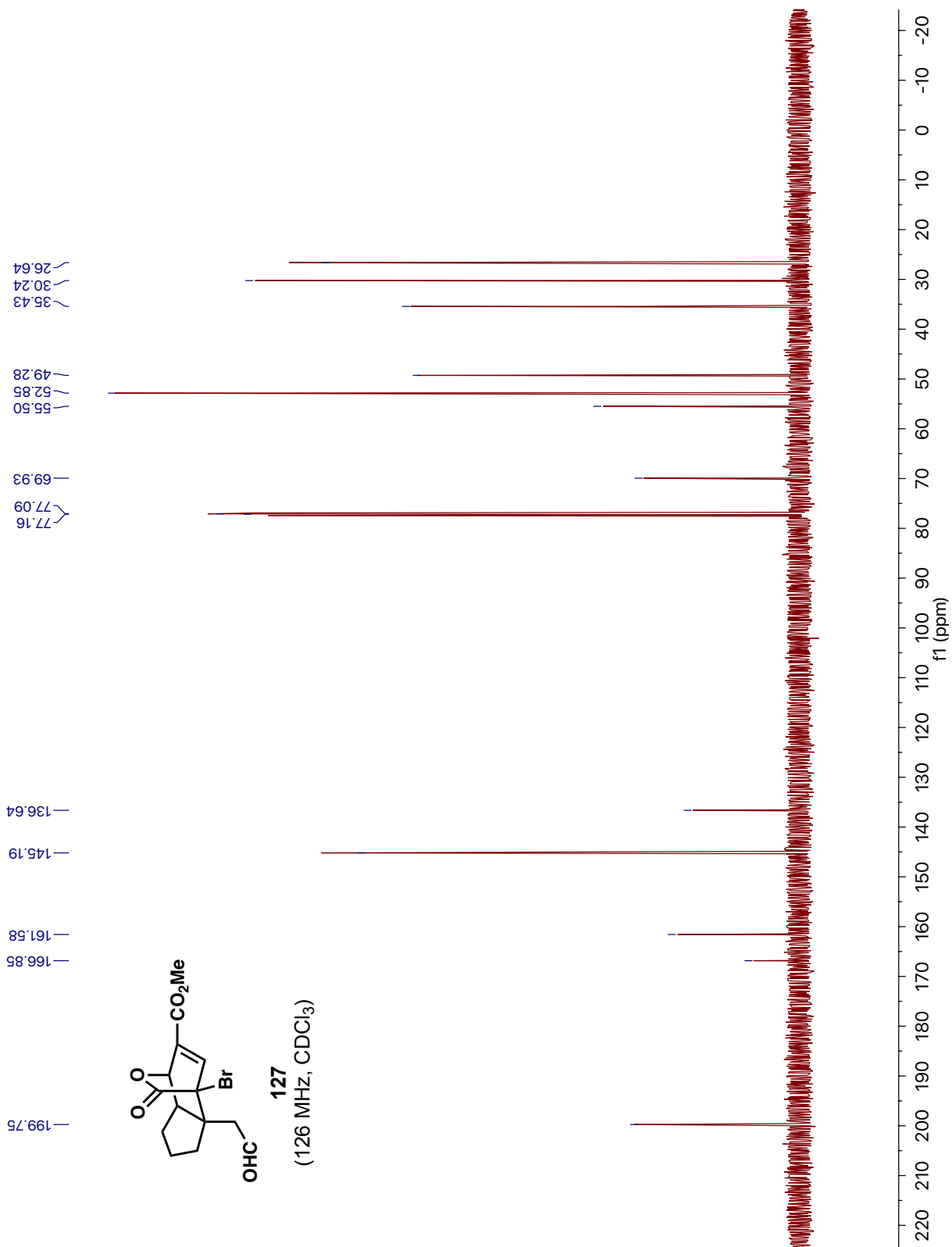


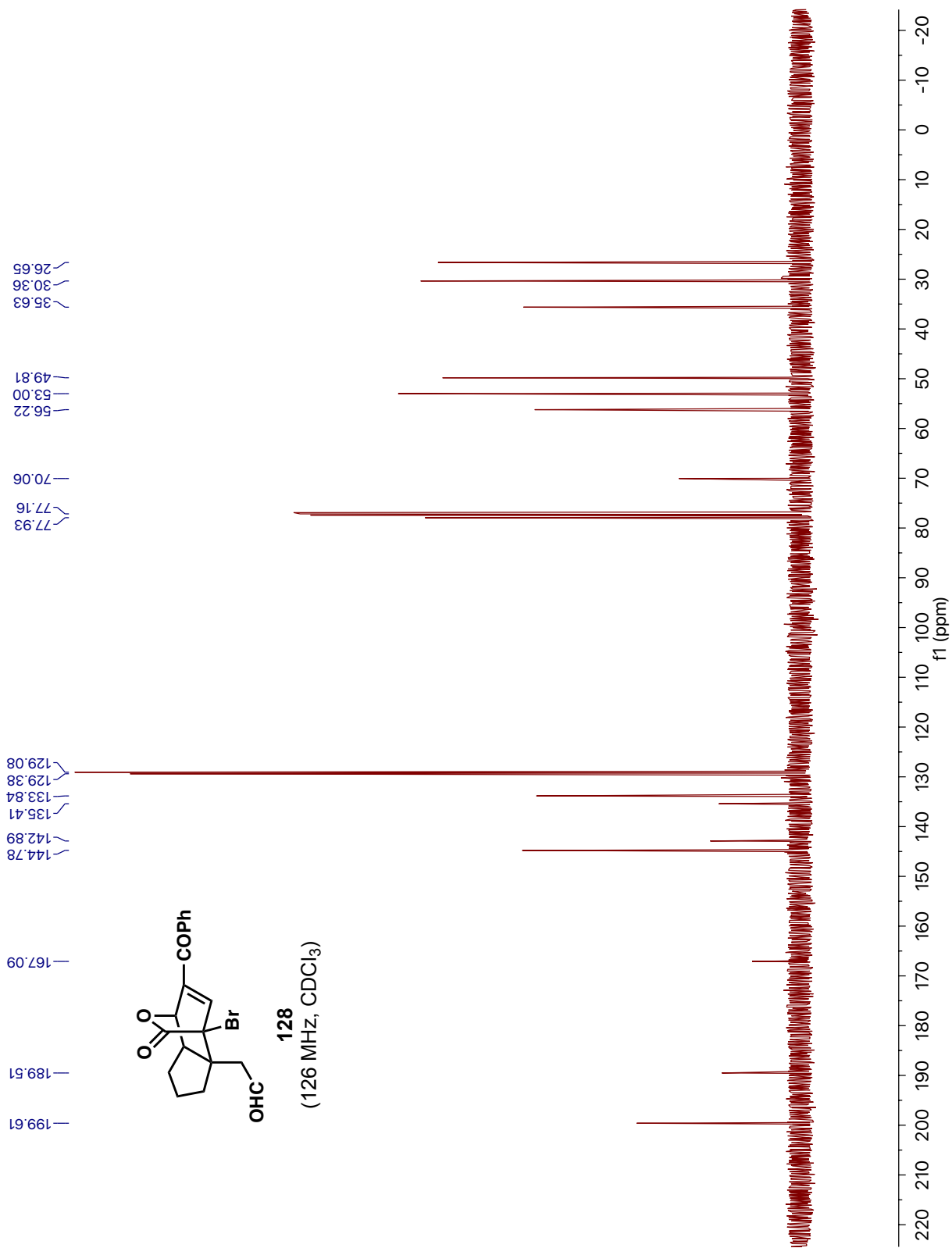


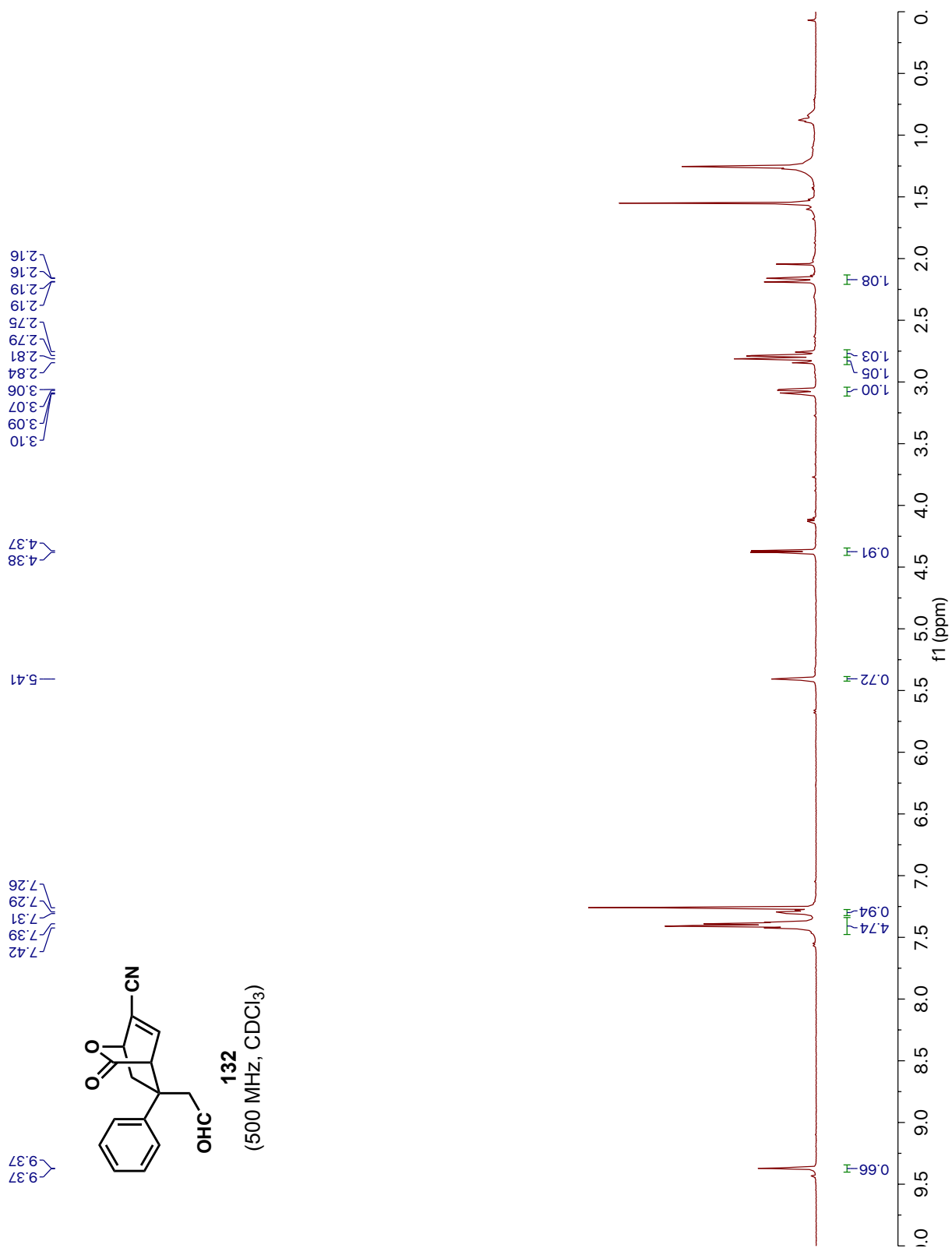


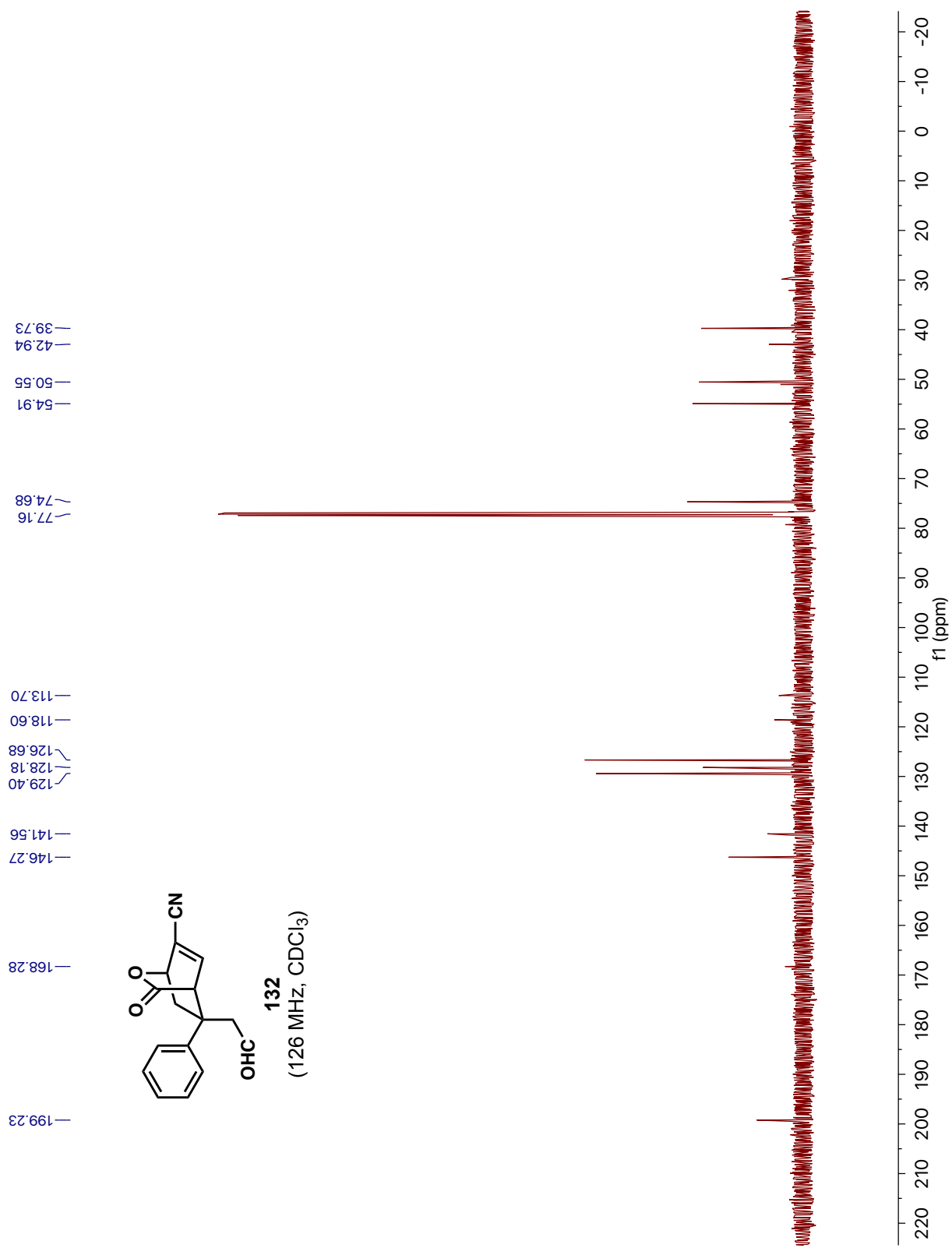


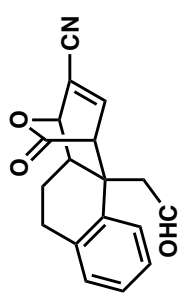
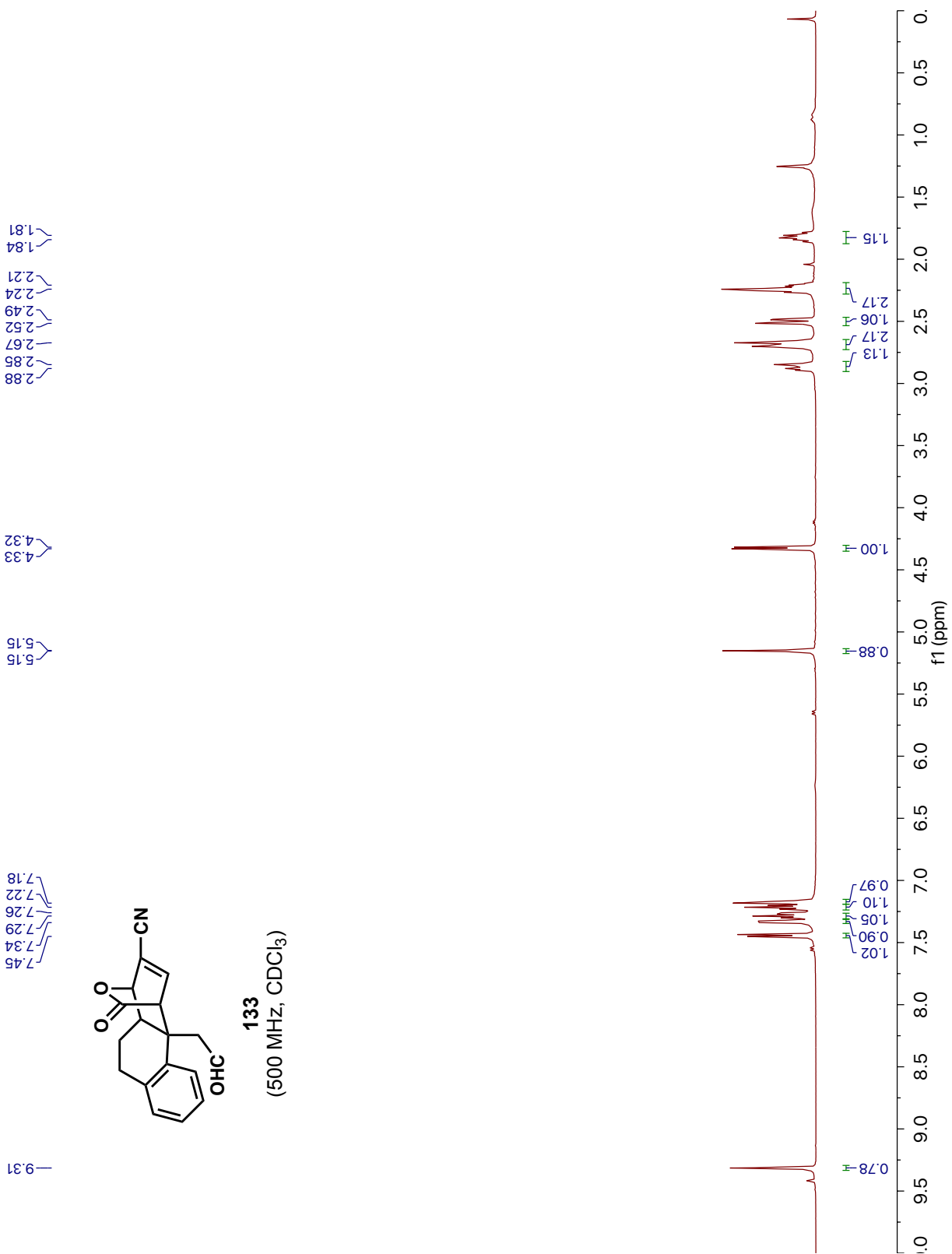




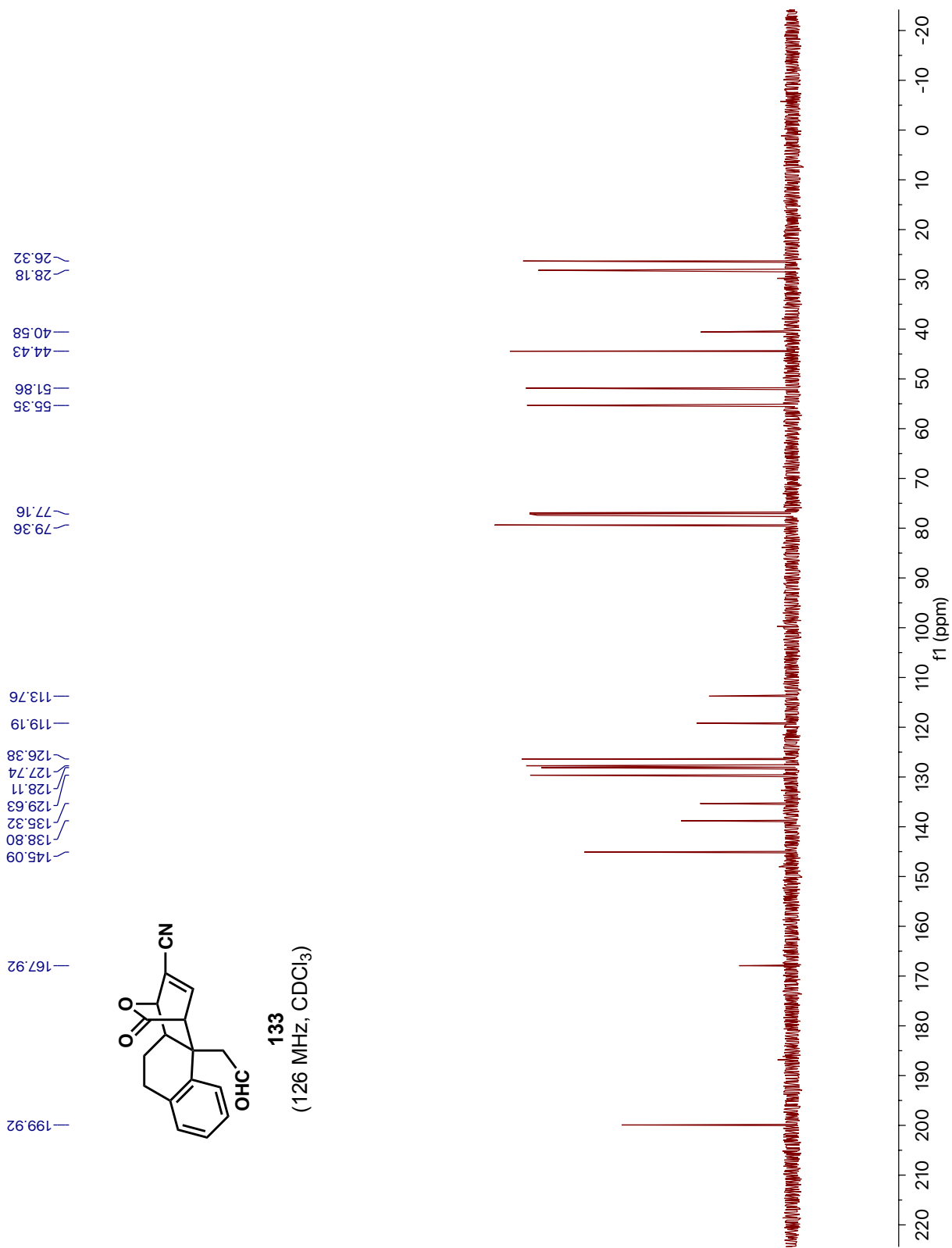


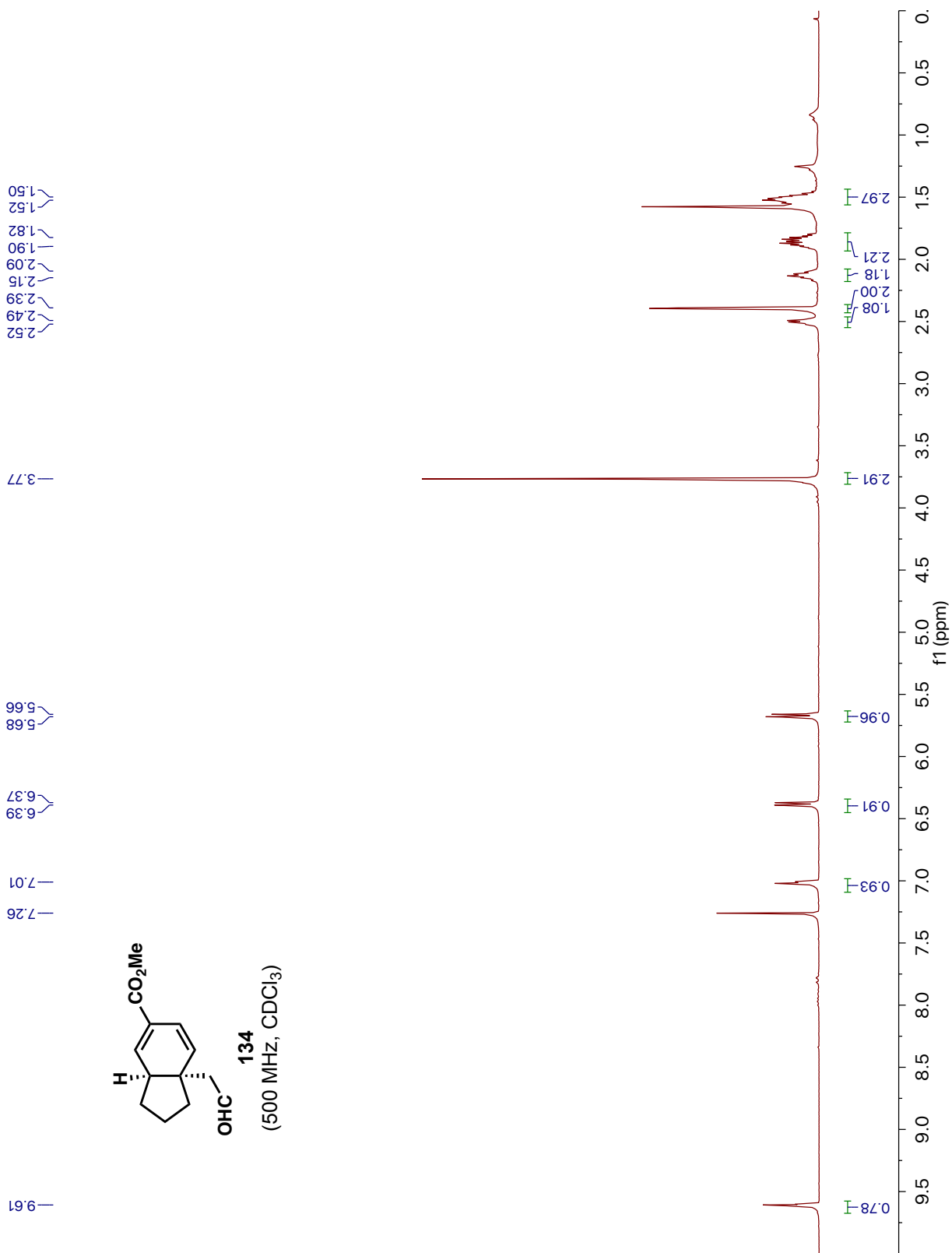


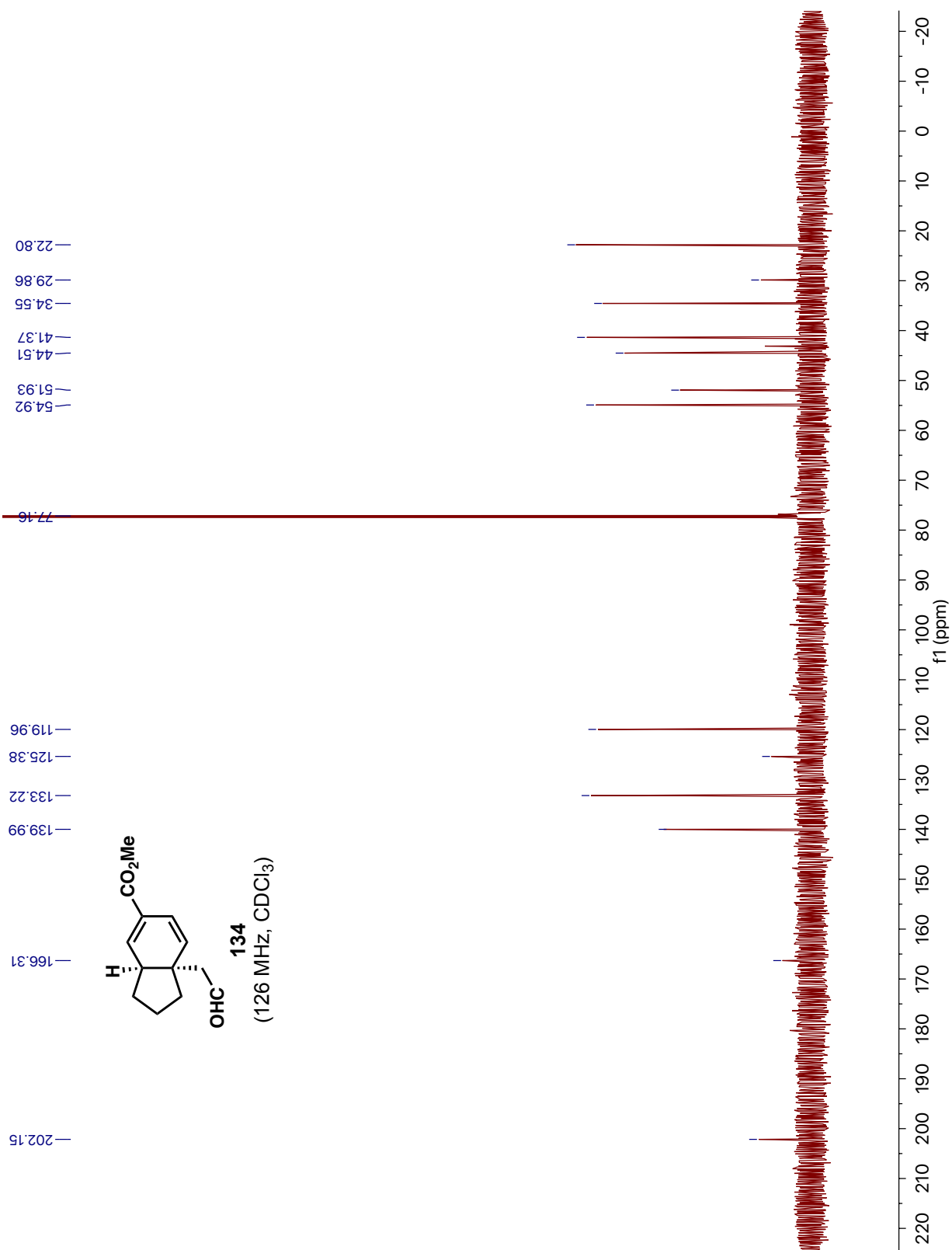


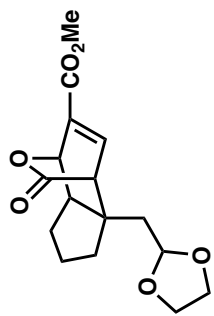


133
(500 MHz, CDCl_3)

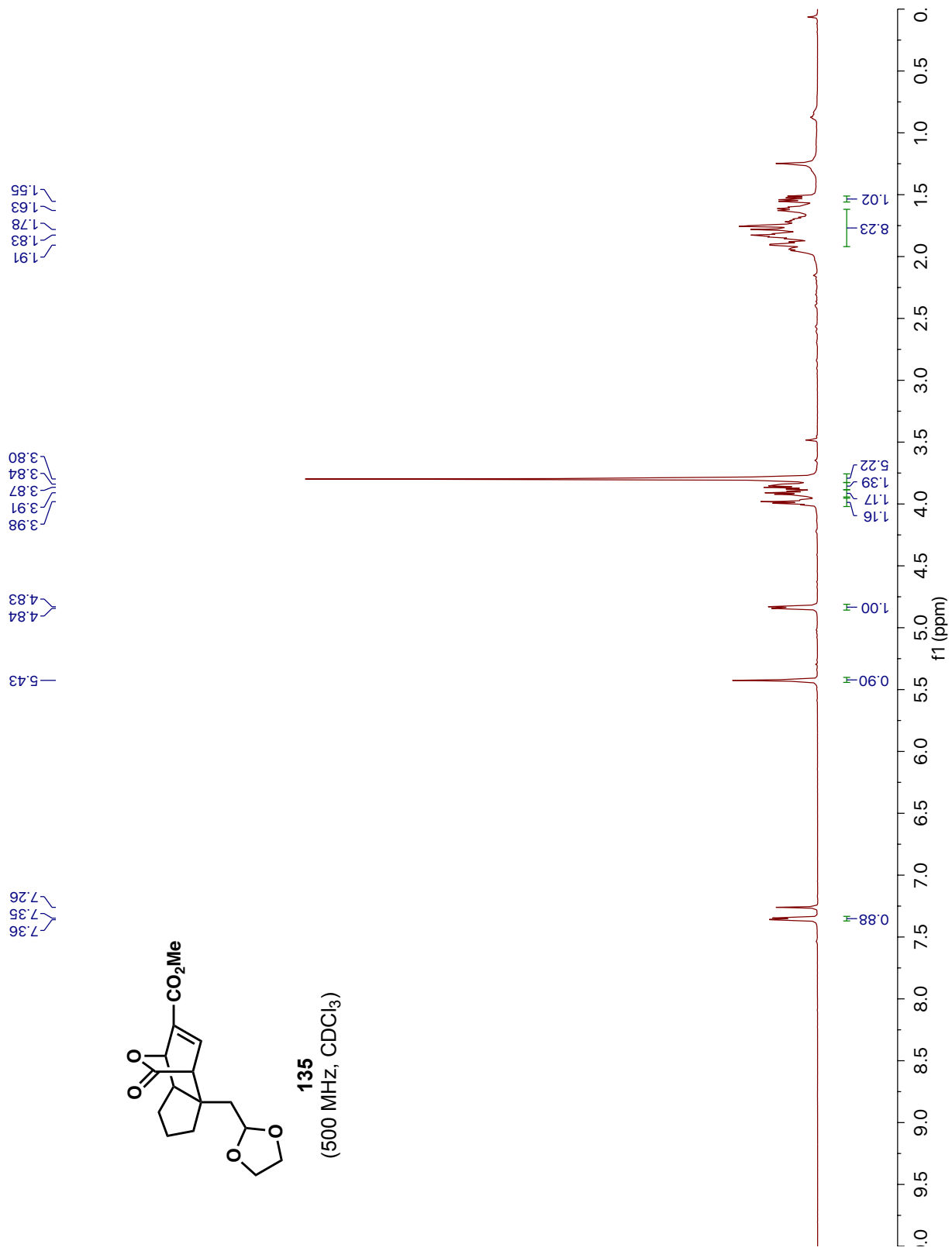


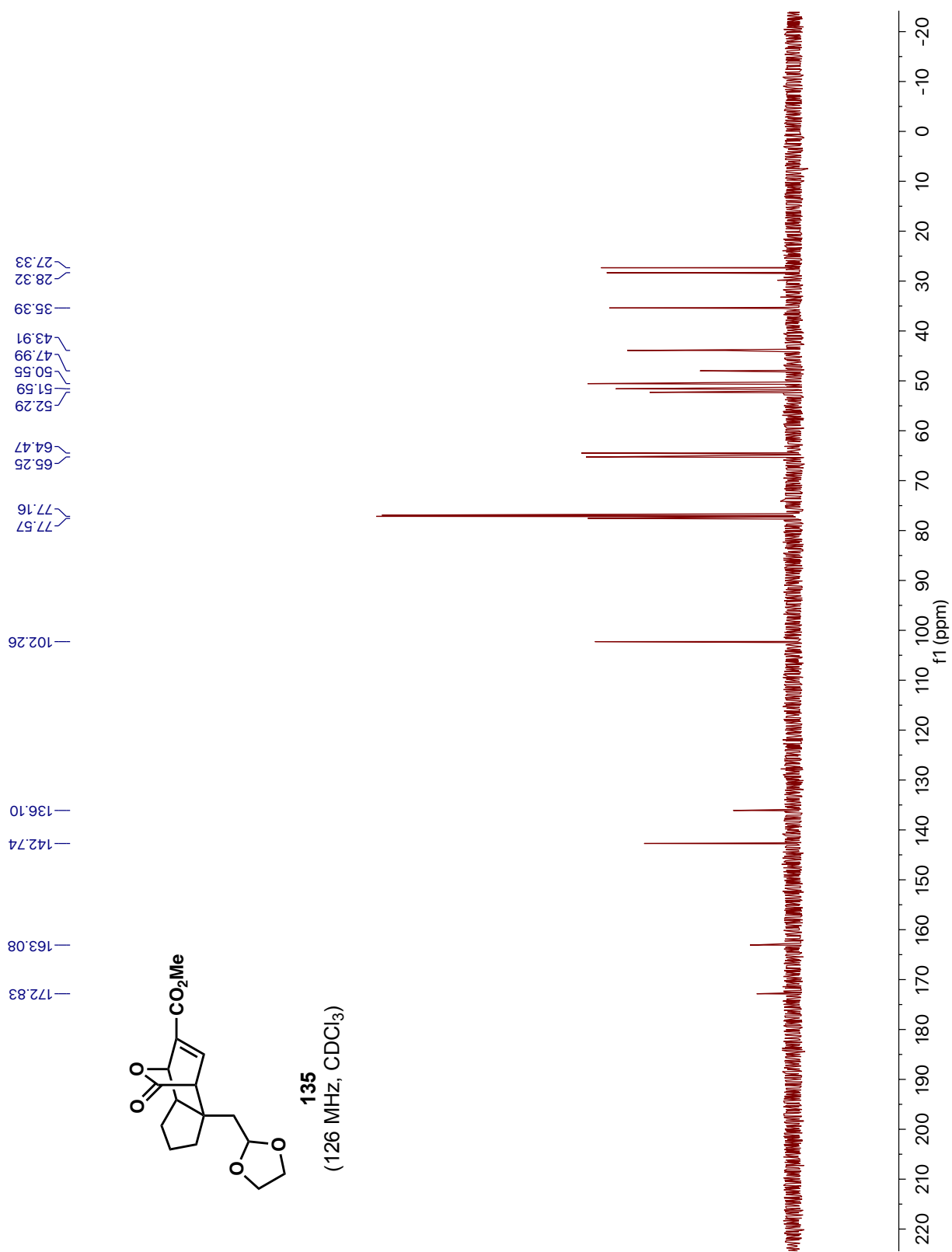






135
(500 MHz, CDCl₃)



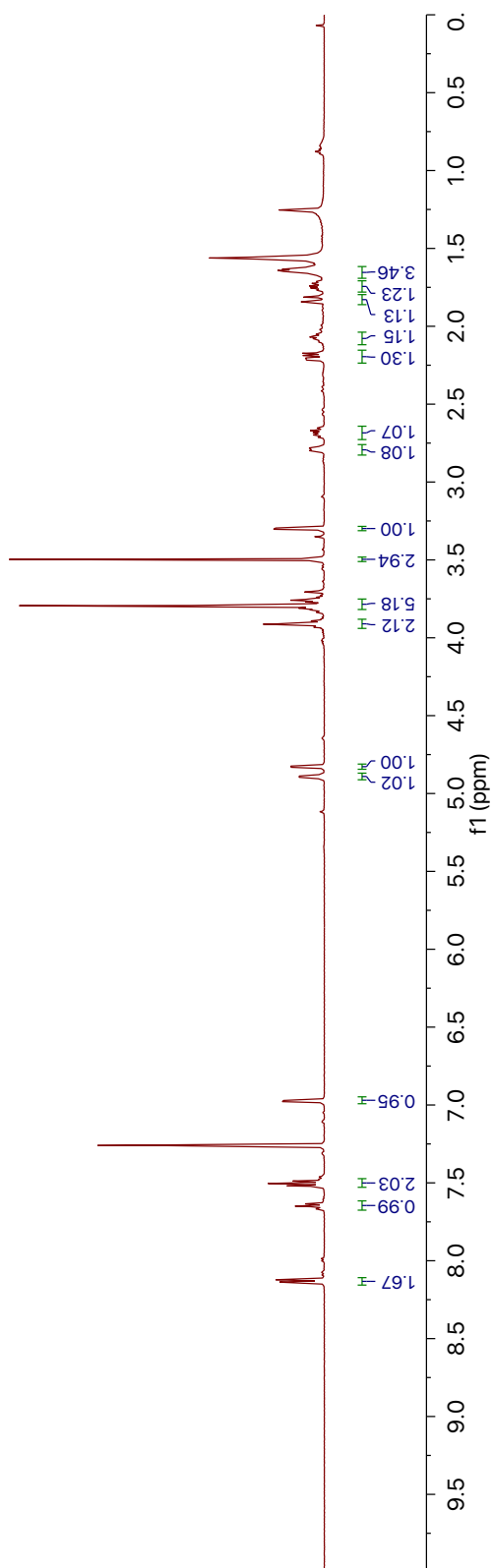
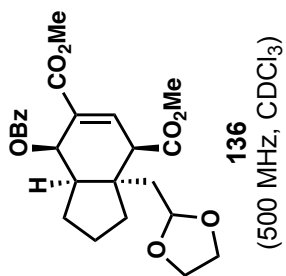


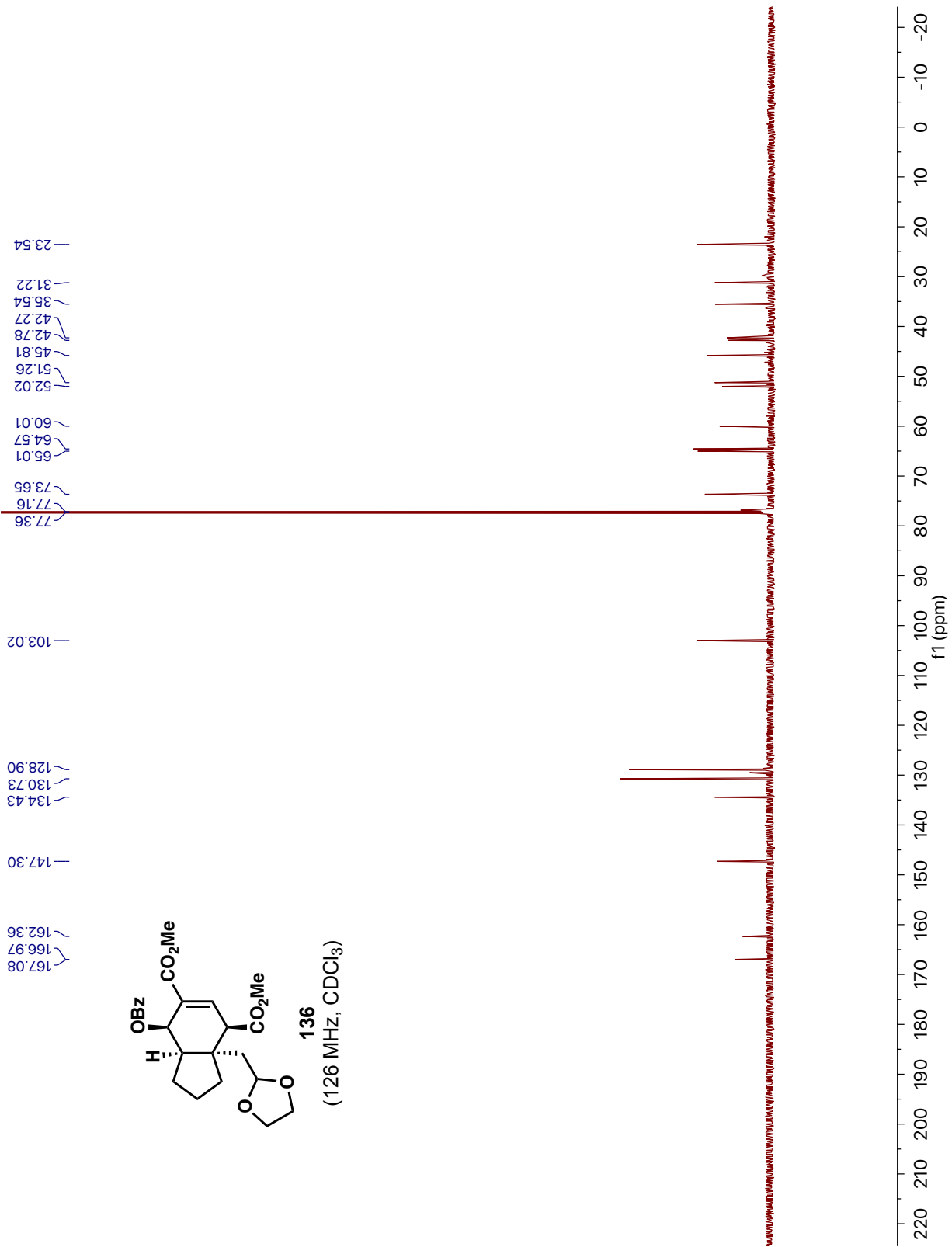
1.63
1.66
1.74
1.84
1.84
2.06
2.17
2.22
2.68
2.78
2.79
3.30
3.50
3.75
3.80
3.91

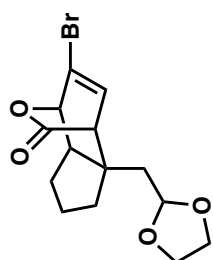
4.83
4.90

6.97
7.26
7.50
7.65

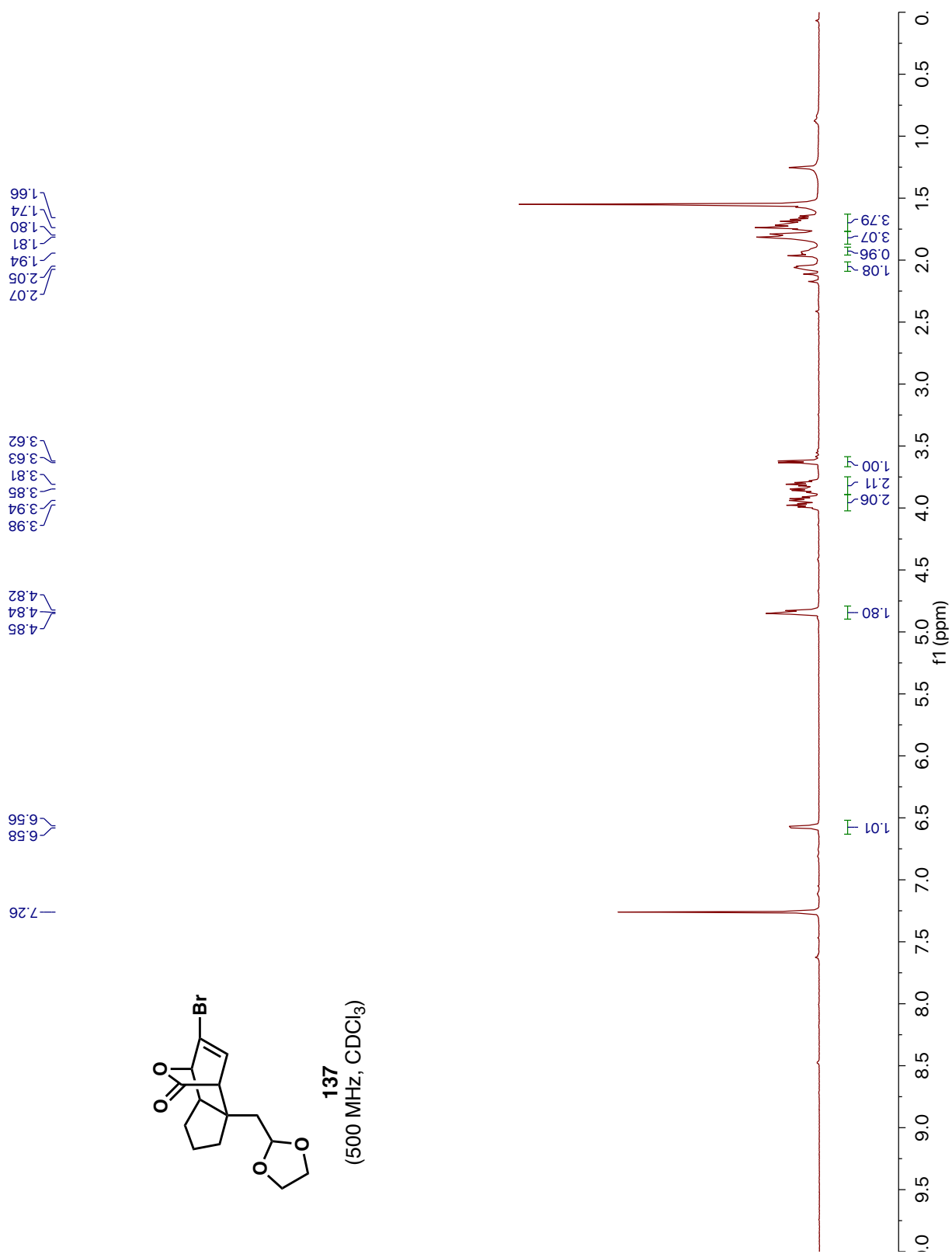
8.14

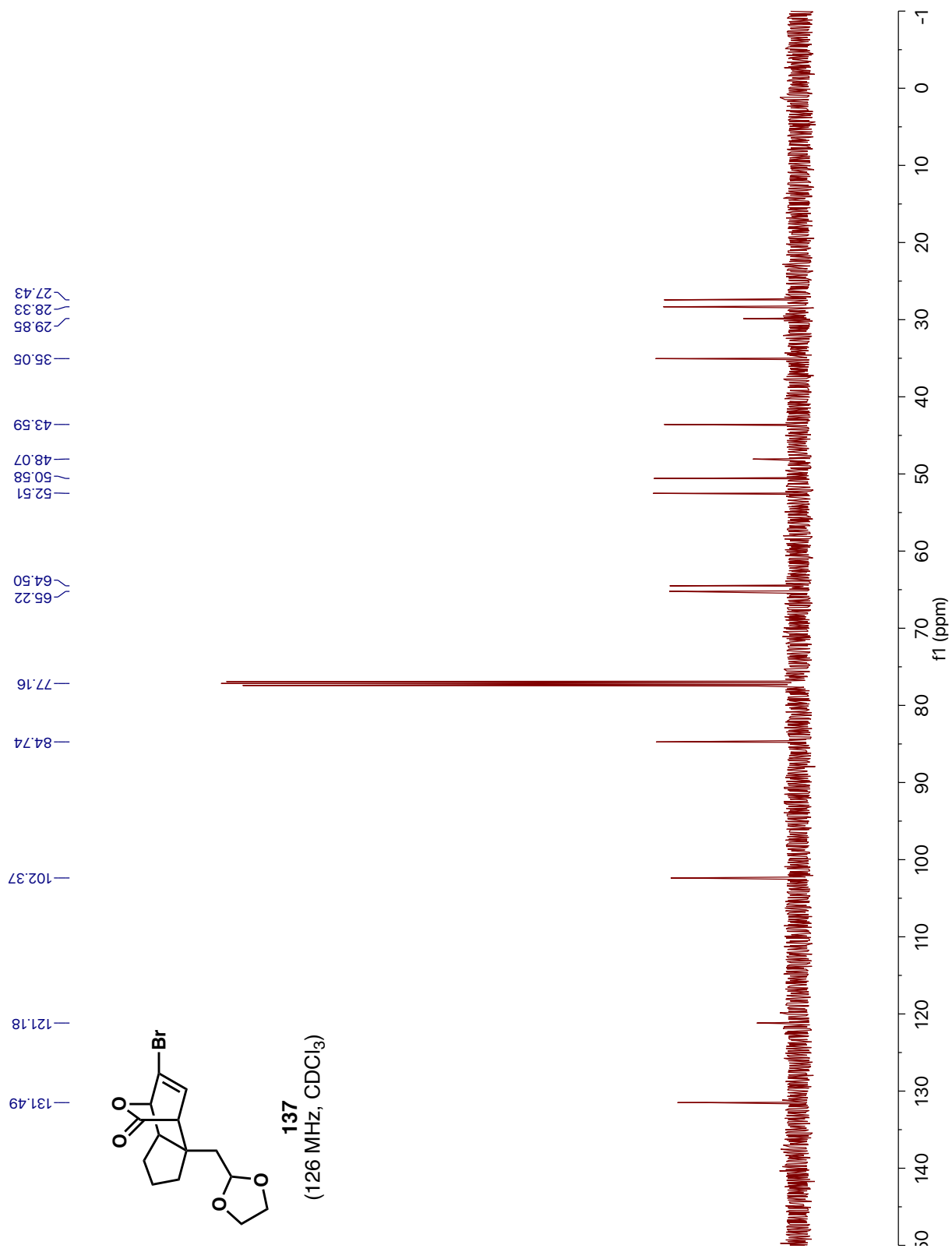


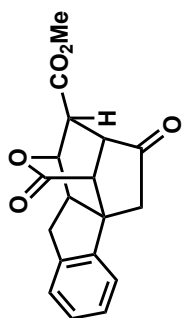




137
(500 MHz, CDCl₃)





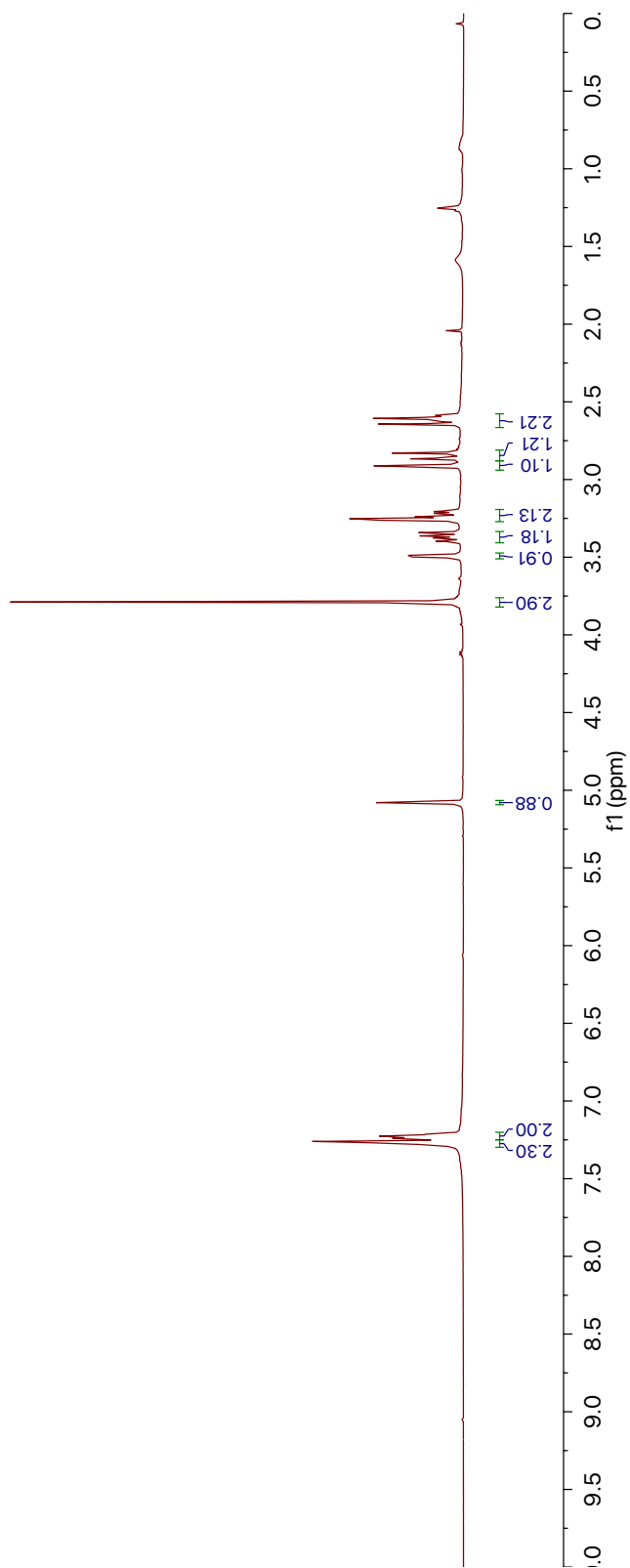


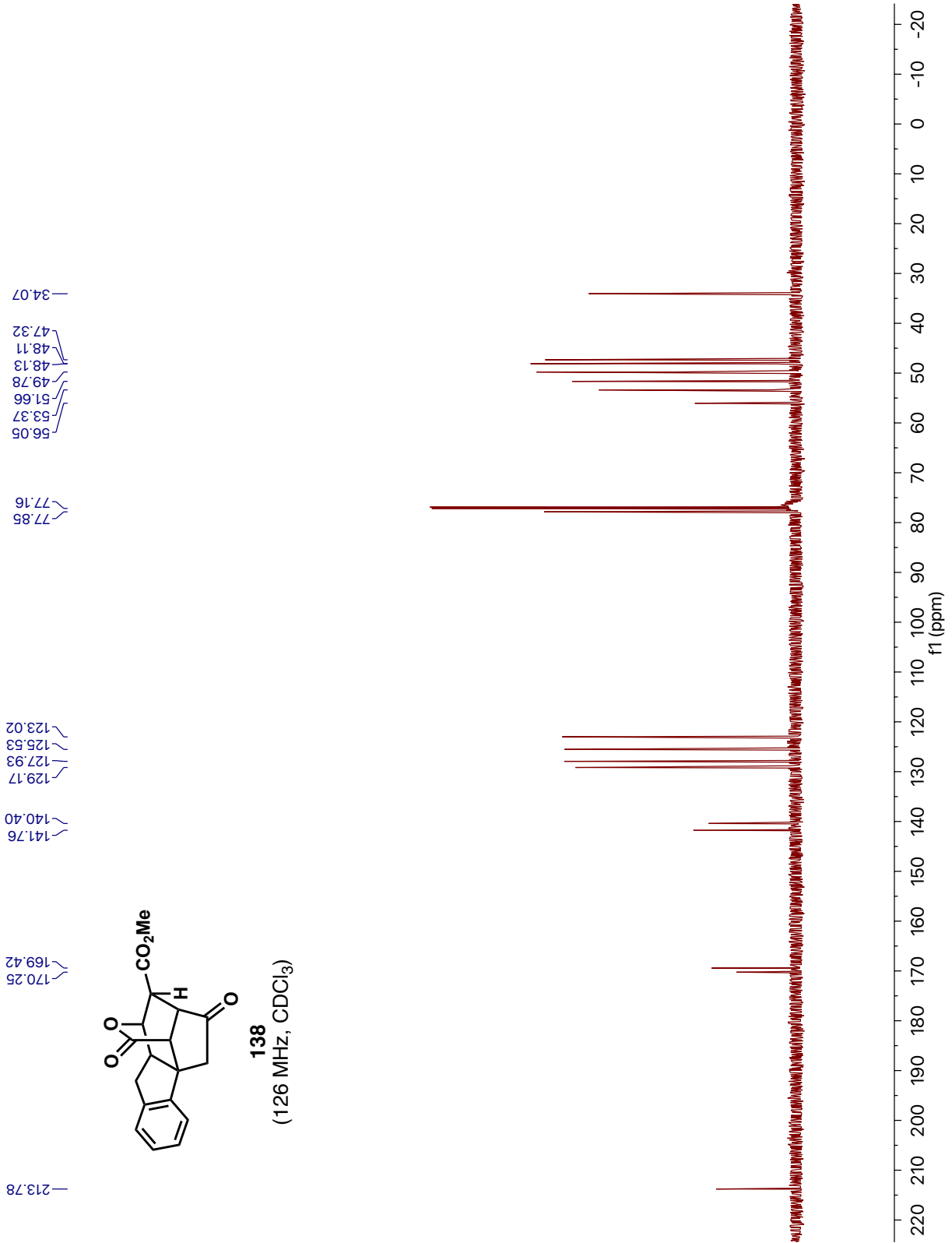
138
(500 MHz, CDCl₃)

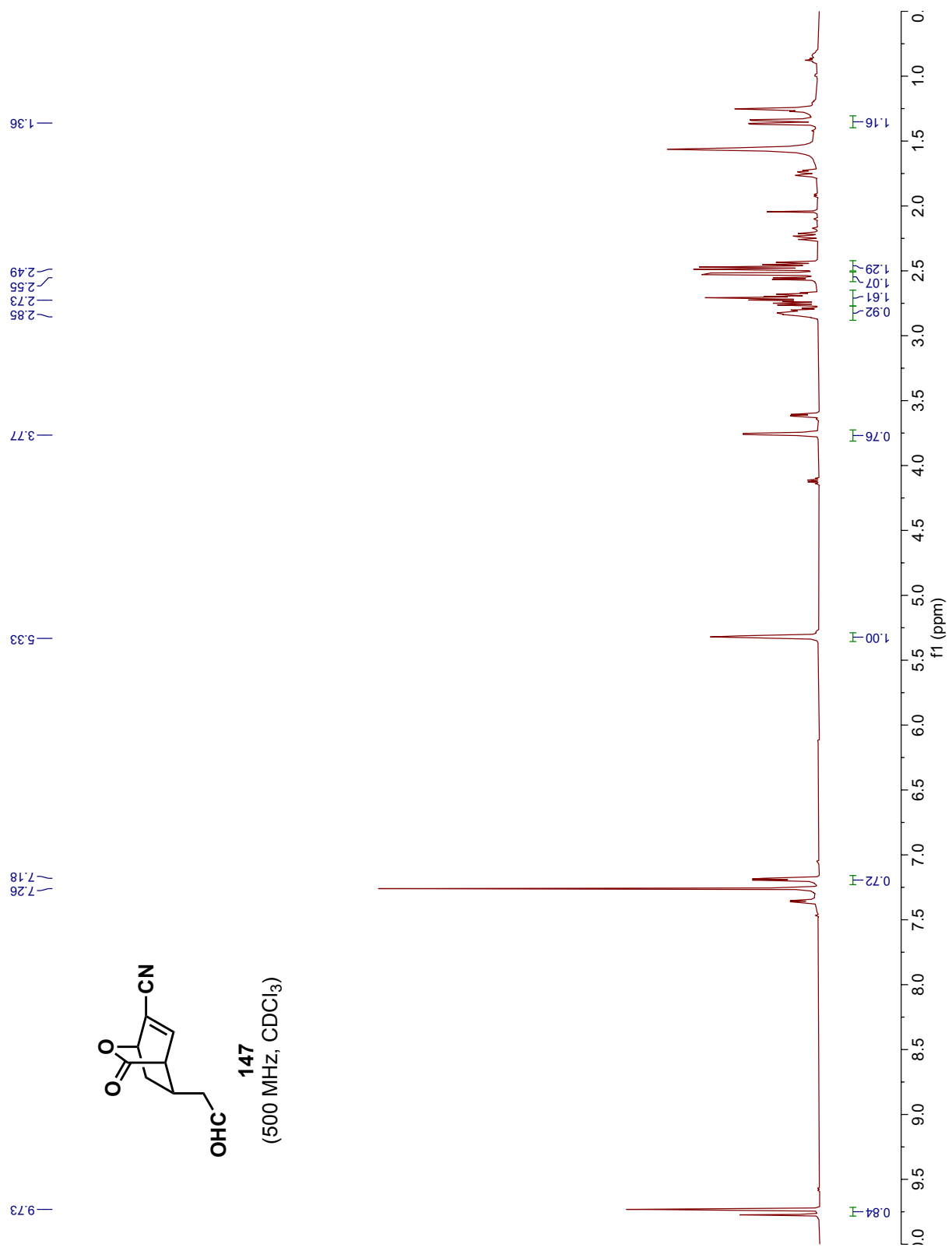
3.79
3.50
3.40
3.36
3.26
3.24
3.21
2.91
2.83
2.64
2.61

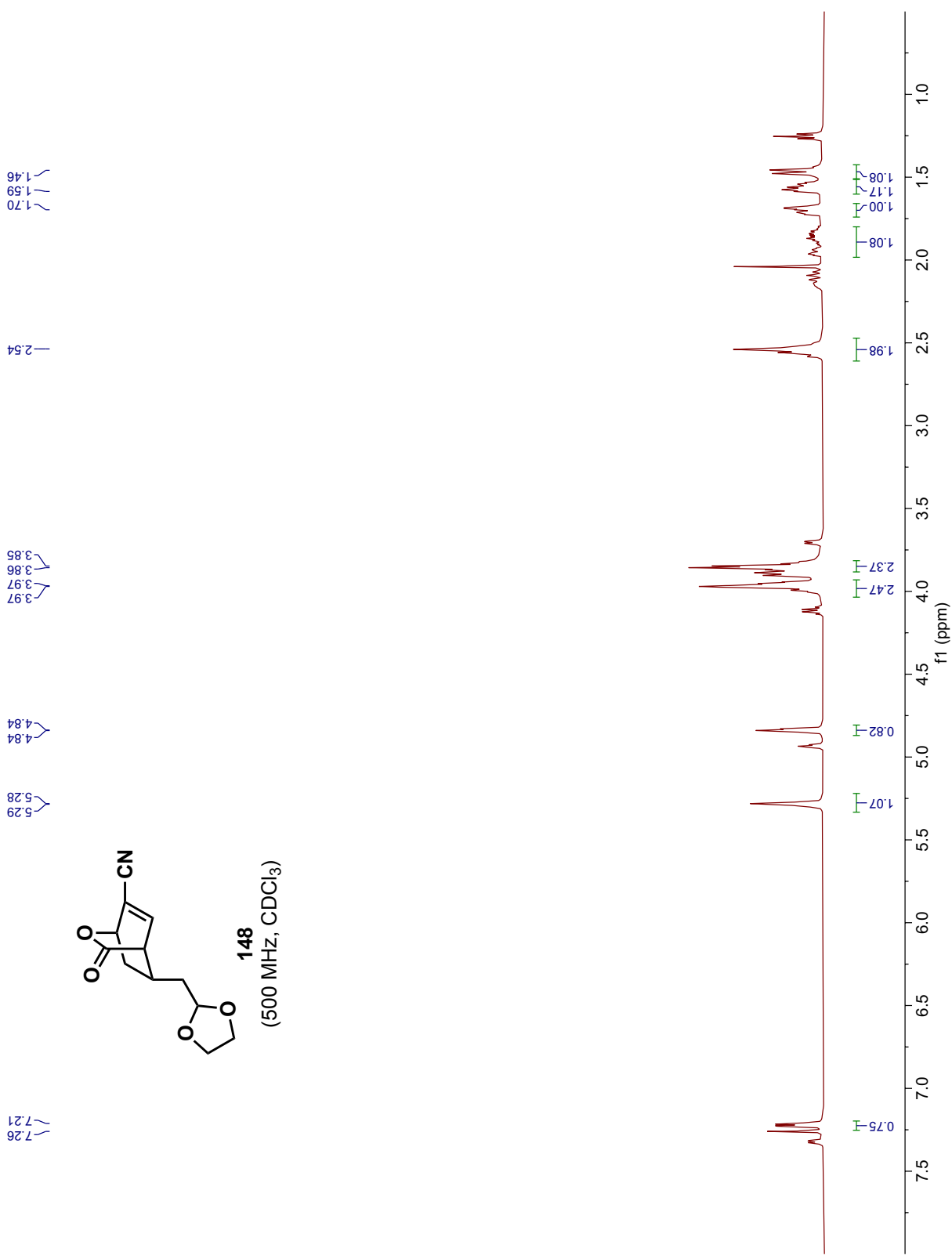
5.08

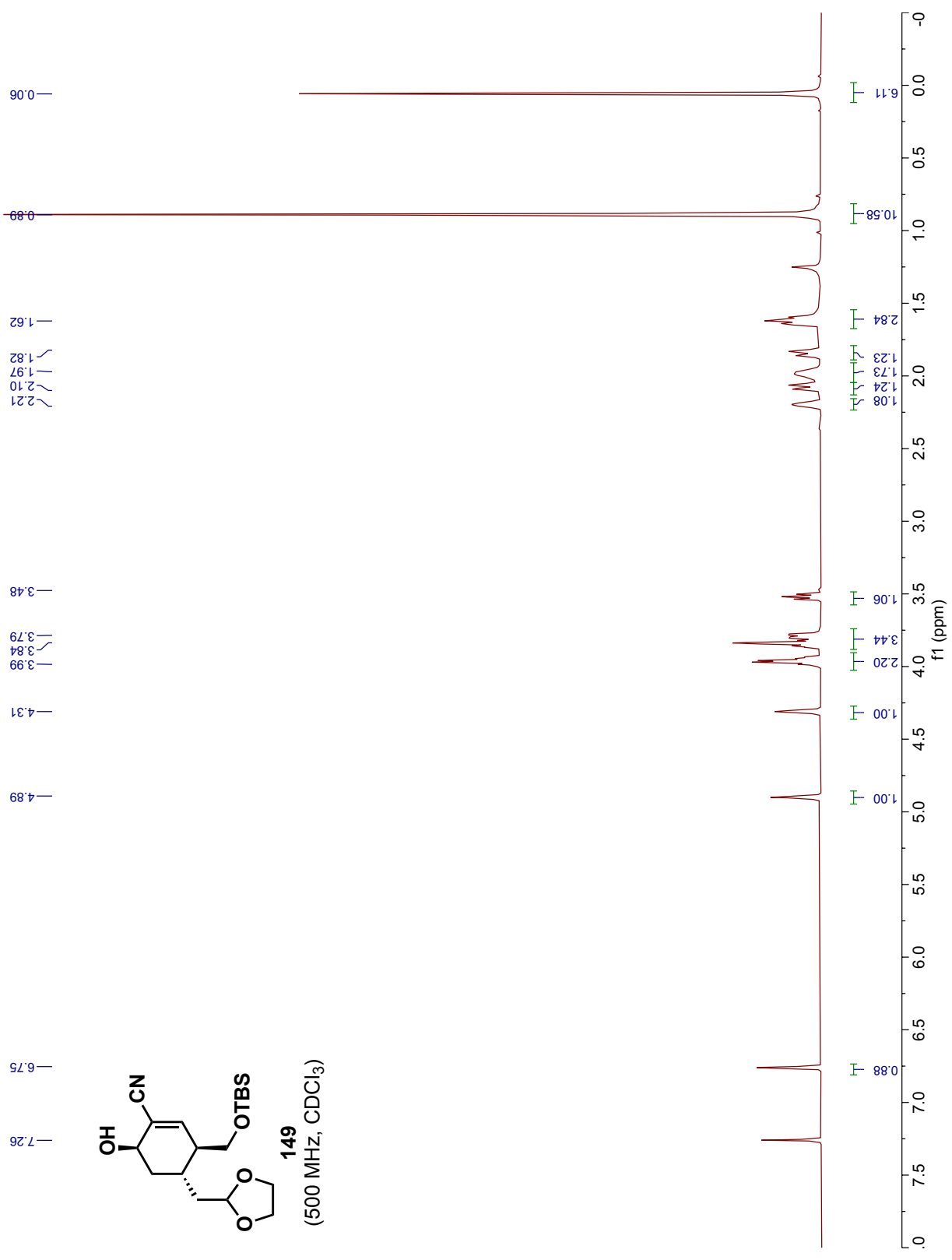
7.28
7.26
7.24
7.23
7.22

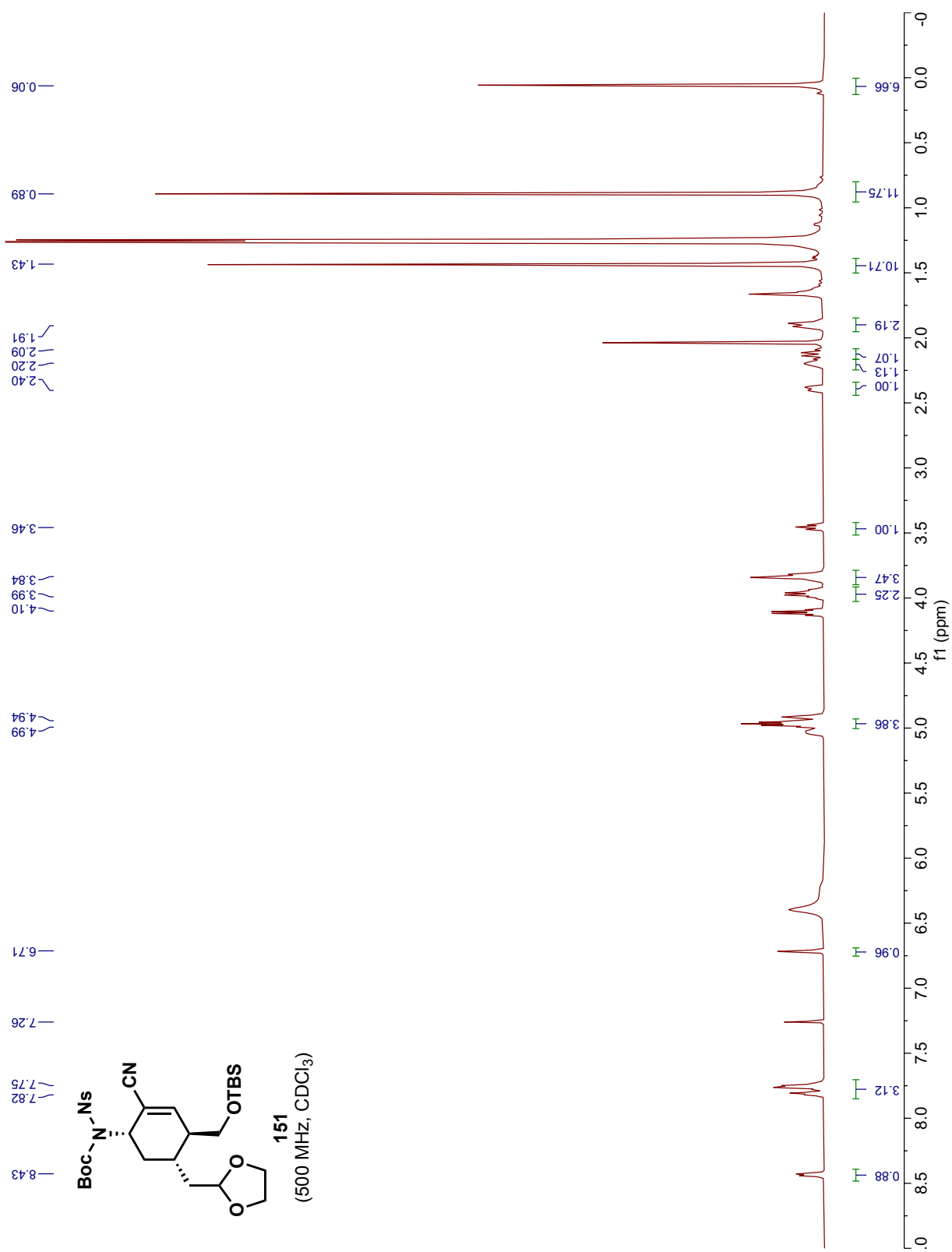


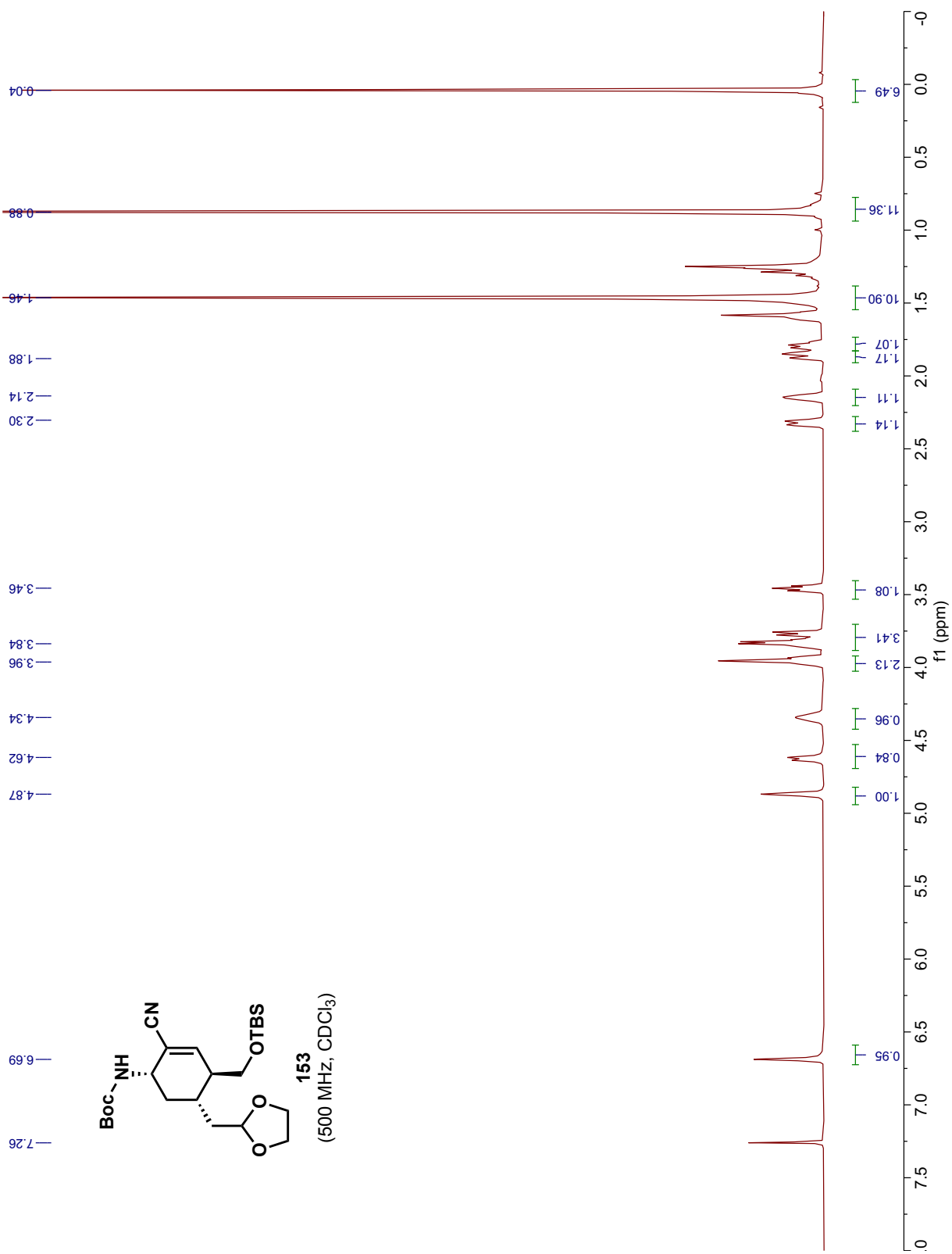


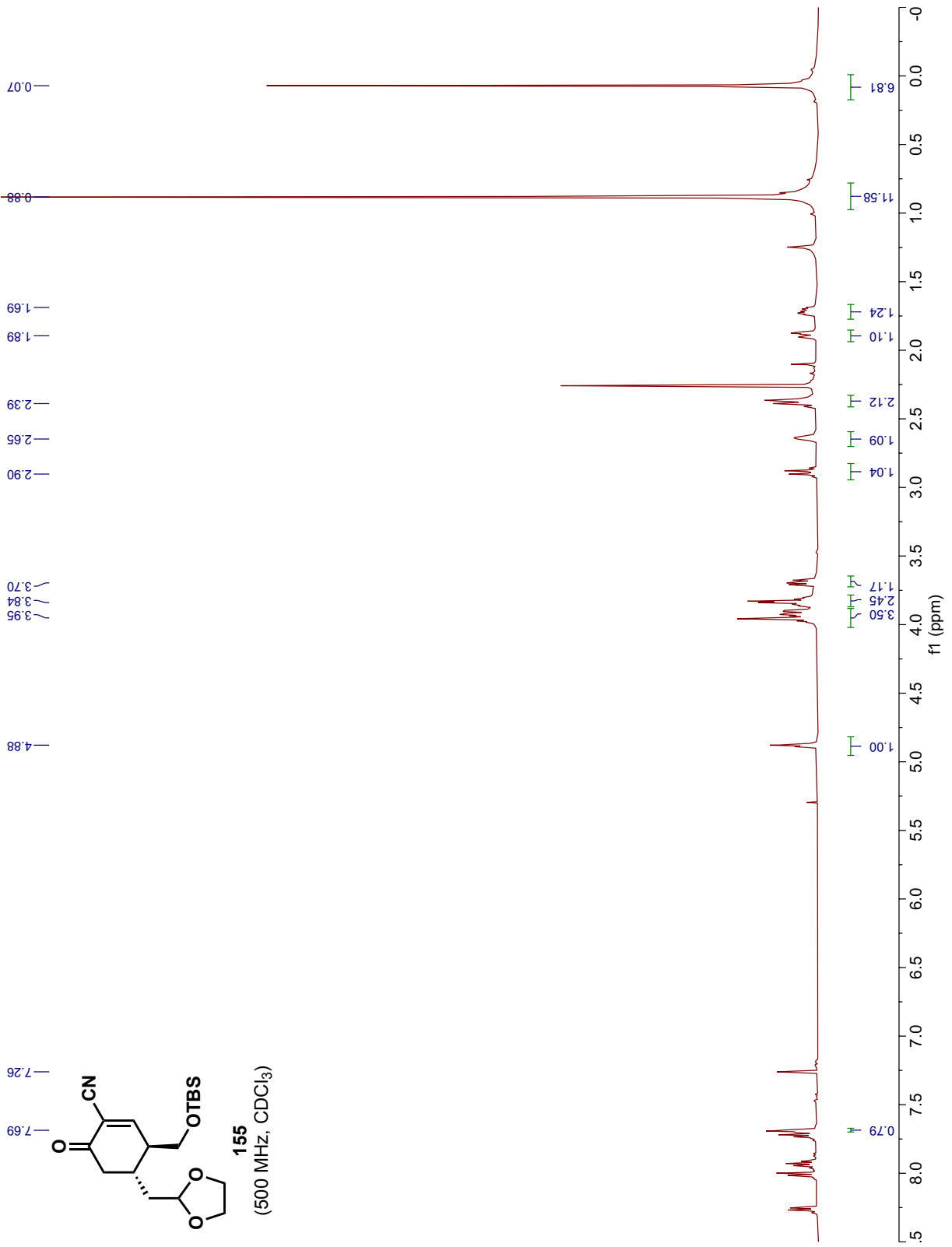
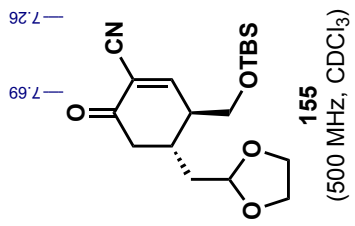


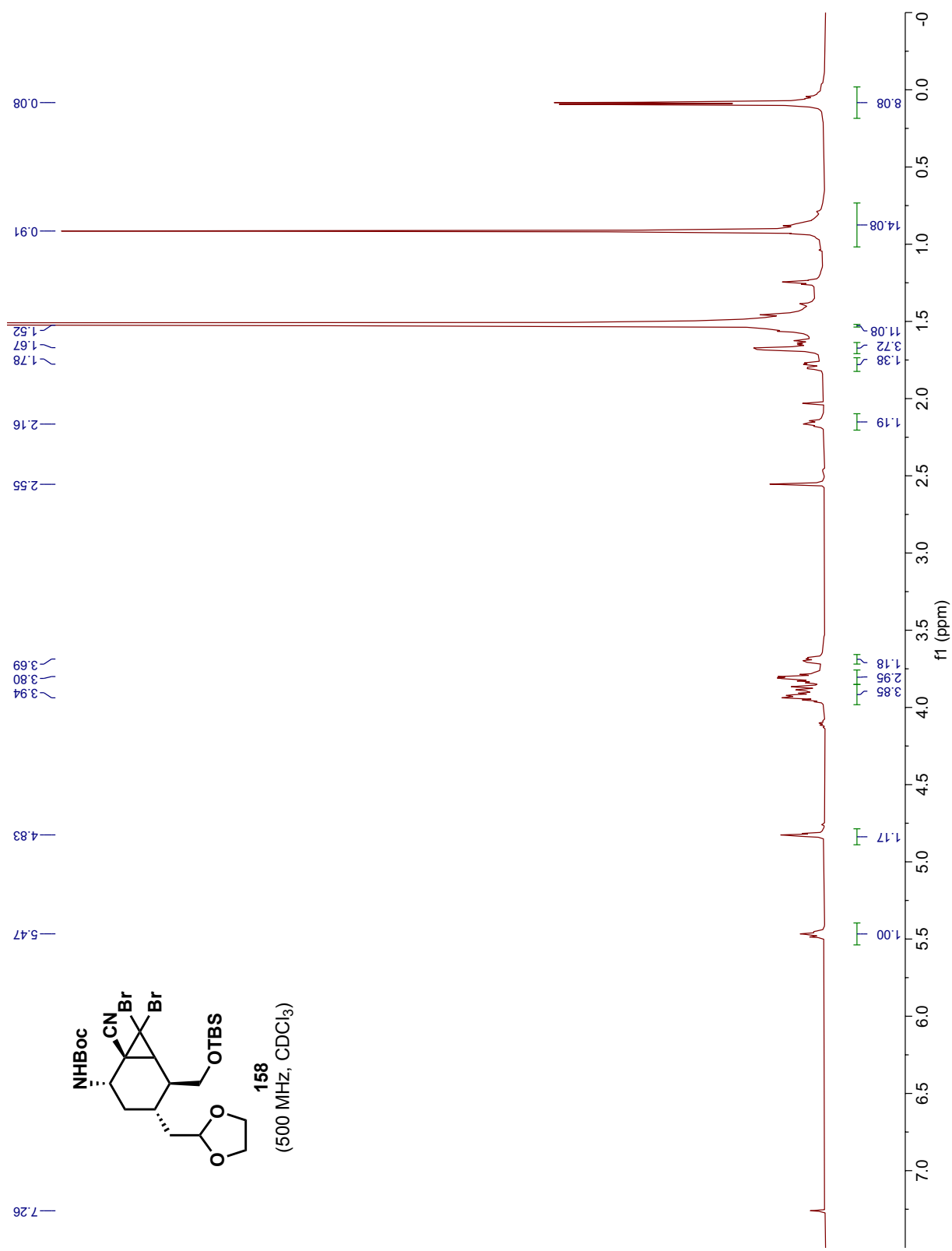


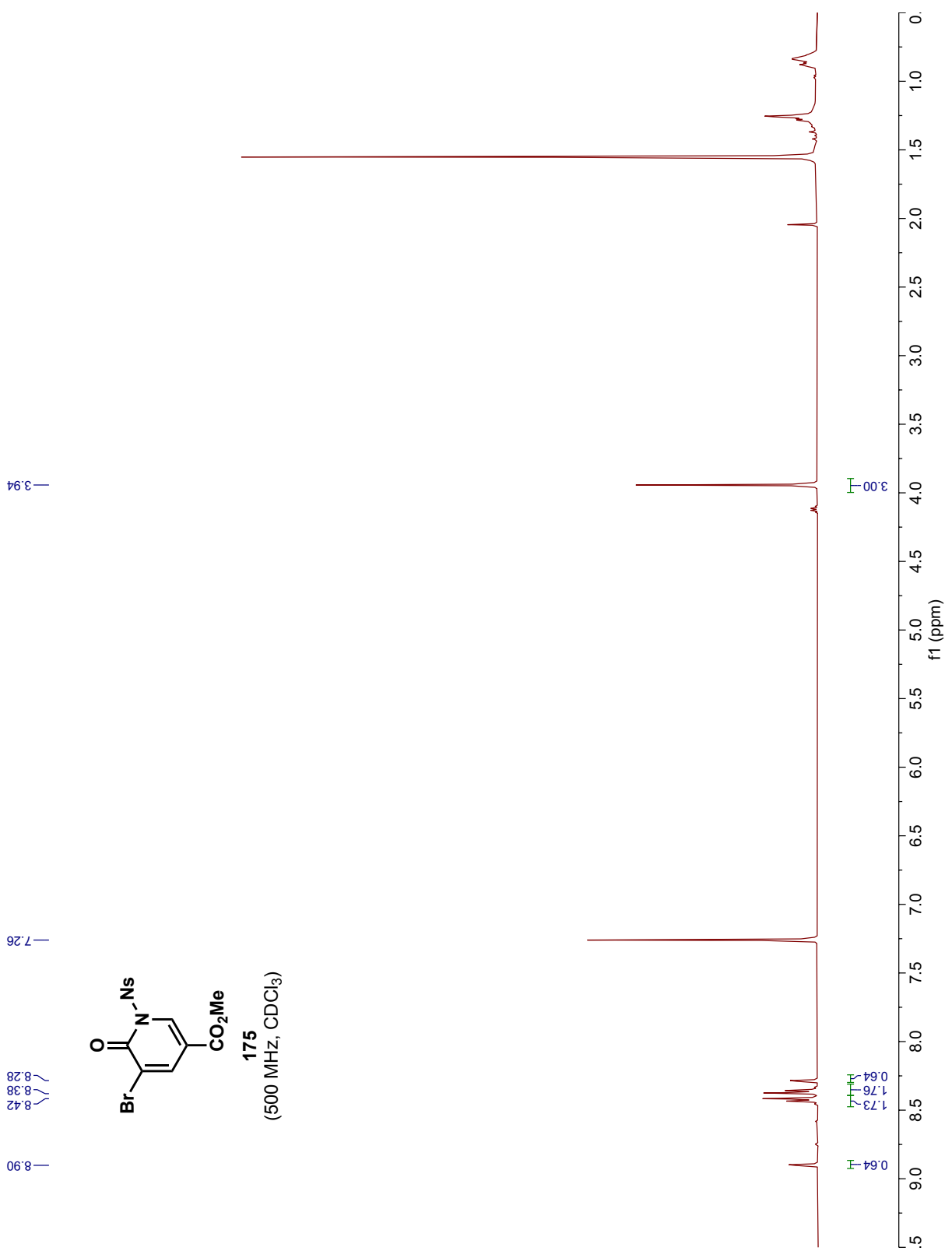


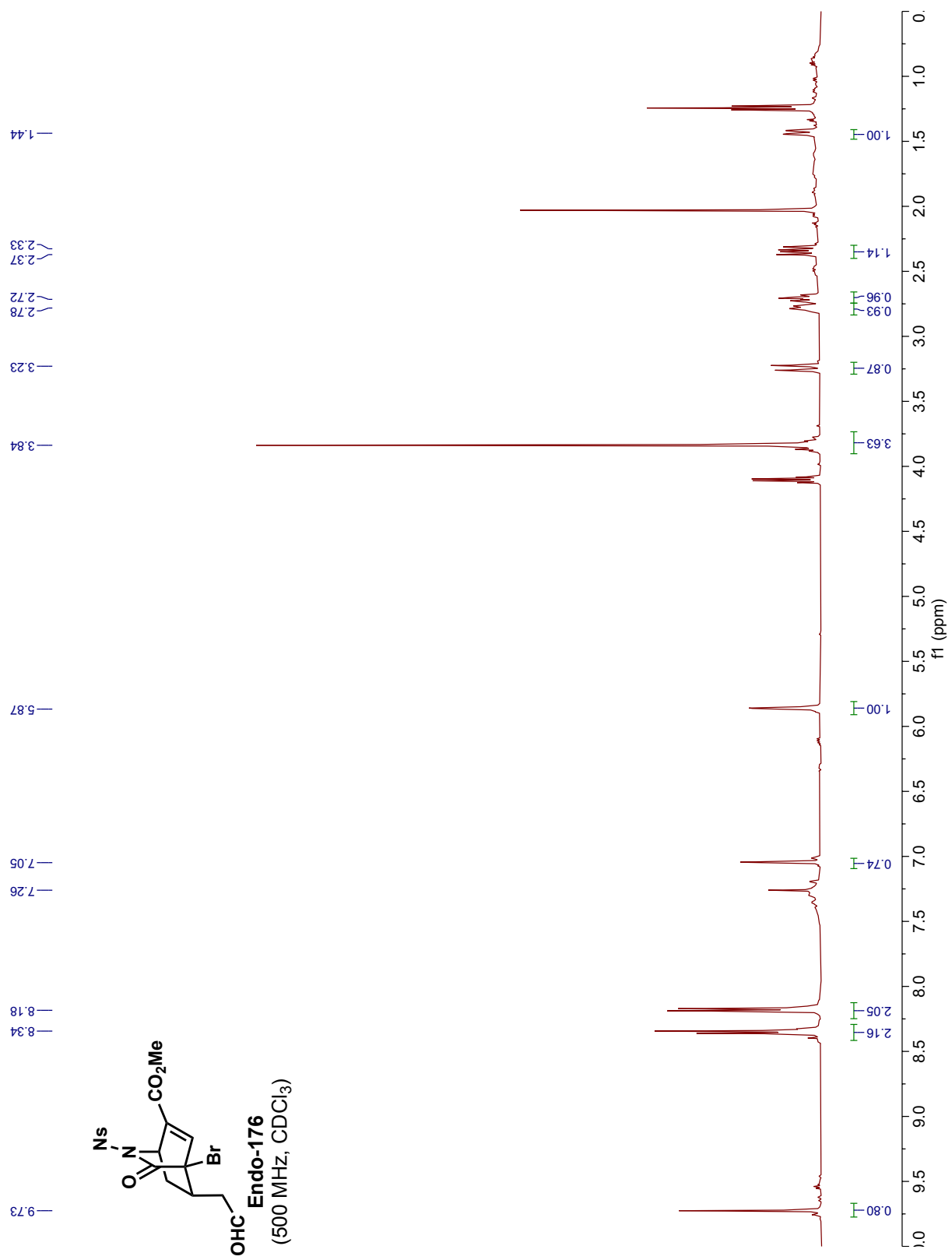


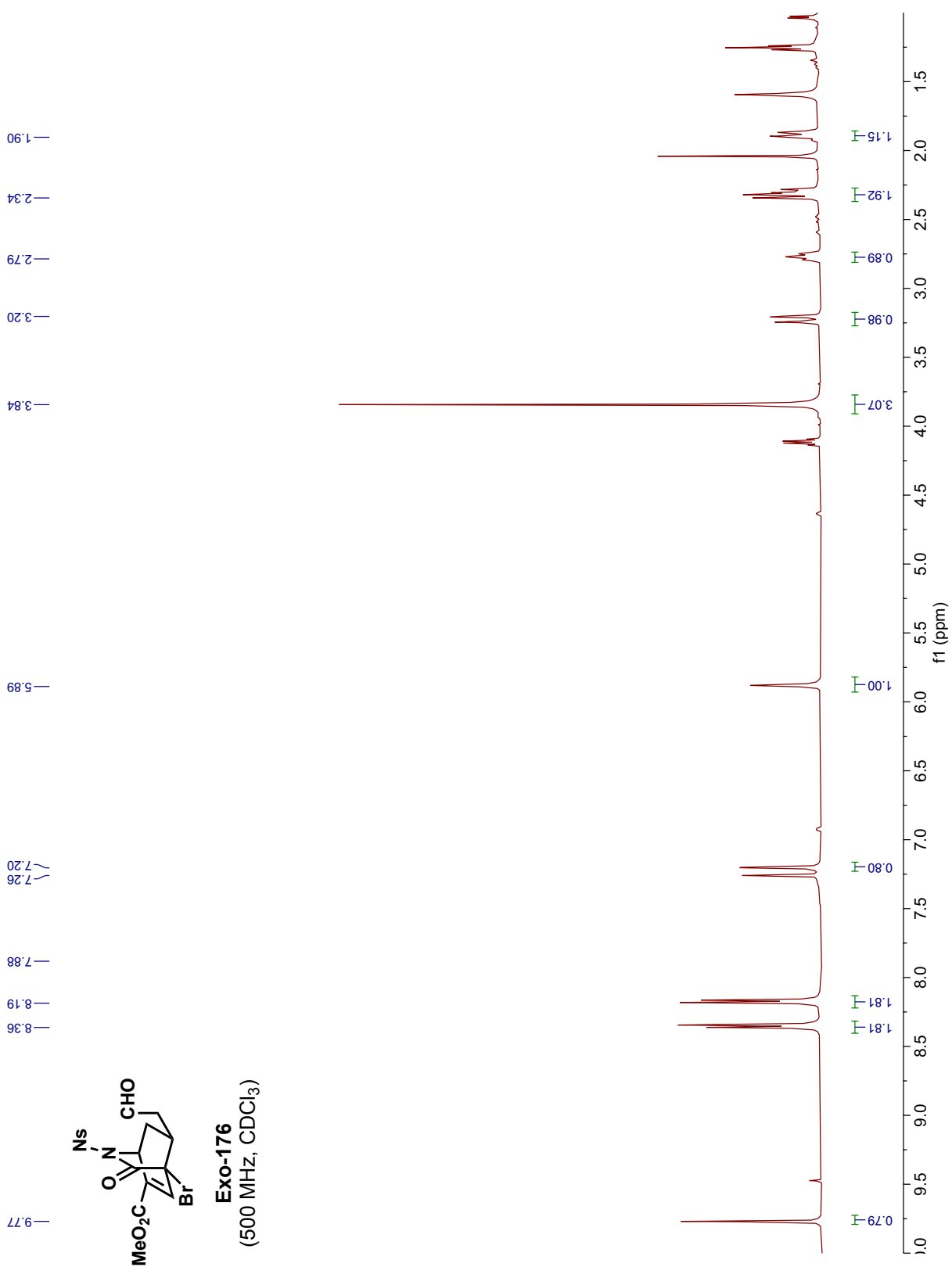






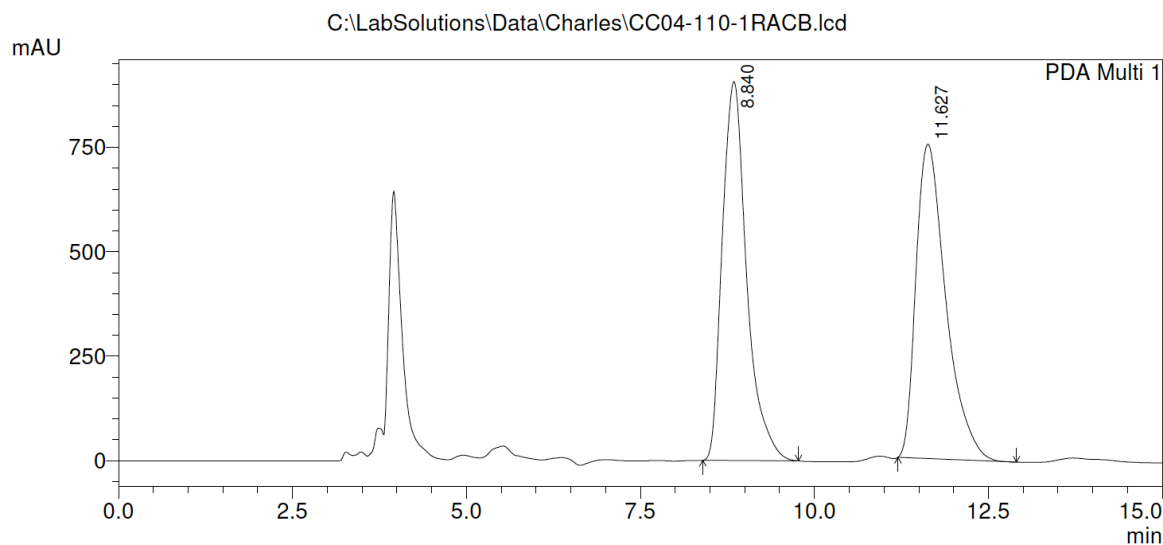






3.14 HPLC Traces (Note: All traces are of the corresponding Wittig products)

Racemic **Endo-88** (Chiralpak IA, Hexanes/*i*PrOH 85:15, 215 nm)

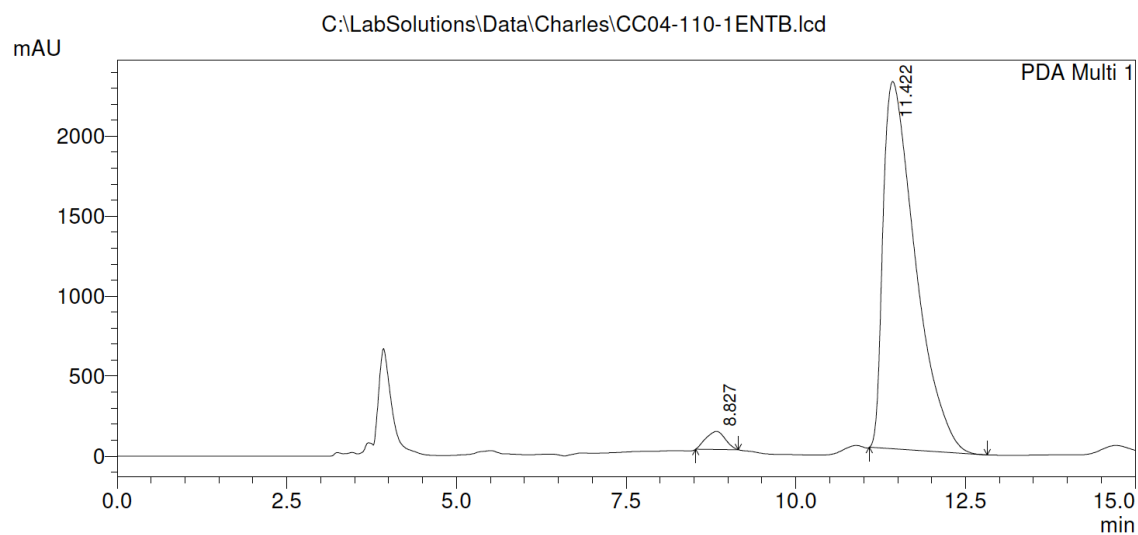


PeakTable

PDA Ch1 215nm 4nm

Peak#	Ret. Time	Area	Height	Area %	Height %
1	8.840	22126644	907466	49.559	54.668
2	11.627	22519980	752489	50.441	45.332
Total		44646624	1659956	100.000	100.000

Enantioenriched **Endo-88** (Chiralpak IA, Hexanes/*i*PrOH 85:15, 215 nm)

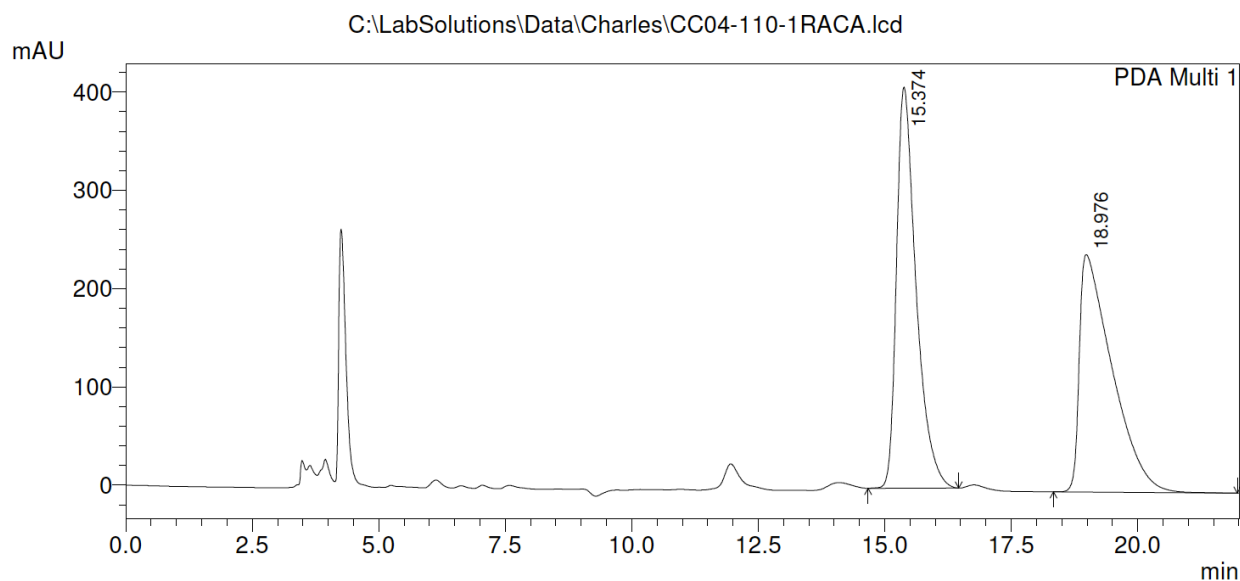


PeakTable

PDA Ch1 215nm 4nm

Peak#	Ret. Time	Area	Height	Area %	Height %
1	8.827	2233008	112841	2.841	4.682
2	11.422	76354430	2297192	97.159	95.318
Total		78587438	2410033	100.000	100.000

Racemic *Exo-88* (Chiralpak IA, Hexanes/*i*PrOH 90:10, 215 nm)

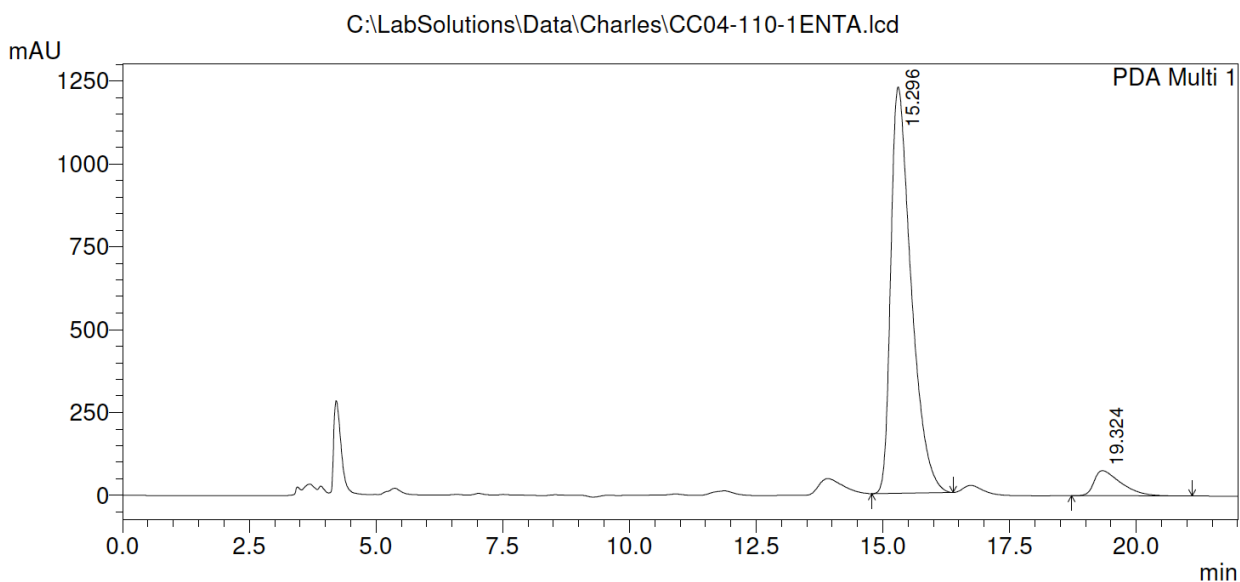


PeakTable

PDA Ch1 215nm 4nm

Peak#	Ret. Time	Area	Height	Area %	Height %
1	15.374	11016577	407996	50.358	62.802
2	18.976	10859945	241660	49.642	37.198
Total		21876522	649656	100.000	100.000

Enantioenriched *Exo-88* (Chiralpak IA, Hexanes/*i*PrOH 90:10, 215 nm)



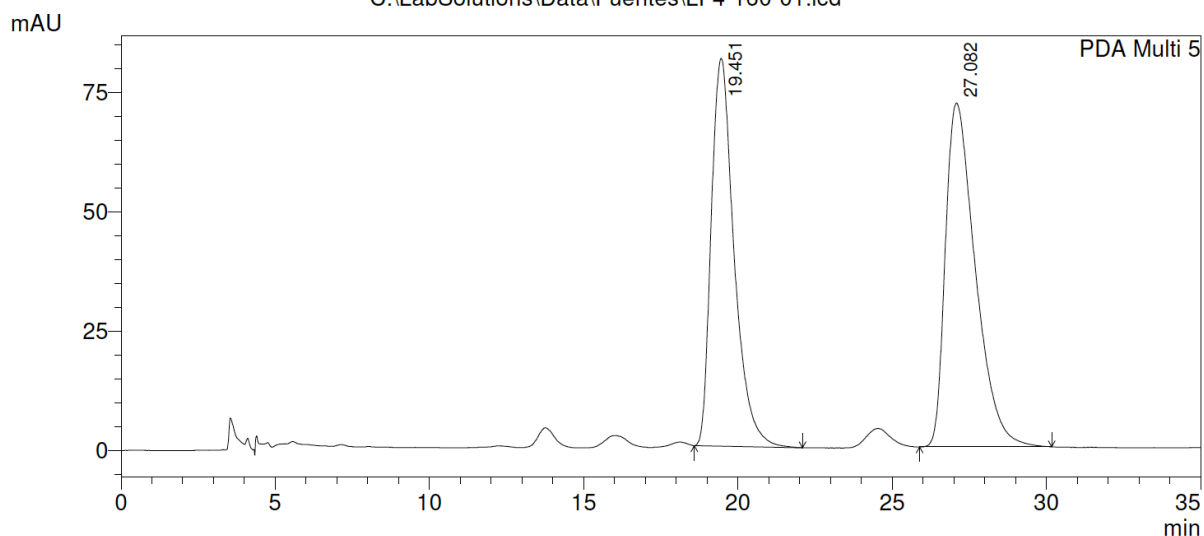
PeakTable

PDA Ch1 215nm 4nm

Peak#	Ret. Time	Area	Height	Area %	Height %
1	15.296	34284306	1225572	92.408	94.159
2	19.324	2816847	76021	7.592	5.841
Total		37101153	1301592	100.000	100.000

Racemic **Endo-102** (Chiralpak IA, Hexanes/*i*PrOH 95:5, 254 nm)

C:\LabSolutions\Data\Fuentes\LF4-160-01.lcd



1 PDA Multi 5/254nm 4nm

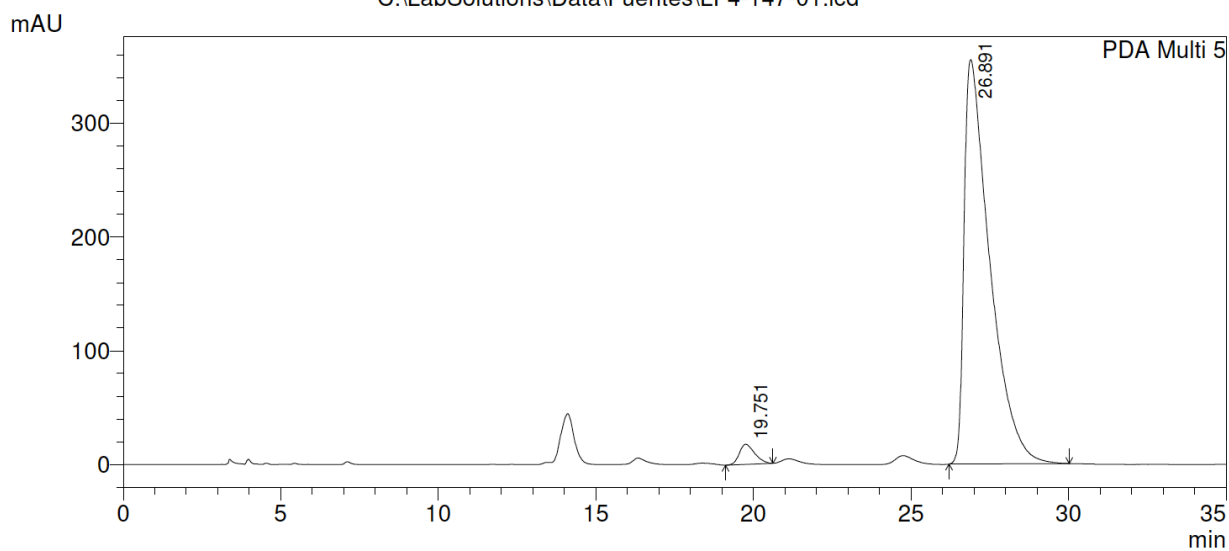
PeakTable

PDA Ch5 254nm 4nm

Peak#	Ret. Time	Area	Height	Area %	Height %
1	19.451	4186247	81240	46.243	52.996
2	27.082	4866430	72055	53.757	47.004
Total		9052677	153295	100.000	100.000

Enantioenriched **Endo-102** (Chiralpak IA, Hexanes/*i*PrOH 95:5, 254 nm)

C:\LabSolutions\Data\Fuentes\LF4-147-01.lcd



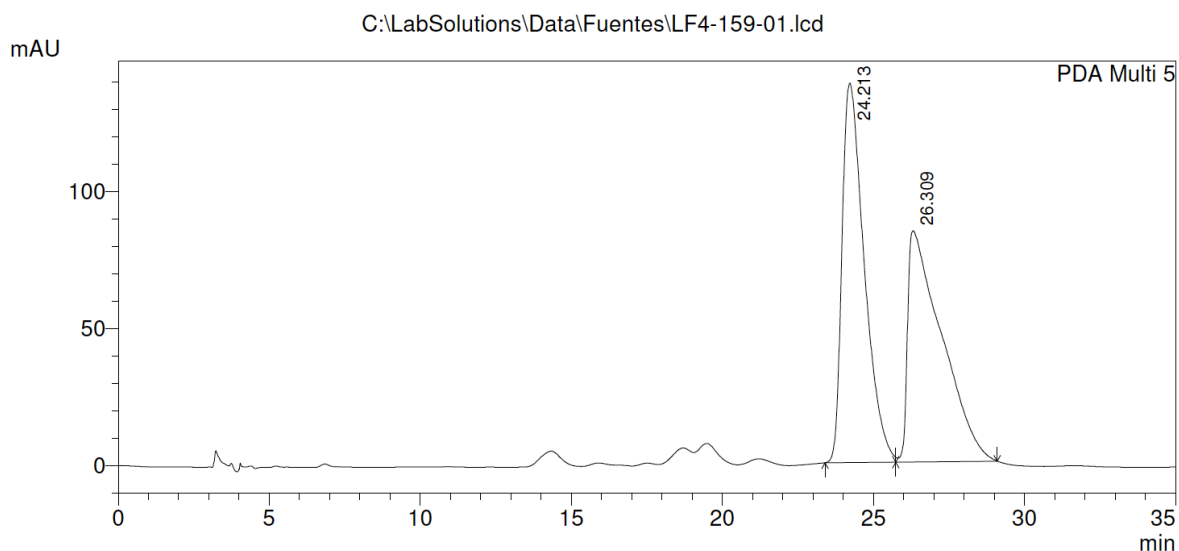
1 PDA Multi 5/254nm 4nm

PeakTable

PDA Ch5 254nm 4nm

Peak#	Ret. Time	Area	Height	Area %	Height %
1	19.751	596314	17664	2.879	4.735
2	26.891	20116790	355351	97.121	95.265
Total		20713105	373014	100.000	100.000

Racemic *Exo-102* (Chiralpak IA, Hexanes/*i*PrOH 95:5, 254 nm)



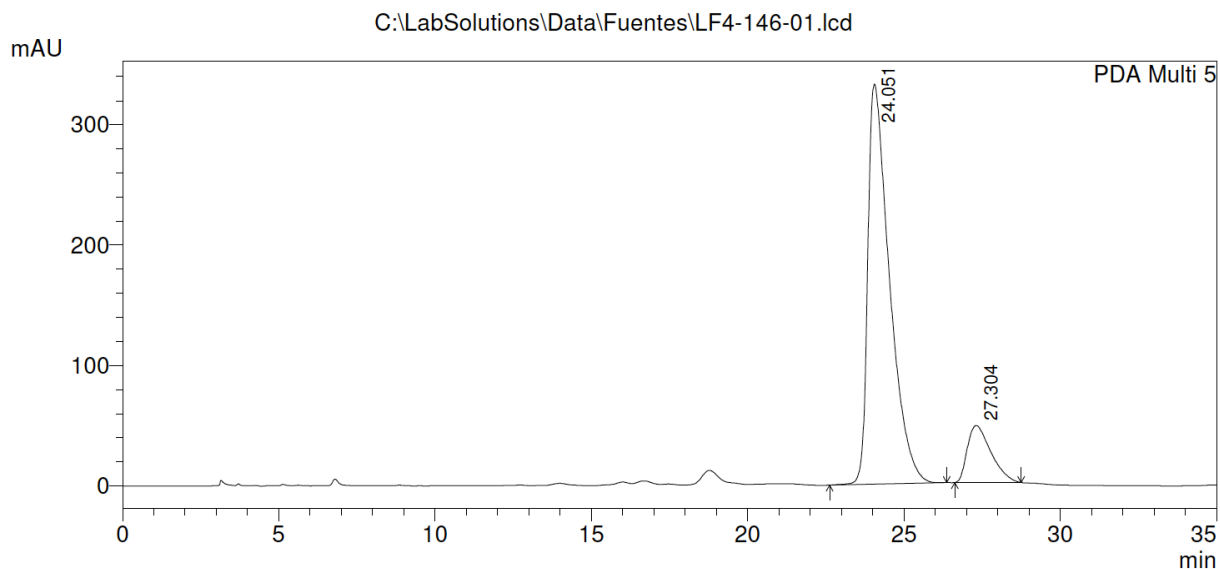
1 PDA Multi 5/254nm 4nm

PeakTable

PDA Ch5 254nm 4nm

Peak#	Ret. Time	Area	Height	Area %	Height %
1	24.213	7093311	138542	51.733	62.132
2	26.309	6618194	84440	48.267	37.868
Total		13711505	222982	100.000	100.000

Enantioenriched *Exo-102* (Chiralpak IA, Hexanes/*i*PrOH 95:5, 254 nm)



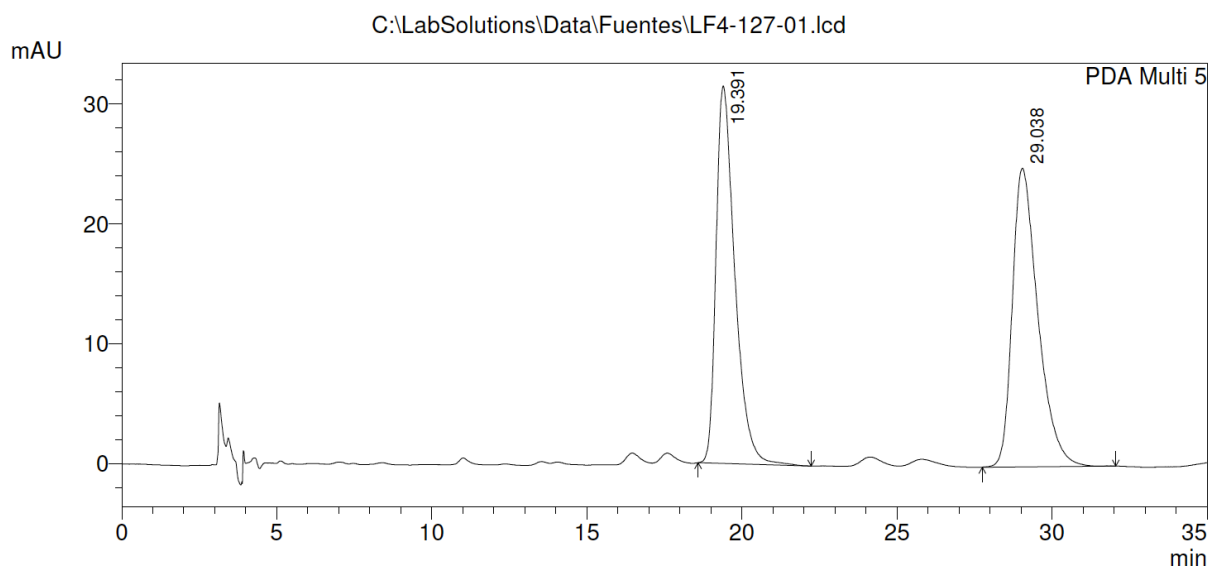
1 PDA Multi 5/254nm 4nm

PeakTable

PDA Ch5 254nm 4nm

Peak#	Ret. Time	Area	Height	Area %	Height %
1	24.051	16033603	332290	86.572	87.527
2	27.304	2486878	47354	13.428	12.473
Total		18520481	379644	100.000	100.000

Racemic **Endo-103** (Chiralpak IA, Hexanes/*i*PrOH 95:5, 254 nm)

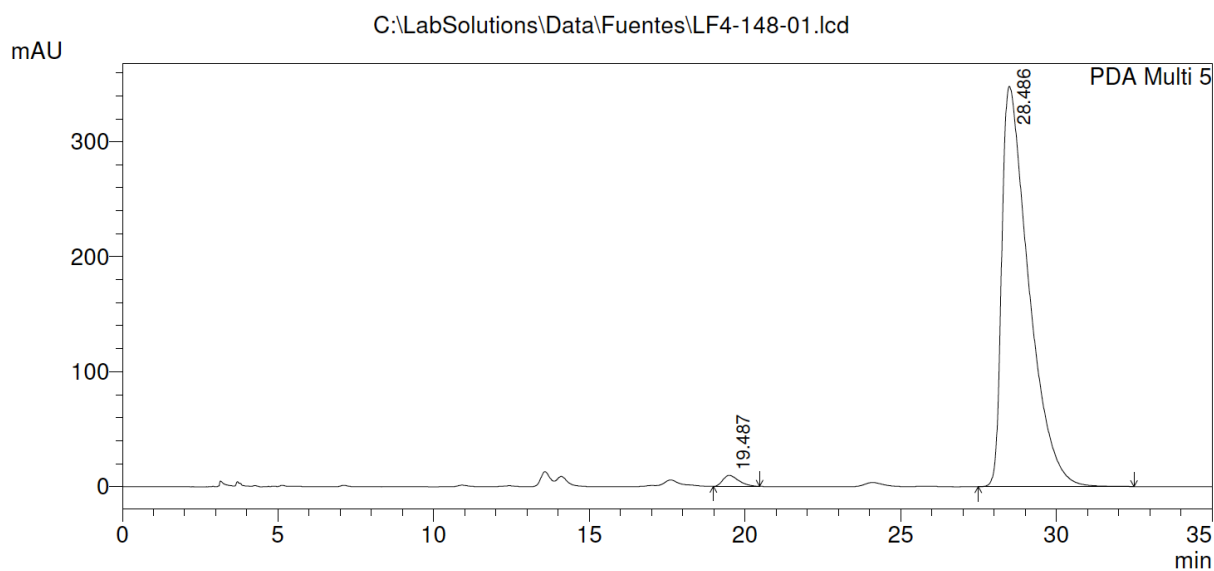


PeakTable

PDA Ch5 254nm 4nm

Peak#	Ret. Time	Area	Height	Area %	Height %
1	19.391	1326560	31475	48.151	55.827
2	29.038	1428418	24904	51.849	44.173
Total		2754978	56379	100.000	100.000

Enantioenriched **Endo-103** (Chiralpak IA, Hexanes/*i*PrOH 95:5, 254 nm)

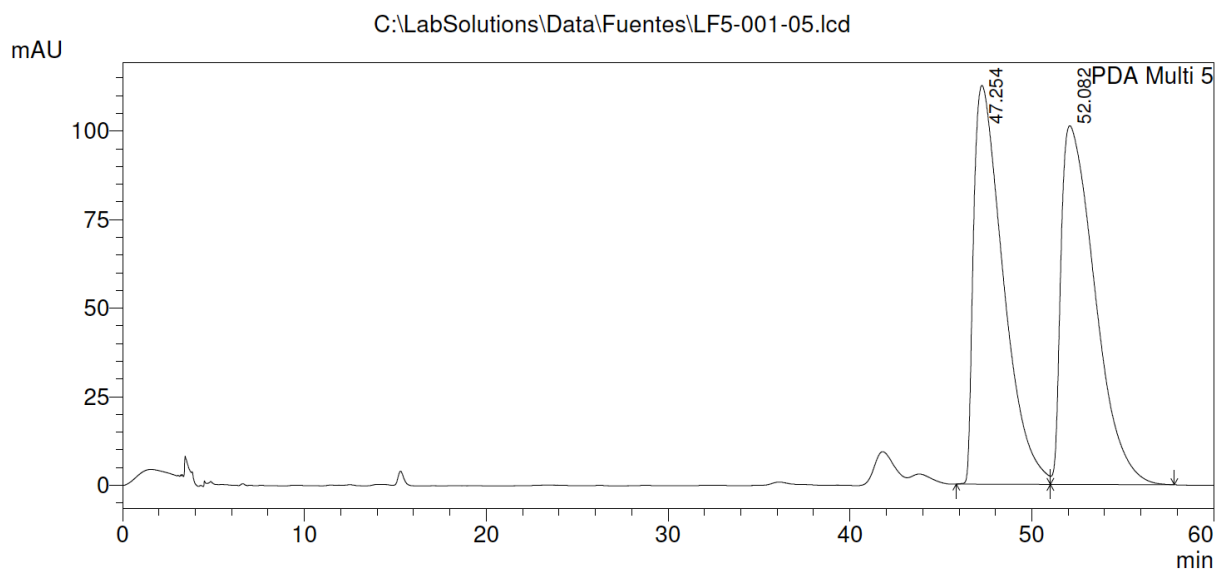


PeakTable

PDA Ch5 254nm 4nm

Peak#	Ret. Time	Area	Height	Area %	Height %
1	19.487	339093	9531	1.595	2.664
2	28.486	20918263	348244	98.405	97.336
Total		21257356	357776	100.000	100.000

Racemic **Endo-104** (Chiralpak AD-H, Hexanes/*i*PrOH 98:2, 254 nm)

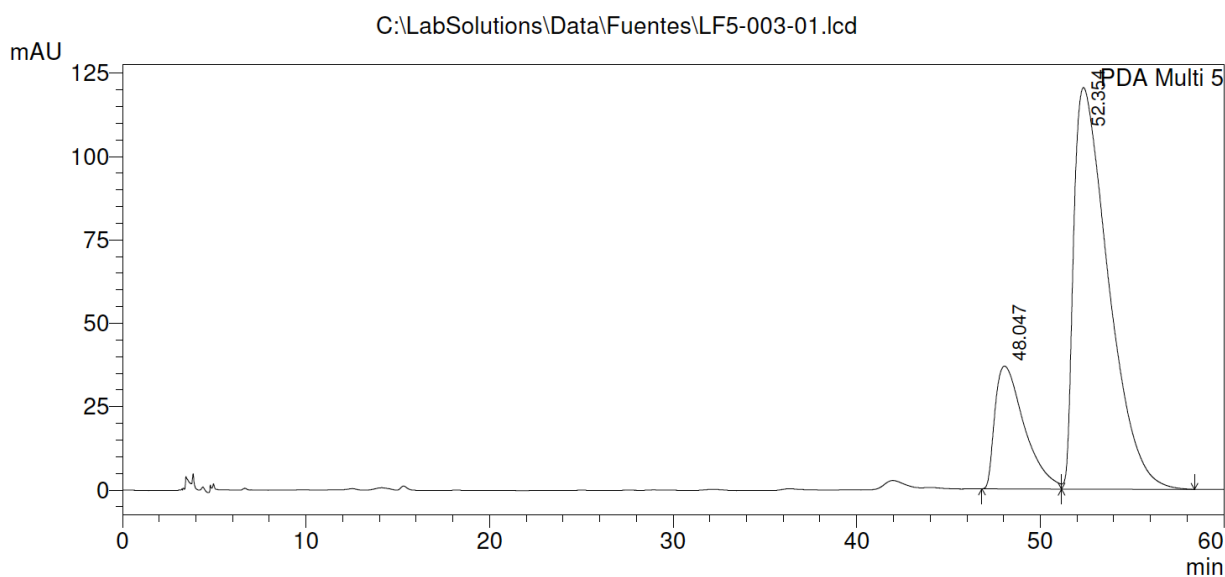


PeakTable

PDA Ch5 254nm 4nm

Peak#	Ret. Time	Area	Height	Area %	Height %
1	47.254	12710315	112585	49.179	52.636
2	52.082	13134708	101309	50.821	47.364
Total		25845024	213894	100.000	100.000

Enantioenriched **Endo-104** (Chiralpak AD-H, Hexanes/*i*PrOH 98:2, 254 nm)

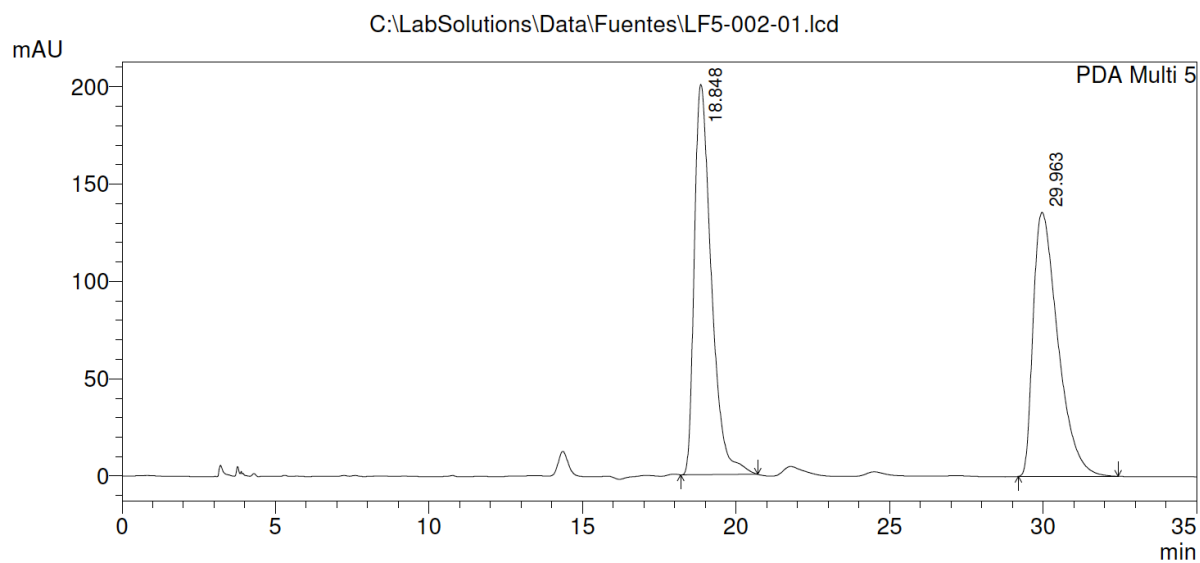


PeakTable

PDA Ch5 254nm 4nm

Peak#	Ret. Time	Area	Height	Area %	Height %
1	48.047	4095815	36791	20.600	23.414
2	52.354	15786664	120341	79.400	76.586
Total		19882479	157132	100.000	100.000

Racemic **Exo-104** (Chiralpak AD-H, Hexanes/*i*PrOH 95:5, 254 nm)

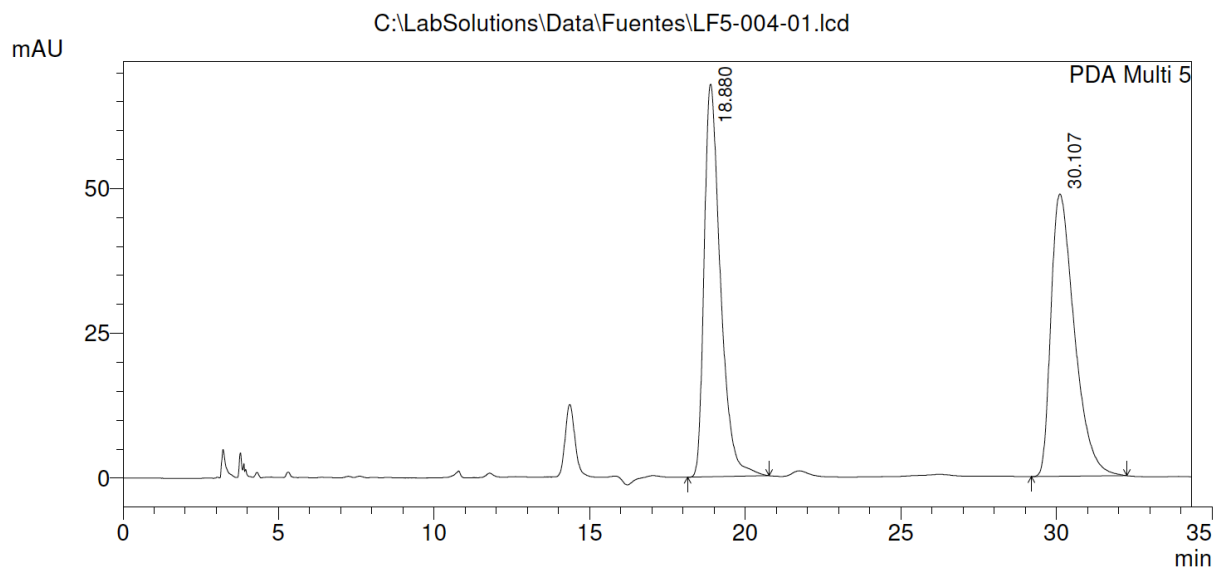


PeakTable

PDA Ch5 254nm 4nm

Peak#	Ret. Time	Area	Height	Area %	Height %
1	18.848	7743431	200541	50.509	59.646
2	29.963	7587340	135679	49.491	40.354
Total		15330771	336220	100.000	100.000

Enantioenriched **Exo-104** (Chiralpak AD-H, Hexanes/*i*PrOH 95:5, 254 nm)

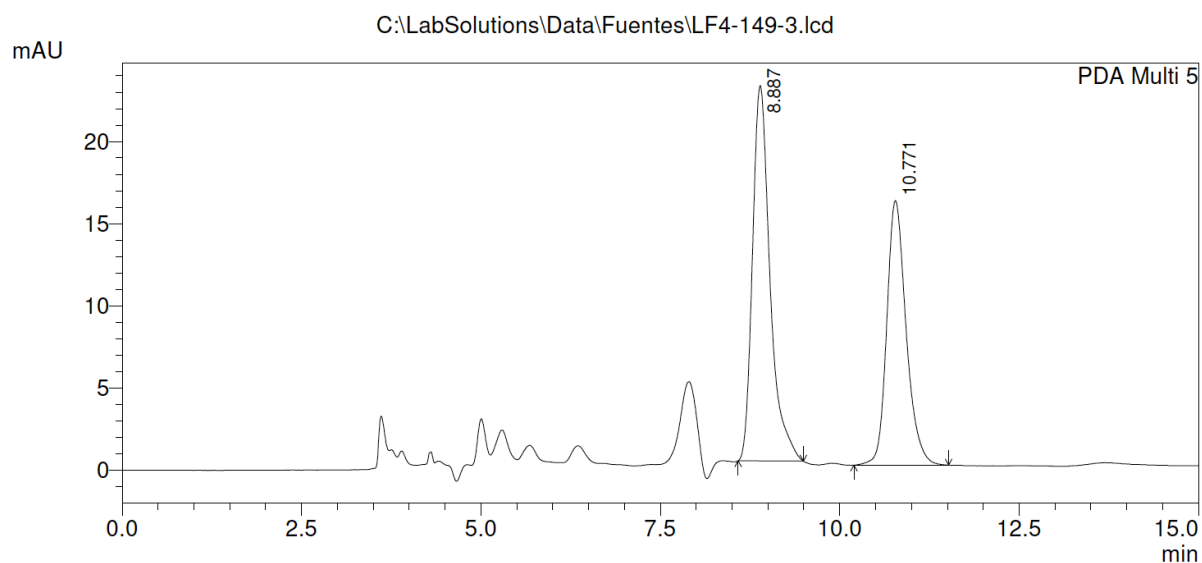


PeakTable

PDA Ch5 254nm 4nm

Peak#	Ret. Time	Area	Height	Area %	Height %
1	18.880	2465971	67753	49.089	58.148
2	30.107	2557515	48765	50.911	41.852
Total		5023486	116518	100.000	100.000

Racemic **Endo-105** (Chiralpak AD-H, Hexanes/*i*PrOH 90:10, 254 nm)

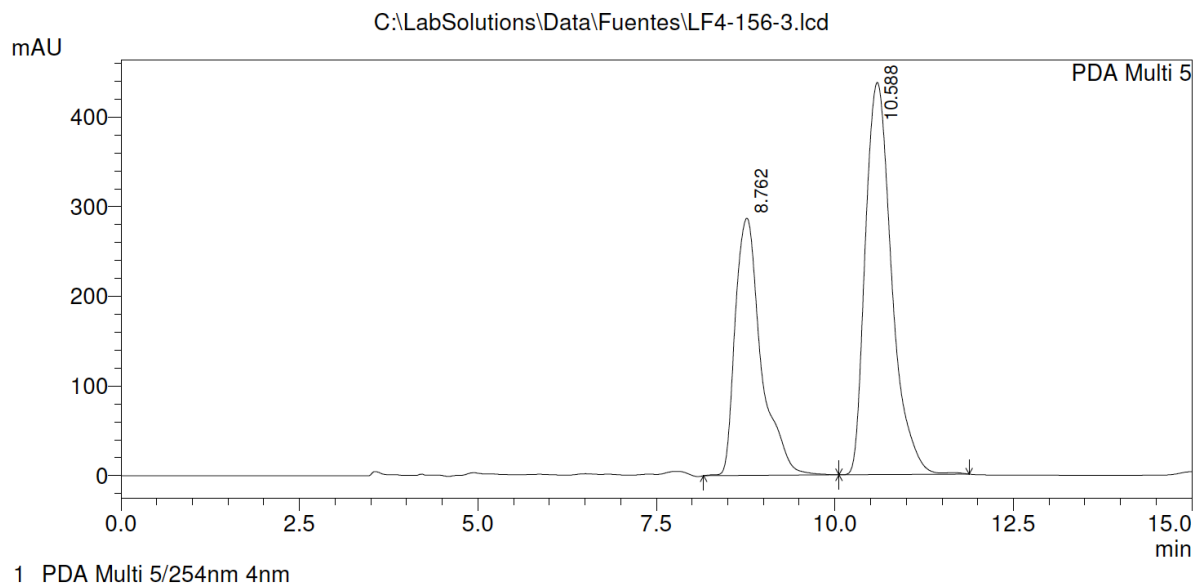


PeakTable

PDA Ch5 254nm 4nm

Peak#	Ret. Time	Area	Height	Area %	Height %
1	8.887	387775	22837	56.163	58.638
2	10.771	302676	16109	43.837	41.362
Total		690451	38946	100.000	100.000

Enantioenriched **Endo-105** (Chiralpak AD-H, Hexanes/*i*PrOH 90:10, 254 nm)

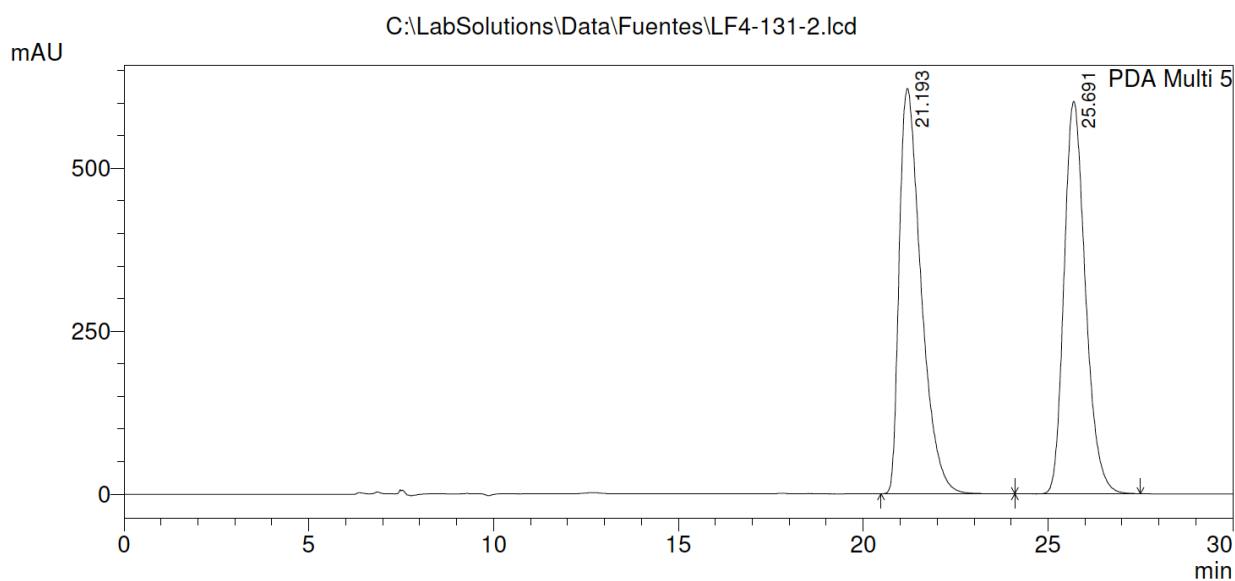


PeakTable

PDA Ch5 254nm 4nm

Peak#	Ret. Time	Area	Height	Area %	Height %
1	8.762	7284760	287052	39.305	39.617
2	10.588	11249382	437517	60.695	60.383
Total		18534142	724569	100.000	100.000

Racemic **Endo-106** (Chiralpak AD-H, Hexanes/*i*PrOH 90:10, 254 nm)



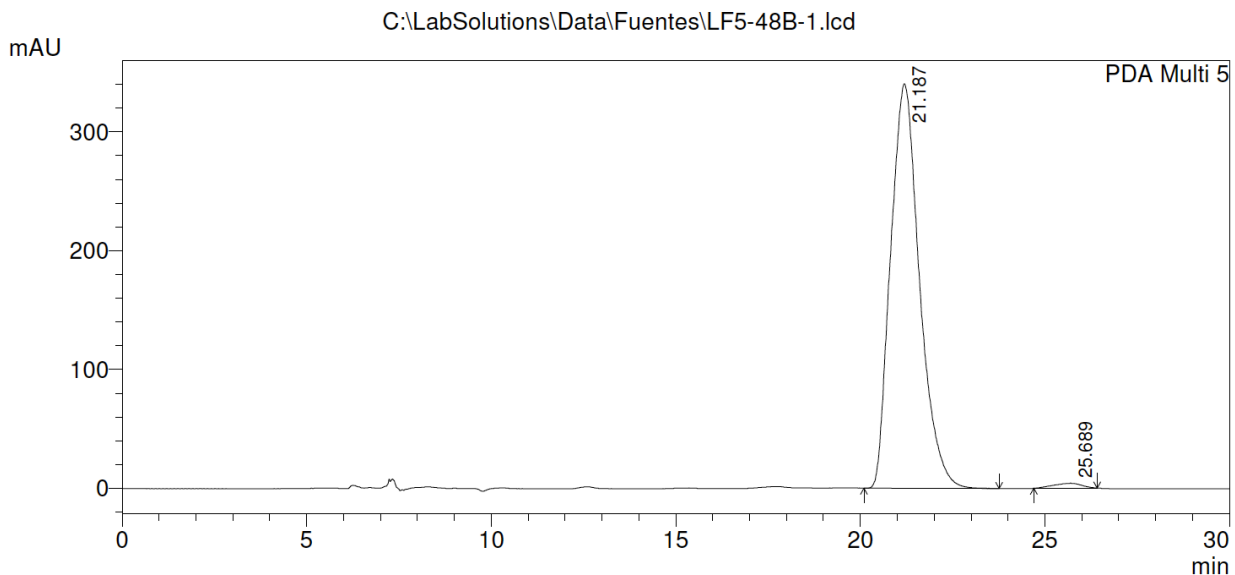
1 PDA Multi 5/254nm 4nm

PeakTable

PDA Ch5 254nm 4nm

Peak#	Ret. Time	Area	Height	Area %	Height %
1	21.193	25489356	621522	51.261	50.816
2	25.691	24235125	601561	48.739	49.184
Total		49724481	1223083	100.000	100.000

Enantioenriched **Endo-106** (Chiralpak AD-H, Hexanes/*i*PrOH 90:10, 254 nm)



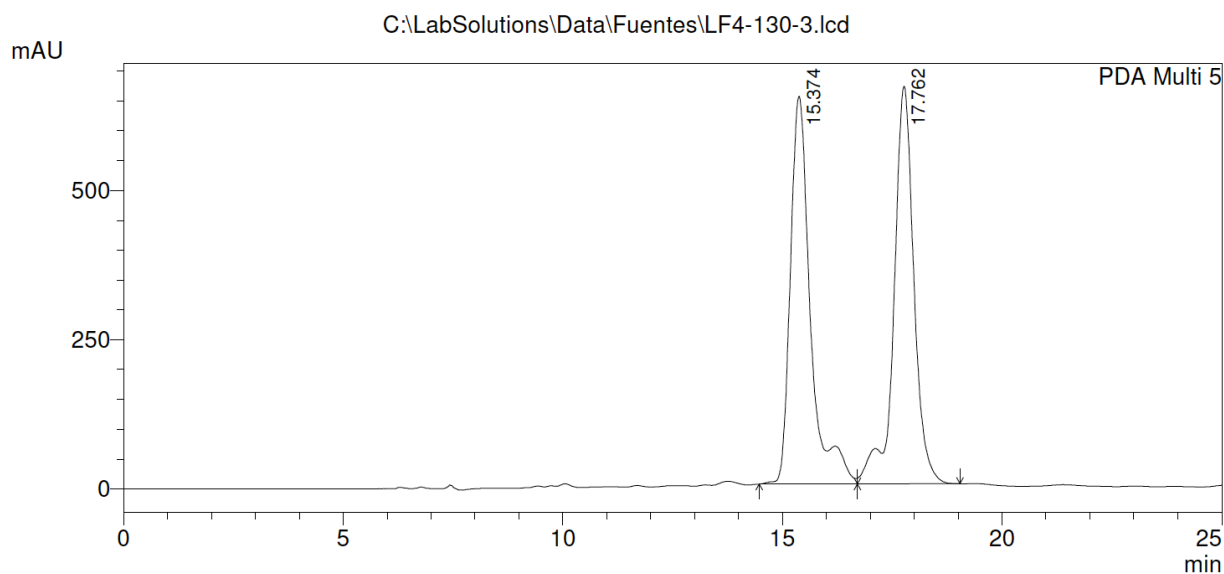
1 PDA Multi 5/254nm 4nm

PeakTable

PDA Ch5 254nm 4nm

Peak#	Ret. Time	Area	Height	Area %	Height %
1	21.187	18521991	340585	98.839	98.802
2	25.689	217473	4130	1.161	1.198
Total		18739464	344715	100.000	100.000

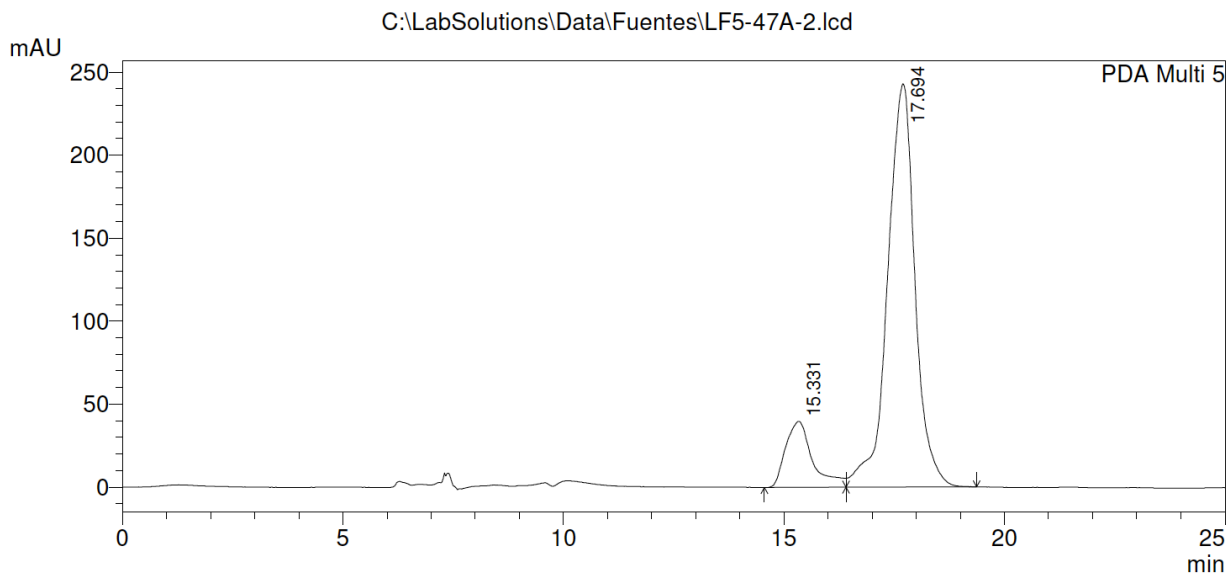
Racemic *Exo-106* (Chiralpak IA, Hexanes/*i*PrOH 95:5, 254 nm)



PeakTable

Peak#	Ret. Time	Area	Height	Area %	Height %
1	15.374	20628486	649720	49.363	49.379
2	17.762	21160831	666053	50.637	50.621
Total		41789316	1315772	100.000	100.000

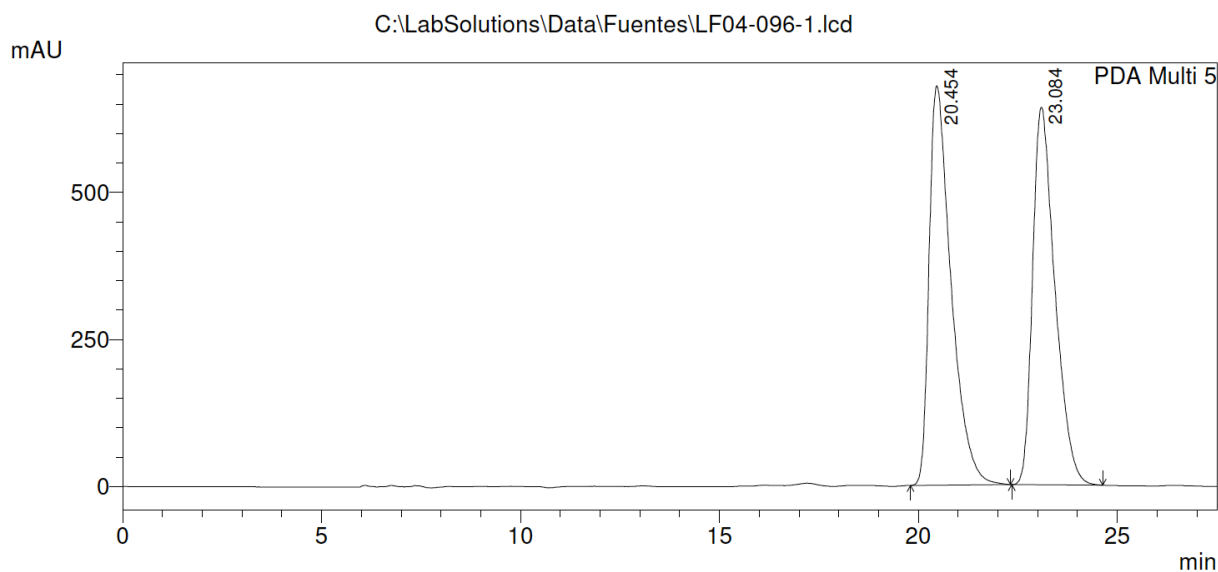
Enantioenriched *Exo-106* (Chiralpak IA, Hexanes/*i*PrOH 95:5, 254 nm)



PeakTable

Peak#	Ret. Time	Area	Height	Area %	Height %
1	15.331	1695204	39752	13.925	14.062
2	17.694	10478688	242937	86.075	85.938
Total		12173892	282689	100.000	100.000

Racemic **Endo-107** (Chiralpak IA, Hexanes/*i*PrOH 90:10, 254 nm)

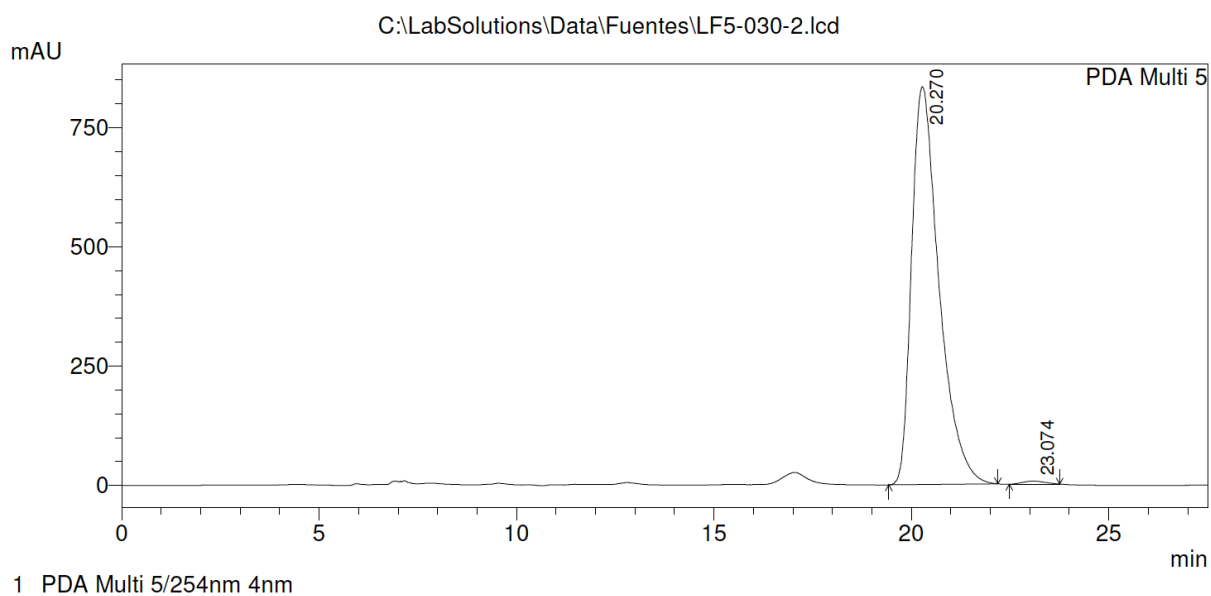


PeakTable

PDA Ch5 254nm 4nm

Peak#	Ret. Time	Area	Height	Area %	Height %
1	20.454	26084674	679301	51.002	51.416
2	23.084	25059770	641879	48.998	48.584
Total		51144444	1321180	100.000	100.000

Enantioenriched **Endo-107** (Chiralpak IA, Hexanes/*i*PrOH 90:10, 254 nm)

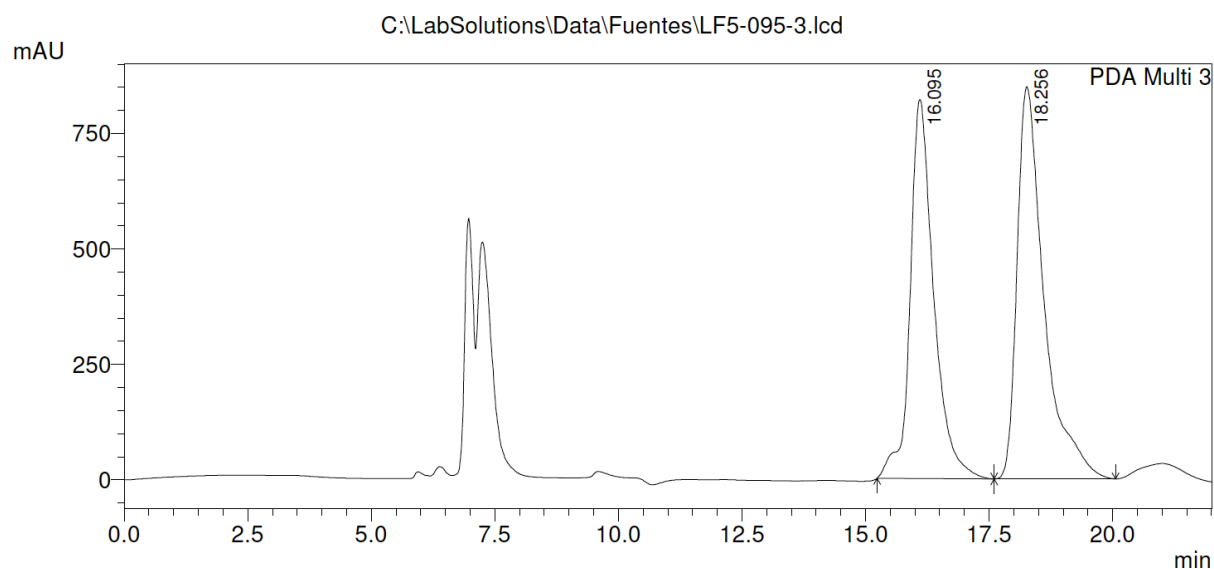


PeakTable

PDA Ch5 254nm 4nm

Peak#	Ret. Time	Area	Height	Area %	Height %
1	20.270	40317539	834739	99.388	99.252
2	23.074	248399	6291	0.612	0.748
Total		40565938	841030	100.000	100.000

Racemic **Exo-107** (Chiralpak IA, Hexanes/*i*PrOH 90:10, 254 nm)

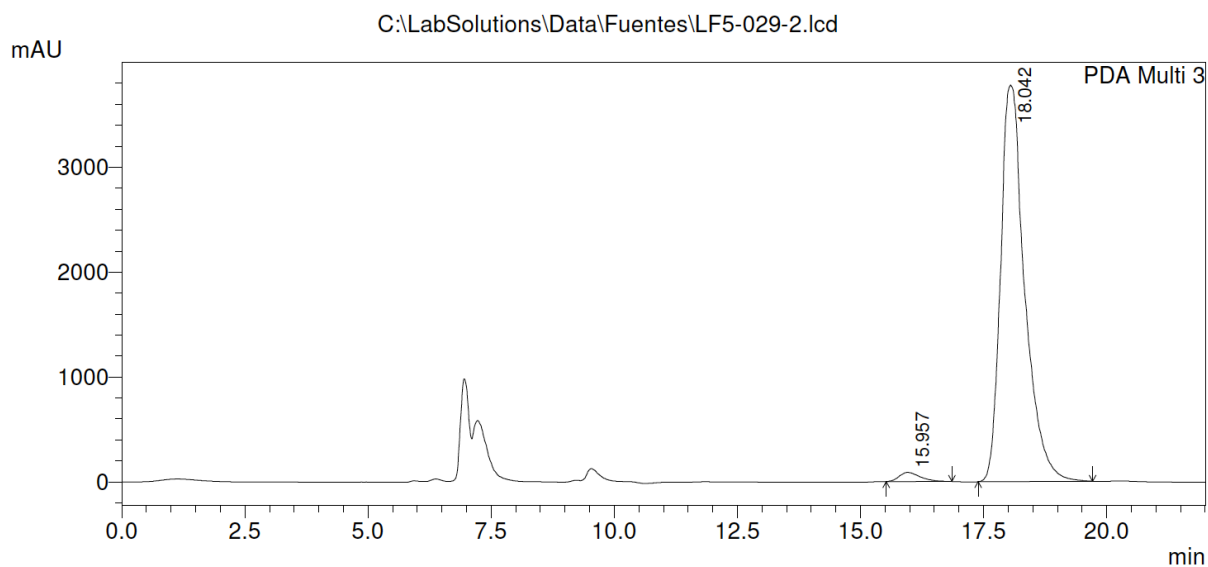


PeakTable

PDA Ch3 215nm 4nm

Peak#	Ret. Time	Area	Height	Area %	Height %
1	16.095	27295212	820986	45.869	49.129
2	18.256	32211134	850099	54.131	50.871
Total		59506347	1671085	100.000	100.000

Enantioenriched **Exo-107** (Chiralpak IA, Hexanes/*i*PrOH 90:10, 254 nm)

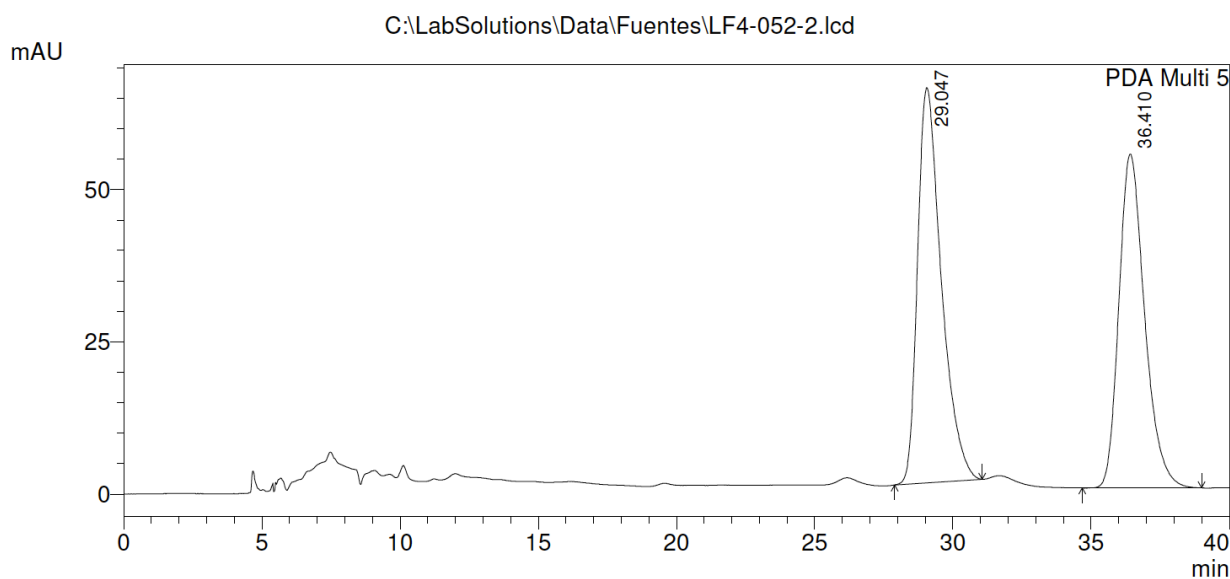


PeakTable

PDA Ch3 215nm 4nm

Peak#	Ret. Time	Area	Height	Area %	Height %
1	15.957	2555408	86561	1.949	2.238
2	18.042	128525507	3782020	98.051	97.762
Total		131080915	3868581	100.000	100.000

Racemic **Endo-108** (Chiralpak AD-H, Hexanes/*i*PrOH 90:10, 254 nm)

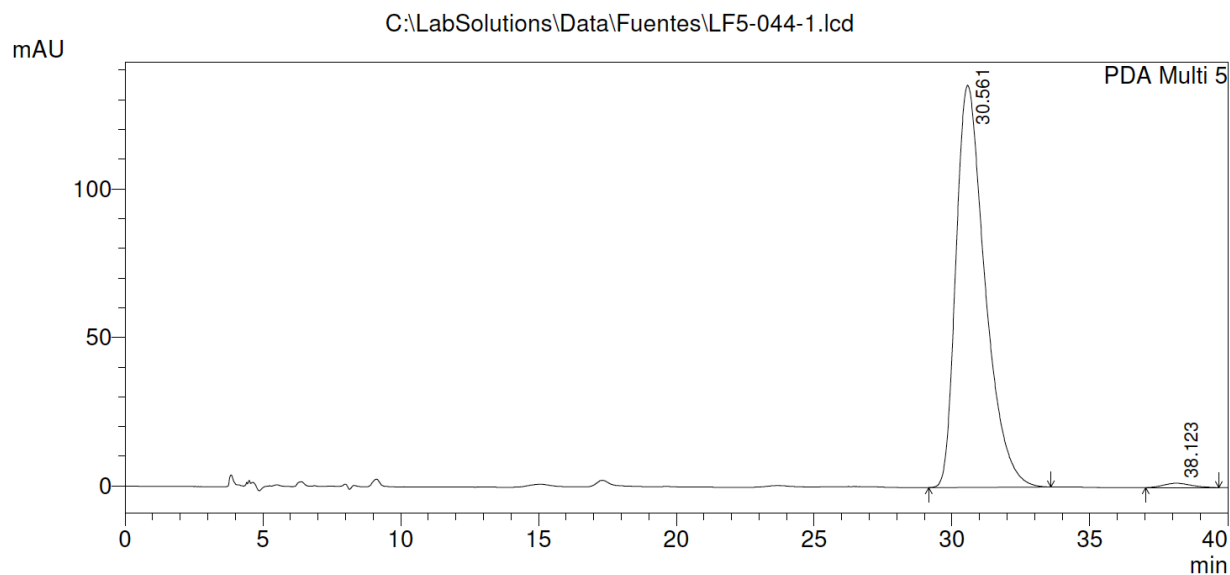


PeakTable

PDA Ch5 254nm 4nm

Peak#	Ret. Time	Area	Height	Area %	Height %
1	29.047	3887734	64921	52.266	54.197
2	36.410	3550634	54866	47.734	45.803
Total		7438367	119787	100.000	100.000

Enantioenriched **Endo-108** (Chiralpak AD-H, Hexanes/*i*PrOH 90:10, 254 nm)

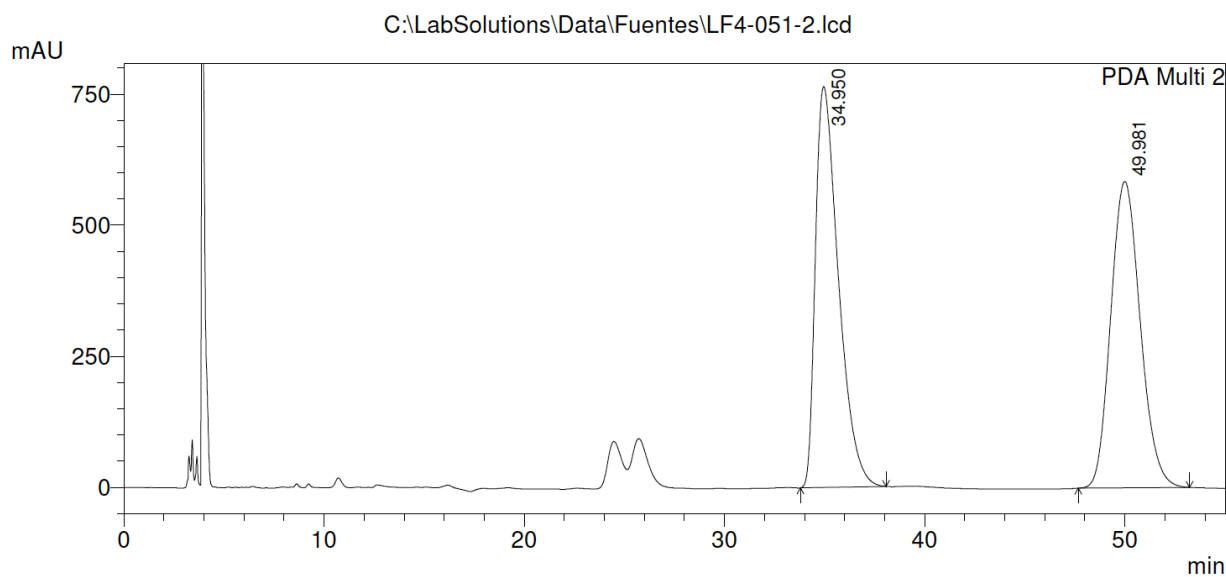


PeakTable

PDA Ch5 254nm 4nm

Peak#	Ret. Time	Area	Height	Area %	Height %
1	30.561	9891240	135294	98.992	98.940
2	38.123	100731	1450	1.008	1.060
Total		9991972	136744	100.000	100.000

Racemic **Exo-108** (Chiralcel OD-H, Hexanes/*i*PrOH 90:10, 254 nm)

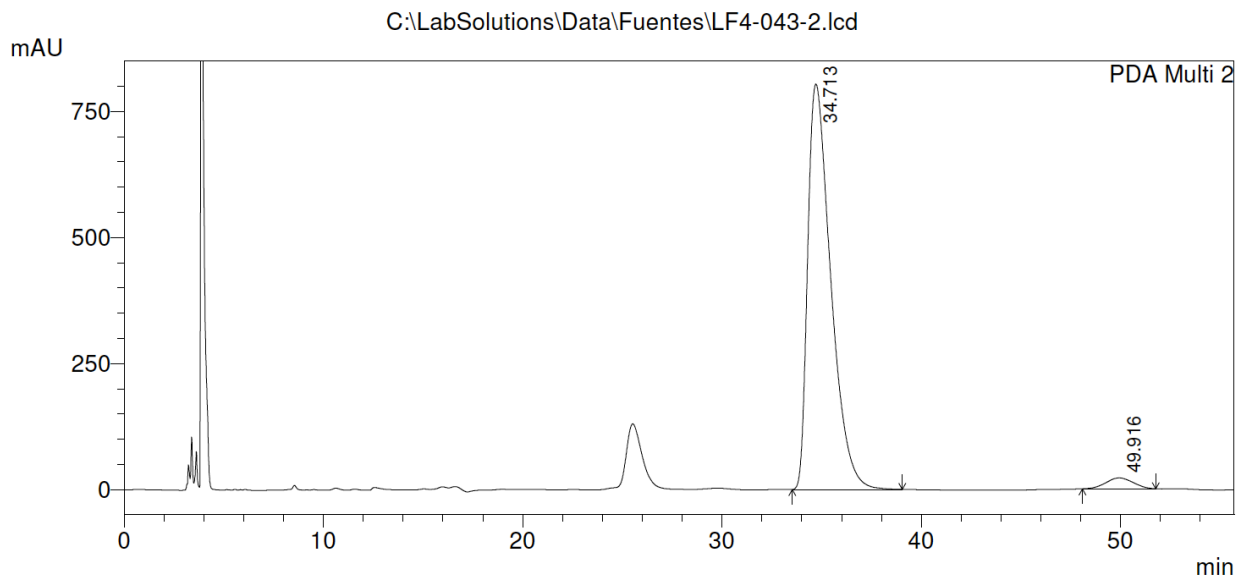


PeakTable

PDA Ch2 205nm 4nm

Peak#	Ret. Time	Area	Height	Area %	Height %
1	34.950	61128309	764734	50.529	56.681
2	49.981	59848104	584447	49.471	43.319
Total		120976413	1349181	100.000	100.000

Enantioenriched **Exo-108** (Chiralcel OD-H, Hexanes/*i*PrOH 90:10, 254 nm)

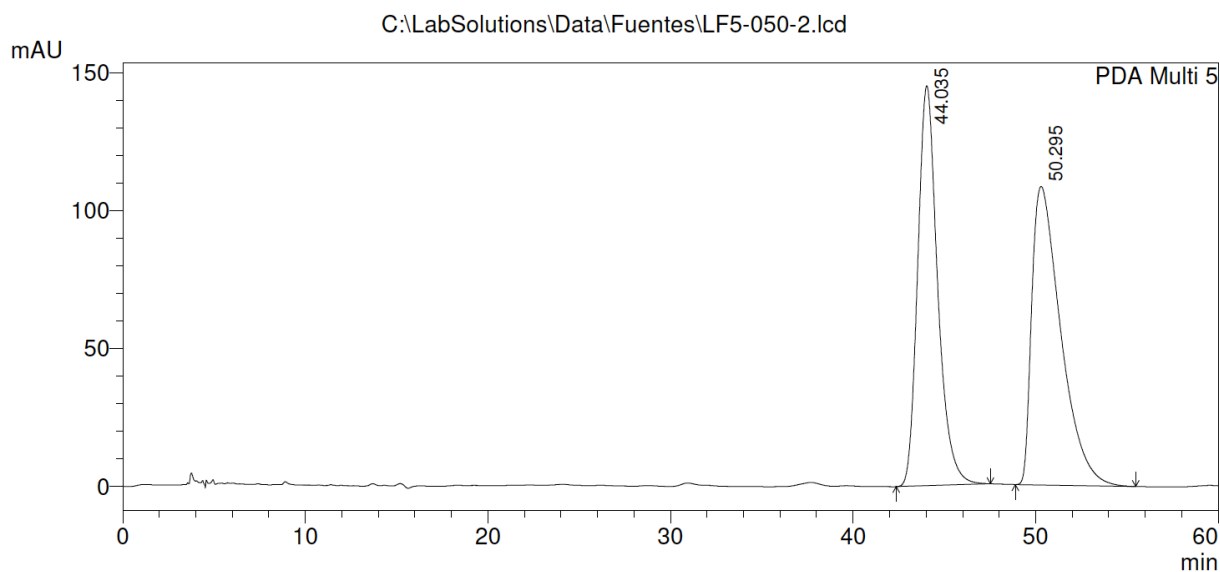


PeakTable

PDA Ch2 205nm 4nm

Peak#	Ret. Time	Area	Height	Area %	Height %
1	34.713	64572698	803809	96.949	97.401
2	49.916	2032032	21451	3.051	2.599
Total		66604730	825260	100.000	100.000

Racemic **Endo-109** (Chiralpak AD-H, Hexanes/*i*PrOH 95:5, 254 nm)

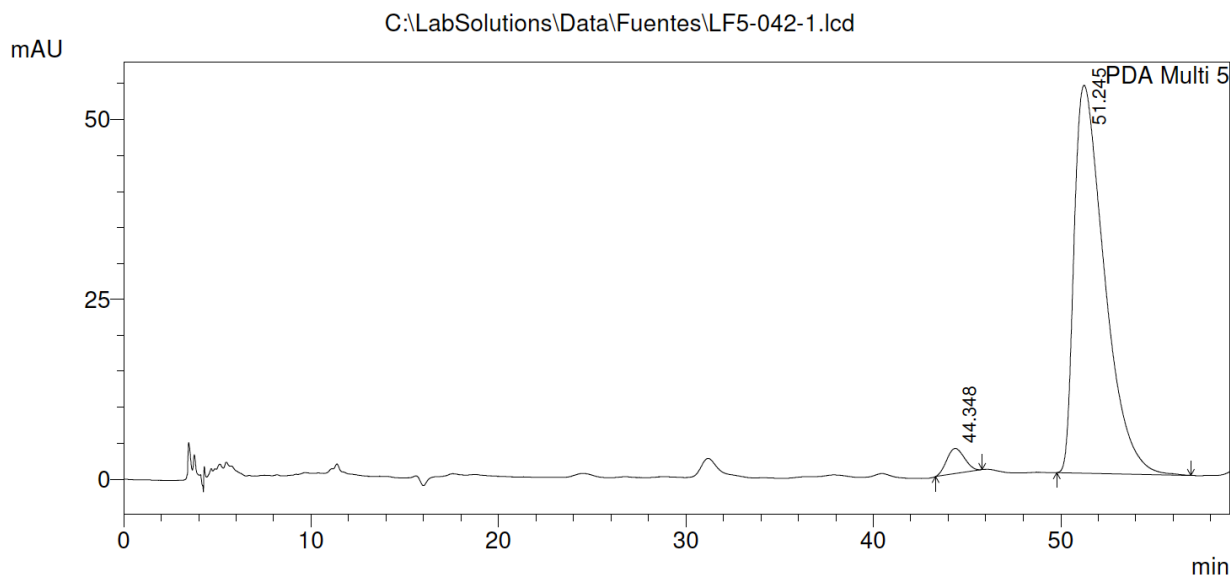


PeakTable

PDA Ch5 254nm 4nm

Peak#	Ret. Time	Area	Height	Area %	Height %
1	44.035	10971847	145002	47.880	57.259
2	50.295	11943420	108238	52.120	42.741
Total		22915267	253240	100.000	100.000

Enantioenriched **Endo-109** (Chiralpak AD-H, Hexanes/*i*PrOH 95:5, 254 nm)

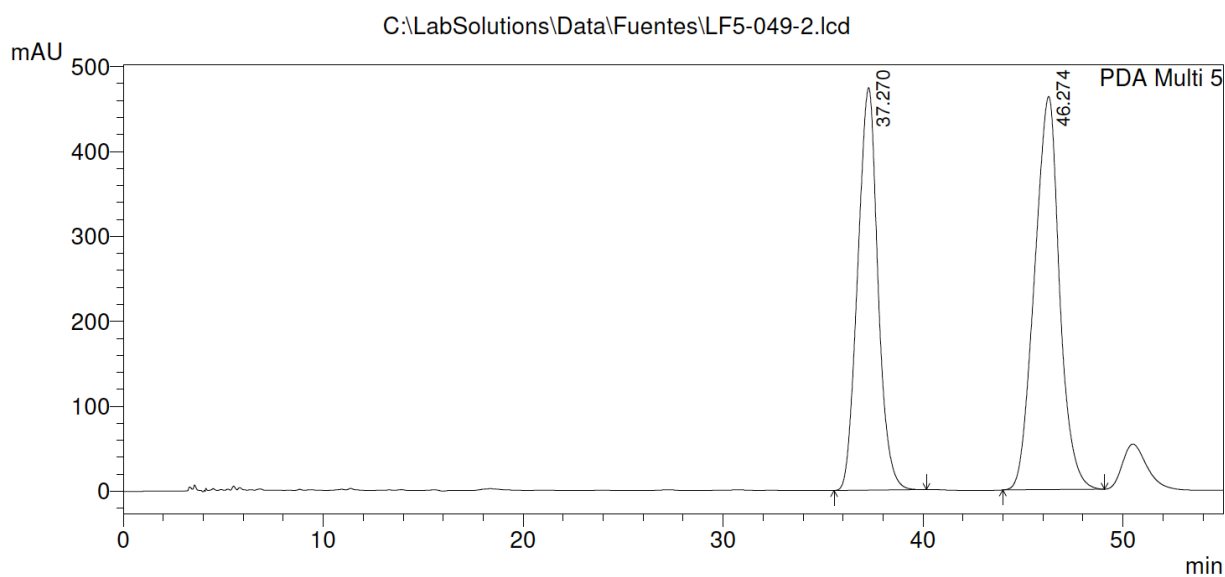


PeakTable

PDA Ch5 254nm 4nm

Peak#	Ret. Time	Area	Height	Area %	Height %
1	44.348	231004	3509	3.673	6.110
2	51.245	6059004	53931	96.327	93.890
Total		6290008	57440	100.000	100.000

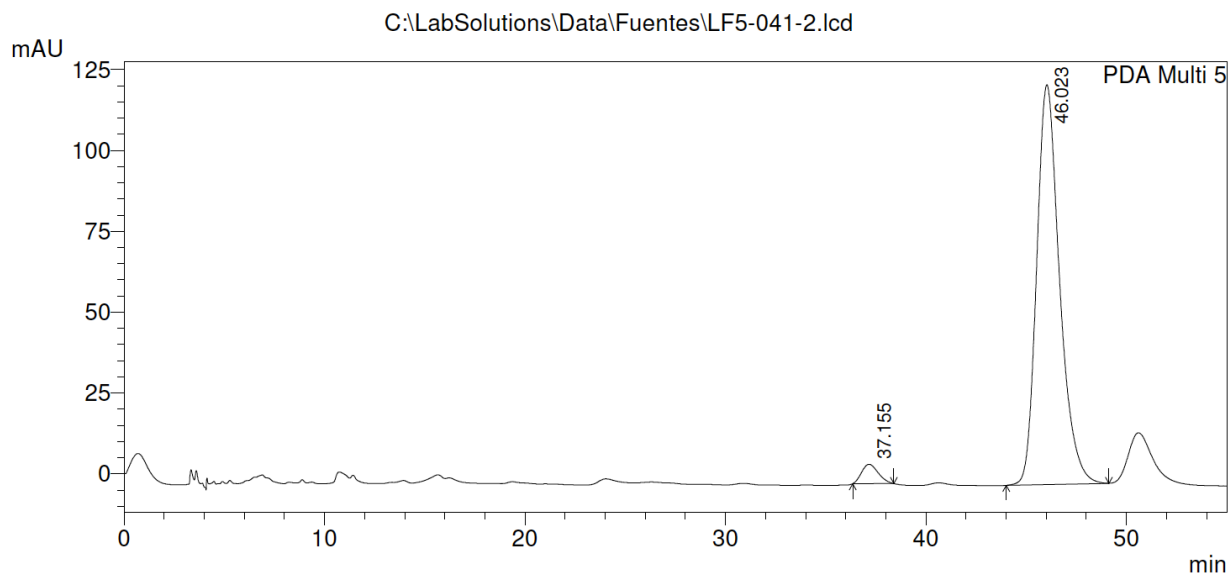
Racemic **Exo-109** (Chiralpak AD-H, Hexanes/*i*PrOH 95:5, 254 nm)



PeakTable

Peak#	Ret. Time	Area	Height	Area %	Height %
1	37.270	33293341	473780	45.246	50.583
2	46.274	40289897	462864	54.754	49.417
Total		73583238	936643	100.000	100.000

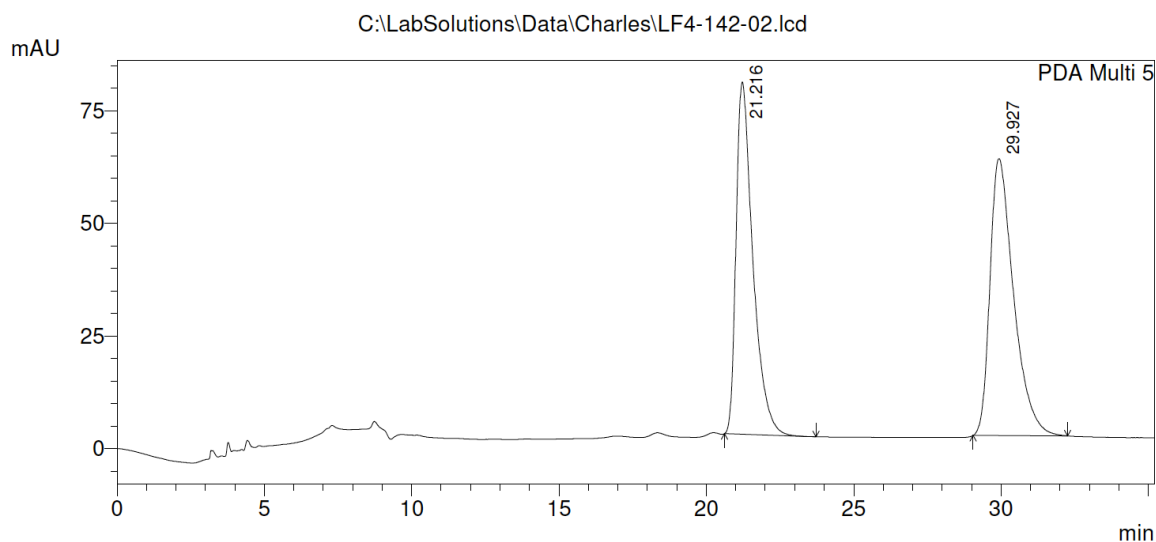
Enantioenriched **Exo-109** (Chiralpak AD-H, Hexanes/*i*PrOH 95:5, 254 nm)



PeakTable

Peak#	Ret. Time	Area	Height	Area %	Height %
1	37.155	344839	6010	3.393	4.634
2	46.023	9819603	123672	96.607	95.366
Total		10164442	129681	100.000	100.000

Racemic **Endo-110** (Chiralpak IA, Hexanes/*i*PrOH 90:10, 254 nm)

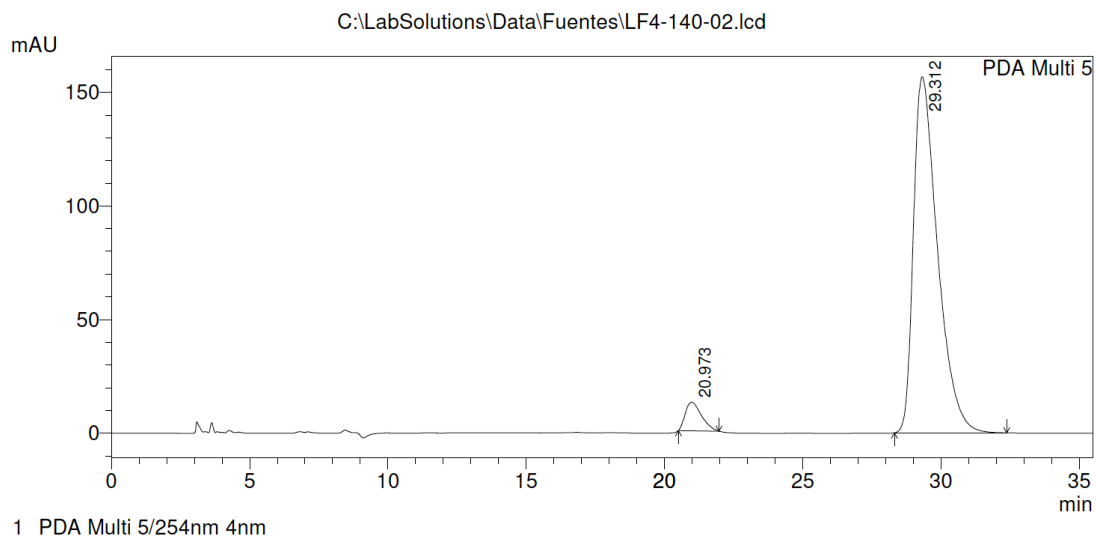


PeakTable

PDA Ch5 254nm 4nm

Peak#	Ret. Time	Area	Height	Area %	Height %
1	21.216	3096217	78135	47.456	55.983
2	29.927	3428145	61435	52.544	44.017
Total		6524362	139570	100.000	100.000

Enantioenriched **Endo-110** (Chiralpak IA, Hexanes/*i*PrOH 90:10, 254 nm)

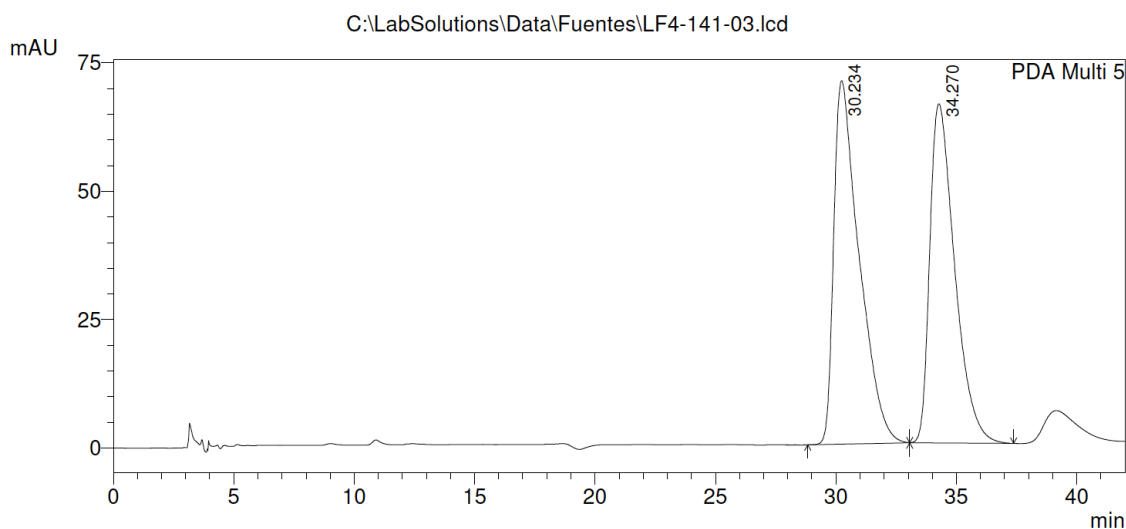


PeakTable

PDA Ch5 254nm 4nm

Peak#	Ret. Time	Area	Height	Area %	Height %
1	20.973	510519	12635	5.098	7.463
2	29.312	9503042	156653	94.902	92.537
Total		10013561	169288	100.000	100.000

Racemic *Exo-110* (Chiralpak IA, Hexanes/*i*PrOH 95:5, 254 nm)



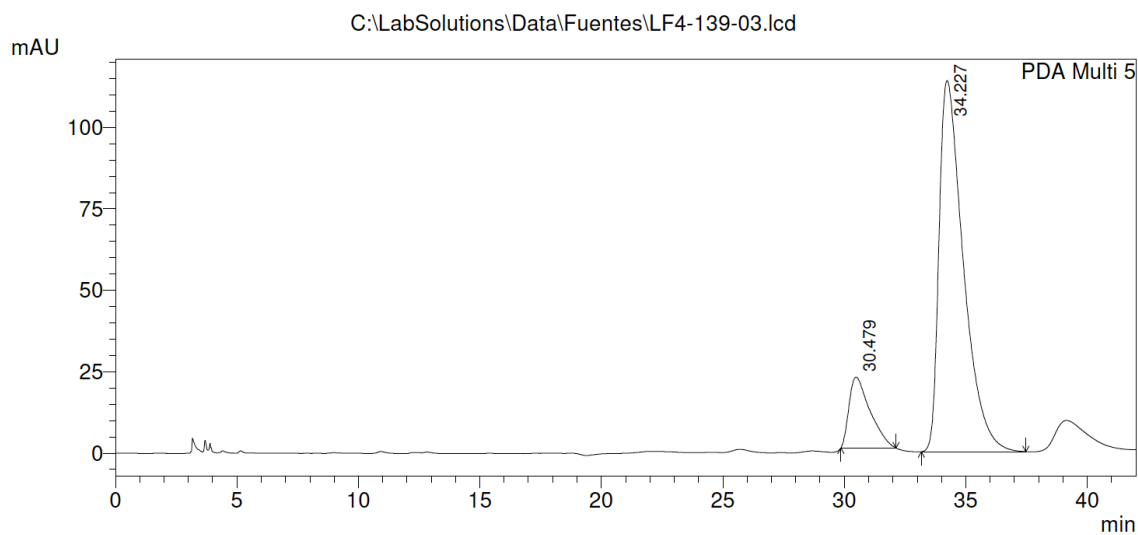
1 PDA Multi 5/254nm 4nm

PeakTable

PDA Ch5 254nm 4nm

Peak#	Ret. Time	Area	Height	Area %	Height %
1	30.234	5180178	70787	52.176	51.738
2	34.270	4748143	66033	47.824	48.262
Total		9928321	136820	100.000	100.000

Enantioenriched *Exo-110* (Chiralpak IA, Hexanes/*i*PrOH 95:5, 254 nm)



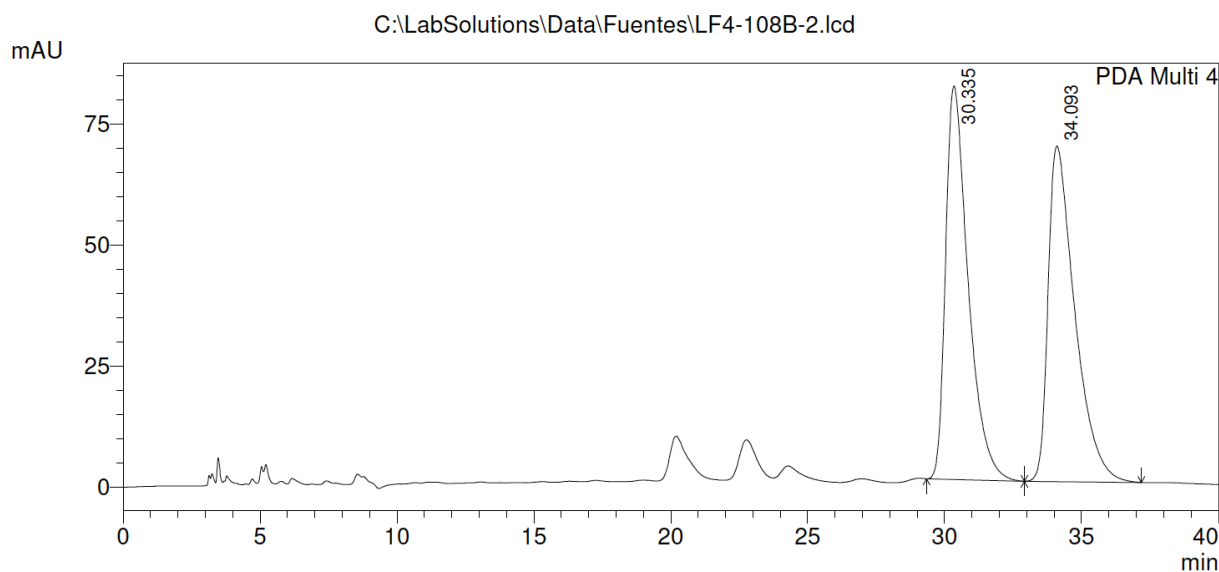
1 PDA Multi 5/254nm 4nm

PeakTable

PDA Ch5 254nm 4nm

Peak#	Ret. Time	Area	Height	Area %	Height %
1	30.479	1310605	21805	14.177	16.053
2	34.227	7933850	114024	85.823	83.947
Total		9244456	135829	100.000	100.000

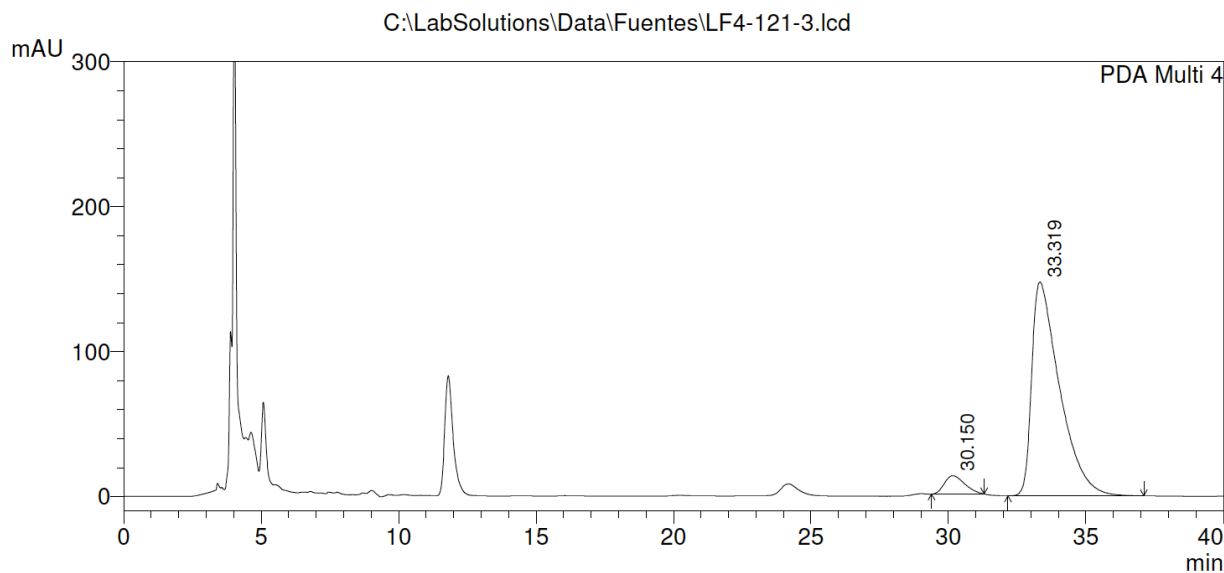
Racemic **Endo-111** (Chiralpak IA, Hexanes/*i*PrOH 90:10, 240 nm)



PeakTable

Peak#	Ret. Time	Area	Height	Area %	Height %
1	30.335	4654265	81250	49.756	53.968
2	34.093	4699978	69301	50.244	46.032
Total		9354243	150552	100.000	100.000

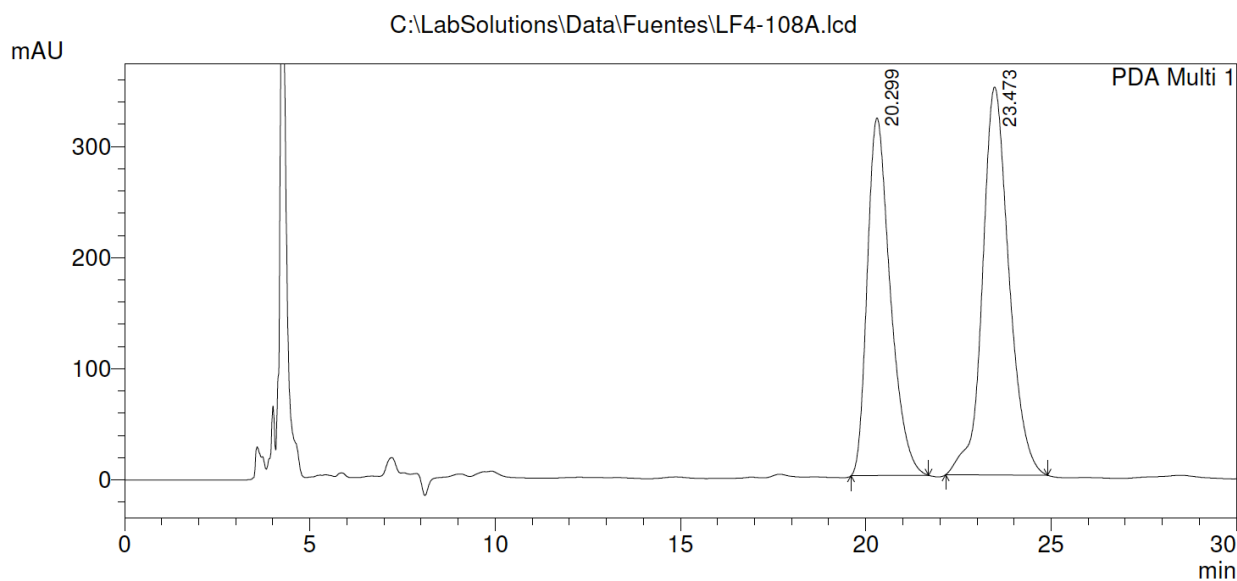
Enantioenriched **Endo-111** (Chiralpak IA, Hexanes/*i*PrOH 90:10, 240 nm)



PeakTable

Peak#	Ret. Time	Area	Height	Area %	Height %
1	30.150	653989	12711	5.908	7.926
2	33.319	10414971	147657	94.092	92.074
Total		11068960	160367	100.000	100.000

Racemic **Exo-111** (Chiralpak AD-H, Hexanes/*i*PrOH 90:10, 215 nm)

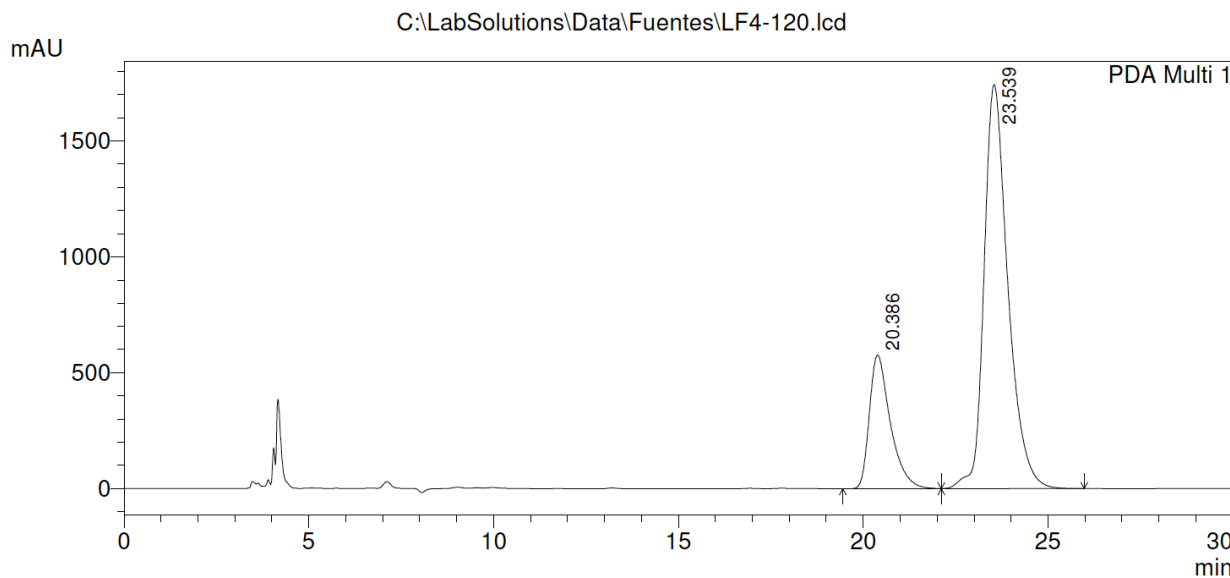


PeakTable

PDA Ch1 215nm 4nm

Peak#	Ret. Time	Area	Height	Area %	Height %
1	20.299	13919500	321665	44.449	47.966
2	23.473	17396187	348941	55.551	52.034
Total		31315688	670606	100.000	100.000

Enantioenriched **Exo-111** (Chiralpak AD-H, Hexanes/*i*PrOH 90:10, 215 nm)

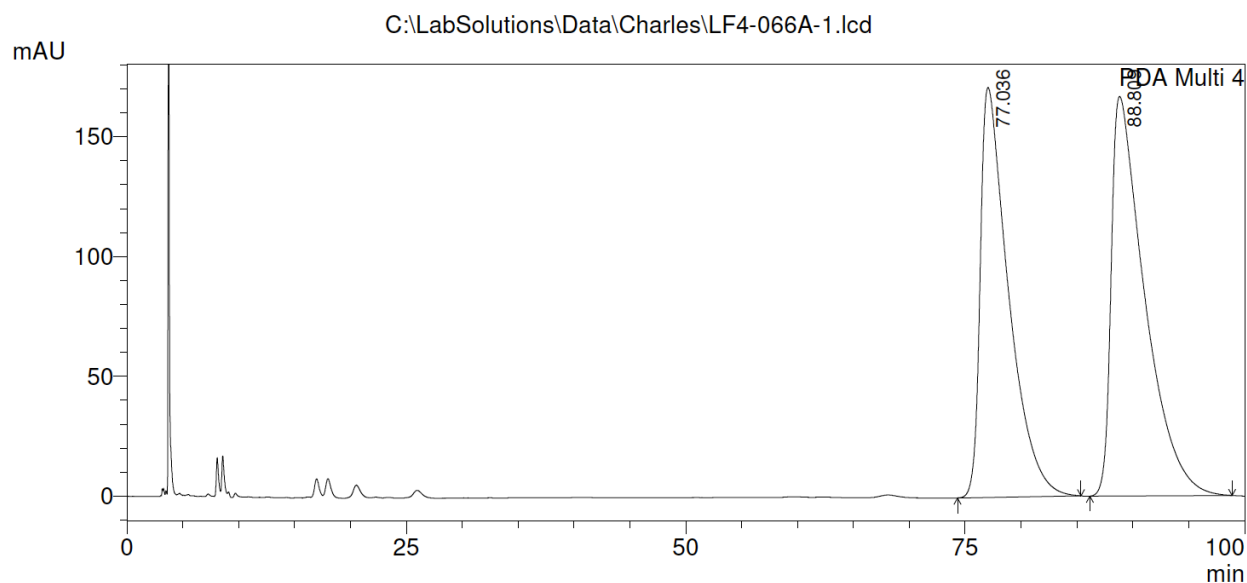


PeakTable

PDA Ch1 215nm 4nm

Peak#	Ret. Time	Area	Height	Area %	Height %
1	20.386	22795884	577566	22.516	24.870
2	23.539	78446427	1744731	77.484	75.130
Total		101242312	2322297	100.000	100.000

Racemic **Endo-112** (Chiralpak IA, Hexanes/*i*PrOH 90:10, 240 nm)

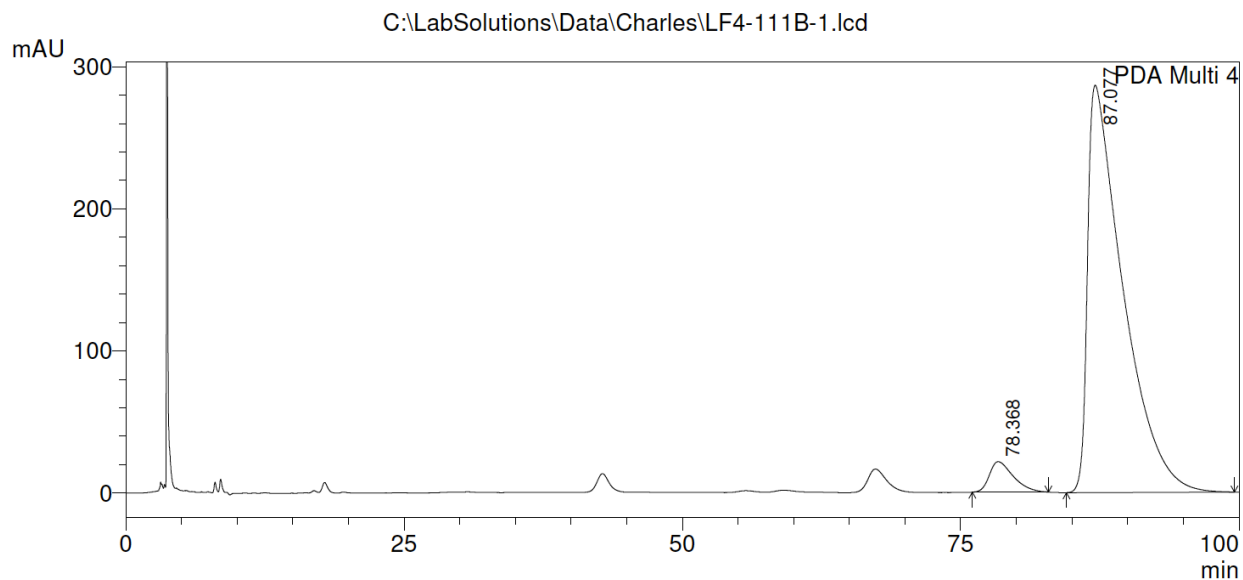


PeakTable

PDA Ch4 240nm 1nm

Peak#	Ret. Time	Area	Height	Area %	Height %
1	77.036	30026202	170982	46.449	50.642
2	88.809	34616570	166649	53.551	49.358
Total		64642771	337630	100.000	100.000

Enantioenriched **Endo-112** (Chiralpak IA, Hexanes/*i*PrOH 90:10, 240 nm)

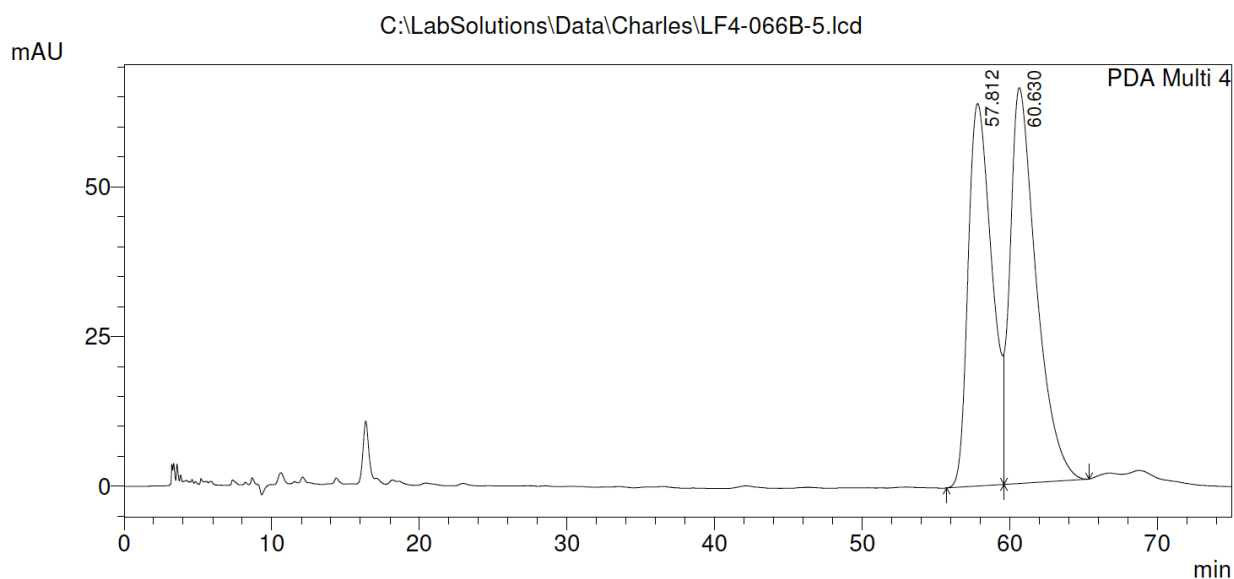


PeakTable

PDA Ch4 240nm 1nm

Peak#	Ret. Time	Area	Height	Area %	Height %
1	78.368	3210085	21464	4.817	6.970
2	87.077	63425016	286499	95.183	93.030
Total		66635101	307964	100.000	100.000

Racemic **Exo-112** (Chiralpak IA, Hexanes/*i*PrOH 90:10, 240 nm)



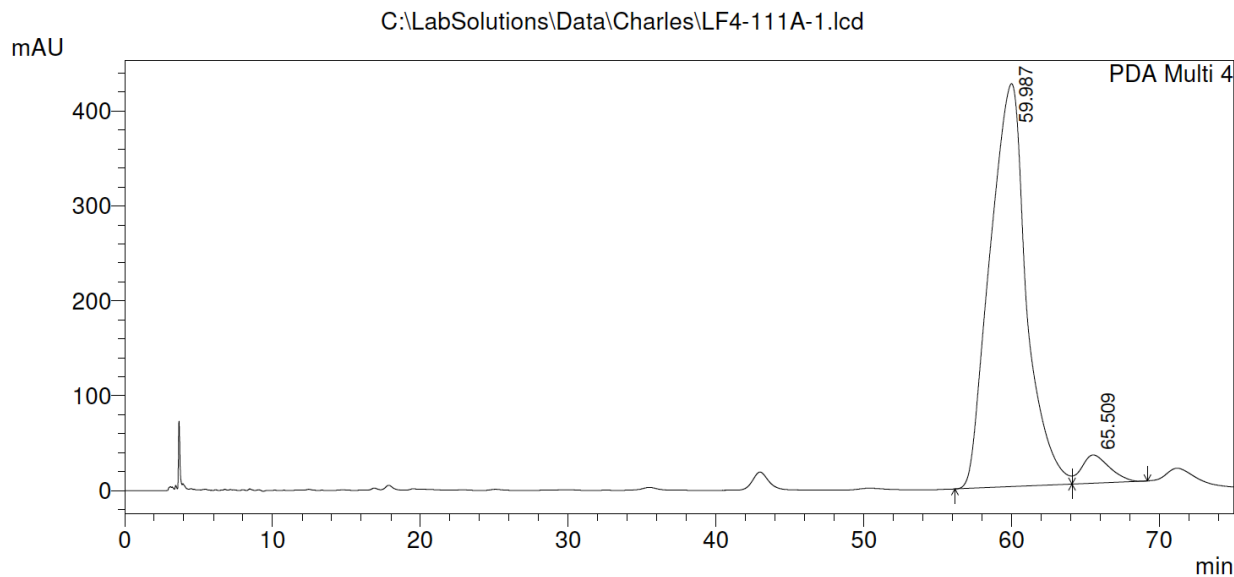
1 PDA Multi 4/240nm 1nm

PeakTable

PDA Ch4 240nm 1nm

Peak#	Ret. Time	Area	Height	Area %	Height %
1	57.812	7179776	63813	46.811	49.149
2	60.630	8158124	66021	53.189	50.851
Total		15337899	129834	100.000	100.000

Enantioenriched **Exo-112** (Chiralpak IA, Hexanes/*i*PrOH 90:10, 240 nm)



1 PDA Multi 4/240nm 1nm

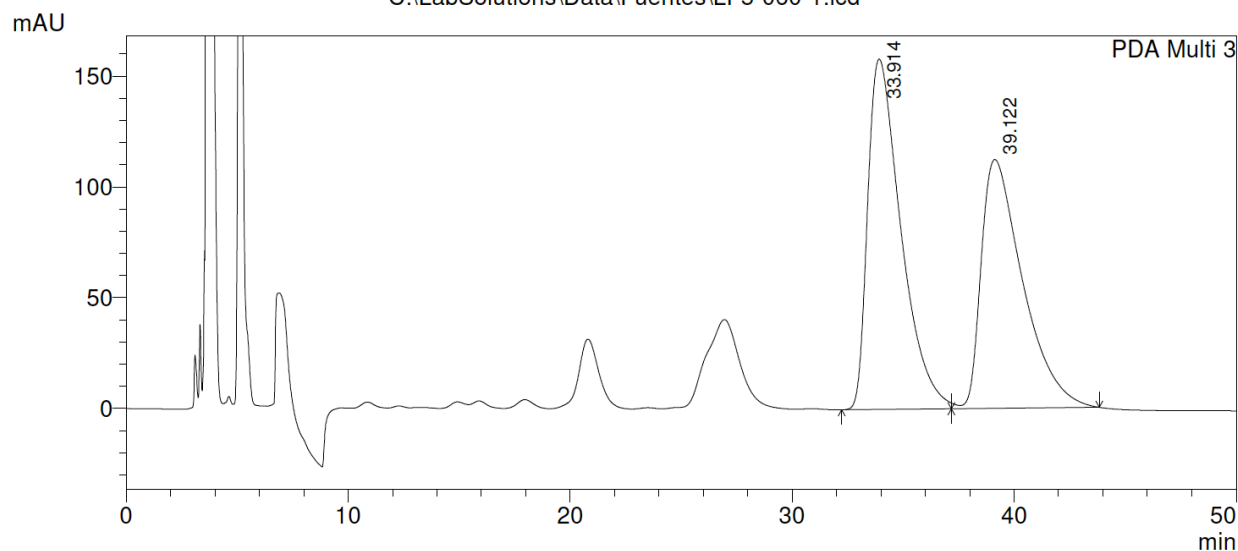
PeakTable

PDA Ch4 240nm 1nm

Peak#	Ret. Time	Area	Height	Area %	Height %
1	59.987	72927723	424839	94.921	93.455
2	65.509	3902348	29751	5.079	6.545
Total		76830070	454590	100.000	100.000

Racemic **Endo-113** (Chiralpak IA, Hexanes/*i*PrOH 90:10, 254 nm)

C:\LabSolutions\Data\Fuentes\LF5-060-1.lcd



1 PDA Multi 3/215nm 4nm

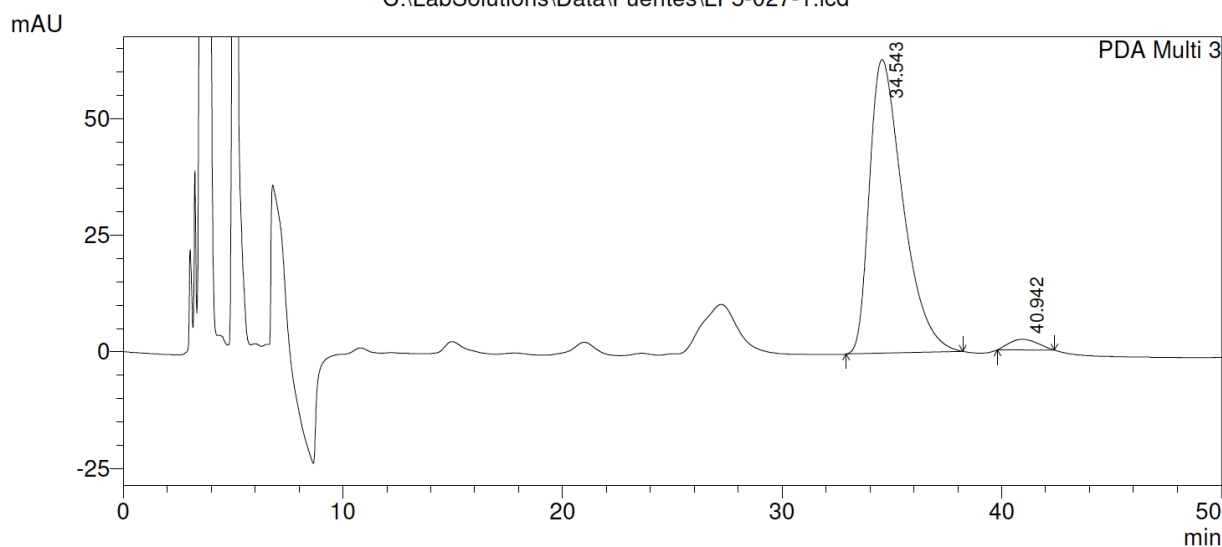
PeakTable

PDA Ch3 215nm 4nm

Peak#	Ret. Time	Area	Height	Area %	Height %
1	33.914	16449145	158000	53.000	58.471
2	39.122	14587018	112221	47.000	41.529
Total		31036162	270220	100.000	100.000

Enantioenriched **Endo-113** (Chiralpak IA, Hexanes/*i*PrOH 90:10, 254 nm)

C:\LabSolutions\Data\Fuentes\LF5-027-1.lcd



1 PDA Multi 3/215nm 4nm

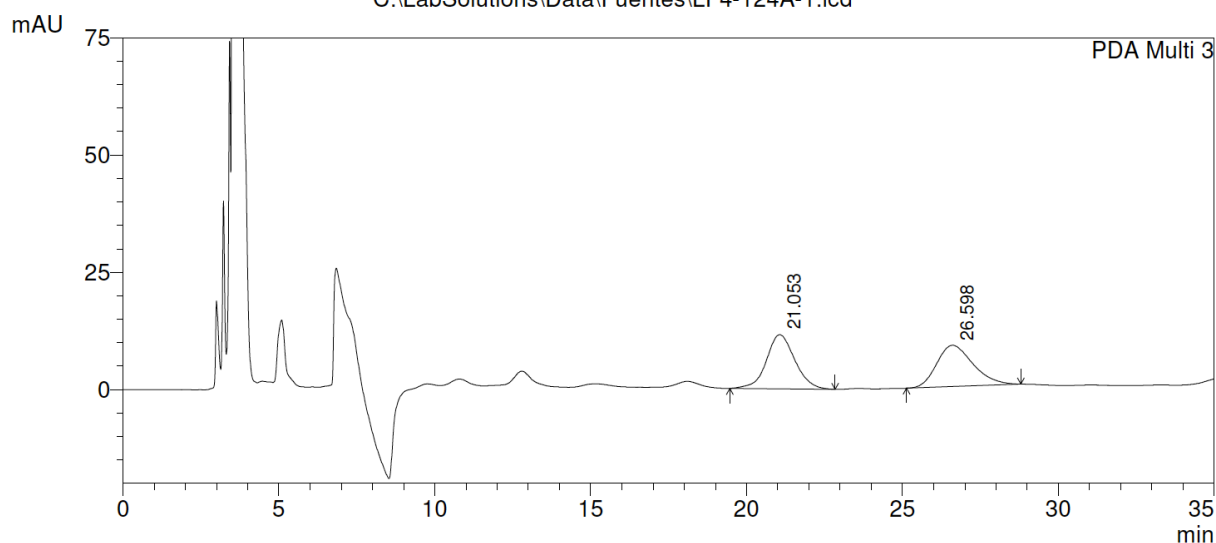
PeakTable

PDA Ch3 215nm 4nm

Peak#	Ret. Time	Area	Height	Area %	Height %
1	34.543	6656396	62889	97.033	96.536
2	40.942	203531	2257	2.967	3.464
Total		6859927	65146	100.000	100.000

Racemic *Exo-113* (Chiralpak IA, Hexanes/*i*PrOH 95:5, 254 nm)

C:\LabSolutions\Data\Fuentes\LF4-124A-1.lcd



1 PDA Multi 3/215nm 4nm

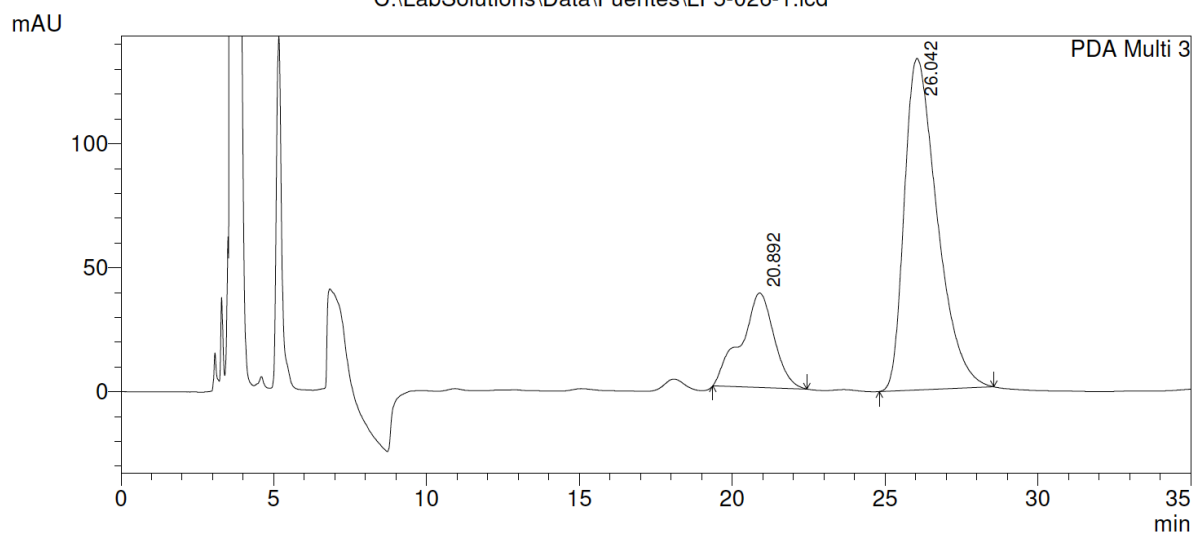
PeakTable

PDA Ch3 215nm 4nm

Peak#	Ret. Time	Area	Height	Area %	Height %
1	21.053	733664	11538	50.642	56.712
2	26.598	715065	8807	49.358	43.288
Total		1448729	20345	100.000	100.000

Enantioenriched *Exo-113* (Chiralpak IA, Hexanes/*i*PrOH 95:5, 254 nm)

C:\LabSolutions\Data\Fuentes\LF5-026-1.lcd



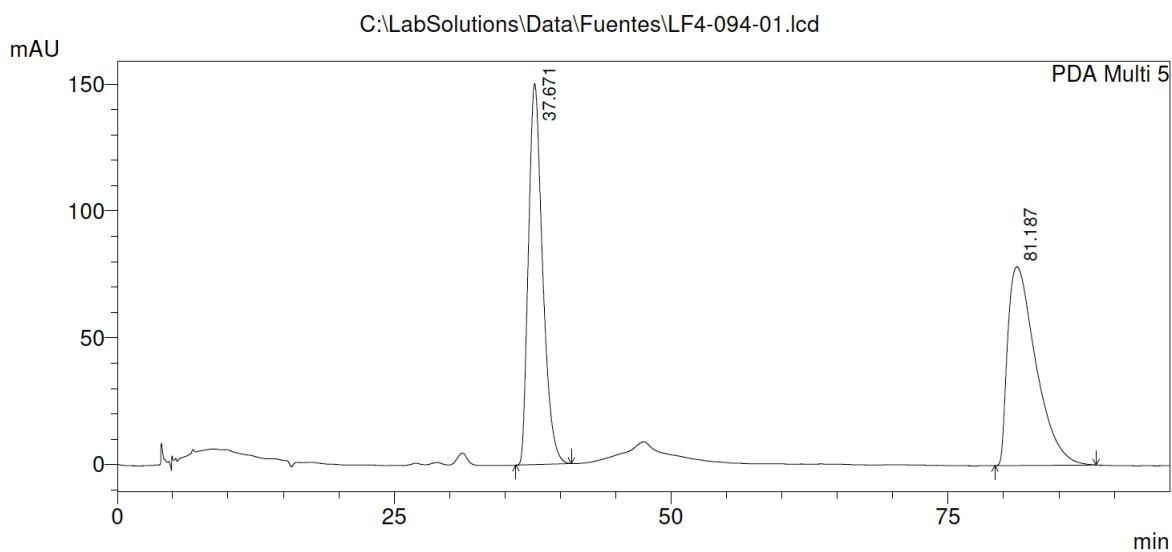
1 PDA Multi 3/215nm 4nm

PeakTable

PDA Ch3 215nm 4nm

Peak#	Ret. Time	Area	Height	Area %	Height %
1	20.892	2883062	38093	22.362	22.181
2	26.042	10009498	133647	77.638	77.819
Total		12892560	171740	100.000	100.000

Racemic **Endo-114** (Chiralpak IA, Hexanes/*i*PrOH 90:10, 254 nm)

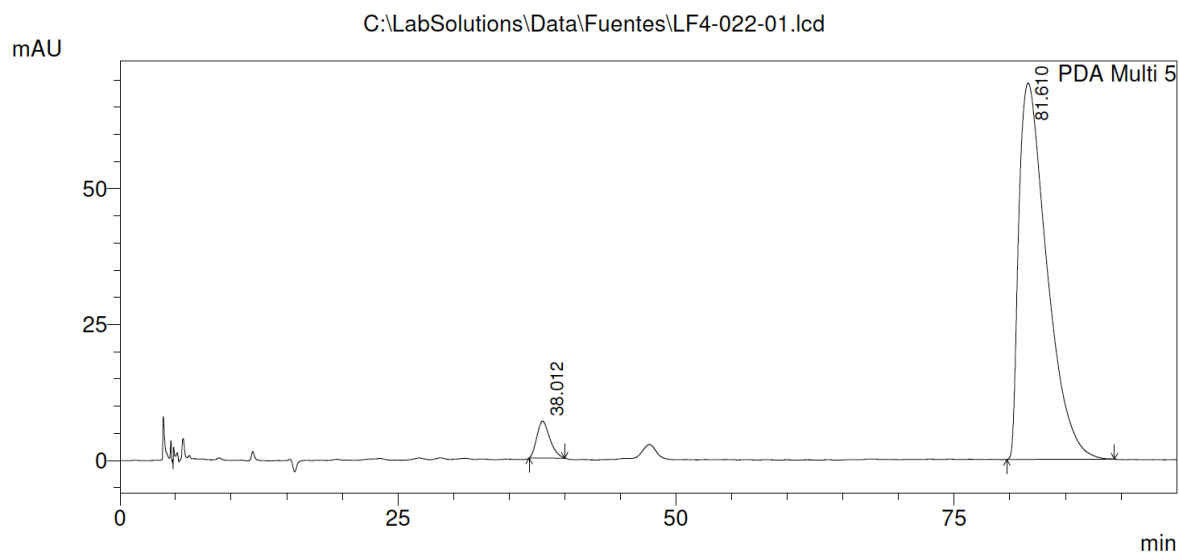


PeakTable

PDA Ch5 254nm 4nm

Peak#	Ret. Time	Area	Height	Area %	Height %
1	37.671	13340007	150462	49.033	65.717
2	81.187	13866256	78493	50.967	34.283
Total		27206263	228955	100.000	100.000

Enantioenriched **Endo-114** (Chiralpak IA, Hexanes/*i*PrOH 90:10, 254 nm)

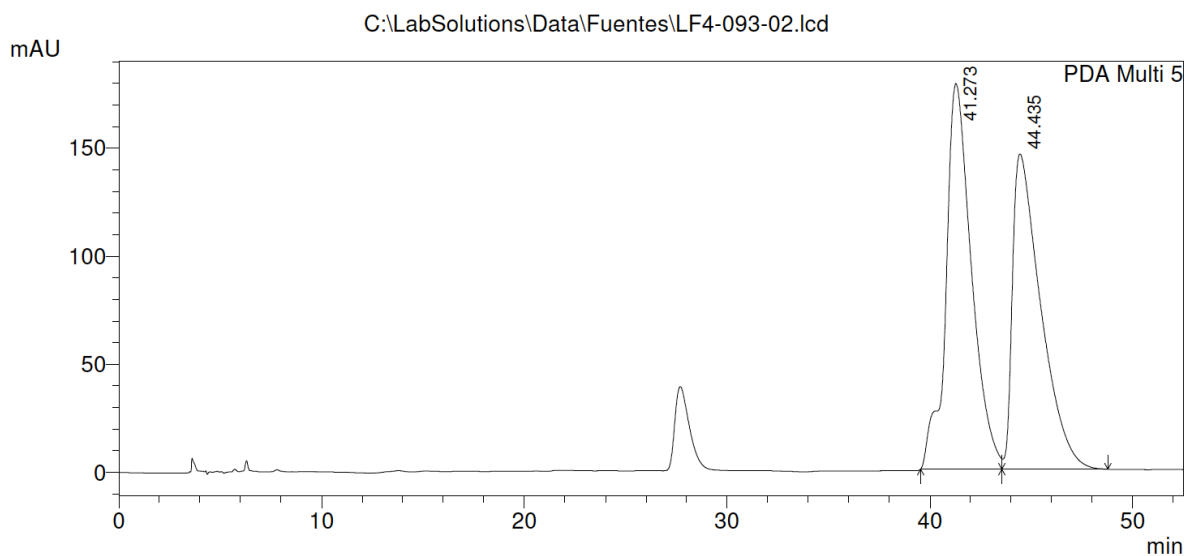


PeakTable

PDA Ch5 254nm 4nm

Peak#	Ret. Time	Area	Height	Area %	Height %
1	38.012	552493	6806	4.367	8.955
2	81.610	12100390	69191	95.633	91.045
Total		12652883	75996	100.000	100.000

Racemic **Exo-114** (Chiralpak IA, Hexanes/*i*PrOH 95:5, 254 nm)

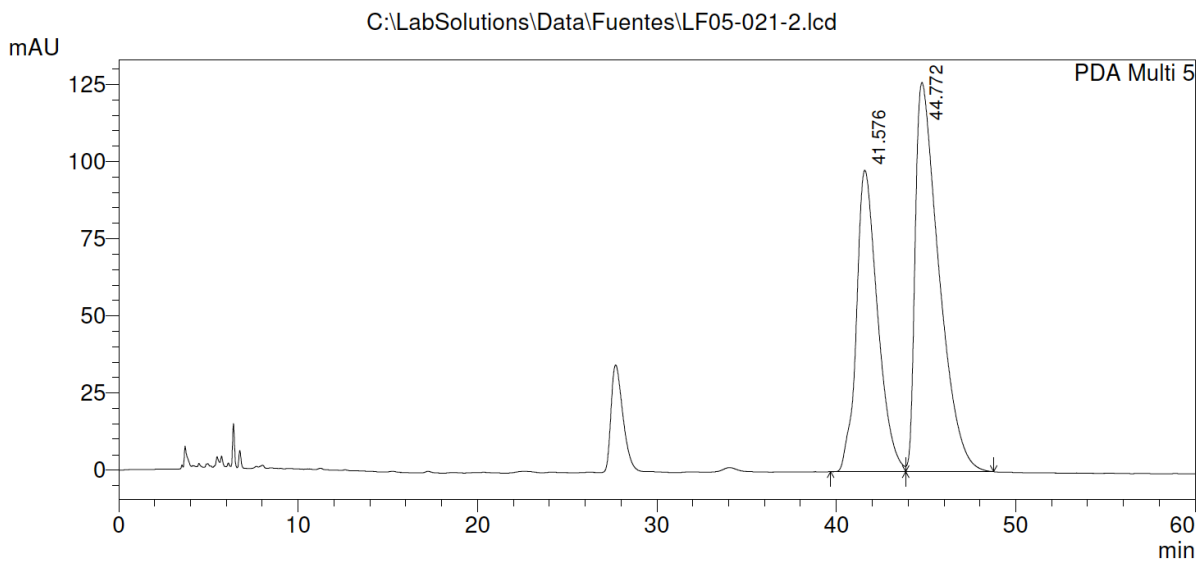


PeakTable

PDA Ch5 254nm 4nm

Peak#	Ret. Time	Area	Height	Area %	Height %
1	41.273	15744595	178469	52.633	55.032
2	44.435	14169112	145833	47.367	44.968
Total		29913708	324302	100.000	100.000

Enantioenriched **Exo-114** (Chiralpak IA, Hexanes/*i*PrOH 95:5, 254 nm)

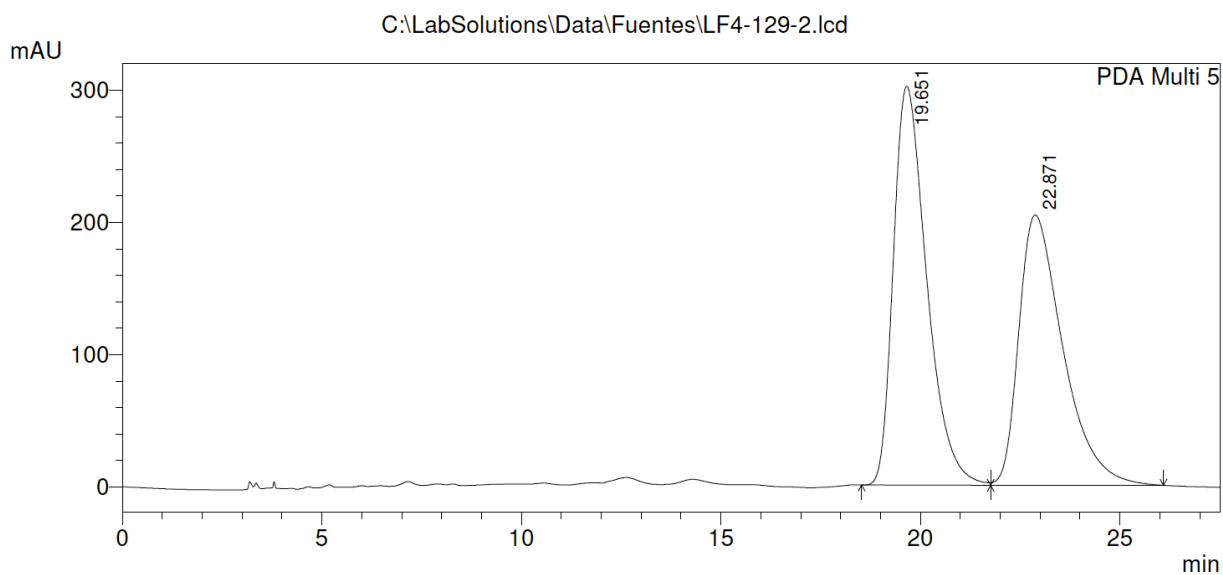


PeakTable

PDA Ch5 254nm 4nm

Peak#	Ret. Time	Area	Height	Area %	Height %
1	41.576	8050678	97766	40.980	43.651
2	44.772	11594724	126205	59.020	56.349
Total		19645402	223972	100.000	100.000

Racemic **Endo-115** (Chiralpak IA, Hexanes/*i*PrOH 90:10, 254 nm)

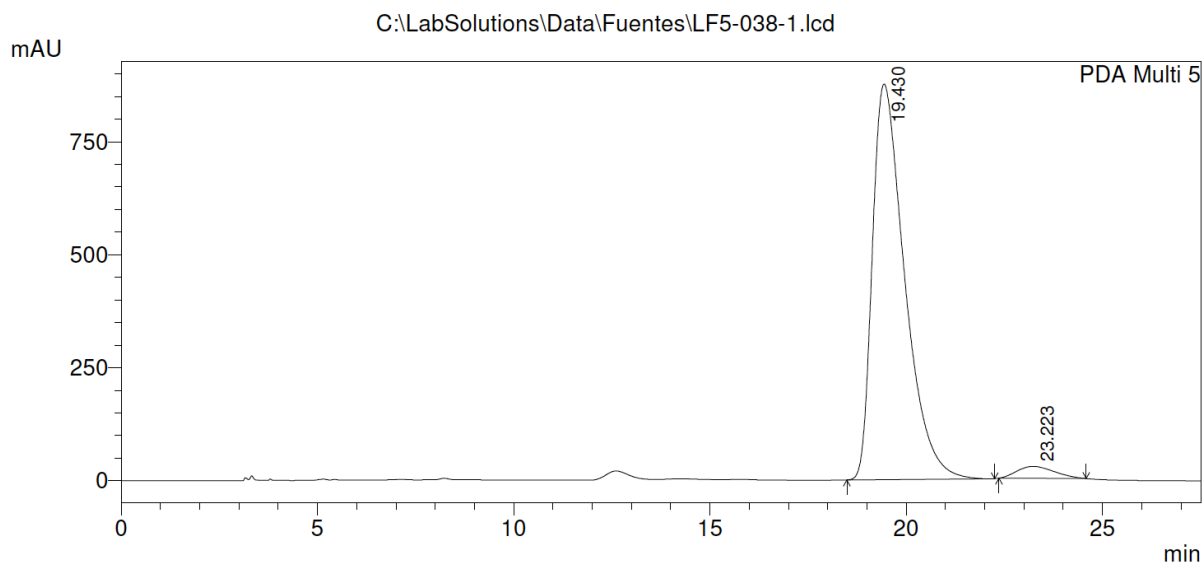


PeakTable

PDA Ch5 254nm 4nm

Peak#	Ret. Time	Area	Height	Area %	Height %
1	19.651	17529401	301587	52.754	59.603
2	22.871	15699446	204407	47.246	40.397
Total		33228846	505994	100.000	100.000

Enantioenriched **Endo-115** (Chiralpak IA, Hexanes/*i*PrOH 90:10, 254 nm)

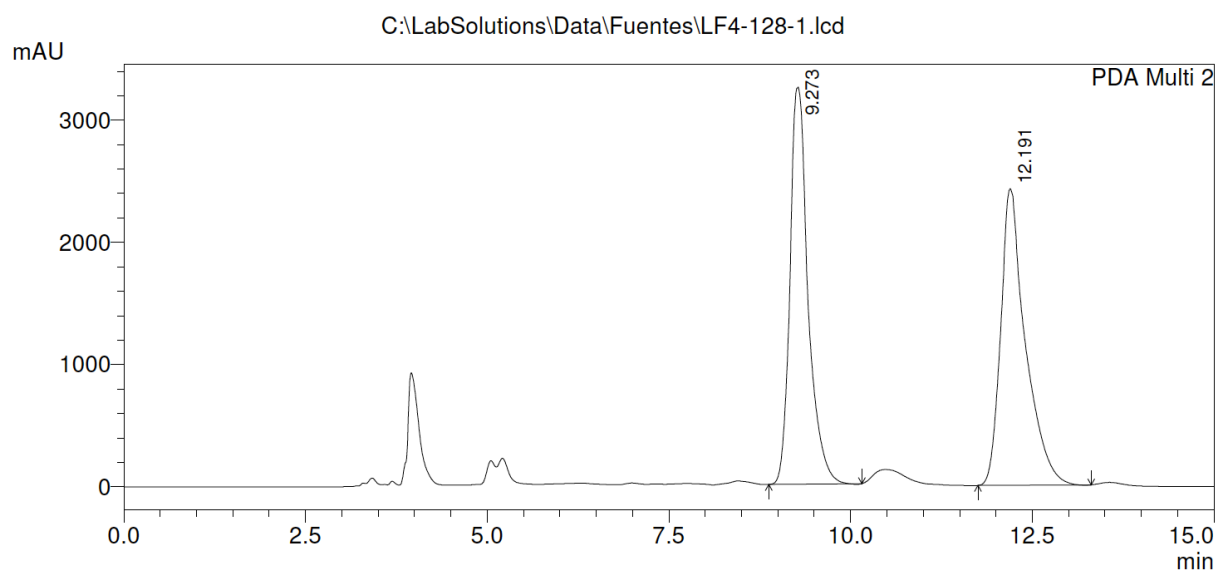


PeakTable

PDA Ch5 254nm 4nm

Peak#	Ret. Time	Area	Height	Area %	Height %
1	19.430	49997400	875455	96.618	97.075
2	23.223	1750061	26375	3.382	2.925
Total		51747461	901830	100.000	100.000

Racemic *Exo-115* (Chiralpak IA, Hexanes/*i*PrOH 95:5, 254 nm)

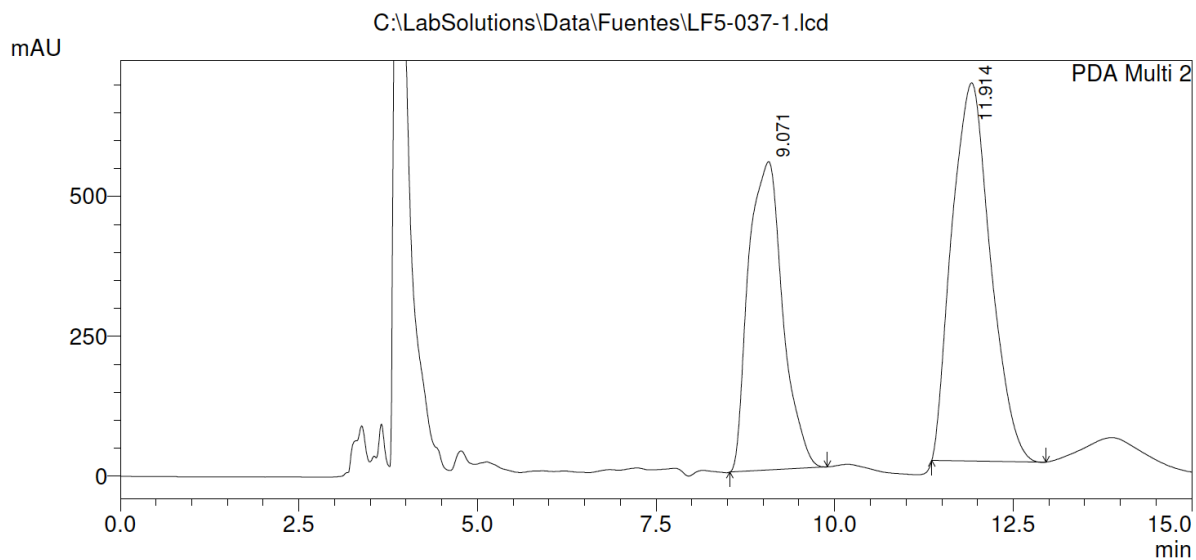


PeakTable

PDA Ch2 205nm 4nm

Peak#	Ret. Time	Area	Height	Area %	Height %
1	9.273	56156396	3250471	49.507	57.249
2	12.191	57274648	2427336	50.493	42.751
Total		113431044	5677806	100.000	100.000

Enantioenriched *Exo-115* (Chiralpak IA, Hexanes/*i*PrOH 95:5, 254 nm)

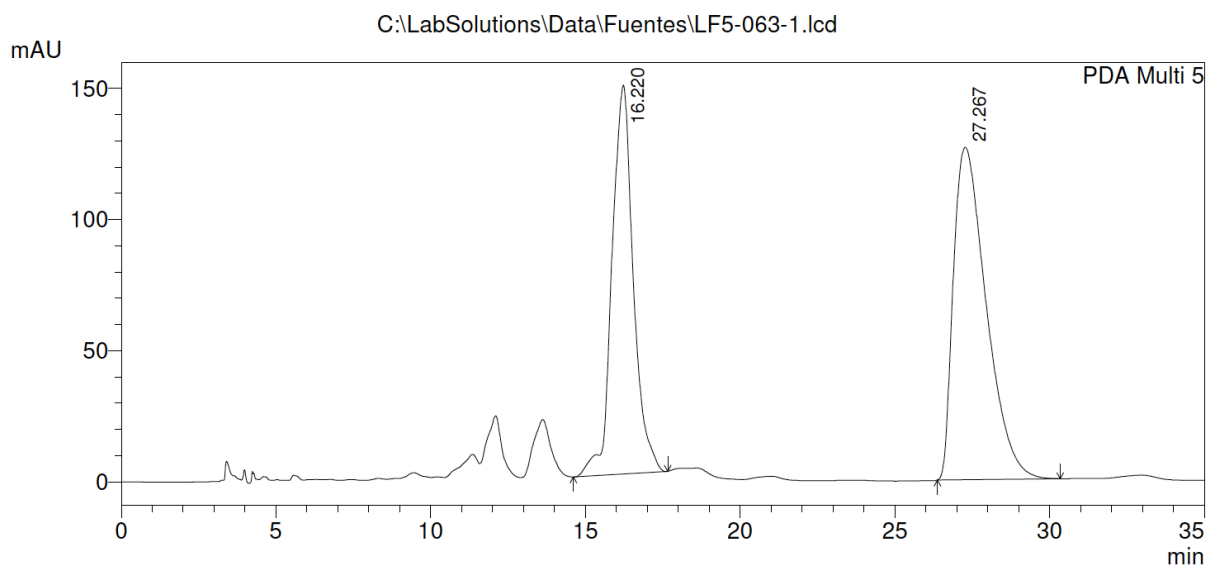


PeakTable

PDA Ch2 205nm 4nm

Peak#	Ret. Time	Area	Height	Area %	Height %
1	9.071	18347380	551309	41.904	44.929
2	11.914	25436502	675770	58.096	55.071
Total		43783882	1227079	100.000	100.000

Racemic **119** (Chiralpak IA, Hexanes/*i*PrOH 95:5, 254 nm)

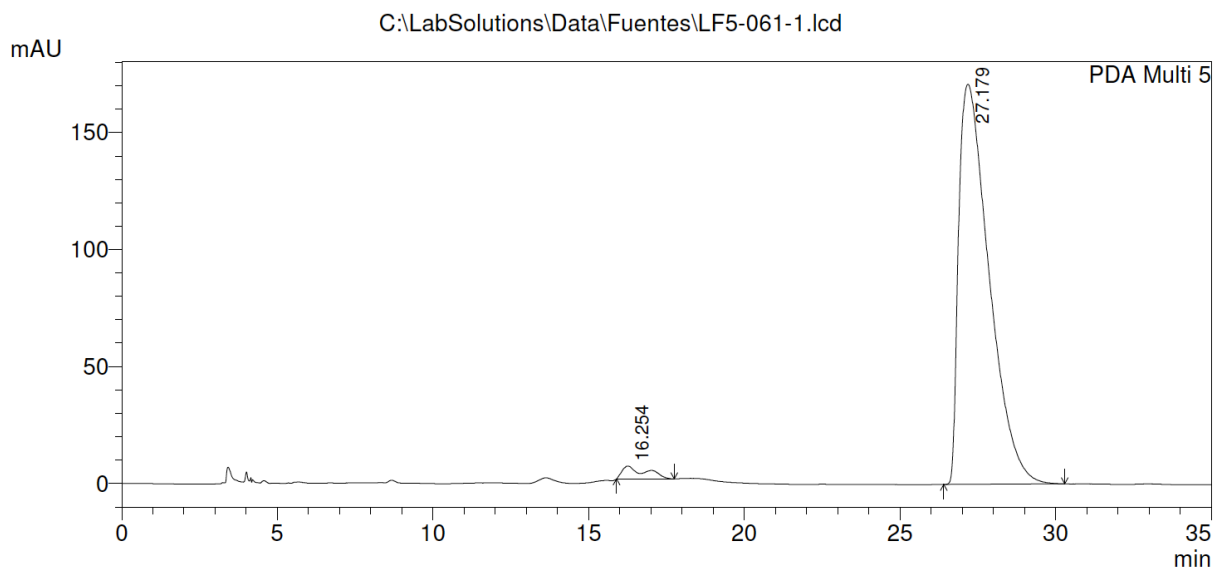


PeakTable

PDA Ch5 254nm 4nm

Peak#	Ret. Time	Area	Height	Area %	Height %
1	16.220	7122348	148356	43.247	53.919
2	27.267	9346824	126792	56.753	46.081
Total		16469173	275149	100.000	100.000

Enantioenriched **119** (Chiralpak IA, Hexanes/*i*PrOH 95:5, 254 nm)

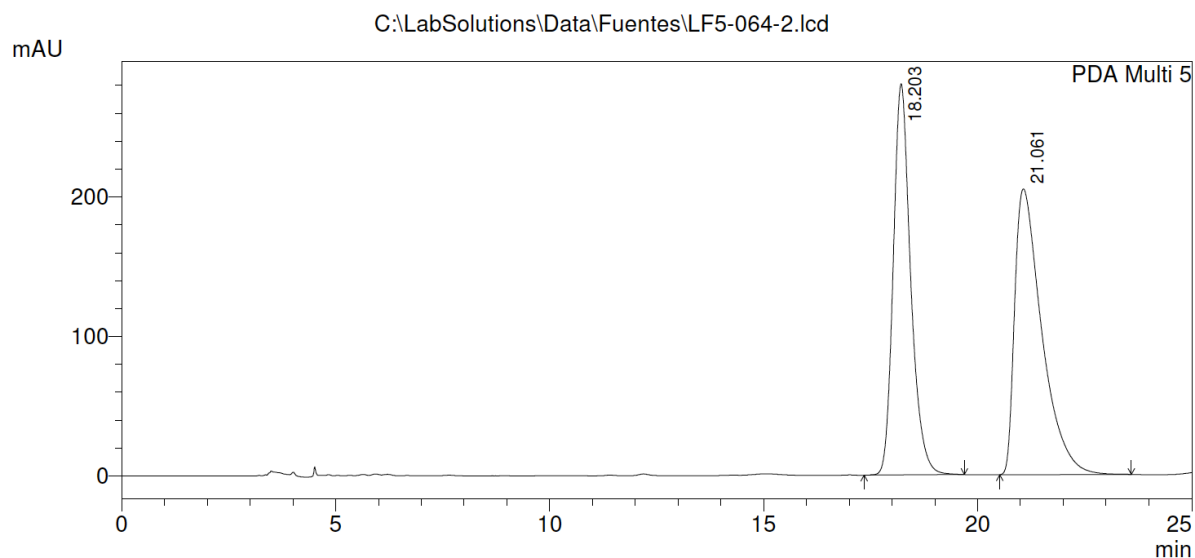


PeakTable

PDA Ch5 254nm 4nm

Peak#	Ret. Time	Area	Height	Area %	Height %
1	16.254	283669	5458	2.391	3.095
2	27.179	11580184	170891	97.609	96.905
Total		11863853	176349	100.000	100.000

Racemic **120** (Chiralpak IA, Hexanes/*i*PrOH 90:10, 254 nm)

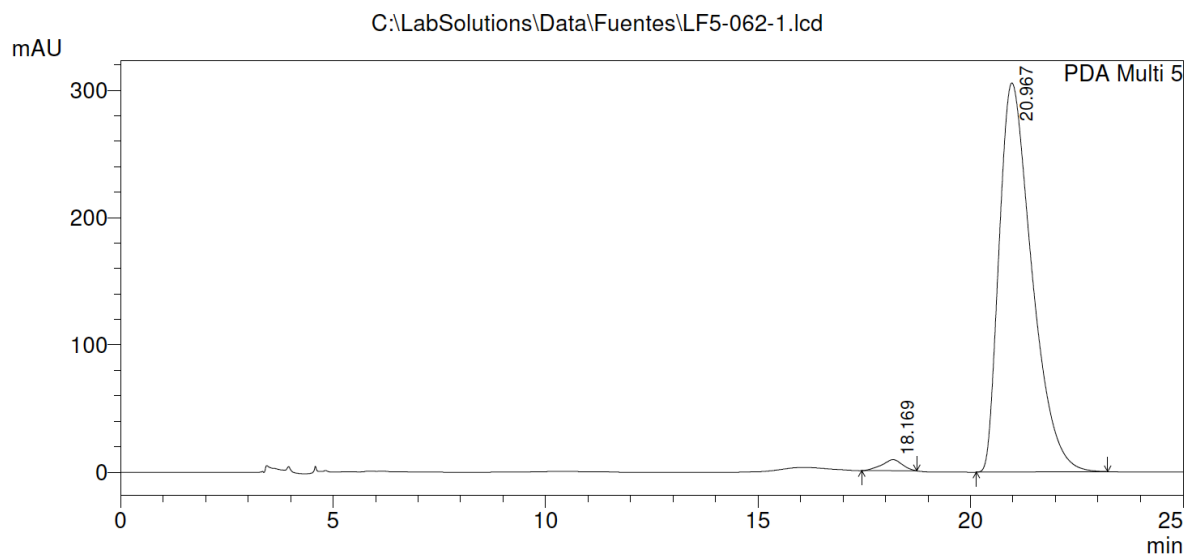


PeakTable

PDA Ch5 254nm 4nm

Peak#	Ret. Time	Area	Height	Area %	Height %
1	18.203	7939134	280392	46.827	57.785
2	21.061	9014991	204843	53.173	42.215
Total		16954124	485235	100.000	100.000

Enantioenriched **120** (Chiralpak IA, Hexanes/*i*PrOH 90:10, 254 nm)



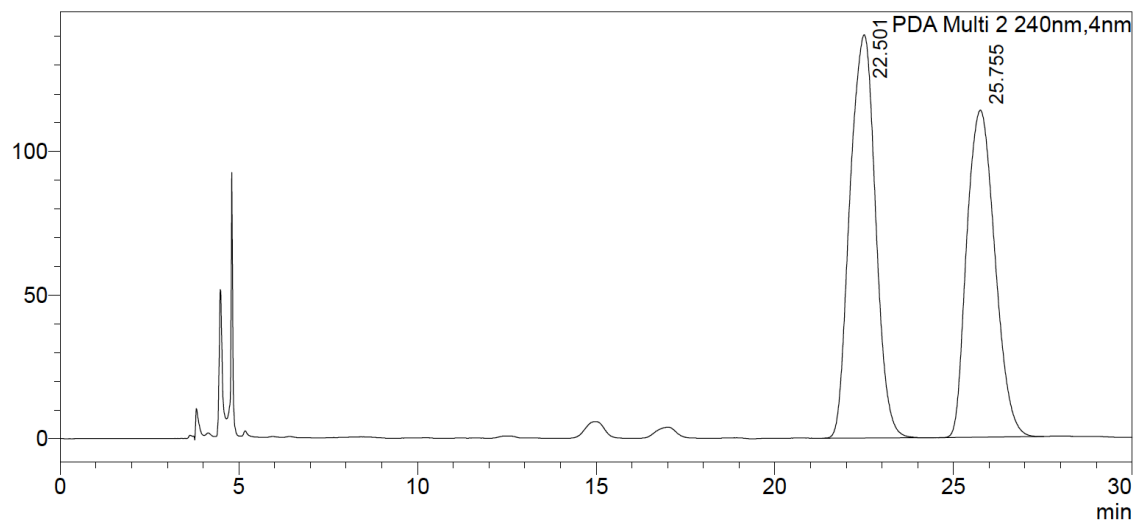
PeakTable

PDA Ch5 254nm 4nm

Peak#	Ret. Time	Area	Height	Area %	Height %
1	18.169	293398	8703	1.768	2.768
2	20.967	16301701	305727	98.232	97.232
Total		16595098	314430	100.000	100.000

Racemic **123** (Chiralpak AD-H, Hexanes/*i*PrOH, 95:5, 240 nm)

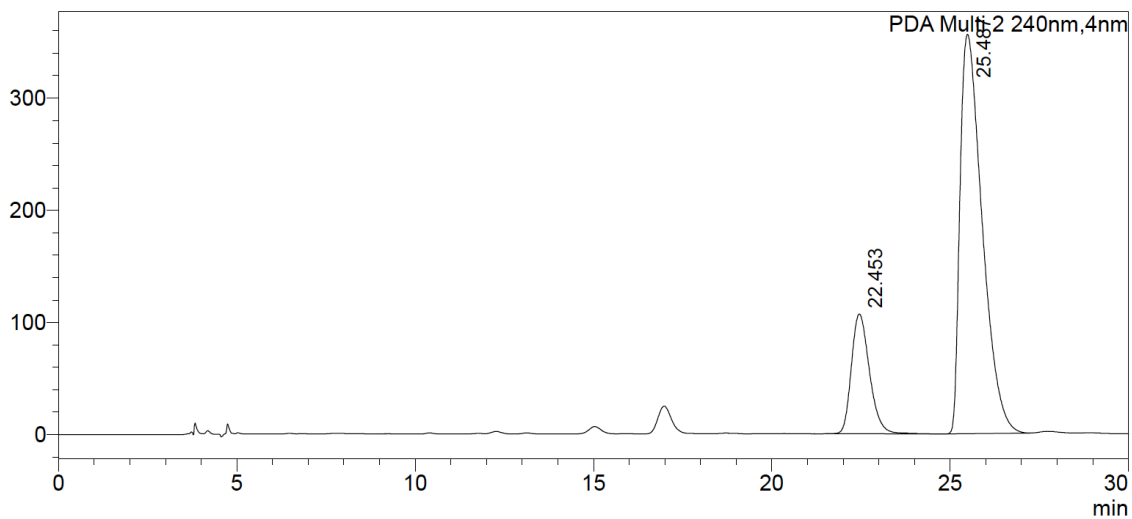
mAU



PDA Ch2 240nm					
Peak#	Ret. Time	Area	Height	Area%	Height%
1	22.501	6987684	140380	52.893	55.215
2	25.755	6223383	113862	47.107	44.785
Total		13211066	254242	100.000	100.000

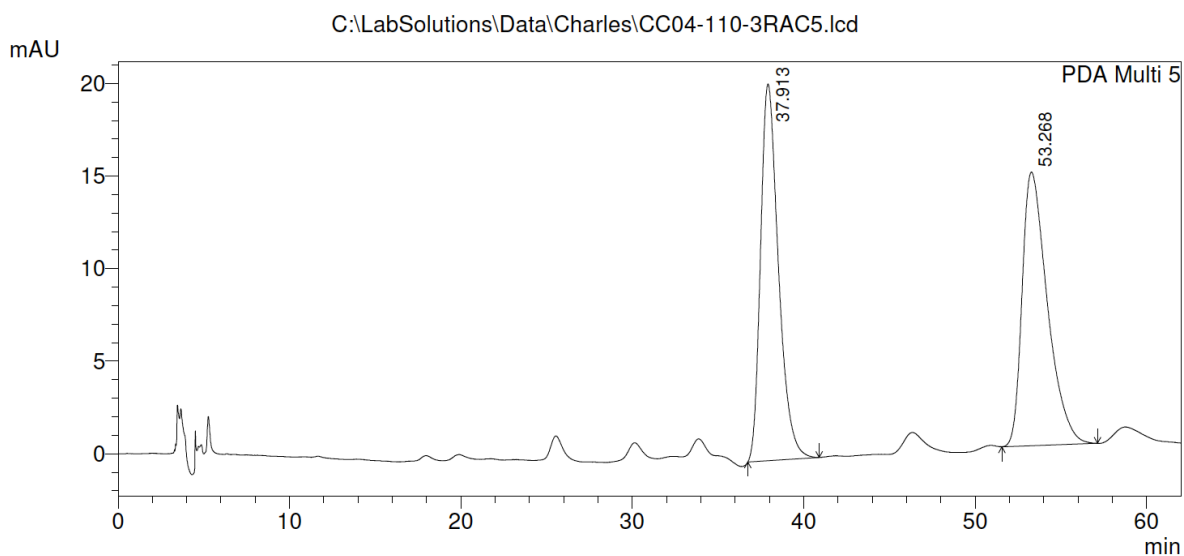
Enantioenriched **123** (Chiralpak AD-H, Hexanes/*i*PrOH, 95:5, 240 nm)

mAU



PDA Ch2 240nm					
Peak#	Ret. Time	Area	Height	Area%	Height%
1	22.453	3777674	106893	19.710	23.087
2	25.487	15388599	356108	80.290	76.913
Total		19166274	463001	100.000	100.000

Racemic **124** (Chiralpak IA, Hexanes/*i*PrOH 97:3, 254 nm)



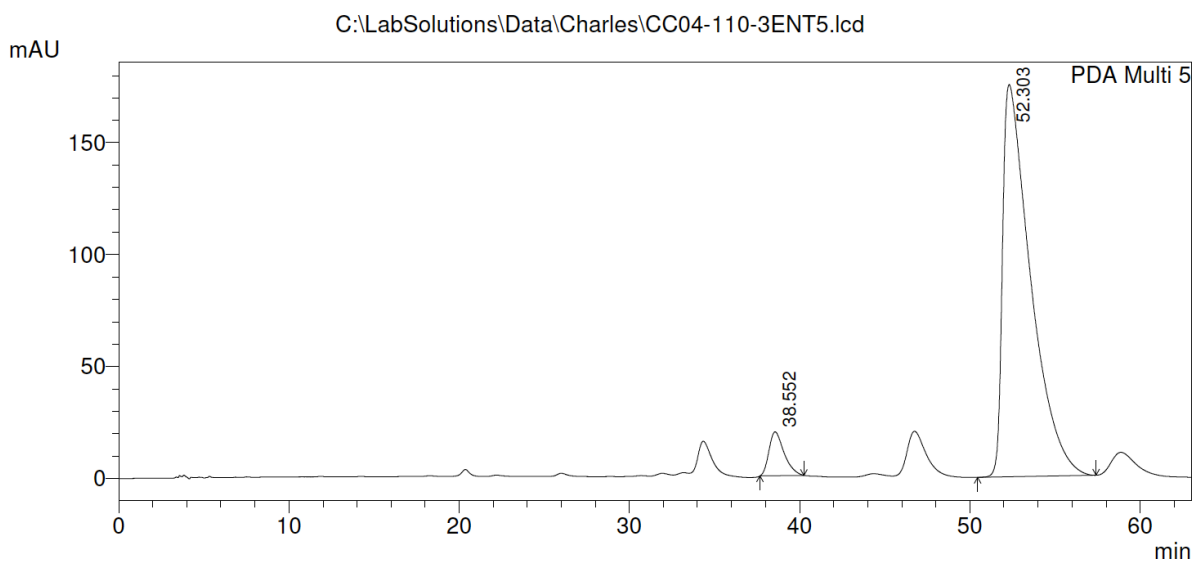
1 PDA Multi 5/254nm 4nm

PeakTable

PDA Ch5 254nm 4nm

Peak#	Ret. Time	Area	Height	Area %	Height %
1	37.913	1474958	20354	49.312	57.936
2	53.268	1516091	14778	50.688	42.064
Total		2991049	35131	100.000	100.000

Enantioenriched **124** (Chiralpak IA, Hexanes/*i*PrOH 97:3, 254 nm)



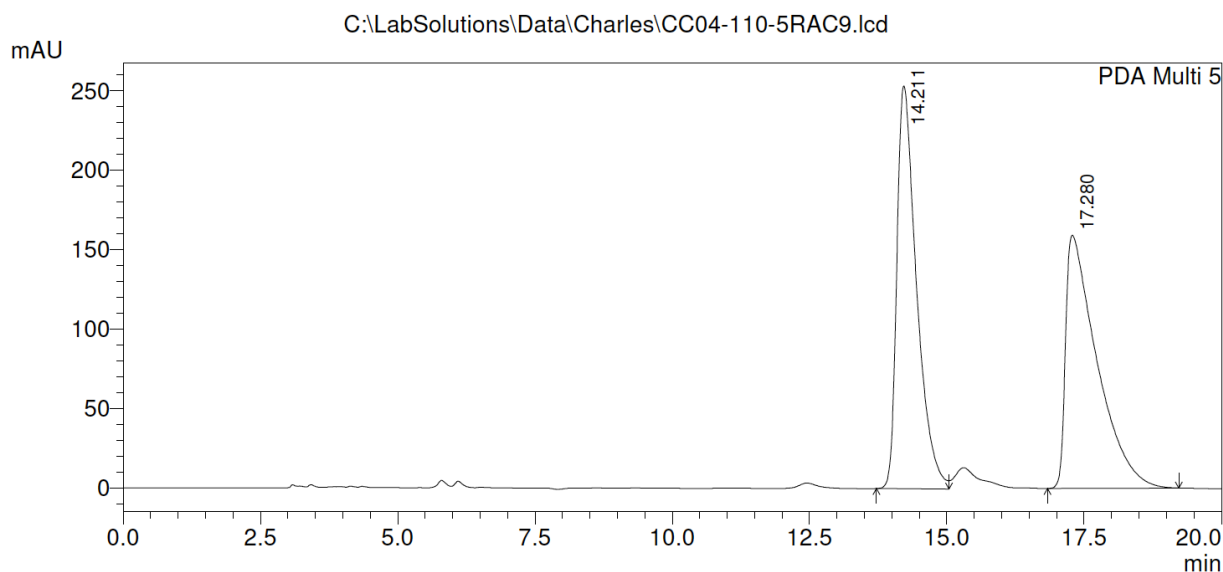
1 PDA Multi 5/254nm 4nm

PeakTable

PDA Ch5 254nm 4nm

Peak#	Ret. Time	Area	Height	Area %	Height %
1	38.552	1214658	19613	5.714	10.066
2	52.303	20044748	175225	94.286	89.934
Total		21259406	194837	100.000	100.000

Racemic **125** (Chiralpak IA, Hexanes/*i*PrOH 88:12, 254 nm)

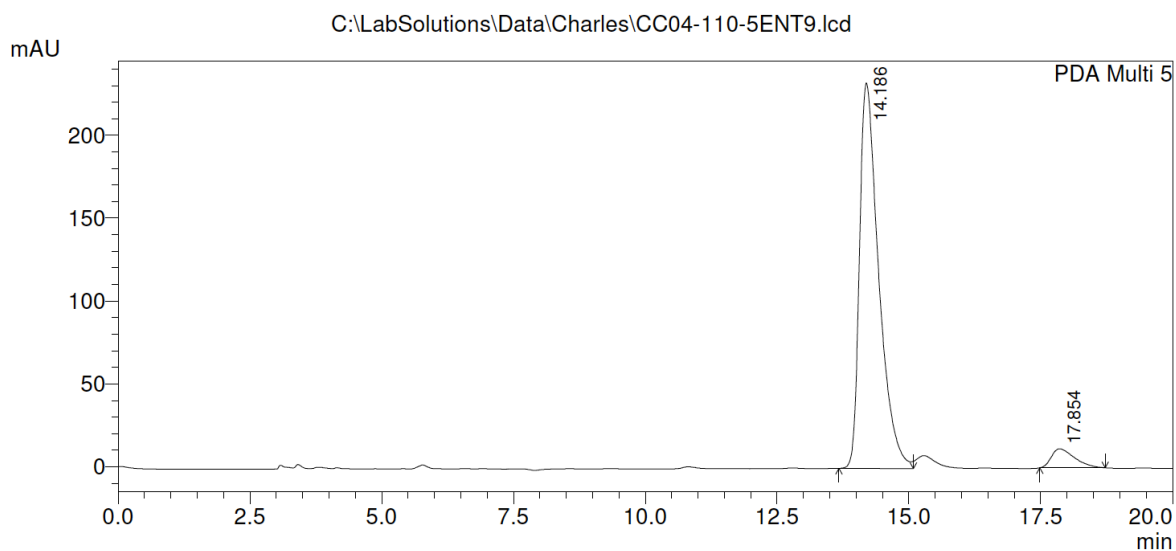


1 PDA Multi 5/254nm 4nm

PeakTable

Peak#	Ret. Time	Area	Height	Area %	Height %
1	14.211	6336270	253594	50.047	61.395
2	17.280	6324427	159460	49.953	38.605
Total		12660697	413054	100.000	100.000

Enantioenriched **125** (Chiralpak IA, Hexanes/*i*PrOH 88:12, 254 nm)



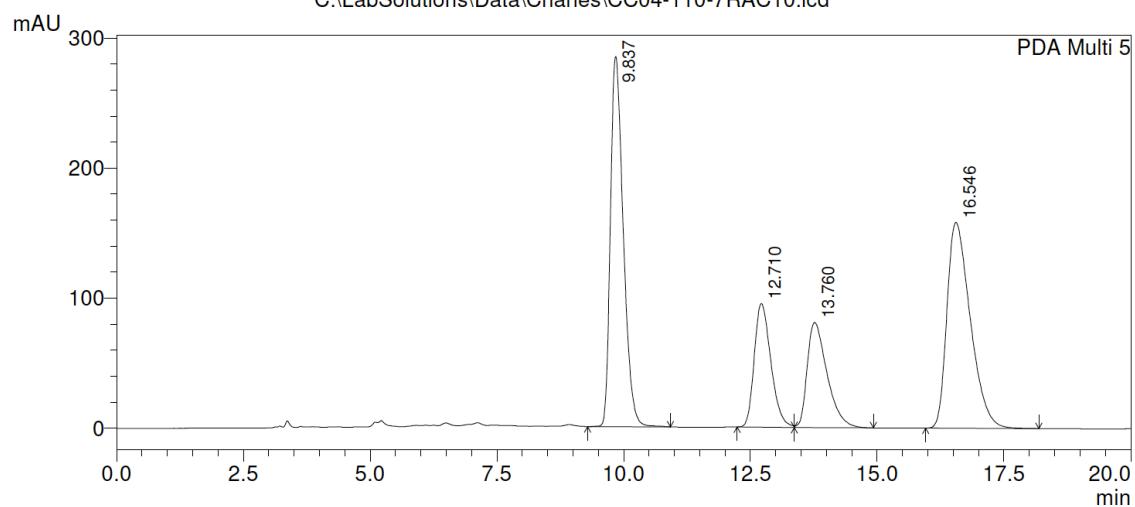
1 PDA Multi 5/254nm 4nm

PeakTable

Peak#	Ret. Time	Area	Height	Area %	Height %
1	14.186	5907117	232612	94.401	95.298
2	17.854	350337	11478	5.599	4.702
Total		6257454	244090	100.000	100.000

Racemic **126** (Chiralcel OD-H, Hexanes/*i*PrOH 90:10, 254 nm)

C:\LabSolutions\Data\Charles\CC04-110-7RAC10.lcd



1 PDA Multi 5/254nm 4nm

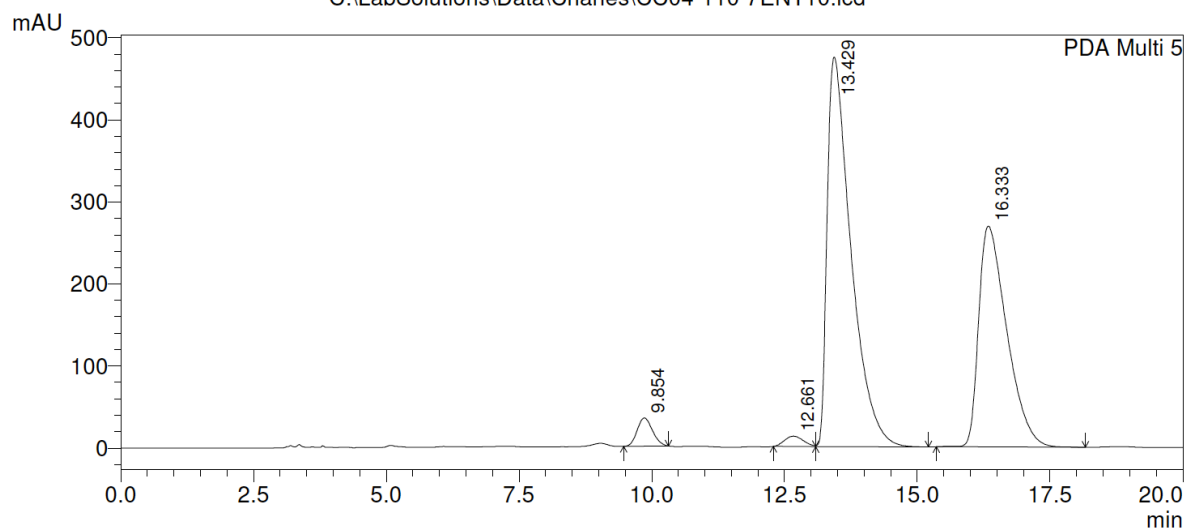
PeakTable

PDA Ch5 254nm 4nm

Peak#	Ret. Time	Area	Height	Area %	Height %
1	9.837	5016277	284652	34.698	46.006
2	12.710	2167971	95064	14.996	15.364
3	13.760	2198582	80732	15.208	13.048
4	16.546	5074045	158287	35.098	25.582
Total		14456874	618734	100.000	100.000

Enantioenriched **126** (Chiralcel OD-H, Hexanes/*i*PrOH 90:10, 254 nm)

C:\LabSolutions\Data\Charles\CC04-110-7ENT10.lcd



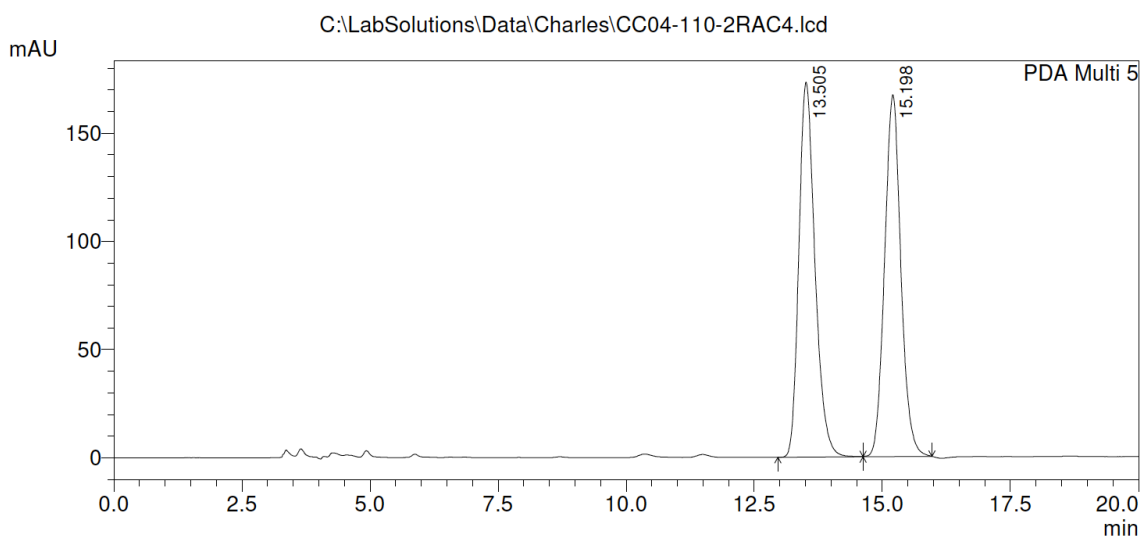
1 PDA Multi 5/254nm 4nm

PeakTable

PDA Ch5 254nm 4nm

Peak#	Ret. Time	Area	Height	Area %	Height %
1	9.854	692226	34429	2.691	4.354
2	12.661	310365	12596	1.206	1.593
3	13.429	14823458	474667	57.616	60.025
4	16.333	9902165	269091	38.488	34.028
Total		25728215	790783	100.000	100.000

Racemic **127** (Chiralpak AD-H, Hexanes/*i*PrOH 95:5, 254 nm)

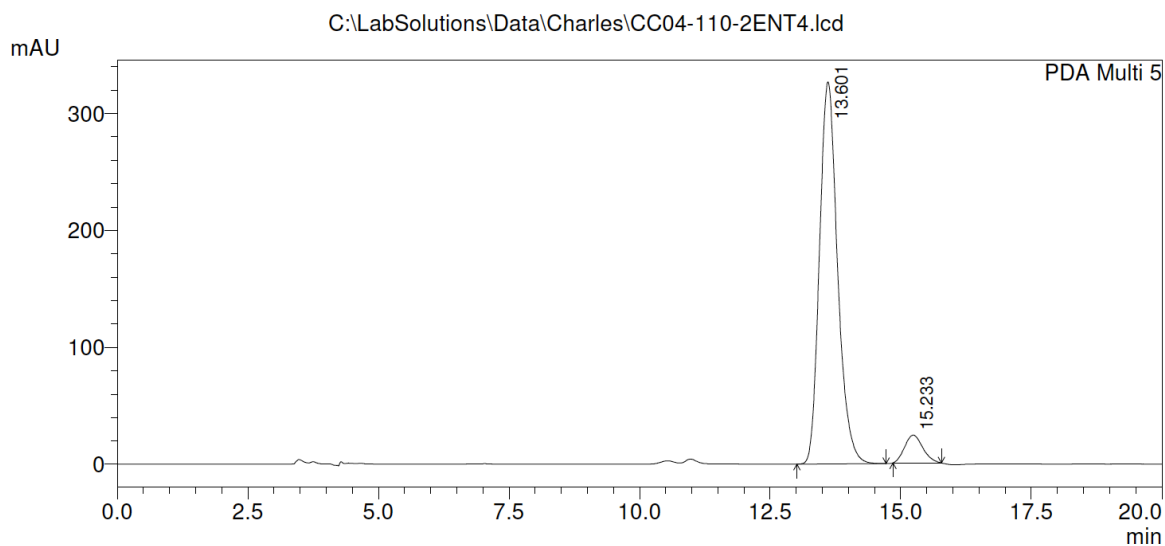


PeakTable

PDA Ch5 254nm 4nm

Peak#	Ret. Time	Area	Height	Area %	Height %
1	13.505	3789793	173302	50.545	50.883
2	15.198	3708070	167286	49.455	49.117
Total		7497863	340588	100.000	100.000

Enantioenriched **127** (Chiralpak AD-H, Hexanes/*i*PrOH 95:5, 254 nm)

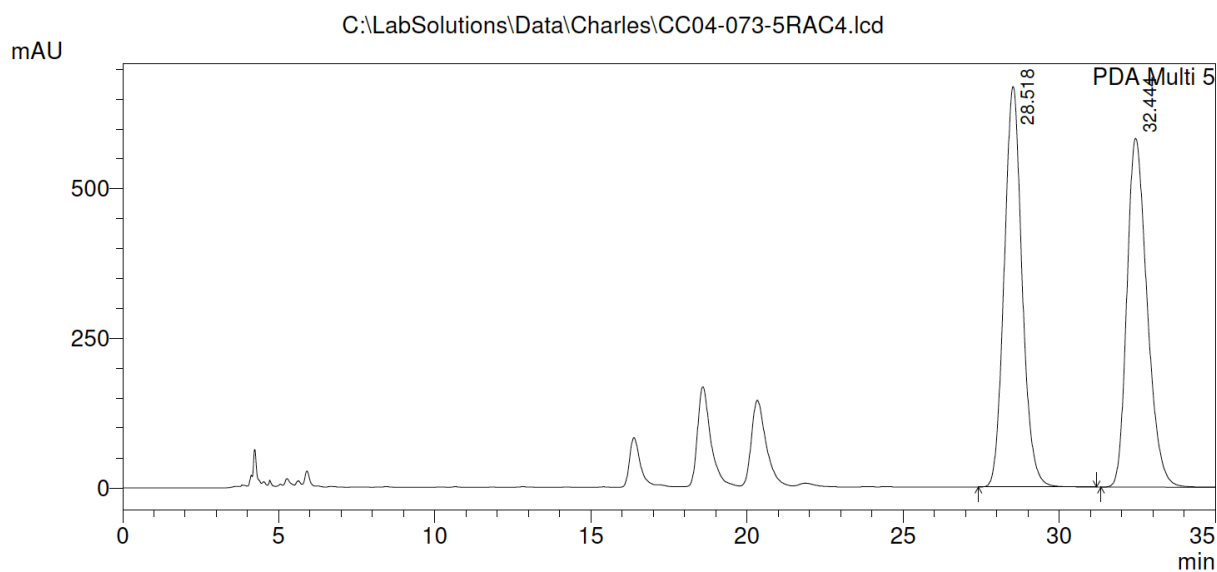


PeakTable

PDA Ch5 254nm 4nm

Peak#	Ret. Time	Area	Height	Area %	Height %
1	13.601	7865847	326769	93.176	93.221
2	15.233	576074	23764	6.824	6.779
Total		8441921	350533	100.000	100.000

Racemic **128** (Chiralpak AD-H, Hexanes/*i*PrOH 95:5, 254 nm)



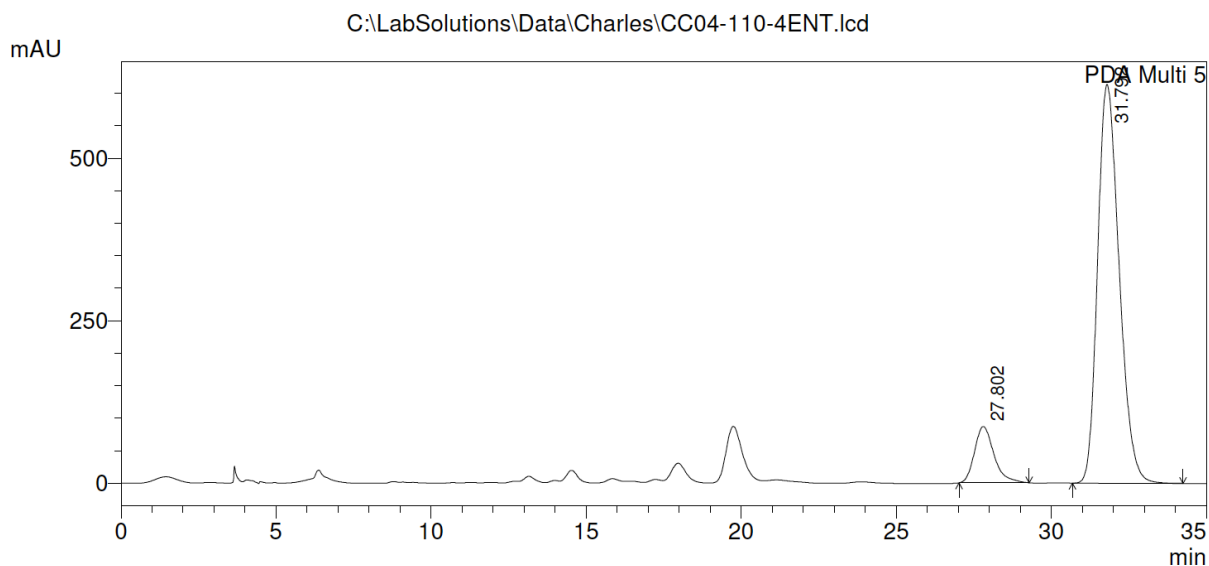
1 PDA Multi 5/254nm 4nm

PeakTable

PDA Ch5 254nm 4nm

Peak#	Ret. Time	Area	Height	Area %	Height %
1	28.518	26744807	669883	50.416	53.447
2	32.444	26303396	583482	49.584	46.553
Total		53048203	1253365	100.000	100.000

Enantioenriched **128** (Chiralpak AD-H, Hexanes/*i*PrOH 95:5, 254 nm)



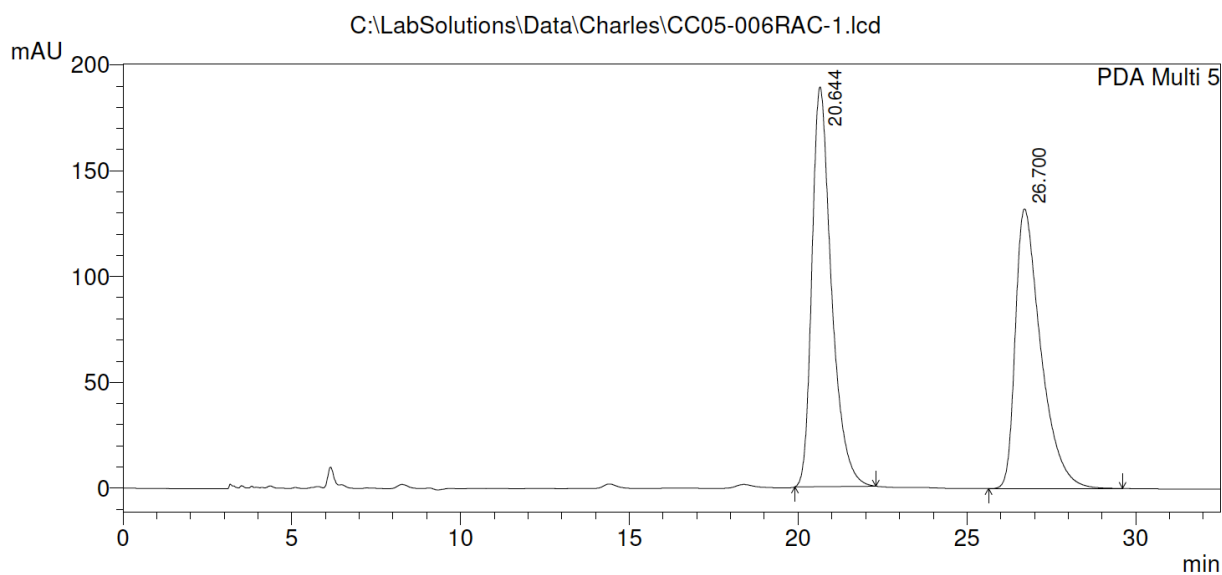
1 PDA Multi 5/254nm 4nm

PeakTable

PDA Ch5 254nm 4nm

Peak#	Ret. Time	Area	Height	Area %	Height %
1	27.802	3784088	86527	11.321	12.363
2	31.792	29642661	613355	88.679	87.637
Total		33426749	699882	100.000	100.000

Racemic **132** (Chiralpak IA, Hexanes/*i*PrOH 90:10, 254 nm)

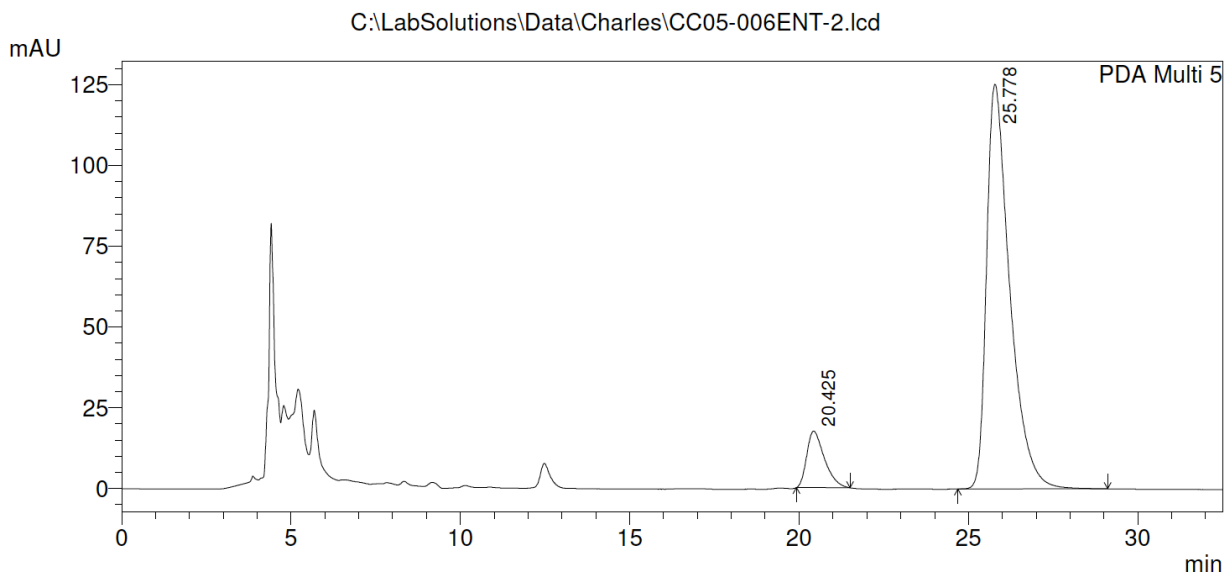


PeakTable

PDA Ch5 254nm 4nm

Peak#	Ret. Time	Area	Height	Area %	Height %
1	20.644	7602453	188892	52.282	58.832
2	26.700	6938674	132177	47.718	41.168
Total		14541128	321069	100.000	100.000

Enantioenriched **132** (Chiralpak IA, Hexanes/*i*PrOH 90:10, 254 nm)

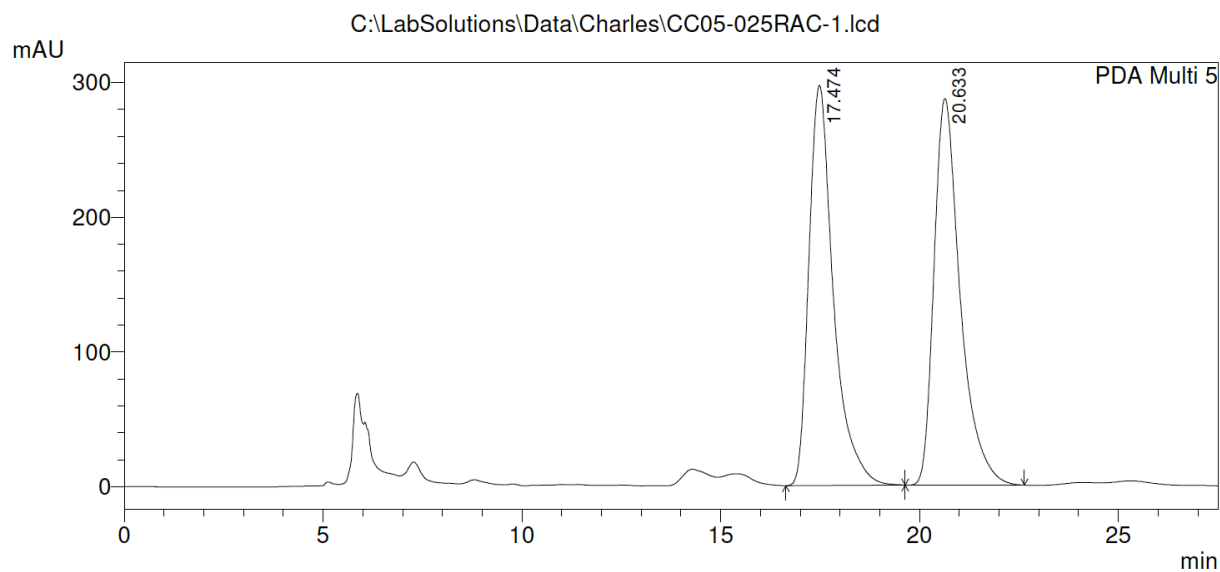


PeakTable

PDA Ch5 254nm 4nm

Peak#	Ret. Time	Area	Height	Area %	Height %
1	20.425	632826	17483	9.598	12.256
2	25.778	5960170	125166	90.402	87.744
Total		6592996	142649	100.000	100.000

Racemic **133** (Chiralpak IA, Hexanes/*i*PrOH 90:10, 254 nm)

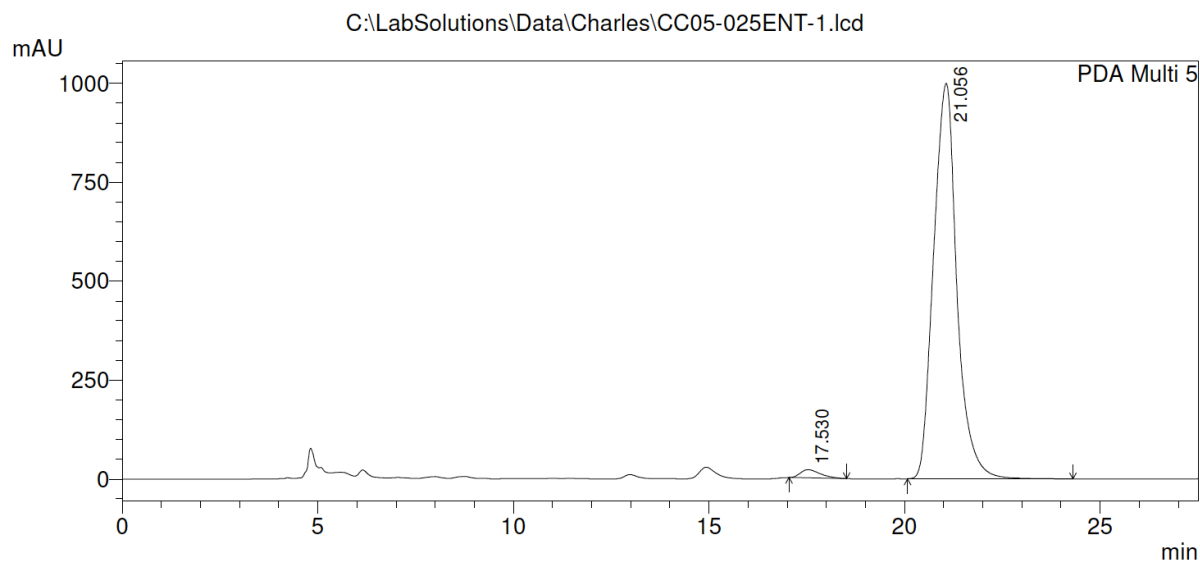


PeakTable

PDA Ch5 254nm 4nm

Peak#	Ret. Time	Area	Height	Area %	Height %
1	17.474	12716112	297063	49.157	50.868
2	20.633	13152424	286920	50.843	49.132
Total		25868536	583983	100.000	100.000

Enantioenriched **133** (Chiralpak IA, Hexanes/*i*PrOH 90:10, 254 nm)

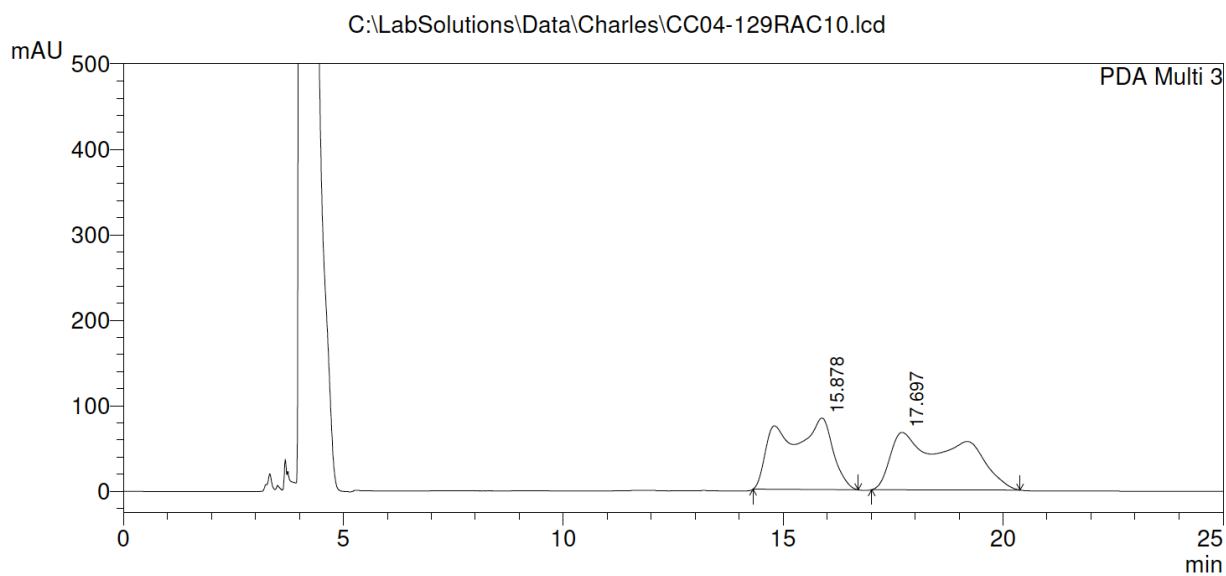


PeakTable

PDA Ch5 254nm 4nm

Peak#	Ret. Time	Area	Height	Area %	Height %
1	17.530	735208	20670	1.747	2.028
2	21.056	41337255	998760	98.253	97.972
Total		42072463	1019430	100.000	100.000

Racemic **134** (Chiralcel OJ-H, Hexanes/*i*PrOH 99:1, 215 nm)



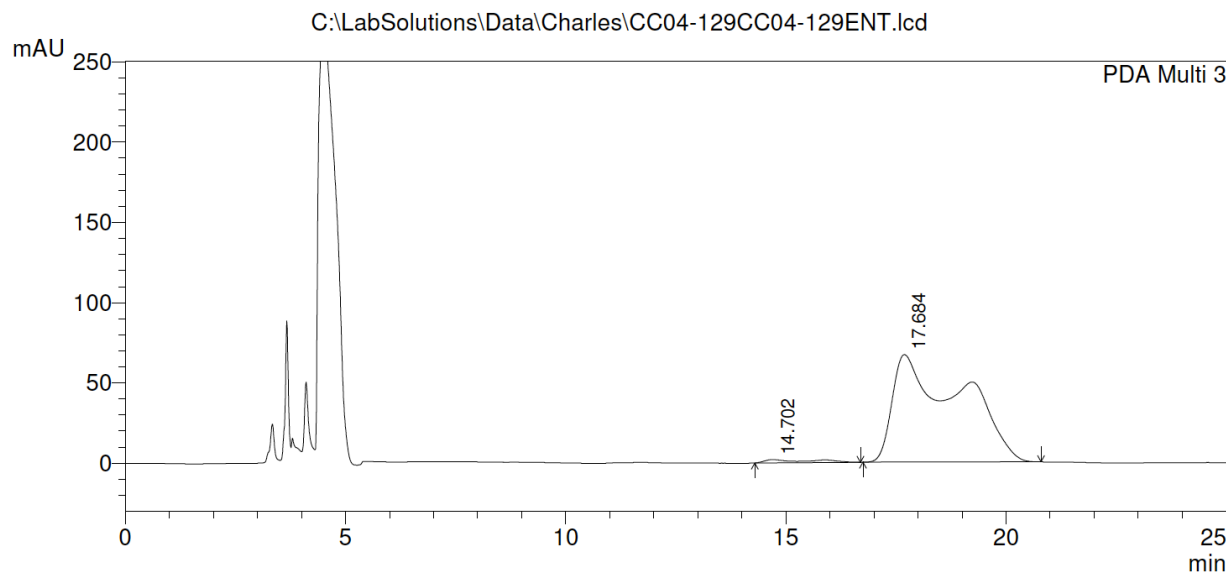
1 PDA Multi 3/215nm 4nm

PeakTable

PDA Ch3 215nm 4nm

Peak#	Ret. Time	Area	Height	Area %	Height %
1	15.878	6678515	83808	47.405	55.533
2	17.697	7409694	67108	52.595	44.467
Total		14088209	150917	100.000	100.000

Enantioenriched **134** (Chiralcel OJ-H, Hexanes/*i*PrOH 99:1, 215 nm)



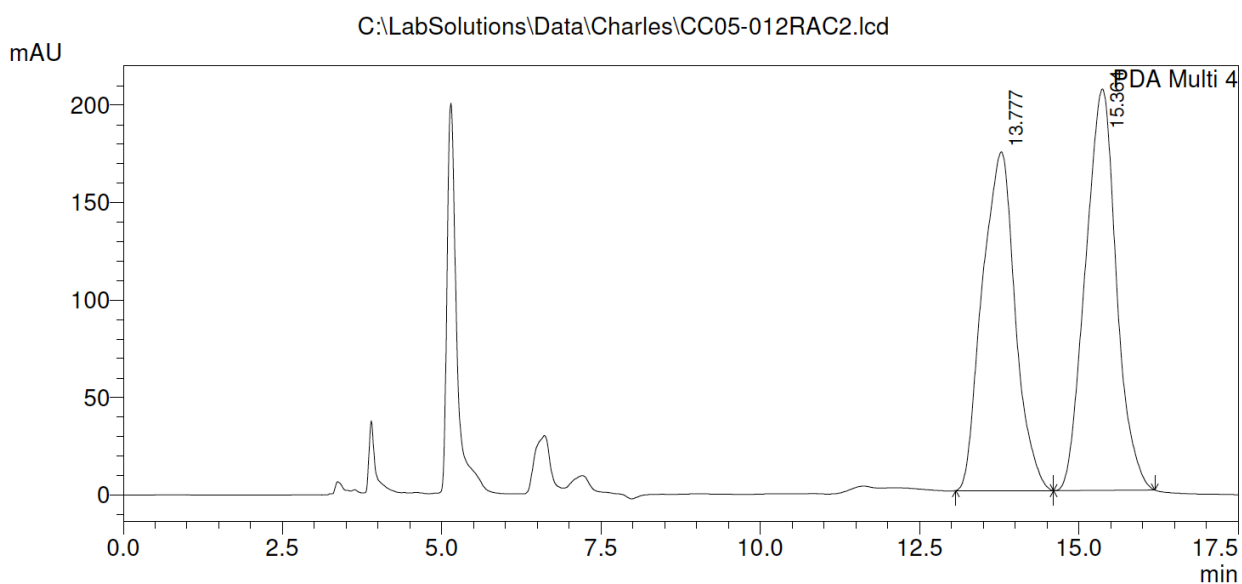
1 PDA Multi 3/215nm 4nm

PeakTable

PDA Ch3 215nm 4nm

Peak#	Ret. Time	Area	Height	Area %	Height %
1	14.702	144308	2041	1.983	2.959
2	17.684	7134381	66956	98.017	97.041
Total		7278689	68998	100.000	100.000

Racemic **136** (Chiralpak AD-H, Hexanes/*i*PrOH 90:10, 240 nm)



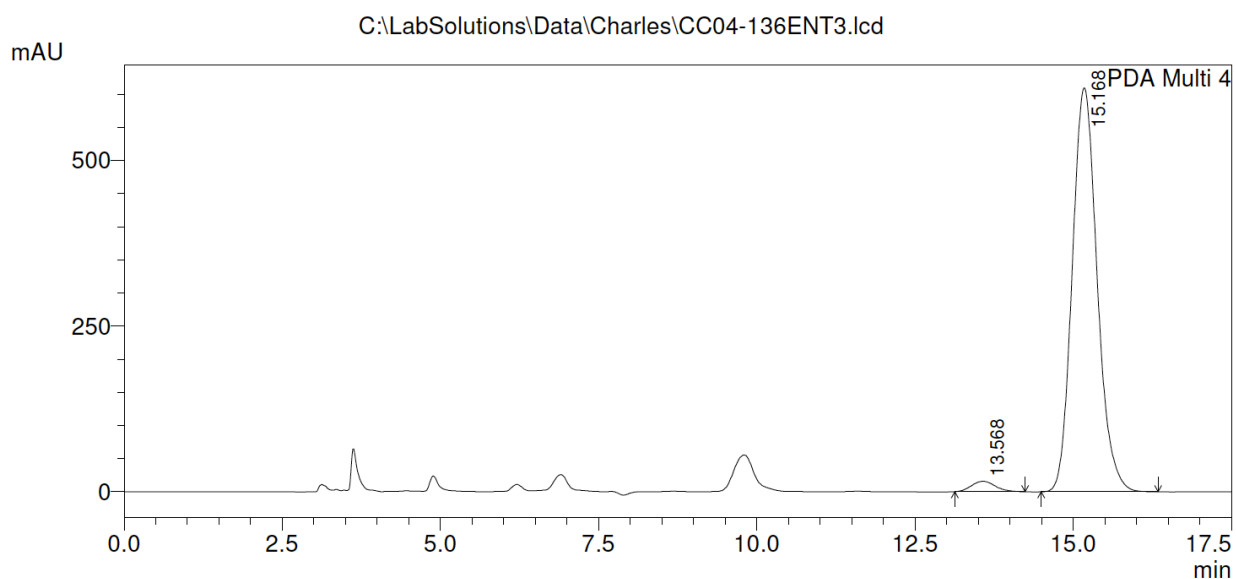
1 PDA Multi 4/240nm 1nm

PeakTable

PDA Ch4 240nm 1nm

Peak#	Ret. Time	Area	Height	Area %	Height %
1	13.777	6255295	173727	47.330	45.769
2	15.364	6961091	205849	52.670	54.231
Total		13216387	379575	100.000	100.000

Enantioenriched **136** (Chiralpak AD-H, Hexanes/*i*PrOH 90:10, 240 nm)



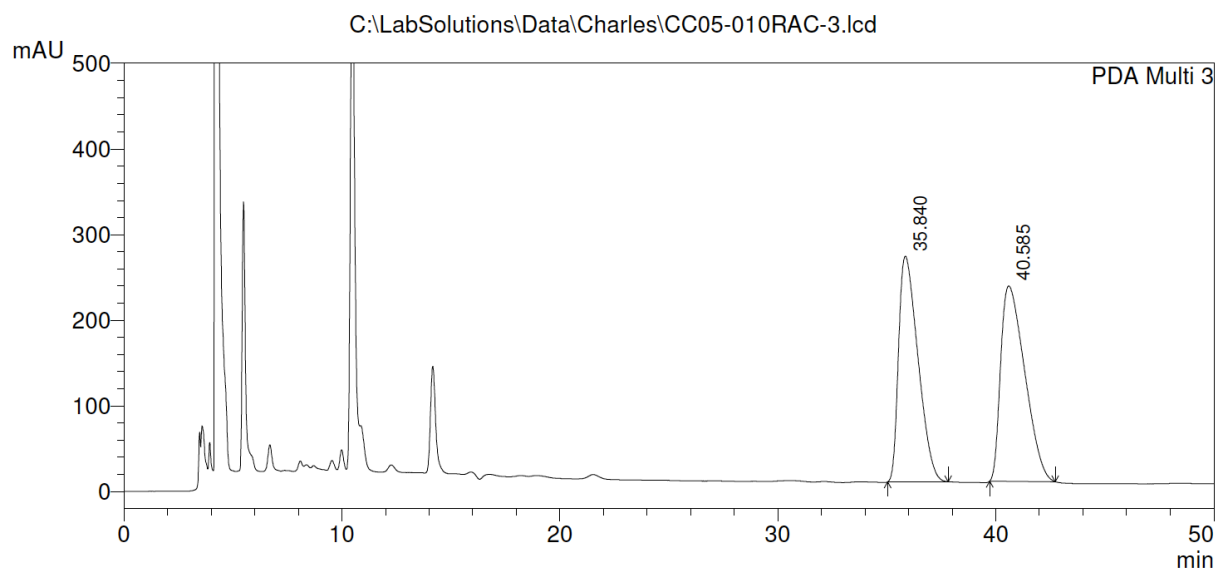
1 PDA Multi 4/240nm 1nm

PeakTable

PDA Ch4 240nm 1nm

Peak#	Ret. Time	Area	Height	Area %	Height %
1	13.568	413230	15703	2.415	2.513
2	15.168	16698964	609100	97.585	97.487
Total		17112195	624803	100.000	100.000

Racemic **137** (Chiralpak AS-H, Hexanes/*i*PrOH 90:10, 215 nm)

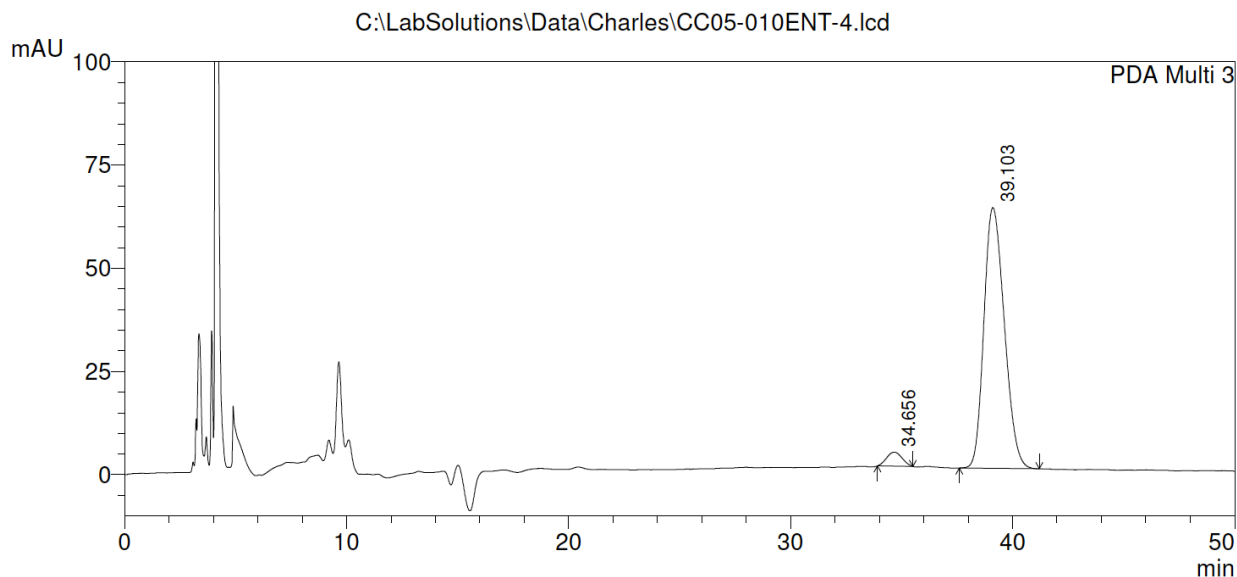


PeakTable

PDA Ch3 215nm 4nm

Peak#	Ret. Time	Area	Height	Area %	Height %
1	35.840	16239806	263521	48.142	53.591
2	40.585	17493105	228210	51.858	46.409
Total		33732910	491730	100.000	100.000

Enantioenriched **137** (Chiralpak AS-H, Hexanes/*i*PrOH 90:10, 215 nm)



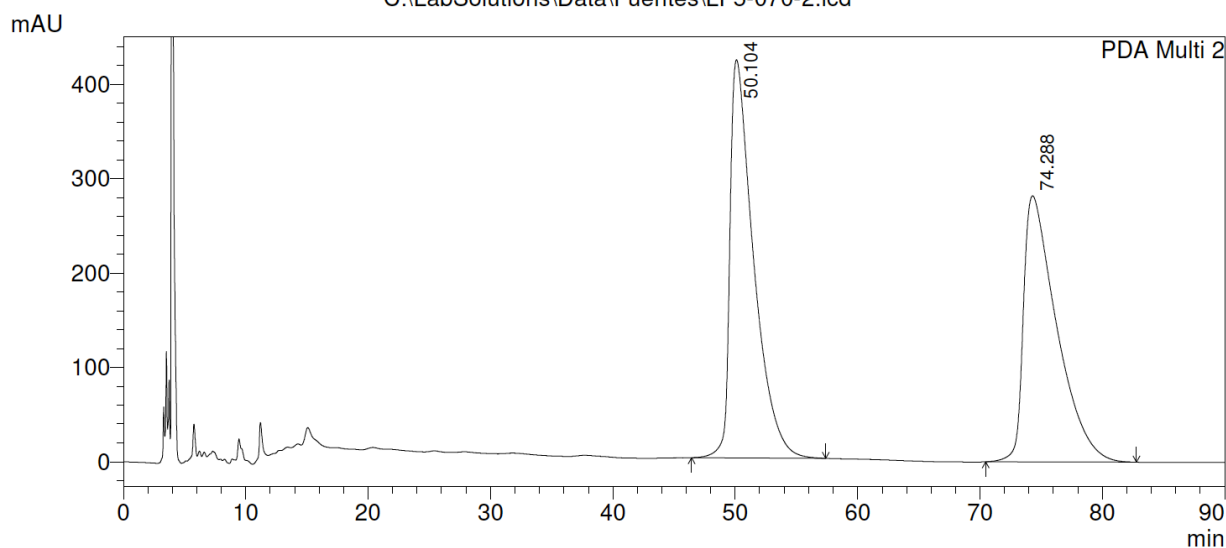
PeakTable

PDA Ch3 215nm 4nm

Peak#	Ret. Time	Area	Height	Area %	Height %
1	34.656	163203	3402	3.882	5.108
2	39.103	4040418	63202	96.118	94.892
Total		4203621	66605	100.000	100.000

Racemic **138** (Chiralcel OD-H, Hexanes/*i*PrOH 90:10, 205 nm)

C:\LabSolutions\Data\Fuentes\LF5-070-2.lcd



1 PDA Multi 2/205nm 4nm

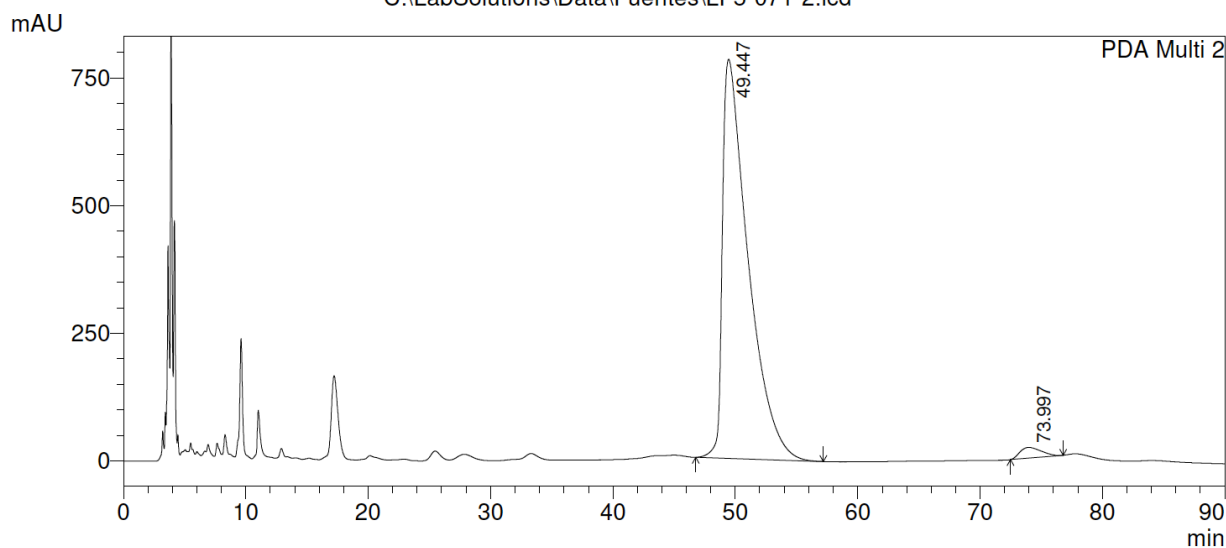
PeakTable

PDA Ch2 205nm 4nm

Peak#	Ret. Time	Area	Height	Area %	Height %
1	50.104	56832069	422211	51.590	59.940
2	74.288	53329972	282181	48.410	40.060
Total		110162041	704392	100.000	100.000

Enantioenriched **138** (Chiralcel OD-H, Hexanes/*i*PrOH 90:10, 205 nm)

C:\LabSolutions\Data\Fuentes\LF5-071-2.lcd



1 PDA Multi 2/205nm 4nm

PeakTable

PDA Ch2 205nm 4nm

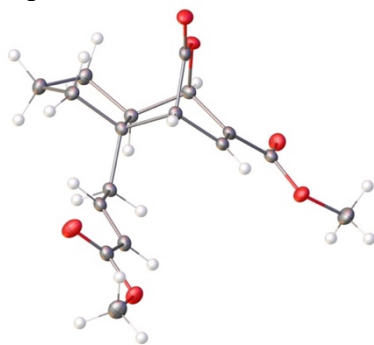
Peak#	Ret. Time	Area	Height	Area %	Height %
1	49.447	113870491	782008	97.835	97.402
2	73.997	2520135	20859	2.165	2.598
Total		116390626	802867	100.000	100.000

3.15 X-Ray Crystallographic Data

(Note: All crystal structures are of the corresponding Wittig products)

General information: The diffraction data were measured at 100 K on a Bruker D8 VENTURE diffractometer equipped with a microfocus Mo-target X-ray tube ($\lambda = 0.71073 \text{ \AA}$) and PHOTON 100 CMOS detector. Data were collected using ϕ and ω scans to survey a hemisphere of reciprocal space. Data reduction and integration were performed with the Bruker APEX3 software package (Bruker AXS, version 2017.3-0, 2018). Data were scaled and corrected for absorption effects using the multi-scan procedure as implemented in SADABS (Bruker AXS, version 2014/5, Krause, Herbst-Irmer, Sheldrick & Stalke, *J. Appl. Cryst.* **2015**, *48*, 3-10). The structure was solved by SHELXT (Version 2014/5: Sheldrick, G. M. *Acta Crystallogr.* **2015**, *A71*, 3-8) and refined by a full-matrix least-squares procedure using OLEX2 (O. V. Dolomanov, L. J. Bourhis, R. J. Gildea, J. A. K. Howard and H. Puschmann. *J. Appl. Crystallogr.* **2009**, *42*, 339-341) (XL refinement program version 2018/1, Sheldrick, G. M. *Acta Crystallogr.* **2015**, *C71*, 3-8). **Specific details for structure refinement:** All atoms were refined with anisotropic thermal parameters. Hydrogen atoms were included in idealized positions for structure factor calculations. All structures are drawn with thermal ellipsoids at 50% probability.

Figure 3.4. ORTEP representation of *Endo-88*.



Crystal data and structure refinement for cu_0682_Cole_AM_0m.

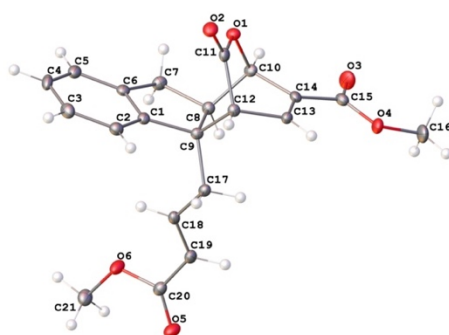
Identification code	cu_0682_Cole_AM_0m
Empirical formula	C ₁₇ H ₂₀ O ₆
Formula weight	320.33
Temperature/K	100(2)
Crystal system	monoclinic
Space group	<i>P</i> 2 ₁
<i>a</i> /Å	7.0910(4)
<i>b</i> /Å	16.2621(9)
<i>c</i> /Å	13.2704(7)
α /°	90
β /°	92.494(2)

Figure 3.4. *continued.*

$\gamma/^\circ$	90
Volume/ \AA^3	1528.82(15)
Z	4
$\rho_{\text{calc}}/\text{cm}^3$	1.392
μ/mm^{-1}	0.881
F(000)	680.0
Crystal size/ mm^3	$0.38 \times 0.31 \times 0.28$
Radiation	CuK α ($\lambda = 1.54178$)
2Θ range for data collection/ $^\circ$	6.666 to 145.374
Index ranges	$-8 \leq h \leq 8, -20 \leq k \leq 20, -16 \leq l \leq 16$
Reflections collected	25135
Independent reflections	6029 [$R_{\text{int}} = 0.0301, R_{\text{sigma}} = 0.0249$]
Data/restraints/parameters	6029/1/419
Goodness-of-fit on F^2	1.042
Final R indexes [$I \geq 2\sigma(I)$]	$R_1 = 0.0275, wR_2 = 0.0705$
Final R indexes [all data]	$R_1 = 0.0280, wR_2 = 0.0709$
Largest diff. peak/hole / $e \text{\AA}^{-3}$	0.20/-0.19
Flack parameter	-0.01(4)
Hooft parameter	0.01(3)
$R_{\text{int}} = \Sigma F_o^2 - \langle F_o^2 \rangle / \Sigma F_o^2 $	
$R_1 = \Sigma F_o - F_c / \Sigma F_o $	
$wR_2 = [\Sigma [w(F_o^2 - F_c^2)^2] / \Sigma [w(F_o^2)^2]]^{1/2}$	
Goodness-of-fit = $[\Sigma [w(F_o^2 - F_c^2)^2] / (n-p)]^{1/2}$	

n: number of independent reflections; p: number of refined parameters

Figure 3.5. ORTEP representation of *Endo-106*.



Crystal data and structure refinement for 0692_cole.

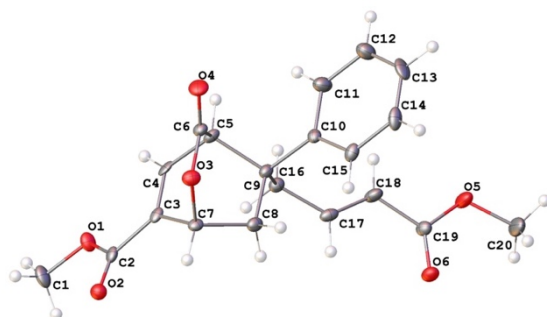
Identification code	0692_cole
Empirical formula	$\text{C}_{21}\text{H}_{20}\text{O}_6$
Formula weight	368.37
Temperature/K	100(2)
Crystal system	orthorhombic
Space group	$P2_12_12_1$
a/ \AA	8.6977(4)

Figure 3.5. *continued.*

b/Å	9.9164(4)
c/Å	20.6241(9)
$\alpha/^\circ$	90
$\beta/^\circ$	90
$\gamma/^\circ$	90
Volume/Å ³	1778.83(13)
Z	4
$\rho_{\text{calc}}/\text{cm}^3$	1.375
μ/mm^{-1}	0.101
F(000)	776.0
Crystal size/mm ³	0.28 × 0.2 × 0.18
Radiation	MoK α ($\lambda = 0.71073$)
2 Θ range for data collection/ $^\circ$	4.558 to 57.466
Index ranges	-10 ≤ h ≤ 11, -13 ≤ k ≤ 12, -27 ≤ l ≤ 27
Reflections collected	6802
Independent reflections	4513 [R _{int} = 0.0480, R _{sigma} = 0.0908]
Data/restraints/parameters	4513/0/254
Goodness-of-fit on F ²	1.040
Final R indexes [I ≥ 2 σ (I)]	R ₁ = 0.0511, wR ₂ = 0.1017
Final R indexes [all data]	R ₁ = 0.0795, wR ₂ = 0.1140
Largest diff. peak/hole / e Å ⁻³	0.30/-0.25
$R_{\text{int}} = \Sigma F_o^2 - \langle F_o^2 \rangle / \Sigma F_o^2 $	
$R_1 = \Sigma F_o - F_c / \Sigma F_o $	
$wR_2 = [\Sigma [w(F_o^2 - F_c^2)^2] / \Sigma [w(F_o^2)^2]]^{1/2}$	
Goodness-of-fit = $[\Sigma [w(F_o^2 - F_c^2)^2] / (n-p)]^{1/2}$	

n: number of independent reflections; p: number of refined parameters

Figure 3.6. ORTEP representation of *Endo-110*.



Crystal data and structure refinement for 0685_cole.

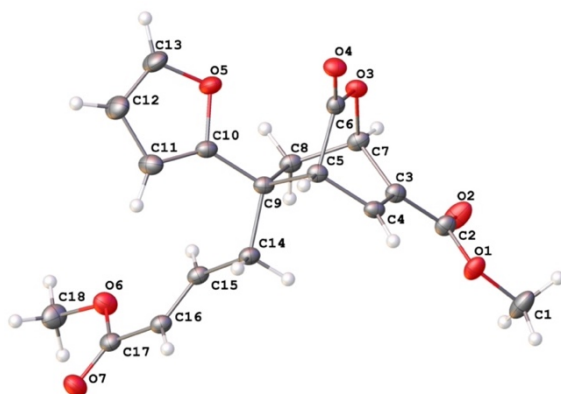
Identification code	0685_cole
Empirical formula	C ₂₀ H ₂₀ O ₆
Formula weight	356.36
Temperature/K	100(2)
Crystal system	monoclinic
Space group	P2 ₁ /c

Figure 3.6. *continued.*

a/Å	11.1979(9)
b/Å	12.5205(10)
c/Å	24.904(2)
$\alpha/^\circ$	90
$\beta/^\circ$	93.401(2)
$\gamma/^\circ$	90
Volume/Å ³	3485.5(5)
Z	8
$\rho_{\text{calc}}/\text{cm}^3$	1.358
μ/mm^{-1}	0.100
F(000)	1504.0
Crystal size/mm ³	0.32 × 0.16 × 0.08
Radiation	MoK α ($\lambda = 0.71073$)
2 Θ range for data collection/ $^\circ$	4.618 to 50.92
Index ranges	-13 ≤ h ≤ 13, -15 ≤ k ≤ 15, -30 ≤ l ≤ 30
Reflections collected	41322
Independent reflections	6449 [$R_{\text{int}} = 0.0939$, $R_{\text{sigma}} = 0.0747$]
Data/restraints/parameters	6449/0/473
Goodness-of-fit on F ²	1.066
Final R indexes [$I \geq 2\sigma(I)$]	$R_1 = 0.0846$, $wR_2 = 0.1990$
Final R indexes [all data]	$R_1 = 0.1373$, $wR_2 = 0.2260$
Largest diff. peak/hole / e Å ⁻³	0.85/-0.31
$R_{\text{int}} = \Sigma F_o^2 - \langle F_o^2 \rangle / \Sigma F_o^2 $	
$R_1 = \Sigma F_o - F_c / \Sigma F_o $	
$wR_2 = [\Sigma [w(F_o^2 - F_c^2)^2] / \Sigma [w(F_o^2)^2]]^{1/2}$	
Goodness-of-fit = $[\Sigma [w(F_o^2 - F_c^2)^2] / (n-p)]^{1/2}$	

n: number of independent reflections; p: number of refined parameters

Figure 3.7. ORTEP representation of *Endo-114*.



Crystal data and structure refinement for 0683_cole.

Identification code	0683_cole
Empirical formula	C ₁₈ H ₁₈ O ₇

Figure 3.7. continued.

Formula weight	346.32
Temperature/K	100(2)
Crystal system	monoclinic
Space group	$P2_1/n$
a/Å	13.6526(8)
b/Å	9.7720(5)
c/Å	24.8831(13)
$\alpha/^\circ$	90
$\beta/^\circ$	101.015(2)
$\gamma/^\circ$	90
Volume/Å ³	3258.6(3)
Z	8
$\rho_{\text{calc}}/\text{cm}^3$	1.412
μ/mm^{-1}	0.109
F(000)	1456.0
Crystal size/mm ³	0.384 × 0.184 × 0.171
Radiation	MoK α ($\lambda = 0.71073$)
2 Θ range for data collection/ $^\circ$	4.49 to 48.29
Index ranges	-15 ≤ h ≤ 15, -11 ≤ k ≤ 11, -28 ≤ l ≤ 28
Reflections collected	45288
Independent reflections	5139 [$R_{\text{int}} = 0.0269$, $R_{\text{sigma}} = 0.0146$]
Data/restraints/parameters	5139/42/505
Goodness-of-fit on F ²	1.064
Final R indexes [$I \geq 2\sigma(I)$]	$R_1 = 0.0357$, $wR_2 = 0.0847$
Final R indexes [all data]	$R_1 = 0.0426$, $wR_2 = 0.0886$
Largest diff. peak/hole / e Å ⁻³	0.20/-0.24
$R_{\text{int}} = \Sigma F_o^2 - \langle F_o^2 \rangle / \Sigma F_o^2 $	
$R_1 = \Sigma F_o - F_c / \Sigma F_o $	
$wR_2 = [\Sigma [w(F_o^2 - F_c^2)^2] / \Sigma [w(F_o^2)^2]]^{1/2}$	
Goodness-of-fit = $[\Sigma [w(F_o^2 - F_c^2)^2] / (n-p)]^{1/2}$	
n: number of independent reflections; p: number of refined parameters	

Figure 3.8. ORTEP representation of *Endo-115*.

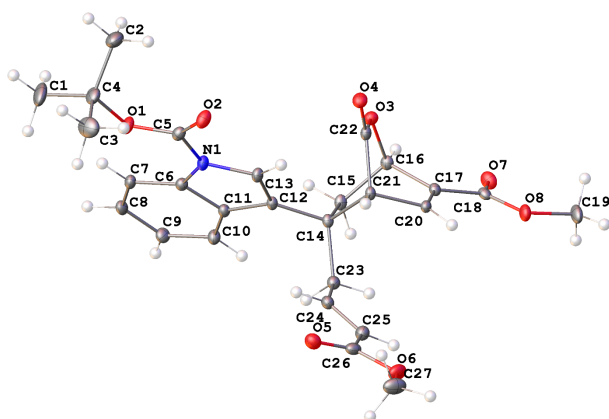


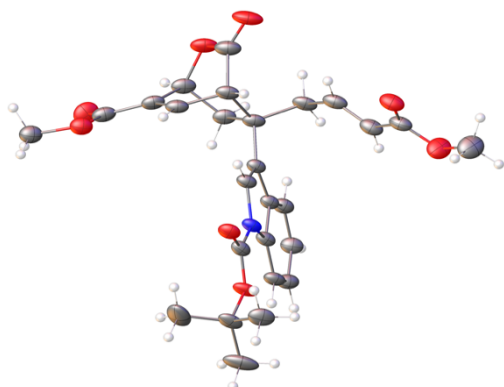
Figure 3.8. *continued.*

Crystal data and structure refinement for 0761_Cole.

Identification code	0761_Cole
Empirical formula	C ₂₇ H ₂₉ NO ₈
Formula weight	495.51
Temperature/K	100(2)
Crystal system	monoclinic
Space group	C2
a/Å	26.9187(10)
b/Å	7.6682(3)
c/Å	12.9814(5)
α/°	90
β/°	108.271(3)
γ/°	90
Volume/Å ³	2544.50(17)
Z	4
ρ _{calc} /cm ³	1.293
μ/mm ⁻¹	0.096
F(000)	1048.0
Crystal size/mm ³	0.37 × 0.29 × 0.17
Radiation	MoKα (λ = 0.71073)
2θ range for data collection/°	5.262 to 61.606
Index ranges	-38 ≤ h ≤ 38, -11 ≤ k ≤ 11, -18 ≤ l ≤ 18
Reflections collected	44278
Independent reflections	7883 [R _{int} = 0.0341, R _{sigma} = 0.0320]
Data/restraints/parameters	7883/1/330
Goodness-of-fit on F ²	1.040
Final R indexes [I ≥ 2σ (I)]	R ₁ = 0.0375, wR ₂ = 0.0836
Final R indexes [all data]	R ₁ = 0.0478, wR ₂ = 0.0876
Largest diff. peak/hole / e Å ⁻³	0.33/-0.18
R _{int} = Σ F _o ² - <F _o ² > / Σ F _o ²	
R ₁ = Σ F _o - F _c / Σ F _o	
wR ₂ = [Σ [w (F _o ² - F _c ²) ²] / Σ [w (F _o ²) ²]] ^{1/2}	
Goodness-of-fit = [Σ [w (F _o ² - F _c ²) ²] / (n-p)] ^{1/2}	

n: number of independent reflections; p: number of refined parameters

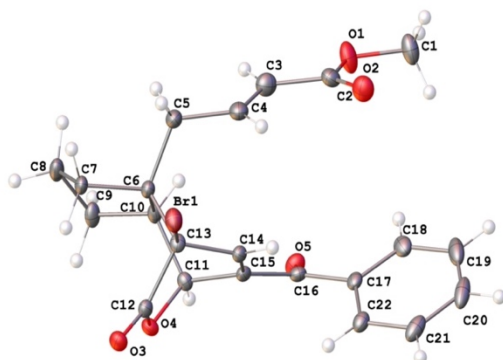
Figure 3.9. ORTEP representation of *Exo-115*.



Crystal data and structure refinement for 0737_Cole.

Identification code	0737_Cole
Empirical formula	C ₂₇ H ₂₉ NO ₈
Formula weight	495.51
Temperature/K	100(2)
Crystal system	monoclinic
Space group	P2 ₁
a/Å	10.1038(7)
b/Å	12.0566(9)
c/Å	10.4153(7)
α/°	90
β/°	97.827(2)
γ/°	90
Volume/Å ³	1256.95(15)
Z	2
ρ _{calc} /cm ³	1.309
μ/mm ⁻¹	0.097
F(000)	524.0
Crystal size/mm ³	0.45 × 0.31 × 0.052
Radiation	MoKα (λ = 0.71073)
2θ range for data collection/°	5.196 to 50.172
Index ranges	-12 ≤ h ≤ 12, -14 ≤ k ≤ 14, -12 ≤ l ≤ 12
Reflections collected	30674
Independent reflections	4414 [R _{int} = 0.0531, R _{sigma} = 0.0377]
Data/restraints/parameters	4414/1/330
Goodness-of-fit on F ²	1.059
Final R indexes [I ≥ 2σ (I)]	R ₁ = 0.0431, wR ₂ = 0.0848
Final R indexes [all data]	R ₁ = 0.0651, wR ₂ = 0.0916
Largest diff. peak/hole / e Å ⁻³	0.17/-0.14
R _{int} = Σ F _o ² - <F _o ² > / Σ F _o ²	
R ₁ = Σ F _o - F _c / Σ F _o	
wR ₂ = [Σ [w (F _o ² - F _c ²) ²] / Σ [w (F _o ²) ²]] ^{1/2}	
Goodness-of-fit = [Σ [w (F _o ² - F _c ²) ²] / (n-p)] ^{1/2}	
n: number of independent reflections; p: number of refined parameters	

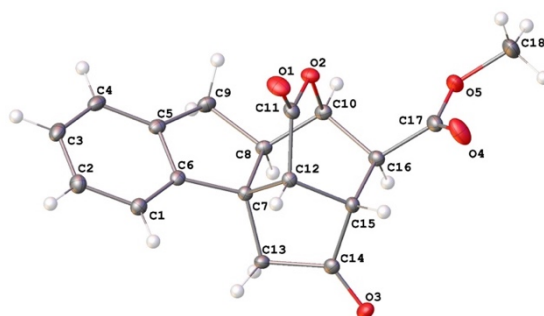
Figure 3.10. ORTEP representation of **128**.



Crystal data and structure refinement for mo_0680_AM_CC04_073_5_0m.

Identification code	mo_0680_AM_CC04_073_5_0m
Empirical formula	C ₃₇ H ₃₂ Br ₂ O ₉
Formula weight	780.44
Temperature/K	100(2)
Crystal system	monoclinic
Space group	<i>P</i> 2 ₁ / <i>c</i>
<i>a</i> /Å	15.4799(6)
<i>b</i> /Å	12.7561(5)
<i>c</i> /Å	17.7032(7)
α /°	90
β /°	110.4710(10)
γ /°	90
Volume/Å ³	3275.0(2)
<i>Z</i>	4
ρ_{calc} /cm ³	1.583
μ /mm ⁻¹	2.533
<i>F</i> (000)	1584.0
Crystal size/mm ³	0.34 × 0.28 × 0.22
Radiation	MoK α (λ = 0.71073)
2 θ range for data collection/°	4.252 to 57.438
Index ranges	-20 ≤ <i>h</i> ≤ 20, -16 ≤ <i>k</i> ≤ 16, -22 ≤ <i>l</i> ≤ 23
Reflections collected	54277
Independent reflections	7686 [<i>R</i> _{int} = 0.0355, <i>R</i> _{sigma} = 0.0334]
Data/restraints/parameters	7686/0/435
Goodness-of-fit on <i>F</i> ²	1.008
Final <i>R</i> indexes [<i>I</i> ≥ 2 σ (<i>I</i>)]	<i>R</i> ₁ = 0.0334, <i>wR</i> ₂ = 0.0669
Final <i>R</i> indexes [all data]	<i>R</i> ₁ = 0.0536, <i>wR</i> ₂ = 0.0726
Largest diff. peak/hole / e Å ⁻³	0.76/-0.34
$R_{\text{int}} = \Sigma F_o^2 - \langle F_o^2 \rangle / \Sigma F_o^2 $	
$R_1 = \Sigma F_o - F_c / \Sigma F_o $	
$wR_2 = [\Sigma [w (F_o^2 - F_c^2)^2] / \Sigma [w (F_o^2)^2]]^{1/2}$	
Goodness-of-fit = $[\Sigma [w (F_o^2 - F_c^2)^2] / (n-p)]^{1/2}$	
n: number of independent reflections; p: number of refined parameters	

Figure 3.11. ORTEP representation of **138**.



Crystal data and structure refinement for 0693_Cole.

Identification code	0693_Cole
Empirical formula	C ₁₈ H ₁₆ O ₅
Formula weight	312.31
Temperature/K	100(2)
Crystal system	monoclinic
Space group	<i>P</i> 2 ₁
<i>a</i> /Å	11.2987(6)
<i>b</i> /Å	10.6941(6)
<i>c</i> /Å	11.9582(7)
α /°	90
β /°	90.7230(10)
γ /°	90
Volume/Å ³	1444.79(14)
<i>Z</i>	4
ρ_{calc} /cm ³	1.436
μ /mm ⁻¹	0.105
<i>F</i> (000)	656.0
Crystal size/mm ³	0.38 × 0.24 × 0.21
Radiation	MoK α (λ = 0.71073)
2 Θ range for data collection/°	4.93 to 57.64
Index ranges	-15 ≤ <i>h</i> ≤ 15, -14 ≤ <i>k</i> ≤ 14, -16 ≤ <i>l</i> ≤ 16
Reflections collected	62679
Independent reflections	7546 [<i>R</i> _{int} = 0.0297, <i>R</i> _{sigma} = 0.0157]
Data/restraints/parameters	7546/1/417
Goodness-of-fit on <i>F</i> ²	1.039
Final <i>R</i> indexes [<i>I</i> ≥ 2 σ (<i>I</i>)]	<i>R</i> ₁ = 0.0312, <i>wR</i> ₂ = 0.0772
Final <i>R</i> indexes [all data]	<i>R</i> ₁ = 0.0334, <i>wR</i> ₂ = 0.0787
Largest diff. peak/hole / e Å ⁻³	0.33/-0.19
$R_{\text{int}} = \Sigma F_o^2 - \langle F_o^2 \rangle / \Sigma F_o^2 $	
$R_1 = \Sigma F_o - F_c / \Sigma F_o $	
$wR_2 = [\Sigma [w (F_o^2 - F_c^2)^2] / \Sigma [w (F_o^2)^2]]^{1/2}$	
Goodness-of-fit = $[\Sigma [w (F_o^2 - F_c^2)^2] / (n-p)]^{1/2}$	
n: number of independent reflections; p: number of refined parameters	

CHAPTER 4

STUDY TOWARDS THE TOTAL SYNTHESIS OF NARELINE

4.1 Introduction

The akuammiline family of indole alkaloids is an extremely diverse class that has been known in the literature for some time.^{1a} In fact, the first report of an isolate from this family was echitamine (**10**) in 1875.² Subsequent work by Henry and Sharp led to the isolation and characterization of the leading members, akuammine (1927)³ and akuammiline (**1**, 1932).⁴

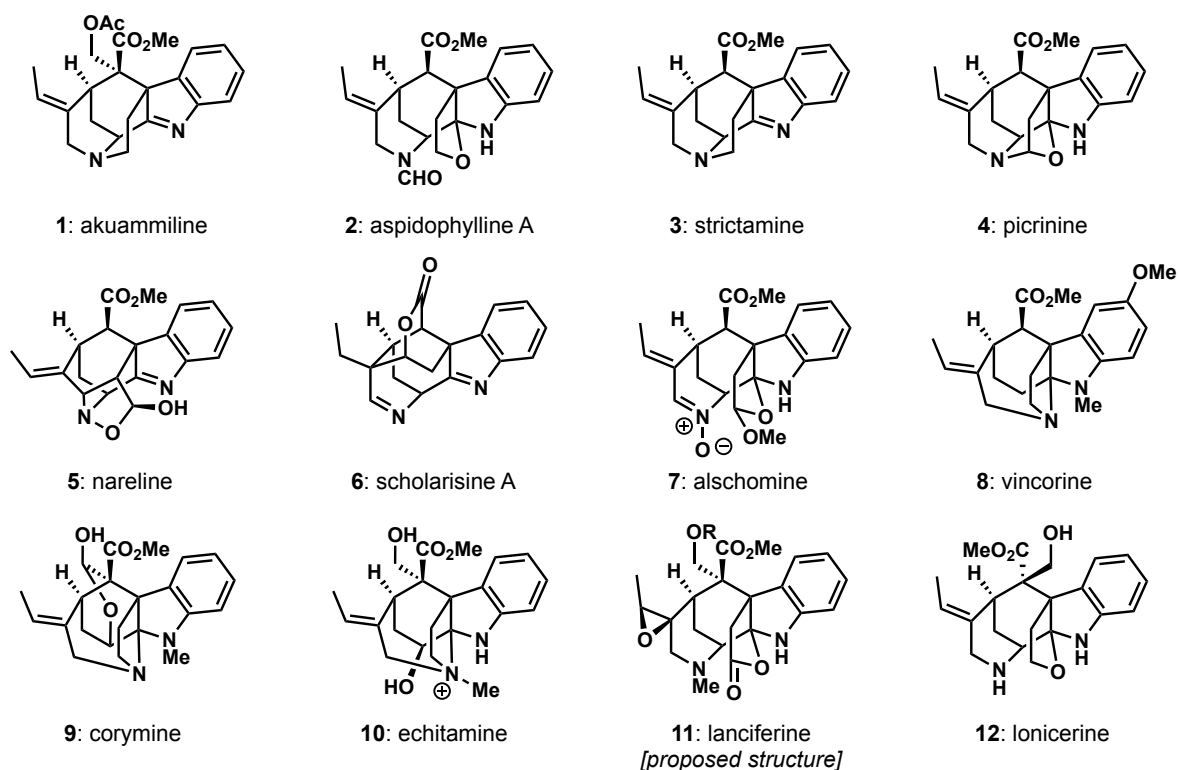


Figure 4.1. The diverse members of the akuammiline alkaloid family of natural products.

These compounds are isolated from several genera of the *Alpocynaee* family of plants, a group which has generated much interest as a result of their roles in traditional medicine in regions of Africa and Southeastern Asia. For example, in southern Asia *Alstonia scholaris*, the source of compounds like nareline (**5**) and scholarisine A (**6**), had long been used in the treatment of illnesses in humans and livestock.⁵ Similarly, in tropical areas of Africa, the seeds of *Picralima klaineana*, known by the native Ghanaian name akuamma, the namesake of the class, have been used to treat malaria.⁴ Several studies to date have reinforced the assorted bioactivity exhibited by various family members, including anticancer, antibacterial, antiviral and anti-inflammatory properties. Strictamine (**3**) and nareline (**5**), for instance, have been shown to

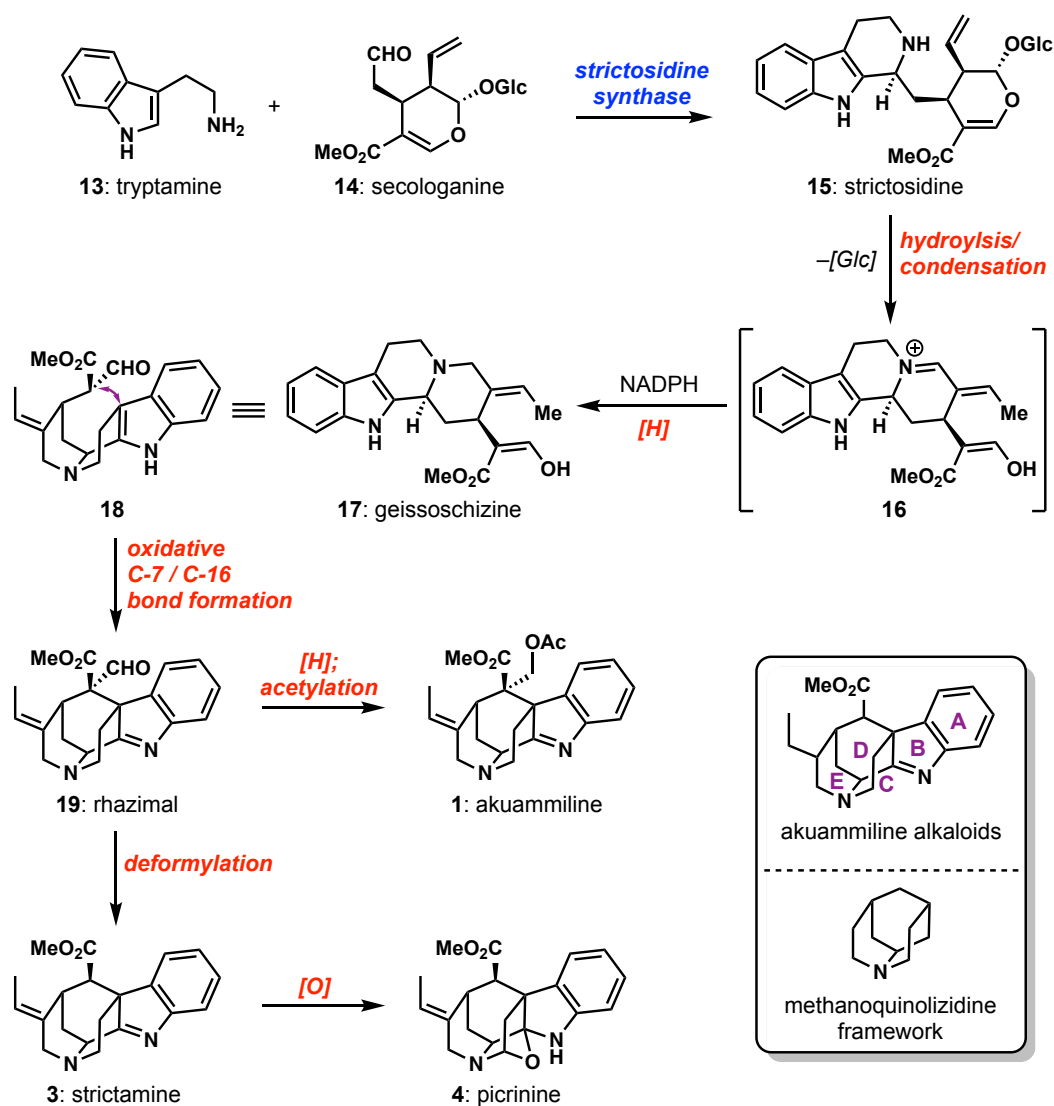
inhibit nuclear factor- κ B (NF- κ B),⁶ while corymine (**9**) can act as a glycine receptor antagonist relevant to CNS inhibition,⁷ and aspidophylline A (**2**) has been shown to reverse drug resistance in cancerous cell lines.⁸

Despite the clear pharmacological drive to pursue such targets, as well as the structural elucidation of several members, the first completed total synthesis of any one member was that of vincorine (**8**) by the Qin group in 2009,⁹ more than a century after the isolation of the inaugural member of the class.¹⁰ However, the last decade has seen an exponential rise in the total synthesis of akuammiline alkaloids, with 20 members having been successfully synthesized and 31 total syntheses reported to date. This chapter serves to present the biosynthetic origins of these natural products, selected total syntheses to elucidate some of the creative, yet concise solutions that have been reported thus far and finally, to delineate our group's own approach to the synthesis of indole alkaloids, alongside our current pursuit of the structurally intriguing alkaloid nareline (**5**).

4.2 Biosynthesis of the Akuammiline Alkaloids

The akuammiline family of alkaloids is believed to arise biosynthetically from geissoschizine (**17**), a common precursor to many monoterpene indole alkaloids.^{1b} This pathway originates via a Pictet-Spengler reaction between tryptamine (**13**) and secologanin (**14**) to produce strictosidine (**15**), catalyzed by the enzyme strictosidine synthase (Scheme 4.1). Following this, a deglycosylation produces aglucon **16**, which itself cannot be isolated but serves as a point of divergence for many polycyclic alkaloids.¹¹ As it relates specifically to the akuammiline family, subsequent condensation and reduction of the iminium ion intermediate via NADPH provides the key precursor geissoschizine (**17**). From here, a crucial oxidative, dearomative C-7/C-16 bond formation provides rhazimal (**19**) and with it, the core methanoquinolizidine framework found in many family members. **19** then serves as the

diversification point, granting access to a variety of akuammiline alkaloids through a series of redox manipulations and/or careful rearrangements.¹²

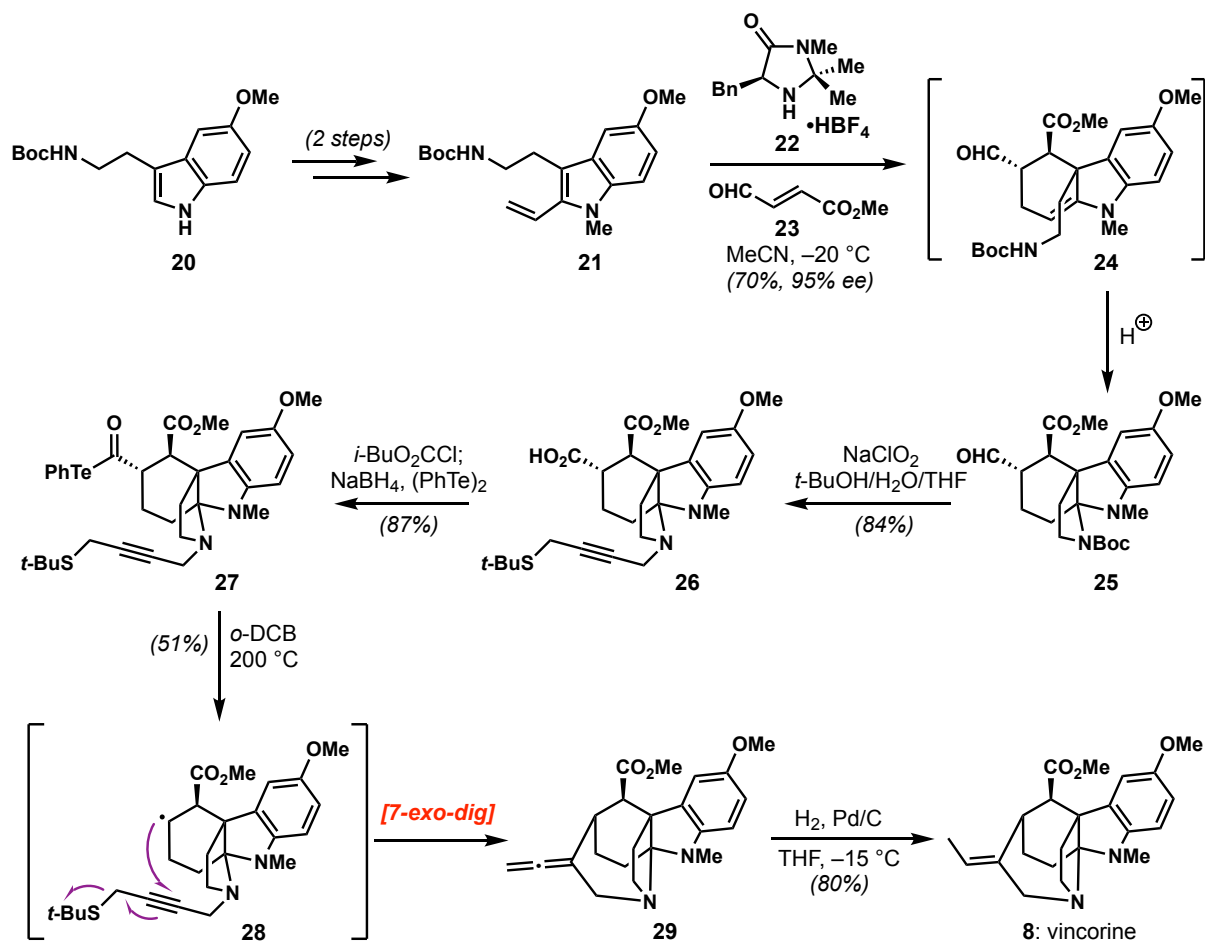


Scheme 4.1. Proposed biosynthesis of the akuammiline alkaloids through key intermediate geissoschizine (17).

4.3 Selected Total Syntheses of the Akuammiline Family of Natural Products

Despite their early isolation and structural determination, efforts towards the total synthesis of akuammiline alkaloids have seen an expansive increase in the last decade. In this section we will look at some selected examples within the literature of recent total syntheses, focused on the diverse strategies used to access the respective scaffolds, as well as certain considerations which informed our own synthetic design. In particular, the synthesis of (–)-vincorine (8) from

the MacMillan group,¹³ the synthesis of (±)-aspidophylline A (**2**)¹⁴ from the Ma group, the synthesis of (±)-strictamine (**3**)¹⁵ from the Zhu group and the synthesis of picrinine (**4**)¹⁶ from the Garg group.

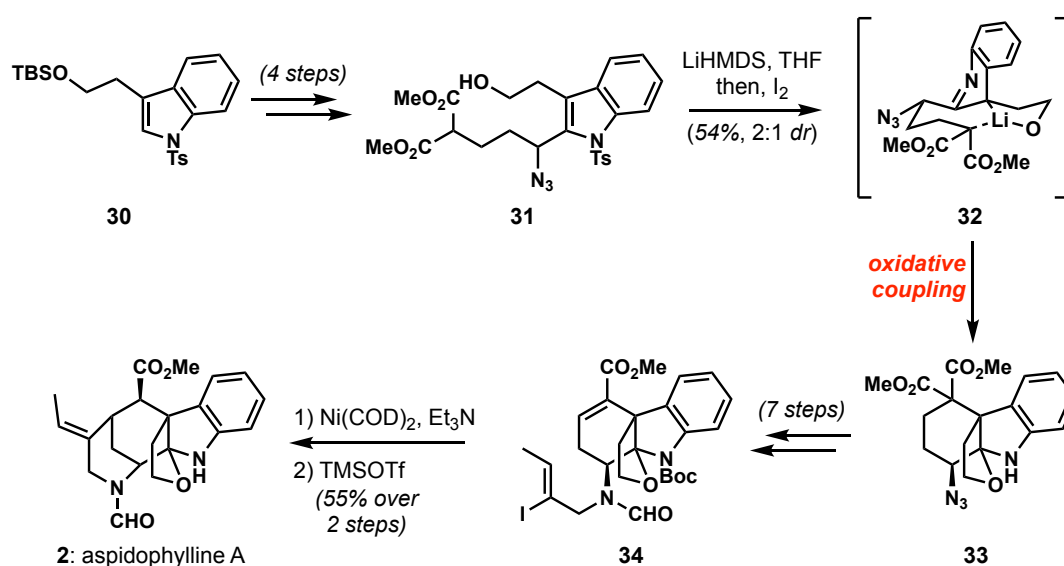


Scheme 4.2. MacMillan synthesis of vincorine (**8**).

The MacMillan synthesis of vincorine (**8**) is noteworthy, both due to its concise nature and the key C-15/C-20 bond formation event to close the final ring.^{13, 17} Although a similar strategy was applied in their synthesis of minfiensine, ring closure initiated at the C-15 site is a quite rare but beneficial tactic.¹⁸ To start, an enantioselective imidazolidinone-catalyzed Diels–Alder reaction between *N*-methyl-indole **21** and highly electron poor dienophile **23** produced cycloadduct **24**, which in one-pot underwent an intramolecular cyclization to form pyrroloindole **25**. From here, the necessary radical precursor was installed via oxidation and acyl telluride formation, and the propargylic side chain introduced through reductive

amination. The choice of acyl telluride, although uncommon, was made after screening other standard radical precursors. In this case, the acyl telluride provided the distinct advantage of thermolytic cleavage to form the desired radical, obviating the need for typical radical initiators or propagators. Therefore at high temperature, acyl telluride decomposition, followed by an intramolecular 7-*exo*-dig cyclization, gave allene **29**. The terminal olefin of the allene could then be reduced under standard hydrogenation conditions performed at low temperature, to afford (–)-vincorine (**8**) in just nine steps from commercial materials.

Aspidophylline A (**2**) represents an intriguing structure within the akuammiline family. Like alschomine (**7**), vincorine (**8**) and lonicerine (**12**), this target exhibits a five-membered heteroatom-containing bridge, cyclized onto the typical indolenine motif. However, distinct from other members such as akuammiline (**1**), strictamine (**3**) and picrinine (**4**), the methanoquinolizidine scaffold is not present, with the C- and E-rings existing completely separate from one another. This bond disconnection has permitted several creative solutions to the total synthesis of this target, six published to date.¹⁹ The Ma synthesis of **2** is particularly interesting, as both the C- and D-rings found within the target are established in a single step, with the remaining ring installed as the final operation.¹⁴



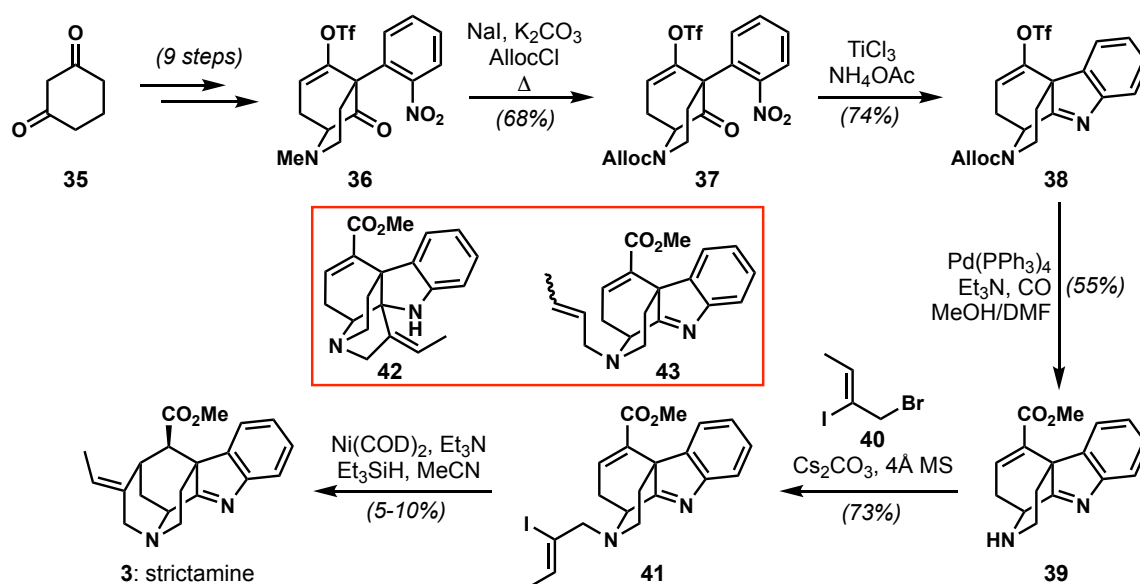
Scheme 4.3. Ma synthesis of aspidophylline A (**2**).

From the TBS-protected tryptophol **30**, the requisite side chain was introduced over four steps in an overall yield of 23%. Following this, an oxidative coupling using LiHMDS and I₂ introduced the tetrahydrocarboazole frame, as well as the furoindole in a single step.²⁰ Interestingly, the free hydroxyl group is necessary for the success of this cyclization, believed to proceed through the chelated intermediate **32** shown in Scheme 4.3. Four additional steps, including a Krapcho decarboxylation, Staudinger reduction and *N*-alkylation provided **34**. Finally, a Ni(0)-mediated 6-*exo*-trig reductive cyclization and Boc-deprotection yielded aspidophylline A (**2**) in 15 steps from known compound **30**. The use of this Ni(0) reductive cyclization E-ring closure is noteworthy, as it is a classic tactic employed by Cook in the synthesis of a number of indole alkaloid natural products, where the corresponding Michael addition proved challenging.²¹ While other studies have shown that this cyclization on similar frameworks can be achieved under anionic and radical conditions, such Ni conditions have been shown to provide solutions where other more typical reaction manifolds have failed (*vide infra*).²²

The shortest total synthesis of strictamine (**3**) reported to date, is that of Zhu and co-workers, as published in 2016.¹⁵ This work is particularly significant, as there are several formal syntheses of this target within the literature, including one from our own group (*vide infra*), that all rely on the final ring-closing event first disclosed by Zhu.²³ It should be noted that concluding E-ring formation is common in the synthesis of many other akuammiline alkaloids, however, doing so while the C-ring has already been established is particularly challenging and the Zhu synthesis of strictamine represents the sole successful example.²⁴

Starting from dimedone (**35**), a series of functional group manipulations lead to the construction of vinyl triflate **36** in nine steps. Conversion **36** to *N*-Alloc-protected **37**, followed by a Lewis acid-mediated reduction/condensation sequence led to **38**. A Pd-catalyzed carbonylation introduced the requisite methyl ester and *N*-alkylation with well-known vinyl

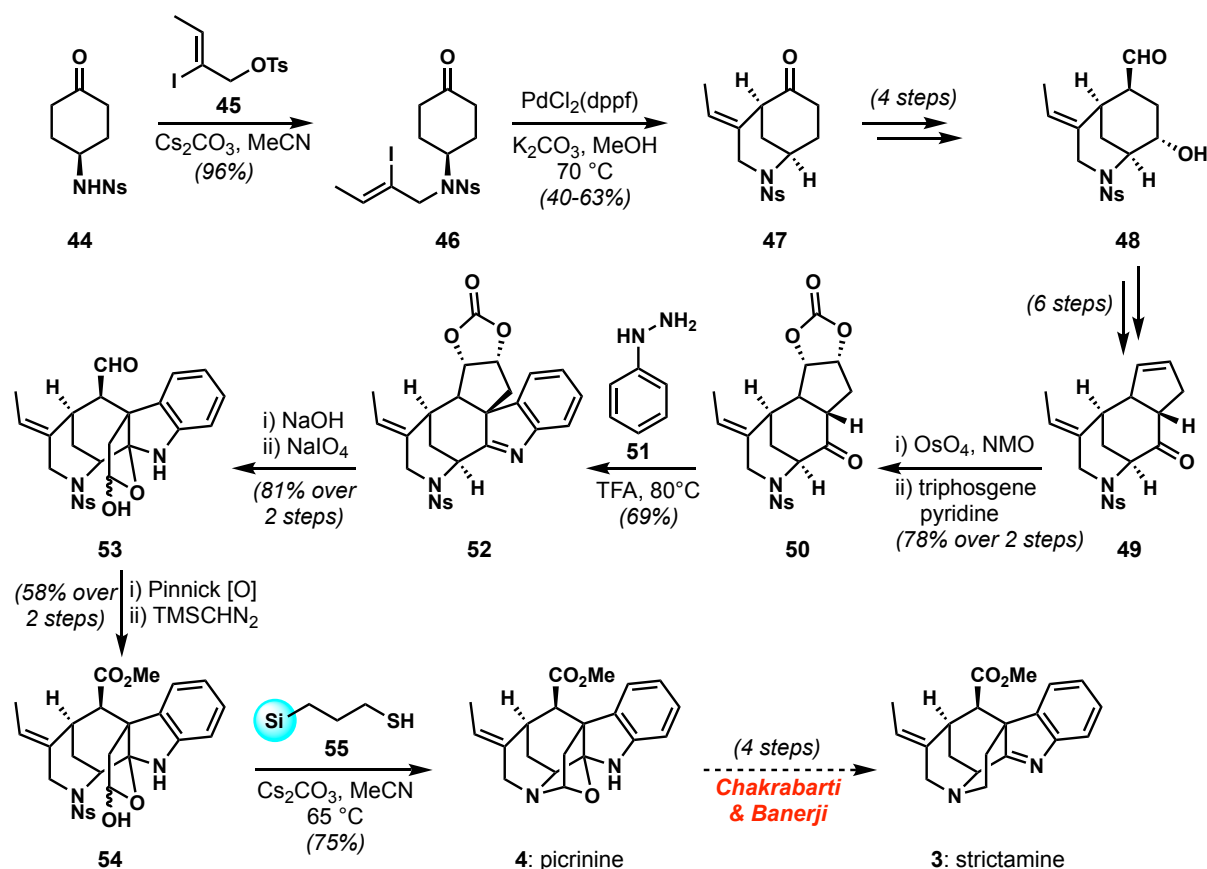
iodide **40**, produced **41**. At this stage, several conditions to effect the desired 6-*exo*-trig cyclization were screened, such as traditional Heck conditions (including Jeffery conditions) and radical conditions.²⁵ However, the only successful result was obtained using stoichiometric Ni(COD)₂, Et₃N and Et₃SiH in MeCN, leading to strictamine (**3**) in 5-10% yield. Despite screening a variety of reaction conditions, the authors were never able to increase the yield of this reaction. This is in part because the reaction suffers from two major side reactions, simple deiodination (**43**) and a 5-*exo*-trig cyclization onto the indolenine moiety to form **42**. Nevertheless, this route resulted in a racemic synthesis of strictamine in 14 steps from commercial materials and clearly demonstrated the challenges associated with the final E-ring formation.



Scheme 4.4. Zhu synthesis of strictamine (**3**).

Despite being structurally similar to strictamine (**3**), picrinine (**4**) represents a unique challenge in the form of the bridged furonindole motif. This is seen in the fact that although there are 5 total syntheses^{19c,24,26,27} and 6 formal syntheses of strictamine,²³ to date there is only one total synthesis of picrinine, published by the Garg group in 2014.¹⁶ Their approach follows a similar strategy to that used in their syntheses of aspidophylline A (**2**), strictamine (**3**), 2(*S*)-cathafoline, akuammiline (**1**) and Ψ -akuammigine.^{19c,28} γ -Aminocyclohexanone **44** was *N*-

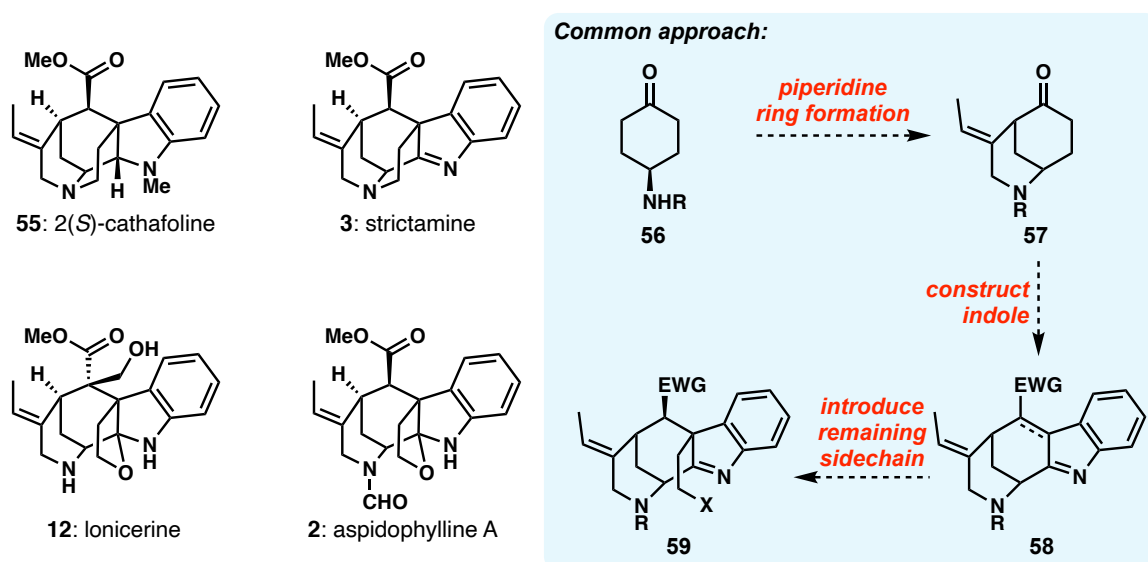
alkylated with tosylate **45** and Pd-catalyzed intramolecular enolate coupling built the bridged piperidine ring **47**. Further functional group manipulations over 10 steps effectively migrated the carbonyl group and introduced the fused cyclopentene **49**. Dihydroxylation and carbonate formation using triphosgene then produced **50**. At this stage, the Garg group utilized their previously established interrupted Fischer indolization, thereby constructing the needed indolenine functionality.^{16b,29} Carbonate hydrolysis and oxidative cleavage of the resultant diol introduced the furoindole precursor in the form of lactol **53**. The aldehyde was then converted to methyl ester **54** via Pinnick oxidation and treatment with TMSCHN₂. Finally, a one-pot Ns removal and intramolecular cyclization forged the remaining hemiaminal bridge, and thereby picrinine (**4**), in 20 steps from commercial materials. It is also worth noting that the total synthesis of picrinine represents the formal synthesis of strictamine via the 4-step sequence originally published by Chakrabarti and Banerji in 1984.³⁰



Scheme 4.5. Garg synthesis of picrinine (**4**) and formal synthesis of strictamine (**3**).

4.4 A Modular Approach to Indole Alkaloid Natural Products

When studying families of indole alkaloid natural products, common structural patterns are often taken advantage of, in order to develop general strategies to access several members of a class using a single approach. For example, an approach which focused on the formation of the methanoquinolizidine skeleton or some slight variant thereof might allow, and in fact has allowed, chemists to gain access to a number of the members within the akuammiline family, some of which are shown in Scheme 4.6.^{19c,28,31,32} The strategy can be delineated as follows, starting from the γ -aminocyclohexanone **56**, *N*-alkylation, followed by an intramolecular cyclization establishes the common bridged piperidine ring **57**. Then, using the ketone as a handle to manipulate functionality about the ring, one can introduce the common indolenine, typically in the form of a Fischer indolization reaction. All that remains is the introduction of a side chain, which can serve to form the final ring of the target as needed. It



Scheme 4.6. Common approach to indole alkaloid natural products with selected examples.

should be said that in some cases the formation of that resulting quaternary center takes place prior to the indole formation, however, the general approach still applies. As is made clear within the literature, this type of strategy and other variants thereof, has allowed for the synthesis of many members within individual subsets. Where such a strategy breaks down

though, is when one considers structures with rearranged frameworks or from different classes altogether.

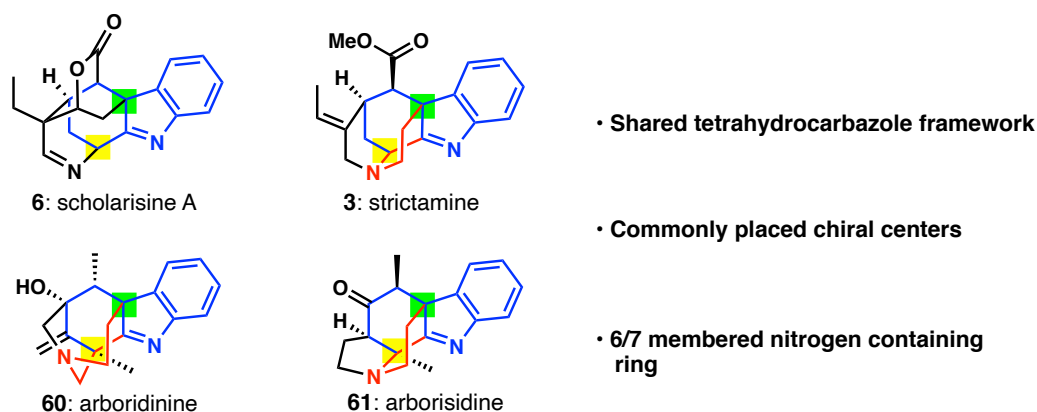
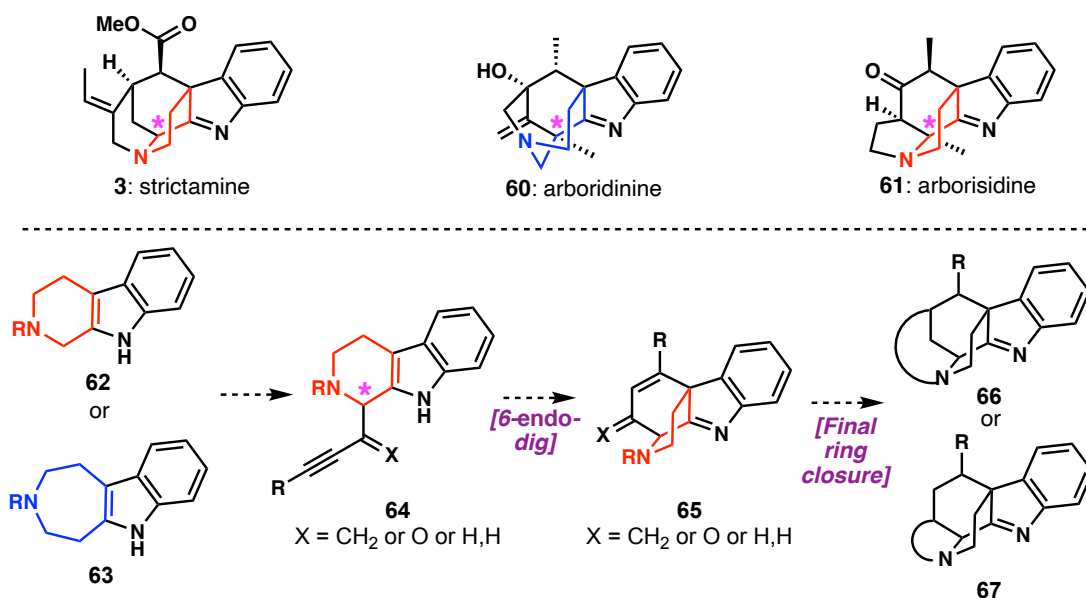


Figure 4.2. Structural features common to many indole alkaloid natural products.

In recent years, our group has adopted a strategy that focuses on individual structural commonalities, as opposed to the overarching skeleton of the target. Figure 4.2 contains four indole alkaloid natural products that, at first glance, might seem somewhat disparate from a structural standpoint but actually demonstrate several key commonalities: 1) they all contain a tetrahydrocarbazole backbone, 2) each contains two commonly placed chiral centers and 3) three of the four structures contain a commonly placed 6/7-membered nitrogen-containing ring. By considering these individual aspects a modular strategy begins to form, one which focuses on generating each of these elements as a means to access the target of interest. This approach is delineated in Scheme 4.7 and has successfully led to the formal synthesis of strictamine (**3**)^{23e} and the inaugural total syntheses of arboridinine (**60**)³³ and arborisidine (**61**),³⁴ each in a stereoselective manner.

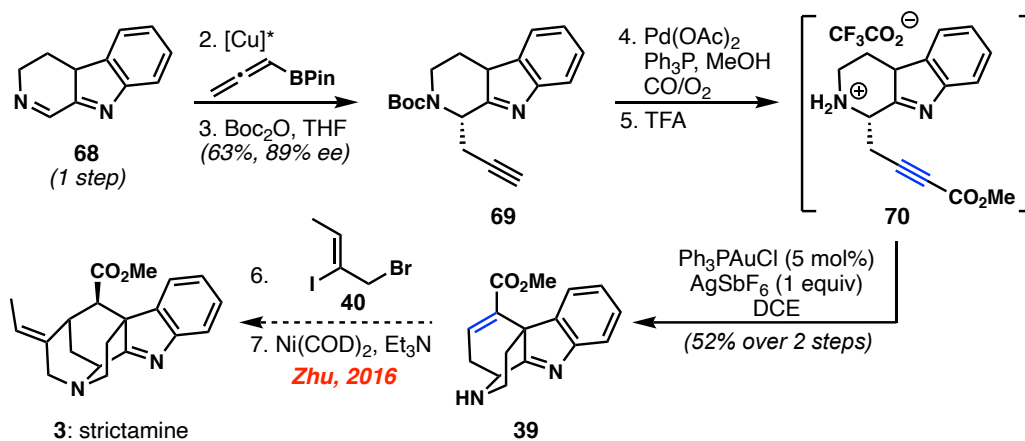
In a forward sense, one begins from the tetrahydro- β -carboline (**62**) or the homologated variant thereof (**63**). Then, a propargyl group is introduced in a stereoselective manner, constructing the first of two key chiral centers. Following this, a Au/Ag-promoted 6-*endo*-dig cyclization forges the requisite carbazole backbone and the second key chiral center. Lastly, based on the functional groups installed along the central frame, the final ring formation



Scheme 4.7. Modular approach to indole alkaloid natural products.

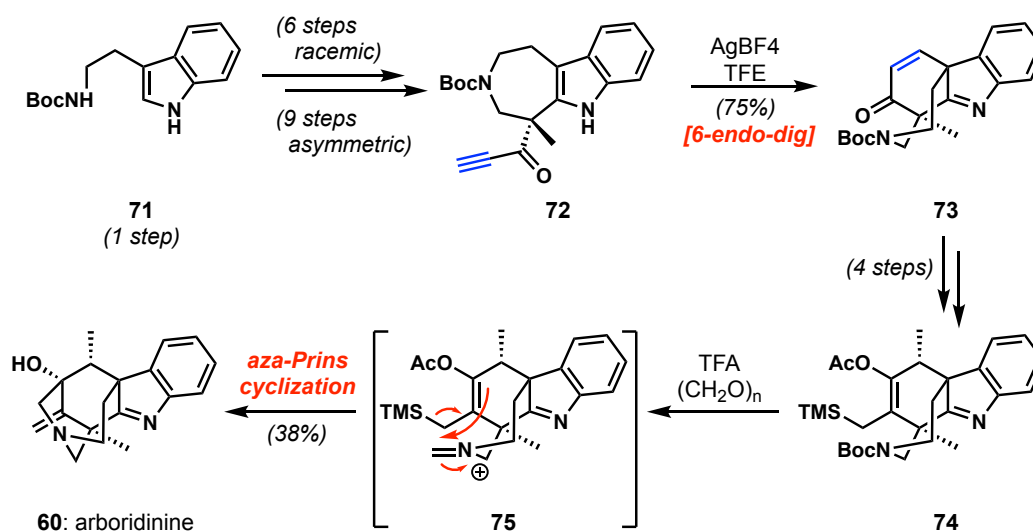
provides the target of interest. The implementation of this approach in practice is discussed below.

Our group's formal synthesis of strictamine is possibly the most straightforward application of this thought process. Starting from dihydro- β -carboline **68**, the propargyl group was introduced in a 1,2-fashion using AllenBpin and a chiral copper catalyst to effect an asymmetric propargylation (63% yield, 85% *ee*). The terminal alkyne then underwent a Pd-mediated carbonylation to introduce the methyl ester group. A subsequent removal of the Boc group with TFA to form intermediate ammonium salt **70** and subjection to Ph₃PAuCl and AgSbF₆ under acidic conditions then afforded the desired carbazole **39**. It is worth noting that the Boc group must be removed prior to the Au-catalyzed cyclization, as the carbonyl can attack the activated alkyne intramolecularly to form a cyclic carbonate. With **39** being an intermediate in the Zhu synthesis of strictamine (*vide supra*),¹⁵ this then represents a 7-step asymmetric formal synthesis of the target.



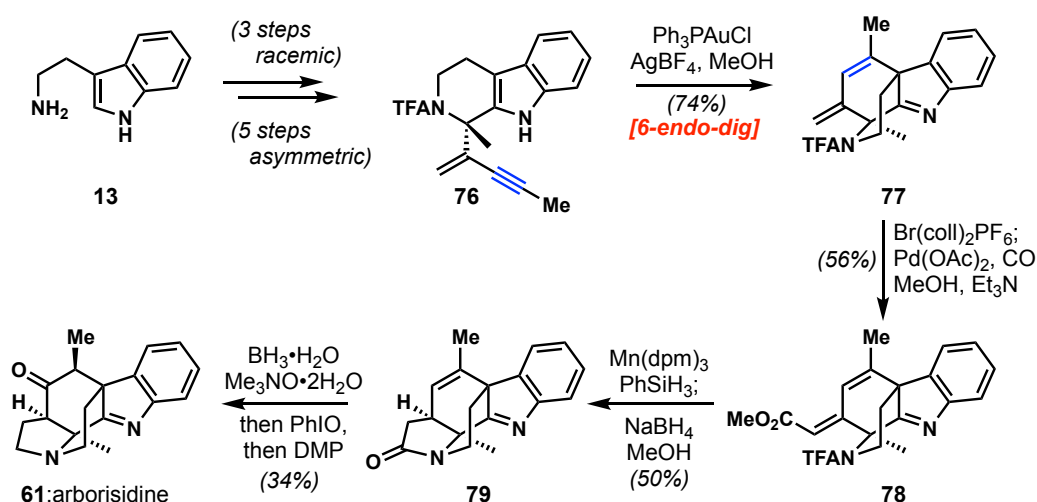
Scheme 4.8. Concise formal synthesis of strictamine (**3**) by Snyder.

Following this, our group published the first total synthesis of arboridinine (**60**). In this case, as opposed to using the 6-membered carboline system, *N*-Boc tryptamine (**71**) was converted over 9 steps to azepane **72** asymmetrically. Here, the ynone underwent a Ag(I)-promoted 6-*endo*-dig cyclization to form enone **73**. Once again, the dihydrocarbazole frame was constructed and both of the previously identified chiral centers installed, after which only one ring remained. The enone was then appropriately functionalized to achieve this goal by converting **73** to allyl silane **74** over four steps. In order to perform this final ring closure, an unprecedented aza-Prins or intramolecular Hosomi-Sakurai allylation was developed and served to both forge the bridged ring system and introduce the bridgehead hydroxyl group.



Scheme 4.9. Snyder synthesis of arboridinine (**60**).

The most recent example though, is the total synthesis of arborisidine (**61**). As can be seen in the examples already presented above, this approach often results in highly concise syntheses, of which that of **61** is the most prominent. From tryptamine (**13**), the cyclization precursor was obtained in just 3 steps racemically and 5 asymmetrically. Enyne **76** efficiently underwent the desired 6-*endo*-dig cyclization to provide diene **77**. The 1,1-disubstituted olefin is then selectively brominated and the resulting vinyl bromide converted to α,β -unsaturated ester **78** via Pd catalysis. At this stage, a selective 1,4-reduction using HAT chemistry afforded the intermediate γ,δ -unsaturated ester, which underwent intramolecular lactam formation upon treatment with NaBH₄ at elevated temperature (**78**→**79**). The remaining oxidation state manipulations were then conducted in one-pot, to grant access to arborisidine (**61**) in seven steps racemically and nine steps asymmetrically.



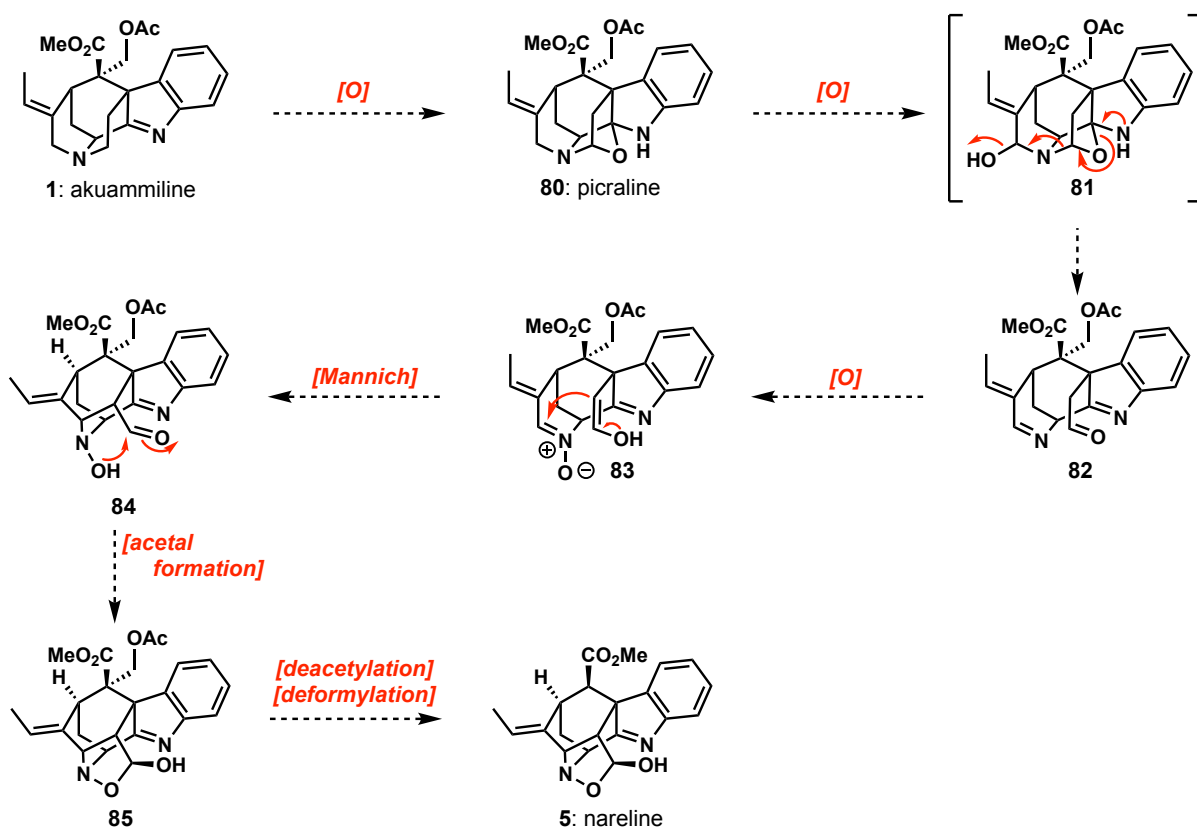
Scheme 4.10. Snyder synthesis of arborisidine (**61**).

In each of these examples, the general approach guided the overall synthetic design, while careful consideration of the functional handles placed throughout the molecule prior to, or following, the 6-*endo*-dig cyclization, helped to expedite formation of the final ring within the target and in each case offered a highly concise synthetic solution. Our hope, then, was to use this strategy to design and execute the synthesis of a new target, nareline (**5**).

4.5 Isolation and Structural Determination of Nareline

In an effort to provide a further proof of concept for this approach to alkaloid synthesis, we set our sights on a target that, although part of the akuammiline family, contains a somewhat distinct framework. Nareline (**5**) was first isolated in 1977 from *Alstonia scholaris* and the structure assigned unambiguously by single-crystal X-ray diffraction.³⁵ In terms of bioactivity, **5** has been shown to exhibit moderate NF- κ B inhibition, as well as antibacterial activity towards *P. aeruginosa* (0.781 μ g/mL) and *K. pneumonia* (1.56 μ g/mL).³⁶ While potential medicinal applications should certainly be considered, the more intriguing feature of nareline (**5**), from a synthetic standpoint, is its structure. **5** contains seven stereocenters, including a single quaternary center, and exhibits a unique azaadamantane frame, distinct from the methanoquinolizidine skeleton typical of the class. But most captivating, perhaps, is the hydroxyisoxazolidine ring, a feature not found in any other akuammiline member and arguably quite rare for any natural product. At the same time, **5** contains all of the structural elements that are considered integral for the approach we hoped to deploy.

Biosynthetically, nareline (**5**) is thought to arise from akuammiline (**1**), whose own origins are described in section 4.2 (*vide supra*). First **1** is proposed to undergo a biosynthetic oxidation to picraline (**80**), which itself undergoes further oxidation to the transient hemiaminal **81**. Cleavage of both *N,O*-linkages and subsequent oxidation then affords the ring opened nitron **83**. This is then proposed to perform an intramolecular Mannich reaction, forging the alternate bridged piperidine ring, followed by acetal formation to construct the hydroxyisoxazolidine and a subsequent deacetylation/deformylation process to generate nareline (**5**).³⁵ Interestingly, although the structure of picrinine (**4**) was known at the time, it was not a postulated intermediate in the proposed biosynthetic pathway.

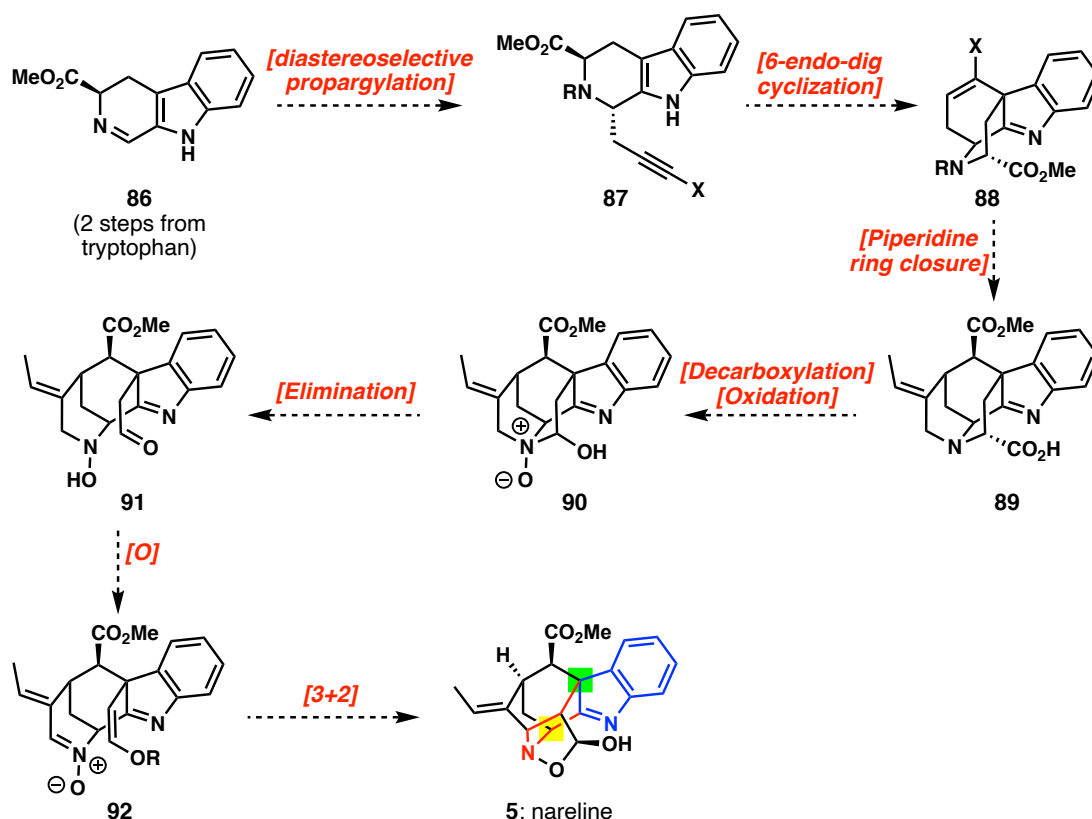


Scheme 4.11. Proposed biosynthesis of nareline (5) from akuammiline (1).

4.6 Retrosynthesis of Nareline

Our approach to nareline (5) sought to take advantage of the group's previously developed route to strictamine (3) to access a functionalized version of this alkaloid. This would then set the stage for an oxidative rearrangement to convert the methanoquinolizidine frame to the desired aza-adamantane core of nareline (5). The route is presented as a proposed forward synthesis for clarity (Scheme 4.12). Starting from dihydro- β -carboline **86**, a diastereoselective propargylation would install the first crucial chiral center and provide the cyclization precursor **87**. A subsequent Au-promoted 6-*endo*-dig cyclization then would form the tetrahydrocarbazole frame and install the second crucial chiral center. Then, using the Ni(0)-mediated reductive cyclization reported by Zhu,¹⁵ we hoped to construct the methanoquinolizidine frame and gain access to a structure that could be termed "carboxy"-strictamine (**89**). We proposed to use this carboxylate group as a handle to perform a

decarboxylation/oxidation sequence and prepare *N*-oxide **90**. Such a compound should be poised to undergo a Cope-type elimination to form the corresponding hydroxylamine (**91**). A final oxidation to the nitron and intramolecular [3+2] cycloaddition, would then deliver nareline (**5**) in a concise manner.^{37,38}

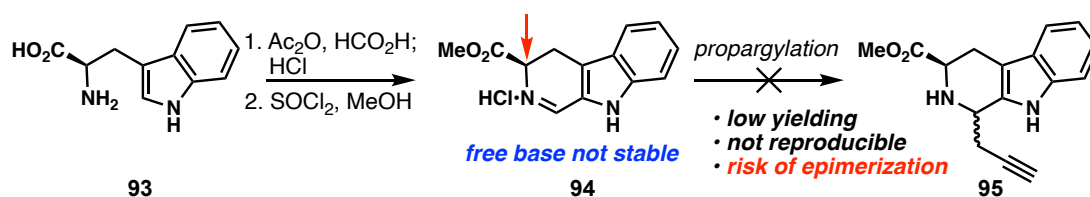


Scheme 4.12. Proposed route to nareline (**5**).

4.7 Initial Approach: β -Carboline Propargylation

As indicated above, we hoped to align the opening steps of our approach with those used in our groups own synthesis of strictamine (**3**), with the only difference being the placement of a functional handle α to the amine, in this case a methyl ester. In two steps from D-tryptophan we could access the desired dihydro- β -carboline as its hydrochloride salt (**94**, Scheme 4.13).³⁹ However, any attempt to introduce a propargyl group was unsuccessful. This was not a complete surprise, as studies on such 1,2-additions to β -carbolines have demonstrated that

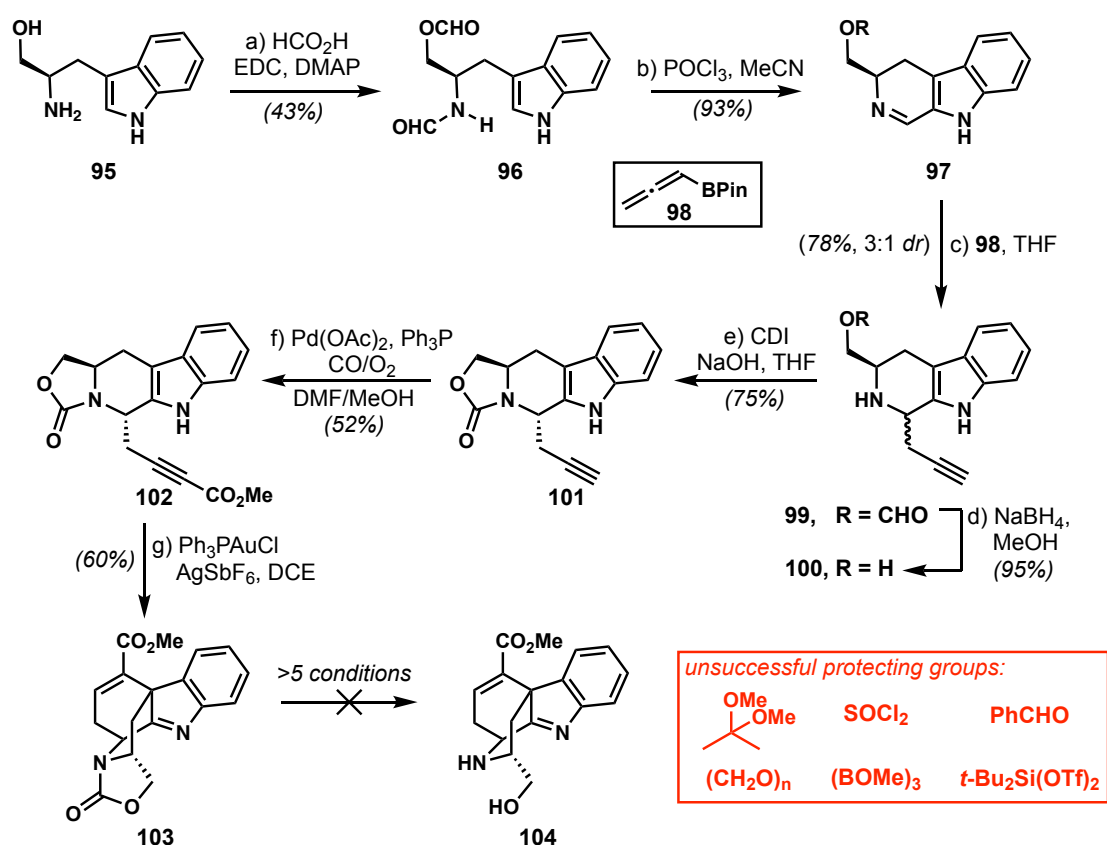
activation of the imine moiety is required, typically in the form of a Lewis acid additive or acyl chloride.^{40,41} Such activation is quite challenging when employing the corresponding hydrochloride salt. On the other hand, the free-base form of **94** is itself highly unstable, owing to the acidity of the α -proton of the ester, as well as the propensity for oxidative aromatization.³⁹ Despite several attempts involving the use of additives that might allow for *in situ* free base formation, only minimal conversion or decomposition was observed. In addition, there was the potential for epimerization in both the starting material and the product, which would, in turn, defeat the purpose of using of a chiral pool starting material and impact the stereoselectivity of the route overall.³⁹



Scheme 4.13. Initial explorations into propargylation of β -carboline **94**.

As a solution to this problem, we instead looked to the analogous aminoalcohol (**100**). Based on a modified procedure from Song and co-workers, tryptophanol (**95**) could be converted to the corresponding carboline (**97**) via EDC coupling with formic acid and subsequent Bischler–Napieralski reaction.⁴² **97** was obtained with partial loss of the formate group, likely due to the acidity of the Bischler–Napieralski reaction conditions, paired with the labile nature of formic esters. As such, we proceeded to perform the propargylation by treatment with **98** at 23 °C and subsequent exposure to NaBH₄ to cleave the formate group and afford **100** in good yield as a 3:1 mixture of diastereomers. This species was then protected as the cyclic carbamate (**101**) and the diastereomers were separated, of which only the major diastereomer was carried forward. Carbonylation of the terminal alkyne under Pd-catalysis gave the desired ynoate **102** in modest yield and subsequent treatment with Ph₃PAuCl and AgSbF₆ then provided the desired 6-*endo*-dig cyclization product.^{23e} From this point, we had

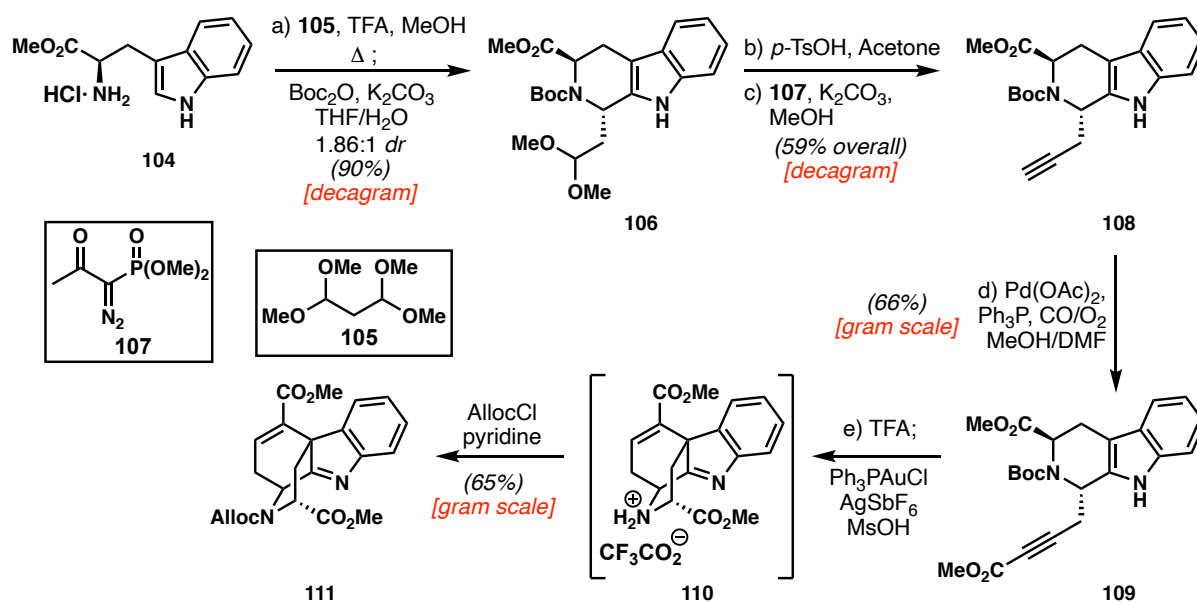
hoped to remove the carbamate protecting group and oxidize to the desired amino acid intermediate, as outlined in our synthetic design. Unfortunately, we were unable to cleave the cyclic carbamate even under forcing conditions (LiOH, THF, 80°C), at which point decomposition pathways began to prevail. The obvious choice at this stage was to introduce a protecting group that could be more easily removed later in the sequence. To our surprise, installation of other groups proved to be quite challenging, often resulting in minimal conversion of the starting material. Realizing that this route might result in a series of unnecessary protecting group and oxidation state manipulations, we decided instead to introduce the propargyl group in a somewhat more traditional manner.



Scheme 4.14. Aminoalcohol approach to Au-cyclization product **103**: (a) HCO₂H (2.4 equiv.), EDC (2.6 equiv.), DMAP (0.2 equiv.), CH₂Cl₂, 23 °C, 12 h, 43%; (b) POCl₃ (2.0 equiv.), MeCN, 0 °C, 4 h, 93%; (c) **98** (1.5 equiv.), THF, 23 °C, 12 h, 78%, 3:1 *dr*; (d) NaBH₄ (2.5 equiv.), MeOH, 0 °C to 23 °C, 3 h, 95%; (e) CDI (3.0 equiv.), NaOH (10% w/v), THF, 23 °C, 5 h, 75%; (f) Pd(OAc)₂ (0.3 equiv.), Ph₃P (0.6 equiv.), CO/O₂, DMF, MeOH, 23 °C, 16 h, 52%; (g) Ph₃PAuCl (0.1 equiv.), AgSbF₆ (1.0 equiv.), 1,2-DCE, 23 °C, 16 h, 60%.

4.8 Pictet–Spengler Approach to the [Au]-Cyclization Precursor

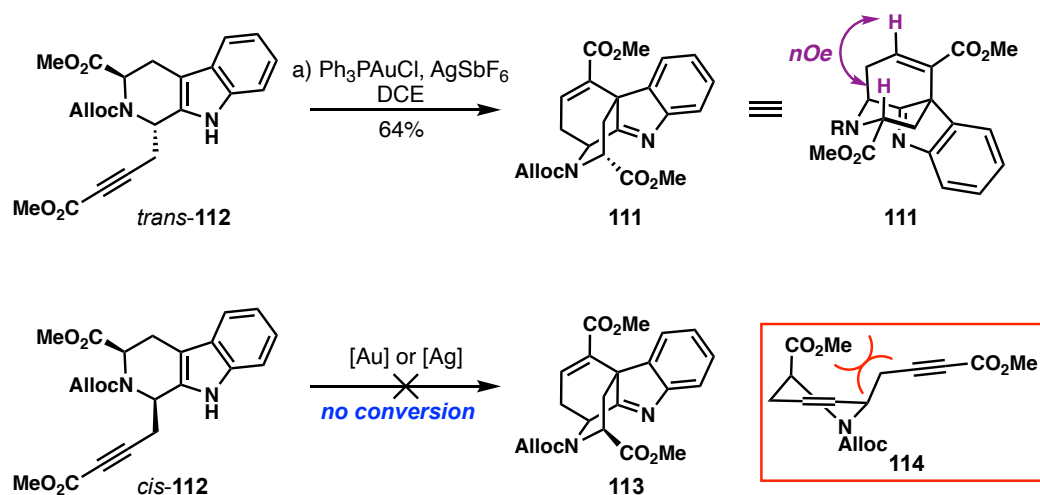
Noting the challenges arising from the proposed β -carboline starting point, we instead envisioned the introduction of some side chain through a Pictet–Spengler reaction that could be elaborated to the desired 6-*endo*-dig cyclization precursor. In practice, a Pictet–Spengler reaction could be performed with tryptophan methyl ester hydrochloride (**104**) and 1,1,3,3-tetramethoxypropane (**105**) under acidic conditions, to give the cyclized intermediate as a ~2:1 mixture of diastereomers, favoring the *cis*-species.⁴³ This could be treated in the same pot with Boc₂O and K₂CO₃ to afford the desired acetal (**102**), at which point the diastereomers were separated. Since the stereochemistry at this center had no bearing on our proposed route, we carried both isomers forward. Note that the yields presented in Scheme 4.15 are those for the *trans*-diastereomer. Following Boc-protection, cleavage of the dimethyl acetal with *p*-TsOH and treatment with Ohira–Bestmann reagent affords the desired alkyne (**108**) (59% over two steps). Once again, in a similar fashion to our synthesis of strictamine, Pd-mediated carbonylation of the terminal alkyne then provides the Au-cyclization precursor **109**. As



Scheme 4.15. Pictet–Spengler approach to 6-*endo*-dig cyclization product **111**: (a) **105** (1.5 equiv.), TFA, MeOH, 80 °C, 16 h, then Boc₂O (1.2 equiv.), K₂CO₃ (4.0 equiv.), THF/H₂O (1:1), 23 °C, 20 h, 90%, 1.86:1 *dr*; (b) *p*-TsOH (0.5 equiv.), acetone/H₂O (10:1), 60 °C, 1 h; (c) **107** (1.5 equiv.), K₂CO₃ (2.0 equiv.), MeOH, 0 °C to 23 °C, 16 h, 59% over 2 steps; (d) Pd(OAc)₂ (0.3 equiv.), Ph₃P (0.6 equiv.), CO/O₂, DMF, MeOH, 23 °C, 16 h, 66%; (e) TFA, CH₂Cl₂, then Ph₃PAuCl (0.05 equiv.), AgSbF₆ (1.0 equiv.), MsOH (2.0 equiv.), 1,2-DCE, 23 °C, 18 h, then pyridine (10.0 equiv.), AllocCl (2.0 equiv.), 23 °C, 24 h, 65%.

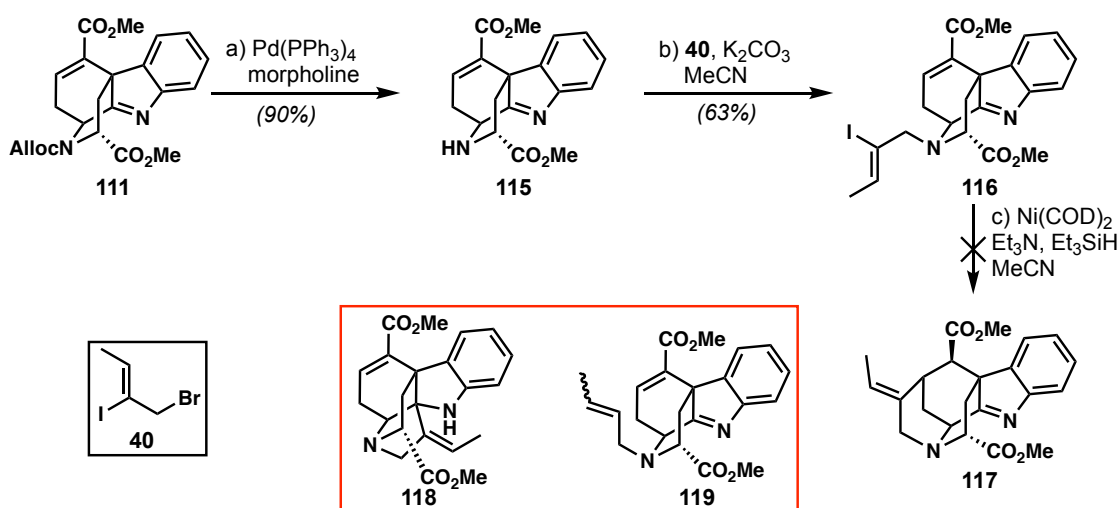
discussed earlier, the Boc group is not compatible with this chemistry as it acts as a nucleophile, trapping the activated alkyne as a cyclic carbonate. Therefore, in a one-pot three-step sequence, the substrate is treated with TFA to both remove the Boc-group and form the corresponding ammonium salt upon concentration of the reaction mixture. This salt can then be directly treated with Ph_3PAuCl and AgSbF_6 to effect the desired 6-*endo*-dig cyclization. The reaction mixture containing ammonium salt **110** is then basified with an excess of pyridine and subsequently treated with AllocCl , thereby delivering the desired Alloc-protected Au-cyclization product **111**.

While this sequence proceeded smoothly with *trans*-**109**, the *cis*-diastereomer showed no conversion of the intermediate ammonium salt. In order to decouple the three transformations and better understand this discrepancy in reactivity, the Alloc-protected cyclization precursors *trans*-**112** and *cis*-**112** were prepared. Interestingly, while the conversion of the *trans*-diastereomer proceeded smoothly in 64% yield, the *cis*-diastereomer showed no conversion to the desired product. This disparity in reactivity can be rationalized through a simplified cyclohexene model as shown in Scheme 4.16. In order to achieve the transition state for the desired transformation, the substituents about the cyclohexene ring would have to adopt a highly unfavorable diaxial orientation, likely inhibiting this reaction pathway.



Scheme 4.16. 6-*endo*-dig cyclization of *cis*- and *trans*-**112**: (a) Ph_3PAuCl (0.1 equiv.), AgSbF_6 (1.0 equiv.), 1,2-DCE, 23 °C, 16 h, 64%.

Nonetheless, with **111** in hand, we then focused on completion of the methanoquinolizidine frame. Notwithstanding the low yield of the reported Zhu conditions (5-10%), we viewed this as the most direct path forward. Thus, removal of the Alloc group with Pd(PPh₃)₄ and *N*-alkylation with allylic bromide **40**,²¹ delivered the desired vinyl iodide **116** in good yield. Unfortunately, when applying these conditions to our system we observed none of the desired 6-*exo*-trig reductive cyclization product. Instead, we only obtained the analogous side products to those observed by the Zhu group, namely, deiodination (**119**) and 5-*exo*-trig cyclization onto the indolenine ring (**118**).¹⁵



Scheme 4.17. Attempt at Ni-mediated 6-*exo*-dig cyclization with **116**: (a) Pd(PPh₃)₄ (0.1 equiv.), morpholine (10.0 equiv.), THF, 0 °C, 30 mins, 90%; (b) **40** (3.0 equiv.), K₂CO₃ (6.5 equiv.), MeCN, 80 °C, 1 h, 63%; (c) Ni(COD)₂ (2.0 equiv.), Et₃N (4.0 equiv.), MeCN, then Et₃SiH (2.0 equiv.), 23 °C, 1.5 h.

4.9 Imposing Structural Rigidity

The challenge of the proposed 6-*exo*-trig cyclization is made clear when **41** is drawn as its chair conformer (Figure 4.3). In this representation, the vinyl iodide side chain is quite distant from the desired reaction site and much closer to the indolenine, likely giving rise to the preferred 5-*exo*-trig cyclization pathway to afford **118**. In order to place the vinyl iodide side chain proximal to the β-position of the enoate, **41** would have to adopt a boat conformation as well as undergo nitrogen inversion, a series of steps which likely pose significant energy

barriers. As shown in the total syntheses of other akuammiline alkaloids such as aspidophylline A (**2**), if the C-ring is not present such a cyclization process is facile, typically occurring under a variety of conditions including anionic, radical and transition metal-mediated processes.^{14,19b,19d, 19e}

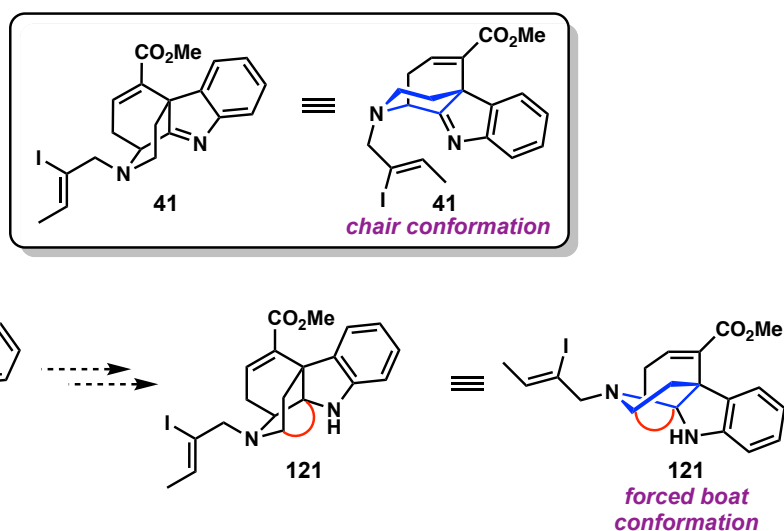
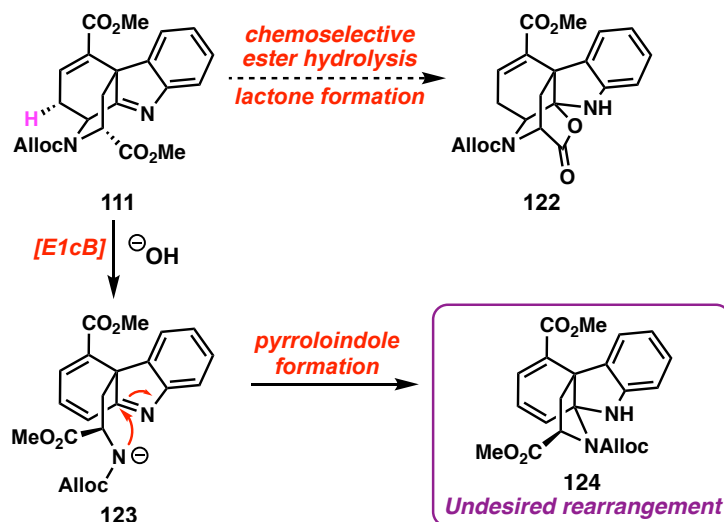


Figure 4.3. Conformation about the bridged piperidine ring and the implication on the potential for cyclization.

While we could potentially go through a series of steps involving cleavage of the newly formed C-ring, closure of the E-ring and then C-ring reinstallation, such a process would be both step intensive as well as take away from the overall elegance of the approach. We instead decided to tune the substrate in an effort to remove the previously described barriers to cyclization. From this perspective, we proposed that the α -aminoester could serve as a functional handle through which to introduce a bridged ring system (Figure 4.3). This would then create a forced boat conformation and bring the side chain closer the desired site of reactivity. It should also be mentioned that this effectively removes the possibility of the undesired 5-*exo*-trig cyclization.

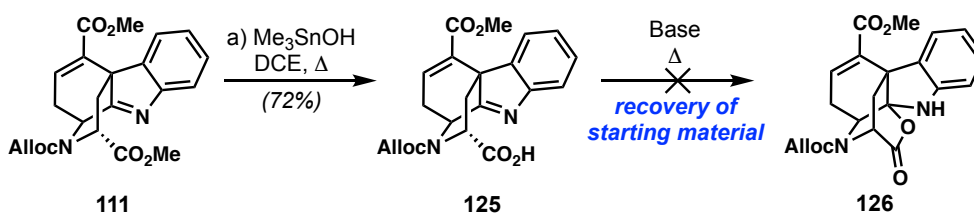
Based on our system, the most logical tactic would be the formation of a bicyclic lactone bridge (**122**, Scheme 4.18). This could be obtained through a chemoselective ester hydrolysis and intramolecular lactone formation. However, when subjected to a variety of basic conditions, the only observed product was an undesired rearrangement to pyrroloindole **124**.

Such a rearrangement was also observed in our group's study towards strictamine and is proposed to occur via an E1cB-elimination leading to the dienolate **123**, followed by pyrroloindole formation.^{23c} This results in a structure much more similar to the framework of vincorine (**8**) or echitamine (**10**).



Scheme 4.18. Proposed bicyclic lactone intermediate and observed undesired rearrangement product (**124**).

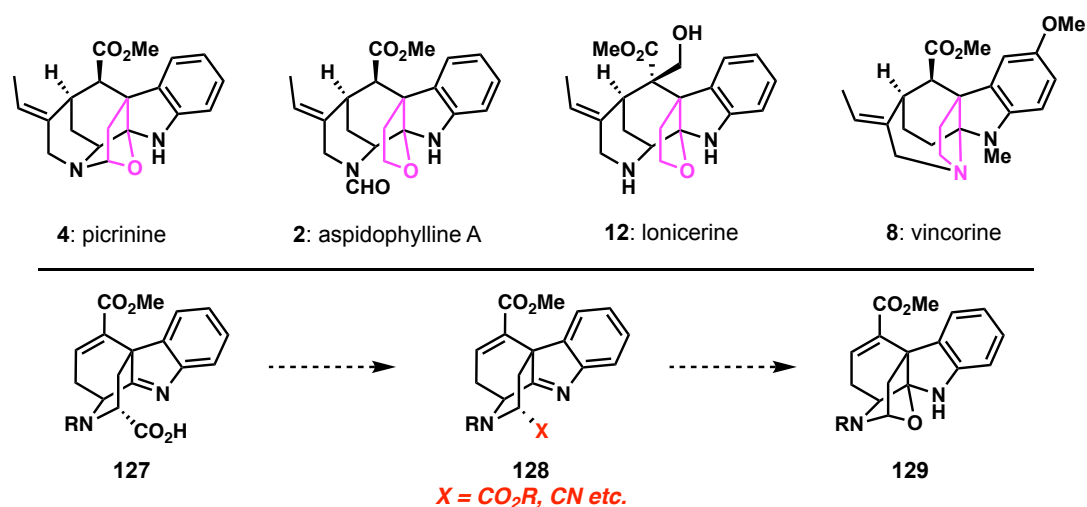
Since this result precluded any base-mediated ester hydrolysis, we instead looked to Me_3SnOH , a reagent developed by the Nicolaou group for selective methyl ester hydrolysis.⁴⁴ Pleasingly, with a large excess of Me_3SnOH at elevated temperature, we observed selective hydrolysis of the α -amino ester in good yield. We believe that the chemoselectivity obtained here is a result of both sterics, with the α,β -unsaturated ester being hindered by the neighboring quaternary center, as well as favorable α -heteroatom chelation from the adjacent nitrogen atom. Surprising to us, was that the acid (**125**) would not perform the proposed intramolecular lactone



Scheme 4.19. Chemoselective ester hydrolysis and failed attempt at intramolecular lactonization: (a) Me_3SnOH (6.0 equiv.) 1,2-DCE, 90 °C, 32 h.

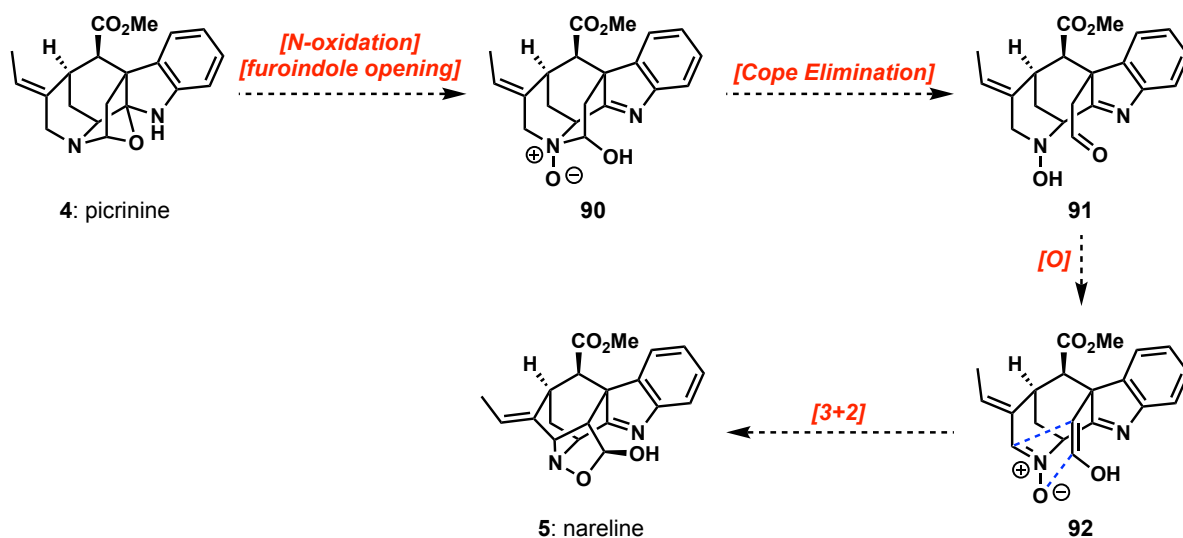
formation. Even when separately exposed to base at elevated temperature, the starting material was recovered unchanged.

In looking through the structure of various indole alkaloids, we realized that while six-membered rings of this type are rare, five-membered rings are quite common, with picrinine (**4**)⁴⁵ being the most representative example of our desired substrate framework. With this in mind, we proposed instead to convert the carboxylic acid into some more activated handle through which we could introduce a single bridging heteroatom. More importantly, this offered the realization that if we could introduce this additional ring system we might be able access picrinine (**4**) *en route* to our original target.



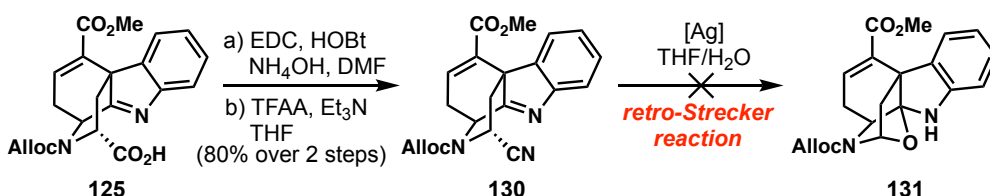
Scheme 4.20. Common 5-membered ring motif found in many akuammine alkaloids and proposed installation of furoindole ring in **129**.

We envisioned the connection between picrinine (**4**) and nareline (**5**) as presented in Scheme 4.21.³⁸ Following *N*-oxidation and opening of the furoindole, the intermediate hemiaminal **90** could undergo a Cope-type elimination to provide hydroxylamine **91**. Oxidation of this intermediate to the corresponding nitron (**92**), followed by an intramolecular [3+2] cycloaddition would deliver nareline (**5**). Alternatively, this final step could be achieved through an intramolecular Mannich reaction and subsequent acetal formation, in a similar fashion to that proposed in the original biosynthesis (Scheme 4.11).



Scheme 4.21. Proposed connection between picrinine (**4**) and nareline (**5**).

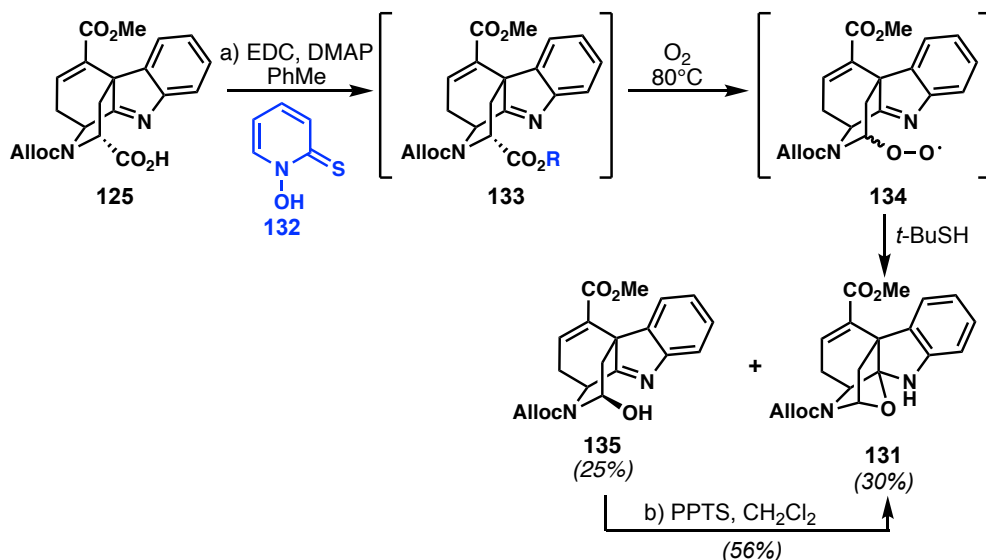
Our first approach involved a proposed retro-Strecker process. In this sense, carboxylic acid **125** was first converted to the primary amide and then dehydrated by treatment with TFAA to afford the α -aminonitrile. Upon treatment with Ag(I) in an aqueous THF solution, we hoped this species would undergo a retro-Strecker process to form in the intermediate iminium species, which could be trapped by H₂O to form the desired bridge.⁴⁶ Unfortunately, when subjected to AgNO₃ in THF/H₂O (1:1) no conversion of the starting material was observed. This is likely a result of the electron withdrawing group on the nitrogen atom, destabilizing the proposed iminium ion intermediate. We further considered removing the Alloc group and alkylating the nitrogen atom, but with the desired side chain containing a requisite halide atom, the proposed Ag(I) conditions would be incompatible.



Scheme 4.22. Preparation of α -aminonitrile and failed attempt at retro-Strecker reaction to form furoindole **140**: (a) EDC (2.5 equiv.), HOBT (2.5 equiv.), NH₄OH (30% w/v), DMF; (b) TFAA (1.0 equiv.), Et₃N (2.0 equiv.), THF, 0°C to 23 °C, 30 min, 80% over 2 steps.

We decided, instead, to pursue this transformation using radical chemistry. Using a Barton decarboxylation or some variant thereof, we believed that the ensuing carbon centered radical could capture oxygen *in situ* to form the alkylhydroperoxide which, upon cleavage,

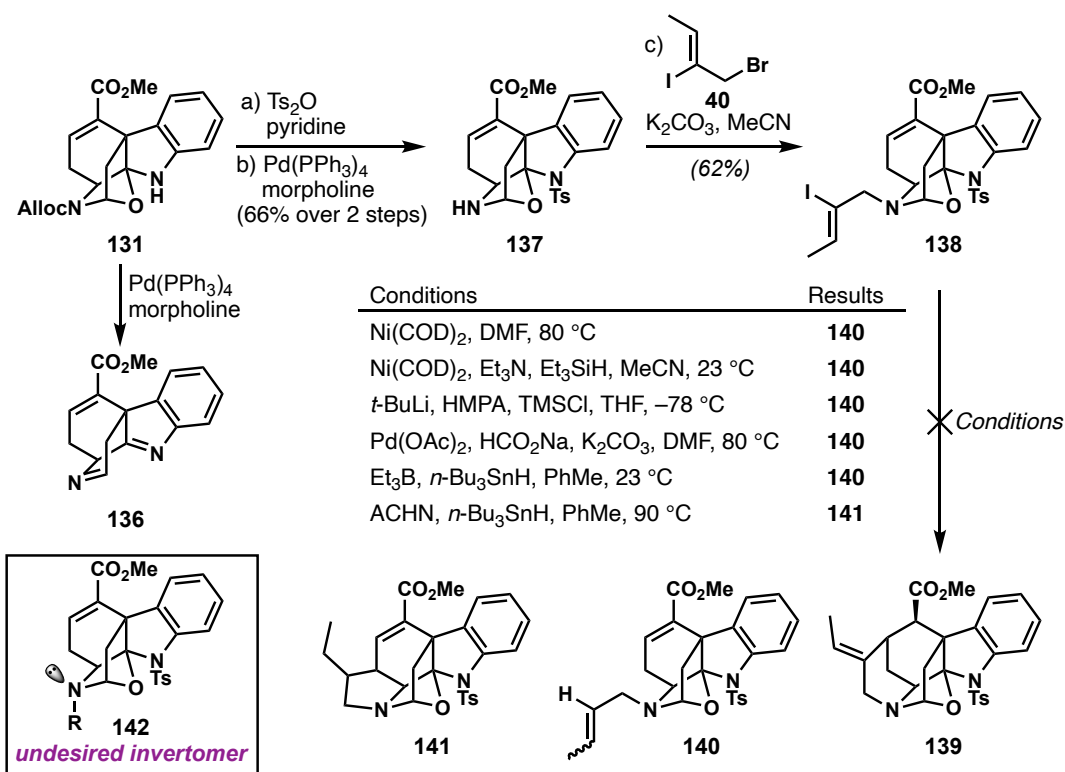
would cyclize to form the desired furoindole. This sequence proceeded as expected to provide furoindole **131** in 30% alongside 25% of the undesired epimer **135**.⁴⁷ Although the yield is low, we found that we could convert **135** to the desired **131** by treatment with PPTS in CH₂Cl₂/H₂O (10:1), thereby increasing the material throughput.



Scheme 4.23. One-pot Barton decarboxylation/oxidation sequence to afford furoindole **131**: (a) EDC (1.5 equiv.), DMAP (1.5 equiv.), 2-mercaptopyridine *N*-oxide (2.0 equiv.), PhMe, 23 °C, 16 h, then O₂, 80 °C, 5 h, then *t*-BuSH (20.0 equiv.), 55%; (b) PPTS (3.0 equiv.), CH₂Cl₂/H₂O (10:1), 23 °C, 24 h, 56%.

4.10 Attempts to Close the *E*-Ring with Furoindole **131**

With this material in hand, the next goal was introduction of the vinyl iodide side chain to re-attempt the proposed 6-*exo*-trig cyclization. Unfortunately, when treated with Pd(PPh₃)₄, the intermediate aminal, following loss of the Alloc group proved highly unstable and underwent dehydration to form aldimine **136**. In order to increase the stability of this species, indoline **131** was protected as the corresponding tosyl sulfonamide, after which the Alloc group could be removed under standard conditions. Subsequent *N*-alkylation then provided the desired cyclization precursor **138**. Scheme 4.24 presents the variety of conditions employed to effect the desired reductive cyclization. However, in almost every case, the only observed product was deiodination. Surprisingly, when ACHN was used as the radical initiator, a product was obtained, in which the proton signal of the β-position of the enoate was still present but

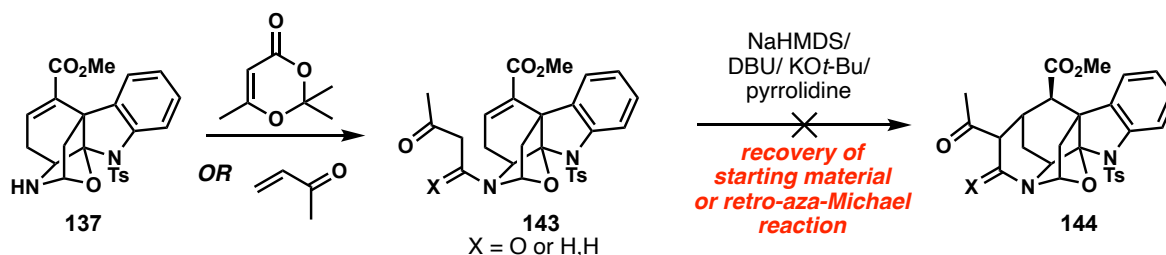


Scheme 4.24. Studies on the 6-*exo*-dig cyclization of furoindole **138**: (a) Ts₂O (1.5 equiv.), pyridine, CH₂Cl₂, 0 °C to 23 °C, 2 h, 76%; (b) Pd(PPh₃)₄ (0.1 equiv.), morpholine (10.0 equiv.), THF, 0 °C, 30 min, 90%; (c) **40** (3.0 equiv.), K₂CO₃ (6.5 equiv.), MeCN, 80 °C, 1 h, 62%.

the proton signal of the trisubstituted olefin had disappeared. This structure has tentatively been assigned as **141**, based on similar pyrrolizidine ring formations as reported by the Parsons group, as well as an analogous result from Zhu and co-workers in their synthesis of aspidophylline A (**2**).^{19b,48} The proposed mechanism of formation is generation of the vinyl radical, followed by a 1,5-HAT process to form the stabilized secondary allylic radical. This species can then perform a 5-*exo*-trig cyclization to construct the proposed pyrrolidine ring. Based on these results, as presented in Scheme 4.24, we believe that although we have been able to enforce the boat conformation, nitrogen inversion remains a problem, with the side chain likely pointed away from the desired reaction site (**142**).

We instead tried to perform an intramolecular Michael addition. Such a process, if conducted under reversible base conditions, might allow for the proposed ring formation, if the transformation was overall thermodynamically favorable. To test this theory, we prepared the aza-Michael adduct of **137** with methyl vinyl ketone, as well as the corresponding β -ketoamide

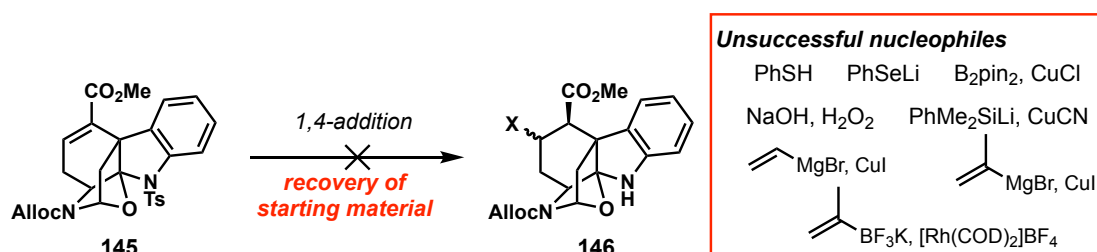
using diketene acetone adduct. Despite several attempts, including reversible base conditions, irreversible bases and Stork enamine chemistry, we only ever observed recovery of the starting material and in some cases amine **137**, via a simple retro-aza-Michael process.



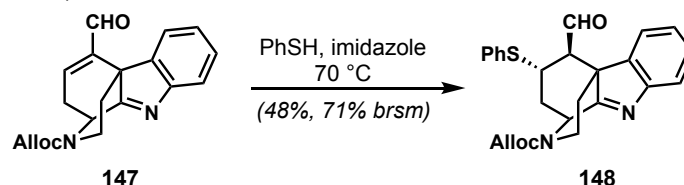
Scheme 4.25. Attempts at intramolecular Michael addition.

4.11 Studies on Conjugate Additions to **145**

At this point it was clear that the proposed ring formation was unlikely to take place as designed. As such, we decided to approach the problem from a different perspective. All of the attempts reported above view the α,β -unsaturated ester as the electrophilic site through which intramolecular delivery of the nucleophile would achieve the desired ring closure. We instead posited that we could introduce a nucleophile through an intermolecular 1,4-addition, which could serve as a handle to construct the final ring. Our first thought was to introduce a radical precursor, either an aryl sulfide or aryl selenide. Once introduced, the ring formation could be



Snyder, 2015 (unpublished)

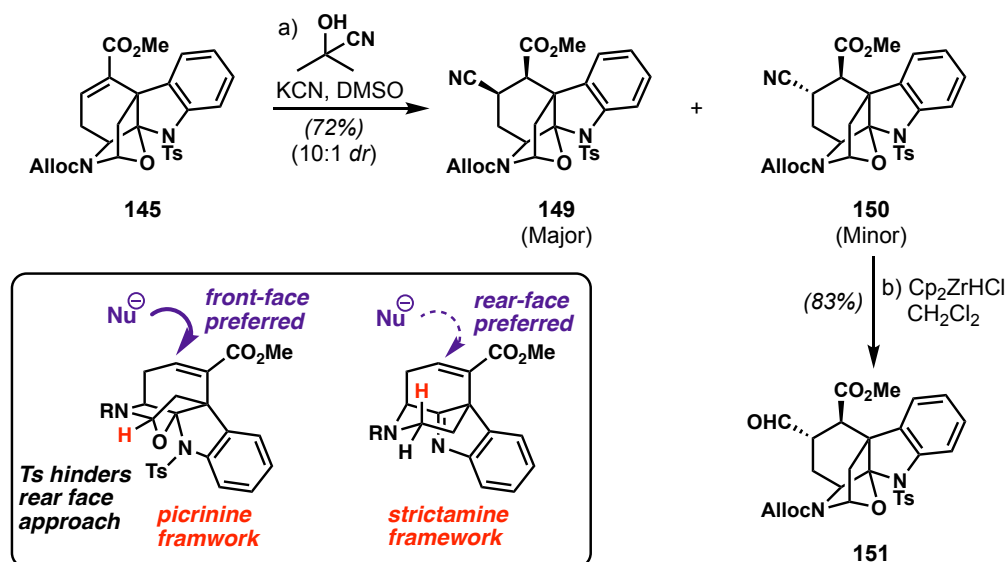


Scheme 4.26. Unsuccessful conjugate additions to **145** and an example from our group.

conducted in a similar fashion to the MacMillan group in their approach to vincorine (**8**, Scheme 4.2) or minfeinsine. Unfortunately, attempts to introduce such heteroatoms only saw recovery of the starting enoate **145**. Along similar lines, we attempted to introduce an oxygen atom at the β -position, either through direct epoxidation or the conjugate addition of PhMe_2SiLi or B_2pin_2 and subsequent oxidation. Such efforts, once again, showed only recovery of the starting material. We then attempted to introduce carbon-based nucleophiles that could be used as a point of elaboration to complete the ring. However, traditional Gilman reagents as well as transition metal-mediated processes, all showed no conversion of the starting material. It is worth noting that a similar consideration was made in our group's approach to strictamine. In that case, the only successful 1,4-addition was between the enal **147** and thiophenol.⁴⁹ The failures observed are in part expected as a result of the steric hinderance of the system and the fact that α,β -unsaturated esters in general are not potent Michael acceptors.

To our surprise, while screening the series of nucleophiles discussed above, we found that we could introduce cyanide in a 1,4-fashion. After optimizing the conditions for this transformation, it was shown that a combination of acetone cyanohydrin and KCN in DMSO afforded the desired adduct in good yield and in a 10:1 *dr*.⁵⁰ The stereochemistries of the major and minor diastereomers were assigned via NOESY analysis, as well as the characteristic *trans*-diaxial coupling ($J = 12.2$ Hz) observed in the ^1H NMR of **150**. We found it surprising that the *syn*-product would be favored in this transformation, especially as the *anti*-product was formed predominantly in the strictamine framework (**148**, Scheme 4.26). Scheme 4.27 presents a possible rationale for this stereooutcome. In the strictamine framework, the stereoselectivity is guided likely by the axial proton positioned in front of the β -position of the Michael acceptor. On the other hand, in the case of the picrinine framework, the boat conformation enforced by the bridging oxygen atom forces this proton into a pseudo-equatorial position and reduces the

steric encumbrance of this face. We also believe that the presence of the tosyl group on the rear face of the molecule, makes this seemingly unlikely front face approach the preferred one.

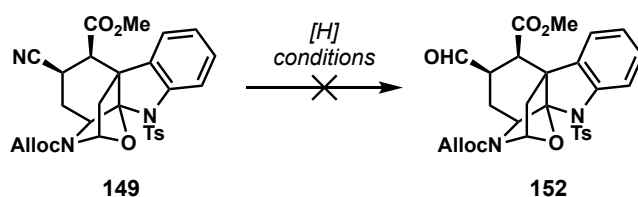


Scheme 4.27. Conjugate addition of cyanide to **145** and rationale for observed stereoselectivity: (a) acetone cyanohydrin (4.0 equiv.), KCN (1.0 equiv.), DMSO, 30 °C, 16 h, 72%, 10:1 dr; (b) Cp₂ZrHCl (2.5 equiv.), CH₂Cl₂, 23 °C, 30 min, 83%.

4.12 Current Progress and Future Outlook

Scalable and reliable access to the *syn*-1,4-adduct **149** was a welcomed result, as the newly introduced nitrile could be elaborated in order to complete the E-ring. As shown in Table 4.1 however, the steric hindrance experienced by the nitrile functional group made further functionalization challenging. A variety of reduction conditions were tested to achieve the selective conversion of the nitrile (**149**) to the corresponding aldehyde (**152**). Typical hydride-based conditions either showed no conversion of the starting material or, in the case of LiAlH₄, gave selective ester reduction to the corresponding primary alcohol, leaving the nitrile untouched. A variety of hydrogenation conditions were also screened, with the only observed reactivity being the reduction of the olefin present in the Alloc protecting group. As a demonstration of the vastly different steric environments of **149** and **150**, we were able to perform the selective reduction effected by Schwartz' reagent (Cp₂ZrHCl) to the corresponding

aldehyde in good yield under mild conditions (83% yield, 23 °C, 15 min), while in the case of **149**, no conversion was observed.



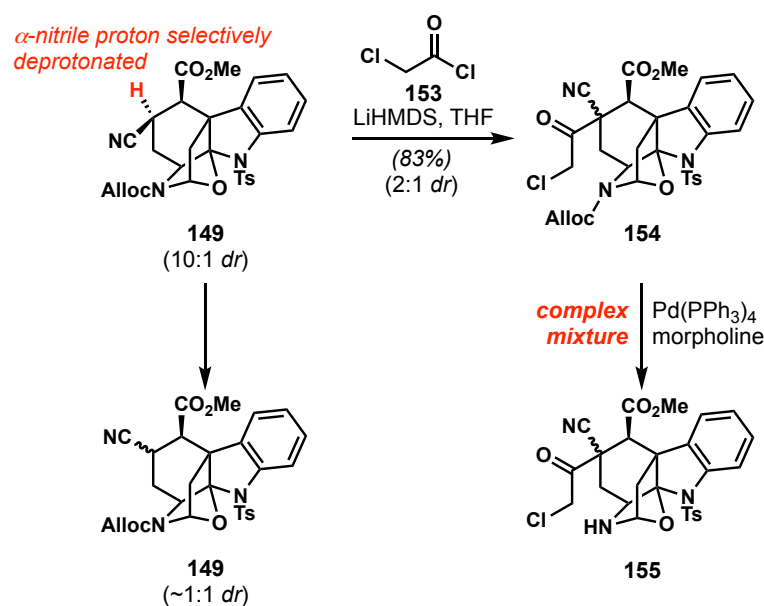
Conditions	Result
LiAlH ₄ , THF, -78 °C to 0 °C	ester reduction
DIBAL-H, THF, -78 °C	no conversion
NaH, ZnCl ₂ , THF	decomp.
i-PrCl, FeCl ₃ , CH ₂ Cl ₂ ; Et ₃ SiH	decomp.
NaBH ₄ , CoCl ₂ , MeOH	decomp.
Ra-Ni, NaH ₂ PO ₂ , pyr./AcOH/H ₂ O	allyl group reduced
H ₂ , Pd/C, Pd(OH) ₂ , MeOH/AcOH/H ₂ O	decomp.
PtO ₂ , HCO ₂ H, 80 °C	allyl group reduced
Cp ₂ ZrHCl (2 eq.), CH ₂ Cl ₂	no conversion

Table 4.1. Screening conditions for selective nitrile reduction.

While pursuing any avenue for further functionalization of nitrile **149**, we observed that if treated with base at low temperature the α -proton of the nitrile is selectively deprotonated and upon quench proton capture takes place indiscriminantly, converting the major diastereomer to a 1:1 epimeric mixture. We were then able to demonstrate that α -alkylation of the nitrile to form the corresponding quaternary center was in fact possible, here using chloroacetyl chloride (**153**) as the electrophile. Notwithstanding the lack of facial selectivity for electrophile capture, the ability to introduce the necessary side chain is notable. But despite this achievement, when removing the Alloc group under standard conditions, a complex mixture resulted.

Realizing that the desired alkylation could take place intermolecularly, we wondered whether an electrophile tethered to the nitrogen atom might offer a means to complete the E-ring, in an intramolecular fashion. In this respect, we have prepared to date, several *N*-alkylated substrates that could serve to perform the proposed cyclization. As of yet, there isn't sufficient data to indicate successful formation of the E-ring, however, tentative crude ¹H NMR shows

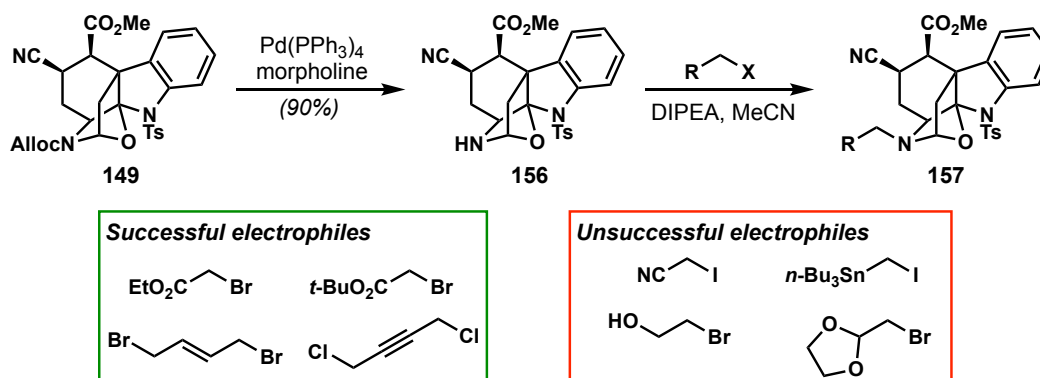
promise for this approach. If such a cyclization were successful, the remaining transformations to access picrinine would include formation of the trisubstituted alkene and removal of the



Scheme 4.28. Observed epimerization of nitrile **149** and α -functionalization to introduce desired sidechain.

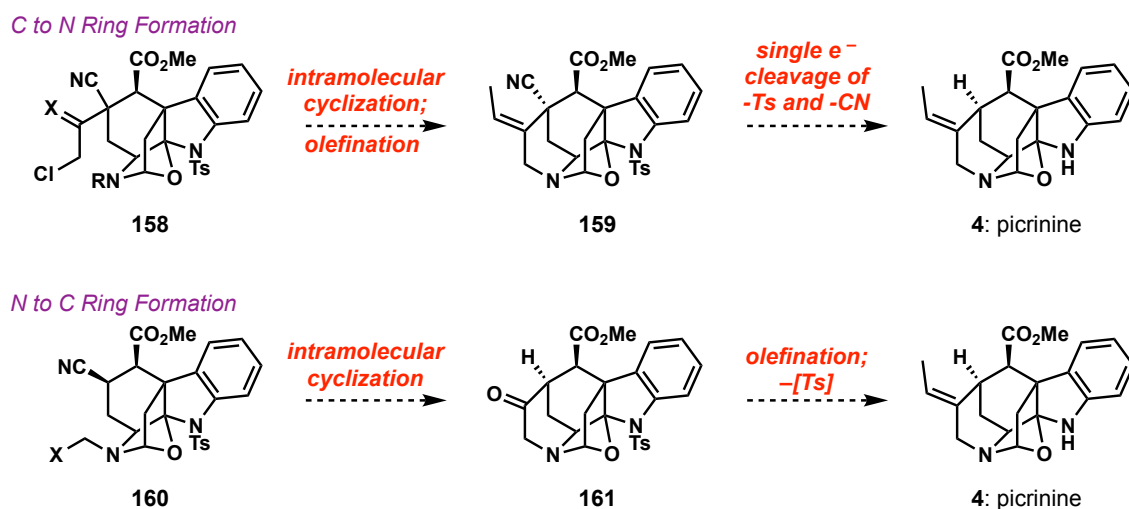
bridgehead nitrile and tosyl sulfonamide groups. The latter of these transformations, we believe, can be performed in a single operation under dissolving metal conditions or some other single electron process.

With substrate **149** in hand, we would also like to explore the potential of the nitrile group to act as an electrophile. Although this would seem to be a similar strategy as the previously attempted with enoate **145**, the increased proximity of the nitrile group to the nitrogen atom would increase the chance for successful cyclization. In addition, the ketone that



Scheme 4.29. Alkylation of secondary amine **156** with various alkyl halides.

would be formed via an intramolecular nucleophilic addition, could serve as a precursor to the ethylidene group found in the target. After this, removal of the tosyl group is the only remaining operation.

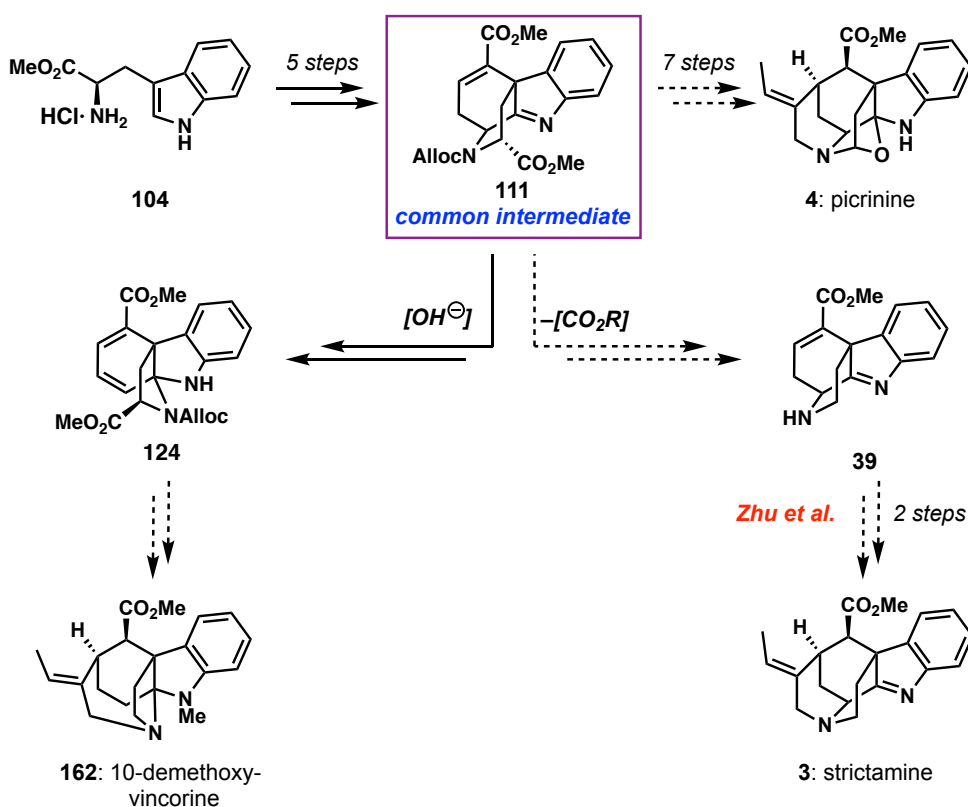


Scheme 4.30. Proposed end-game strategy to access picrinine (4).

4.13 Conclusion

Within this chapter we have detailed our studies towards the indole alkaloids nareline (5) and picrinine (4). The modular approach developed by our group enabled us to access furoindole 149 in just nine steps from commercial materials, in a scalable and reliable fashion. In the pursuit of this target, we have advanced chemical understanding in a number of areas. For example, the one-pot Barton decarboxylation/oxidation sequence has allowed for installation of a bridging heteroatom in a single step. We have also demonstrated that although the α,β -unsaturated ester remains unreactive to many typical Michael donors, we are able to introduce cyanide in a 1,4-fashion with an unexpected facial selectivity, one that could potentially advance the synthesis of the desired target. Possibly most significant, is the hypothetical biosynthetic link proposed between nareline (5) and picrinine (4), a result of challenges related to completion of the methanoquinolizidine skeleton.

In fact, the unpredicted reactivity of this system has shown that this route could give rise to a number of akuammiline alkaloids, from one common intermediate. As shown in Scheme 4.31, tetrahydrocarbazole **111**, obtained in just 5 steps from tryptophan methyl ester, offers formal access to strictamine (**3**), following Alloc removal and decarboxylation. On the other hand, treatment with base promotes the previously discussed rearrangement to pyrroloindole **124**. Such a species contains all of the requisite functionality to deliver 10-demethoxyvincorine (**162**) in short order. And of course, in a proposed seven steps, **111** could lead to the desired picrinine (**4**) and with it, the potential to synthesize nareline (**5**).



Scheme 4.31. **111** as a proposed intermediate to access a wide variety of akuammiline alkaloids.

While the remaining transformations needed to deliver **4**, and the proposed synthesis of **5** thereafter, are daunting challenges, efforts such as these are a necessity in natural product synthesis, not just to reach the end goal of concise and elegant syntheses but as a means to broaden chemical knowledge, inform future prospects and inspire others in the field.

4.14 References

1. For selected reviews on akuammiline alkaloids, see: (a) Ramírez, A.; García-Rubio, S. *Curr. Med. Chem.* **2003**, *10*, 1891; (b) Eckermann, R.; Gaich, T. *Synthesis* **2013**, *45*, 2813; (c) Smith, J. M.; Moreno, J.; Boal, B. W.; Garg, N. K. *Angew. Chem. Int. Ed.* **2015**, *54*, 400; (d) Adams, G. L.; Smith III, A. B., The chemistry of the akuammiline alkaloids. *The Alkaloids: Chemistry and Biology* **2016**, *76*, 171; (e) Joule, J. A. in *Chemistry of Heterocyclic Compounds: A Series of Monographs. The Sarpagine-Akuammiline Group, Vol. XXV, Part IV* (Ed.: J. E. Saxon), Wiley Chichester, **1994**, 201.
2. Gorup-Besanez, V. *Liebigs Ann.* **1875**, *176*, 88.
3. Henry, T. A.; Sharp, T. M. *J. Chem. Soc.* **1927**, 1950.
4. Henry, T. A. *J. Chem. Soc.* **1932**, 2759.
5. Baliga, M. S. *Chin. J. Integ. Med.* **2012**, 1.
6. Hou, Y.; Cao, X.; Wang, L.; Cheng, B.; Dong, L.; Luo, X.; Bai, G.; Gao, W. *J. Chromatogr. B* **2012**, *908*, 98.
7. Leewanich, P.; Tohda, M.; Matsumoto, K.; Subhadhirasakul, S.; Takayama, H.; Aimi, N.; Watanabe, H. *Eur. J. Pharm.* **1997**, *332*, 321.
8. Subramaniam, G.; Hiraku, O.; Hayashi, M.; Koyano, T.; Komiyama, K.; Kam, T.-S. *J. Nat. Prod.* **2007**, *70*, 1783.
9. Zhang, M.; Huang, X.; Shen, L.; Qin, Y. *J. Am. Chem. Soc.* **2009**, *131*, 6013.
10. For examples of early studies towards akuammiline alkaloids, see: (a) Dolby, L. J.; Esfandiari, Z. *J. Org. Chem.* **1972**, *37*, 43; (b) Dolby, L. J.; Nelson, S. J. *J. Org. Chem.* **1973**, *38*, 2882; (c) Lévy, J.; Sapi, J.; Laronze, J.-Y.; Royer, D.; Toupet, L. *Synlett* **1992**, 601; (d) Bosch, J.; Bennasar, M.-L. *Synlett* **1995**, 587; (e) Bennasar, M.-L.; Zulaica, E.; Ramírez, A.; Bosch, J. *J. Org. Chem.* **1996**, *61*, 1239.
11. (a) Battersby, A. R.; Thompson, M.; Glüsenkamp, K. H.; Tietze, L. F. *Chem. Ber.* **1981**, *114*, 3430; (b) Battersby, A. R.; Westcoltt, N. D.; Glüsenkamp, K. H.; Tietze, L. F. *Chem. Ber.* **1981**, *114*, 3439; (c) Scott, A. I. *Acc. Chem. Res.* **1970**, *3*, 151; (d) Stöckigt, J.; Barleben, L.; Panjekar, S.; Loris, E. A. *Plant Physiol. Biochem.* **2008**, *46*, 340.
12. Ahmad, Y.; Fatima, K.; Le Quesne, P. W. *Phytochemistry* **1983**, *22*, 1017.
13. Horning, B. D.; MacMillan, D. W. *J. Am. Chem. Soc.* **2013**, *135*, 6442.
14. Teng, M.; Zi, W.; Ma, D. *Angew. Chem. Int. Ed.* **2014**, *53*, 1814.
15. Ren, W.; Wang, Q.; Zhu, J. *Angew. Chem. Int. Ed.* **2016**, *55*, 3500.

16. (a) Smith, J. M.; Moreno, J.; Boal, B. W.; Garg, N. K. *J. Am. Chem. Soc.* **2014**, *136*, 4504; (b) Smith, J. M.; Moreno, J.; Boal, B. W.; Garg, N. K. *J. Org. Chem.* **2015**, *80*, 8954.
17. Zi, W.; Xie, W.; Ma, D. *J. Am. Chem. Soc.* **2012**, *134*, 9126.
18. Jones, S. B.; Simmons, B.; MacMillan, D. W. *J. Am. Chem. Soc.* **2009**, *131*, 13606.
19. (a) Zu, L.; Boal, B. W.; Garg, N. K. *J. Am. Chem. Soc.* **2011**, *133*, 8877; (b) Ren, W.; Wang, Q.; Zhu, J. *Angew. Chem. Int. Ed.* **2014**, *53*, 1818; (c) Moreno, J.; Picazo, E.; Morrill, L. A.; Smith, J. M.; Garg, N. K. *J. Am. Chem. Soc.* **2016**, *138*, 1162; (d) Jiang, S. Z.; Zeng, X. Y.; Liang, X.; Lei, T.; Wei, K.; Yang, Y. R. *Angew. Chem. Int. Ed.* **2016**, *55*, 4044; (e) Wang, T.; Duan, X.; Zhao, H.; Zhai, S.; Tao, C.; Wang, H.; Li, Y.; Cheng, B.; Zhai, H. *Org. Lett.* **2017**, *19*, 1650.
20. For the original report of the oxidative coupling, see: (a) Baran, P. S.; Richter, J. M. *J. Am. Chem. Soc.* **2004**, *126*, 7450. For applications in synthesis see: (b) Zuo, Z.; Xie, W.; Ma, D. *J. Am. Chem. Soc.* **2010**, *132*, 13226; (c) Zuo, Z.; Ma, D. *Angew. Chem. Int. Ed.* **2011**, *50*, 12008.
21. Yu, S.; Berner, O. M.; Cook, J. M. *J. Am. Chem. Soc.* **2000**, *122*, 7827.
22. Zhang, B.; Wang, X.; Li, C. *J. Am. Chem. Soc.* **2020**, *142*, 3269.
23. (a) Nishiyama, D.; Ohara, A.; Chiba, H.; Kumagai, H.; Oishi, S.; Fujii, N.; Ohno, H. *Org. Lett.* **2016**, *18*, 1670; (b) Eckermann, R.; Breunig, M.; Gaich, T. *Chem. Commun.* **2016**, *52*, 11363; (c) Xiao, T.; Chen, Z.-T.; Deng, L.-F.; Zhang, D.; Liu, X.-Y.; Song, H.; Qin, Y. *Chem. Commun.* **2017**, *53*, 12665; (d) Eckermann, R.; Breunig, M.; Gaich, T. *Chem. Eur. J.* **2017**, *23*, 3938; (e) Smith, M. W.; Zhou, Z.; Gao, A. X.; Shimbayashi, T.; Snyder, S. A. *Org. Lett.* **2017**, *19*, 1004; (f) Sato, K.; Takanashi, N.; Kogure, N.; Kitajima, M.; Takayama, H. *Heterocycles* **2018**, *97*, 365; (g) Ding, H.; Gao, B.; Yao, F.; Zhang, Z. *Angew. Chem. Int. Ed.* **2021**, DOI: 10.1002/anie.202101752.
24. Xie, X.; Wei, B.; Li, G.; Zu, L. *Org. Lett.* **2017**, *19*, 5430.
25. (a) Rawal, V. H.; Michoud, C.; Monestel, R. *J. Am. Chem. Soc.* **1993**, *115* (7), 3030-3031. (b) Rawal, V. H.; Iwasa, S. *J. Org. Chem.* **1994**, *59*, 2685; (c) Birman, V. B.; Rawal, V. H. *Tetrahedron Lett.* **1998**, *39*, 7219.
26. Chen, Z.-T.; Xiao, T.; Tang, P.; Zhang, D.; Qin, Y. *Tetrahedron* **2018**, *74*, 1129.
27. Li, W.; Chen, Z.; Yu, D.; Peng, X.; Wen, G.; Wang, S.; Xue, F.; Liu, X. Y.; Qin, Y. *Angew. Chem. Int. Ed.* **2019**, *58*, 6059.
28. Picazo, E.; Morrill, L. A.; Susick, R. B.; Moreno, J.; Smith, J. M.; Garg, N. K. *J. Am. Chem. Soc.* **2018**, *140*, 6483.
29. Susick, R. B.; Morrill, L. A.; Picazo, E.; Garg, N. K. *Synlett* **2017**, *28*, 1.

30. Banerji, J.; Chakrabarti, R. *Indian J. Chem., Sect. B* **1984**, *23B*, 453.
31. Li, Y.; Zhu, S.; Li, J.; Li, A. *J. Am. Chem. Soc.* **2016**, *138*, 3982.
32. Wang, D.; Hou, M.; Ji, Y.; Gao, S. *Org. Lett.* **2017**, *19*, 1922.
33. Gan, P.; Pitzten, J.; Qu, P.; Snyder, S. A. *J. Am. Chem. Soc.* **2018**, *140*, 919.
34. Zhou, Z.; Gao, A. X.; Snyder, S. A. *J. Am. Chem. Soc.* **2019**, *141*, 7715.
35. Morita, Y.; Hesse, M.; Schmid, H.; Banerji, A.; Banerji, J.; Chatterjee, A.; Oberhänsli, W. E. *Helv. Chim. Acta* **1977**, *60*, 1419.
36. (a) Liu, L.; Chen, Y.-Y.; Qin, X.-J.; Wang, B.; Jin, Q.; Liu, Y.-P.; Luo, X.-D. *Fitoterapia* **2015**, *105*, 160; (b) Yang, J.; Fu, J.; Liu, X.; Jiang, Z.-H.; Zhu, G.-Y. *Fitoterapia* **2018**, *124*, 73.
37. Zhang, X. M.; Tu, Y. Q.; Zhang, F. M.; Shao, H.; Meng, X. *Angew. Chem. Int. Ed.* **2011**, *50*, 3916.
38. A similar connection has been proposed between **4** and **5**: Adams, G. L.; Carroll, P. J.; Smith III, A. B. *J. Am. Chem. Soc.* **2013**, *135*, 519.
39. Maclaren, J. *Aust. J. Chem.* **1989**, *42*, 813-821.
40. For examples of additions to β -carbolines involving acyl chlorides see: (a) Martin, S. F.; Benage, B.; Hunter, J. E. *J. Am. Chem. Soc.* **1988**, *110*, 5925; (b) Martin, S. F.; Clark, C. W.; Corbett, J. W. *J. Org. Chem.* **1995**, *60*, 3236; (c) Birman, V. B.; Rawal, V. H. *J. Org. Chem.* **1998**, *63*, 9146; (d) Deiters, A.; Pettersson, M.; Martin, S. F. *J. Org. Chem.* **2006**, *71*, 6547.
41. For examples of additions to β -carbolines involving Lewis acids see: (a) Knölker, H.-J.; Cämmerer, S. *Tetrahedron Lett.* **2000**, *41*, 5035; (b) González-Gómez, Á. *Tetrahedron Lett.* **2005**, *46*, 7267; (c) Kolundžić, F.; Murali, A.; Pérez-Galán, P.; Bauer, J. O.; Strohmam, C.; Kumar, K.; Waldmann, H. *Angew. Chem. Int. Ed.* **2014**, *53*, 8122.
42. Song, G.; Zhu, X.; Li, J.; Hu, D.; Zhao, D.; Liao, Y.; Lin, J.; Zhang, L.-H.; Cui, Z.-N. *Bioorg. Med. Chem. Lett.* **2017**, *25*, 5709.
43. Liu, J.; Wang, Y.; Yang, Y.; Jiang, X.; Zhao, M.; Wang, W.; Wu, G.; Wu, J.; Zheng, M.; Peng, S. *ChemMedChem* **2011**, *6*, 2312.
44. Nicolaou, K.; Estrada, A. A.; Zak, M.; Lee, S. H.; Safina, B. S. *Angew. Chem. Int. Ed.* **2005**, *44*, 1378.
45. Chatterjee, A.; Mukherjee, B.; Ray, A.; Das, B. *Tetrahedron Lett.* **1965**, *6*, 3633.
46. For selected examples of similar retro-Strecker reactions see: (a) Fukuyama, T.; Nunes, J. J. *J. Am. Chem. Soc.* **1988**, *110*, 5196; (b) Katoh, T.; Kirihara, M.; Yoshino, T.;

- Terashima, S. *Tetrahedron Lett.* **1993**, *34*, 5751; (c) Scott, J. D.; Williams, R. M. *J. Am. Chem. Soc.* **2002**, *124*, 2951; (d) Wu, Y.-C.; Zhu, J. *Org. Lett.* **2009**, *11*, 5558; (e) Korotkov, A.; Li, H.; Chapman, C. W.; Xue, H.; MacMillan, J. B.; Eastman, A.; Wu, J. *Angew. Chem. Int. Ed.* **2015**, *54*, 10604; (f) Xu, S.; Wang, G.; Zhu, J.; Shen, C.; Yang, Z.; Yu, J.; Li, Z.; Lin, T.; Sun, X.; Zhang, F., A. *Eur. J. Org. Chem.* **2017**, 975.
47. For the original report of this transformation see: (a) Barton, D. H.; Crich, D.; Motherwell, W. B. *Tetrahedron* **1985**, *41*, 3901. For selected examples of applications in synthesis see: (b) Corey, E.; Hong, B.-C. *J. Am. Chem. Soc.* **1994**, *116*, 3149; (c) Hatakeyama, S.; Kawamura, M.; Takano, S. *J. Am. Chem. Soc.* **1994**, *116*, 4081; Feng, M.; Jiang, X. *Chem. Commun.* **2014**, *50*, 9690.
48. (a) Borthwick, A. D.; Caddick, S.; Parsons, P. J. *Tetrahedron Lett.* **1990**, *31*, 6911; (b) Lathbury, D. C.; Parsons, P. J.; Pinto, I. *J. Chem. Soc., Chem. Commun.* **1988**, 81.
49. Smith, M. W. *Strategies for the Concise Synthesis of the Akuammiline Alkaloids*. Columbia University, 2015.
50. For selected examples of 1,4-additions of cyanide to α,β -unsaturated esters see: (a) Bhagwat, S. S.; Gude, C.; Cohen, D. S.; Lee, W.; Furness, P.; Clarke, F. H. *J. Med. Chem.* **1991**, *34*, 1790; (b) Olga Hankovszky, H.; Hideg, K.; Cecilla Sar, P.; Judit Lovas, M.; Jerkovich, G. *Synthesis* **1990**, 59.

4.15 Experimental Section

General Procedures. All reactions were carried out under an argon atmosphere with dry solvents under anhydrous conditions, unless otherwise noted. Dry tetrahydrofuran (THF), toluene, diethyl ether (Et₂O), dichloromethane (CH₂Cl₂), and acetonitrile (CH₃CN) were obtained by passing commercially available pre-dried, oxygen-free formulations through activated alumina columns. Yields refer to chromatographically and spectroscopically (¹H and ¹³C NMR) homogeneous materials, unless otherwise stated. Reagents were purchased at the highest commercial quality and used without further purification, unless otherwise stated. Reactions were magnetically stirred and monitored by thin-layer chromatography (TLC) carried out on 0.25 mm E. Merck silica gel plates (60F-254) using UV light as visualizing agent, and an ethanolic solution of phosphomolybdic acid and cerium sulfate or a solution of KMnO₄ in aq. NaHCO₃ and heat as developing agents. SiliCycle silica gel (60, academic grade, particle size 0.040–0.063 mm) was used for flash column chromatography. Preparative thin-layer chromatography separations were carried out on 0.50 mm E. Merck silica gel plates (60F-254). NMR spectra were recorded on Bruker 400 and 500 MHz instruments and calibrated using residual undeuterated solvent as an internal reference. The following abbreviations were used to explain the multiplicities: s = singlet, d = doublet, t = triplet, q = quartet, br = broad, app = apparent. IR spectra were recorded on a Perkin-Elmer 1000 series FT-IR spectrometer. High-resolution mass spectra (HRMS) were recorded on Agilent 6244 ToF-MS using ESI (Electrospray Ionization) at the University of Chicago Mass Spectroscopy Core Facility. All *ee* values were determined by HPLC on Daicel Chiralcel or Chiralpak columns.

Formamide 96. To a solution of the tryptophanol (600.0 mg, 3.15 mmol, 1.0 equiv.), in CH₂Cl₂ (30 mL) at 0 °C was added HCO₂H (0.3 mL, 7.56 mmol, 2.4 equiv.), EDC (1.57 g, 8.19 mmol, 2.6 equiv.) and DMAP (76.9 mg, 0.63 mmol, 0.2 equiv.) successively. The mixture was

warmed to 23 °C and stirred for 12 h. Upon completion the reaction was diluted with CH₂Cl₂ (15 mL), washed with 1M HCl (2 × 15 mL), saturated aq. NaHCO₃ (2 × 15 mL) and brine (2 × 15 mL). The organic layer was dried over Na₂SO₄ and concentrated *in vacuo*. The crude residue was further purified by flash column chromatography (silica gel, hexane/EtOAc, 1:1) to afford the desired formamide **96** (325 mg, 43% yield) as a pale yellow foam. **96**: ¹H NMR (500 MHz, CDCl₃) δ 8.18 (d, *J* = 1.2 Hz, 1 H), 8.13 (d, *J* = 0.9 Hz, 1 H), 7.65 (dp, *J* = 7.9, 0.8 Hz, 1 H), 7.39 (dt, *J* = 8.1, 0.9 Hz, 1 H), 7.22 (ddd, *J* = 8.2, 7.0, 1.2 Hz, 1 H), 7.15 (ddd, *J* = 8.0, 7.0, 1.1 Hz, 1 H), 7.07 (d, *J* = 2.4 Hz, 1 H), 5.71 (d, *J* = 8.7 Hz, 1 H), 5.30 (s, 2 H), 4.69 (h, *J* = 5.4 Hz, 1 H), 4.29 – 4.24 (m, 1 H), 4.23 – 4.18 (m, 1 H), 3.14 – 3.08 (m, 1 H), 3.03 (dd, *J* = 14.7, 7.6 Hz, 1 H).

Aminoalcohol 100. To a suspension of formamide **96** (500.0 mg, 2.03 mmol, 1.0 equiv.) in MeCN (4 mL) at 0 °C was added POCl₃ (0.4 mL, 4.06 mmol 2.0 equiv.) in MeCN (2 mL) over 1 h. Once the addition was complete, the reaction mixture was stirred for an additional 3 h at 0 °C. Upon completion the reaction poured directly into 1 M HCl. The aqueous layer was neutralized with solid NaHCO₃ until pH 7 was reached. The aqueous layer was then extracted with CH₂Cl₂ (3 × 10 mL) and the combined layers dried over Na₂SO₄ and concentrated *in vacuo*. The crude residue (326 mg) was transferred to a flame-dried flask and dissolved in THF (10 mL). To this was added **98** (0.5 mL, 2.45 mmol, 1.5 equiv.) and the reaction stirred at 23 °C for 12 h. Upon consumption of the starting material, the reaction mixture was concentrated directly and redissolved in MeOH (15 mL). The solution was cooled to 0 °C and NaBH₄ (154.2 mg, 4.08 mmol, 2.5 equiv.) was added portion-wise. The reaction was warmed to 23 °C and stirred for 3 h, after which it was concentrated, diluted with CH₂Cl₂ (15 mL) and washed with H₂O (2 × 10 mL), saturated aq. NaHCO₃ (2 × 10 mL) and brine (2 × 10 mL). The organic layer was dried over Na₂SO₄ and concentrated *in vacuo* to afford the desired aminoalcohol **100** (330

mg, 68% yield over 3 steps). **100**: $^1\text{H NMR}$ (500 MHz, CDCl_3) δ 8.48 (s, 1 H), 7.50 – 7.45 (m, 1 H), 7.35 (dt, $J = 8.2, 0.9$ Hz, 1 H), 7.18 (ddd, $J = 8.1, 7.1, 1.3$ Hz, 1 H), 7.10 (ddd, $J = 8.0, 7.1, 1.0$ Hz, 1 H), 4.34 (dq, $J = 6.7, 2.3$ Hz, 1 H), 3.89 (dd, $J = 10.7, 3.7$ Hz, 1 H), 3.62 (dd, $J = 10.7, 8.6$ Hz, 1 H), 3.21 (ddt, $J = 10.9, 8.1, 3.9$ Hz, 1 H), 2.75 (dddd, $J = 13.8, 9.2, 4.3, 2.2$ Hz, 2 H), 2.60 (ddd, $J = 16.5, 8.9, 2.7$ Hz, 1 H), 2.47 (ddd, $J = 15.0, 10.9, 2.4$ Hz, 1 H), 2.26 (t, $J = 2.7$ Hz, 1 H).

Carbamate 101. To a suspension of **100** (80.0 mg, 0.33 mmol, 1.0 equiv.) in THF (1.5 mL) was added CDI (160.5 mg, 0.99 mmol, 3.0 equiv.) and the reaction mixture stirred for 5 h. Following this, the reaction mixture was concentrated and neutralized with NaOH (10% w/v, 3.5 mL) and stirred for an additional 1 h. The mixture was subsequently brought to pH 6 using 1 M HCl and the aqueous solution extracted with EtOAc (3 \times 5 mL). The combined organic layers were dried over Na_2SO_4 and concentrated *in vacuo* to give a crude residue which was further purified by flash column chromatography (silica gel, hexanes/EtOAc, 4:1), affording **101** (65.8 mg, 75% yield). **101**: $^1\text{H NMR}$ (500 MHz, CDCl_3) δ 8.62 (s, 1 H), 7.50 (d, $J = 7.6$ Hz, 1 H), 7.39 (dd, $J = 8.2, 2.7$ Hz, 1 H), 7.23 (ddd, $J = 8.2, 6.9, 1.3$ Hz, 1 H), 7.17 – 7.13 (m, 1 H), 4.91 – 4.82 (m, 1 H), 4.60 – 4.52 (m, 1 H), 4.15 – 4.06 (m, 2 H), 3.77 (dt, $J = 16.5, 2.9$ Hz, 1 H), 3.15 – 3.06 (m, 1 H), 2.82 – 2.71 (m, 1 H), 2.66 (ddd, $J = 16.4, 9.2, 2.6$ Hz, 1 H), 2.21 (t, $J = 2.7$ Hz, 1 H).

Ynoate 102. To a flame-dried 500 mL flask was added $\text{Pd}(\text{OAc})_2$ (10.0 mg, 0.045 mmol, 0.3 equiv.) and Ph_3P (23.6 mg, 0.09 mmol, 0.6 equiv.) and the solids suspended in MeOH (0.9 mL) and DMF (1.6 mL) under Ar. **101** (40.0 mg, 0.15 mmol, 1.0 equiv.) was then added to this mixture and the reaction placed under an atmosphere of CO/O_2 (~1:1) and stirred at 23 $^\circ\text{C}$ for 16 h. Once complete, the reaction was quenched by the addition of H_2O (5 mL) and the contents

transferred to a separatory funnel, diluting with Et₂O (10 mL) and H₂O (5 mL). The layers were separated, and the aqueous layer was further extracted with Et₂O (5 × 5 mL). The combined organic layers were washed with H₂O (3 × 5 mL), brine (5 mL), dried over Na₂SO₄ and concentrated *in vacuo*. The resultant crude product was further purified by flash column chromatography (silica gel, Hexanes/EtOAc, 4:1) to give ynoate **102** (20.8 mg, 52% yield) as a pale-yellow oil. **102**: ¹H NMR (500 MHz, CDCl₃) δ 8.52 (s, 1H), 7.50 (d, *J* = 8.1 Hz, 1 H), 7.42 – 7.35 (m, 1 H), 7.25 – 7.21 (m, 1 H), 7.15 (tdd, *J* = 7.4, 3.5, 1.8 Hz, 1 H), 4.97 – 4.90 (m, 1H), 4.57 (t, *J* = 2.6 Hz, 1 H), 4.12 (ddt, *J* = 9.4, 7.2, 3.0 Hz, 2 H), 3.77 (s, 3 H), 3.64 (dq, *J* = 17.2, 2.8 Hz, 1 H), 3.19 – 3.02 (m, 2 H), 2.86 – 2.73 (m, 1 H).

Indolenine 103. To a 4 mL scintillation vial containing Ph₃PAuCl (2.5 mg, 0.0046 mmol, 0.1 equiv.) was added 1,2-DCE (0.2 mL) followed by AgSbF₆ (15.8 mg, 0.046 mmol, 1.0 equiv.). This mixture was stirred for 15 min after which **102** (15.0 mg, 0.046 mmol, 1.0 equiv.) was added as a solution in 1,2-DCE (0.5 mL). The reaction was stirred for 16 h at 23 °C, after which it was quenched by the addition of saturated aq. NaHCO₃ (1 mL) and stirred for 30 min. The mixture was then diluted with CH₂Cl₂ (3 mL) and H₂O (3 mL). The layers were separated and the aqueous layer was further extracted with CH₂Cl₂ (3 × 2 mL). The combined organic layers were dried over Na₂SO₄ and concentrated *in vacuo* to afford a crude residue which was further purified flash column chromatography (silica gel, hexanes/EtOAc, 2:1) to afford **103** (9.0 mg, 60% yield). **103**: ¹H NMR (500 MHz, CDCl₃) δ 7.91 (d, *J* = 7.6 Hz, 1 H), 7.61 (d, *J* = 7.6 Hz, 1H), 7.39 (t, *J* = 7.5 Hz, 1 H), 7.28 (d, *J* = 8.1 Hz, 1 H), 6.82 (dd, *J* = 5.1, 2.3 Hz, 1 H), 4.99 (s, 1 H), 4.49 (t, *J* = 8.3 Hz, 1 H), 3.88 (t, *J* = 9.1 Hz, 1 H), 3.80 (s, 3 H), 3.73 (d, *J* = 12.9 Hz, 1 H), 3.67 – 3.55 (m, 1 H), 2.81 – 2.70 (m, 2 H), 2.44 (dd, *J* = 13.6, 6.0 Hz, 1 H).

Carboline 106. To a 1L flask was added tryptophan methyl ester hydrochloride salt (40.0 g, 157.0 mmol, 1.0 equiv.), MeOH (200 mL) and TFA (40 mL) and the resulting suspension stirred for 30 min. Following this, 1,1,3,3-tetramethoxypropane (32.0 mL, 196.9 mmol, 1.25 equiv.) was added and the mixture heated to 80 °C for 16 h. The reaction mixture was then concentrated *in vacuo* to give a deep red oil that was carried forward without further purification. The crude product was dissolved in THF/H₂O (1:1 v/v, 320 mL) and K₂CO₃ (86.8 g, 628.0 mmol, 4.0 equiv.) and Boc₂O (41.1 g, 188.4 mmol, 1.2 equiv.) were added (*caution*: vigorous effervescence upon the addition of K₂CO₃). After 20 h the layers were separated and the aqueous layer was extracted with EtOAc (3 × 100 mL). The combined organic layers were then washed with brine (100 mL), dried over Na₂SO₄ and concentrated *in vacuo* to give the crude product as a 1.86:1 mixture of diastereomers, which was further purified by flash column chromatography (silica gel, Hexanes/Acetone, 9:1) to give the desired Boc-protected dihydro- β -carboline **106** (19.75 g, 30% yield) as pale-yellow amorphous solid. **106**: ¹H NMR (400 MHz, CDCl₃) δ 8.46 (s, 1 H), 7.49 (d, *J* = 7.7 Hz, 1 H), 7.33 (dt, *J* = 8.1, 0.9 Hz, 1 H), 7.16 (td, *J* = 7.6, 1.3 Hz, 1 H), 7.14 – 7.06 (m, 1 H), 5.17 (s, 1 H), 4.85 – 4.50 (m, 2 H), 3.62 (s, 3 H), 3.43 (s, 3 H), 3.39 (s, 3 H), 3.14 – 3.05 (m, 1 H), 2.51 (ddd, *J* = 14.0, 5.9, 4.5 Hz, 1 H), 1.90 (d, *J* = 17.2 Hz, 1 H), 1.61 – 1.39 (m, 9 H), 1.28 (q, *J* = 5.6 Hz, 1 H).

Alkyne 108. To a 2L flask containing **106** (18.20 g, 43.4 mmol, 1.0 equiv.) was added acetone (900 mL) and H₂O (90 mL). To the resulting solution was added *p*-TsOH·H₂O (4.12 g, 21.7 mmol, 0.5 equiv.) and the reaction mixture heated to 60 °C for 1 h. The contents of the flask were then concentrated to ~ 200 mL, quenched with saturated aq. NaHCO₃ (150 mL) and transferred to a separatory funnel. The aqueous layer was then extracted with EtOAc (3 × 150 mL) and the combined organic layers dried over Na₂SO₄ and concentrated *in vacuo* to provide the desired aldehyde **106**, which was carried forward without any further purification.

To a flame dried flask containing **107** (7.92 g, 41.3 mmol, 1.5 equiv.) in MeOH (200 mL) at 0 °C was added K₂CO₃ (7.60 g, 55.0 mmol, 2.0 equiv.). This mixture was stirred for 30 min after which a portion of aldehyde (10.22 g, 27.5 mmol, 1.0 equiv.) was added as a solution in MeOH (70 mL) dropwise. After 1 h the reaction was warmed to 23 °C and stirred for 16 h. Upon completion the reaction mixture was filtered over celite and concentrated *in vacuo*. The crude material was dissolved in EtOAc (150 mL) and washed with H₂O (100 mL). The aqueous layer was then extracted with EtOAc (2 × 100 mL). The organic layers were combined, washed with brine, dried over Na₂SO₄ and concentrated *in vacuo*. The resultant crude mixture was further purified by flash column chromatography (silica gel, Hexanes/Acetone, 7:1 → 5:1) to give **108** as a cream-colored crystalline solid (5.96 g, 59% yield). **108**: ¹H NMR (400 MHz, CDCl₃) δ 8.20 (s, 1H), 7.51 (d, *J* = 7.8 Hz, 1 H), 7.39 – 7.31 (m, 1 H), 7.18 (ddd, *J* = 8.2, 7.1, 1.3 Hz, 1 H), 7.12 (ddd, *J* = 8.1, 7.1, 1.1 Hz, 1 H), 5.21 (s, 1 H), 5.04 – 4.80 (m, 1 H), 3.57 (s, 3 H), 3.38 (d, *J* = 15.4 Hz, 1 H), 3.16 (d, *J* = 16.5 Hz, 2 H), 2.58 (s, 1 H), 2.10 (s, 1 H), 1.47 (s, 9 H).

Ynoate 109. To a flame-dried 500 mL flask was added Pd(OAc)₂ (1.09 g, 4.85 mmol, 0.3 equiv.) and Ph₃P (2.55 g, 9.72 mmol, 0.6 equiv.) and the solids suspended in MeOH (80 mL) and DMF (160 mL) under Ar. **108** (5.96 g, 16.2 mmol, 1.0 equiv.) was then added to this mixture and the reaction placed under an atmosphere of CO/O₂ (~1:1) and stirred at 23 °C for 48 h. Once complete, the reaction was quenched by the addition of H₂O (150 mL) and the contents transferred to a separatory funnel, diluting with Et₂O (200 mL) and H₂O (50 mL). The layers were separated, and the aqueous layer was further extracted with Et₂O (5 × 100 mL). The combined organic layers were washed with H₂O (3 × 100 mL), brine (100 mL), dried over Na₂SO₄ and concentrated *in vacuo*. The resultant crude product was further purified by flash column chromatography (silica gel, Hexanes/EtOAc, 4:1) to give the desired ynoate **109** (4.55

g, 66% yield) as a pale-yellow oil. **109**: $^1\text{H NMR}$ (400 MHz, CDCl_3) δ 8.17 (s, 1 H), 7.51 (d, $J = 7.8$ Hz, 1 H), 7.41 – 7.28 (m, 1 H), 7.19 (ddd, $J = 8.2, 7.1, 1.3$ Hz, 1 H), 7.12 (td, $J = 7.5, 1.1$ Hz, 1 H), 5.38 – 5.16 (m, 1 H), 5.11 – 4.84 (m, 1H), 3.76 (s, 3 H), 3.56 (s, 3 H), 3.40 (d, $J = 15.4$ Hz, 1 H), 3.22 (d, $J = 17.2$ Hz, 2 H), 2.90 (dd, $J = 16.9, 7.9$ Hz, 1 H), 1.47 (s, 9 H).

Indolenine 111. To a solution of ynoate **109** (2.5 g, 5.86 mmol, 1.0 equiv.) in CH_2Cl_2 (270 mL) at 0 °C was added TFA (30 mL) dropwise. The reaction mixture was then warmed to 23 °C and stirred for 1 h after which the reaction contents were directly concentrated. The resultant crude TFA salt was dissolved in 1,2-DCE (45 mL) and MsOH (0.8 mL, 11.72 mmol, 2.0 equiv.) was added at 23 °C. In a separate flame-dried flask a solution of Ph_3PAuCl (0.15 mg, 0.293 mmol, 0.05 equiv.) in 1,2-DCE (15 mL) was prepared. AgSbF_6 (2.0 g, 5.86 mmol, 1.0 equiv.) was added and the resultant suspension stirred at 23 °C for 15 min, after which the previously prepared solution of the TFA salt was added and the reaction mixture stirred for 18 h at 23 °C. Upon consumption of starting ammonium salt, the reaction mixture was cooled to 0 °C and pyridine (4.7 mL, 58.6 mmol, 10.0 equiv.) was added dropwise followed by the addition of AllocCl (1.25 mL, 11.72 mmol, 2.0 equiv.). The reaction flask was then warmed to 23 °C and stirred at this temperature for 24 h. Upon completion, the reaction was quenched by the addition of saturated aq. NaHCO_3 (50 mL), the layers separated, and the aqueous layer extracted with CH_2Cl_2 (3 \times 25 mL). The combined organic layers were dried over Na_2SO_4 and concentrated *in vacuo*. The crude residue was then further purified by flash column chromatography (silica gel, hexanes/EtOAc, 3:2) to give the desired enoate **111** (1.56 g, 65% yield) as yellow amorphous solid. **111**: $^1\text{H NMR}$ (500 MHz, CDCl_3) δ 7.91 (d, $J = 7.6$ Hz, 1 H), 7.65 (d, $J = 7.7$ Hz, 1 H), 7.43 – 7.36 (m, 1 H), 7.29 – 7.22 (m, 1 H), 6.97 – 6.92 (m, 1 H), 6.06 – 5.80 (m, 1 H), 5.44 – 5.21 (m, 3 H), 4.69 (s, 2 H), 4.53 – 4.34 (m, 1 H), 3.82 (s, 3 H), 3.60 (s, 1 H), 3.28 (dd, $J = 13.6, 6.1$ Hz, 1 H), 3.08 – 3.00 (m, 1 H), 2.84 – 2.67 (m, 1 H).

Vinyl iodide 116. To a solution of amine **111** (10.0 mg, 0.031 mmol, 1.0 equiv.) in MeCN (0.3 mL) was added K₂CO₃ (28.0 mg, 0.202 mmol, 6.5 equiv.) and **40** (24.0 mg, 0.092 mmol, 3.0 equiv.) and the mixture heated to 80 °C for 1 h. Upon completion the reaction mixture was concentrated and directly purified by flash column chromatography (silica gel, hexanes/EtOAc, 2:1) to afford desired vinyl iodide **116** as an orange oil (10.0 mg, 63% yield). **116**: ¹H NMR (400 MHz, CDCl₃) δ 7.89 (d, *J* = 7.5 Hz, 1 H), 7.66 (d, *J* = 7.7 Hz, 1 H), 7.39 (td, *J* = 7.6, 1.3 Hz, 1 H), 7.23 (dd, *J* = 7.5, 1.1 Hz, 1 H), 7.03 (t, *J* = 3.5 Hz, 1 H), 6.00 (q, *J* = 6.4 Hz, 1 H), 4.15 (d, *J* = 1.4 Hz, 1 H), 3.97 (dd, *J* = 11.5, 3.3 Hz, 1 H), 3.77 (s, 3 H), 3.70 (s, 3 H), 3.32 (q, *J* = 1.3 Hz, 2 H), 3.06 – 2.95 (m, 2 H), 2.81 – 2.71 (m, 1 H), 1.81 (dt, *J* = 6.4, 1.2 Hz, 3 H), 1.79 – 1.74 (m, 1 H).

Amine 118. (*Reaction performed in a glovebox*) To a 4 mL scintillation vial containing **116** (12.5 mg, 0.025 mmol, 1.0 equiv.) was added MeCN (1.25 mL). Et₃N (0.014 mL, 0.10 mmol, 4.0 equiv.) and Ni(COD)₂ (13.7 mg, 0.05 mmol, 2.0 equiv.) were added in succession. The reaction mixture was stirred for 20 min, after which Et₃SiH (0.008 mL, 0.05 mmol, 2.0 equiv.) was added and the contents stirred for an additional 1 h. Once complete, the reaction was quenched with saturated aq. NaHCO₃ (2 mL) and diluted with CH₂Cl₂ (2 mL). The layers were separated and the aqueous layer was further extracted with CH₂Cl₂ (2 × 3 mL). The combined organic layers were dried over Na₂SO₄ and concentrated *in vacuo*. The crude residue was further purified by preparative thin layer chromatography (silica gel, CH₂Cl₂/MeOH, 9:1) to afford the 5-*exo*-trig product **118** and deiodinated product **119**. **118**: ¹H NMR (400 MHz, CDCl₃) δ 7.25 (d, *J* = 1.3 Hz, 1 H), 7.06 (td, *J* = 7.6, 1.3 Hz, 1 H), 6.89 (t, *J* = 3.7 Hz, 1 H), 6.74 (td, *J* = 7.5, 1.0 Hz, 1 H), 6.65 (d, *J* = 7.8 Hz, 1 H), 5.34 – 5.25 (m, 1 H), 3.86 – 3.78 (m, 1 H), 3.76 (s, 3 H), 3.69 – 3.60 (m, 1 H), 3.55 (s, 3 H), 3.50 (d, *J* = 7.0 Hz, 1 H), 3.38 (d, *J* = 15.9 Hz, 1 H),

2.96 – 2.82 (m, 2 H), 2.79 – 2.69 (m, 1 H), 2.36 (t, $J = 12.6$ Hz, 1 H), 1.03 (dt, $J = 7.5, 1.9$ Hz, 3 H).

Pyrroloindole 124. To a solution of indolenine **111** (10.0 mg, 0.024 mmol, 1.0 equiv.) in THF (1.0 mL) was added 1 M LiOH (1.2 mL, 1.2 mmol, 50.0 equiv.). After 1 h the reaction mixture was partitioned between EtOAc (3 mL) and H₂O (3 mL), the layers separated and the aqueous layer extracted with EtOAc (2 × 2 mL). The combined organic layers were dried over Na₂SO₄ and concentrated *in vacuo* to afford the rearranged product **124** (9.8 mg, 98% yield). **124**: ¹H NMR (500 MHz, CDCl₃) δ 7.53 (dd, $J = 7.7, 1.3$ Hz, 1 H), 7.02 (td, $J = 7.6, 1.3$ Hz, 1 H), 6.88 (dd, $J = 6.0, 0.8$ Hz, 1 H), 6.76 (d, $J = 9.7$ Hz, 1 H), 6.68 (td, $J = 7.5, 1.1$ Hz, 1 H), 6.63 (d, $J = 7.7$ Hz, 1 H), 6.03 (dt, $J = 9.7, 5.6$ Hz, 1 H), 5.82 (ddt, $J = 17.2, 10.8, 5.5$ Hz, 1 H), 5.74 (s, 1 H), 5.21 (dd, $J = 17.2, 1.5$ Hz, 1 H), 5.15 (dd, $J = 10.5, 1.3$ Hz, 1 H), 4.60 (ddt, $J = 13.4, 5.4, 1.5$ Hz, 1 H), 4.54 (ddt, $J = 13.3, 5.6, 1.5$ Hz, 1 H), 4.41 (d, $J = 9.0$ Hz, 1 H), 3.74 (s, 3 H), 3.55 (d, $J = 13.4$ Hz, 1 H), 3.18 (s, 3 H), 2.48 (dd, $J = 13.3, 9.1$ Hz, 1 H).

Carboxylic Acid 125. To a solution of **111** (0.900 g, 2.27 mmol, 1.0 equiv.) in 1,2-DCE (12 mL) was added Me₃SnOH (1.25 g, 6.82 mmol, 3.0 equiv.), the reaction flask was fitted with a reflux condenser and the reaction contents heated to 90 °C. After 16 h an additional portion of Me₃SnOH (1.25 g, 6.82 mmol, 3.0 equiv.) was added and the reaction temperature maintained for 16 h. Upon completion the contents of the reaction flask were loaded directly onto a silica plug and eluted with CH₂Cl₂/MeOH (9:1). The material was taken forward without further purification.

Aminonitrile 130. To a solution of carboxylic acid **125** (52.0 mg, 0.129 mmol, 1.0 equiv.) in DMF (2.5 mL) was added EDC (61.9 mg, 0.323 mmol, 2.5 equiv.) and HOBt (43.6 mg, 0.323 mmol, 2.5 equiv.). Following this, aq. NH₄OH (30% v/v, 0.25 mL) was added dropwise and the reaction was allowed to stir for 2 h. Upon completion the reaction was diluted with H₂O (5 mL) and EtOAc (5 mL) and the aqueous layer extracted with EtOAc (3 × 5 mL). The combined organic layers were dried over Na₂SO₄ and concentrated *in vacuo* to provide a crude residue which was carried forward without further purification.

To a flame-dried flask was added the crude primary amide, and THF (1.0 mL), followed by Et₃N (0.03 mL, 0.212 mmol, 2.0 equiv.). The mixture was then cooled to 0 °C and TFAA (0.015 mL, 0.106 mmol, 1.0 equiv.) dropwise. The reaction was warmed to 23 °C and stirred for 30 min, after which it was quenched by the addition of saturated aq. NaHCO₃ (2 mL). The layers were separated and the aqueous layer extracted with CH₂Cl₂ (2 × 2 mL). The combined organic layers were dried over Na₂SO₄ and concentrated *in vacuo*. The crude residue was then further purified by flash column chromatography (silica gel, hexanes/EtOAc, 3:2) to afford the desired aminonitrile **130** (41.6 mg, 80% yield) as a pale yellow oil. **130**: ¹H NMR (500 MHz, CDCl₃) δ 7.90 (d, *J* = 7.6 Hz, 1 H), 7.70 (d, *J* = 7.7 Hz, 1 H), 7.43 (td, *J* = 7.6, 1.2 Hz, 1 H), 7.29 (td, *J* = 7.6, 1.1 Hz, 1 H), 6.89 (dd, *J* = 5.3, 2.3 Hz, 1 H), 5.98 (ddt, *J* = 16.4, 10.4, 5.8 Hz, 1 H), 5.40 (dt, *J* = 17.2, 1.4 Hz, 1 H), 5.32 (dq, *J* = 7.0, 3.8 Hz, 2 H), 4.84 – 4.69 (m, 3 H), 3.81 (s, 3 H), 3.44 – 3.36 (m, 1 H), 3.26 – 3.12 (m, 1 H), 2.83 – 2.74 (m, 1 H), 2.08 (dd, *J* = 14.2, 7.2 Hz, 1 H).

Furoindole 131. To a flame dried flask containing **125** (400.0 mg, 1.01 mmol, 1.0 equiv.), EDC (287.5 mg, 1.5 mmol, 1.5 equiv.), DMAP (183.2 mg, 1.5 mmol, 1.5 equiv.) and 2-mercaptopyridine *N*-oxide (256.3 mg, 2.0 mmol, 2.0 equiv.) was added toluene (30 mL) and

CH₂Cl₂ (5 mL). The reaction mixture was placed under Ar and stirred at 23 °C for 16 h after which the contents were warmed to 80 °C and continuously sparged with O₂. Upon completion the reaction was cooled to 23 °C, *t*-BuSH (2.25 mL, 20 mmol, 20 equiv.) was added, and the reaction mixture stirred for 1 h. Saturated aq. NH₄Cl (30 mL) was added, and the mixture transferred to a separatory funnel. The layers were separated, and the aqueous layer extracted with EtOAc (3 × 20 mL). The combined organic layers were washed with brine (20 mL), dried over Na₂SO₄ and concentrated *in vacuo*. The crude residue was further purified by flash column chromatography (silica gel, hexanes/EtOAc, 4:1) to afford **131** (110.5 mg, 30% yield) and the epimer **135** (92.0 mg, 25% yield) as a pale yellow amorphous solid. **131**: ¹H NMR (400 MHz, CDCl₃) δ 7.58 (d, *J* = 7.6 Hz, 1 H), 7.12 (td, *J* = 7.7, 1.3 Hz, 1 H), 6.86 (t, *J* = 7.6 Hz, 1 H), 6.74 (d, *J* = 7.8 Hz, 1 H), 6.71 – 6.64 (m, 1 H), 5.93 (ddt, *J* = 16.3, 10.8, 5.6 Hz, 1 H), 5.82 – 5.58 (m, 1 H), 5.31 (d, *J* = 17.2 Hz, 1 H), 5.24 (d, *J* = 10.5 Hz, 1 H), 4.61 (s, 2H), 4.06 (s, 1 H), 3.73 (s, 3 H), 3.28 – 3.12 (m, 1 H), 3.08 (s, 1 H), 2.57 (q, *J* = 11.9 Hz, 2 H). **135**: ¹H NMR (400 MHz, CDCl₃) δ 7.86 (dd, *J* = 7.7, 1.3 Hz, 1 H), 7.66 (d, *J* = 7.7 Hz, 1 H), 7.39 (td, *J* = 7.6, 1.3 Hz, 1 H), 7.23 (td, *J* = 7.6, 1.2 Hz, 1 H), 6.98 – 6.93 (m, 1 H), 5.93 (s, 1 H), 5.46 (s, 1 H), 5.35 (d, *J* = 16.8 Hz, 1 H), 5.25 (d, *J* = 10.5 Hz, 1 H), 4.83 (dd, *J* = 10.0, 6.9 Hz, 1 H), 4.66 (s, 2 H), 3.82 (s, 3 H), 3.41 (s, 1 H), 2.86 – 2.68 (m, 2 H), 1.48 (dd, *J* = 13.7, 10.1 Hz, 1 H).

Furoindole 131. To a solution of **135** (92.0 mg, 0.25 mmol, 1.0 equiv.) in CH₂Cl₂/H₂O (9:1, 1.25 mL) at 23 °C was added PPTS (3.0 equiv.) and the mixture stirred at this temperature for 24 h. After, the reaction was quenched by the addition of saturated aq. NaHCO₃ (2 mL), diluted with CH₂Cl₂ (2 mL) and transferred to a separatory funnel. The layers were separated, and the aqueous layer was further extracted with CH₂Cl₂ (3 × 2 mL). The combined organic layers were dried over Na₂SO₄ and concentrated *in vacuo* to give a crude residue which was further purified by flash column chromatography (silica gel, hexanes/EtOAc, 3:2). This afforded the

desired carbinolamine **131** (51.6 mg, 56% yield) as a pale yellow amorphous solid whose ^1H NMR spectrum matched that obtained via the Barton decarboxylation/oxidation sequence.

Aldimine 136. To a solution of **131** (3.0 mg, 0.008 mmol, 1.0 equiv.) in THF (0.1 mL) was added $\text{Pd}(\text{PPh}_3)_4$ (4.7 mg, 0.004 mmol, 0.5 equiv.) and morpholine (0.007 mL, 0.08 mmol, 10.0 equiv.) sequentially. After 15 min the reaction was diluted with saturated NH_4Cl (2 mL) and EtOAc (2 mL). The aqueous layer was extracted with EtOAc (2×2 mL) and the organic layers were combined, dried over Na_2SO_4 and concentrated *in vacuo*. The crude residue was further purified by flash column chromatography (silica gel, $\text{CH}_2\text{Cl}_2/\text{MeOH}$, 19:1) to afford aldimine **136** as a yellow oil. **136:** ^1H NMR (500 MHz, CDCl_3) δ 7.95 (dt, $J = 7.5, 1.1$ Hz, 1 H), 7.83 (d, $J = 2.5$ Hz, 1 H), 7.71 – 7.67 (m, 1 H), 7.40 (td, $J = 7.6, 1.3$ Hz, 1 H), 7.24 (dd, $J = 7.5, 1.2$ Hz, 1 H), 6.82 (dd, $J = 5.0, 2.3$ Hz, 1 H), 5.15 – 5.07 (m, 1 H), 3.98 – 3.89 (m, 1 H), 3.80 (s, 3 H), 3.13 – 3.03 (m, 1 H), 2.99 – 2.90 (m, 2 H), 2.33 – 2.24 (m, 1 H).

Sulfonamide 145. Pyridine (2.5 mL) was added to a flame-dried flask containing **131** (85.0 mg, 0.23 mmol, 1.0 equiv.) and the solution cooled to 0 °C. Ts_2O (113.0 mg, 0.346 mmol, 1.5 equiv.) was added in one portion and the reaction contents stirred at 0 °C for 30 min. The reaction was then warmed to 23 °C and stirred at this temperature for 2 h, after which the reaction was quenched by the slow addition of saturated aq. NaHCO_3 (5 mL). The mixture was transferred to a separatory funnel and diluted with EtOAc (5 mL). The layers were separated, and the aqueous layer was extracted with EtOAc (3×5 mL). The combined organic layers were dried over Na_2SO_4 and concentrated *in vacuo*, the residue was then diluted with toluene (10 mL) and concentrated once more in order to remove residual pyridine. The crude product was further purified by flash column chromatography (silica gel, hexanes/EtOAc, 4:1) to provide the desired sulfonamide **145** (91.4 mg, 76% yield) as a pale-yellow amorphous solid.

145: ^1H NMR (500 MHz, CDCl_3) δ 7.97 (d, $J = 8.1$ Hz, 2 H), 7.59 (d, $J = 7.7$ Hz, 1 H), 7.45 (d, $J = 8.2$ Hz, 1 H), 7.28 (s, 1 H), 7.17 (t, $J = 7.8$ Hz, 1 H), 6.99 (t, $J = 7.6$ Hz, 1 H), 6.73 (dd, $J = 5.7, 2.3$ Hz, 1 H), 5.96 (s, 1 H), 5.83 – 5.64 (m, 1 H), 5.33 (d, $J = 17.6$ Hz, 1 H), 5.27 (s, 1 H), 5.07 (s, 1 H), 4.63 (s, 2 H), 3.71 (s, 3 H), 3.34 – 3.06 (m, 1 H), 3.00 – 2.85 (m, 1 H), 2.56 (d, $J = 12.2$ Hz, 1 H), 2.48 (dd, $J = 12.4, 2.8$ Hz, 1 H), 2.39 (s, 3 H).

Vinyl iodide 138. To a solution of amine **137** (11.8 mg, 0.027 mmol, 1.0 equiv.) in MeCN (0.3 mL) was added K_2CO_3 (24.2 mg, 0.176 mmol, 6.5 equiv.) and **40** (21.1 mg, 0.081 mmol, 3.0 equiv.) and the mixture heated to 80 °C for 1 h. Upon completion the reaction mixture was concentrated and directly purified by flash column chromatography (silica gel, hexanes/EtOAc, 2:1) to afford desired vinyl iodide **138** as an orange oil (10.2 mg, 62% yield). **138:** ^1H NMR (400 MHz, CDCl_3) δ 7.99 (d, $J = 8.4$ Hz, 2 H), 7.58 (dd, $J = 7.7, 1.4$ Hz, 1 H), 7.39 (d, $J = 8.2$ Hz, 1 H), 7.28 (dd, $J = 8.7, 0.7$ Hz, 2 H), 7.16 – 7.10 (m, 1 H), 6.96 (td, $J = 7.6, 1.1$ Hz, 1 H), 6.75 – 6.73 (m, 1 H), 5.95 (q, $J = 6.4$ Hz, 1 H), 4.68 (d, $J = 3.2$ Hz, 1 H), 4.06 (d, $J = 3.9$ Hz, 1 H), 3.71 (s, 3 H), 3.69 – 3.63 (m, 1 H), 3.48 (dt, $J = 14.0, 1.5$ Hz, 1 H), 2.84 – 2.72 (m, 1 H), 2.65 – 2.56 (m, 1 H), 2.48 (d, $J = 11.5$ Hz, 1 H), 2.39 (s, 3 H), 2.38 – 2.33 (m, 1 H), 1.81 (d, $J = 6.4$ Hz, 3 H).

Aminoketone 143. To a 4 mL scintillation vial containing **137** (10.0 mg, 0.023 mmol, 1.0 equiv.) in MeOH (0.5 mL) was added Et_3N (0.005 mL, 0.034 mmol, 1.5 equiv.) and methyl vinyl ketone (0.002 mL, 0.024 mmol, 1.1 equiv.) and the reaction stirred at 23 °C for 16 h. Upon completion the contents of the vial were concentrated and purified directly by column to afford the desired aminoketone **143** as a yellow oil. **143:** ^1H NMR (500 MHz, CDCl_3) δ 8.00 – 7.95 (m, 2 H), 7.56 (dd, $J = 7.7, 1.4$ Hz, 1 H), 7.42 (d, $J = 8.4$ Hz, 1 H), 7.27 (d, $J = 8.9$ Hz, 2 H), 7.13 (ddd, $J = 8.4, 7.5, 1.4$ Hz, 1 H), 6.96 (td, $J = 7.6, 1.0$ Hz, 1 H), 6.74 – 6.69 (m, 1 H),

4.69 (t, $J = 1.8$ Hz, 1 H), 4.03 – 4.00 (m, 1 H), 3.68 (s, 3 H), 3.64 (t, $J = 6.2$ Hz, 1 H), 3.12 (ddd, $J = 12.6, 8.2, 5.7$ Hz, 1 H), 3.02 (ddd, $J = 12.7, 8.3, 6.7$ Hz, 1 H), 2.91 – 2.82 (m, 1 H), 2.65 – 2.56 (m, 2 H), 2.38 (s, 3 H), 2.35 (d, $J = 1.9$ Hz, 2 H), 2.17 (s, 3 H).

Nitrile 149. A solution of **145** (100.0 mg, 0.191 mmol, 1.0 equiv.) in DMSO (2 mL) in a flame-dried flask was heated to 50 °C. To this reaction was added acetone cyanohydrin (65.0 mg, 0.764 mmol, 4.0 equiv.) and KCN (12.5 mg, 0.191 mmol, 1.0 equiv.) sequentially. The reaction contents were cooled to 30 °C and stirred at this temperature for 16 h. Upon completion the reaction was quenched by the addition of saturated aq. NH_4Cl (2 mL) and transferred to a separatory funnel, diluting with EtOAc (3 mL). The aqueous layer was extracted with EtOAc (3 \times 3 mL), dried over Na_2SO_4 and concentrated *in vacuo*. The crude residue was purified by flash column chromatography (silica gel, hexane/EtOAc, 4:1) to afford the desired nitrile **149** (76.7 mg, 72% yield, 10:1 *dr*) as a yellow oil. **149** (major): ^1H NMR (400 MHz, CDCl_3) δ 7.94 (d, $J = 8.4$ Hz, 2 H), 7.52 (d, $J = 2.6$ Hz, 1 H), 7.39 (dd, $J = 7.6, 1.4$ Hz, 1 H), 7.29 (d, $J = 8.0$ Hz, 2 H), 7.25 – 7.17 (m, 1 H), 7.02 (td, $J = 7.6, 1.0$ Hz, 1 H), 5.98 (ddd, $J = 16.2, 11.1, 5.7$ Hz, 1 H), 5.90 – 5.62 (m, 1 H), 5.49 – 5.18 (m, 2 H), 5.07 (s, 1 H), 4.70 (s, 2 H), 3.77 (s, 3 H), 3.42 (s, 1 H), 3.21 (d, $J = 13.7$ Hz, 1 H), 3.14 – 2.90 (m, 1 H), 2.64 (d, $J = 5.7$ Hz, 1 H), 2.48 (d, $J = 13.3$ Hz, 1 H), 2.39 (s, 3 H), 2.29 – 2.16 (m, 1 H). **150** (minor): ^1H NMR (500 MHz, CDCl_3) δ 7.92 (d, $J = 8.4$ Hz, 2 H), 7.55 (d, $J = 8.3$ Hz, 1 H), 7.38 (dd, $J = 9.5, 6.2$ Hz, 1 H), 7.28 (d, $J = 8.3$ Hz, 2 H), 7.07 – 7.00 (m, 1 H), 6.90 (dd, $J = 7.6, 1.3$ Hz, 1 H), 5.98 (ddt, $J = 16.3, 11.1, 5.8$ Hz, 1 H), 5.76 (s, 2 H), 5.37 (d, $J = 17.3$ Hz, 1 H), 5.34 – 5.29 (m, 1 H), 5.07 (d, $J = 3.4$ Hz, 1 H), 4.69 (d, $J = 6.3$ Hz, 2 H), 3.74 (s, 3 H), 3.07 (s, 2 H), 2.84 (d, $J = 13.3$ Hz, 1 H), 2.60 (d, $J = 12.2$ Hz, 1 H), 2.43 (d, $J = 5.3$ Hz, 1 H), 2.39 (s, 3 H), 2.22 (dd, $J = 13.3, 3.4$ Hz, 1 H).

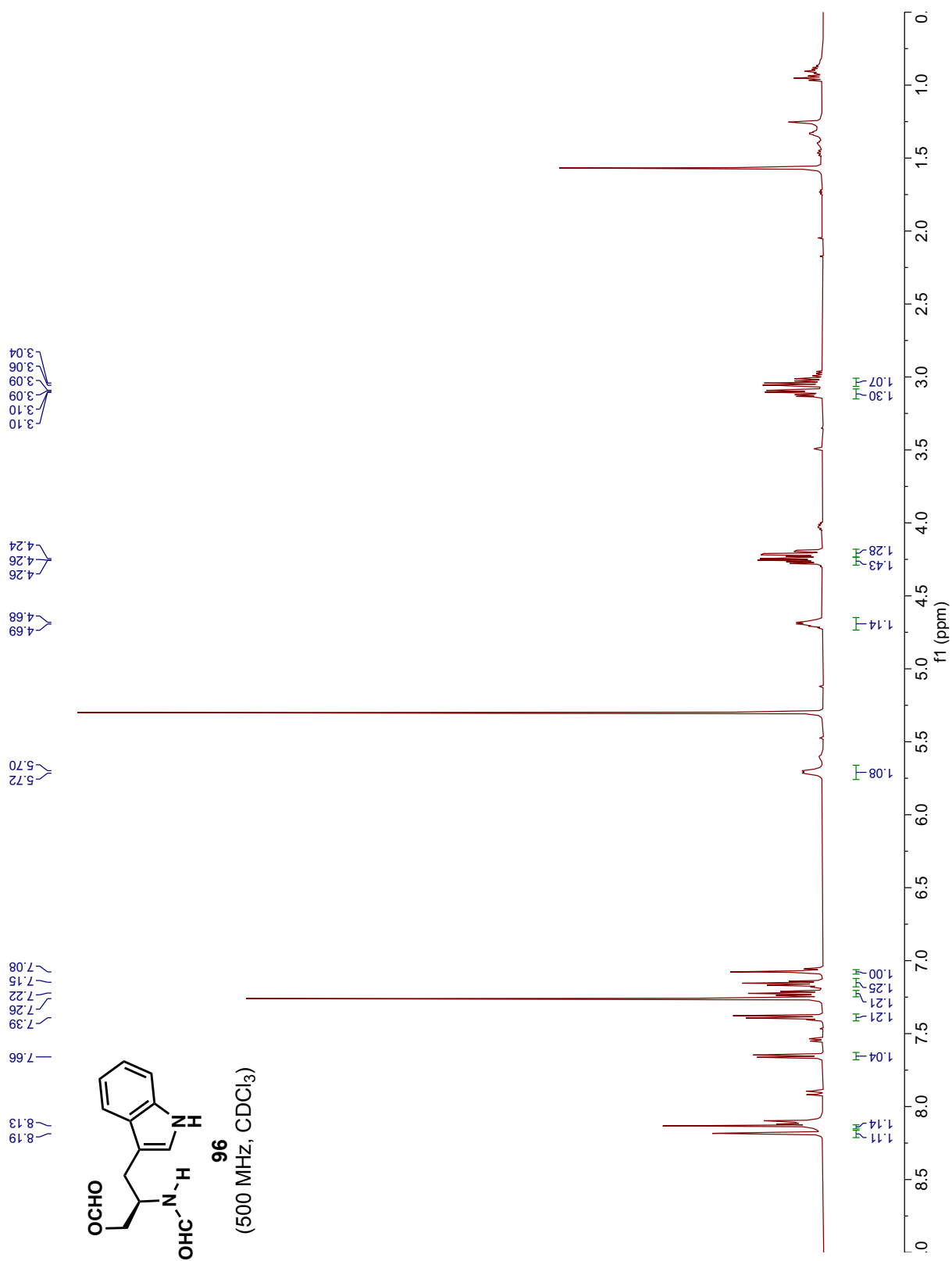
Aldehyde 151. To a solution of **150** (5.0 mg, 0.01 mmol, 1.0 equiv.) in CH₂Cl₂ (0.1 mL) was added Schwartz' reagent (6.7 mg, 0.026 mmol, 2.5 equiv.). After 30 min, the solution was loaded onto a TLC plate and the compound extracted from the silica with EtOAc (3 × 3 mL). The filtrate was concentrated *in vacuo* to afford the desired aldehyde **151** as a yellow oil (4.8 mg, 83% yield). **151**: ¹H NMR (500 MHz, CDCl₃) δ 9.64 (d, *J* = 1.2 Hz, 1 H), 7.94 (dd, *J* = 9.3, 2.9 Hz, 2 H), 7.54 (d, *J* = 8.4 Hz, 1 H), 7.29 (s, 2 H), 7.22 (d, *J* = 8.0 Hz, 1 H), 7.02 (t, *J* = 7.4 Hz, 1 H), 6.93 (d, *J* = 7.5 Hz, 1 H), 5.99 (ddt, *J* = 16.3, 10.7, 5.7 Hz, 1 H), 5.37 (d, *J* = 17.5 Hz, 1 H), 5.31 (d, *J* = 8.2 Hz, 1 H), 5.14 (s, 1 H), 4.69 (d, *J* = 7.1 Hz, 2 H), 3.66 (s, 3 H), 2.96 (s, 1 H), 2.78 (d, *J* = 13.1 Hz, 1 H), 2.52 (d, *J* = 11.7 Hz, 1 H), 2.38 (s, 3 H), 2.24 – 2.17 (m, 1 H), 2.02 (s, 1 H), 1.92 – 1.80 (m, 1 H).

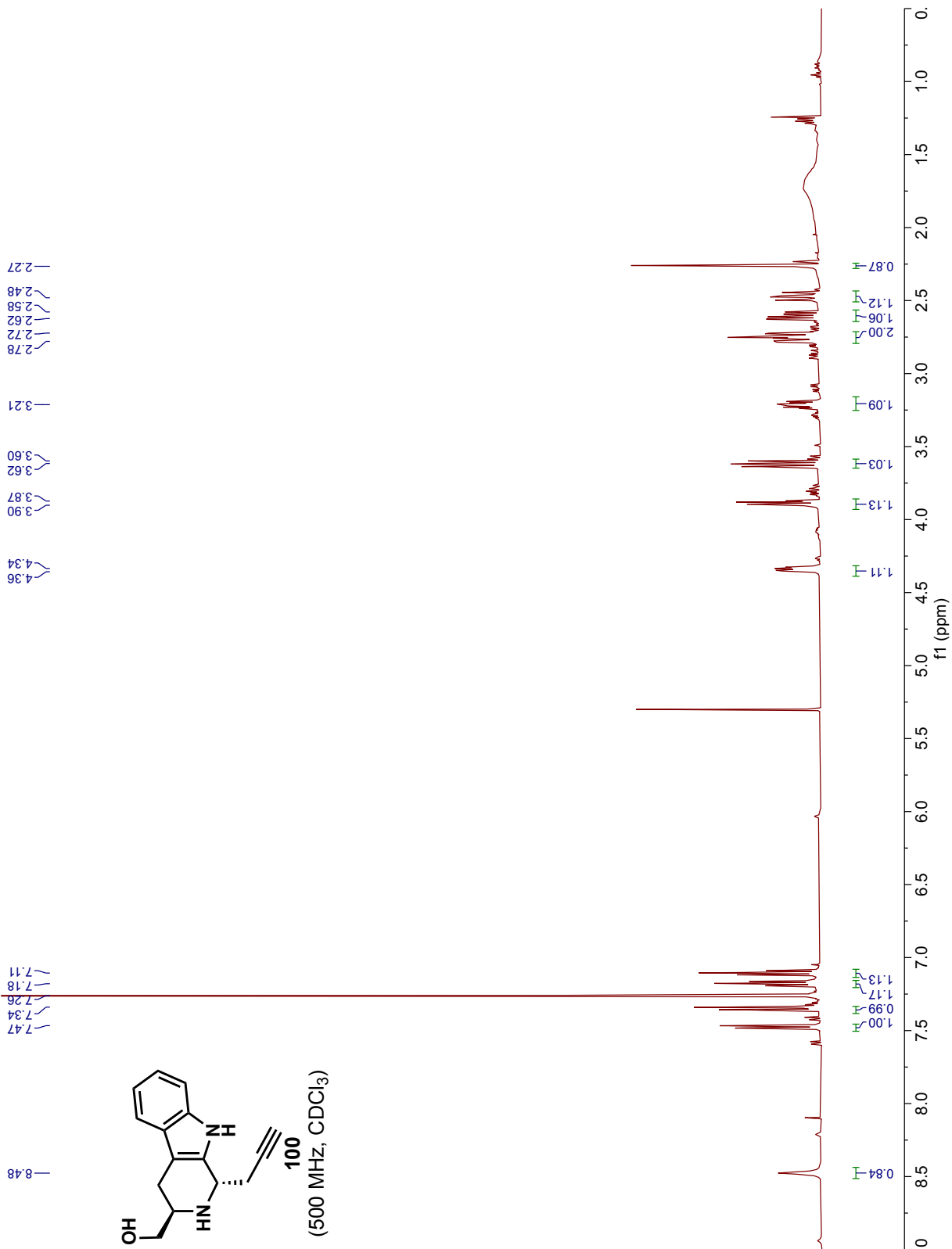
α-Chloroketone 154. A solution of **149** (5.5 mg, 0.01 mmol, 1.0 equiv.) in THF (0.2 mL) was cooled to –78 °C and LiHMDS (1.0 M in THF, 0.015 mL, 1.5 equiv.) added dropwise. After stirring for 1 h, chloroacetyl chloride (0.001 mL, 0.012 mmol, 1.0 equiv.). The reaction was slowly warmed to –40 °C after which the reaction was stirred for 1 h. Upon consumption of the starting material the reaction was quenched by the addition of saturated aq. NH₄Cl (1 mL). The reaction was diluted with EtOAc (1 mL) and the layers separated. The aqueous layer was further extracted with EtOAc (2 × 2 mL), the organic layers combined, dried over Na₂SO₄ and concentrated *in vacuo*. The crude residue was further purified by flash column chromatography (silica gel, hexanes/EtOAc, 2:1) to afford the desired product as a yellow oil (5.5 mg, 87% yield, ~2:1 *dr*). **154**: ¹H NMR (400 MHz, CDCl₃) δ 7.93 (d, *J* = 7.7 Hz, 2 H), 7.57 (s, 1 H), 7.30 (d, *J* = 8.2 Hz, 2 H), 7.04 (t, *J* = 7.5 Hz, 1 H), 7.00 – 6.90 (m, 1 H), 6.10 – 5.91 (m, 1 H), 5.87 – 5.59 (m, 1 H), 5.32 (d, *J* = 14.9 Hz, 2 H), 5.21 – 5.08 (m, 1H), 4.71 (s, 2 H), 4.10 – 4.01 (m, 2 H), 3.74 (s, 3 H), 3.70 – 3.55 (m, 1 H), 2.91 – 2.73 (m, 1 H), 2.40 (s, 3 H), 2.26 (dd, *J* = 12.7, 9.2 Hz, 1 H).

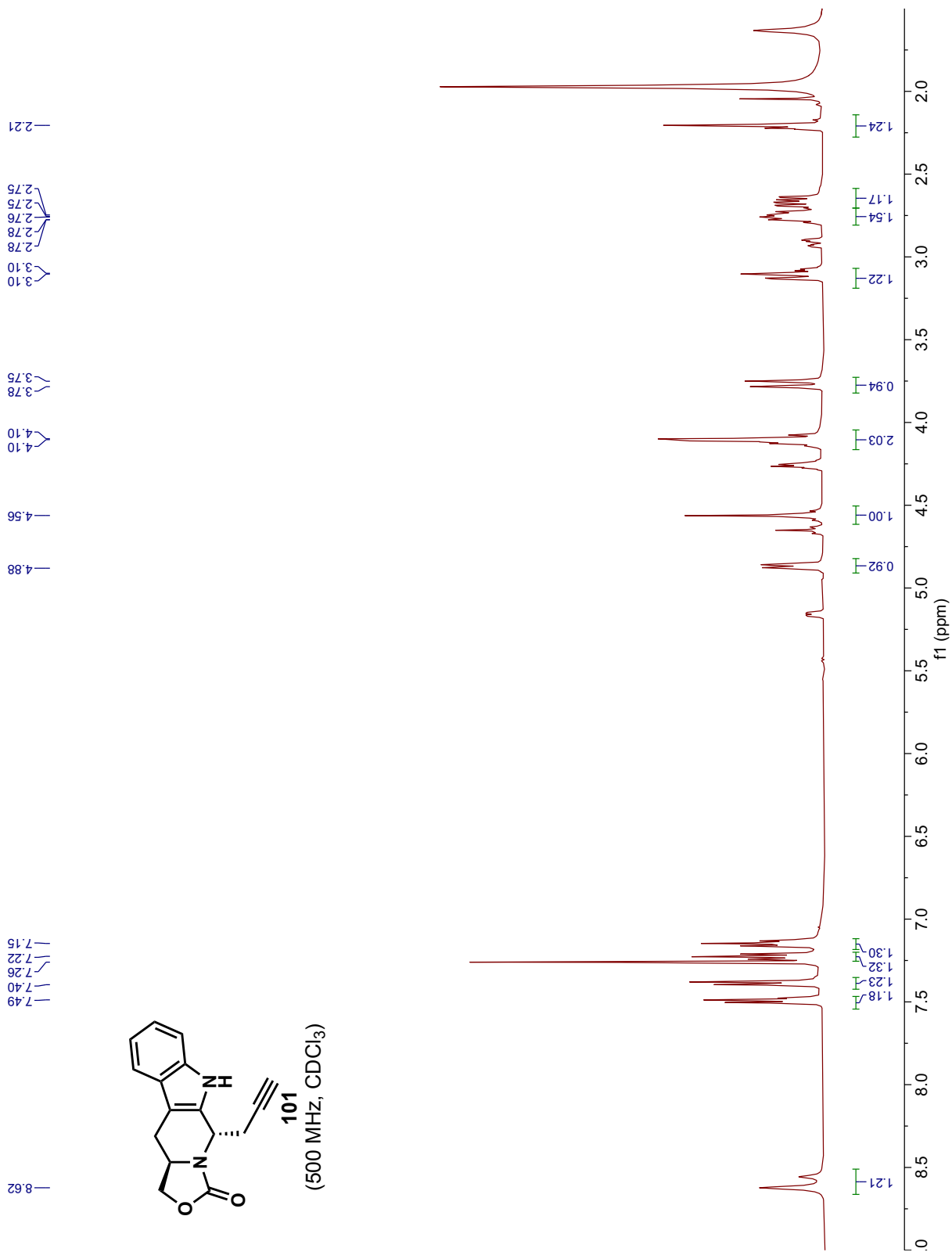
Aminoester 157-1. To a solution of **156** (15.0 mg, 0.032 mmol, 1.0 equiv.) in MeCN (0.5 mL) was added Hünig's base (0.02 mL, 0.096 mmol, 3.0 equiv.) and bromoethyl acetate (0.006 mL, 0.048 mmol, 1.5 equiv.). The solution was heated to 60 °C and stirred for 12 h, after which it was cooled to 23 °C, concentrated *in vacuo* and purified directly by flash column chromatography (silica gel, hexanes/EtOAc, 3:1), to afford the desired aminoester as a pale yellow amorphous solid. **157-1**: ¹H NMR (500 MHz, CDCl₃) δ 7.98 (d, *J* = 8.4 Hz, 2 H), 7.49 (d, *J* = 8.2 Hz, 1 H), 7.37 (dd, *J* = 7.6, 1.3 Hz, 1 H), 7.29 (d, *J* = 8.2 Hz, 2 H), 7.18 (td, *J* = 7.9, 1.4 Hz, 1 H), 7.05 – 6.96 (m, 1 H), 4.22 (q, *J* = 7.1 Hz, 2 H), 4.16 (dd, *J* = 4.0, 1.8 Hz, 1 H), 3.76 (s, 3 H), 3.66 (d, *J* = 16.4 Hz, 1 H), 3.53 (d, *J* = 16.4 Hz, 1 H), 3.45 – 3.39 (m, 1 H), 3.21 – 3.15 (m, 1 H), 2.67 – 2.59 (m, 2 H), 2.39 (s, 3 H), 2.38 – 2.34 (m, 1 H), 2.16 – 2.12 (m, 1 H).

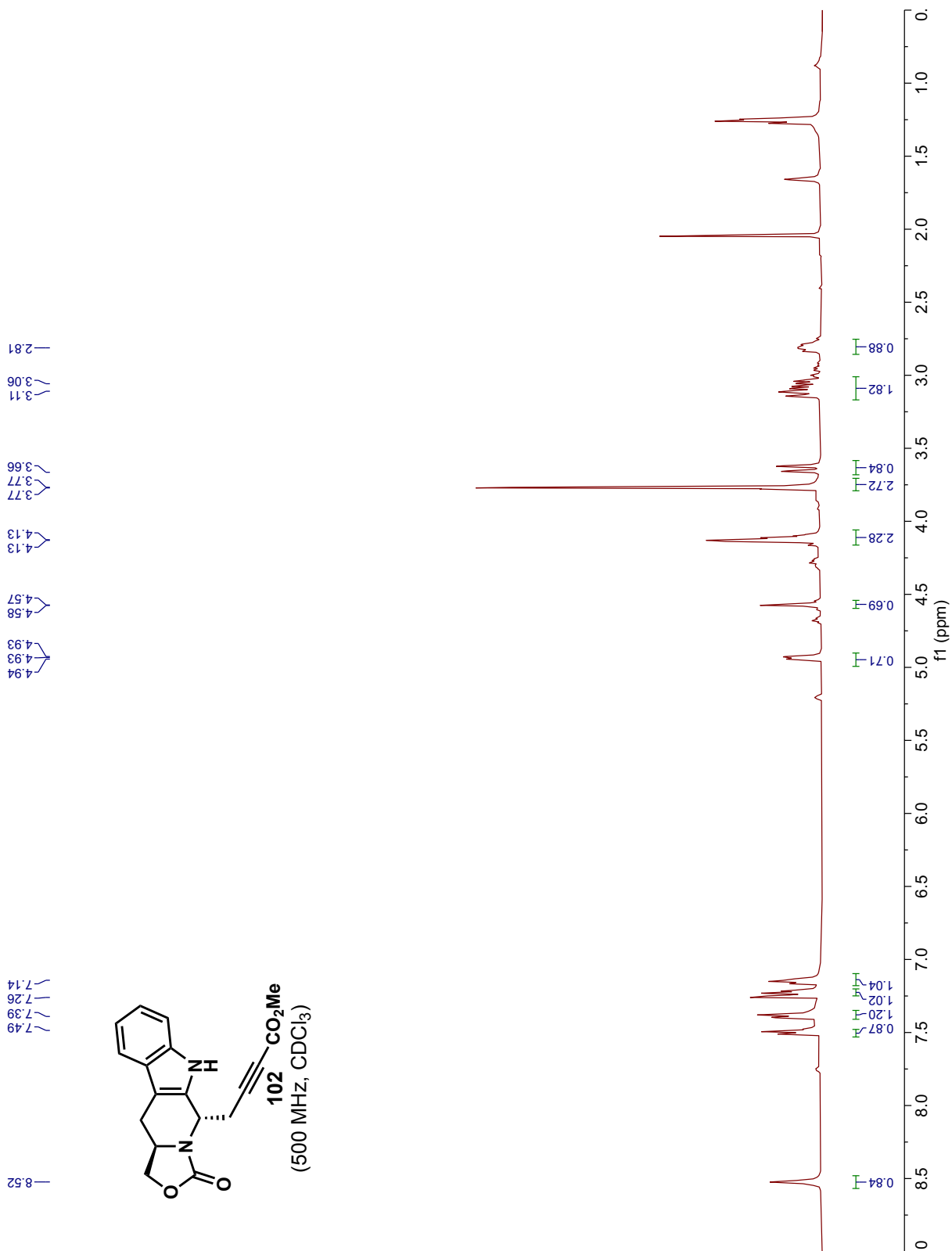
Allylic Bromide 157-2. To a solution of **156** (5.7 mg, 0.012 mmol, 1.0 equiv.) in MeCN (0.25 mL) was added Hünig's base (0.0065 mL, 0.036 mmol, 3.0 equiv.) and 1,4-dibromo-*trans*-2-butene (3.9 mL, 0.018 mmol, 1.5 equiv.). The solution was heated to 60 °C and stirred for 1 h, after which it was cooled to 23 °C, concentrated *in vacuo* and purified directly by flash column chromatography (silica gel, hexanes/EtOAc, 3:1), to afford the desired allylic bromide as a pale yellow amorphous solid. **157-2**: ¹H NMR (500 MHz, CDCl₃) δ 7.96 (d, *J* = 8.2 Hz, 2 H), 7.49 (d, *J* = 8.1 Hz, 1 H), 7.36 (d, *J* = 7.4 Hz, 1 H), 7.30 (d, *J* = 8.1 Hz, 2 H), 7.18 (t, *J* = 7.6 Hz, 1 H), 6.99 (dd, *J* = 7.9, 6.9 Hz, 1 H), 6.05 – 5.91 (m, 2 H), 4.71 (d, *J* = 3.6 Hz, 1 H), 4.02 (d, *J* = 2.4 Hz, 1 H), 3.99 (d, *J* = 7.1 Hz, 2 H), 3.76 (s, 3 H), 3.49 (dd, *J* = 13.8, 6.1 Hz, 1 H), 3.43 – 3.33 (m, 2 H), 3.09 (d, *J* = 13.0 Hz, 1 H), 2.60 (d, *J* = 5.6 Hz, 1 H), 2.40 (s, 3 H), 2.36 (s, 1 H), 2.34 (dd, *J* = 13.1, 3.7 Hz, 1 H), 2.19 – 2.11 (m, 1 H).

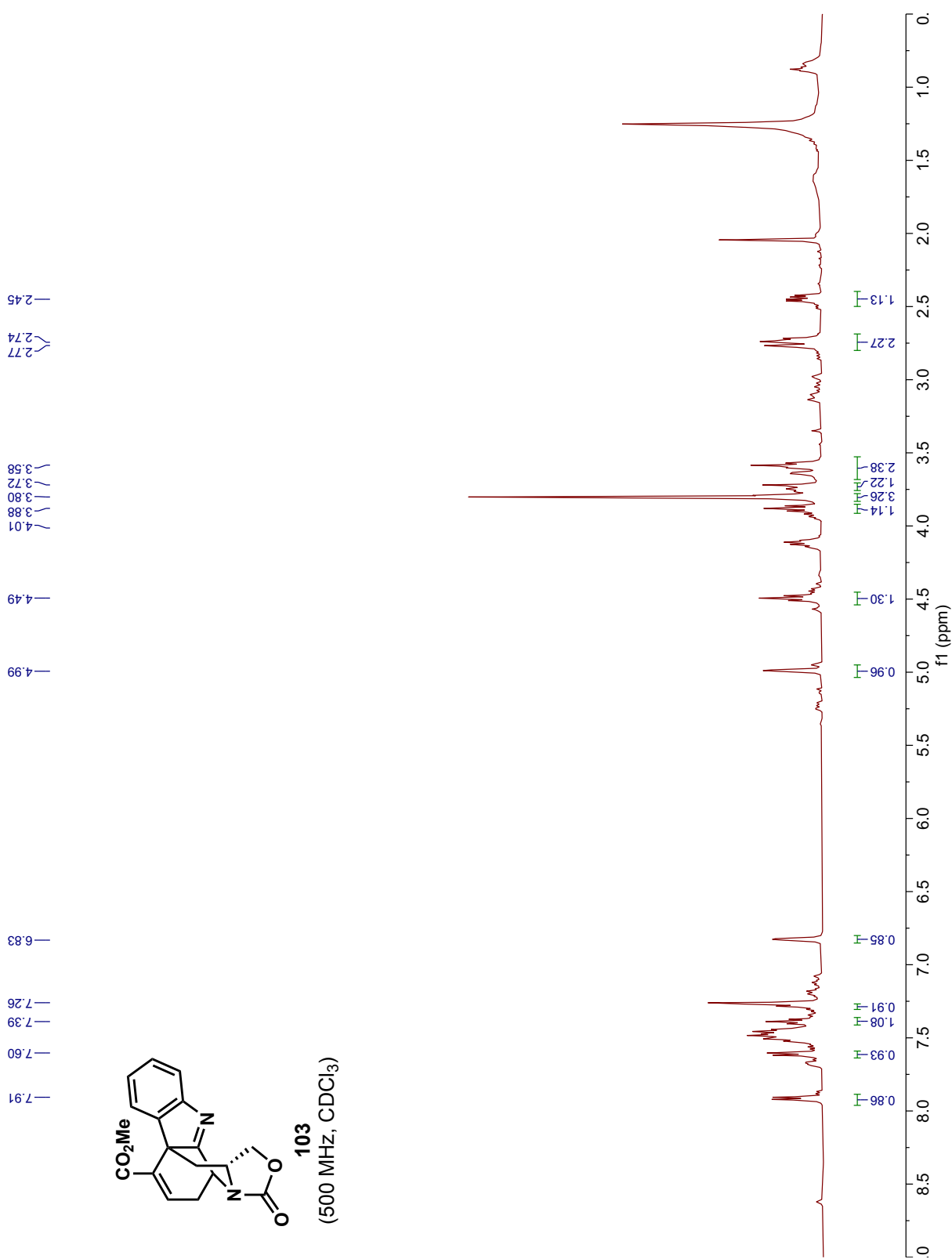
4.16 ^1H NMR Data

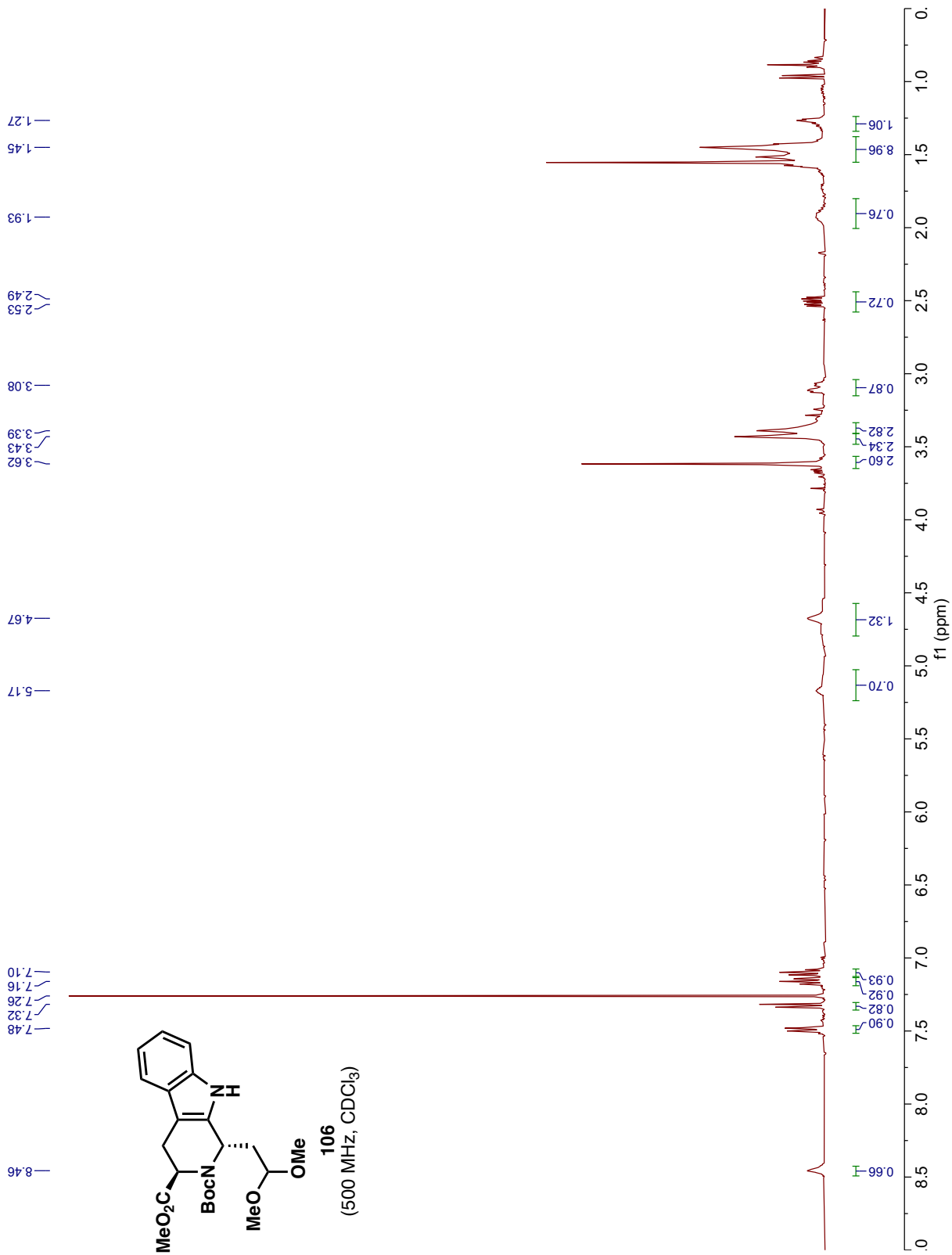


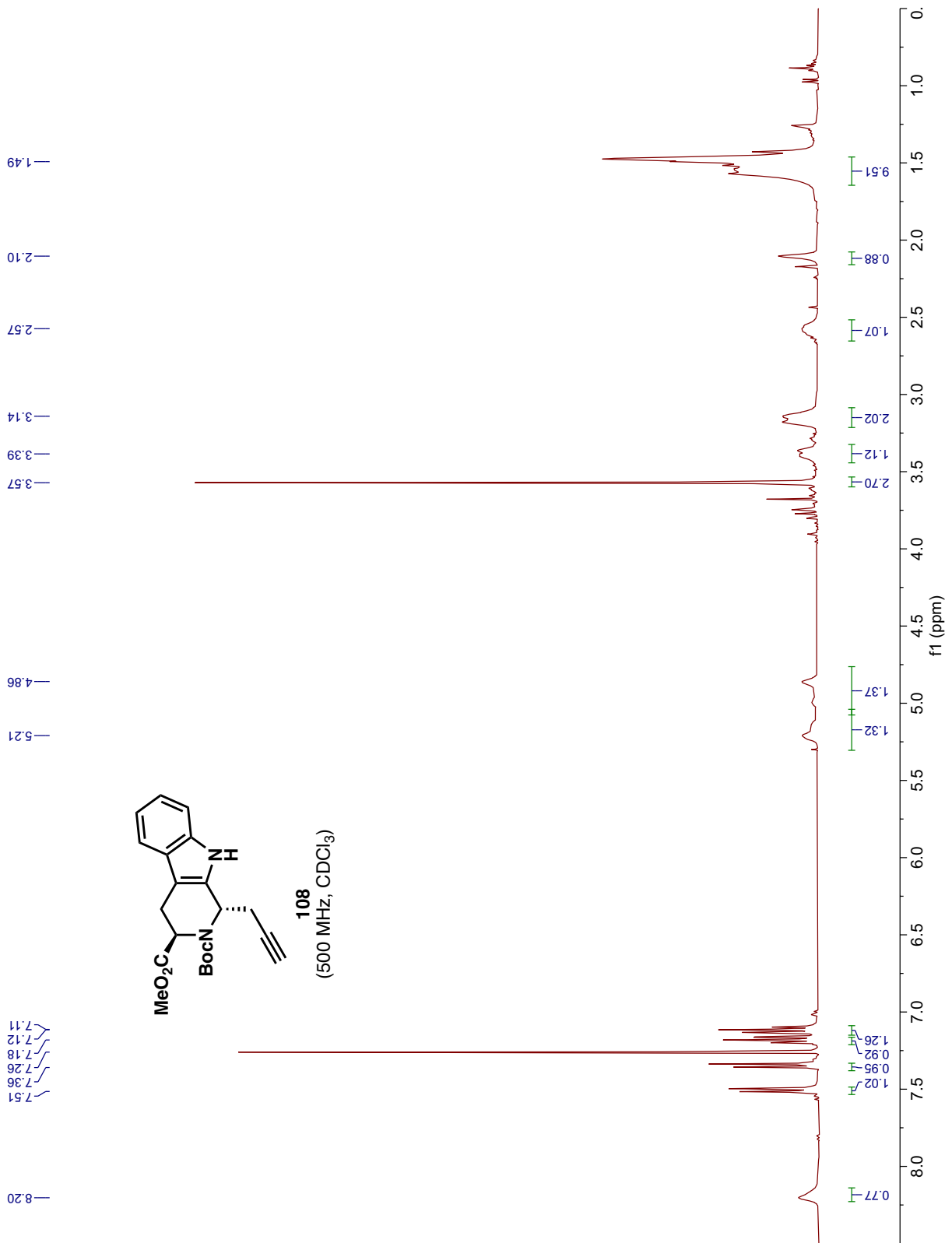


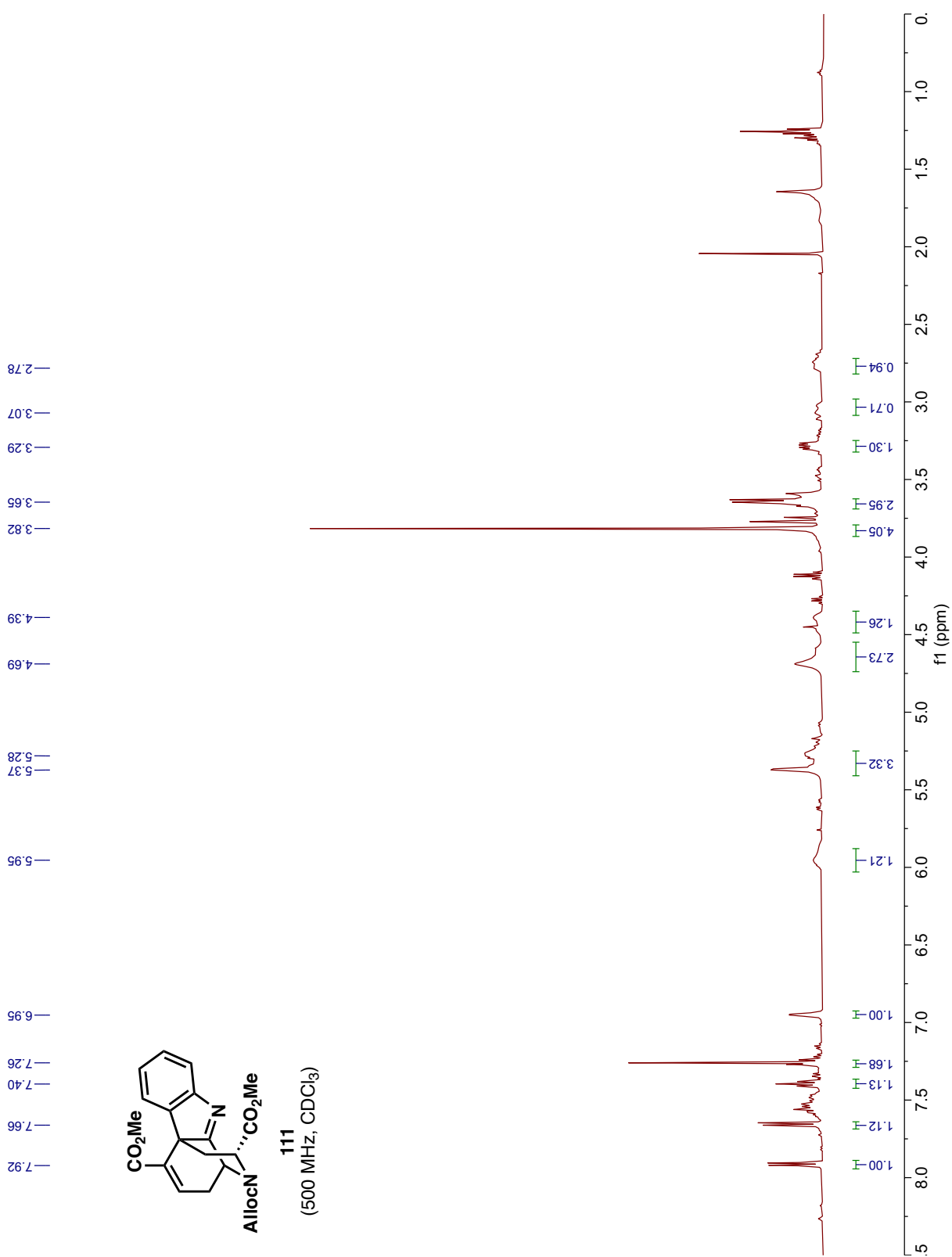


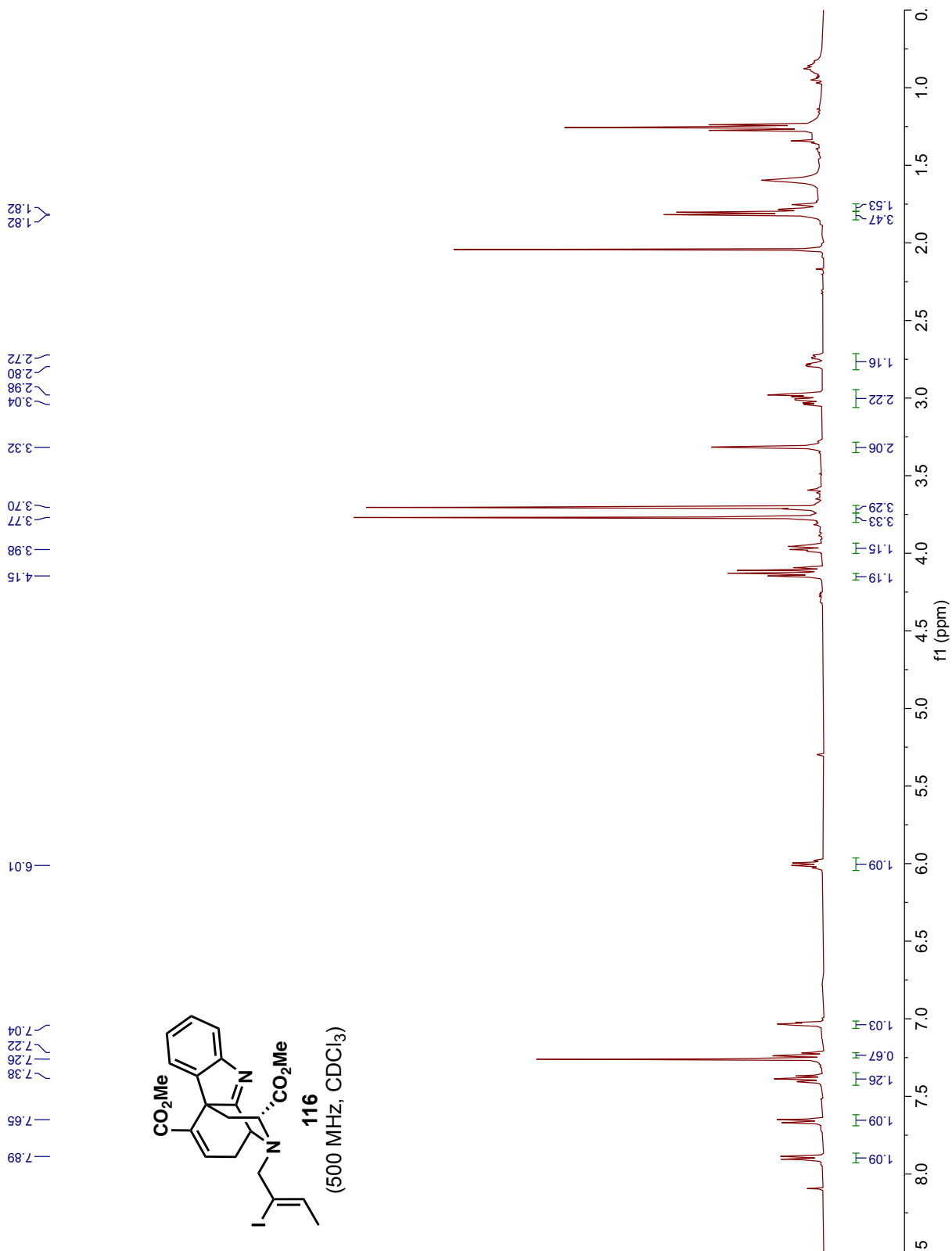


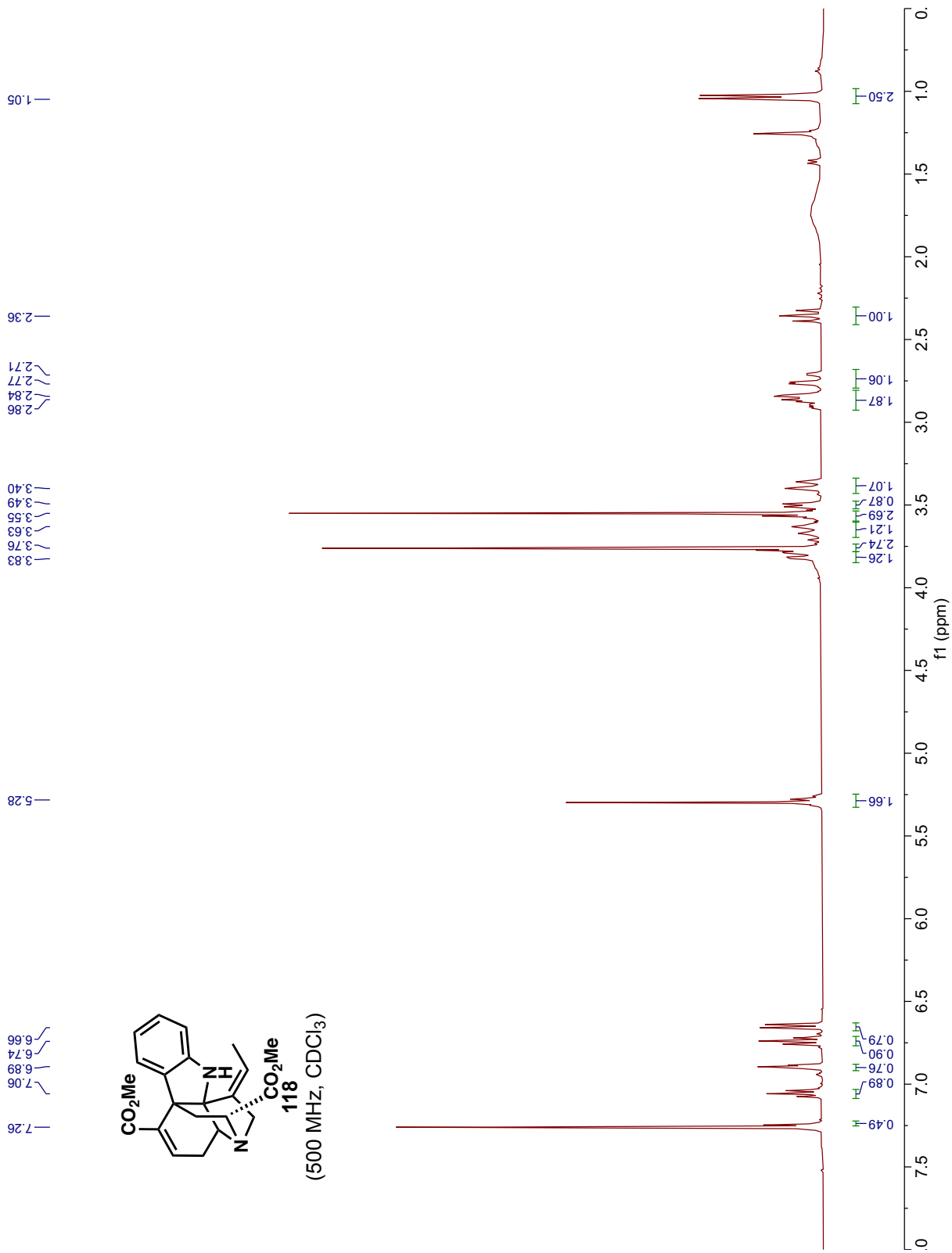


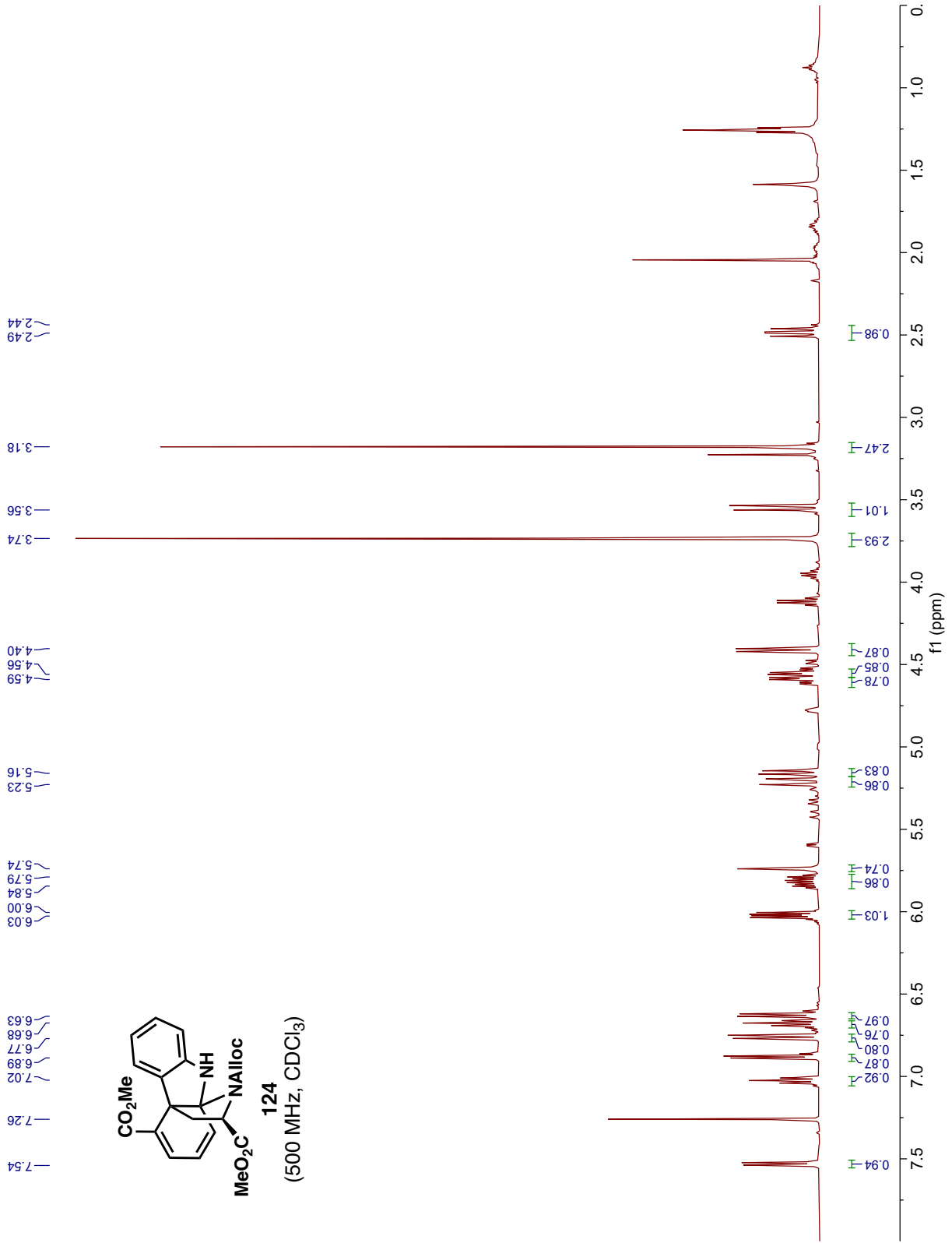


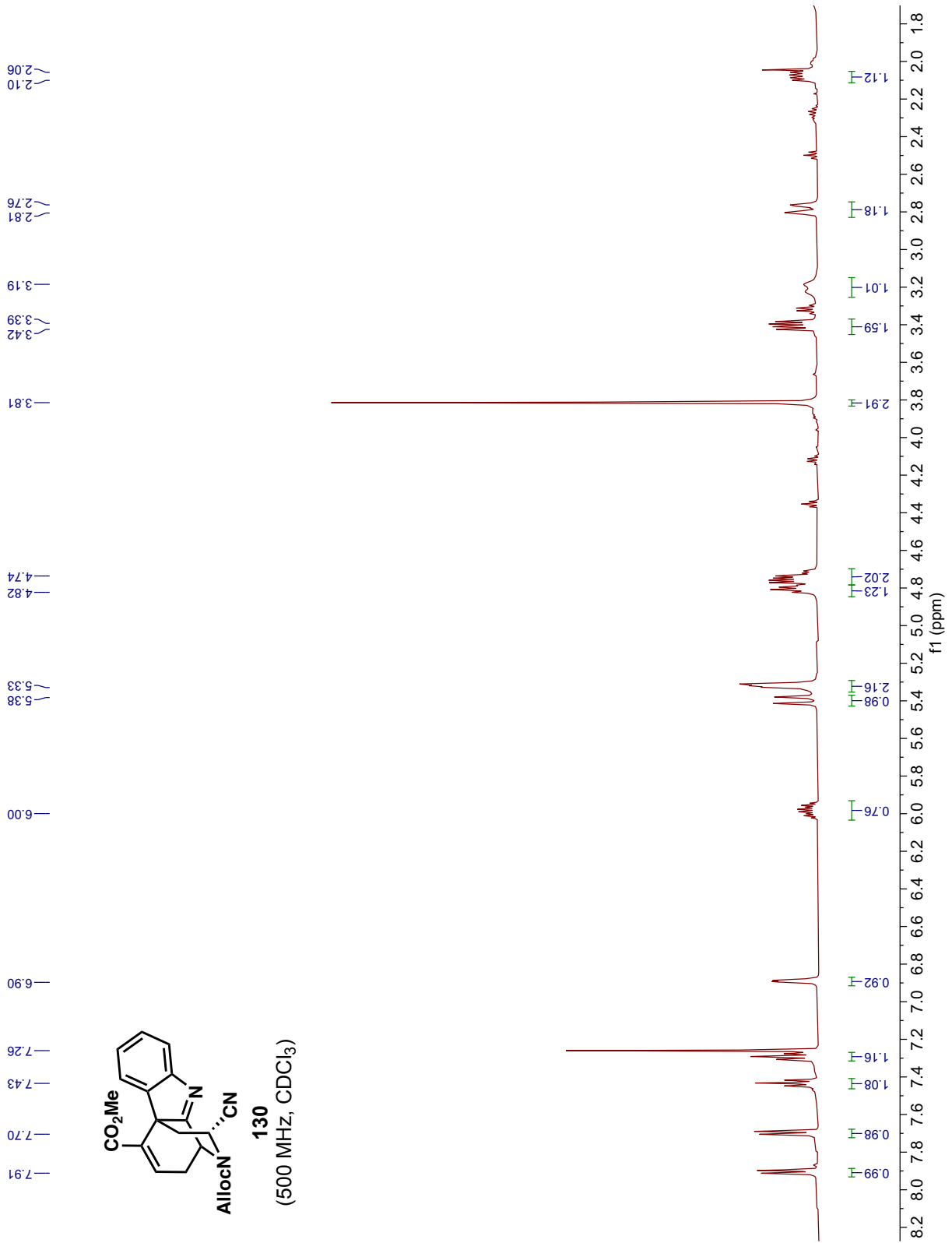


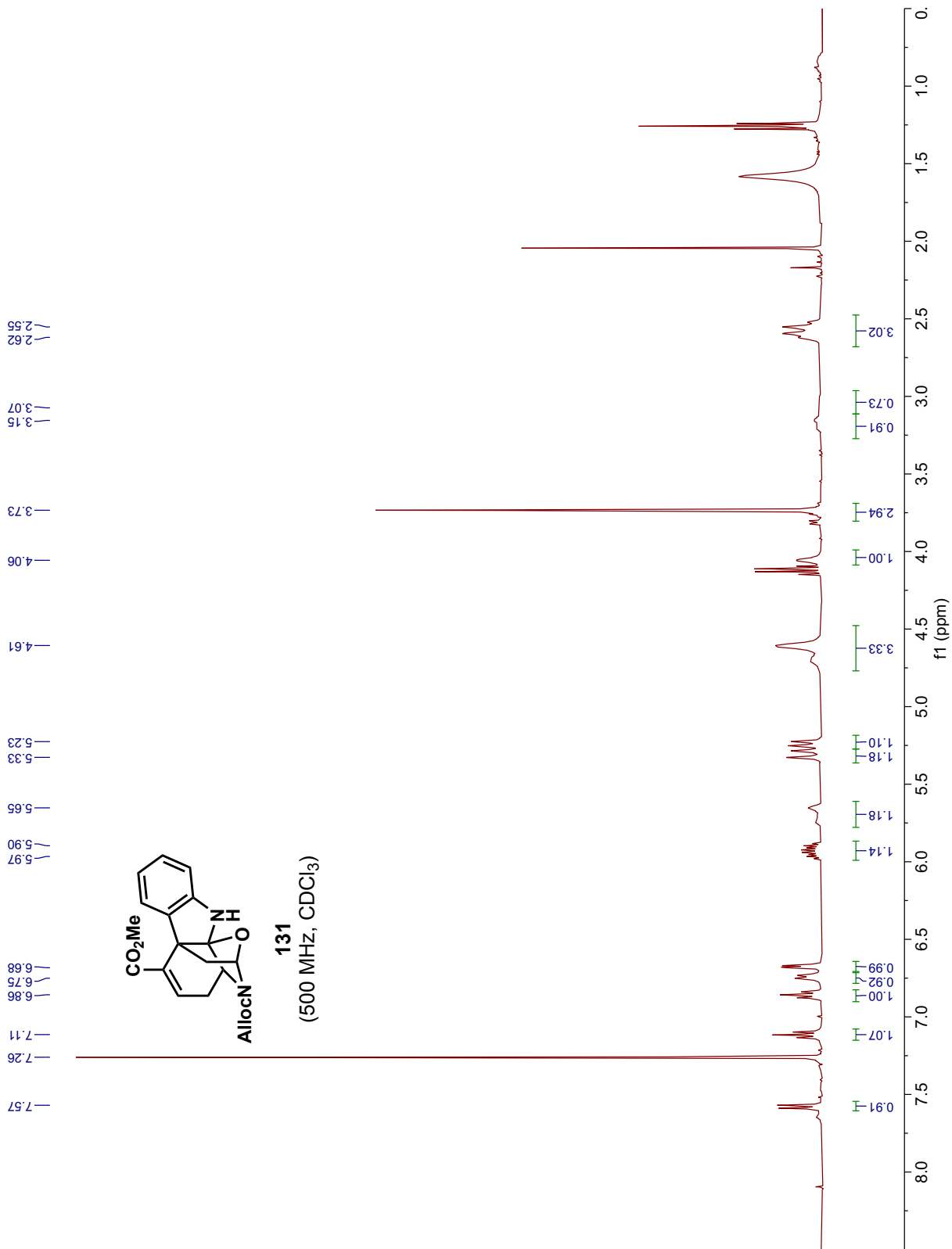


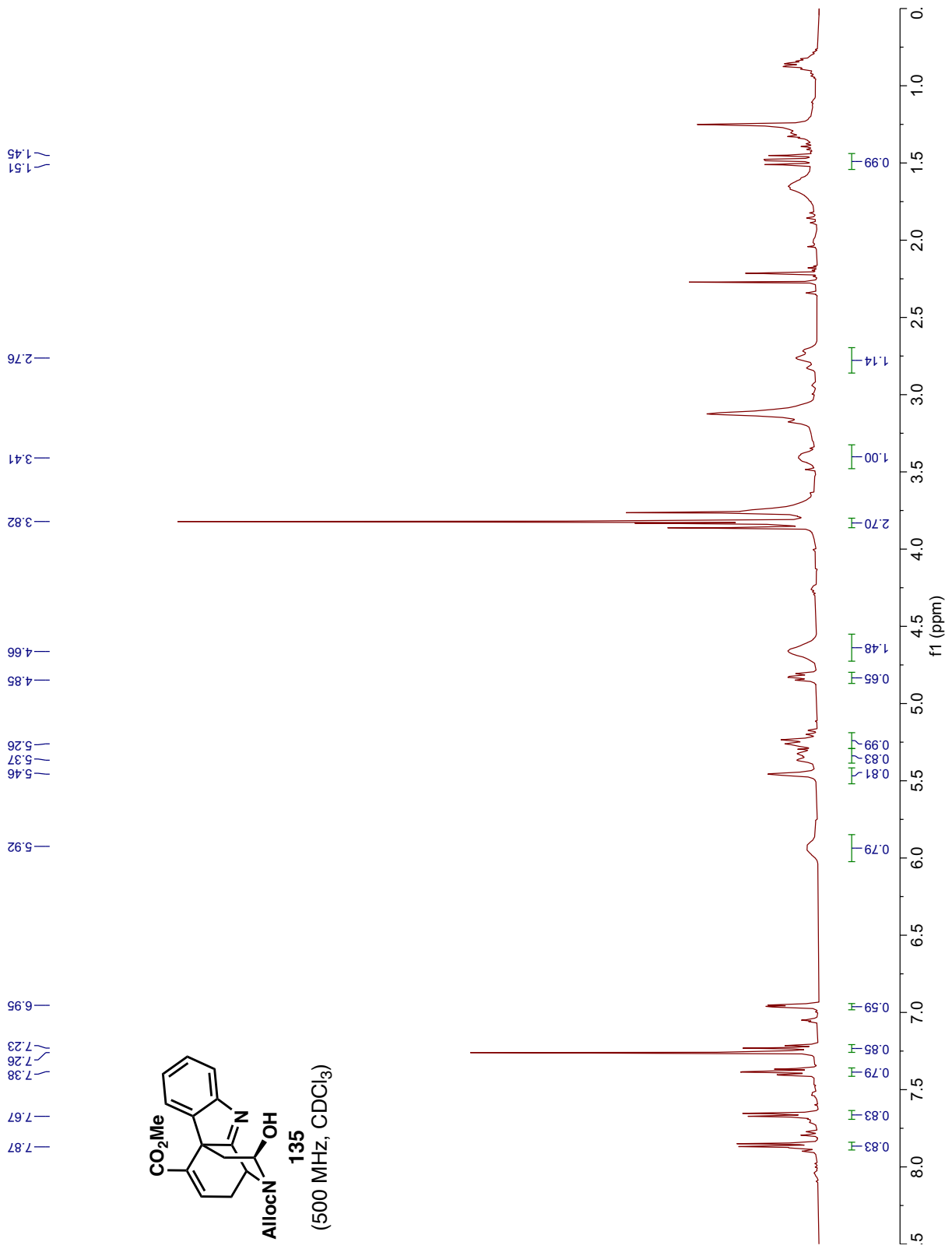


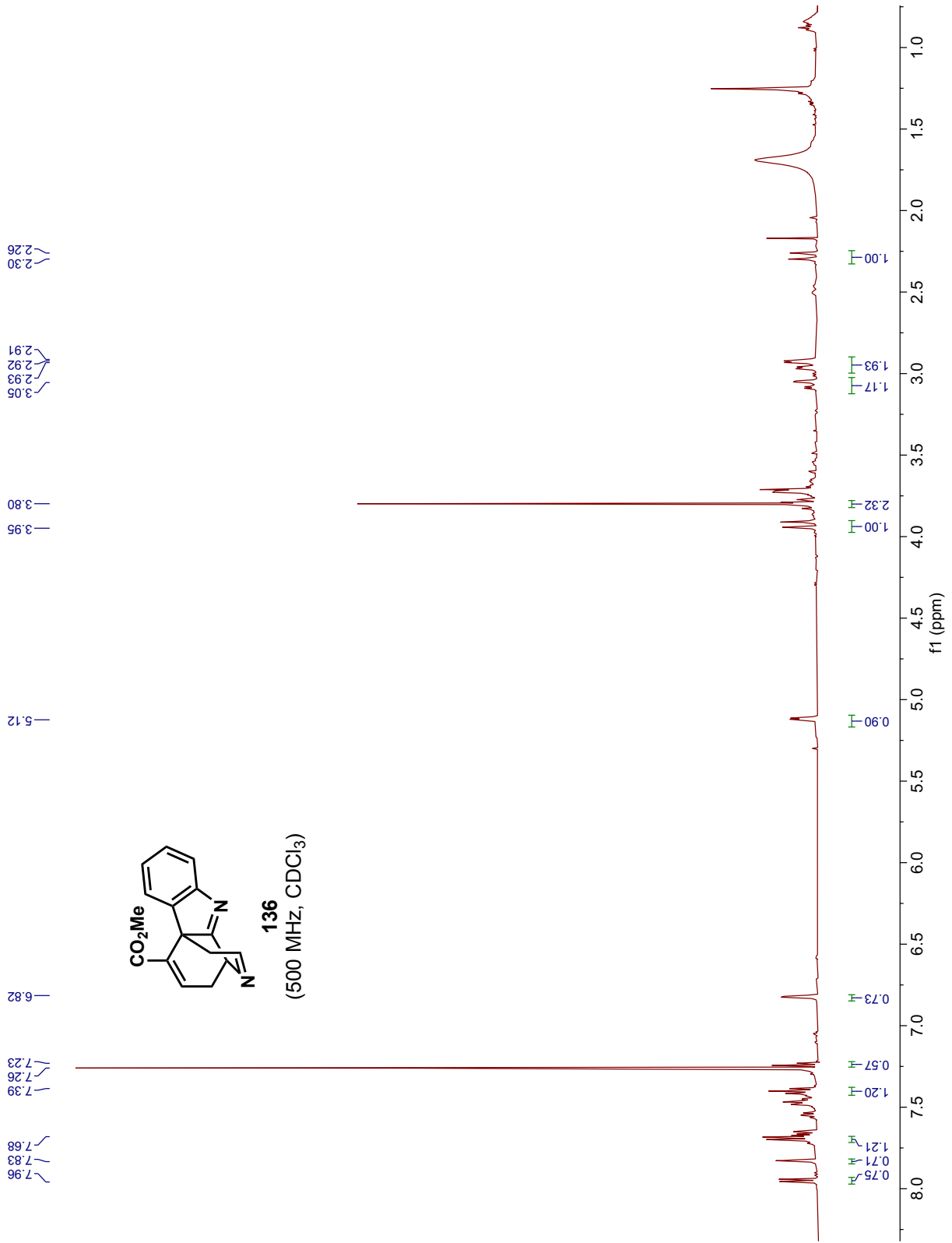


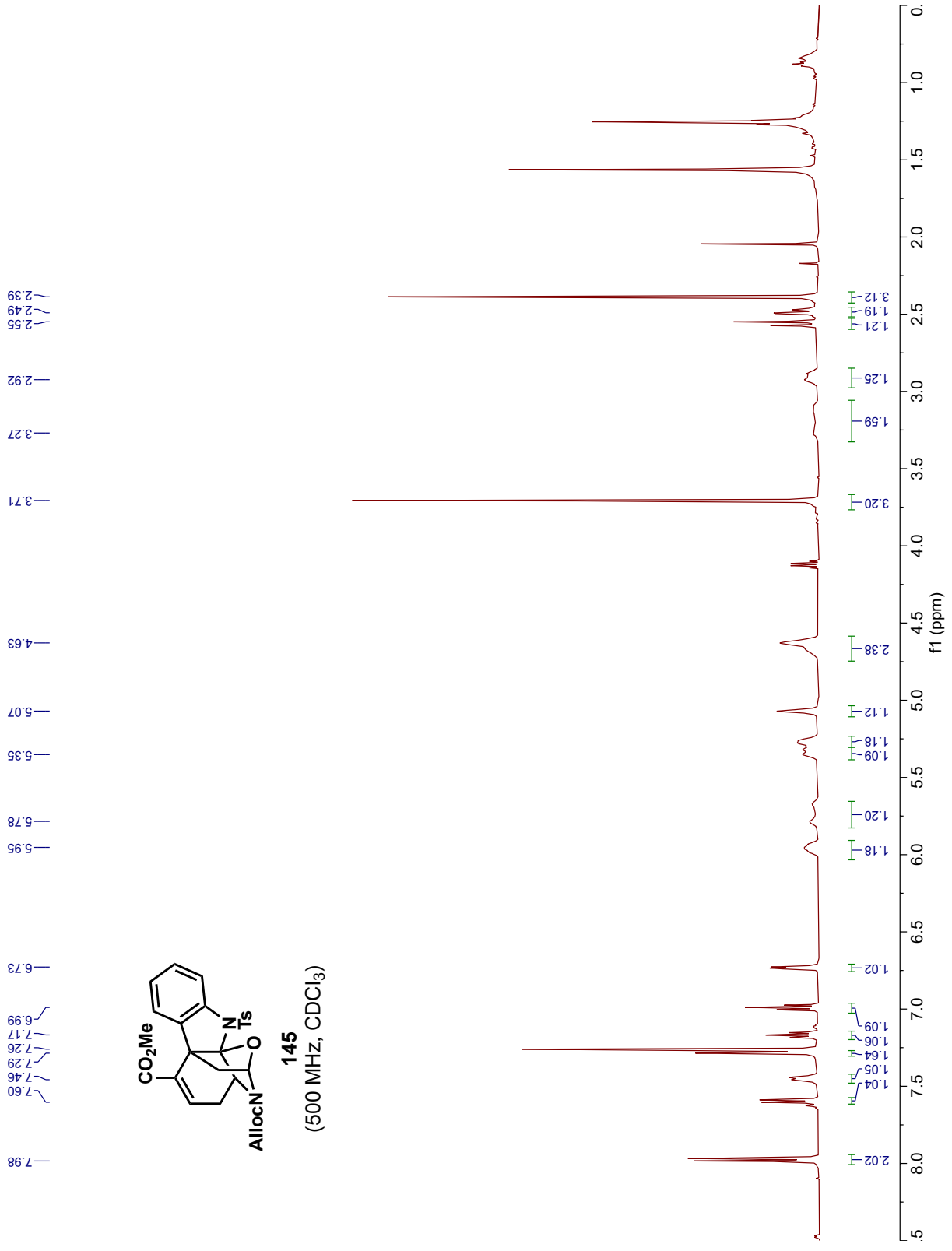


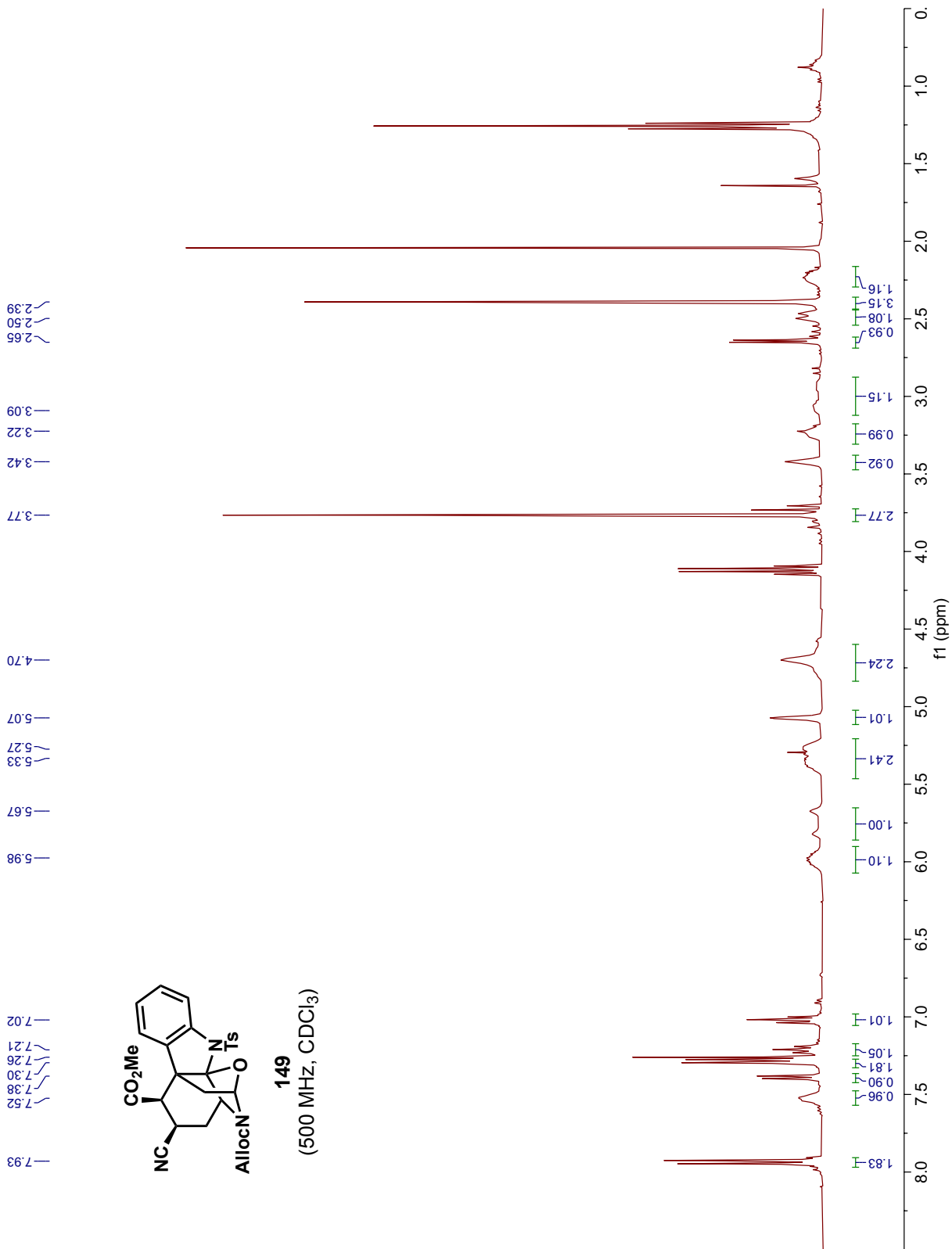


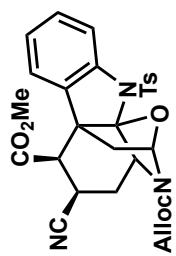












149
(500 MHz, CDCl₃)

